

**Luminescent Cyclometallated Ir(III) Complexes:  
Synthesis, Characterisation and Applications.**

**Thesis Submitted for the Degree of  
Doctor of Philosophy**

**by**

**Shalini Singh**

**at the  
University of Leicester**

**November 2010**

# **Title: Luminescent Cyclometallated Ir(III) Complexes: Synthesis, Characterisation and Applications**

**Author: Shalini Singh**

## **ABSTRACT**

A range of luminescent Ir(III) complexes  $[\text{Ir}(\text{C}^{\wedge}\text{N})_2(\text{X}^{\wedge}\text{Y})]^{n+}$  ( $n = 0, 1$ ) containing different cyclometallated ( $\text{C}^{\wedge}\text{N}$ ) and ancillary ( $\text{X}^{\wedge}\text{Y}$ ) ligands has been synthesised. All new compounds were fully characterised by  $^1\text{H}$  and  $^{13}\text{C}$  NMR spectroscopy, mass spectrometry and elemental analyses and several compounds have been structurally characterised by X-ray crystallography. The photophysical and electrochemical properties of the complexes were also studied.

Chapter one provides an introduction to luminescent transition metal complexes, in particular Ru(II) and Ir(III) complexes and gives an overview of the factors controlling the emission wavelengths of cyclometallated Ir(III) complexes and their applications, particularly as biological labels and probes. Chapter two discusses the synthesis and properties of  $[\text{Ir}(\text{C}^{\wedge}\text{N})_2(\text{bipy})]^+$  and shows that substituents para to the metal on the cyclometallated phenyl have a significant effect on the emission wavelength. Chapter three describes complexes  $[\text{Ir}(\text{C}^{\wedge}\text{N})_2(\text{X}^{\wedge}\text{Y})]^{n+}$  ( $n = 1$ ,  $\text{X}^{\wedge}\text{Y}$  = pyridine imine;  $n = 0$ ,  $\text{X}^{\wedge}\text{Y}$  = pyrrolylimine) and the effect of substituents on the redox properties and emission wavelength. Some of these complexes have been employed in live-cell imaging. In Chapter four the synthesis, characterisation and application of  $[\text{Ir}(\text{C}^{\wedge}\text{N})_2(\text{phen}^{\text{cat}}\text{-OH})]^+$  complexes as molybdate sensors is discussed.

Chapter five describes the synthesis of  $[\text{Ir}(\text{C}^{\wedge}\text{N})_2(\text{X}^{\wedge}\text{Y})]^{n+}$  ( $n = 0, 1$ ) containing a homochiral  $\text{X}^{\wedge}\text{Y}$  ligand i.e. (S)-soxH, (S)-pepH, (S)-phglyH, (+)-tfacH and (S)-ppea. The complexes are all formed as 1:1 mixtures of diastereomers with  $\Delta$  or  $\Lambda$  chirality at the metal. Diastereomers containing the (S)-sox and (S)-pep ligands can often be separated via crystallisation or column chromatography. Treatment of a single diastereomer ( $\Lambda\text{S}$  or  $\Delta\text{S}$ ) with an appropriate acid removes the sox or pep ligand hence provides a route to complexes with only metal-centred chirality, for example  $\Lambda$ - and  $\Delta$ - $[\text{Ir}(\text{ppz})_2(\text{bipy})]^+$ .

## Acknowledgements

I would like to express my deep and sincere gratitude to my supervisor, Dr D. L. Davies for his invaluable help, motivation, patience and guidance throughout this project. His wide knowledge and his logical way of thinking have been of great value for me. I could not have imagined having a better advisor and mentor for my Ph.D study.

My sincere thanks goes to Dr M. P. Lowe for his time, and assistance in the use of the flourimeter. I would also like to thank our collaborators in Ruhr University Bochum, Prof. Dr. Nils Metzler-Nolte and especially Annika Gross for live-cell imaging and in the University of York, Dr Anne-K. Duhme-Klair and co-workers for molybdate sensing studies.

I would like to thank all the people who have been involved in this project, Dr G. A. Griffith for 2D NMR spectra and Mr K. Singh for the X-ray structure determinations. Thanks are also due to Dr G. A. Eaton for the mass spectra.

My thanks are also extended to A. Armitage for the synthesis of some of the pyridineimine complexes, i.e. **3.14g**(*o*/*m*-C<sub>6</sub>H<sub>4</sub>Br), **3.14g**(*m*-C<sub>6</sub>H<sub>4</sub>OH) and **3.14g**(*p*-C<sub>6</sub>H<sub>4</sub>CO<sub>2</sub>Me) (see **Chapter 3**). Complex **5.5a** was synthesised by C. Daly (see **Chapter 5**). I would also like to thank everyone I have worked with in the lab for making it such a pleasurable experience, namely Youcef, Graeme, Rachel and Nitika.

I owe my loving thanks to my husband Hemant K. Singh and my daughter Saanvi. Without their encouragement and understanding it would never have been possible for me to finish this work. My special gratitude is due to my family (especially my father) in India for their loving support.

## Statement

This thesis is based on work conducted by the author, in the Department of Chemistry of the University of Leicester, during the period between January 2007 and January 2010. Live-cell imaging was done by the collaborators, Prof. Dr. Nils Metzler-Nolte and Annika Gross at Ruhr University Bochum, and molybdate sensing studies were carried out by Dr Anne-K. Duhme-Klair and co-workers at the University of York.

My thanks to A. Armitage and C. Daly for preliminary work in the area and specifically for the preparation of **3.14g(*o*/m-C<sub>6</sub>H<sub>4</sub>Br)**, **3.14g(*m*-C<sub>6</sub>H<sub>4</sub>OH)** and **3.14g(*p*-C<sub>6</sub>H<sub>4</sub>CO<sub>2</sub>Me)** and **5.5a**.

All the work described in the thesis is original unless otherwise stated in the text or in the references. This work is not being presented for any other degree.

Signed: \_\_\_\_\_

Date: \_\_\_\_\_

*Shalini Singh*

## Abbreviations

### NMR

bd	broad doublet
bs	broad singlet
bsept	broad septet
d	doublet
dd	doublet of doublets
ddd	doublet of doublet of doublets
dt	doublet of triplets
m	multiplet
s	singlet
sept	septet
septd	septet of doublets
t	triplet
td	triplet of doublets
tt	triplet of triplets
COSY	correlated spectroscopy
HMBC	heteronuclear multiple bond coherence
HSQC	heteronuclear single quantum correlation
NMR	nuclear magnetic resonance
NOE	nuclear Overhauser effect
NOESY	nuclear Overhauser effect spectroscopy
TOCSY	total correlation spectroscopy
ppm	parts per million
$\delta$	delta (NMR Chemical Shift)

### Other Techniques

CSP	chiral stationary phase
DFT	density functional theory
DSSC	dye sensitized solar cells
ELISA	enzyme-linked immunosorbent assay
ES-MS	electrospray mass spectrometry

FAB-MS	fast atom bombardment mass spectrometry
HPLC	high performance liquid chromatography
TLC	thin layer chromatography

## Others

<i>cf.</i>	compare
<i>d.e.</i>	diastereomeric excess
<i>e.e.</i>	enantiomeric excess
equiv	equivalent
<i>fac</i>	facial
HOMO	highest occupied molecular orbital
hr	hour
ILCT	intra ligand charge transfer
LC	ligand centred
LLCT	ligand to ligand charge transfer
LUMO	lowest unoccupied molecular orbital
MC	metal centred
<i>mer</i>	meridional
min	minute
ml	millilitre
MLCT	metal to ligand charge transfer
OLED	organic light emitting diode
PMT	photomultiplier tube
SCE	standard calomel electrode
sh	shoulder

## Chemical

acac	anion of pentane-2,4-dione
BINOL	[1,1']-binaphthalenyl-2,2'-diol
bipy	2,2'-bipyridine
bipy- <sup>t</sup> Bu <sub>2</sub>	4,4'-di- <i>tert</i> -butyl-2,2'-bipyridine
BSA	bovine serum albumin
DABCO	1,4-diazabicyclo[2.2.2]octane

DCM	dichloromethane
DMSO	dimethylsulfoxide
dppz	dipyrido[3,2-a:2',3'c]phenazine
dps	4,7-diphenyl-1,10-phenanthrolinedisulfonic acid disodium salt
GFP	green fluorescent proteins
HSA	human serum albumin
Ig	immunoglobulin
<sup>i</sup> Pr	isopropyl
iq	isoquinoline-3-carboxylate
NHS	N-hydroxysuccinimide
phen	phenanthroline
pmpz	3,5-dimethyl-1-phenyl-1H-pyrazole
ppy	2-phenylpyridine
ppz	1-phenylpyrazole
py	pyridine
<sup>t</sup> Bu	t-butyl
terpy	2,2';6',2"-terpyridine
TFA	trifluoroacetic acid
THF	tetrahydrofuran
TMS	trimethylsilane
topy	2-(p-tolyl)pyridine
TRISPHAT	tris-(tetrachlorobenzenediolato)phosphate(V)
(+)-tfacH	(+)-3-(trifluoroacetyl)-camphor
(S)-pepH	( <i>S,E</i> )-2-((1-phenylethylimino)methyl)phenol
(S)-phglyH	( <i>S</i> )-(+)-2-phenylglycine
(S)-soxH	( <i>S</i> )-2-(4-isopropyl-4,5-dihydrooxazol-2-yl)phenol

## List of contents

<b>Chapter 1 General Introduction</b>	1
1.1 Luminescence	1
1.2 Luminescent Transition Metal Complexes	2
1.2.1 Luminescent Ru (II) and Os (II) complexes	6
1.2.2 Luminescent Pt (II) complexes	10
1.2.3 Luminescent Re (I) complexes	11
1.2.4 Luminescent bis-tridentate Ir(III) complexes	12
1.3 Luminescent Ir(III) complexes, $[\text{Ir}(\text{C}^{\wedge}\text{N})_3]$ and $[\text{Ir}(\text{C}^{\wedge}\text{N})_2(\text{X}^{\wedge}\text{Y})]^n$ ( $n = 0, +1, -1$ )	13
1.3.1 Synthesis of Ir (III) complexes i.e. $[\text{Ir}(\text{C}^{\wedge}\text{N})_3]$ and $[\text{Ir}(\text{C}^{\wedge}\text{N})_2(\text{X}^{\wedge}\text{Y})]^{n+}$	16
1.3.2 Emission in Ir (III) complexes i.e. $[\text{Ir}(\text{C}^{\wedge}\text{N})_3]$ and $[\text{Ir}(\text{C}^{\wedge}\text{N})_2(\text{X}^{\wedge}\text{Y})]^{n+}$	19
1.3.2.1 Tuning of luminescent wavelength by variation of $\text{X}^{\wedge}\text{Y}/\text{XY}$ ligands	19
1.3.2.2 Tuning of luminescent wavelength by variation of $\text{C}^{\wedge}\text{N}$ ligands	21
1.3.2.3 Effect of conjugation	23
1.3.2.4 Tuning of emission by varying substituents	25
1.3.2.5 Colour Tuning	29
1.4 Bioconjugation	31
1.4.1 Transition metal complexes as labels	34
1.4.1.1 Protein and Hormone labels	34
1.4.1.2 Biotin complexes	38
1.4.1.3 DNA probes and labels	39
1.4.2 Applications of transition metal complexes in live cell imaging	44
<b>Chapter 2 Synthesis and Characterisation of bis-cyclometallated Ir(III) diimine complexes <math>[\text{Ir}(\text{C}^{\wedge}\text{N})_2(\text{X}^{\wedge}\text{Y})]^+</math></b>	55
2.1 Introduction	55
2.1.1 Microwave Chemistry	58
2.2 Results and Discussion	60
2.2.1 Synthesis of $[\text{Ir}(\text{C}^{\wedge}\text{N})_2\text{Cl}]_2$	61

2.2.2 Synthesis and characterisation of diimine complexes $[\text{Ir}(\text{C}^{\text{N}})_2(\text{X}^{\text{Y}})]^+$ ( $\text{X}^{\text{Y}}$ = bipy and dps)	65
2.2.2.1 Electrochemistry of Ir(III) diimine complexes $[\text{Ir}(\text{C}^{\text{N}})_2(\text{bipy})]^+$ (2.7a-f)	71
2.2.2.2 Photophysical properties of $[\text{Ir}(\text{C}^{\text{N}})_2(\text{bipy})]^+$ (2.7a-f) and $[\text{Ir}(\text{C}^{\text{N}})_2(\text{dps})]^+$ complexes (2.8a,g)	73
2.3 Experimental	79
2.4 Bibliography	87
 <b>Chapter 3 Synthesis, Characterisation and Properties of <math>[\text{Ir}(\text{C}^{\text{N}})_2(\text{X}^{\text{Y}})]^{\text{n}+}</math></b>	
(n = 0, 1) (n = 1, X^Y = pyridineimine; n = 0, X^Y = pyrrolylimine)	90
3.1 Introduction	90
3.2 Results and Discussion	93
3.2.1 Synthesis and characterisation of $[\text{Ir}(\text{C}^{\text{N}})_2(\text{pyridineimine})]^+$ (3.14)	93
3.2.1.1 Electrochemistry of $[\text{Ir}(\text{C}^{\text{N}})_2(\text{pyridineimine})]^+$ (3.14)	111
3.2.1.2 Photophysical properties of $[\text{Ir}(\text{C}^{\text{N}})_2(\text{pyridineimine})]^+$ (3.14)	115
3.2.2 Synthesis and characterisation of $[\text{Ir}(\text{C}^{\text{N}})_2(\text{pyrrolylimine})]$ (3.15)	122
3.2.2.1 Electrochemistry of $[\text{Ir}(\text{C}^{\text{N}})_2(\text{pyrrolylimine})]$ (3.15)	126
3.2.2.2 Photophysical properties of $[\text{Ir}(\text{C}^{\text{N}})_2(\text{pyrrolylimine})]$ (3.15)	129
3.2.3 Live-cell imaging	132
3.3 Experimental	136
3.4 Bibliography	156
 <b>Chapter 4 Bis-cyclometallted Ir(III) complexes for use as Oxometallate Sensors</b>	
4.1 Introduction	158
4.2 Results and Discussion	163
4.2.1 Synthesis and Characterisation	163
4.2.2 Photophysical properties of $[\text{Ir}(\text{C}^{\text{N}})_2(\text{phencat-OMe})]^+$ (4.9) and $[\text{Ir}(\text{C}^{\text{N}})_2(\text{phencat-OH})]^+$ (4.11) complexes.	169
4.2.3 Molybdate sensing	172

4.3 Experimental	174
4.4 Bibliography	179
<b>Chapter 5 Homochiral bis-cyclometallated Ir(III) complexes</b>	<b>181</b>
5.1 Introduction	181
5.2 Results and Discussion	187
5.2.1 Synthesis and resolution of Ir(III) diastereomers	187
5.2.2 Synthesis of homochiral dimers and homochiral complexes	211
5.3 Experimental	216
5.4 Bibliography	232

# **Chapter One:**

## **General Introduction**

## Chapter 1 General Introduction

### 1.1 Luminescence

When a molecule absorbs energy in the form of electromagnetic radiation, an electron is excited to a higher energy level ( $S_1$  or  $S_2$ ), it can return to the ground state ( $S_0$ ) by a number of routes with emission of light. This process is known as luminescence.

Luminescence can be schematically illustrated with the classical Jablonski diagram (Fig. 1.1), which was firstly proposed by Alexander Jablonski in 1935.<sup>1</sup>

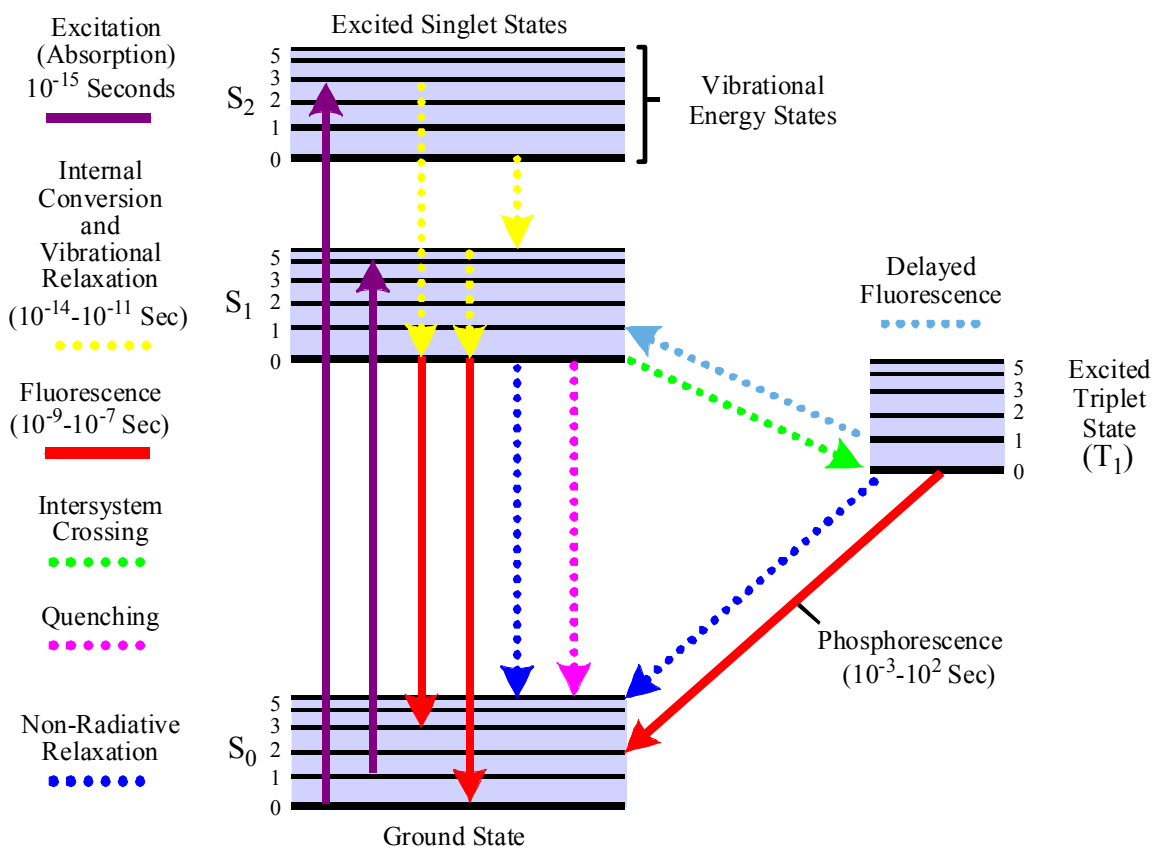


Fig. 1.1: Jablonski energy diagrams

There are three main types of luminescence described below:

**(i) Fluorescence** – This occurs if the electron decays immediately from  $S_1$  to  $S_0$ . An electron in the excited state is paired anti-parallel with an electron in a ground state so the return of this electron is spin allowed and hence the emission of a photon is very rapid. The time scale for fluorescence is  $10^{-9}$ - $10^{-7}$  sec.

**(ii) Phosphorescence** – Occurs when the electron in the excited state  $S_1$  undergoes a spin conversion and jumps to a forbidden triplet excited state  $T_1$  (intersystem crossing) then emission from the excited triplet state occurs with lower energy (longer wavelength) relative to fluorescence. It is a forbidden transition hence the time scale is longer as compared to fluorescence ( $10^{-3}$ - $10^2$  sec).

**(iii) Delayed Fluorescence** – Occurs when the electron first decays into the triplet state and then crosses back over into the lowest singlet excited state before returning to the ground state.

Most organic molecules that emit light, including  $\pi$ -conjugated ligands, do so from singlet excited states; therefore the emission is a spin allowed process termed fluorescence. The  $d^6$  and  $d^8$  second and third row transition metal ions [Re(I), Ru(II), Os(II), Rh(III), Ir(III), and Pt(II)] can induce intersystem crossing by strong spin-orbit coupling, which means the excited states are a hybrid of singlet (spin allowed) and triplet (spin forbidden) states that leads to the relaxation of spin selection rules. The presence of some triplet contribution leads to slower emission and consequently prolongs the emissive lifetimes. The long lived emission allows time resolved detection methods of analysis to be employed, which gets round the problem of background interference from other fluorescent bio-molecules and also offers the potential for lifetime based sensing and imaging.<sup>2</sup>

## 1.2 Luminescent Transition Metal Complexes

To understand the luminescence of  $d^6$  transition metal complexes, it is useful to consider a localised molecular orbital model of the excited states. **Fig. 1.2** shows the orbitals and spectroscopic states diagram for a low spin  $d^6$  octahedral complex ( $ML_6$ ).<sup>3,4</sup> The octahedral crystal field of the ligands splits the five degenerate d-orbitals into a triply degenerate  $t_{2g}$  level and a doubly degenerate  $e_g^*$  level. The magnitude of the splitting ( $\Delta$ ) is dependent on the crystal field strength of the ligands and the central metal ion. In the strong field configuration, the ground state is  $t_{2g}^6$  and as all spins are paired it is a singlet ( $S_0$ ). The lowest excited states are derived from promoting an electron to one of the unoccupied orbitals. There are three types of excited states: metal centred d-d states, ligand based  $\pi$ - $\pi^*$  states and charge transfer states. Metal centred d-d states arise from promoting a bonding electron from the  $t_{2g}$  level to  $e_g^*$  level ( $t_{2g}^5 e_g^{*1}$ ) and give rise to weak (Laporte forbidden) absorption bands ( $\epsilon = ca. 100 \text{ L mol}^{-1} \text{ cm}^{-1}$ ). Thus d-d emission is characterised by long radiative lifetimes and negligible quantum yields. Ligand based  $\pi$ - $\pi^*$  states derive from

promoting a bonding  $\pi$ -electron to an antibonding  $\pi^*$  level. These transitions are highly intense and are localised on the ligands. Charge transfer states involve either metal to ligand charge transfer (MLCT) by promoting an electron from a metal orbital to a ligand orbital ( $t_{2g}^5\pi^{*1}$ ) or ligand to metal charge transfer (LMCT) which involves promoting an electron from a ligand to a metal orbital ( $\pi^1e_g^1$ ). These transitions have significant absorptions in the visible region ( $\epsilon = ca. 20,000 - 25,000 \text{ L mol}^{-1} \text{ cm}^{-1}$ ).<sup>3,4</sup>

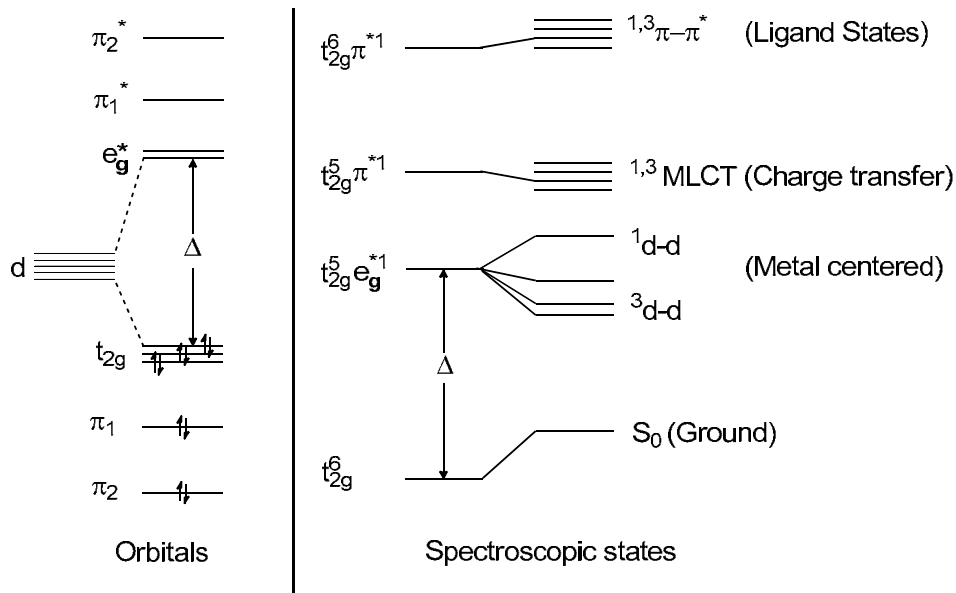


**Fig. 1.2:** Simplified orbital and state diagrams for a  $d^6$  metal in an octahedral environment.<sup>3,4</sup>

For a metal complex to be luminescent, it has to meet certain criteria: (i) the lowest excited state must be either a charge transfer (CT) or ligand  $\pi-\pi^*$ , this avoids photochemical instability associated with unstable d-d excited states, (ii) spin-orbit coupling should be high to enhance the emission to be more allowed and permit radiative decay to compete more effectively with non-radiative decay, which precludes first transition series complexes, (iii) the crystal field should be strong enough to raise the d-d state above the MLCT state, to avoid thermal excitation. For example; in iron complexes,  $[\text{FeL}_3]^{2+}$ , the d-d states are lower than the MLCT (**Fig. 1.3**), therefore, these complexes are non-luminescent. In contrast,  $[\text{RuL}_3]^{2+}$  complexes are luminescent, because the d-d states are above the MLCT states and do not serve as a major route of non-radiative decay. In  $[\text{OsL}_3]^{2+}$  complexes, the d-d levels are higher still and are not accessible, which makes these complexes highly photostable but their MLCT levels are lower with respect to ruthenium complexes which make them weakly luminescent in general. This can be explained on the

basis of the energy gap law which states that as the energy of the excited state becomes closer to the ground state, the rate of non-radiative decay increases.<sup>3</sup> Hence, Os(II) polypyridine complexes typically have long wavelength emission due to a low energy MLCT state and also have a rapid rate of non-radiative decay. The quantum efficiency of metal complexes is dependent on the radiative and non-radiative relaxation of the excited states. Non-radiative relaxation occurs on a much faster time scale than radiative transitions.<sup>3,5</sup>

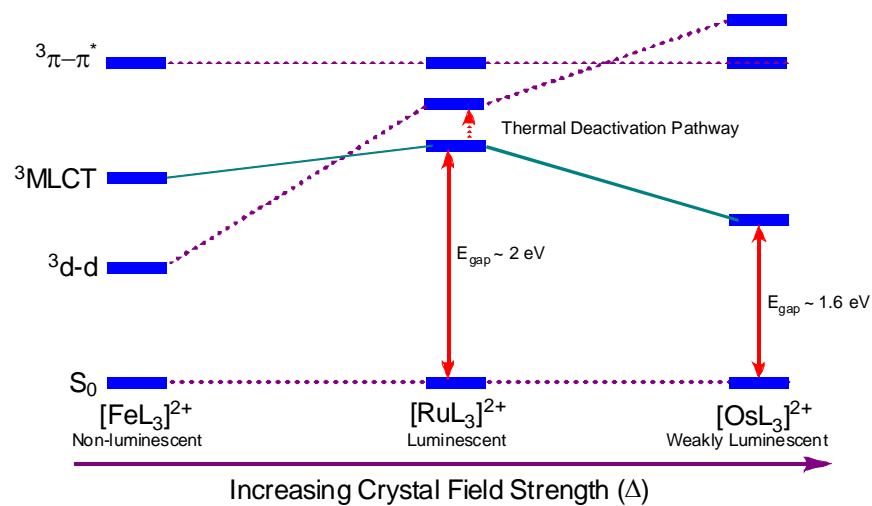


**Fig. 1.3:** Lowest energy triplet states for metal ligand complexes with increasing crystal field strength.<sup>6</sup>

The relative levels of the MLCT and d-d states also determine the sensitivity of excited state decay times to temperature. If the d-d states are close to the MLCT level, then they are thermally accessible. In such cases increasing the temperature results in decreasing the lifetimes, due to the thermal population of the d-d states followed by rapid non-radiative decay. Osmium complexes are less sensitive to temperature due to high, and hence thermally inaccessible, d-d levels. It is well established now, that metal perturbed  ${}^3\text{LC}$  ( ${}^3\pi\text{-}\pi^*$ ) excited states, which can be fairly emissive at 77 K in a rigid matrix, are rarely emissive at room temperature in fluid solution, because these are effectively deactivated by thermal population to upper-lying  ${}^3\text{MC}$  ( ${}^3\text{d-d}$ ) levels, which finally deactivate by fast non-radiative transition to the ground state.<sup>7</sup>

Solvent can also have a profound effect on the emission spectra of polar metal complexes. Though the effects of solvent and environment on emission are complex, in

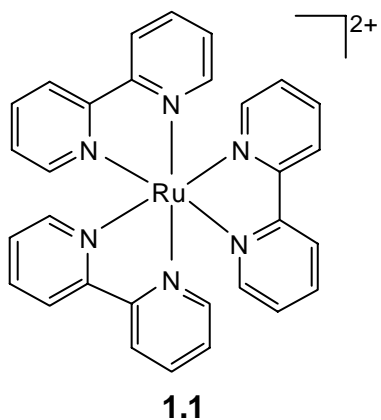
general, polar complexes display a large sensitivity to solvent polarity while non polar molecules are much less sensitive to solvent polarity. Considering only the solvent effects, polar solvents shift the emission to lower energy due to stabilization of the excited state by the polar solvent molecules. Typically, the lumophore has a larger dipole moment in the excited state ( $\mu_E$ ) than in the ground state ( $\mu_G$ ). Following excitation, the solvent dipoles can reorient or relax around  $\mu_E$ , which lowers the energy of the excited state. This effect becomes larger with the increase of polarity of the solvent; therefore emission shifts to lower energies (or longer wavelengths) with increase in the polarity of the solvent.

As discussed above, luminescent transition metal complexes have interesting photophysical properties and have attracted much attention in the past few decades because of their diverse applications. For example, they can be used as photo-sensitizers in solar energy conversion,<sup>8-10</sup> in chemi/electroluminescent systems,<sup>11</sup> emissive dopants in organic light emitting devices (OLEDs),<sup>12-19</sup> photocatalysts for CO<sub>2</sub> reduction,<sup>20, 21</sup> luminescent sensors<sup>22-26</sup>, biological labels,<sup>27-29</sup> and biological probes.<sup>30</sup> These applications have focused mainly on a few key 2<sup>nd</sup> and 3<sup>rd</sup> row transition metals [*i.e.* Re(I), Ru(II), Os(II), Pt(II), Rh(III) and Ir(III)] that have certain desirable luminescent properties such as; long emission life times (0.1 to  $> 100$   $\mu$ sec), high quantum yields (0.01 to nearly 1) and large Stokes shifts. Long emission lifetimes help to discriminate the ubiquitous background fluorescence of bio-molecules ( $\tau = \sim$  nsec) from the emission of the complex ( $\tau = \sim$   $\mu$ sec), by giving a delay before detection which is difficult for organic fluorophores owing to their shorter lifetimes. The Stokes shift is the difference between the band maxima of the absorption and emission arising from the same electronic transition; therefore, a large Stokes shift helps to isolate the excitation and emission wavelengths.

The capacity to make neutral, cationic and anionic complexes increases their versatility for different applications. For example, neutral complexes tend to be more volatile and have good miscibility in organic materials which make them ideal for the fabrication of organic light emitting diodes (OLEDs) using direct vacuum deposition, while cationic complexes are good for light emitting electrochemical cells (LECs) as these require an excess of mobile ions in the emissive layer. Luminescent Ir(III) complexes, in particular, have an advantage over many other metal complexes as they have greater structural variety and hence ability to tune the emission over a wide range of wavelength through variation of ligand structure and substituents,<sup>31-33</sup> this will be discussed in more detail in **Section 1.3.2**.

The next section will consider selected examples of luminescent complexes of Ru(II), Os(II), Pt(II), Re(I) and Ir(III). In particular, comparisons will be drawn between diimine complexes containing bipy or terpy ligands and analogous complexes in which one pyridine is replaced by a cyclometallated phenyl. The effect of this change and other substituents on the ligands on luminescence will be discussed.

### 1.2.1 Luminescent Ru (II) and Os (II) complexes

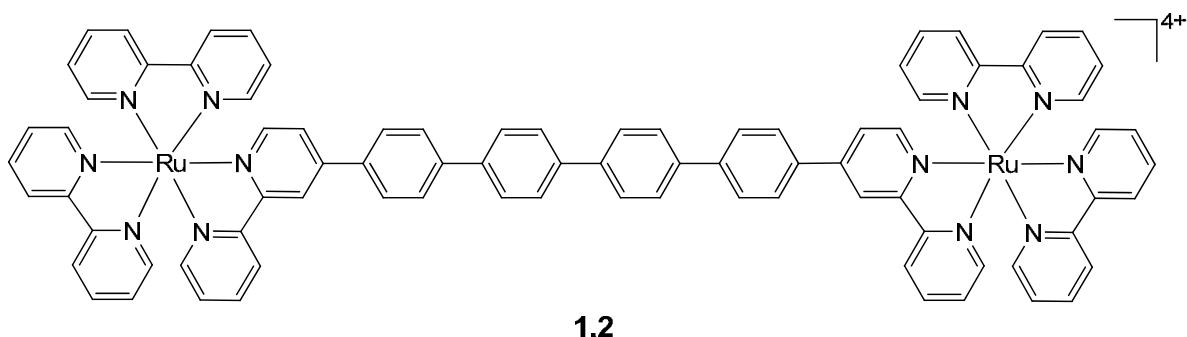


Electrochemical studies of  $[\text{Ru}(\text{bipy})_3]^{2+}$  (**1.1**) show that it undergoes a reversible metal-centred Ru(II)/(III) oxidation process ( $E_{\text{Ox}} = +1.28$  V) and a reversible reduction ( $E_{\text{Red}} = -1.33$  V) which is ligand centred (bipy).<sup>9</sup> Therefore, Ru  $t_{2g}$  orbitals are the highest occupied molecular orbitals (HOMO) and the lowest unoccupied molecular orbital (LUMO) resides on the bipy.<sup>34</sup> Consequently, the lowest energy electronic transition is a metal to ligand charge transfer  $^3\text{MLCT}$  transition.<sup>35</sup> Upon excitation at 452 nm,  $[\text{Ru}(\text{bipy})_3]^{2+}$  emits at 605 nm with an emission life time ( $\tau$ ) of 153 ns in air equilibrated acetonitrile and a quantum yield ( $\phi$ ) of 0.062.<sup>36</sup>

Since the luminescence of  $[\text{Ru}(\text{bipy})_3]^{2+}$  (**1.1**) was first reported,<sup>37</sup> tris(diimine) and related ruthenium complexes have received a wealth of attention due to their attractive photophysical and photochemical properties. The combination of properties like high chemical, thermal and photochemical stability, reversible redox behaviour, substantial UV-visible light absorption and long lived metal to ligand charge transfer (MLCT) excited states make  $[\text{Ru}(\text{bipy})_3]^{2+}$  and its analogues ideal for diverse applications.  $[\text{Ru}(\text{bipy})_3]^{2+}$  in particular is the most widely studied luminescent complex in existence. For example,  $[\text{Ru}(\text{bipy})_3]^{2+}$  and its derivatives have been investigated extensively as model compounds for studies of photochemical processes,<sup>10, 34</sup> light harvesting processes that mimic

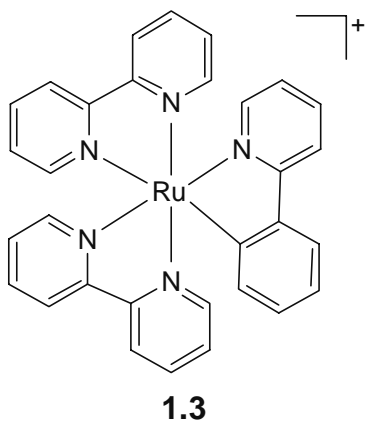
photosynthesis,<sup>38-41</sup> as photo-sensitizers in conversion of solar energy into chemical or electrical energy,<sup>8, 9, 41,42</sup> as oxygen sensors,<sup>43, 44</sup> as biological labels,<sup>45</sup> and probes,<sup>46</sup> and in cell imaging.<sup>2, 47</sup> (Note - applications of  $[\text{Ru}(\text{bipy})_3]^{2+}$  and/or its derivatives as oxygen sensors and biological labels and probes will be discussed in more detail in later sections).

De Cola *et al.* reported an electroluminescent device using a semiconducting polymer combined with a derivative of  $[\text{Ru}(\text{bipy})_3]^{2+}$  (**1.2**) which showed fully reversible voltage dependent switching between green and red light emission.<sup>48</sup> The HOMO levels of the polymer and of the complex **1.2** are almost isoenergetic, whereas the LUMO of **1.2** is about 0.5 eV lower in energy than that of the polymer. The device emits pure red light from complex **1.2** when the indium tin oxide (ITO) contact is biased positively (forward bias), and green light from the polymer when the ITO contact is biased negatively (reverse bias).



Exploiting the rich electrochemical properties of  $[\text{Ru}(\text{bipy})_3]^{2+}$ , Kalyanasundaram and Gratzel successfully demonstrated the production of dihydrogen and dioxygen from dissociation of water using  $[\text{Ru}(\text{bipy})_3]^{2+}$ .<sup>49</sup> In recent years, one of the most actively scrutinized aspects of solar energy conversion has been concerned with the design and optimisation of dye sensitized solar cells (DSSCs).<sup>50, 51</sup> In 1991, Gratzel and co-workers reported a revolutionary type of solar cell which mimics the “electron pump mechanism” of photosynthesis based on a ruthenium complex sensitizer in place of chlorophyll and titanium dioxide semiconductor as an analogue of a biological membrane.<sup>35</sup>

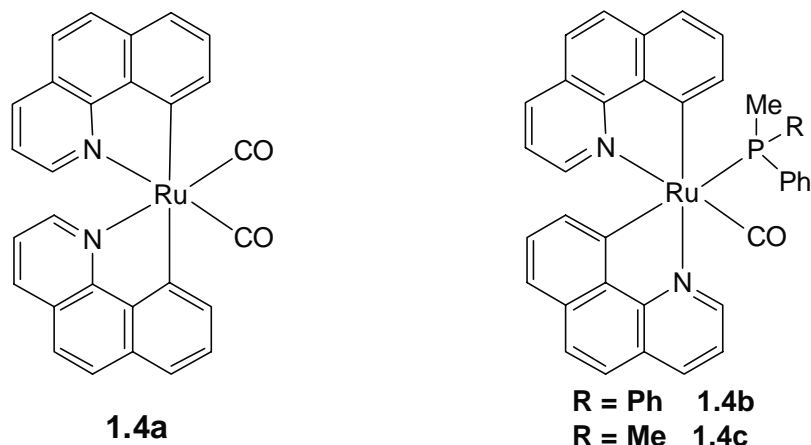
Recently, luminescent transition metal complexes containing cyclometallated ligands, such as 2-phenylpyridine (Hppy) and benzo-(h)-quinoline (Hbzq) etc, have received a great deal of attention. Cyclometallated ligands exhibit higher field strength than bipy due to the strong donor capability of the metallated carbon.<sup>16, 52</sup> This raises the energy of the metal centred d-d excited states, hence reduces deactivation by non radiative



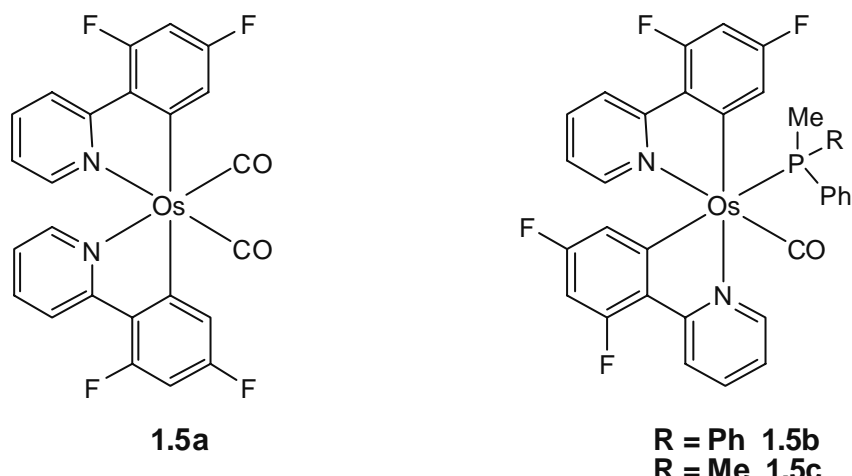
decay and offers increased luminescence compared to bipy complexes.<sup>9</sup> Moreover, cyclometallation also shifts the emission towards longer wavelengths, which is a desirable factor in DSSCs to harness a greater fraction of the solar spectrum.<sup>53, 54</sup> Following this idea, the viability of using cyclometallated Ru complexes in DSSCs has been explored and been found to be very promising.<sup>8, 9</sup> Cyclometallated complex,  $[\text{Ru}(\text{ppy})(\text{bipy})_2]^+$  (**1.3**) undergoes a reversible oxidation ( $E_{\text{Ox}} = +0.46$  V) assigned as a Ru(II)/(III) couple and a reversible reduction ( $E_{\text{Red}} = -1.60$  V) localised on the bipy similar to  $[\text{Ru}(\text{bipy})_3]^{2+}$ . Hence, substitution of one bipy ligand in **1.1** with ppy in **1.3** leads to a shift of the oxidation and reduction waves by about -0.8 V and -0.3 V, respectively, with respect to **1.1** (*i.e.* raising both the HOMO and the LUMO levels), which is ascribed to the additional electron density on the metal centre and the change in the overall charge of the complex (*i.e.* **1.1** is dicationic, whilst **1.3** is monocationic). The shift of the reduction potential upon cyclometallation is a consequence of enhanced  $\pi$ -backbonding to the pyridyl rings resulting from the increased electron density at the metal centre.<sup>9</sup> The incorporation of a  $\sigma$ -bond in **1.3** also leads to intense absorption bands in the visible region of the spectrum, and a red shift in the emission compared to **1.1** due to a significantly reduced HOMO-LUMO gap. These features offer much promise for light-harvesting applications.<sup>9</sup>

In addition to mono-cyclometallated complexes, bis-cyclometallated complexes of Ru(II) such as **1.4a-c** have also been investigated.<sup>55, 56</sup> Complex **1.4a** is non emissive at room temperature in degassed  $\text{CH}_2\text{Cl}_2$  solution but emits at 77 K in a  $\text{CH}_2\text{Cl}_2$  matrix while complexes **1.4b** and **1.4c** show emission both at room temperature (in  $\text{CH}_2\text{Cl}_2$ ) and at 77 K (in a  $\text{CH}_2\text{Cl}_2$  matrix). This can be understood in terms of the  $\pi$ -acceptor properties of

the ligands. According to DFT calculations, the lowest lying  $T_1$  state of complex **1.4a** is dominated by the ligand centred  $\pi-\pi^*$  transitions while those of complex **1.4b** and **1.4c** possess a considerable proportion of MLCT character. CO is a better  $\pi$ -acceptor ligand than phosphine, therefore, leaves a much reduced electron density on the metal and hence a lesser amount of the MLCT contribution to the excited state. The greater contribution of  $\pi-\pi^*$  in the  $T_1$  state suppresses the spin-orbit coupling and leads to non-radiative deactivation and hence no emission in the fluid state at room temperature.<sup>16</sup>

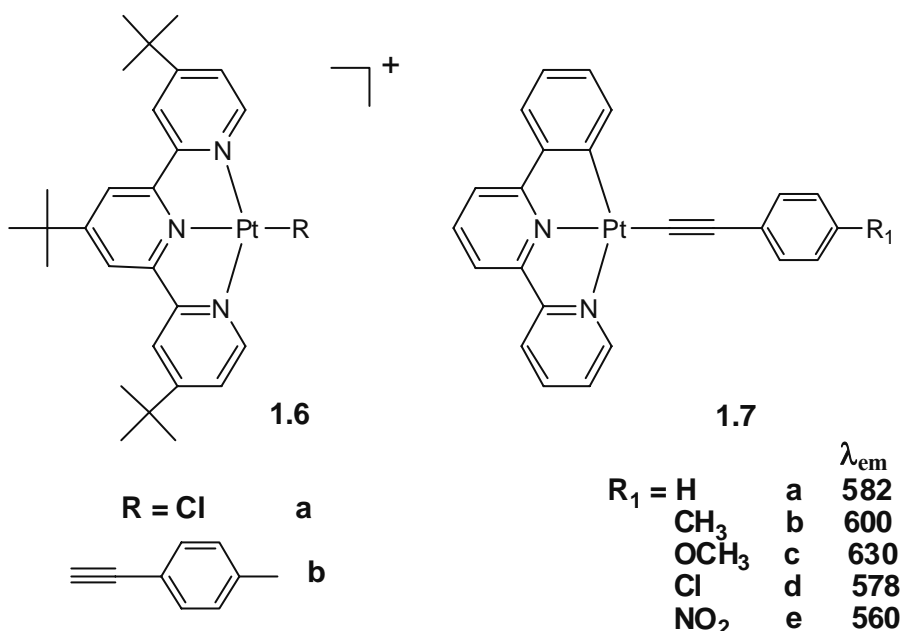


The related osmium complex **1.5a** is more emissive than the second row Ru(II) congener due to an increase of separation between the metal centred d-d orbitals and the lowest lying excited states.<sup>16</sup> Phosphine-substituted complexes (**1.5b** and **1.5c**) show a red shift compared to the dicarbonyl complex (**1.5a**) due to a decrease in the  $\pi$  accepting strength of phosphine, which in turn pushes up the metal  $d\pi$  energy level. Substituting  $\text{PPh}_2\text{Me}$  in **1.5b** with the less  $\pi$ -accepting  $\text{PPhMe}_2$  ligand in **1.5c**, results in a further red shift.



### 1.2.2 Luminescent Pt (II) complexes

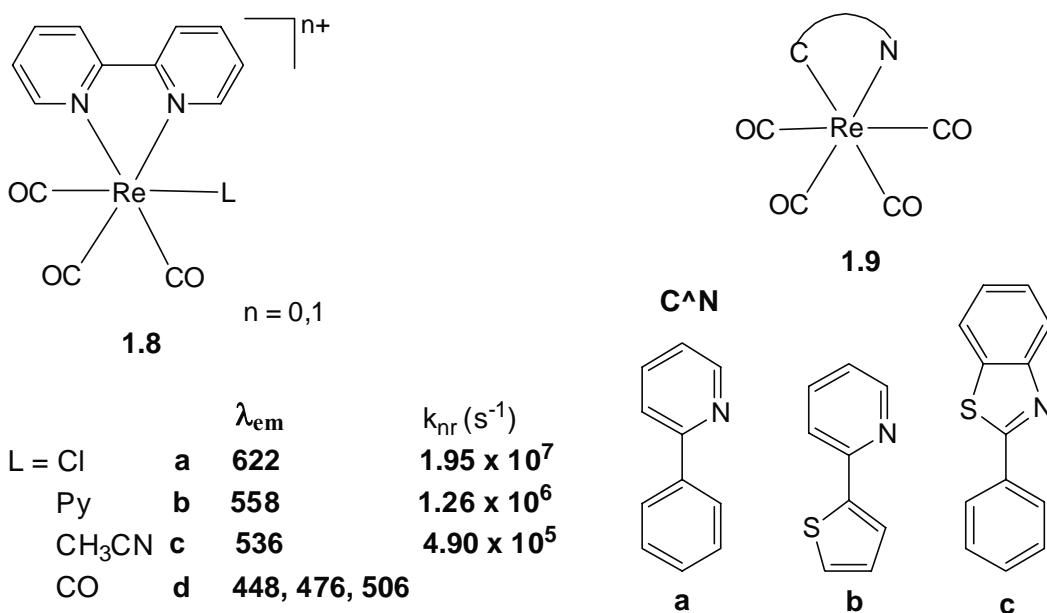
Recently, Ventura *et al.*<sup>57</sup> synthesised Pt(II) complexes (**1.6a,b**) and found that both complexes absorb in the ranges 300-360 nm and 360-450 nm corresponding to  $\pi-\pi^*$  and  $^1\text{MLCT}$  transitions, respectively. Complex **1.6a** produces a weak MLCT emission at 491 nm. Replacement of the chloride with the strong field acetylide (**1.6b**) raises the energy of the d-d states, thereby reducing non-radiative decay pathways and giving an increase in quantum yields. A red shift is also observed in **1.6b** with respect to **1.6a**.



As found for Ru(II) complexes, cyclometallated Pt(II) complexes have better emissive properties compared to the terpy analogs *i.e.* these complexes show intense emission and have higher quantum yields. All complexes **1.7a-e** show long lived yellow to red emission, which can be  $^3\text{MLCT}$ ,  $^3\pi\pi^*$  (alkynyl) and/or  $^3\pi\pi^*$  (cyclometallating ligand) emission depending on the relative energies of the Pt d-orbitals and the  $\pi-\pi^*$  orbitals of the ligands. Electron withdrawing substituents such as  $\text{Cl}$ ,  $\text{NO}_2$  on the phenyl of the alkyne increase the HOMO-LUMO gap and cause a blue shift in emission, while electron donating substituents (*i.e.*  $\text{CH}_3$ ,  $\text{OCH}_3$ ) cause a red shift. Emission quantum yields of all of these complexes are comparable to  $[\text{Ru}(\text{bipy})_3]^{2+}$ <sup>36, 58</sup> and significantly higher than  $[\text{PtR}(\text{terpy})]^+$  (**1.6a,b**)<sup>57</sup> however, the presence of  $\text{tBu}$  groups on the terpy ligand in complexes **1.6a,b** may also have some influence.

### 1.2.3 Luminescent Re (I) complexes

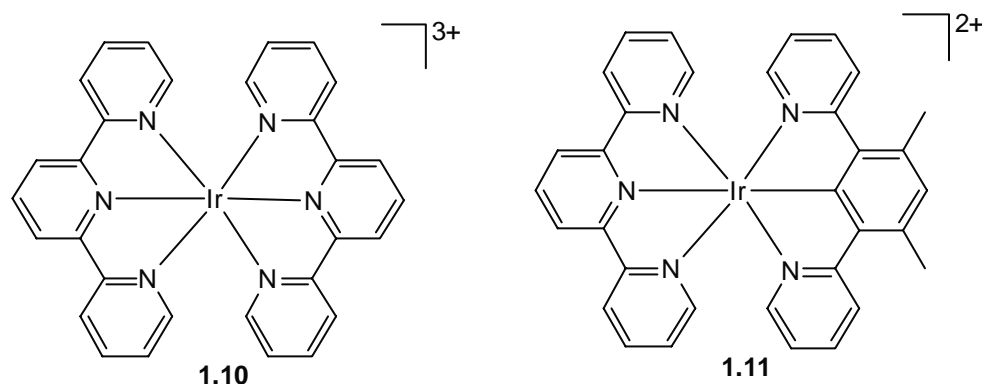
The complexes *fac*-[Re(CO)<sub>3</sub>(bipy)L]<sup>n+</sup> (**1.8a-c**) are luminescent and the electronic states responsible for emission have been assigned to <sup>3</sup>MLCT.<sup>59</sup> The photophysical properties can be tailored by varying the nature of the ancillary ligand (L). The radiative decay rates of **1.8a-c** are relatively independent of the non-chromophoric ligand L but the nonradiative decay rates (K<sub>nr</sub>) are strongly dependent on L, and on the emission energy. The emission energy increases from complex **1.8a** to **1.8c** and, hence, the rate of nonradiative decay (K<sub>nr</sub>) decreases, as predicted by the energy gap law. Re (I) complexes are used for bio-imaging and will be discussed in more detail in **Section 1.4.2**.



The MLCT states of cyclometallated Re(I) complexes (**1.9a,b**) are lower in energy than [Re(CO)<sub>4</sub>(bipy)]<sup>+</sup> (**1.8d**).<sup>60, 61</sup> This is due to the decrease in the  $\pi$ -acceptor strength on going from N to C<sup>-</sup> and increased  $\sigma$ -donor character of the anionic ligand. According to DFT calculations, the HOMO is primarily located on the phenyl atomic orbitals admixed with a metal *d*-orbital contribution and the LUMO exhibits mostly  $\pi^*$  character with the electron density distributed over the entire C<sup>-</sup>N ligand. The complex **1.9c** has been successfully employed in an OLED device which showed electroluminescence very similar to the room temperature emission.<sup>62</sup>

#### 1.2.4 Luminescent bis-tridentate Ir(III) complexes

This section will consider luminescent Ir(III) bis-tridentate complexes such as  $[\text{Ir}(\text{terpy})_2]^{3+}$  **1.10** and cyclometallated analogue **1.11**, and their derivatives; tris bidentate complexes will be considered in **Section 1.3**. Luminescent complex  $[\text{Ir}(\text{terpy})_2]^{3+}$  **1.10**, was first reported by Demas and co-workers in 1990.<sup>63</sup> Since then a lot of research has been carried out on the synthesis and characterisation of its cyclometallated and non-cyclometallated derivatives to understand their excited states and for various applications such as efficient singlet oxygen sensitizers,<sup>64</sup> as sensors,<sup>23, 65</sup> and as sensitizers in dye-sensitised solar cells.<sup>66</sup> Applications of derivatives of complex **1.10** as pH and Cl<sup>-</sup> ion sensors will be discussed in more detail in **Chapter 4**.



Complex **1.10** displays a green-blue emission upon excitation in the near-UV region.<sup>64</sup> The emission is primarily considered to be LC ( $\pi-\pi^*$ ) in nature. This contrasts with  $[\text{Ru}(\text{terpy})_2]^{2+}$ , for which the lowest lying excited states are  $^3\text{MLCT}$  and lower in energy than the Ir analogue. The differing behaviour stems from the different oxidation states of these two d<sup>6</sup> metal ions, whereas formal oxidation of Ru(II) to Ru(III) is relatively facile, the higher oxidation potential of Ir(III)/(IV) raises the MLCT states to energies higher than those of  $^3\text{LC}$  states.

It is expected that substituting one of the pyridyl rings in **1.10** with a cyclometallating phenyl ring (*e.g.* **1.11**) may lead to an increase in the MLCT character of the emissive state; however, this is not the case, since **1.11** displays very weak emission, even at 77 K.<sup>64, 67</sup> The quantum yield for **1.11** was found to be lower than **1.10** ( $< 10^{-2}$  *vs*  $3 \times 10^2$ , respectively). This is rationalised on the basis of DFT calculations which indicate that in **1.11**, the HOMO is localised on the N<sup>3</sup>C<sup>3</sup>N ligand with only a small contribution from the metal, whilst the LUMO is localised on the N<sup>3</sup>N<sup>3</sup>N ligand.

Given the small contribution of metal character to the excited state, the radiative rate constant ( $K_r$ ) is expected to be small, accounting for the weak emission.

### 1.3 Luminescent Ir(III) complexes, $[\text{Ir}(\text{C}^{\wedge}\text{N})_3]$ and $[\text{Ir}(\text{C}^{\wedge}\text{N})_2(\text{X}^{\wedge}\text{Y})]^n$ ( $n = 0, +1, -1$ )

There are 4 main types of tris-bidentate homoleptic and heteroleptic Ir(III) complexes discussed in the literature -  $[\text{Ir}(\text{C}^{\wedge}\text{N})_3]$ ,  $[\text{Ir}(\text{C}^{\wedge}\text{N})_2(\text{X}^{\wedge}\text{Y})]$ ,  $[\text{Ir}(\text{C}^{\wedge}\text{N})(\text{X}^{\wedge}\text{Y})_2]$  and  $[\text{Ir}(\text{X}^{\wedge}\text{Y})_3]$ . However, there are much fewer examples of complexes of the type  $[\text{Ir}(\text{C}^{\wedge}\text{N})(\text{X}^{\wedge}\text{Y})_2]$ ,<sup>68</sup> and  $[\text{Ir}(\text{X}^{\wedge}\text{Y})_3]$  ( $\text{X}^{\wedge}\text{Y}$  = acac, pyridyl azolate),<sup>69</sup> due to their difficult synthesis and purification. Although in some cases similar complexes are also known for Rh, the Ir complexes are much more studied and Rh complexes have similar properties, hence, only Ir complexes are discussed. This area of chemistry has experienced a huge growth in recent years, this was prompted by the report in 1998 by Thompson *et al.* that luminescent bis- and tris-cyclometallated Ir(III) complexes can be used as phosphors in OLEDs.<sup>17</sup>

The homoleptic complexes  $[\text{Ir}(\text{C}^{\wedge}\text{N})_3]$  and heteroleptic ones  $[\text{Ir}(\text{C}^{\wedge}\text{N})_2(\text{X}^{\wedge}\text{Y})]^{n+}$  ( $n = 0, 1$ ) have attractive photophysical and photochemical properties, they often show intense phosphorescence at room temperature with phosphorescent life times of microseconds ( $\tau \sim \mu\text{s}$ ) which are relatively long compared to fluorescent life times, but are shorter than phosphorescent life times of common organic lumophores ( $\tau \geq \text{milliseconds}$ ).<sup>70, 71</sup> Moreover these complexes possess high quantum yields for emission due to spin-orbit coupling and large Stokes shifts. Because of these properties, these complexes have been applied in different fields such as dopants in emissive layer of organic light emitting diodes (OLEDs),<sup>12-19</sup> luminescent sensors,<sup>24, 72-76</sup> photocatalysts for  $\text{CO}_2$  reduction,<sup>20, 21</sup> biological labels,<sup>27, 77, 78</sup> and probes,<sup>79-81</sup> singlet oxygen sensitizers,<sup>82-84</sup> for charge transfer reactions in DNA<sup>85-87</sup> and as sensitizers in dye-sensitised solar cells.<sup>88-90</sup>

A wide variety of bidentate ( $\text{X}^{\wedge}\text{Y}$ ) ligands and cyclometallated ( $\text{HC}^{\wedge}\text{N}$ ) ligands have been used to coordinate to the Ir(III) metal centre. By altering either the cyclometallated ligands and/or the ancillary ligands on the metal and also substituents on the ligands, the emission wavelength can be controlled and hence a wide region of the visible spectrum can be covered. The  $\text{X}^{\wedge}\text{Y}$  ligands can be neutral (**L1-9 Fig. 1.4**) or anionic (**L10-19 Fig. 1.5**), which make cationic complexes  $[\text{Ir}(\text{C}^{\wedge}\text{N})_2(\text{X}^{\wedge}\text{Y})]^+$  and neutral ones  $[\text{Ir}(\text{C}^{\wedge}\text{N})_2(\text{X}^{\wedge}\text{Y})]$  respectively.

**Fig. 1.4: Neutral  $X^{\wedge}Y$  ligands**

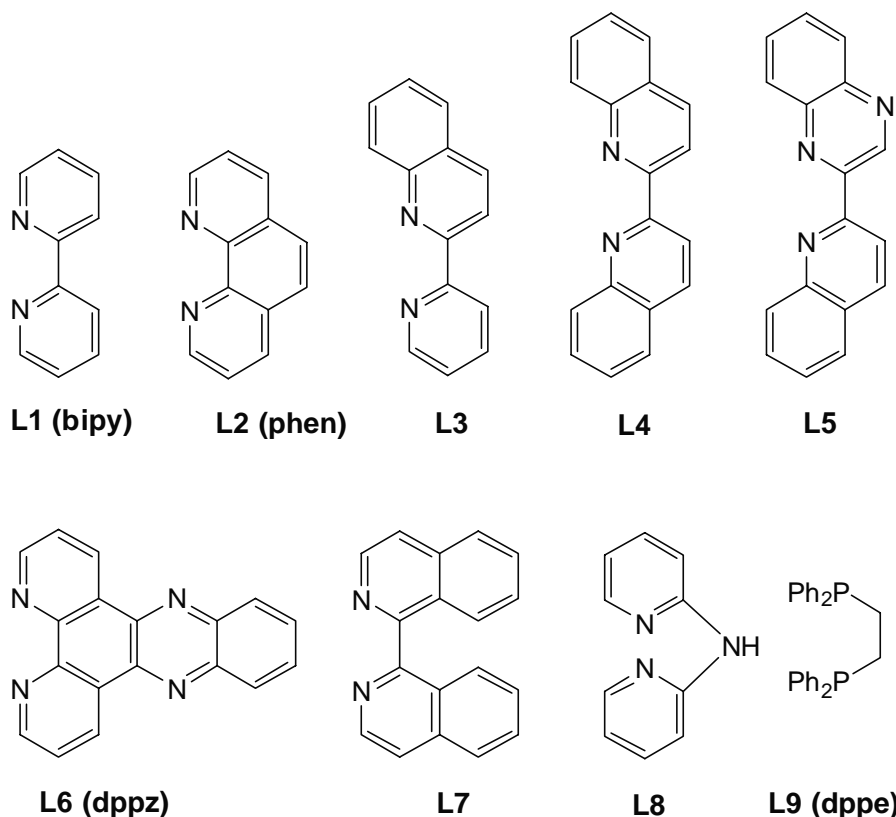
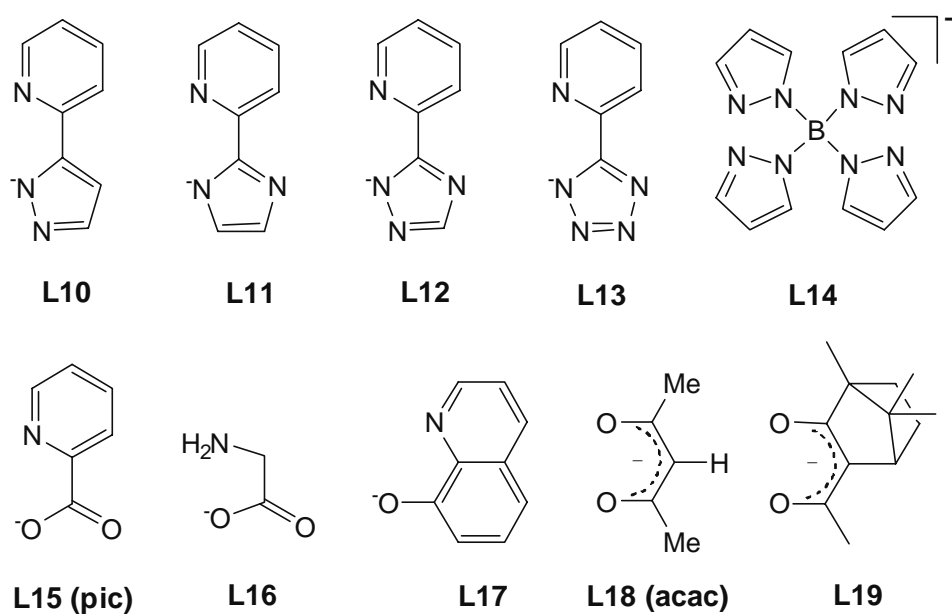
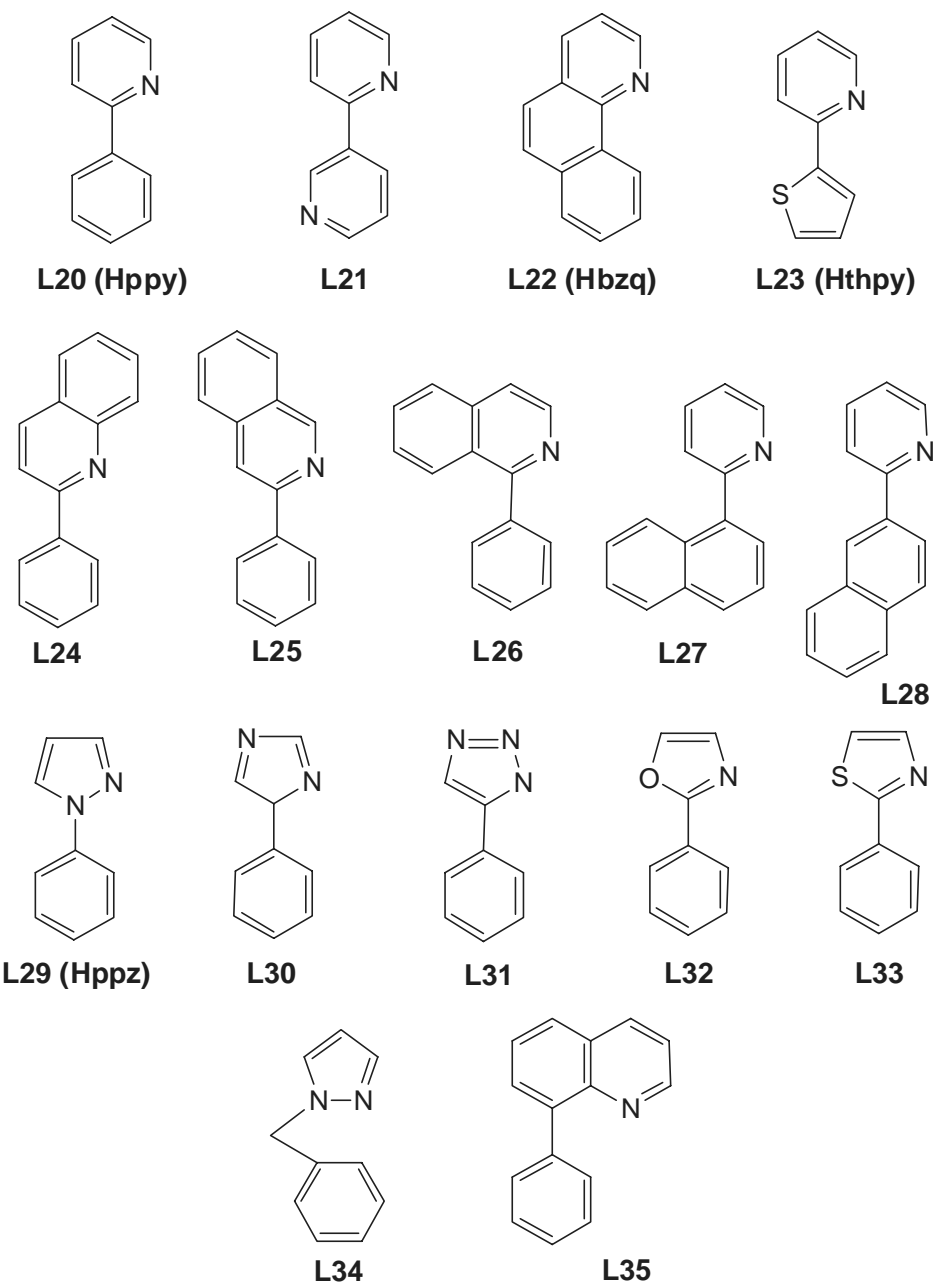


**Fig. 1.5: Anionic  $X^{\wedge}Y$  ligands**



Similarly, a wide range of  $\text{HC}^{\wedge}\text{N}$  ligands are also available, *e.g.* **L20-35** (Fig. 1.6), the vast majority of which coordinate to the Ir, forming a 5-membered metallacycle through activation of the *ortho* C-H bond of a phenyl ring that is adjacent to the heterocycle. Metallation of a heterocycle *e.g.* pyridine (**L21**) and thiophene (**L23**) is also possible, as formation of a 6-membered metallacycle *e.g.* (**L34** and **L35**), though these are less common.

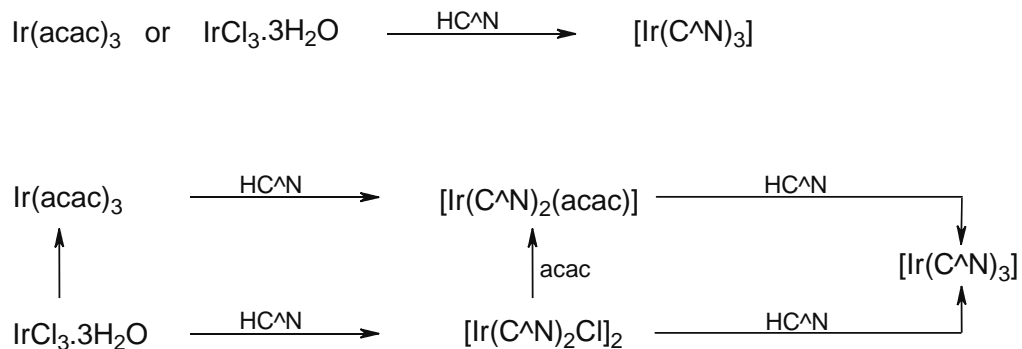
**Fig. 1.6: Cyclometallating ( $\text{HC}^{\wedge}\text{N}$ ) ligands**



Hence, an enormous number of possible complexes can be made by choosing different  $\text{HC}^{\wedge}\text{N}$  and  $\text{X}^{\wedge}\text{Y}$  ligands (high structural variety). Further tuning is then possible by having electron donating or electron withdrawing substituents on various positions on the  $\text{X}^{\wedge}\text{Y}$  and/or  $\text{HC}^{\wedge}\text{N}$  ligands. (Effect of substituents will be discussed in **Section 1.3.2.4**). Therefore, through judicious choice of  $\text{HC}^{\wedge}\text{N}$  and  $\text{X}^{\wedge}\text{Y}$  ligands, the excited states of both homoleptic and heteroleptic Ir(III) complexes can be tuned to display all three primary colours (red, blue and green).<sup>31, 33</sup> Hence they can be used in full colour displays.

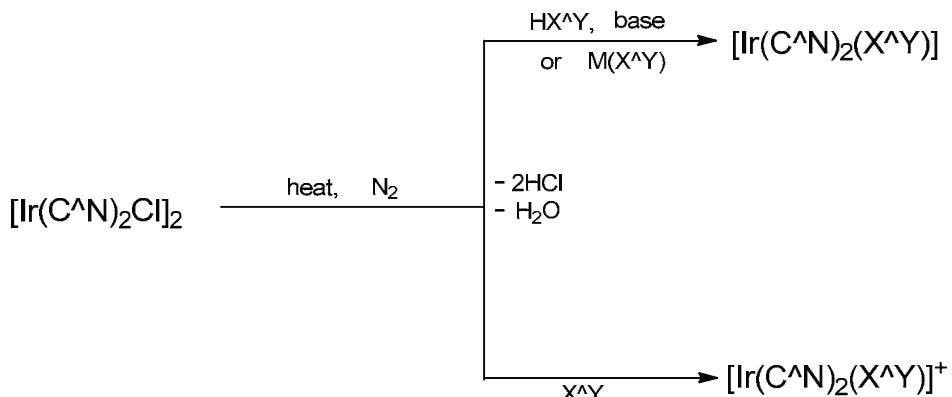
### 1.3.1 Synthesis of Ir (III) complexes i.e. $[\text{Ir}(\text{C}^{\wedge}\text{N})_3]$ and $[\text{Ir}(\text{C}^{\wedge}\text{N})_2(\text{X}^{\wedge}\text{Y})]^{n+}$

In general, the synthesis of Ir(III) coordination complexes requires relatively harsh conditions due to the kinetic inertness associated with the low-spin  $d^6$  electronic configuration of the  $3+$  metal centre.<sup>19, 64, 91</sup> Tris-cyclometallated Ir(III) complexes  $[\text{Ir}(\text{C}^{\wedge}\text{N})_3]$  can be prepared directly by reaction of either  $\text{Ir}(\text{acac})_3$ <sup>92-94</sup> or  $\text{IrCl}_3 \cdot 3\text{H}_2\text{O}$ <sup>94, 95</sup> with a large excess of the cyclometallating ligand in glycerol at reflux temperatures, or in two steps by isolation of the intermediate bis-cyclometallated complexes  $[\text{Ir}(\text{C}^{\wedge}\text{N})_2(\text{acac})]$ <sup>96</sup> or  $[\text{Ir}(\text{C}^{\wedge}\text{N})_2\text{Cl}]_2$ ,<sup>97, 98</sup> respectively (**Scheme 1.1**). In 1984, Watts *et al.* synthesised the chloro-bridged dimer  $[\text{Ir}(\text{ppy})_2\text{Cl}]_2$  by heating  $\text{IrCl}_3 \cdot 3\text{H}_2\text{O}$  with 2-phenylpyridine in ethoxyethanol/water at reflux for 24 hours at  $135\text{ }^{\circ}\text{C}$ .<sup>91</sup> Since the  $[\text{Ir}(\text{C}^{\wedge}\text{N})_2]$  fragment is chiral, the chlorobridged dimers can in principle have either meso ( $\Delta\Lambda$ ) or racemic isomers ( $\Delta\Delta/\Lambda\Lambda$ ), these will be discussed in more detail in **Chapters 2 and 5**.



The dimers  $[\text{Ir}(\text{C}^{\wedge}\text{N})_2\text{Cl}]_2$ <sup>98, 99</sup> are easily prepared in high yields ( $> 85\%$ ) from  $\text{IrCl}_3\cdot 3\text{H}_2\text{O}$ , and can then be converted in high yield to  $[\text{Ir}(\text{C}^{\wedge}\text{N})_2(\text{O}^{\wedge}\text{O})]$ .<sup>19, 71</sup> This route is much more efficient than going *via*  $[\text{Ir}(\text{acac})_3]$  which itself is prepared from  $\text{IrCl}_3\cdot 3\text{H}_2\text{O}$  but only in low yield ( $< 20\%$ ).<sup>100, 101</sup> Preparing  $[\text{Ir}(\text{C}^{\wedge}\text{N})_3]$  in two steps from  $\text{IrCl}_3\cdot 3\text{H}_2\text{O}$  gives overall yields between 75 and 80%<sup>98</sup> vs 45-60% using a one pot method.<sup>95</sup> In addition, the second step from  $[\text{Ir}(\text{C}^{\wedge}\text{N})_2\text{Cl}]_2$  can be carried out at much lower temperatures using Ag salts.<sup>102</sup> Also, the one pot method uses a much larger excess of the cyclometallating ligand as solvent (up to 60 times<sup>95</sup>) compared with only 2-3 times excess in each step during the two step procedure.<sup>19, 71</sup> Hence, the two step method starting from  $\text{IrCl}_3\cdot 3\text{H}_2\text{O}$  is the preferred method.<sup>96</sup>

Cationic heteroleptic complexes  $[\text{Ir}(\text{C}^{\wedge}\text{N})_2(\text{X}^{\wedge}\text{Y})]^+$  are easily synthesised from  $[\text{Ir}(\text{C}^{\wedge}\text{N})_2\text{Cl}]_2$  by reaction with neutral ligands  $\text{X}^{\wedge}\text{Y}$ .<sup>103</sup> The corresponding neutral analogues are accessed by reaction of  $[\text{Ir}(\text{C}^{\wedge}\text{N})_2\text{Cl}]_2$  either with  $\text{HX}^{\wedge}\text{Y}$  in the presence of base or with salts  $\text{M}(\text{X}^{\wedge}\text{Y})$  ( $\text{M} = \text{Na, K}$ ) (**Scheme 1.2**).<sup>104</sup> All these reactions occur under relatively mild conditions (from RT to  $< 100\text{ }^{\circ}\text{C}$ ).



**Scheme 1.2**

In principle, complexes  $[\text{Ir}(\text{C}^{\wedge}\text{N})_2(\text{X}^{\wedge}\text{Y})]^{n+}$  ( $n = 0, 1$ ) can exist in various geometrical isomers (**Fig. 1.7**) each of which has two enantiomers ( $\Lambda$  and  $\Delta$ ). However, in practice only one of these isomers has been reported in the literature *i.e.* **1**. In this case the two cyclometallating ligand carbon atoms are mutually *cis* and the nitrogens are mutually *trans*. Presumably, the strong *trans* effect of the carbon atoms makes isomer **2** less favourable, however, the absence of isomers **3** is less easy to explain on thermodynamic grounds. Tris-cyclometallated Ir(III) complexes  $[\text{Ir}(\text{C}^{\wedge}\text{N})_3]$  exist as *mer*

isomers (type **1**, where  $X = C$ ,  $Y = N$ ) (also equivalent to type **3**  $X = C$ ,  $Y = N$ ) and *fac* isomers (type **3**, where  $X = N$ ,  $Y = C$ ).

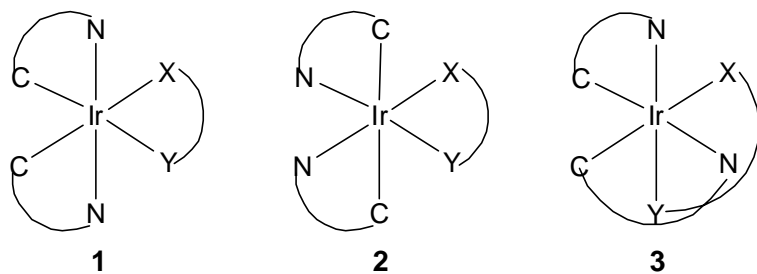
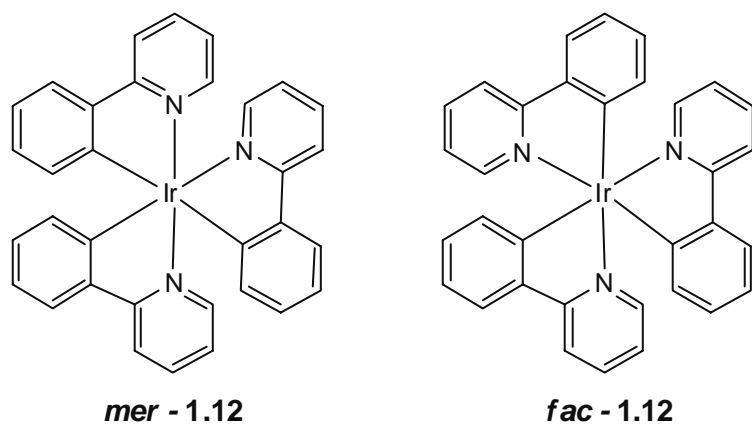


**Fig. 1.7:** Possible isomers of bis-cyclometallated Ir(III) complexes  $[\text{Ir}(\text{C}^{\wedge}\text{N})_2(\text{X}^{\wedge}\text{Y})]$

*Fac* and *mer* isomers of  $[\text{Ir}(\text{C}^{\wedge}\text{N})_3]$  are easily distinguished by  $^1\text{H}$  NMR spectroscopy since the *fac* isomers have  $\text{C}_3$ -symmetry, so, give only one set of ligand signals. Thompson *et al.* have demonstrated that controlling the reaction conditions can impart significant control on the isomer ratio (*fac/mer*). In general, the *fac* isomer is preferred at higher temperatures ( $> 200$  °C) and the *mer* isomer at lower temperature ( $< 150$  °C). At high temperatures, the *mer* isomer can be efficiently converted into the *fac* isomer, demonstrating that the *fac* isomer is the thermodynamically more stable isomer.<sup>96</sup> In 2007, McGee and Mann proposed a mechanism to explain the formation of *mer* and *fac* isomers.<sup>105</sup> They suggested that in the presence of sufficient base (excess ligand) formation of the *mer* isomer is preferred. They confirmed this by reacting Hppy with  $[\text{Ir}(\text{ppy})_2(\text{OH})]_2$ , the bridging hydroxides act as an internal base and the product is exclusively *mer*  $[\text{Ir}(\text{ppy})_3]$ . However, reaction of  $[\text{Ir}(\text{ppy})_2(\text{NCMe})_2](\text{PF}_6)$  with Hppy (1.1 equivalents) at 100 °C gave exclusively *fac*  $[\text{Ir}(\text{ppy})_3]$ . Thus, the presence of base prevents isomerisation of the bis-cyclometallated fragment which is required for formation of the *fac* isomer. This mechanism has subsequently been supported by van Koten *et al.*<sup>97</sup> Presumably, the observation of predominantly the *mer* isomer in previous preparations reflects the use of excess ligand which acts a base, thus, hindering isomerisation. *Fac/mer* isomerisation will also be discussed again in **Chapter 5**.

### 1.3.2 Emission in Ir (III) complexes *i.e.* $[\text{Ir}(\text{C}^{\wedge}\text{N})_3]$ and $[\text{Ir}(\text{C}^{\wedge}\text{N})_2(\text{X}^{\wedge}\text{Y})]^{\text{n}^+}$

Cyclometallated complex  $[\text{Ir}(\text{ppy})_3]$  (**1.12**) has been extensively studied and applied in fabricating green organic light emitting and electrochemiluminescent devices.<sup>106-108</sup> The strong emission occurring at  $\lambda_{\text{em}}$  514 nm is believed to originate from the triplet state possessing both intraligand  $\pi$ - $\pi^*$  and metal to ligand charge transfer (MLCT) character.<sup>107, 108</sup> Moreover, as discussed earlier  $[\text{Ir}(\text{ppy})_3]$  exists as two isomers, *fac* and *mer*, which have different electrochemical and photophysical properties.<sup>96</sup> The *mer* isomer is easier to oxidise and the emission is broad and red shifted relative to the *fac* isomer. The luminescent quantum efficiency and emission lifetime of the *mer* isomer is significantly lower than the *fac* isomer. This large difference between the properties of two isomers has been explained by an efficient bond breaking process for the *mer* excited state, acting as an effective quenching pathway and giving subsequent isomerisation to the *fac* form.<sup>96</sup>



#### 1.3.2.1 Tuning of luminescent wavelength by variation of $\text{X}^{\wedge}\text{Y}/\text{XY}$ ligands

The cationic, neutral and anionic Ir(III) complexes *i.e.*  $[\text{Ir}(\text{ppy})_2(\text{XY})]^{\text{n}}$  ( $\text{n} = 0, +1, -1$ ) (**1.13a-h**) can be used to illustrate the effect of the ancillary ligand on the emission wavelength and electrochemical properties (**Table 1.1**). The oxidation potentials range from 0.85 to 1.19 V for the neutral complexes and between 1.25 and 1.45 V for the cationic ones, giving a full range of *ca.* 0.6 V with the cationic complexes being harder to oxidise as expected. In comparison the reduction potentials go from -1.42 to -2.36 a range of almost a volt. The smaller range and the quasi-reversible nature of the oxidations are consistent with the oxidation being mainly metal based,  $\text{Ir}^{\text{III}} \rightarrow \text{Ir}^{\text{IV}}$  with some contribution from the Ir-C  $\sigma$ -bond. Thus, the HOMO mainly resides on the

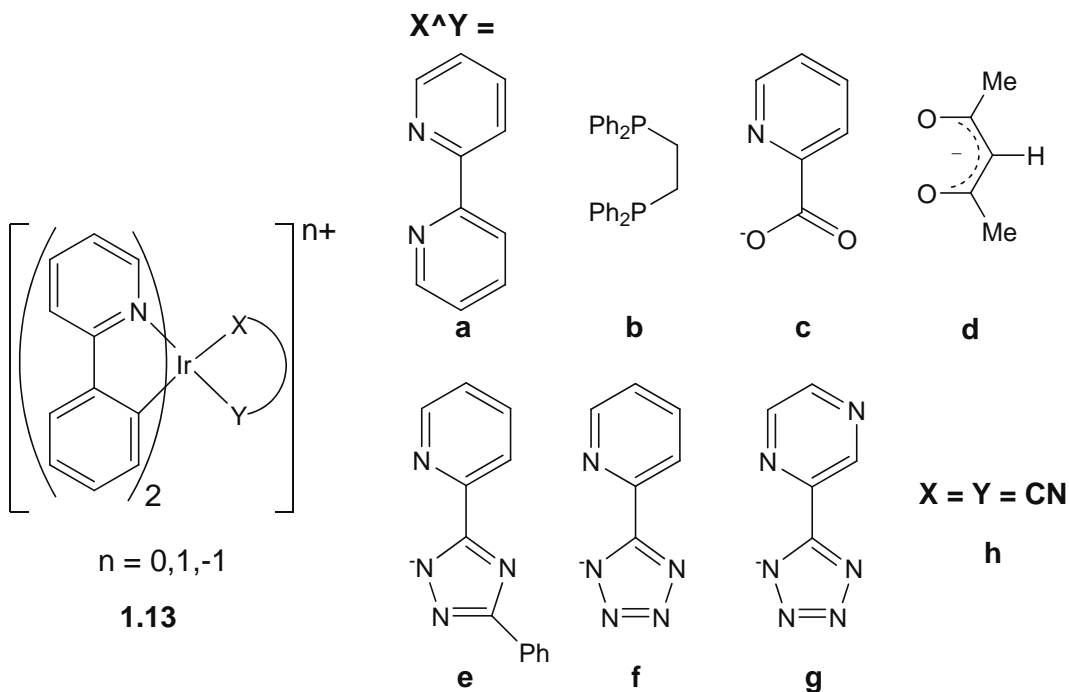


**Table 1.1:** Emission wavelength and redox properties of  $[\text{Ir}(\text{C}^{\text{N}}\text{N})_2(\text{X}^{\text{Y}})]^{\text{n}}$  ( $\text{n} = 0, +1, -1$ ).

Entry	Complex	$\lambda_{\text{em}} (\text{nm})$	$E^{1/2}_{\text{Ox}}$	$E^{1/2}_{\text{Red}}$	$\Delta E^{1/2}$	References
1	<b>[1.13a]<sup>+</sup></b>	580	1.25	-1.42	2.67	<sup>109-111</sup>
2	<b>[1.13b]<sup>+</sup>*</b>	458	1.45	-2.04	3.49	<sup>112</sup>
3	<b>1.13c</b>	505	0.99	-1.94	2.93	<sup>109, 113</sup>
4	<b>1.13d</b>	516	0.85	-2.10	2.95	<sup>109, 114</sup>
5	<b>1.13e</b>	489, 517	1.06	-2.11	3.17	<sup>33</sup>
6	<b>1.13f</b>	481, 510	1.13	-2.00	3.13	<sup>115</sup>
7	<b>1.13g</b>	601	1.19	-1.47, -2.28	2.66, 3.47	<sup>115</sup>
8	<b>[1.13h]<sup>-</sup></b>	476	0.92	-2.36	3.28	<sup>112</sup>

<sup>a</sup>The potentials are given *vs* SCE. <sup>b\*</sup> - C<sup>N</sup> ligand has a methyl substituent on the phenyl ring *para* to the pyridine.

Ir. The wider range ( $\sim 1$  V) for the reduction potentials reflects the fact that the reduction actually occurs on the X<sup>Y</sup> ligand in some cases. The most positive reduction potential is, as expected, for the cationic complex  $[\text{Ir}(\text{ppy})_2(\text{bipy})]^+$  **1.13a** and reduction occurs on the bipy. DFT calculations confirm that, the HOMO resides on the Ir and Ir-C  $\sigma$ -bond, while the LUMO is mainly on the diimine and partly on the pyridyl ring of the cyclometallating ligand (ppy). Substituting bipy (**1.13a**) with a diphosphine ligand (dppe) in **1.13b** affects the reduction potential more than the oxidation potential (0.62 V *vs* 0.20 V, respectively) (**Table 1.1**, entries 1, 2), therefore, it has more effect on the

LUMO. Hence, in  $[\text{Ir}(\text{ppy})_2(\text{dppe})]^+$ , the LUMO resides mainly on the pyridyl ring of cyclometallating ligand. Moreover, the higher HOMO-LUMO gap for **1.13b** is consistent with the observed blue shift of emission.

The neutral complexes (**1.13c-f**) have a larger  $\Delta E^{1/2}$  than cationic complex **1.13a** mainly due to a more negative reduction, *i.e.* raised LUMO (**Table 1.1**, entries 1, 3-6), which leads to a blue shift in emission. Substituting the pyridine ring of the  $\text{X}^{\wedge}\text{Y}$  ligand in **1.13f** with a pyrazine ring in **1.13g** has very little effect on the oxidation potentials, however it leads to a large positive shift in the reduction potential, since pyrazine is much easier to reduce than pyridine, (**Table 1.1**, entries 6 and 7) and this causes a red shift in the emission. DFT calculations confirm that the excited states vary according to the nature of the  $\text{X}^{\wedge}\text{Y}$  ligand. Using picolinate (pic **1.13c**) and pyridylazolates (**1.13e-g**) as the ancillary ligands, the LUMO resides mainly on the  $\text{X}^{\wedge}\text{Y}$  ligand and partially on the pyridyl ring of the ppy.<sup>104, 115-117</sup> In contrast, when  $\text{X}^{\wedge}\text{Y} = \text{acac}$  (**1.13d**), the LUMO is mostly localised on the pyridyl ring of ppy.<sup>104, 117, 118</sup> Anionic complex **1.13h** has a bigger  $\Delta E^{1/2}$  than either the cationic complex (**1.13a**) or the neutral complexes (**1.13c-g**), hence, the emission is most blue shifted. Thus, in general, the HOMO-LUMO energy gap broadly increases in the order, cationic (diimine) < neutral < anionic complexes, which is also consistent with their emission wavelengths (see **Table 1.1**).

### 1.3.2.2 Tuning of luminescent wavelength by variation of $\text{C}^{\wedge}\text{N}$ ligands

As mentioned above, in cationic Ir(III) complexes  $[\text{Ir}(\text{C}^{\wedge}\text{N})_2(\text{bipy})]^+$ , the HOMO resides on the Ir and Ir-C  $\sigma$ -bond while the LUMO resides mainly on the bipy ligand and possibly on the  $\text{C}^{\wedge}\text{N}$  ligand if it contains a group with a low lying  $\pi^*$ -orbital *e.g.* pyridine. Replacement of 2-phenyl pyridine in (**1.14a**) with 2-phenyl pyrazole in (**1.14b**) changes the oxidation potential more than the reduction potential (0.12V vs 0.04V) (**Table 1.2**, entries 1, 2), which suggests that it mainly affects the HOMO. Pyrazole is less electron donating than pyridine, therefore it lowers the HOMO causing a blue shift.

In neutral acetylacetonato (acac) complexes  $[\text{Ir}(\text{C}^{\wedge}\text{N})_2(\text{acac})]$  **1.15a,b**, substituting the pyridine ring of **1.15a** with a pyrazole ring **1.15b** causes a similar 0.12V increase in oxidation potential but a more dramatic shift (0.21V) of the reduction potential to more negative voltage. This leads to a larger value of  $\Delta E^{1/2}$  for the ppz complex **1.15b** hence a blue shift is expected. However a slight red shift is observed

(entries 3 and 4) which suggests the electrochemical data should only be used as a guide (the triplet emission is not equivalent to the HOMO-LUMO gap).

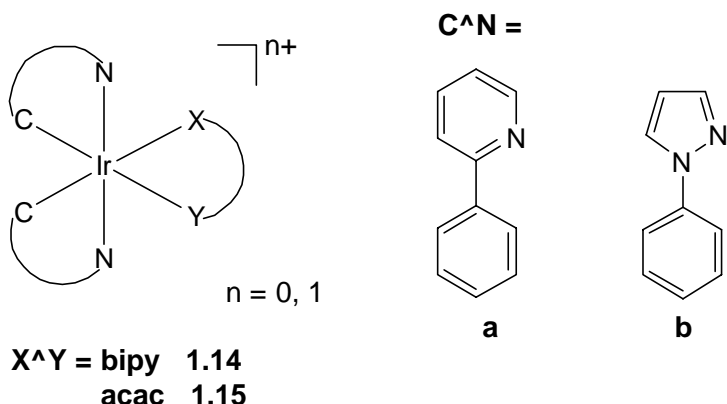


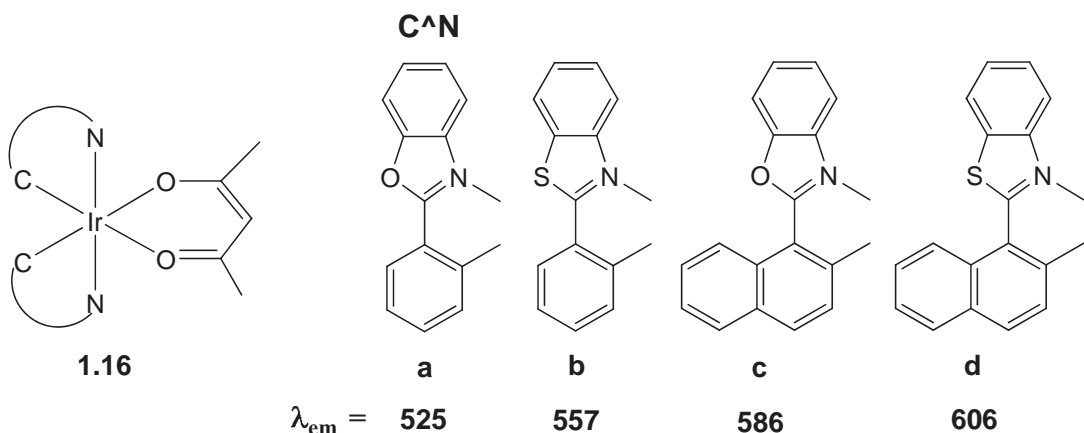
**Table 1.2:** Emission wavelength and redox properties of  $[\text{Ir}(\text{C}^{\text{N}})_2(\text{X}^{\text{Y}})]^{n+}$  ( $n = 0, 1$ )

Entry	Complex	$\lambda_{\text{em}} (\text{nm})$	$E^{1/2}_{\text{Ox}}$	$E^{1/2}_{\text{Red}}$	$\Delta E^{1/2}$	References
1	<b>1.14a</b>	580	1.25	-1.42	2.67	<sup>109-111</sup>
2	<b>1.14b</b>	554	1.37	-1.38	2.75	<sup>32</sup>
3	<b>1.15a</b>	516	0.85	-2.10	2.95	<sup>109, 114</sup>
4	<b>1.15b</b>	520	0.97	-2.31	3.28	<sup>104</sup>

<sup>a</sup>Both the emission and redox measurements were carried out in  $\text{CH}_2\text{Cl}_2$ .

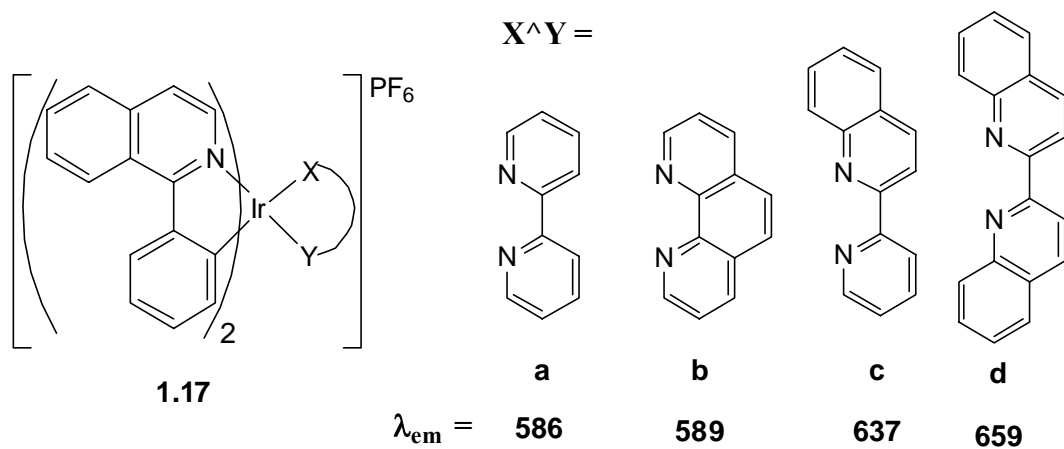
Thus, overall, complexes **1.14** and **1.15** illustrate the complex interplay between  $\text{C}^{\text{N}}$  and  $\text{X}^{\text{Y}}$  ligands. In cationic complexes  $[\text{Ir}(\text{C}^{\text{N}})_2(\text{bipy})]^+$ , ppz (**1.14b**) causes a considerable blue shift (-26 nm) with respect to ppy (**1.14a**) whilst in neutral complexes  $[\text{Ir}(\text{C}^{\text{N}})_2(\text{acac})]$ , it causes a slight red shift (+4 nm) which suggests that the excited states are different in the two types of complex *i.e.* in the cationic complexes the HOMO resides on the Ir and Ir-C  $\sigma$ -bond and the LUMO resides mainly on the bipy while in the acac complexes, both the HOMO and the LUMO reside on the  $\text{C}^{\text{N}}$  ligand.

Thompson and co-workers synthesized a series of complexes  $[\text{Ir}(\text{C}^{\text{N}})_2(\text{acac})]$  (**1.16a-d**) containing different cyclometallated ligands.<sup>19</sup> The substitution of O by S in the chromophores leads to a red shift in the emission because of the higher polarizability of S relative to O in the ligand based excited state. Further, increasing the conjugation of the ligand *i.e.* substituting a phenyl group with a naphthyl group also leads to a red shift (*cf.* **1.16a** and **1.16c**, or **1.16b** and **1.16d**). The effect of conjugation is discussed in more detail in **Section 1.3.2.3**.



### 1.3.2.3 Effect of conjugation

Recently, Zhao *et al.* synthesised a series of complexes  $[\text{Ir}(\text{piq})_2(\text{X}^{\wedge}\text{Y})]\text{PF}_6$  (piq = 1-phenylisoquinoline and  $\text{X}^{\wedge}\text{Y}$  = bipy, phen derivatives) (**1.17a-d**) and studied the effect on emission of increasing conjugation of the  $\text{X}^{\wedge}\text{Y}$  ligand.<sup>103</sup> The emission wavelength of the complexes varies from 586 to 659 nm, **1.17a** to **1.17d**, respectively. Hence, it is concluded that increasing the  $\pi$ -conjugation of the  $\text{X}^{\wedge}\text{Y}$  ligand leads to a red shift in emission consistent with the LUMO being centred on the  $\text{X}^{\wedge}\text{Y}$  ligand. These results also have been supported by density functional theory (DFT) calculations.<sup>103</sup>



As discussed above for complexes **1.16**, increasing conjugation on the C<sup>4</sup>N ligand can also be used to produce a red shift in the emission as in analogous complexes **1.18a-e** (**Table 1.3**, entries 1-5). The LUMO is on the cyclometallated ligand and the energy of this level decreases as the  $\pi$ -conjugation length increases.

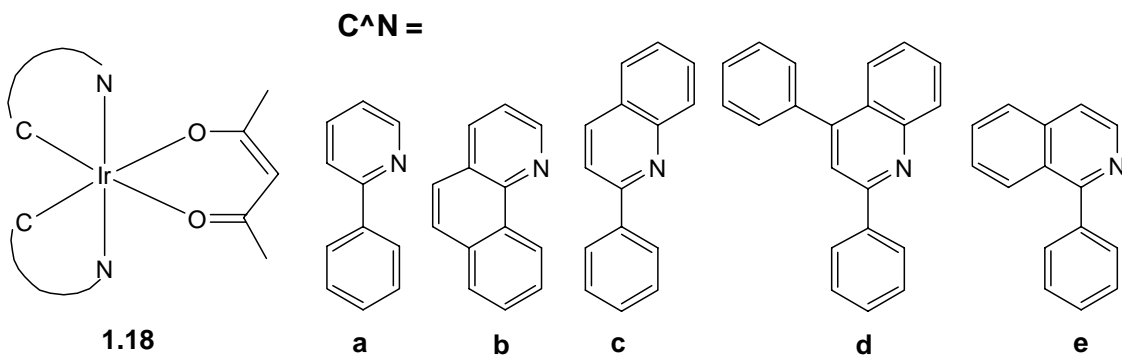
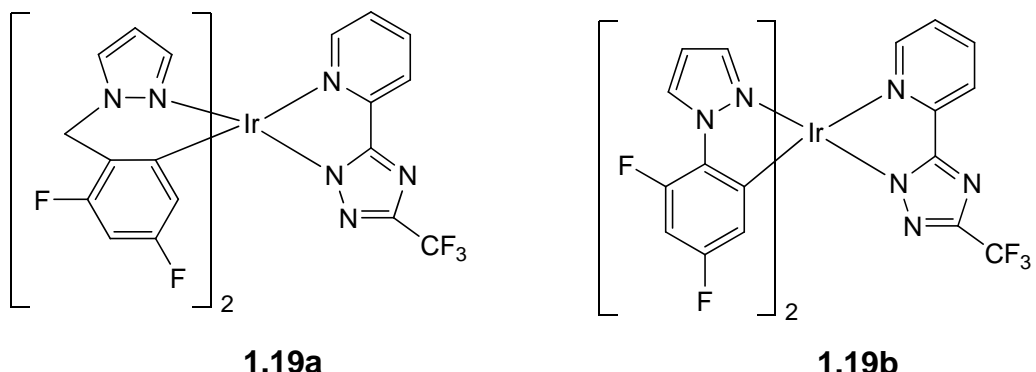


**Table 1.3:** Emission wavelengths of  $[\text{Ir}(\text{C}^{\text{N}})^2(\text{acac})]$  complexes **1.18a-e**.

Entry	Complex	$\lambda_{\text{em}} (\text{nm})$	References
1	<b>1.18a</b>	516	<sup>19</sup>
2	<b>1.18b</b>	548	<sup>19</sup>
3	<b>1.18c</b>	599	<sup>119, 120</sup>
4	<b>1.18d</b>	614	<sup>120</sup>
5	<b>1.18e</b>	622	<sup>119</sup>

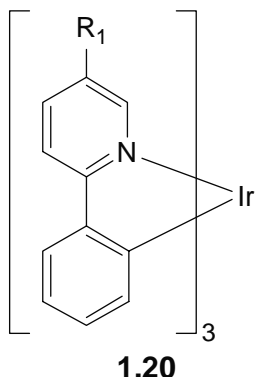
As discussed earlier, in neutral complexes, both the HOMO and the LUMO involve the  $\text{C}^{\text{N}}$  ligand, hence it is very difficult to adjust the energy of just the HOMO or the LUMO without having any effect on the other, due to conjugation in the  $\text{C}^{\text{N}}$  ligand. To overcome this intrinsic problem, in 2008, Y. Chi and co-workers reported **1.19a** with a non-conjugated  $\text{C}^{\text{N}}$  ligand in which the two chromophores were linked with a methylene spacer.<sup>121</sup> This destabilizes the  $\pi^*$  orbitals of the non-conjugated  $\text{C}^{\text{N}}$  ligand, causing a blue shift in emission for **1.19a**<sup>121</sup> ( $\lambda_{\text{em}} = 437, 460$  (sh) nm) compared with **1.19b**<sup>122</sup> ( $\lambda_{\text{em}} = 457$  nm) with a conjugated  $\text{C}^{\text{N}}$  ligand.



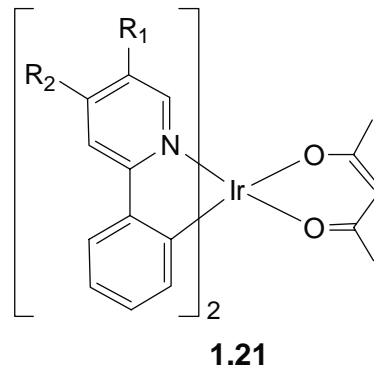
### 1.3.2.4 Tuning of emission by varying substituents

As discussed earlier, oxidation of  $[\text{Ir}(\text{C}^{\wedge}\text{N})_2(\text{X}^{\wedge}\text{Y})]^{n+}$  ( $n = 0, 1$ ) occurs mainly on the Ir and the Ir-C  $\sigma$ -bond and thus the HOMO mainly resides on the d-orbitals of Ir and partly over the phenyl ring of cyclometallated ( $\text{C}^{\wedge}\text{N}$ ) ligand. Therefore, putting substituents on the phenyl ring of the  $\text{C}^{\wedge}\text{N}$  ligand will mostly affect the HOMO. The situation is more complicated for the LUMO since in cationic complexes ( $\text{X}^{\wedge}\text{Y} = \text{diimine}$ ) the LUMO is mainly on the diimine, but in neutral complexes the LUMO may be mainly on the  $\text{C}^{\wedge}\text{N}$  or mainly on the  $\text{X}^{\wedge}\text{Y}$  ligand, hence the effect of substituents on the  $\text{X}^{\wedge}\text{Y}$  ligand or the heterocyclic part of  $\text{C}^{\wedge}\text{N}$  is more difficult to predict. Indeed, in some of these cases the effect of substituents can be sufficient to shift the LUMO from the  $\text{C}^{\wedge}\text{N}$  to the  $\text{X}^{\wedge}\text{Y}$  ligand or vice versa. Selected examples are discussed below, however, complexes of type  $[\text{Ir}(\text{C}^{\wedge}\text{N})_2(\text{diimine})]^+$  will be considered in **Chapter 2**.

In tris-cyclometallated complexes  $[\text{Ir}(\text{ppy})_3]$  **1.20a-c**, the HOMO resides on the Ir and Ir-C  $\sigma$ -bond while the LUMO resides on the pyridyl ring of ppy ligand. Liu *et al.* studied the effect of varying substituents on the pyridyl ring.<sup>123</sup> A strong electron withdrawing substituent (*e.g.* CN in **1.20b**) lowers the LUMO decreasing the HOMO-LUMO gap leading to a red shift in emission with respect to the unsubstituted complex **1.20a**. In contrast, with OMe, the emission was relatively unaffected suggesting the HOMO-LUMO gap is relatively unchanged.



$\text{R}_1 = \text{H}$       a  
 $\text{R}_1 = \text{CN}$     b  
 $\text{R}_1 = \text{OMe}$    c

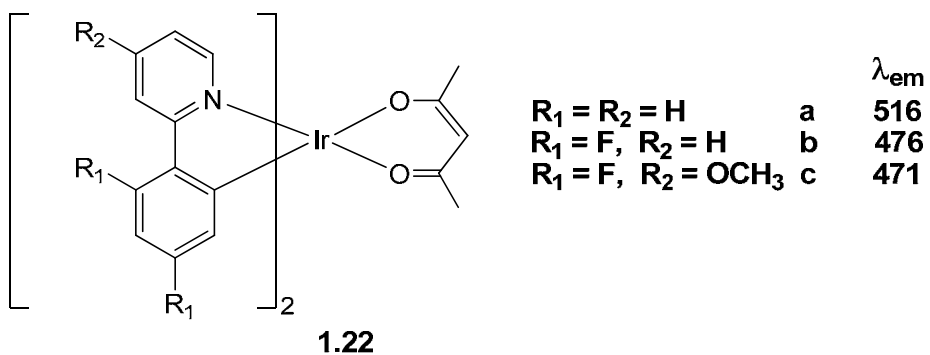


		$\lambda_{\text{em}}$
$\text{R}_1 = \text{H}$	$\text{R}_2 = \text{H}$	a    516
$\text{R}_1 = \text{H}$ ,	$\text{R}_2 = \text{C}_6\text{F}_5$	b    578
$\text{R}_1 = \text{C}_6\text{F}_5$ ,	$\text{R}_2 = \text{H}$	c    559

Similarly, in complexes **1.21** the LUMO resides on the pyridyl ring, therefore, electron withdrawing substituents on the pyridine are expected to cause a red shift.

Tsuzuki and co-workers demonstrated that the position of the substituent also effects the emission.<sup>124</sup> Thus, the strongly electron withdrawing  $C_6F_5$  substituent on the pyridine in **1.21b** and **1.21c** leads to a lowering of the LUMO energy and results in a red shift of emission with respect to the unsubstituted complex **1.21a**. DFT calculations suggest that the increased shift for **1.21b** compared with **1.21c** is because the LUMO is more concentrated on the *para*- position with respect to N, therefore, substitution on this position has a greater effect. This indicates that the emission wavelength is tunable according to the position as well as the electronic properties of the substituent.

Lasker and co-workers reported that for the analogous complexes (**1.22a-c**) the effect of substituents on the phenyl and pyridine can be additive.<sup>125</sup> Thus, **1.22b** with F substituents *meta* to the metallated carbon lowers the HOMO level giving a blue shift compared to **1.22a**. Complex **1.22c** also contains an electron donating substituent on the pyridine ring which raises the LUMO giving an increased blue shift.



A more complicated situation arises in complexes  $[\text{Ir}(\text{dfppy})_2(\text{acac}^*)]$  (**1.23a-c**) containing different substituents on the *acac* ligand.<sup>126</sup> Redox properties were measured using cyclic voltammetry (**Table 1.4**) and the energy gaps ( $\Delta E^{1/2}$ ) are consistent with the maximum emission wavelengths. For example, **1.23a** has the largest band gap and this has the shortest  $\lambda_{em}$  (482 nm), while the smallest band gap is for complex **1.23c** which has the longest  $\lambda_{em}$  (586 nm). By combining the experimental results with DFT calculations, they determined the detailed electronic structures and emission processes involved. For the emission, the transition of complex **1.23a** is  $[\text{d}(\text{Ir}) + \pi(\text{C}^{\wedge}\text{N}) \rightarrow \pi^*(\text{C}^{\wedge}\text{N})]$  and for complexes **1.23b** and **1.23c**, it is  $[\text{d}(\text{Ir}) + \pi(\text{X}^{\wedge}\text{Y}) \rightarrow \pi^*(\text{X}^{\wedge}\text{Y})]$ . Hence, in **1.23a** the LUMO is mainly on the pyridine whereas in **1.23b,c** it is mainly on the

acac; *i.e.* this is an example where substituents have changed the location of the LUMO from the C<sup>N</sup> ligand to the X<sup>Y</sup> ligand.

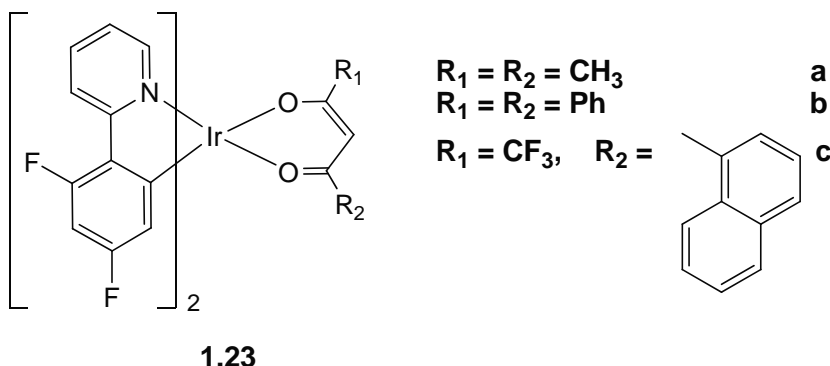


**Table 1.4:** Electrochemical and photophysical properties of  $[\text{Ir}(\text{dfppy})_2(\text{acac}^*)]$  complexes (1.23a-c)<sup>126</sup>

Complex	$E^{1/2}_{\text{ox}}$ [V]	$E^{1/2}_{\text{Red}}$ [V]	$\Delta E^{1/2}$ [V]	$\lambda_{\text{em}}$ (nm)	$E_{\text{em}}$ [eV]
<b>1.23a</b>	1.24	-1.98	3.22	482	2.57
<b>1.23b</b>	0.74	-1.60	2.34	557	2.23
<b>1.23c</b>	0.83	-1.21	2.04	586	2.11

The situation can be even more complicated than described above. For example, De Cola *et al.* recently described the luminescent behaviour of complexes **1.24a-e**.<sup>33</sup> All the complexes **1.24b-e** contain electron withdrawing substituents (F or CF<sub>3</sub>) on the phenyl and show the expected increase in oxidation potential, hence have a lower HOMO, compared to the unsubstituted complex **1.24a**. The reduction potentials are more similar, indicating less effect of the electron withdrawing substituents on the LUMO (**Table 1.5**) hence have larger gaps and blue shifts compared to **1.24a** as expected. Complex **1.24b** with fluorine substituents at the 3 and 5 positions (*meta* to the metallated carbon) shows the expected blue shift compared to **1.24a**. On the other hand **1.24c**, with F atoms on the 2 and 4 positions, (*ortho* and *para*) with respect to Ir-C, shows a negligible blue shift compared to **1.24a** suggesting possibly that inductive and conjugative effects cancel out to some extent. Surprisingly the CF<sub>3</sub> substituted complexes show an opposite trend. Complex **1.24e**, shows the expected strong blue shift compared to **1.24a**. However, **1.24d**, with 3,5-substituted CF<sub>3</sub> groups actually shows a red shift. Looking at the electrochemical data it is difficult to rationalise the

emission wavelengths of **1.24d**, it has the largest HOMO-LUMO gap but the longest wavelength emission. It is worth remembering that the electrochemical reduction involves addition of an extra electron to the complex whilst the emission corresponds to an internal electron that has been excited to a higher energy state. As mentioned previously this emphasises the complexity of the excited states and the limitations of using the electrochemistry to probe them.

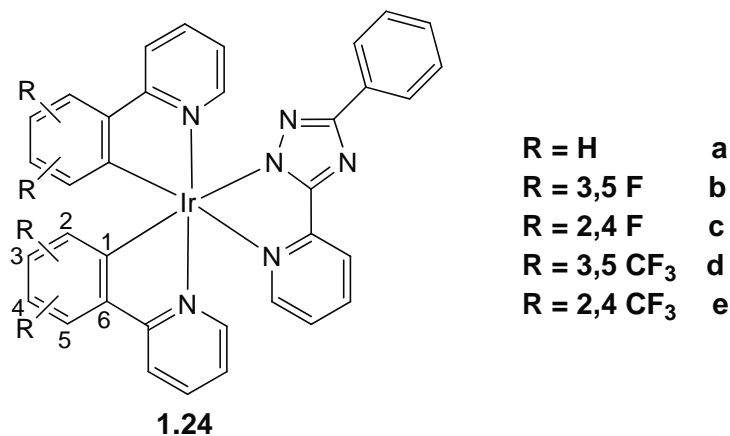


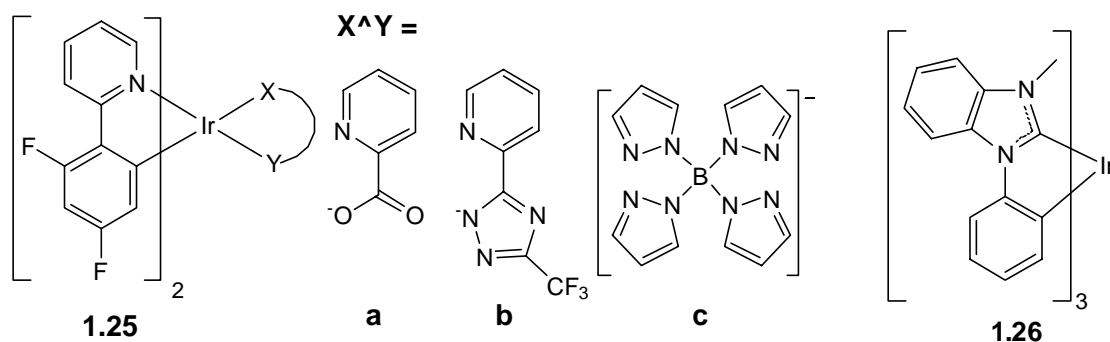
**Table 1.5:** Electrochemical and photophysical properties of  $[\text{Ir}(\text{C}^{\text{N}})^2(\text{X}^{\text{Y}})]$  complexes (**1.24a-e**)<sup>33</sup>

Complex	$E^{1/2}_{\text{ox}}$ [V]	$E^{1/2}_{\text{Red}}$ [V]	$\Delta E^{1/2}$ [V]	$\lambda_{\text{em}}$ (nm)	$E_{\text{em}}$ [eV]
<b>1.24a</b>	1.06	-2.11	3.17	489, 517	2.54
<b>1.24b</b>	1.41	-2.05	3.46	461, 491	2.69
<b>1.24c</b>	1.26	-2.10	3.36	484, 518	2.56
<b>1.24d</b>	1.52	-2.02	3.54	511, 544	2.42
<b>1.24e</b>	1.58	-1.93	3.51	466, 499	2.66

In conclusion, it is possible to tune the emission wavelength through modifications of the HOMO and LUMO electron densities by controlling the nature and position of substituents on either the  $\text{C}^{\text{N}}$  and/or the  $\text{X}^{\text{Y}}$  ligands. As mentioned above, since, the position of the HOMO and the LUMO can vary depending on the particular ligands it is not possible to have a simple general rule for example, electron withdrawing substituents always give a blue shift.

### 1.3.2.5 Colour Tuning

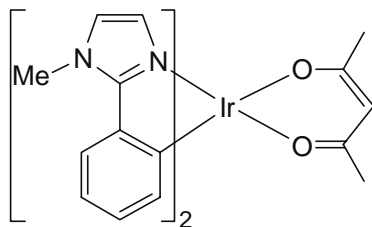
As shown in **Section 1.3.2.4**, changing the nature and position of substituents has provided a mechanism to tune the emission to a particular region of the spectrum. Having said this, the vast majority of complexes  $[\text{Ir}(\text{C}^{\wedge}\text{N})_3]$  and  $[\text{Ir}(\text{C}^{\wedge}\text{N})_2(\text{X}^{\wedge}\text{Y})]$  emit in the red and green regions and there are relatively few reports of room temperature blue phosphorescence. To achieve blue emission clearly requires a large HOMO-LUMO band gap, the most common strategies to achieve this are to introduce electron withdrawing groups on the phenyl ring of the cyclometallating ligand as discussed in **section 1.3.2.4**, or to use a stronger donor ligand *e.g.* an N-heterocyclic carbene,<sup>127-129</sup> in place of the pyridine in the cyclometallating ligand (*i.e.*  $\text{C}^{\wedge}\text{N}$  becomes  $\text{C}^{\wedge}\text{C}$ ), or to use strong field monodentate  $\text{XY}$  ligands (*e.g.*  $\text{CN}$ ).<sup>112, 130</sup>



A particularly successful example of the use of electron withdrawing substituents is **1.25a** ( $\lambda_{\text{em}} = 466 \text{ nm}$ )<sup>68, 131, 132</sup> which proved to be an excellent dopant for sky blue phosphorescent OLEDs. Moreover, improvements were made by changing the picolinate (pic) with other ancillary ligands, such as pyridyl azolate to afford **1.25b** ( $\lambda_{\text{em}} = 459 \text{ nm}$ )<sup>68, 121</sup> or tetrakis(1-pyrazolyl)borate to afford **1.25c** ( $\lambda_{\text{em}} = 460 \text{ nm}$ ).<sup>68, 121</sup> These modifications have produced a further blue shift of approximately 6-7 nm compared with **1.25a**, however the quantum yield is significantly reduced. Applying an alternative strategy, Holmes and co-workers reported complex **1.26** in which the pyridine is replaced with an N-heterocyclic carbene, which emits in the deep blue region ( $\lambda_{\text{em}} = <400 \text{ nm}$ ).<sup>128</sup>

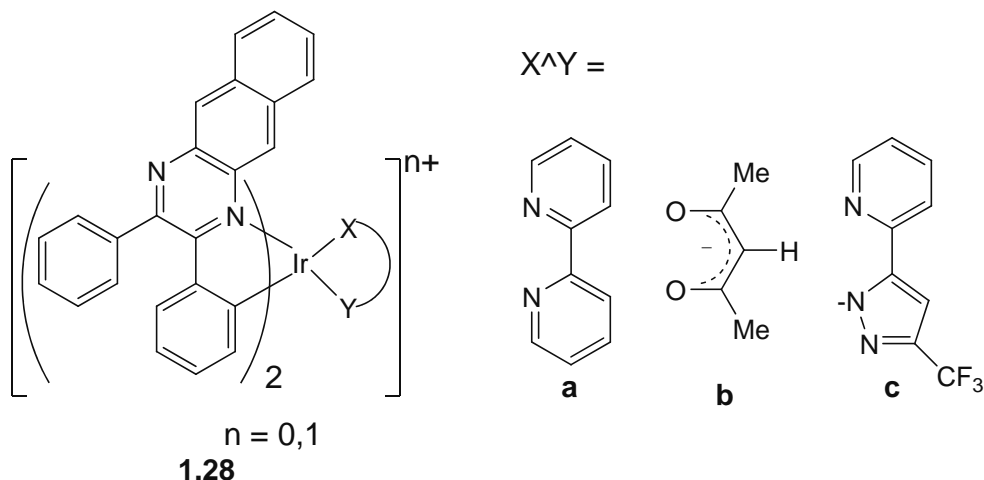
Another big challenge in OLED research is the production of single emitter white light-emitting devices (WOLEDs) which are one of the most appealing solutions

for low energy consumption solid state lighting. Currently, most WOLEDs are obtained by combining the emission from red, green and blue or sky blue and orange emitters.<sup>133, 134</sup> This requires more complex device architecture and production processes, as compared to single emitter based OLEDs, which has so far greatly hindered their market entry. Therefore, the development of a white light emitting luminescent single transition metal complex is very much desired. In 2009, Nazeeruddin and co-workers reported complex **1.27**,<sup>135</sup> which upon excitation within the ligand ( $\pi$ - $\pi^*$ ) and MLCT absorption bands, shows a broad and structureless emission covering the spectral range from 440 to 800 nm, with a maximum intensity at 570 nm. The emission spectrum is independent of excitation wavelength and concentration (which excludes the presence of an excimer). These photophysical results point toward a single broad emitting centre. Though the device efficiency based on complex **1.27** is rather low, the preparation of a single component white light emitting phosphorescent emitter is significant as it demonstrates the large potential that simple single transition metal complexes have for the development of WOLEDs.



**1.27**

The other significant challenge in terms of tuning the emission wavelength is to move the emission into the near infrared region. Infrared light can penetrate tissue more than visible light so may be desirable in imaging or possibly in phototherapeutic applications. Studies of complexes with emission in the near infrared region (NIR) are relatively rare; the most plausible reason is that decreasing the energy gap towards the near infrared leads to faster non-radiative decay according to the energy gap law. Recently, Chen *et al.* reported some complexes (**1.28a-c**) in which emission is into the near infrared region ( $\lambda_{\text{max}} = \sim 910\text{-}920\text{ nm}$ ) at room temperature by extending the  $\pi$ -conjugation and introducing an electronegative N atom in the C<sup>N</sup> ligand, which lowers the LUMO to a considerable extent.<sup>136</sup>



In summary, the emission wavelength (colour) of cyclometalated Ir(III) complexes  $[Ir(C^N)_2(XY)]^{n^+}$  ( $n = 0, 1$ ) can be tuned through the entire visible region and into the near infrared by varying either the  $C^N$  ligand and/or the  $X^Y$  ligand. Furthermore, the electronic effects of the substituents and their position can significantly influence the photophysical properties. Owing to their rich photophysical and electrochemical properties, these complexes will continue to be used in diverse applications such as; emissive dopants in OLEDs, as sensors and as biological labels and probes which are discussed further in the next section.

#### 1.4 Bioconjugation

Bioconjugation refers to the process of labelling biomolecules with a moiety (label) for the purpose of detection/analysis or for gaining insight into biological recognition.<sup>27</sup> Hence, the label should have some property *e.g.* luminescent, electroactive or radioactive which can be easily detected. Bioconjugation involves the reaction of a functional group on the label with target functional groups of the biomolecules, resulting in the formation of stable covalent bond(s). For example, NHS ester, isothiocyanate and aldehyde groups react readily with amines, whilst iodoacetamide and maleimide react with thiol, and amines react with carboxylic acid groups of biomolecules.<sup>78, 137</sup> (**Fig. 1.8**)

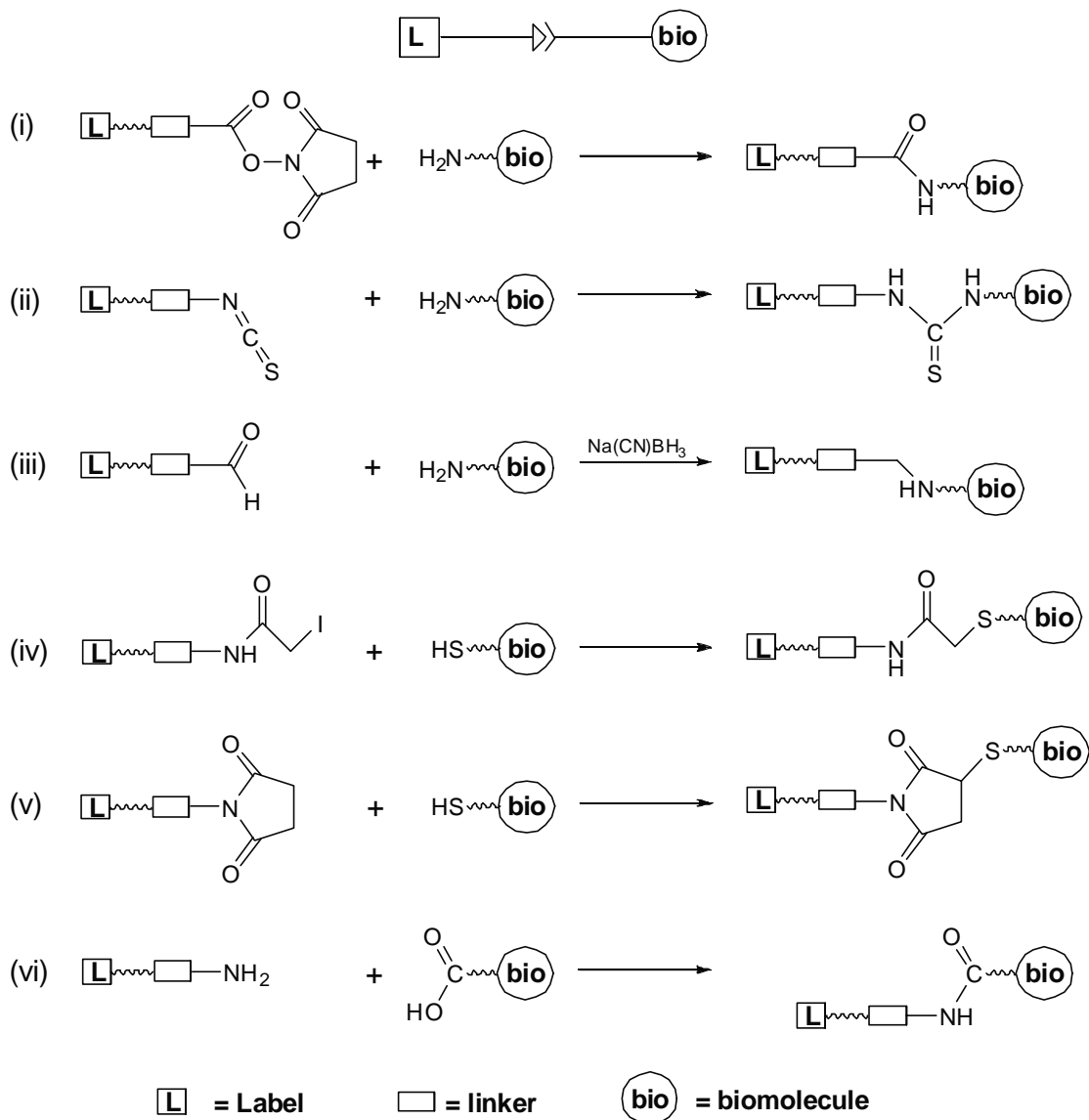


**Fig. 1.8** Examples of typical reactions used in bioconjugation

Traditionally, labelling of biomolecules has relied heavily on radioactive isotopes owing to their high detection sensitivity. In early studies, radiolabelling of proteins involved the incorporation of unstable  $\beta$ -emitting  $^3\text{H}$  or  $^{14}\text{C}$  containing amino acids. Later on the majority of these studies utilized  $\gamma$ -emitting isotopes of iodine *i.e.*  $^{125}\text{I}$  and  $^{131}\text{I}$ , which created probes with higher specific activities, for detection of proteins at low concentrations.<sup>138</sup> Similarly, radioactive markers have also been used for DNA labelling. Owing to the high sensitivity of  $^{32}\text{P}$ , it is the most commonly used radiolabel for DNA, but  $^{33}\text{P}$  and  $^{35}\text{S}$  are also used. However, radioisotopes have been gradually replaced by non-radioactive labelling reagents, particularly luminescent ones, in view of their longer shelf lives and lower potential health hazards.

Many luminescent organic molecules have been developed as labels for different biomolecules. Fluorescein (**a**)<sup>139</sup>, rhodamine (**b**)<sup>139</sup> (**Fig. 1.9**) and their derivatives are the most common fluorescent organic labels for antibodies, proteins and DNA, for use in fluorescence microscopy, flow cytometry and ELISA (enzyme-linked immunosorbent assay). Recently green fluorescent proteins, combined with genetic engineering and cloning techniques have revolutionized the design of imaging agents and probes for the study of protein and peptide conformations and interactions.<sup>140, 141</sup> For both small organic fluorophores and GFPs, the extinction coefficients and quantum yields are very high, however, they can suffer from small Stokes shifts, short emission lifetimes and susceptibility to photobleaching. Hence, there is still a need for new fluorophores with improved photophysical properties.

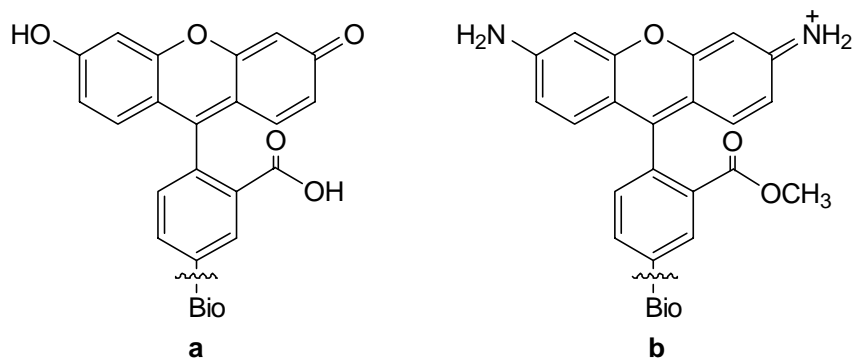


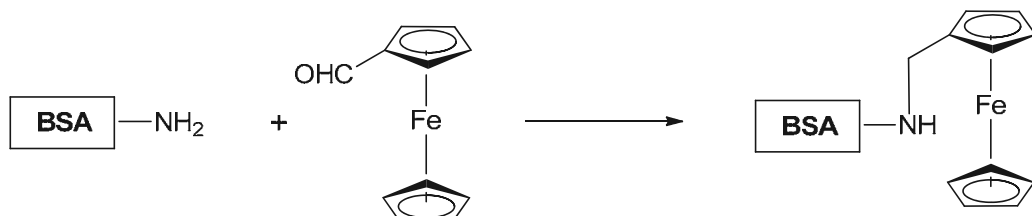
**Fig. 1.9** Fluorescein and rhodamine showing point of attachment to biomolecules.

Lanthanide complexes have also been used as luminescent labels.<sup>142</sup> Direct excitation of many lanthanides is problematic due to low extinction coefficients and free lanthanide ions usually do not luminesce in aqueous solutions as a result of the efficient deactivation pathway associated with the surrounding water molecules. However, both these problems can be improved by the use of suitably designed ligands (chelate or multidentate) which themselves are highly light absorbing. These lanthanide chelate complexes can have intense luminescence and long emission lifetimes (ms). Hence, lanthanide bioconjugates have been used in fluorescence microscopy.<sup>142, 143</sup> Transition metal complexes have also attracted attention due to their ease of synthesis, complex stability, desirable photophysical properties and ability to tune the properties by changing the ligands. The next section will discuss the use of transition metal bioconjugates as biological labels and probes.

### 1.4.1 Transition metal complexes as labels

#### 1.4.1.1 Protein and Hormone labels

Labelling of biomolecules with transition metals has received much attention for bioanalytical applications.<sup>144</sup> The first bioconjugates of transition metals were various ferrocene amino acids including ferrocenyl alanine and p-ferrocenylphenylalanine, reported in 1957 by Schlogl.<sup>145</sup> Since then, a range of ferrocene derived bioconjugates including of proteins (**Scheme 1.3**) and nucleic acids, have been synthesised and tested for various applications in biochemistry.<sup>146</sup> The interactions of ferrocene conjugates can be monitored by changes in the  $\text{Fe}^{2+}/\text{Fe}^{3+}$  redox potential of the complexes upon conjugation. One of the most important uses of ferrocene bioconjugates is in glucose sensors, due to the necessity, for glucose monitoring for diabetics.

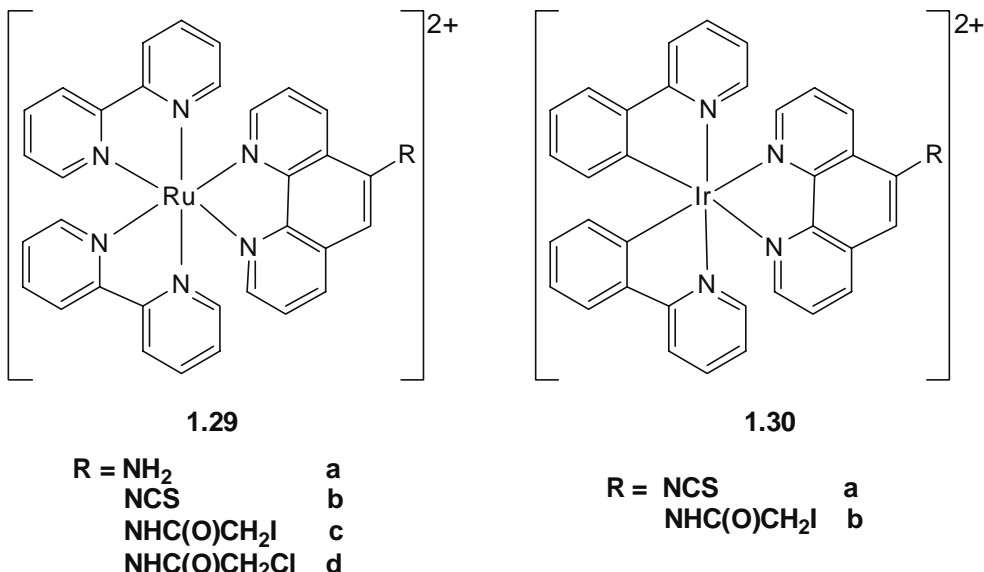


**Scheme 1.3**

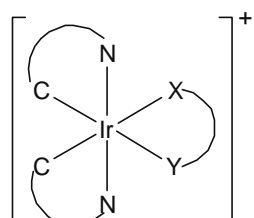
As mentioned above, luminescent labels have become very popular in recent times. Luminescent transition metal complexes possess large Stokes shifts (hundreds of nm), long emission lifetimes (100 ns to ms), and enhanced photostability (lower photobleaching) with respect to organic fluorophores.<sup>38, 70, 71, 147, 148</sup> In comparison to lanthanide complexes, they benefit from easy excitation (high  $\epsilon$ ) as a result of allowed excitation transitions ( $\pi-\pi^*$  or MLCT), and higher quantum yields (up to 80% in fluid solution at room temperature) which provide brighter images at lower concentrations.<sup>148, 149</sup> Therefore, these are attractive candidates as lumophores for application in fluorescence microscopy.

Various luminescent transition metals have been used to make metal bioconjugates by following the reactions shown in **Fig. 1.8**. Emission can be affected by bioconjugation and by the type of linker, which is discussed further in **Section 1.4.1.2**. A range of biomolecules have been labelled with transition metals, for example, proteins *e.g.* human serum albumin (HSA) and bovine serum albumin (BSA),<sup>77, 78</sup>

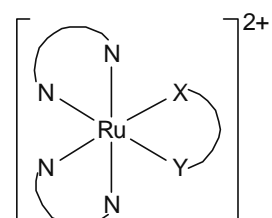
antibodies *e.g.* immunoglobulin (Ig),<sup>78, 150</sup> hormones *e.g.* estradiol,<sup>151, 152</sup> vitamins *e.g.* biotin,<sup>151, 153</sup> and DNA,<sup>45</sup> and specific examples are discussed in more detail below.



In 1992, Vos and co-workers reported complexes (**1.29a,b**) which were used to label various proteins such as poly(L-lysine), BSA, HSA and IgG.<sup>150</sup> Lakowicz also reported bioconjugation of Ru(II) polypyridine complex **1.29c** to HSA and IgG.<sup>154</sup> Complex **1.29d** was unable to label HSA presumably since chloride is a poorer leaving group than iodide. Upon photoexcitation, all the bioconjugates display intense and long lived emission in aqueous buffer at room temperature. Conjugates of **1.29c** have longer emission lifetimes than that of precursor complex (**1.29c**) under ambient, air-saturated conditions, which suggests that the label is well encapsulated by each protein and a low exposure to the solvent environment results in inefficient quenching by water and/or oxygen. It was not until 2001 that Lo reported bioconjugates of analogous Ir complexes (**1.30a,b**), which were used to label HSA and DNA (see later in **Section 1.4.1.3**).<sup>77</sup> Similar to the Ru analogues, the HSA-conjugates of complexes **1.30a** and **1.30b** exhibit only a small decrease in emission lifetimes in the presence of water and/or oxygen unlike the free labels, which was again ascribed to the good-shielding of the bioconjugates within the protein matrix. Since then, the same group has labelled various proteins and hormones with a range of cyclometallated Ir (III) complexes.<sup>26, 78, 155-157</sup>

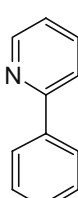


1.31

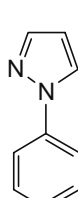


1.32

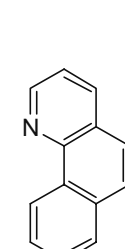
$C^N =$



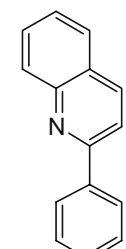
a



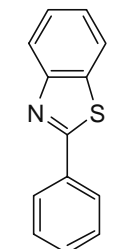
b



c

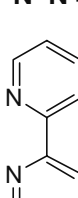


d

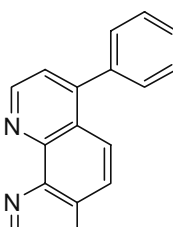


e

$N^N =$

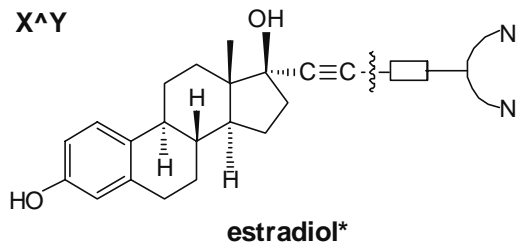


a



b

$X^Y$



estradiol\*

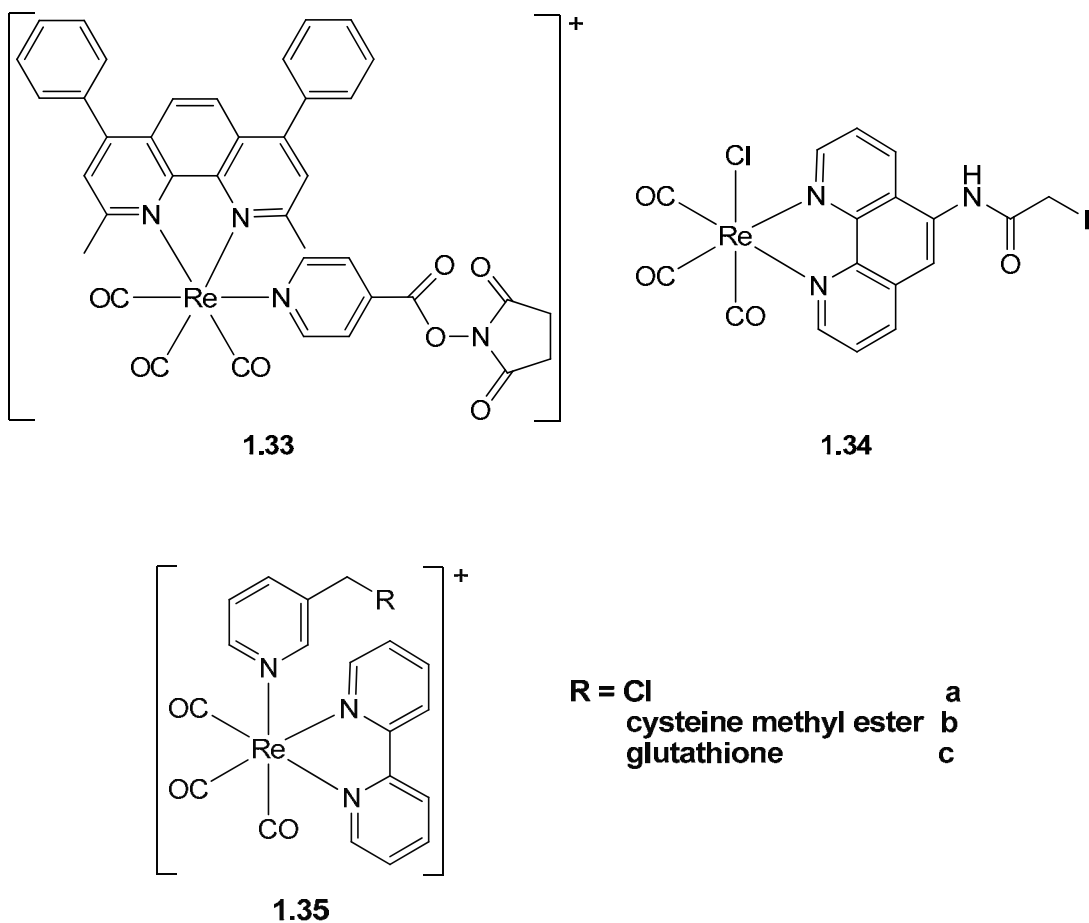
$\text{N} \text{---} \text{N} = \text{bipy}$

$\square = \text{linker}$

Early studies of metal bioconjugates were mainly interested in demonstrating attachment of metal complexes to biomolecules and measuring the effect on emission. In more recent studies the metal bioconjugates are actually being applied to study biochemical interactions, for example probing hormone receptor interactions. The estrogens are a group of hormones including estrone, estriol and estradiol, which is the major estrogen in humans.<sup>158</sup> The concentration of estradiol receptors is a useful diagnostic tool for many breast cancers<sup>152</sup> and thus luminescent labelled estradiol derivatives have been reported.<sup>152, 156</sup> Lo *et al.* synthesized some Ir(III) (1.31a-e)<sup>156</sup> and Ru(II) (1.32a,b)<sup>152</sup> complexes and examined their potential as luminescent probes for estrogen receptors. All the estradiol complexes displayed emission enhancement in the presence of ER $\alpha$  (estrogen receptor) due to the specific binding to ER $\alpha$ . The emission enhancement was ascribed to the increase in the hydrophobicity and rigidity of their local environment. The binding constants ( $K_a$ ) of the estradiol complexes to ER $\alpha$  ( $\sim 1.0$

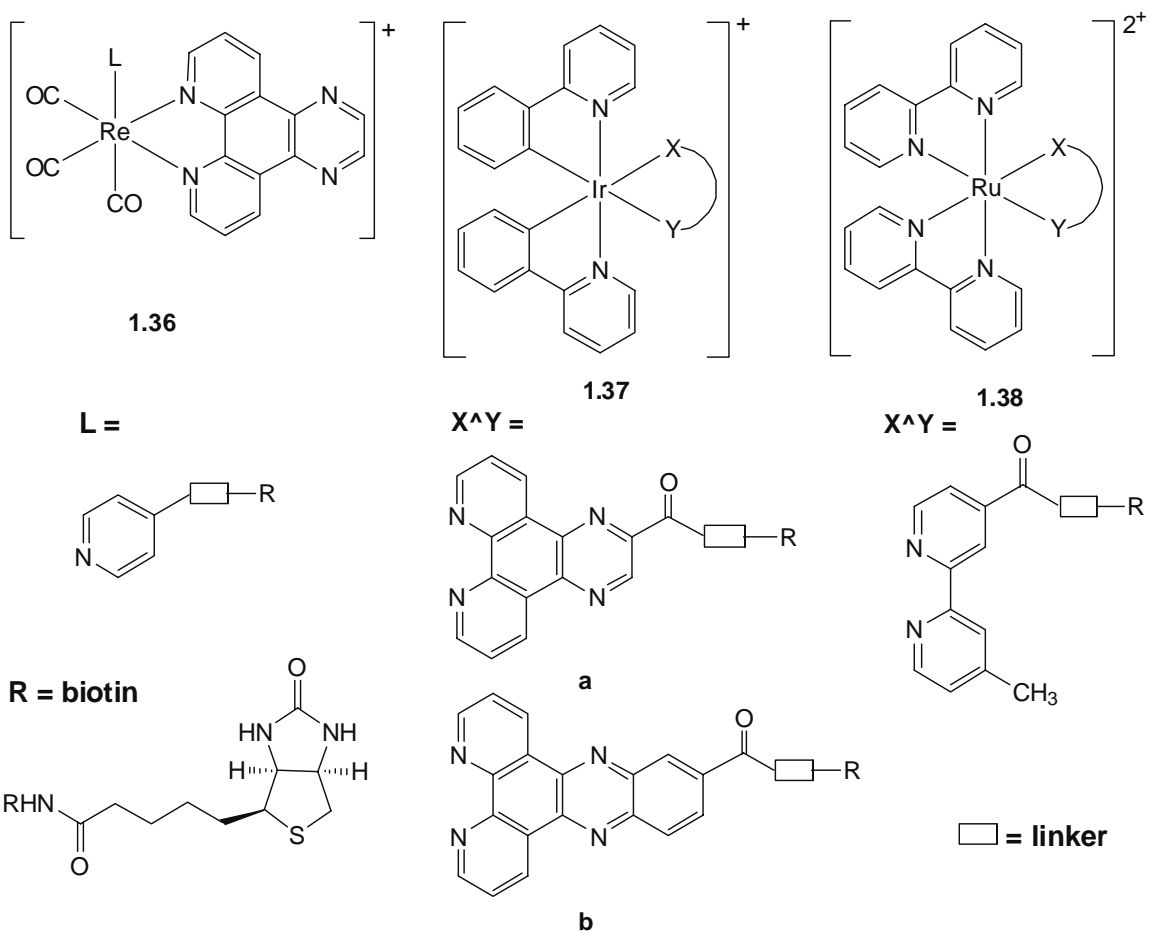
to  $2.1 \times 10^7 \text{ M}^{-1}$  for **1.31** and  $\sim 10^6 \text{ M}^{-1}$  for **1.32**) are smaller than that of free estradiol ( $K_a = 5 \times 10^9 \text{ M}^{-1}$ ), this was attributed to the bulky metal fragments increasing the steric hindrance between the complexes and the receptor.

In 1997, the first luminescent Re(I) protein conjugates (HSA and bovine-IgG) were made from NHS ester<sup>159</sup> and iodoacetamide<sup>160</sup> activated complexes **1.33** and **1.34**. These bioconjugates showed intense and long lived emission similar to the free complexes. The HSA-conjugate of **1.33** displays highly polarized emission in the absence of rotational diffusion in air-equilibrated aqueous solution. The steady state polarization of the bioconjugate was sensitive to the binding of anti-HSA (antibody), resulting in a significant increase in luminescence polarization. Consequently, HSA-conjugate of **1.33** can be used as a tracer in a competitive immunoassay with unlabelled HSA acting as an antigen. Later, Coogan and co-workers reported complex (**1.35a**) which reacts with thiol groups of the biomolecules such as cysteine (**1.35b**) and glutathione (**1.35c**).<sup>161</sup> Complex **1.35a** was also used in cell imaging (see later).



### 1.4.1.2 Biotin complexes

Avidin is a glycoprotein isolated from chicken egg white which has four identical subunits, and can bind up to four biotin molecules (Vitamin H) with high affinity ( $K_d = ca. 10^{-15} M$ ). As a result, the avidin-biotin system has been widely utilized in many bio-analytical applications.<sup>162</sup> To use the biotin/avidin recognition in bioanalytical applications requires labelling of the biotin or avidin. Biomolecules can be biotinylated and then detected by avidin that has been suitably labelled.<sup>162</sup> The alternative of labelling the biotin is problematic if organic fluorophores are used due to self quenching by fluorescent resonance energy transfer (FRET) when bound to avidin. In contrast, luminescent transition metal complexes have large Stokes shifts which disfavour RET quenching hence these can also be used in biotin labelling.



<sup>162</sup>Lo *et al.* reported biotinylated complexes of Re(I) (**1.36**),<sup>163</sup> Ir(III) (**1.37**),<sup>164</sup> and Ru(II) (**1.38**),<sup>165</sup> which displayed intense emission at room temperature in organic solvents but were non-emissive in aqueous buffer. The binding of the complexes to

avidin was studied by the standard HABA assay. All the complexes displayed enhanced emission intensities and extended lifetimes upon binding to avidin. Complexes with longer spacer arms exhibited less significant emission enhancement because they remained more exposed to the polar buffer after binding to the protein. The  $K_d$  of the adducts of the Ir-biotin complexes **1.37a** and **1.37b** were  $2.0 \times 10^{-7}$  M and  $8.2 \times 10^{-7}$  M respectively, which are about 8 orders of magnitude larger than that of native biotin  $K_d = ca. 10^{-15}$  M, and about 2 orders of magnitude larger than Re-biotin adducts ( $\sim 10^{-9}$  M). This suggests that the binding of the Ir-biotin complexes **1.37** to avidin is more hindered by the extended planar nature of the X<sup>Y</sup> ligand compared to L in Re-biotin complexes **1.36** having the variable linkers. The  $K_d$  for Ru(II) biotin complex (**1.38**) ( $\sim 10^{-11}$  M) is  $10^3$  to  $10^4$  times lower than the Ir(III) complexes indicating a stronger binding with avidin;<sup>162</sup> this can be ascribed to a smaller X<sup>Y</sup> ligand and the higher cationic charge of Ru(II) complexes relative to the Ir(III) complexes.

As illustrated above, the rich photophysical properties of transition metal complexes are ideal for exploitation as biological labels. The flexibility to control independently the photophysical properties and chemical properties *e.g.* charge, hydrophobicity, through careful choice of ligands and metals means that it is likely that luminescent transition metal complexes will continue to be used in the design of new biological labels to probe biological systems.

#### 1.4.1.3 DNA probes and labels

Over the last 25 years, interactions between nucleic acids and transition metal complexes have been studied extensively for various bioanalytical and pharmaceutical purposes notably by Barton's group and there have been a number of comprehensive reviews on the subject.<sup>78-81, 166</sup> This section summarises some examples of luminescent transition metal complexes that have been employed as DNA probes and labels, *cis*-platin and the therapeutic interactions of transition metal complexes will not be discussed. In the following section probes will be used to describe complexes that interact with DNA through non-covalent interactions and labels to complexes that are covalently bound to DNA or a nucleotide.

Octahedral polypyridyl transition metal complexes such as  $[\text{Fe}(\text{bipy})_3]^{2+}$ ,  $[\text{Ru}(\text{bipy})_3]^{2+}$  and  $[\text{Ru}(\text{phen})_3]^{2+}$  (**Fig. 1.10**) have received considerable attention as DNA conformational probes.<sup>30</sup> The exact mode of binding of  $[\text{Ru}(\text{phen})_3]^{2+}$  to DNA is

somewhat controversial, it has been ascribed to groove binding, intercalation and insertion.<sup>79, 167</sup> Rodger *et al.* suggests that all three occur and the ratio of these is dependent on the degree of saturation of the DNA by the complex.<sup>167</sup> The complex has a preference for GC rich sequences and there is a small but significant preference for binding by the right-handed  $\Delta$ -isomer.

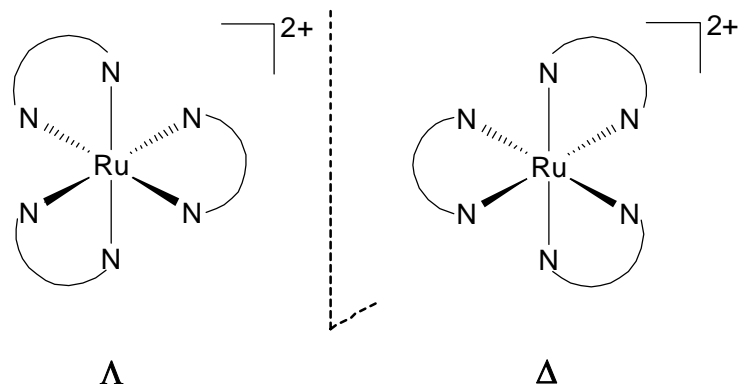


**Fig. 1.10:** Enantiomers of  $[\text{Ru}(\text{N}^{\wedge}\text{N})_3]^{2+}$  ( $\text{N}^{\wedge}\text{N}$  = bipy, phen)

$[\text{Ru}(\text{bipy})_3]^{2+}$  shows no emission enhancement in the presence of DNA, therefore, extended planar ligands with high aromaticity *e.g.* dppz (**Fig. 1.11**) were designed to increase intercalative binding. The resultant metallo-intercalators *e.g.*  $[\text{Ru}(\text{bipy})_2(\text{dppz})]^{2+}$  have become immensely powerful tools to probe nucleic acids.<sup>168</sup> Re(I),<sup>169</sup> Ru(II)<sup>80, 168</sup> and Ir(III)<sup>164</sup> complexes of dppz do not luminesce in aqueous solution due to the ability of water molecules to deactivate the excited state through hydrogen bonding. However, upon introduction of double helical DNA to an aqueous solution of these complexes, emission is observed, reflecting the shielding of the

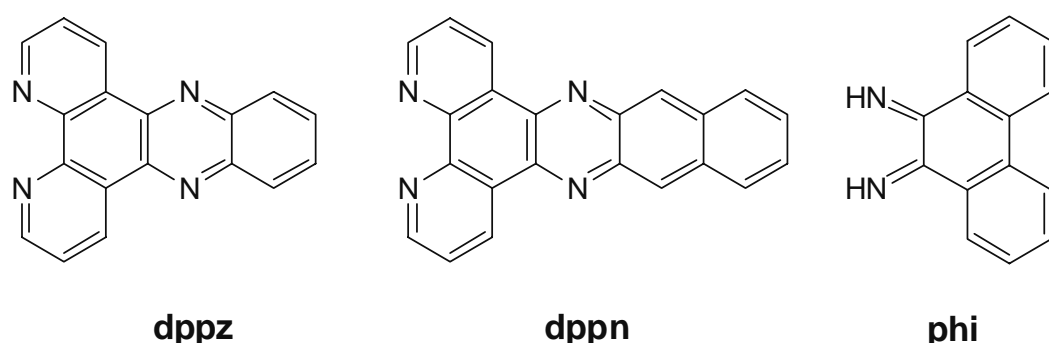
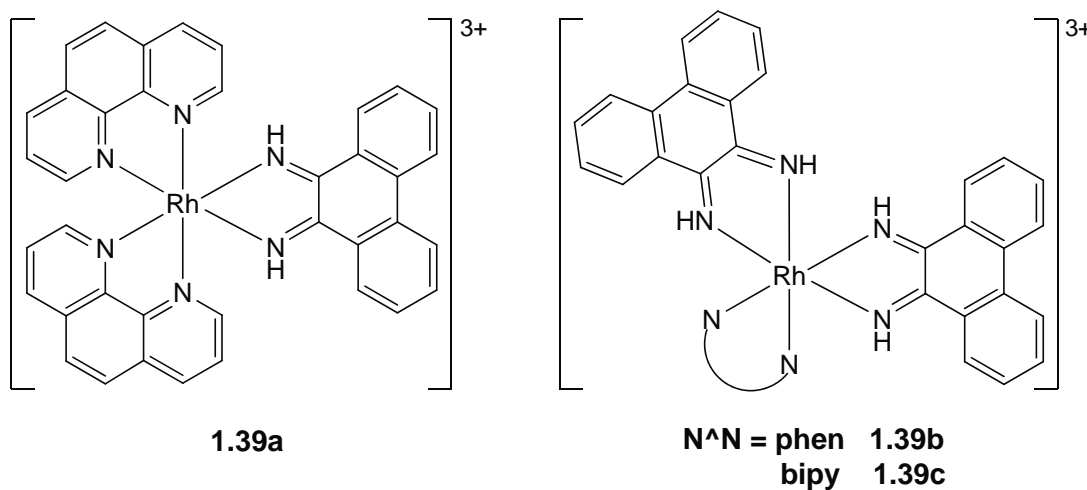


**Fig. 1.11:** Structures of extended planar diimine ligands *i.e.* dppz, dppn and phi

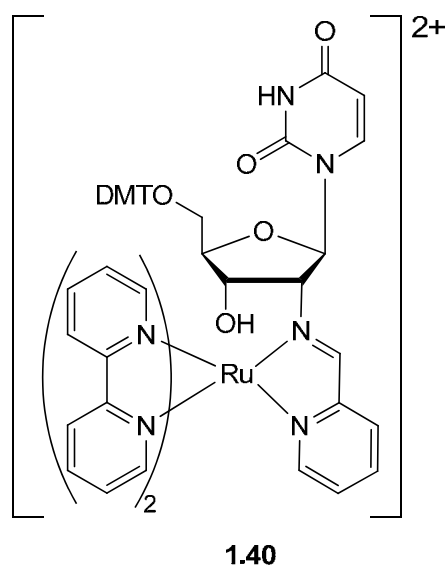
intercalating ligand from bulk solvent. Thus, intercalation results in, i) the protection of the diimine (dppz) ligands from the water molecules, ii) a more hydrophobic environment, iii) a higher rigidity of the local surroundings of the complexes. All these factors lead to enhanced emission intensity *e.g.*  $> 10^4$  times for  $[\text{Ru}(\text{bipy})_2(\text{dppz})]^{2+}$ . This has been termed a “light switch effect” by Barton.<sup>168</sup> It is quite remarkable and provides the basis for a valuable photophysical probe of nucleic acids. The intrinsic binding constants for  $[\text{Re}(\text{CO})_3(4\text{-Mepy})(\text{dppz})]^+$  and  $[\text{Ir}(\text{ppy})_2(\text{dppz})]^+$  are smaller than that of  $[\text{Ru}(\text{bipy})_2(\text{dppz})]^{2+}$ ,<sup>164</sup> which can be ascribed to the lower cationic charge of the Re(I) and Ir(III) complexes. The binding constant of complex  $[\text{Ir}(\text{ppy})_2(\text{dppn})]^+$  is higher than that of  $[\text{Ir}(\text{ppy})_2(\text{dppz})]^+$  which is due to the larger planar surface area of the dppn ligand. Similar observations have been reported for related Re(I)-dppz and -dppn complexes.<sup>169</sup> Therefore, extending the ligand from dppz to dppn enhances intercalation, which results in higher binding constants.



9,10-phenanthrenequinone (phi) has also been used as an intercalating ligand. However, in contrast to the dppz ligand, transition metal complexes of phi intercalate with the long axis of the phi ligand parallel to the long axis of the base pair. The first report on DNA binding by the complexes of phi ligand were based on Ru(II) systems, but subsequent work has largely concerned Rh(III) complexes.<sup>79, 80</sup> Barton and co-workers reported that the complexes **1.39a-c** bind to DNA ( $K_b \geq 10^7 \text{ M}^{-1}$ ) and upon photo-excitation, all of the complexes efficiently cleave duplex DNA at the site of intercalation.<sup>80</sup> Complex **1.39a** shows site selectivity upon binding to DNA, whereas the close analogues **1.39b** and **1.39c** show no sequence or structure selectivity. This is attributed to the steric bulk of the phen ligands in complex **1.39a**, which block a portion

of the aromatic surface of the phi from intercalation and the complex is considered to bind tightly only at sites which are more open in the major groove. There are no steric clashes with the helix in complexes **1.39b** and **1.39c**; hence, they do not show any selectivity.

Fluorescence resonance energy transfer (FRET) is a popular microscopy technique used to measure the proximity of two fluorophores. It involves the transfer of excited state energy from a donor fluorophore to an acceptor fluorophore through nonradiative dipole-dipole coupling. Upon transfer of energy, the acceptor molecule enters an excited state from which it decays emissively. Thus, by exciting the donor and then monitoring the relative donor and acceptor emission, one can determine when FRET has occurred and at what efficiency. Barton and co-workers studied metal to metal FRET in DNA.<sup>170</sup> They reported total luminescence quenching of  $[\text{Ru}(\text{phen})_2(\text{dppz})]^{2+}$  by complex **1.39c**, when the complexes were covalently tethered to opposite 5'-ends of a 15 base pair DNA duplex and interpreted their results as indicative of fast long range electron transfer from the intercalated excited state electron donor  $[\text{Ru}(\text{phen})_2(\text{dppz})]^{2+*}$  to the intercalated acceptor **1.39c**.



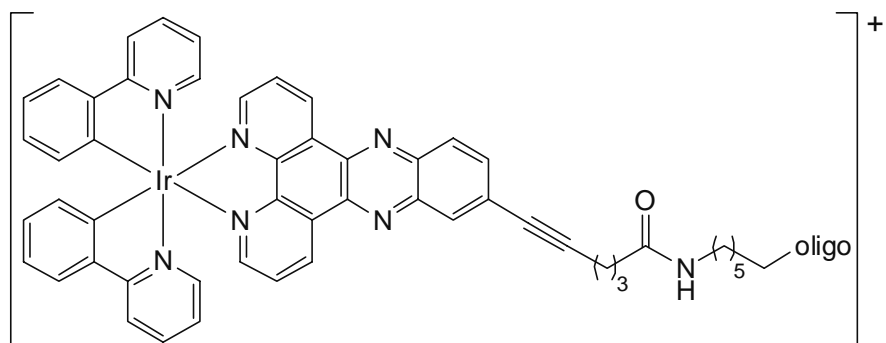
To investigate the transition metal complexes as DNA labels, Meade and co-workers designed a chelating uridine-based nucleoside from the reaction of an amine functionalised uridine and 2-pyridinecarboxaldehyde, which was then coordinated to a  $[\text{Ru}(\text{bipy})_2]^{2+}$  moiety to give complex **1.40**.<sup>45</sup> This nucleoside was linked to a solid

support and converted to an 11-mer oligonucleotide 5'-TCTCCTACACU<sub>Ru</sub>-3'. This displayed similar emission properties in aqueous buffer as that of complex **1.40**. The oligonucleotide was hybridised with its complementary strand and the duplex formed again showed similar emission properties, which suggests that the photo-excited complex does not oxidise guanine, which is the most easily oxidised base, being the most facile electron donor of the DNA bases. Also, the addition of quencher  $[\text{Ru}(\text{NH}_3)_6]^{3+}$ , which is known to generate a potent Ru(III) oxidant from excited Ru(II) polypyridine species, does not lead to detectable guanine oxidation. For  $[\text{Ru}(\text{NH}_3)_6]^{3+}$ , the bimolecular quenching constant determined for the quenching of photoexcited duplex **1.40** is an order of magnitude smaller compared to the value measured for the quenching of  $[\text{Ru}(\text{bipy})_3]^{2+}$  ( $1.1 \times 10^8 \text{ M}^{-1} \text{ s}^{-1}$  vs  $2.0 \times 10^9 \text{ M}^{-1} \text{ s}^{-1}$ , respectively). However, the driving force estimate ( $\Delta G_q$ ) for the single electron transfer from  $[\text{Ru}(\text{NH}_3)_6]^{3+}$  to photoexcited duplex **1.40** is much smaller than the value calculated for  $[\text{Ru}(\text{bipy})_3]^{2+}$  (~ -0.24 eV vs -0.92 eV, respectively). Therefore, addition of oxidative quencher to this assembly fails to result in any oxidative damage to DNA, despite generating a Ru(III) species that is a powerful oxidant. These properties make complex **1.40** a valuable probe for DNA mediated electron transfer studies.

As discussed earlier, Lo and co-workers reported the first bioconjugated cyclometallated Ir(III) complexes (**1.30a,b**), which were used to label DNA. The free complexes are insoluble in water which prevents studying their photophysical properties in aqueous solutions, however, the labelled DNA species were soluble in aqueous buffer and exhibited intense, long lived emissions. These labelled oligonucleotides were hybridized with their unmodified complementary oligonucleotides to give luminescent double stranded DNA molecules. The photophysical properties of these duplexes are similar to those of the labelled probes, which is indicative of negligible influence of the labels on the hybridisation.

Taking advantage of the powerful photochemistry of bis-cyclometallated Ir(III) complexes, Barton and co-workers showed that  $[\text{Ir}(\text{ppy})_2(\text{dppz}^*)]^+$  (**1.41**), functionalised through a modified dppz ligand, serves both as a photo-oxidant and reductant of distal DNA bases.<sup>87</sup> They designed Ir-DNA conjugates containing two modified bases embedded in an AT tract, a <sup>CP</sup>A ( $\text{N}^6$ -cyclopropyladenine) for hole injection and either a <sup>Br</sup>U (5-bromouridine) or a <sup>CP</sup>C ( $\text{N}^4$ -cyclopropylcytosine), as an electron trap. Upon excitation, the excited Ir(III) complex irreversibly oxidises a <sup>CP</sup>A base from a distance

within the same DNA assembly. The subsequent reduced metallic species is, in turn, able to reduce distal  $^{3\text{Br}}\text{U}$  or  $^{3\text{CP}}\text{C}$  bases.



1.41

In summary, transition metal complexes have been studied extensively as probes and labels for DNA. The rich photophysical and photochemical properties of these metal complexes will continue to find applications in DNA recognition studies and photoinduced electron transfer studies. It seems likely that future systems will show further enhancements in both binding affinity and selectivity.

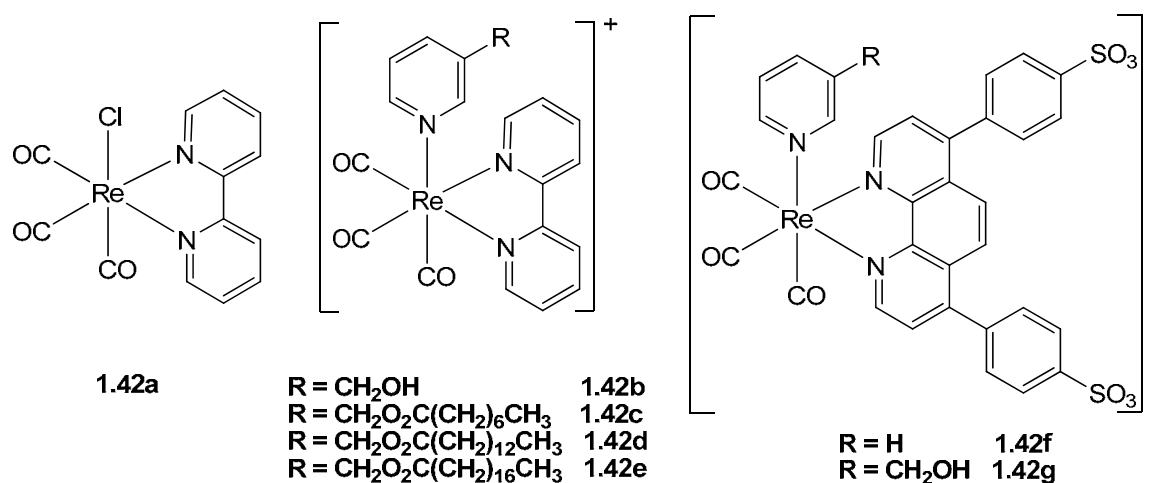
#### 1.4.2 Applications of transition metal complexes in live cell imaging

Various transition metal complexes have been employed for cell imaging due to their attractive photophysical properties and the area has recently been reviewed.<sup>149</sup> To render metal complexes suitable for imaging applications, it is necessary to address some of the essential criteria for fluorophores such as cellular uptake, toxicity and localisation.

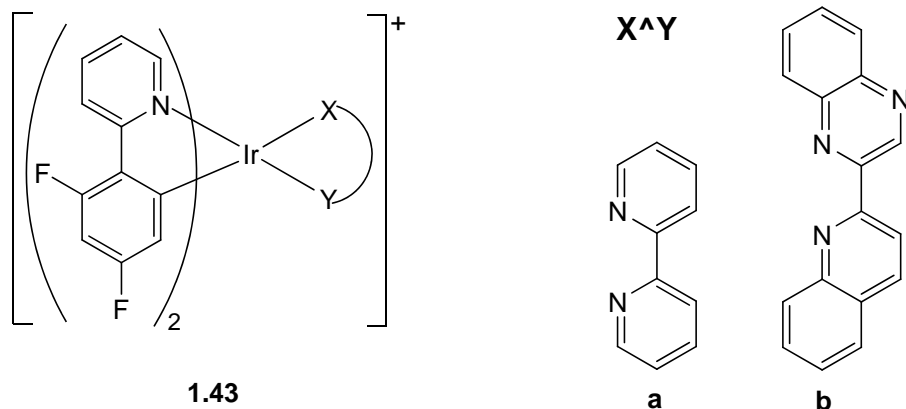
In 1997, Levine and co-workers reported the application of  $[\text{Ru}(\text{bipy})_3]^{2+}$  in quantitative imaging of oxygen in single cells (macrophages) using Fluorescence Lifetime Imaging Microscopy (FLIM).<sup>2</sup> They showed that the behaviour of this complex in the presence of oxygen could be described as a dynamic quenching process, and that its lifetime is insensitive to pH, ion concentrations and cellular contents.  $[\text{Ru}(\text{bipy})_3]^{2+}$  was found to partition heterogeneously inside the cells, leading to a non-uniform fluorescence intensity, however, a uniform lifetime was observed throughout the cell, suggesting that the oxygen concentration was constant.

In 2007, Coogan and co-workers reported the first application of Re-complexes  $[\text{Re}(\text{CO})_3(\text{X}^{\text{Y}}\text{L})]$  (1.42a-g) in cell imaging.<sup>171</sup> They synthesised a range of lipophilic

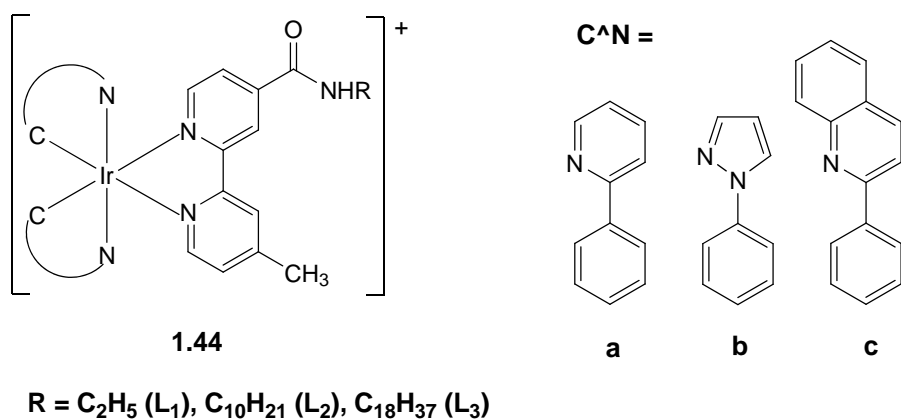
and hydrophilic cationic, neutral and anionic complexes in order to delineate toxicity and cellular uptake. The choice of ligands is vital in controlling toxicity. The neutral complex (**1.42a**) showed high toxicity, presumably due to the easy substitution of chloride by donor groups on biomolecules. The steryl complex **1.42e** also showed high toxicity at moderate concentrations, but at lower concentrations this complex and other shorter chain analogues (**1.42b-d**) showed good uptake and low toxicity. Anionic complexes (**1.42f,g**) were of lower toxicity than the cationic complexes (**1.42b-e**) and accumulated in the digestive vacuoles by phagocytosis; while cationic complexes showed distribution throughout the cells localizing in membranes and membrane structures in the cytoplasm.



The first report of the application of Ir(III) complexes (**1.43**) in cell imaging came in 2008 from Li and co-workers.<sup>172</sup> They used fluorine substituents on the cyclometallated ligands to assist cellular uptake. Incubation of HeLa cells with **1.43a** and **1.43b** resulted in intense intracellular Ir-derived luminescence, localized in the cytoplasm rather than the membranes or nucleus.



Subsequently, Lo *et al.* reported some cyclometallated Ir(III) complexes (**1.44a-c,L<sub>1-3</sub>**) with varying alkyl chain lengths to control lipophilicity (longer chains more lipophilic).<sup>157</sup> All of the complexes showed similar luminescence in a variety of media and their interactions with membranes were studied using artificial vesicles prior to cellular uptake. Complex **1.44cL<sub>3</sub>** with the longest alkyl chain, showed the lowest cellular uptake; therefore, to minimise cytotoxicity, this was used for live cell imaging experiments with HeLa cells. The complex was mostly distributed inside the cytoplasm with a lower proportion of nuclear uptake.



As discussed earlier, the same group also published some Ru estradiol complexes (**1.32a-b**) and investigated their cellular uptake and cytotoxicity toward HeLa cell line.<sup>152</sup> The highly lipophilic estradiol complex **1.32b** is anticipated to facilitate the cellular uptake. The cytotoxicity of these complexes was much lower than *cis*-platin and they were applied in live cell imaging with HeLa cells. Emission of the complexes was maintained after the uptake. Upon excitation, all the cell samples incubated with **1.32a,b** displayed intense emission. Good internalisation was observed, attributed to high lipophilicity and they were distributed in the cytoplasm with low nuclear uptake and concentrated in the perinuclear region suggesting interaction of these species with the endoplasmic reticulum and Golgi apparatus.<sup>152</sup>

One of the commonest strategies to improve cellular uptake is to attach a biotin moiety to exogenous species as the biotinylated species can be actively transported into cells by some of the mechanisms which exist for biotin uptake. Recently, the cellular uptake of Re-biotin complexes was examined by fluorescence microscopy, the complexes localised in the perinuclear region of the cell as a result of possible interactions with hydrophobic organelles such as Golgi apparatus.<sup>173</sup>

In conclusion,  $d^6$  transition metal complexes have great potential for applications in fluorescence live cell imaging due to attractive photophysical properties, easy cellular uptake and lower cytotoxicity than *cis*-platin. In addition, the longer emission lifetimes for metal complexes compared with most organic fluorophores means there is potential for lifetime imaging microscopy as described earlier for  $O_2$  concentration mapping with Ru complexes.<sup>2</sup> Further developments in the use of metal complexes for cell imaging are likely.

In summary, it can be seen that luminescent transition metal complexes have interesting photophysical properties, the earliest and the most extensively studied systems are Ru(II) polypyridine complexes, despite their  $^3MLCT$  emission being somewhat limited in the orange-red region. Other metal complexes such as those of Re(I), Os(II), Pt(II) and Rh(III) have now also been explored for diverse applications such as OLEDs, photosensitisers, sensors, biological labels and probes. As discussed in **Section 1.3**, there has been an explosion of interest in the photoluminescence properties of Ir(III) complexes *i.e.*  $[Ir(C^N)_2(X^Y)]^{n+}$  ( $n = 0, 1$ ), in the last few years. However, the use of these complexes for biological recognition is still in its infancy and has not been explored as extensively as the  $d^6$  Ru(II) analogues. Perhaps most importantly, the Ir(III) complexes have greater structural variety and hence more scope to tune the emission over a wide range of wavelength through variation of ligand structure and substituents.

In **Chapter 2** and **3** the synthesis and characterisation of a range of cationic and neutral, luminescent Ir(III) complexes,  $[Ir(C^N)_2(X^Y)]^{n+}$  ( $n = 0, 1$ ) are described. The emission wavelength is tuned by varying either the cyclometallated ( $C^N$ ) ligands or by varying substituents on the  $C^N$  or  $X^Y$  ligands, individually. Some of these complexes have been employed in the live cell imaging. **Chapter 4** includes the synthesis and application of some related complexes as molybdate sensors and **Chapter 5** describes attempts to separate lambda and delta isomers of complexes  $[Ir(C^N)_2(X^Y)]^{n+}$  ( $n = 0, 1$ ).

## 1.5 Bibliography

1. A. Jablonski, *Z. Physik*, 1935, **95**, 460.
2. H. Gerritsen, R. Sanders, A. Draaijer, C. Ince and Y. Levine, *Journal of Fluorescence*, 1997, **7**, 11-15.
3. J. N. Demas and B. A. DeGraff, *Anal. Chem.*, 1991, **63**, A829-A837.
4. J. N. Demas and B. A. DeGraff, *Coord. Chem. Rev.*, 2001, **211**, 317-351.

5. J. V. Caspar, E. M. Kober, B. P. Sullivan and T. J. Meyer, *J. Am. Chem. Soc.*, 1982, **104**, 630-632.
6. J. R. Lakowicz and B. R. Masters, *Journal of Biomedical Optics*, 2008, **13**, 029901-029902.
7. G. Calogero, G. Giuffrida, S. Serroni, V. Ricevuto and S. Campagna, *Inorg. Chem.*, 1995, **34**, 541-545.
8. T. Bessho, E. Yoneda, J. H. Yum, M. Guglielmi, I. Tavernelli, H. Imai, U. Rothlisberger, M. K. Nazeeruddin and M. Graetzel, *J. Am. Chem. Soc.*, 2009, **131**, 5930-5934.
9. P. G. Bomben, K. C. D. Robson, P. A. Sedach and C. P. Berlinguette, *Inorg. Chem.*, 2009, **48**, 9631-9643.
10. K. Kalyanasundaram, *Coord. Chem. Rev.*, 1982, **46**, 159-244.
11. J. Slinker, D. Bernards, P. L. Houston, H. D. Abruna, S. Bernhard and G. G. Malliaras, *Chem. Commun.*, 2003, 2392-2399.
12. L. Flamigni, A. Barbieri, C. Sabatini, B. Ventura and F. Barigelli, *Photochemistry and photophysics of coordination compounds: Iridium*, 2007.
13. P.-T. Chou and Y. Chi, *Chemistry*, 2007, **13**, 380-395.
14. Y. You and S. Y. Park, *Dalton Trans.*, 2009, 1267-1282.
15. E. Baranoff, J. H. Yum, M. Graetzel and M. K. Nazeeruddin, *J. Organomet. Chem.*, 2009, **694**, 2661-2670.
16. Y. Chi and P.-T. Chou, *Chem Soc Rev*, 2010, **39**, 638-655.
17. M. A. Baldo, D. F. O'Brien, Y. You, A. Shoustikov, S. Sibley, M. E. Thompson and S. R. Forrest, *Nature*, 1998, **395**, 151-154.
18. C. Adachi, M. A. Baldo, S. R. Forrest and M. E. Thompson, *Appl. Phys. Lett.*, 2000, **77**, 904-906.
19. S. Lamansky, P. Djurovich, D. Murphy, F. Abdel-Razzaq, H. E. Lee, C. Adachi, P. E. Burrows, S. R. Forrest and M. E. Thompson, *J. Am. Chem. Soc.*, 2001, **123**, 4304-4312.
20. K. A. Belmore, R. A. Vanderpool, J. C. Tsai, M. A. Khan and K. M. Nicholas, *J. Am. Chem. Soc.*, 1988, **110**, 2004-2005.
21. N. D. Silavwe, A. S. Goldman, R. Ritter and D. R. Tyler, *Inorg. Chem.*, 1989, **28**, 1231-1236.
22. G. Di Marco, M. Lanza, A. Mamo, I. Stefio, C. Di Pietro, G. Romeo and S. Campagna, *Anal. Chem.*, 1998, **70**, 5019-5023.
23. W. Goodall and J. A. G. Williams, *J. Chem. Soc., Dalton Trans.*, 2000, **17**, 2893-2895.
24. M. C. DeRosa, D. J. Hodgson, G. D. Enright, B. Dawson, C. E. B. Evans and R. J. Crutchley, *J. Am. Chem. Soc.*, 2004, **126**, 7619-7626.
25. M. Schmittel and H. Lin, *Inorg. Chem.*, 2007, **46**, 9139-9145.
26. K. K. W. Lo, K. Y. Zhang, S. K. Leung and M. C. Tang, *Angew. Chem., Int. Ed.*, 2008, **47**, 2213-2216.
27. K. K. W. Lo, C. K. Chung, T. K. M. Lee, L. H. Lui, K. H. K. Tsang and N. Y. Zhu, *Inorg. Chem.*, 2003, **42**, 6886-6897.
28. K. K. W. Lo, C. K. Chung and N. Y. Zhu, *Chem. Eur. J.*, 2003, **9**, 475-483.
29. J. M. Hsieh, M. L. Ho, P. W. Wu, P. T. Chou, T. T. Tsai and Y. Chi, *Chem. Commun.*, 2006, 615-617.
30. B. Norden, P. Lincoln, B. Akerman and E. Tuite, *Metal Ions in Biological Systems: Probing Nucleic Acids by Metal Complexes of Small Molecules*, Marcel Decker, New York, 1996.
31. M. S. Lowry and S. Bernhard, *Chem. Eur. J.*, 2006, **12**, 7970-7977.

32. A. B. Tamayo, S. Garon, T. Sajoto, P. I. Djurovich, I. M. Tsyba, R. Bau and M. E. Thompson, *Inorg. Chem.*, 2005, **44**, 8723-8732.

33. P. Coppo, E. A. Plummer and L. De Cola, *Chem. Commun.*, 2004, 1774-1775.

34. V. Balzani, A. Juris, M. Venturi, S. Campagna and S. Serroni, *Chem. Rev.*, 1996, **96**, 759-833.

35. L. Spiccia, G. B. Deacon and C. M. Kepert, *Coord. Chem. Rev.*, 2004, **248**, 1329-1341.

36. J. D. Slinker, A. A. Gorodetsky, M. S. Lowry, J. J. Wang, S. Parker, R. Rohl, S. Bernhard and G. G. Malliaras, *J. Am. Chem. Soc.*, 2004, **126**, 2763-2767.

37. J. P. Paris and W. W. Brandt, *J. Am. Chem. Soc.*, 1959, **81**, 5001-5002.

38. A. Juris, V. Balzani, F. Barigelletti, S. Campagna, P. Belser and A. von Zelewsky, *Coord. Chem. Rev.*, 1988, **84**, 85-277.

39. F. R. Keene, *Coord. Chem. Rev.*, 1997, **166**, 121-159.

40. V. Balzani and A. Juris, *Coord. Chem. Rev.*, 2001, **211**, 97-115.

41. M. Grätzel, *Coord. Chem. Rev.*, 1991, **111**, 167-174.

42. Y. D. Zhao, A. Richman, C. Storey, N. B. Radford and P. Pantano, *Anal. Chem.*, 1999, **71**, 3887-3893.

43. Z. Rosenzweig and R. Kopelman, *Anal. Chem.*, 1995, **67**, 2650-2654.

44. M. J. P. Leiner, *Anal. Chim. Acta*, 1991, **255**, 209-222.

45. E. S. Krider, J. J. Rack, N. L. Frank and T. J. Meade, *Inorg. Chem.*, 2001, **40**, 4002-4009.

46. J. K. Barton, A. T. Danishefsky and J. M. Goldberg, *J. Am. Chem. Soc.*, 1984, **106**, 2172-2176.

47. J. W. Dobrucki, *Journal of Photochemistry and Photobiology B: Biology*, 2001, **65**, 136-144.

48. S. Welter, K. Brunner, J. W. Hofstraat and L. De Cola, *Nature*, 2003, **421**, 54-57.

49. K. Kuppuswamy and G. Michael, *Angewandte Chemie International Edition in English*, 1979, **18**, 701-702.

50. M. K. Nazeeruddin, A. Kay, I. Rodicio, R. Humphry-Baker, E. Mueller, P. Liska, N. Vlachopoulos and M. Graetzel, *J. Am. Chem. Soc.*, 1993, **115**, 6382-6390.

51. K. Kalyanasundaram and M. Grätzel, *Coord. Chem. Rev.*, 1998, **177**, 347-414.

52. M. C. Tseng, J. L. Ke, C. C. Pai, S. P. Wang and W. L. Huang, *Polyhedron*, 2006, **25**, 2160-2166.

53. N. Robertson, *Chemsuschem*, 2008, **1**, 977-979.

54. R. Neil, *Angew. Chem. Int. Ed.*, 2008, **47**, 1012-1014.

55. Z. Qian-Feng, C. Ka-Man, D. W. Ian and L. Wa-Hung, *Eur. J. Inorg. Chem.*, 2005, **2005**, 4780-4787.

56. E. Y. Li, Y.-M. Cheng, C.-C. Hsu, P.-T. Chou, G.-H. Lee, I. H. Lin, Y. Chi and C.-S. Liu, *Inorg. Chem.*, 2006, **45**, 8041-8051.

57. B. Ventura, A. Barbieri, A. Zanelli, F. Barigelletti, J. B. Seneclauze, S. p. Diring and R. Ziessel, *Inorg. Chem.*, 2009, **48**, 6409-6416.

58. W. Lu, B. X. Mi, M. C. W. Chan, Z. Hui, C. M. Che, N. Y. Zhu and S. T. Lee, *J. Am. Chem. Soc.*, 2004, **126**, 4958-4971.

59. J. V. Caspar and T. J. Meyer, *J. Phys. Chem.*, 1983, **87**, 952-957.

60. F. W. M. Vanhelmont, G. F. Strouse, H. U. Gudel, A. C. Stuckl and H. W. Schmalle, *J. Phys. Chem. A*, 1997, **101**, 2946-2952.

61. F. W. M. Vanhelmont and H. U. Gudel, *Inorg. Chem.*, 1997, **36**, 5512-5517.

62. R. Czerwieniec, A. Kapturkiewicz and J. Nowacki, *Inorg. Chem. Commun.*, 2005, **8**, 1101-1104.

63. N. P. Ayala, C. M. Flynn, L. Sacksteder, J. N. Demas and B. A. Degraff, *J. Am. Chem. Soc.*, 1990, **112**, 3837-3844.

64. J. A. G. Williams, A. J. Wilkinson and V. L. Whittle, *Dalton Trans.*, 2008, 2081-2099.

65. M. Licini and J. A. G. Williams, *Chem. Commun.*, 1999, 1943-1944.

66. E. I. Mayo, K. Kilsa, T. Tirrell, P. I. Djurovich, A. Tamayo, M. E. Thompson, N. S. Lewis and H. B. Gray, *Photochem. Photobiol.*, 2006, **5**, 871-873.

67. A. J. Wilkinson, H. Puschmann, J. A. K. Howard, C. E. Foster and J. A. G. Williams, *Inorg. Chem.*, 2006, **45**, 8685-8699.

68. Y. Cheng-Han, C. Yi-Ming, C. Yun, H. Chia-Jung, F. Fu-Chuan, W. Ken-Tsung, C. Pi-Tai, C. Chih-Hao, T. Ming-Han and W. Chung-Chih, *Angew. Chem. Int. Ed.*, 2007, **46**, 2418-2421.

69. Y. S. Yeh, Y. M. Cheng, P. T. Chou, G. H. Lee, C. H. Yang, Y. Chi, C. F. Shu and C. H. Wang, *ChemPhysChem*, 2006, **7**, 2294-2297.

70. S. L. Murov, I. Carmichael and G. L. Hug, *Handbook of photochemistry*, New York, 1993.

71. S. Lamansky, P. Djurovich, D. Murphy, F. Abdel-Razzaq, R. Kwong, I. Tsyba, M. Bortz, B. Mui, R. Bau and M. E. Thompson, *Inorg. Chem.*, 2001, **40**, 1704-1711.

72. K. K.-W. Lo, J. S.-Y. Lau, D. K.-K. Lo and L. T.-L. Lo, *Eur. J. Inorg. Chem.*, 2006, 4054-4062.

73. M. Gaetano Di, L. Maurizio, P. Marco and C. Sebastiano, *Adv. Mater.*, 1996, **8**, 576-580.

74. L. Chih-Wei, W. Yu-Hsiu, L. Cheng-Hsuan, Y. Meng-Ju, C. Chun-Yen, C. Pi-Tai, C. Chi-Shun, C. Yun, C. Yu-Chun and H. Jong-Kai, *Small*, 2008, **4**, 218-224.

75. H. L. Chen, Q. Zhao, Y. B. Wu, F. Y. Li, H. Yang, T. Yi and C. H. Huang, *Inorg. Chem.*, 2007, **46**, 11075-11081.

76. M. Schmittel and H. W. Lin, *Inorg. Chem.*, 2007, **46**, 9139-9145.

77. K. K. W. Lo, D. C. M. Ng and C. K. Chung, *Organometallics*, 2001, **20**, 4999-5001.

78. K. K. W. Lo, *Photofunctional transition metal complexes*, 2007, **123**, 205-245

79. C. Metcalfe and J. A. Thomas, *Chem. Soc. Rev.*, 2003, **32**, 215-224.

80. K. E. Erkkila, D. T. Odom and J. K. Barton, *Chem. Rev.*, 1999, **99**, 2777-2795.

81. F. Pierard and A. Kirsch-De Mesmaeker, *Inorg. Chem. Commun.*, 2006, **9**, 111-126.

82. J. N. Demas, E. W. Harris, C. M. Flynn and D. Diemente, *J. Am. Chem. Soc.*, 1975, **97**, 3838-3839.

83. J. N. Demas, E. W. Harris and R. P. McBride, *J. Am. Chem. Soc.*, 1977, **99**, 3547-3551.

84. R. M. Gao, D. G. Ho, B. Hernandez, M. Selke, D. Murphy, P. I. Djurovich and M. E. Thompson, *J. Am. Chem. Soc.*, 2002, **124**, 14828-14829.

85. F. W. Shao and J. K. Barton, *J. Am. Chem. Soc.*, 2007, **129**, 14733-14738.

86. F. W. Shao, B. Elias, W. Lu and J. K. Barton, *Inorg. Chem.*, 2007, **46**, 10187-10199.

87. B. Elias, J. C. Genereux and J. K. Barton, *Angew. Chem. Int. Ed.*, 2008, **47**, 9067-9070.

88. L. Flamigni, J. P. Collin and J. P. Sauvage, *Acc. Chem. Res.*, 2008, **41**, 857-871.

89. M. S. Lowry, J. I. Goldsmith, J. D. Slinker, R. Rohl, R. A. Pascal, G. G. Malliaras and S. Bernhard, *Chemistry of Materials*, 2005, **17**, 5712-5719.

90. W.-Y. Wong, *J. Organomet. Chem.*, 2009, **694**, 2644-2647.

91. S. Sprouse, K. A. King, P. J. Spellane and R. J. Watts, *J. Am. Chem. Soc.*, 1984, **106**, 6647-6653.

92. K. Dedeian, P. I. Djurovich, F. O. Garces, G. Carlson and R. J. Watts, *Inorg. Chem.*, 1991, **30**, 1685-1687.

93. V. Adamovich, J. Brooks, A. Tamayo, A. M. Alexander, P. I. Djurovich, B. W. D'Andrade, C. Adachi, S. R. Forrest and M. E. Thompson, *New J. Chem.*, 2002, **26**, 1171-1178.

94. V. V. Grushin, N. Herron, D. D. LeCloud, W. J. Marshall, V. A. Petrov and Y. Wang, *Chem. Commun.*, 2001, 1494-1495.

95. R. Ragni, E. A. Plummer, K. Brunner, J. W. Hofstraat, F. Babudri, G. M. Farinola, F. Naso and L. De Cola, *Journal of Materials Chemistry*, 2006, **16**, 1161-1170.

96. A. B. Tamayo, B. D. Alleyne, P. I. Djurovich, S. Lamansky, I. Tsyba, N. N. Ho, R. Bau and M. E. Thompson, *J. Am. Chem. Soc.*, 2003, **125**, 7377-7387.

97. A. R. McDonald, M. Lutz, L. S. von Chrzanowski, G. P. M. van Klink, A. L. Spek and G. van Koten, *Inorg. Chem.*, 2008, **47**, 6681-6691.

98. M. Lepeltier, H. Le Bozec, V. Guerchais, T. K.-M. Lee and K. K.-W. Lo, *Organometallics*, 2005, **24**, 6069-6072.

99. M. Nonoyama, *Bull. Chem. Soc. Jpn.*, 1974, **47**, 767-768.

100. M. A. Bennett and T. R. B. Mitchell, *Inorg. Chem.*, 1976, **15**, 2936-2938.

101. H. Oonishi, *jpn. kokai tokkyo koho*, 1995, **JP07316176**, 3.

102. H.-C. Böttcher, M. Graf, H. Krüger and C. Wagner, *Inorg. Chem. Commun.*, 2005, **8**, 278-280.

103. Q. Zhao, S. Liu, M. Shi, C. Wang, M. Yu, L. Li, F. Li, T. Yi and C. Huang, *Inorg. Chem.*, 2006, **45**, 6152-6160.

104. T. Fei, X. Gu, M. Zhang, C. L. Wang, M. Hanif, H. Y. Zhang and Y. G. Ma, *Synth. Met.*, 2009, **159**, 113-118.

105. K. A. McGee and K. R. Mann, *Inorg. Chem.*, 2007, **46**, 7800-7809.

106. T. Hofbeck and H. Yersin, *Inorg. Chem.*, 2010, **49**, 9290-9299.

107. A. Tsuboyama, H. Iwawaki, M. Furugori, T. Mukaiide, J. Kamatani, S. Igawa, T. Moriyama, S. Miura, T. Takiguchi, S. Okada, M. Hoshino and K. Ueno, *J. Am. Chem. Soc.*, 2003, **125**, 12971-12979.

108. T. Sajoto, P. I. Djurovich, A. B. Tamayo, J. Oxgaard, W. A. Goddard and M. E. Thompson, *J. Am. Chem. Soc.*, 2009, **131**, 9813-9822.

109. B. Beyer, C. Ullbricht, D. Escudero, C. Friebe, A. Winter, L. Gonzalez and U. S. Schubert, *Organometallics*, 2009, **28**, 5478-5488.

110. J. I. Goldsmith, W. R. Hudson, M. S. Lowry, T. H. Anderson and S. Bernhard, *J. Am. Chem. Soc.*, 2005, **127**, 7502-7510.

111. F. Neve, M. La Deda, F. Puntoriero and S. Campagna, *Inorg. Chim. Acta*, 2006, **359**, 1666-1672.

112. J. Li, P. I. Djurovich, B. D. Alleyne, M. Yousufuddin, N. N. Ho, J. C. Thomas, J. C. Peters, R. Bau and M. E. Thompson, *Inorg. Chem.*, 2005, **44**, 1713-1727.

113. A. R. McDonald, D. Mores, C. D. Donega, C. A. van Walree, R. Gebbink, M. Lutz, A. L. Spek, A. Meijerink, G. P. M. van Klink and G. van Koten, *Organometallics*, 2009, **28**, 1082-1092.

114. J. Nishida, H. Echizen, T. Iwata and Y. Yamashita, *Chem. Lett.*, 2005, **34**, 1378-1379.

115. S. Stagni, S. Colella, A. Palazzi, G. Valenti, S. Zacchini, F. Paolucci, M. Marcaccio, R. Q. Albuquerque and L. De Cola, *Inorg. Chem.*, 2008, **47**, 10509-10521.

116. M. L. Xu, R. Zhou, G. Y. Wang, Q. Xiao, W. S. Du and G. B. Che, *Inorg. Chim. Acta*, 2008, **361**, 2407-2412.

117. H. Jang, C. H. Shin, N. G. Kim, K. Y. Hwang and Y. Do, *Synth. Met.*, 2005, **154**, 157-160.

118. L. Y. Zhang, B. Li, L. F. Shi and W. L. Li, *Opt. Mater.*, 2009, **31**, 905-911.

119. F. M. Hwang, H. Y. Chen, P. S. Chen, C. S. Liu, Y. Chi, C. F. Shu, F. I. Wu, P. T. Chou, S. M. Peng and G. H. Lee, *Inorg. Chem.*, 2005, **44**, 1344-1353.

120. F. I. Wu, H. J. Su, C. F. Shu, L. Y. Luo, W. G. Diau, C. H. Cheng, J. P. Duan and G. H. Lee, *Journal of Materials Chemistry*, 2005, **15**, 1035-1042.

121. Y. H. Song, Y. C. Chiu, Y. Chi, Y. M. Cheng, C. H. Lai, P. T. Chou, K. T. Wong, M. H. Tsai and C. C. Wu, *Chem. Eur. J.*, 2008, **14**, 5423-5434.

122. C. H. Yang, S. W. Li, Y. Chi, Y. M. Cheng, Y. S. Yeh, P. T. Chou, G. H. Lee, C. H. Wang and C. F. Shu, *Inorg. Chem.*, 2005, **44**, 7770-7780.

123. X. D. Liu, J. K. Feng, A. M. Ren, L. Yang, B. Yang and Y. G. Ma, *Opt. Mater.*, 2006, **29**, 231-238.

124. T. Tsuzuki, N. Shirasawa, T. Suzuki and S. Tokito, *Adv. Mater.*, 2003, **15**, 1455-1458.

125. I. R. Laskar, S. F. Hsu and T. M. Chen, *Polyhedron*, 2005, **24**, 189-200.

126. X. Gu, T. Fei, H. Y. Zhang, H. Xu, B. Yang, Y. G. Ma and X. D. Liu, *Eur. J. Inorg. Chem.*, 2009, 2407-2414.

127. T. Sajoto, P. I. Djurovich, A. Tamayo, M. Yousufuddin, R. Bau, M. E. Thompson, R. J. Holmes and S. R. Forrest, *Inorg. Chem.*, 2005, **44**, 7992-8003.

128. R. J. Holmes, S. R. Forrest, T. Sajoto, A. Tamayo, P. I. Djurovich, M. E. Thompson, J. Brooks, Y. J. Tung, B. W. D'Andrade, M. S. Weaver, R. C. Kwong and J. J. Brown, *Appl. Phys. Lett.*, 2005, **87**, 243507.

129. C. F. Chang, Y. M. Cheng, Y. Chi, Y. C. Chiu, C. C. Lin, G. H. Lee, P. T. Chou, C. C. Chen, C. H. Chang and C. C. Wu, *Angew. Chem., Int. Ed.*, 2008, **47**, 4542-4545.

130. K. Dedeian, J. M. Shi, E. Forsythe, D. C. Morton and P. Y. Zavalij, *Inorg. Chem.*, 2007, **46**, 1603-1611.

131. R. J. Holmes, S. R. Forrest, Y. J. Tung, R. C. Kwong, J. J. Brown, S. Garon and M. E. Thompson, *Appl. Phys. Lett.*, 2003, **82**, 2422-2424.

132. S. Tokito, T. Iijima, Y. Suzuri, H. Kita, T. Tsuzuki and F. Sato, *Appl. Phys. Lett.*, 2003, **83**, 569-571.

133. M. Suzuki, S. Tokito, M. Kamachi, K. Shirane and F. Sato, *Journal of Photopolymer Science and Technology*, 2003, **16**, 309-314.

134. S. Tokito, T. Iijima, T. Tsuzuki and F. Sato, *Appl. Phys. Lett.*, 2003, **83**, 2459-2461.

135. H. J. Bolink, F. De Angelis, E. Baranoff, C. Klein, S. Fantacci, E. Coronado, M. Sessolo, K. Kalyanasundaram, M. Gratzel and M. K. Nazeeruddin, *Chem Commun (Camb)*, 2009, 4672-4674.

136. H. Y. Chen, C. H. Yang, Y. Chi, Y. M. Cheng, Y. S. Yeh, P. T. Chou, H. Y. Hsieh, C. S. Liu, S. M. Peng and G. H. Lee, *Can. J. Chem.*, 2006, **84**, 309-318.

137. J. G. Cannon, *Journal of Medicinal Chemistry*, 1997, **40**, 631-631.

138. D. S. Wilbur, *Bioconjugate Chemistry*, 1992, **3**, 433-470.

139. R. Alford, H. M. Simpson, J. Duberman, G. C. Hill, M. Ogawa, C. Regino, H. Kobayashi and P. L. Choyke, *Molecular Imaging*, 2009, **8**, 341-354.

140. M. Zimmer, *Chem Soc Rev*, 2009, **38**, 2823-2832.

141. Y. T. Roger *Angew. Chem. Int. Ed.*, 2009, **48**, 5612-5626.

142. C. P. Montgomery, B. S. Murray, E. J. New, R. Pal and D. Parker, *Acc. Chem. Res.*, 2009, **42**, 925-937.

143. B. Song, C. D. B. Vandevyver, A. S. Chauvin and J. C. G. Bunzli, *Org. Biomol. Chem.*, 2008, **6**, 4125-4133.

144. G. Jaouen, *Bioorganometallics: biomolecules, labelling, medicine*, Wiley-VCH, 2006.

145. K. Schlogl, *Monatsh. Chem.*, 1957, **88**, 601-602.

146. H. Q. A. Lê, S. Chebil, B. Makrouf, H. Sauriat-Dorizon, B. Mandrand and H. Korri-Youssoufi, *Talanta*, **81**, 1250-1257.

147. M. S. Lowry, W. R. Hudson, R. A. Pascal and S. Bernhard, *J. Am. Chem. Soc.*, 2004, **126**, 14129-14135.

148. D. J. Stufkens and A. Vlcek, *Coord. Chem. Rev.*, 1998, **177**, 127-179.

149. V. Fernandez-Moreira, F. L. Thorp-Greenwood and M. P. Coogan, *Chem. Commun.*, 2010, **46**, 186-202.

150. E. M. Ryan, R. O'Kennedy, M. M. Feeney, J. M. Kelly and J. G. Vos, *Bioconjugate Chemistry*, 1992, **3**, 285-290.

151. K. K. W. Lo, K. H. K. Tsang, K. S. Sze, C. K. Chung, T. K. M. Lee, K. Y. Zhang, W. K. Hui, C. K. Li, J. S. Y. Lau, D. C. M. Ng and N. Zhu, *Coord. Chem. Rev.*, 2007, **251**, 2292-2310.

152. K. K. W. Lo, T. K. M. Lee, J. S. Y. Lau, W. L. Poon and S. H. Cheng, *Inorg. Chem.*, 2008, **47**, 200-208.

153. K. K. W. Lo, J. S. W. Chan, L. H. Lui and C. K. Chung, *Organometallics*, 2004, **23**, 3108-3116.

154. F. N. Castellano, J. D. Dattelbaum and J. R. Lakowicz, *Anal. Biochem.*, 1998, **255**, 165-170.

155. K. K. W. Lo and J. S. Y. Lau, *Inorg. Chem.*, 2007, **46**, 700-709.

156. K. K. W. Lo, K. Y. Zhang, C. K. Chung and K. Y. Kwok, *Chem. Eur. J.*, 2007, **13**, 7110-7120.

157. K. K. W. Lo, P. K. Lee and J. S. Y. Lau, *Organometallics*, 2008, **27**, 2998-3006.

158. E. Caron, C. Sheedy and A. Farenhorst, *J Environ Sci Health B*, **45**, 145-151.

159. X. Q. Guo, F. N. Castellano, L. Li, H. Szmacinski, J. R. Lakowicz and J. Sipior, *Anal. Biochem.*, 1997, **254**, 179-186.

160. J. D. Dattelbaum, O. O. Abugo and J. R. Lakowicz, *Bioconjugate Chemistry*, 2000, **11**, 533-536.

161. A. J. Amoroso, R. J. Arthur, M. P. Coogan, J. B. Court, V. Fernandez-Moreira, A. J. Hayes, D. Lloyd, C. Millet and S. J. A. Pope, *New J. Chem.*, 2008, **32**, 1097-1102.

162. K. K. W. Lo, W. K. Hui, C. K. Chung, K. H. K. Tsang, T. K. M. Lee, C. K. Li, J. S. Y. Lau and D. C. M. Ng, *Coord. Chem. Rev.*, 2006, **250**, 1724-1736.

163. K. K.-W. Lo and W.-K. Hui, *Inorg. Chem.*, 2005, **44**, 1992-2002.

164. K. K. W. Lo, C. K. Chung and N. Y. Zhu, *Chem. Eur. J.*, 2006, **12**, 1500-1512.

165. K. K.-W. Lo and T. K.-M. Lee, *Inorg. Chem.*, 2004, **43**, 5275-5282.

166. K. K. W. Lo, W. K. Hui, C. K. Chung, K. H. K. Tsang, D. C. M. Ng, N. Y. Zhu and K. K. Cheung, *Coord. Chem. Rev.*, 2005, **249**, 1434-1450.

167. D. Z. M. Coggan, I. S. Haworth, P. J. Bates, A. Robinson and A. Rodger, *Inorg. Chem.*, 1999, **38**, 4486-4497.

168. A. E. Friedman, J. C. Chambron, J. P. Sauvage, N. J. Turro and J. K. Barton, *J. Am. Chem. Soc.*, 1990, **112**, 4960-4962.

169. K. K.-W. Lo and K. H.-K. Tsang, *Organometallics*, 2004, **23**, 3062-3070.
170. P. Lincoln, E. Tuite and B. Norden, *J. Am. Chem. Soc.*, 1997, **119**, 1454-1455.
171. A. J. Amoroso, M. P. Coogan, J. E. Dunne, V. Fernandez-Moreira, J. B. Hess, A. J. Hayes, D. Lloyd, C. Millet, S. J. A. Pope and C. Williams, *Chem. Commun.*, 2007, 3066-3068.
172. M. Yu, Q. Zhao, L. Shi, F. Li, Z. Zhou, H. Yang, T. Yi and C. Huang, *Chem Commun (Camb)*, 2008, 2115-2117.
173. K. K. W. Lo, M. W. Louie, K. S. Sze and J. S. Y. Lau, *Inorg. Chem.*, 2008, **47**, 602-611.

## **Chapter Two:**

# **Synthesis and Characterisation of bis-cyclometallated Ir(III) diimine complexes $[\text{Ir}(\text{C}^{\wedge}\text{N})_2(\text{X}^{\wedge}\text{Y})]^+$**

## Chapter 2 Synthesis and Characterisation of bis-cyclometallated Ir(III) diimine complexes $[\text{Ir}(\text{C}^{\wedge}\text{N})_2(\text{X}^{\wedge}\text{Y})]^+$

### 2.1 Introduction

As discussed in **Chapter 1**, different groups have investigated the effects of varying substituents on the phenyl ring of cyclometallated ligands to tune the emission wavelength. The majority of studies have involved substituents on the position *para* to the heterocycle (position 3 **Fig. 2.1**)<sup>1-6</sup> or both positions *meta* to the metallated carbon (3 and 5)<sup>2, 3, 7-13</sup> or on the *ortho* and *para* positions with respect to the metallated carbon (2 and 4).<sup>7, 8, 14</sup> However, there are very few reports on varying the substituents only on the *para* position with respect to the metallated carbon (4 in **Fig. 2.1**).<sup>3, 5, 15</sup> In all subsequent discussion the terms *ortho*, *meta* and *para* will be relative to the metal unless stated otherwise.

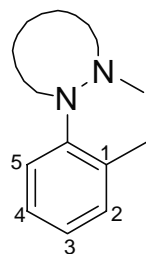
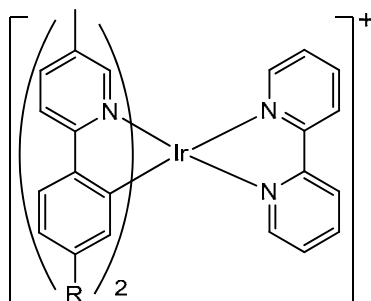


**Fig. 2.1:** Possible sites of substitution (*ortho*, *meta*, *para*) on the  $\text{C}^{\wedge}\text{N}$  fragment.

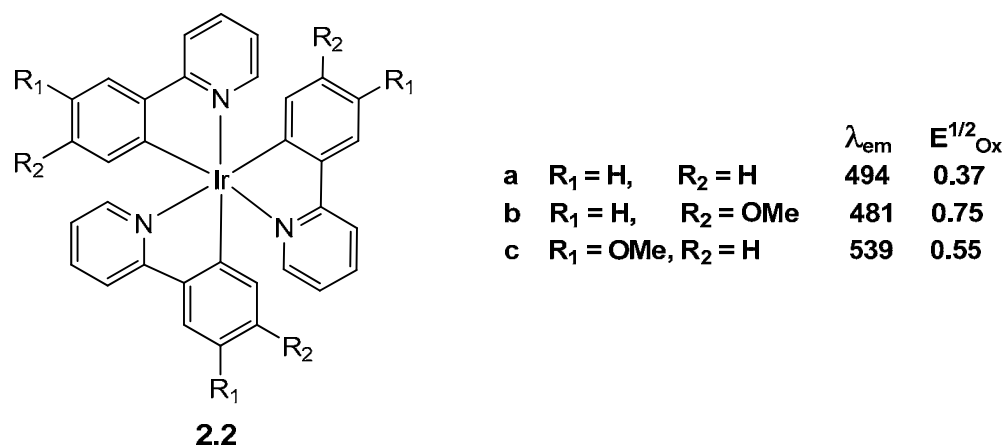
Synthetically, substitution at position 3 is much easier than at position 4 since cyclometallation can only give one isomer (see later). Lowry *et al.* studied the effect of varying substituents at position 3 in  $[\text{Ir}(\text{C}^{\wedge}\text{N})_2(\text{bipy})]^+$  (**2.1a-f**).<sup>1</sup> The electron withdrawing substituents (F, Cl, Br, Ph) cause a blue shift whilst OMe causes a slight red shift with respect to the unsubstituted complex. Emission maxima of these complexes were correlated with the  $\Delta E$  obtained from DFT calculations, and were found to be consistent.



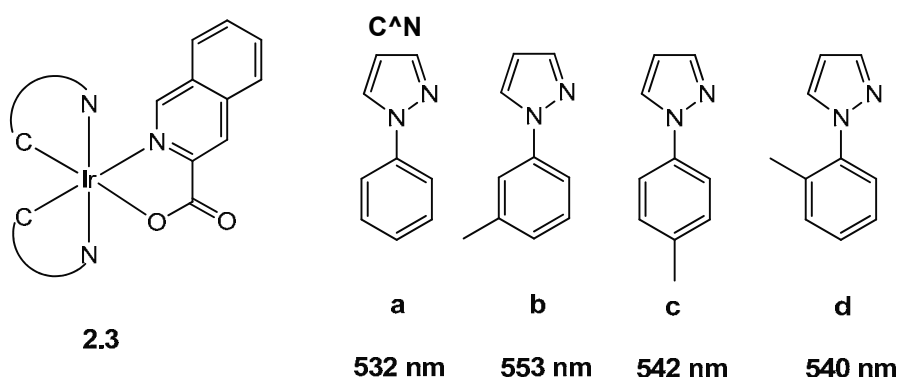
**2.1**

		$\lambda_{\text{em}}$
$\text{R} = \text{H}$	<b>a</b>	587
$= \text{F}$	<b>b</b>	558
$= \text{Cl}$	<b>c</b>	553
$= \text{Br}$	<b>d</b>	553
$= \text{Ph}$	<b>e</b>	582
$= \text{OMe}$	<b>f</b>	593

In the majority of cases, substitution at position 4 (*para* to M) has a more significant effect on emission than at position 3 (*meta* to M).<sup>5, 16, 17</sup> For example complex **2.2b**, with OMe *meta* to the metal shows a blue shift relative to **2.2a**, while **2.2c**, in which OMe is at the *para* position, shows a considerable red shift.<sup>18</sup> From the electrochemical data **2.2c** destabilizes the HOMO by 0.2 V as compared to **2.2b**. These observations can be rationalized by considering the value of the Hammett substituent constant for the OMe substituent. Thus, when OMe is in the *meta* position (**2.2b**), it is an acceptor group ( $\sigma = 0.12$ ) due to the an *inductive* effect, whereas in the *para* position (**2.2c**), OMe is a donor group ( $\sigma = -0.27$ ) due to a *conjugative* effect.

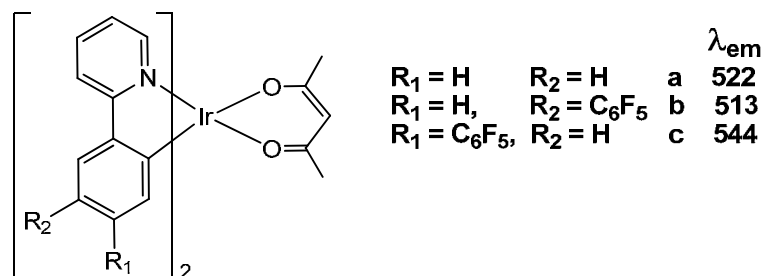


Using complexes **2.3** Kwon and co-workers also demonstrated that the position of the substituent affects the wavelength of the emission.<sup>5</sup> Thus, compared to unsubstituted complex **2.3a** methyl substitution in the phenyl ring causes a red shift in emission by raising the HOMO, however, the *para*-substituted complex (**2.3b** 553 nm) is more red shifted than *meta*-substituted ones (**2.3c,d** 542 and 540 respectively). DFT calculations suggest that the HOMO has large coefficients on the *ortho* and *para* positions (and nodes in the *meta* positions) of the phenyl of the ppz ligand, therefore,



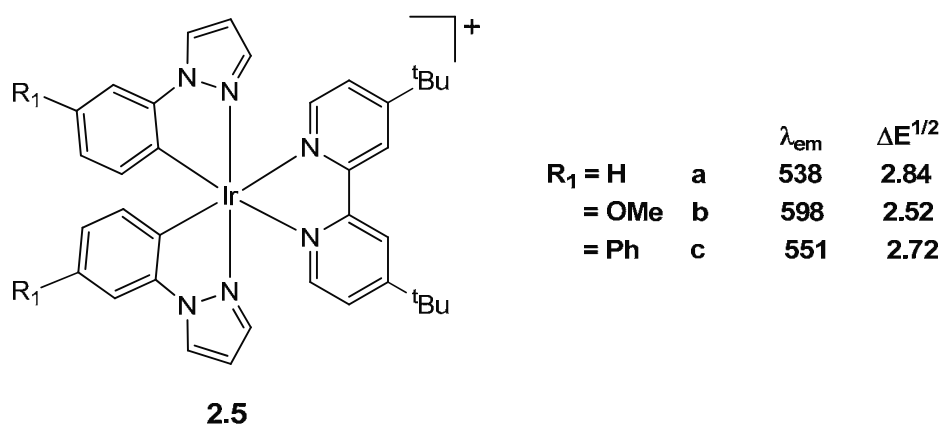
incorporation of a methyl at the *para* position should raise the HOMO more than substitution at the *meta* position as observed experimentally.<sup>5</sup>

Tsuzuki *et al.* studied the effect of C<sub>6</sub>F<sub>5</sub> substitution on the phenyl in complexes **2.4a-c**<sup>16</sup> (Substitution on the pyridine was discussed in **Chapter 1, 1.21a-c**). Substitution on the *para* position (**2.4b**) resulted in a blue shift of emission with respect to the unsubstituted complex **2.4a** consistent with lowering the HOMO, however, substitution on the *meta* position (**2.4c**) surprisingly resulted in a significant red shift. This is consistent with the LUMO having a significant coefficient on the meta positions of the phenyl hence being lowered in energy by the electron withdrawing substituent, as found in a related neutral complex.<sup>8</sup>



**2.4**

Thompson *et al.* studied the effect of varying substituents on the phenyl ring at the *para* position in complexes [Ir(ppz-R<sub>1</sub>)<sub>2</sub>(bipy-<sup>t</sup>Bu<sub>2</sub>)]<sup>+</sup> (**2.5a-c**)<sup>19</sup> and found that the emission wavelength can be tuned over a range of 60 nm (538 nm for R = H, **2.5a** vs 598 nm for R = OMe, **2.5b**). These results are consistent with the electrochemical results since **2.5b** is easier to oxidize by about over 0.3 V. Complex **2.5c** shows a smaller red shift (13 nm) relative to **2.5a**.



### 2.1.1 Microwave Chemistry

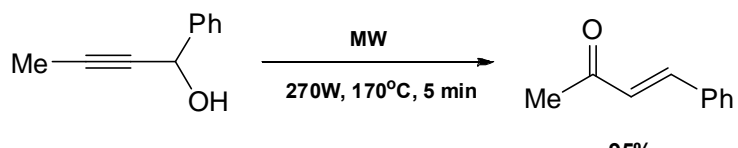
Microwaves are electromagnetic radiation with a frequency between 0.3-300 GHz, corresponding to a wavelength range of 3 mm to 30 cm and an energy range of approximately  $6 \times 10^{-25}$  to  $6 \times 10^{-23}$  J. However, all commercial and domestic microwave systems operate on a frequency of 2.45 GHz ( $\lambda = 12.24$  cm) to avoid interference with telecommunication networks.<sup>20,21</sup>

Microwave Chemistry was first introduced in the 1960s to carry out analytical processes such as ashing, digestion and fat analysis. During the 1980s microwave chemical synthesis advanced and its application was extended to include the synthesis of organic compounds,<sup>22, 23</sup> organometallic compounds<sup>24, 25</sup> and nano particles.<sup>26</sup> However, the use of domestic microwave ovens has some drawbacks, such as lack of control and the possibility of explosions. The introduction of specifically designed and constructed equipment in the mid 1990s such as the Explorer<sup>TM</sup> and Discovery<sup>TM</sup> from CEM, countered the problems with safety and increased the reproducibility, this allowed the synthetic application of microwaves to become established.

Microwaves have energy corresponding to the spacing of vibrational and rotational energy levels in molecules. They are absorbed by molecules that either have a dipole moment or an ionic component, which causes the dipoles of the molecules to align with an applied electric field. This field oscillates and the dipoles attempt to realign themselves. The agitation and resultant collisions causes internal heating. The ability of a molecule to interact with the electromagnetic wave depends upon its dielectric constant and the speed at which the dipoles reorient in an electric field; most small molecules have a frequency of reorientation equivalent to the frequency of microwave radiation.<sup>21</sup> The energy is lost as heat as a result of molecular friction and dielectric loss, this heat is formed directly and rapidly, heating the entire vessel uniformly, without requiring heat transfer through the vessel walls that occurs in conventional heating.

Microwave synthesis has some advantages over conventional heating such as reduced reaction times and often leads to higher product yields and enhanced product purities by reducing unwanted side reactions. For example the Pd-catalyzed Suzuki coupling of aryl bromides to phenyl boronic acid, using microwave heating increased the yield from 55% to 80%.<sup>27</sup> Similarly, the reaction shown in **Scheme 2.1** gives a yield

of 95% upon microwave irradiation (270 W for 5 mins)<sup>28</sup> whilst the comparable thermal reaction at 170 °C gave just 2% of the product.



**Scheme 2.1**

Another advantage of microwave heating is that reactions are more energy efficient as less heat is dissipated, due to direct heating of the reaction medium, without the need for oil bath/hotplate systems. Microwave heating is an ideal method for accelerating chemical reactions under increased pressure conditions as an alternative to microsealed tubes. It is possible to heat a solvent above the conventional boiling point of the solvent. For example, ethanol has a conventional boiling point of 79 °C, but microwave heating in a closed vessel can rapidly lead to temperatures of 164 °C and a pressure of 176 psi leading to a thousand-fold acceleration of the reaction rate.<sup>29</sup>

Since 1986, when Gedye and Giguere<sup>22, 23</sup> published their first article on microwave assisted syntheses, there has been a steadily growing interest in this research area. As mentioned earlier, this has mainly focused on organic syntheses and metal-catalysed reactions; however coordination and organometallic complexes have also been made. For example, the literature synthesis of  $[\text{Ru}(\text{bipy})_3]^{2+}$  requires 72h, reflux in EtOH, to give a 95% yield,<sup>30</sup> whilst the microwave synthesis requires only 10 mins, in MeOH, to give an 87% yield.<sup>30</sup> There are only a few reports of the syntheses of cyclometallated Ir(III) complexes using microwave irradiation.<sup>31-33</sup> The first example of a microwave method for the synthesis of cyclometallated Ir(III) complexes was reported by Konno and Sasaki in 2003.<sup>31</sup> The complexes  $[\text{Ir}(\text{ppy})_3]$  and  $[\text{Ir}(\text{ppy})_2\text{Cl}]_2$  could be made selectively from  $\text{IrCl}_3$  and an excess of Hppy in ethylene glycol by controlling the excess of Hppy used (more favoured  $[\text{Ir}(\text{ppy})_3]$ ) and the time of microwave irradiation (from 1 to 30 min).

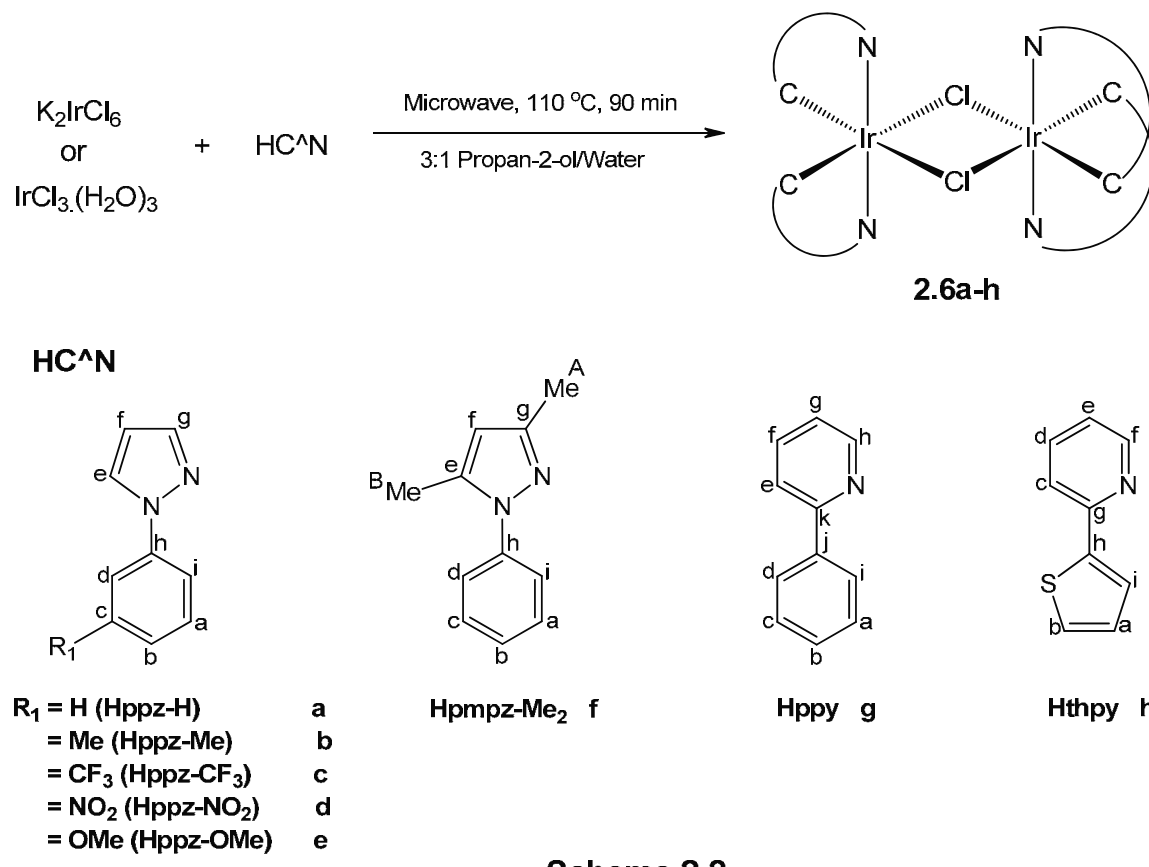
This **Chapter** will contain a description of the synthesis and luminescent properties of  $[\text{Ir}(\text{C}^{\text{N}})_2(\text{X}^{\text{Y}})]^+$  ( $\text{X}^{\text{Y}} = \text{diimine}$ ) complexes. The ability to tune the emission wavelength will be explored by varying substituents on the  $\text{C}^{\text{N}}$ , particularly

substituents on the phenyl *para* to the metal. The use of microwave irradiation for the syntheses is also reported.

## 2.2 Results and Discussion

### 2.2.1 Synthesis of $[\text{Ir}(\text{C}^{\wedge}\text{N})_2\text{Cl}]_2$

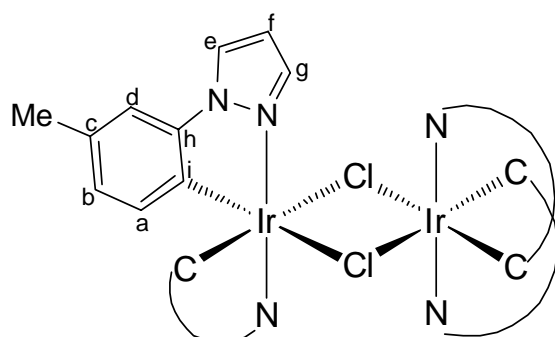
As discussed in **Chapter 1**, Watts *et al.* showed that heating  $\text{IrCl}_3\cdot(\text{H}_2\text{O})_3$  with an excess of  $\text{HC}^{\wedge}\text{N}$  in 2-ethoxyethanol/water (3:1) at reflux for 24 hours at  $135\text{ }^{\circ}\text{C}$  gave dimers  $[\text{Ir}(\text{C}^{\wedge}\text{N})_2\text{Cl}]_2$  in good yields;<sup>34</sup> whilst a microwave method (**Section 2.1.1**) required a 10 fold excess of  $\text{HC}^{\wedge}\text{N}$ .<sup>31</sup> Hence, the use of microwave irradiation as a route to  $[\text{Ir}(\text{C}^{\wedge}\text{N})_2\text{Cl}]_2$  was investigated using only 2.4-3 equiv of  $\text{HC}^{\wedge}\text{N}$  ligand.



**Scheme 2.2**

The synthesis closely follows the Watts route except that in some cases  $\text{K}_2\text{IrCl}_6$  was used instead of  $\text{IrCl}_3$  and microwave irradiation was used in place of conventional heating. The first attempts retained ethoxyethanol/water as solvent, however some of the dimers were reasonably soluble in this solvent mixture and recovery of the soluble fraction was difficult due to the high boiling point of ethoxyethanol. The use of a dedicated microwave synthesis machine allows experiments to be conducted above the

boiling point of the solvents under pressure. Hence, the reactions of  $\text{IrCl}_3\cdot(\text{H}_2\text{O})_3$  or  $\text{K}_2\text{IrCl}_6$  with various cyclometallating ligands ( $\text{HC}^{\wedge}\text{N} = \text{Hppz-R}_1$ ,  $\text{R}_1 = \text{H, Me, CF}_3$ ,  $\text{NO}_2$ ,  $\text{OMe}$ ;  $\text{Hpmpz-Me}_2$ ,  $\text{Hppy}$ , and  $\text{Hthpy}$ ) were carried out in isopropanol/water at  $110\text{ }^{\circ}\text{C}$  under microwave irradiation for 90 mins, to form the dimers **2.6a-h** with yields of greater than 85% (**Scheme 2.2**). However, the dimer from the  $\text{CF}_3$  analog of **2.6f** could not be synthesised presumably due to the strong electron withdrawing groups present on the pyrazole which means it does not coordinate strongly to the metal.

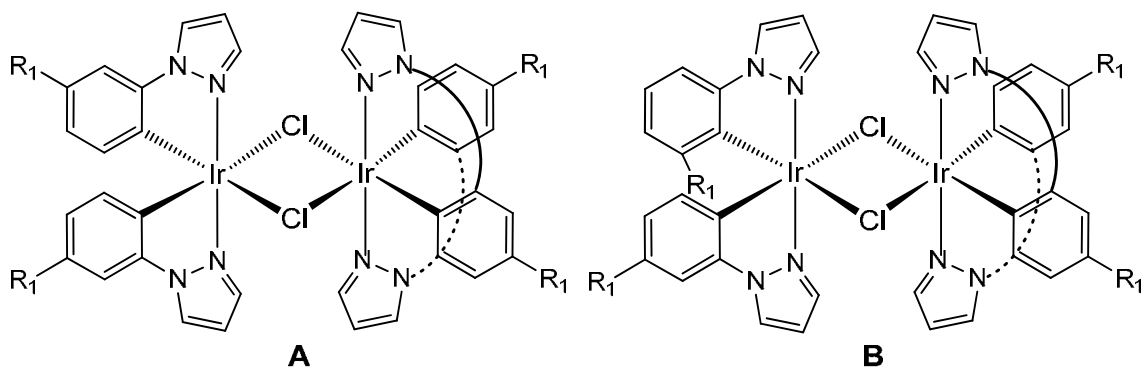


**2.6b**

Dimers **2.6a,g,h** are known and our data is consistent with that published.<sup>34-36</sup> Dimers **2.6b,e,f** have also been reported as intermediates but with no characterisation,<sup>5</sup> therefore, we now give a full assignment of the NMR spectra (see experimental). The yields are slightly improved, *e.g.* the yield reported for dimer **2.6g**, in the literature is 72%<sup>34</sup> while the microwave yield is 93%. Dimers **2.6c,d** are new compounds and have been fully characterised. The  $^1\text{H}$  and  $^{13}\text{C}$  NMR spectra of **2.6b-e** are very similar to each other, therefore, only the assignment of **2.6b** is explained in detail, significant features of the others are discussed and full data for all is given in the experimental, **Section 2.3**. The  $^1\text{H}$  NMR spectrum of **2.6b** shows, a singlet relative integration 3H, three 1H signals for the pyrazole and three 1H doublets due to the cyclometallated phenyl. Thus one proton signal is missing compared to the free ligand and all four ligands are chemically equivalent, though this does not distinguish between *meso* and *racemic* isomers (see later). A TOCSY spectrum of **2.6b** allowed identification of the signals for the phenyl ( $\text{H}_{\text{a,b,d}}$ ) and pyrazole ( $\text{H}_{\text{e-g}}$ ) rings. As expected, on coordination all the pyrazole protons show small shifts (0.1 to 0.2 ppm) to lower field compared to the free ligand, however, the three remaining phenyl protons are considerably shifted upfield (at least 0.6 ppm) consistent with the formal anionic charge on this ring. Protons  $\text{H}_{\text{a}}$  have the largest

upfield shift, being observed at  $\delta$  5.85 (*cf.*  $\delta$  7.32 in the free ligand) since these protons are also affected by the ring current effect of the neighbouring pyrazole ring of the other cyclometallated ligand on the same metal, as noted previously.<sup>37</sup> Hence, this ring current effect is a feature of all such  $[\text{Ir}(\text{C}^{\wedge}\text{N})_2(\text{X}^{\wedge}\text{Y})]^{\text{n}+}$  ( $\text{n} = 0,1$ ) complexes. Having assigned  $\text{H}_a$  the other phenyl protons ( $\text{H}_{\text{b},\text{d}}$ ) were assigned using the COSY and TOCSY spectra.  $\text{H}_d$  shows an NOE to a doublet at  $\delta$  8.08 which is therefore assigned as  $\text{H}_e$  and the COSY spectrum then allows assignment of the other pyrazole protons  $\text{H}_{\text{f},\text{g}}$ . The  $^{13}\text{C}$ –{ $^1\text{H}$ } NMR spectra show the expected number of quaternary and CH signals. The FAB mass spectrum of **2.6b** shows ions at  $m/z$  1084 and 1047 due to  $[\text{M}]^+$  and  $[\text{M}-\text{Cl}]^+$  respectively whilst the ES mass spectrum shows an ion at  $m/z$  589 assigned to  $[\text{Ir}(\text{ppz}-\text{Me})_2(\text{MeCN})_2]^+$  confirming the ease of splitting the dimer in the presence of a coordinating solvent *i.e.* MeCN.

The  $^1\text{H}$  NMR spectra of **2.6c,d** are similar to **2.6b**, with the phenyl protons  $\text{H}_a$  again shifted to highfield, at  $\delta$  6.09 and 6.12 for **2.6c** and **2.6d** respectively due to ring current effects. The reaction with Hppz-OMe gave a mixture of products, careful analysis of the  $^1\text{H}$  NMR spectrum of **2.6e** showed the desired product was present (**A** in **Scheme 2.3** with all ligands equivalent) but with a second product which had four signals for every one of the main product indicating that all the  $\text{C}^{\wedge}\text{N}$  ligands are now different. We assign the minor species as being due to one of the ligands having cyclometallated at a different C atom (*ortho* with respect to metallated carbon, **B**, **Scheme 2.3**). In complex **2.6e**, for isomer **B**, three OMe signals, which are assigned to be rings that have cyclometallated on the desired C atom, have the same chemical shift ( $\delta$  3.66) as that of the OMe signal in isomer **A**, (**Scheme 2.3**), however, the OMe signal for the ligand which has cyclometallated at a different position is at higher field ( $\delta$  3.13) due to the ring currents from the neighbouring pyrazole ring of other  $\text{C}^{\wedge}\text{N}$  ligand on the same Ir atom. Though the ratio of the isomers (**A:B**) was approximately 5:4, each dimer has 4  $\text{C}^{\wedge}\text{N}$  ligands, in the major isomer **A** these are all the same whereas, in the minor isomer **B** 3 are cyclometallated in the same position and one is different. Hence the 5:4 ratio of the isomers corresponds to a ratio of 8:1 metallation *para* or *ortho* with respect to the metal. At lower temperature (70 °C) the ratio was 1:1 whereas at higher temperature (125 °C) it was 1.3:1. The ratio did not change after work up. Recrystallisation gave further enrichment in the major isomer (**A**) up to about a 2:1 ratio.

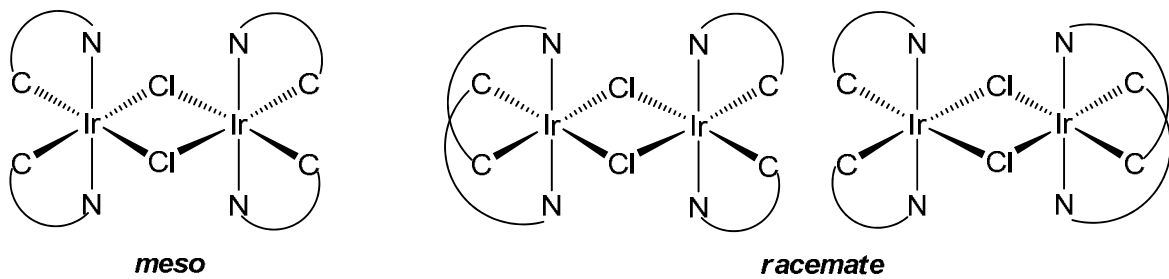


**Scheme 2.3**

Interconversion of the isomers was examined by bubbling HCl gas through a  $\text{CDCl}_3$  solution of a sample of **2.6e** at room temperature for 1 min. Thus, the starting ratio of 1.7:1 (**A:B**) changed to 1:1.4 after several hours, heating of the sample did not alter the ratio significantly. Presumably HCl reverses the cyclometallation providing a path for interconversion of the isomers as suggested for *mer-fac* isomerisation of  $[\text{Ir}(\text{C}^{\text{N}})_3]$  complexes<sup>38, 39</sup> and observed for half-sandwiched cyclometallated complexes of Ir.<sup>40</sup> Since **A** and **B** are isomers the sample still gave a satisfactory microanalysis. Though dimer **2.6e** has been reported as an intermediate it was not characterised.<sup>19</sup> To our knowledge no group have ever reported the observation of two isomers and the assumption seems to have been that cyclometallation only occurs *para* to the substituent.

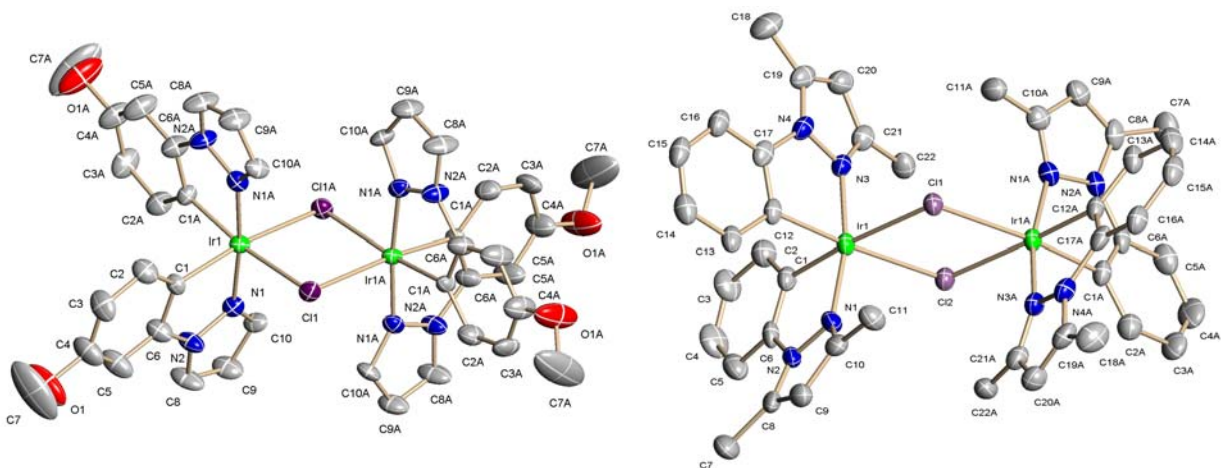
The  $^1\text{H}$  and  $^{13}\text{C}$  NMR spectra of **2.6f** are similar to **2.6a-e** except two of the signals of the pyrazole are replaced by methyl singlets at  $\delta$  2.26 ( $\text{Me}_\text{A}$ ) and 2.85 ( $\text{Me}_\text{B}$ ). Assignment of  $\text{Me}_\text{B}$  was confirmed by an NOE to the phenyl proton  $\text{H}_\text{d}$  on the same cyclometallated ligand. The protons  $\text{H}_\text{a}$  ( $\delta$  6.24) are to highfield of the free ligands (*ca.*  $\delta$  7.4) due to ring current effects, similar to **2.6b**. All the dimers show ions due to  $[\text{M}]^+$  and  $[\text{M}-\text{Cl}]^+$  in the FAB mass spectra and the ES mass spectra show ions due to the monomeric species  $[\text{Ir}(\text{C}^{\text{N}})_2(\text{MeCN})_2]^+$ . For **2.6e** there is no evidence for other species in the mass spectra, again consistent with the minor product being an isomer.

As mentioned in **Chapter 1** the dimers can in principle be either *meso* ( $\Delta\Delta$ ) or *racemic* isomers ( $\Delta\Delta/\Lambda\Lambda$ ) (**Scheme 2.4**). These are indistinguishable by NMR since all



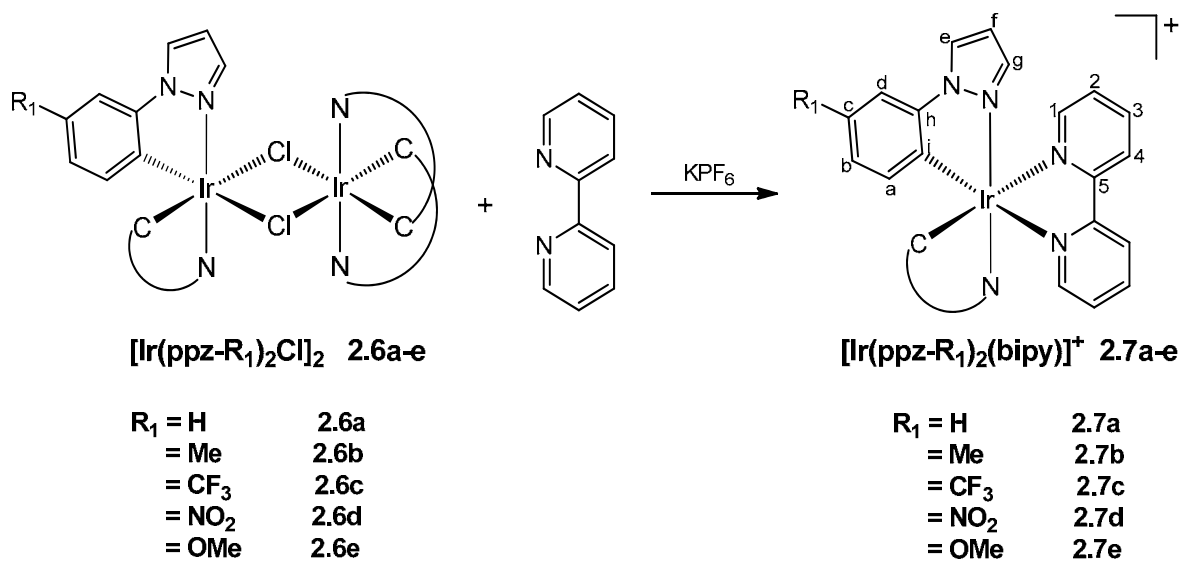
**Scheme 2.4**

the ligands are chemically equivalent in both cases. Crystals of **2.6e** and **2.6f** were obtained from DCM/hexane and were suitable for X-ray diffraction. The structures are shown in **Fig. 2.2** with selected bond lengths (Å) and angles (°). In both cases the Ir atoms are bridged by two Cl atoms along a two-fold axis of rotation and each Ir has a distorted octahedral environment, formed by two chelating ligands with *trans* N—N and *cis* C—C dispositions with the *trans* N—Ir—N angle being less than 180°. The molecules take the *racemic* form ( $\Lambda\Lambda$  for **2.6e** and  $\Delta\Delta$  for **2.6f**), rather than the *meso* form, presumably due to the interligand steric interactions (**Scheme 2.4**). This is consistent with the crystal structures of other similar Ir dimers  $[\text{Ir}(\text{C}^{\text{N}}\text{N})_2\text{Cl}]_2$ .<sup>41-43</sup>



These results show that dimers **2.6a–h** can be synthesised from only a small excess (< 3 equiv) of  $\text{HC}^{\wedge}\text{N}$  using microwave irradiation, and using  $\text{K}_2\text{IrCl}_6$  or  $\text{IrCl}_3$  as a starting material gave comparable yields. Cyclometallation of substituted phenylpyrazoles ( $\text{Hppz}-\text{R}_1$ ) occurs preferentially at the least sterically hindered site to give complexes in which the substituent is *para* to the Ir. For substituents as big as methyl or larger, only the *para* isomer is observed, however, with  $\text{OMe}$  (**2.6e**) the reaction is less selective and some *ortho*-substituted product is also observed. Detection of the minor isomer is made difficult because the symmetry of the molecule is reduced and hence NMR intensities are much smaller than for the major product. This may have lead to the presence of minor isomer being missed in the past. The regioselectivity and sensitivity to steric factors is very similar to that observed in half-sandwich Ir and Rh complexes.<sup>40</sup>

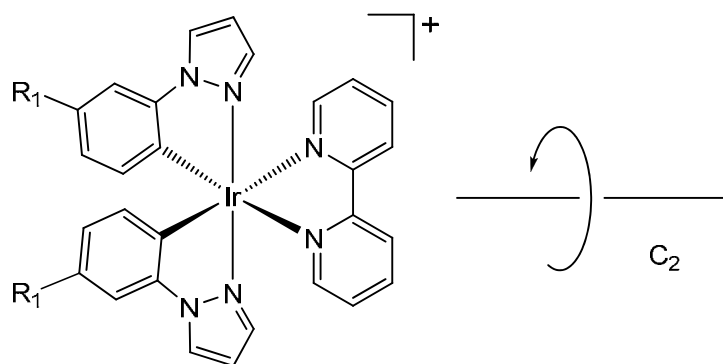
### 2.2.2 Synthesis and characterisation of diimine complexes $[\text{Ir}(\text{C}^{\wedge}\text{N})_2(\text{X}^{\wedge}\text{Y})]^+$ ( $\text{X}^{\wedge}\text{Y}$ = bipy and dps)



**Scheme 2.5**

The reactions of dimers **2.6a–e** with bipy and  $\text{KPF}_6$  were carried out in methanol at 60 °C under microwave irradiation for 20 mins (except for ligand **2.6d** for which a longer reaction time of 65 mins was required for complete conversion), to form compounds **2.7a–e** ( $\text{R}_1 = \text{H, Me, CF}_3, \text{NO}_2, \text{OMe}$ ) in good yields (> 80%) (**Scheme 2.5**). Complex **2.7a** is a known complex<sup>19</sup> (see experimental for full NMR assignment) and  $[\text{Ir}(\text{ppy})_2(\text{bipy})][\text{PF}_6]$  (**2.7g**)<sup>44–46</sup> has also been synthesised for comparison purposes.

All complexes **2.7b-e** have a two-fold axis of symmetry ( $C_2$ ) (Scheme 2.6) as found for the dimers. This is reflected in the  $^1\text{H}$  NMR spectra, *i.e.* both cyclometallating ligands are equivalent as are both halves of the bipy, giving only one set of signals with each signal representing two equivalent protons. In the  $^1\text{H}$  NMR spectra the signals for the cyclometallating ligands in **2.7b-e** are similar to those of the respective dimers **2.6b-e** but an extra four multiplets are observed in the aromatic region due to the bipy ligand. The  $^1\text{H}$  NMR spectra of **2.7b-e** are also very similar to each other except the signal of the phenyl protons, therefore, only the assignment of **2.7b** is explained in detail.



**Scheme 2.6**

A TOCSY spectrum of **2.7b** allowed identification of the signals for the phenyl, pyrazole and pyridyl rings. The phenyl protons are all shifted to lower field compared to the dimer (by *ca.* 0.2 to 0.4 ppm) because cationic complex **2.7b** is deshielded relative to neutral dimer **2.6b**, however, due to a ring current effect (see above)  $\text{H}_a$  is still the most upfield proton, at  $\delta$  6.18 (*cf.*  $\delta$  7.32 in the free ligand). Assignment of  $\text{H}_a$  then allows assignment of the other phenyl protons ( $\text{H}_{b,d}$ ) using the COSY spectrum. The protons  $\text{H}_d$  are observed as a singlet at  $\delta$  7.18 and show an NOE to a multiplet at *ca.*  $\delta$  8.1 which is therefore assigned as pyrazole protons  $\text{H}_e$ . The other pyrazole protons  $\text{H}_f$  and  $\text{H}_g$  are then assigned *via* the COSY spectrum. The chemical shifts of the pyrazole protons  $\text{H}_e$  and  $\text{H}_f$  are almost unchanged from the dimer but  $\text{H}_g$  is observed at  $\delta$  6.83 considerably higher field than in the dimer ( $\delta$  7.82), due to a ring current from the bipy. Assignment of the bipy is possible due to the observation of an NOE between  $\text{H}_a$  and a doublet of doublets at *ca.*  $\delta$  8.21 which is therefore assigned as the bipy proton  $\text{H}_1$  and the COSY spectrum then allows assignment of other bipy protons  $\text{H}_{2-4}$ . Whilst protons  $\text{H}_{2-4}$  are shifted slightly downfield compared to free bipy (0.1 to 0.3

ppm), proton H<sub>1</sub> ( $\delta$  8.21) is observed about 0.5 ppm upfield from the corresponding proton in free bipy ( $\delta$  8.69) due to ring currents from the neighbouring phenyl rings. The  $^{13}\text{C}-\{^1\text{H}\}$  NMR spectra show the expected number of signals. The HSQC is used to identify the carbons with protons attached and HMBC was used to help identify the quaternary carbon atoms. The FAB mass spectrum shows an ion at  $m/z$  663 due to the cation  $[\text{Ir}(\text{ppz-Me})_2(\text{bipy})]^+$ .

As mentioned earlier, the  $^1\text{H}$  NMR spectra of **2.7b-e** are similar to each other and the corresponding dimers **2.6b-e**. The phenyl protons H<sub>a</sub> in **2.7c-e** are still observed at relatively high fields between  $\delta$  6.18 – 6.52, but slightly downfield from the corresponding signals in the dimers. However, all the signals for the pyrazole protons H<sub>g</sub> are observed in a range of  $\delta$  6.77 – 7.02, at higher field than in the dimers ( $\delta$  7.82 – 7.88), due to ring currents from the bipy. Protons H<sub>1</sub> ( $\delta$  8.08 – 8.21) are observed at higher field relative to free bipy ( $\delta$  8.69) due to ring currents from the neighbouring phenyl rings. For **2.7d,e** a second species was observed which we assign as having the substituent on one of the phenyls positioned *para* to the metal and the other one *ortho* which destroys the symmetry and makes all the protons inequivalent. The initial ratio of the isomers **A:B** is 21:1 and 5:1 for **2.7d** and **2.7e** respectively. The observation of a second isomer for **2.7d** suggests there was a minor impurity in the dimer **2.6d** but it was not detected by  $^1\text{H}$  NMR spectroscopy. Interconversion of the isomers was tested with **2.7e**. Thus, bubbling HCl gas through a sample of **2.7e** (**A:B** 7:1) led to no significant change in the isomer ratio. Presumably protonation of an M-C bond in the cationic complex is more difficult than in the neutral dimers. The  $^{13}\text{C}-\{^1\text{H}\}$  NMR spectra of all the complexes **2.7b-e** show the expected number of signals. The FAB mass spectra of all the complexes **2.7b-e** show ions due to the cations  $[\text{Ir}(\text{C}^{\text{N}})_2(\text{bipy})]^+$  and the microanalysis results are satisfactory.

Single crystals of **2.7b** and **2.7c** were each obtained from DCM/hexane and the structures are shown in **Fig. 2.3**. The Ir adopts a distorted octahedral coordination geometry (*trans* N—Ir—N angle  $< 180^\circ$ ) in both the complexes (**Table 2.1**), with *cis* metallated carbons and *trans* pyrazole nitrogen atoms, as revealed by previous structural studies on similar bis-cyclometallated complexes.<sup>47</sup> The Ir—N bipy bond distances are longer than the distances of Ir—N pyrazole for both the complexes, which can be ascribed to the *trans* influence of the Ir—C bonds and has been observed for some other  $[\text{Ir}((\text{C}^{\text{N}})_2(\text{bipy})]^+$  complexes.<sup>47, 48</sup>

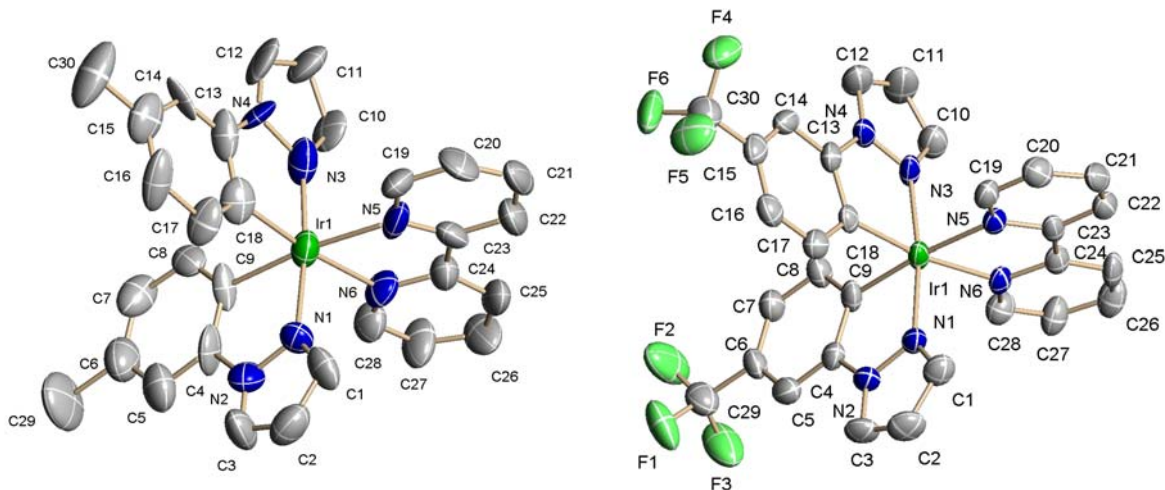
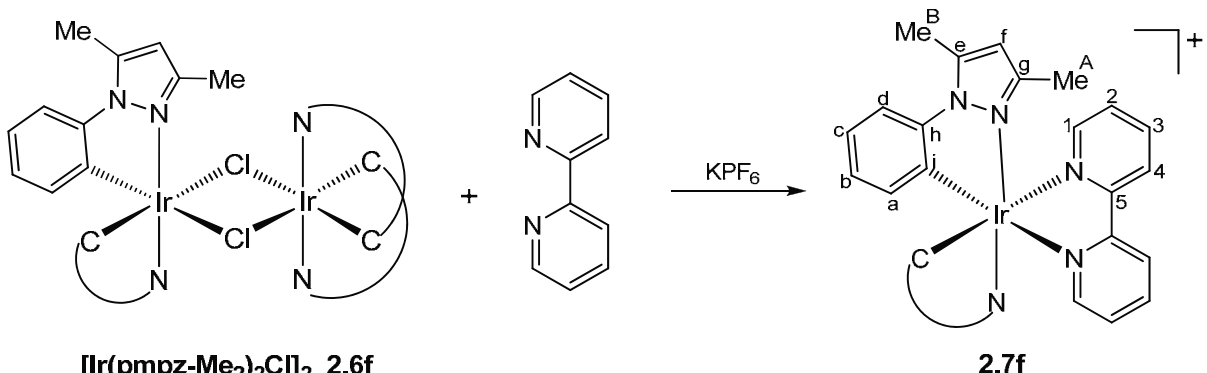


**Fig. 2.3:** X-ray crystal structure for **2.7b** and **2.7c** respectively.

**Table 2.1:** Tabulated bond lengths ( $\text{\AA}$ ) and bond angles ( $^\circ$ ) for **2.7b** and **2.7c** respectively.

( $\text{\AA}$ )	<b>2.7b</b>	<b>2.7c<sup>a</sup></b>	( $^\circ$ )	<b>2.7b</b>	<b>2.7c<sup>a</sup></b>
Ir(1)—N(1)	2.054(10)	2.015(6)	N(1)—Ir(1)—N(3)	173.7(4)	171.7(2)
Ir(1)—N(3)	1.992(12)	2.014(6)	N(1)—Ir(1)—C(9)	80.5(5)	80.3(3)
Ir(1)—N(5)	2.132(12)	2.128(6)	N(3)—Ir(1)—C(18)	80.0(6)	80.3(3)
Ir(1)—N(6)	2.173(10)	2.132(6)	N(5)—Ir(1)—N(6)	77.5(5)	77.3(2)
Ir(1)—C(9)	2.041(11)	2.015(7)			
Ir(1)—C(18)	2.052(15)	2.008(7)			

<sup>a</sup>For **2.7c** there were two independent molecules in the unit cell, therefore the data are an average of values for both structures.

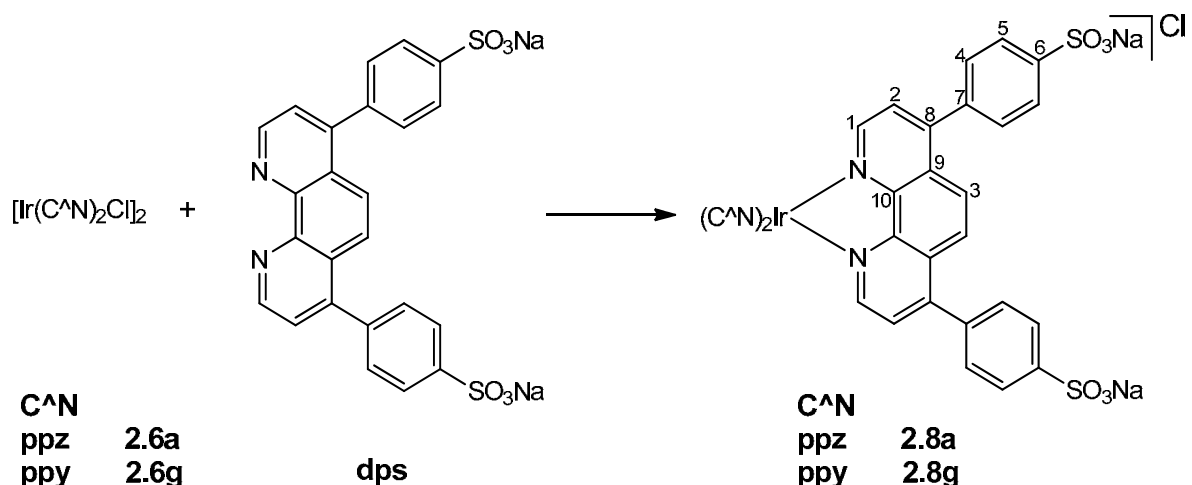


**Scheme 2.7**

The reaction of dimer **2.6f** with bipy and  $\text{KPF}_6$  was carried out in methanol at  $60^\circ\text{C}$  under microwave irradiation for 20 mins, to form compound **2.7f** in good yield (81%) (**Scheme 2.7**). As for the bipy complexes (**2.7a-e**), **2.7f** also has a two-fold axis

of symmetry which is reflected in the  $^1\text{H}$  NMR spectrum. The  $^1\text{H}$  and  $^{13}\text{C}$  NMR spectra of **2.7f** are similar to (**2.7a-e**) except for the signals of the pyrazole rings which now show two methyl signals at  $\delta$  1.47 ( $\text{Me}_\text{A}$ ) and 2.80 ( $\text{Me}_\text{B}$ ) and a 1H singlet at  $\delta$  6.03 ( $\text{H}_\text{f}$ ). The signal for  $\text{Me}_\text{A}$  is upfield with respect to the dimer **2.6f** ( $\delta$  2.26) due to the ring current effects from the bipy, however,  $\text{Me}_\text{B}$  is relatively unaffected ( $\delta$  2.80 vs 2.85 for **2.7f** and **2.6f** respectively). The protons  $\text{H}_\text{a}$  ( $\delta$  6.34) and  $\text{H}_\text{1}$  ( $\delta$  8.01) are to highfield of the free ligands due to ring current effects as found in **2.7b-f**. The COSY spectrum then allows the assignment of the other phenyl ( $\text{H}_{\text{b-d}}$ ) and bipy protons ( $\text{H}_{\text{2-4}}$ ). Assignment of the methyls is confirmed by NOE effects, thus,  $\text{Me}_\text{A}$  at  $\delta$  1.47 shows an NOE to bipy protons  $\text{H}_\text{1}$  and also to  $\text{H}_\text{a}$  on the other  $\text{C}^\text{N}$  ligand, whilst  $\text{Me}_\text{B}$  ( $\delta$  2.80) shows an NOE to the phenyl protons  $\text{H}_\text{d}$  on the same  $\text{C}^\text{N}$  ligand. The  $^{13}\text{C}-\{^1\text{H}\}$  NMR spectra show the expected number of signals and the FAB mass spectrum shows an ion at  $m/z$  691 due to  $[\text{Ir}(\text{pmpz-} \text{Me}_2)_2(\text{bipy})]^+$ .

For applications in biology it may be desirable for the metal complexes to be soluble in water, hence, we were interested in preparing some water-soluble Ir(III) complexes for cell imaging studies. Most ligands that are specifically designed for water solubility contain hydrophilic groups such as carboxylate or sulphonate moieties.<sup>49</sup> Cell imaging studies of Re(I) complexes of 4,7-diphenyl-1,10-phenanthrolinedisulfonic acid disodium salt (dps) were mentioned in **Chapter 1 (Section 1.4.2)**.<sup>50</sup>



**Scheme 2.8**

The dimer **2.6a** reacted with dps in a mixture of DCM/MeOH (1:1.5) at reflux, for 3 hours in the absence of light, to form **2.8a** in 85% yield whilst **2.8g** was

synthesised in 89% yield by the reaction of **2.6f** with dps in methanol at 70 °C under microwave irradiation for 30 mins (**Scheme 2.8**). Both complexes were synthesised as the Cl salts to increase their solubility in water. Complexes **2.8a,g** were considered cationic as the dps ligand was a disodiated sulphonic acid derivative and the complexes gave satisfactory microanalyses based on this formulation.

In the <sup>1</sup>H NMR spectra of **2.8a** and **2.8g** the phenyl protons H<sub>a</sub> are at relatively high field ( $\delta$  6.45 and 6.42 respectively) characteristic of the *cis*-[Ir(C<sup>N</sup>)<sub>2</sub>] fragment as discussed earlier. The proton H<sub>a</sub> of one cyclometallated ligand and the heterocycle proton adjacent to coordinated nitrogen (H<sub>g</sub> or H<sub>h</sub>) of the other cyclometallated ligand show NOEs to the same proton H<sub>1</sub> of the dps ligand, which is a doublet at  $\delta$  8.57 and 8.40 in **2.8a** and **2.8g** respectively. Protons H<sub>3</sub> are easily identified as the only singlet, at  $\delta$  8.22 and 8.20 for **2.8a** and **2.8g** respectively, this signal shows an NOE to a multiplet at *ca.*  $\delta$  7.7 for both **2.8a** and **2.8g**, which is therefore assigned as the phenyl protons H<sub>4</sub> of the dps ligand. The COSY spectrum then allows assignment of protons H<sub>5</sub>. Protons H<sub>4</sub> and H<sub>5</sub> are observed as multiplets rather than doublets. This is possibly due to the exchange of sodium ions in MeOD solvent resulting in a mixture of disodiated and mixed monosodiated / monosulphonic acid complex. The <sup>13</sup>C- $\{{}^1\text{H}\}$  NMR spectra show the expected number of signals for quaternary and CH carbons. The FAB mass spectra show ions at *m/z* 1015 and 1037 respectively for **2.8a** and **2.8g** due to [Ir(C<sup>N</sup>)<sub>2</sub>(dps)]<sup>+</sup> and the microanalysis results are satisfactory.

These reactions show that the diimine complexes **2.7a-f** and **2.8a,g** were successfully synthesized and characterised. The observation of a second isomer for **2.7d** suggests that there was a minor impurity in the dimer **2.6d** but it was not detected by <sup>1</sup>H NMR spectroscopy. The synthesis of complex **2.7e** resulted in a mixture of products corresponding to the mixture of isomers present in the starting dimer **2.6e**. Complexes **2.8a,g** were both highly soluble in water which was desirable for their applications in cell imaging studies discussed later in **Chapter 3**. The electrochemical and photophysical properties of these complexes are discussed in the following sections.

### 2.2.2.1 Electrochemistry of Ir(III) diimine complexes $[\text{Ir}(\text{C}^{\wedge}\text{N})_2(\text{bipy})]^+$ (2.7a-f)

The electrochemical properties of the bipy complexes **2.7a-f** were examined using cyclic voltammetry (**Fig. 2.4**). Complex **2.7a** has a reversible oxidation wave at 1.37 V and a reversible reduction wave at -1.38 V, consistent with published data.<sup>19</sup> In the literature the oxidation is assigned as taking place at Ir with a contribution from the Ir-C  $\sigma$ -bonds while the reduction occurs on the bipy ligand and this was supported by DFT calculations.<sup>19, 47</sup>

All the complexes  $[\text{Ir}(\text{ppz-R}_1)_2(\text{bipy})]^+$  **2.7a-f** except **2.7d** exhibit a reversible reduction wave at a similar potential, between -1.31 and -1.39 V, and a reversible/irreversible oxidative wave between 1.08 and 1.75 V (**Table 2.2**, **Fig. 2.4**). The relatively small range of reduction potentials ( $\sim 0.08$  V) and the reversibility are consistent with the reduction being mainly centred on the bipy, which is similar to that in the literature.<sup>19, 47</sup> Thus, the LUMO mainly resides on the bipy. The irreversible reduction of **2.7d** is attributed to reduction occurring on the  $\text{NO}_2$  substituents, generating a reactive radical, which interferes with the reduction of bipy, hence no reduction value for **2.7d** is quoted in **Table 2.2**.

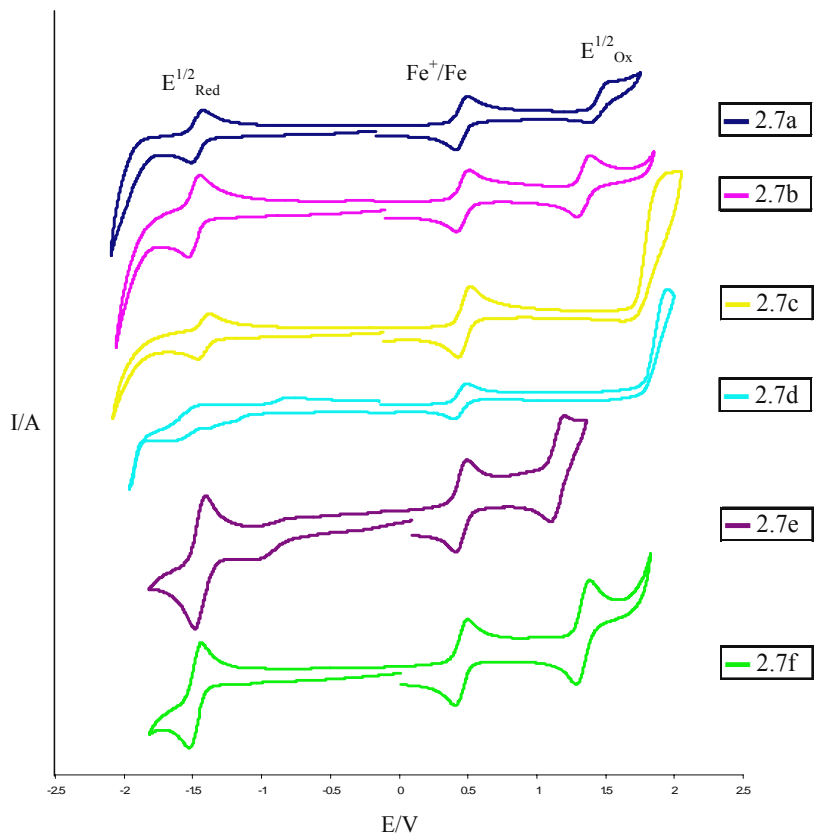


**Fig. 2.4:** Cyclic voltammograms of **2.7a-f** complexes (scan rate = 100 mV/s ).

**Table 2.2:** Redox properties of  $[\text{Ir}(\text{ppz-}\text{R}_1)_2(\text{bipy})]^+$  complexes<sup>a</sup>.

Entry	Complex	$\text{C}^{\wedge}\text{N}$	$E^{1/2}_{\text{Ox}}$	$E^{1/2}_{\text{Red}}$	$\Delta E^{1/2} (\text{V})$
1	<b>2.7a</b>	ppz-H	1.37	-1.38	2.75
2	<b>2.7b</b>	ppz-Me	1.24	-1.39	2.63
3	<b>2.7c</b>	ppz-CF <sub>3</sub>	1.65 <sup>b</sup>	-1.31	2.96
4	<b>2.7d</b>	ppz-NO <sub>2</sub>	1.75 <sup>b</sup>	<sup>c</sup>	
5	<b>2.7e</b>	ppz-OMe	1.08	-1.38	2.46
6	<b>2.7f</b>	pmpz-Me <sub>2</sub>	1.25	-1.37	2.62
7	<b>2.7g</b>	ppy	1.31	-1.35	2.66

<sup>a</sup>In dry acetonitrile (0.1 mol L<sup>-1</sup> of Et<sub>4</sub>NClO<sub>4</sub>), scan rate 100 mV s<sup>-1</sup>, all potentials are quoted *vs* SCE (Cp<sub>2</sub>Fe<sup>+</sup>/Cp<sub>2</sub>Fe *vs* SCE = +0.42 V).<sup>51</sup> A Pt disc was used as a working electrode, counter electrode was a Pt gauze and a silver wire was used as a reference. <sup>b</sup>Irreversible wave, <sup>c</sup>reduction of **2.7d** is a composite of NO<sub>2</sub> and bipy, therefore, difficult to identify and not quoted.

The oxidation potentials span a wider range ( $\sim 0.67$  V) than the reduction potentials, which suggests that substitution on the phenyl of the cyclometallated ligand mainly affects the oxidation, which is consistent with the oxidation being mainly metal based, Ir<sup>III</sup>→Ir<sup>IV</sup> with some contribution from the Ir-C  $\sigma$ -bond. Thus, the HOMO mainly resides on the Ir and partially on the C<sup>^</sup>N ligand, this is consistent with that published for other cationic Ir(III) complexes.<sup>19, 47</sup> For **2.7a,b,e,f** the oxidation is reversible whilst in **2.7c,d** it is irreversible. For **2.7c,d** due to presence of electron withdrawing substituents, after one electron oxidation there may not be enough electron density remaining on the phenyl ring to coordinate to the metal leading to rupture of the Ir-C bond may occur. Moreover, **2.7c,d** show high peak currents for oxidation waves which indicates that there may be an ECE process occurring *i.e.* the product of chemical reaction (oxidation) is also electrochemically active. The fact that no reduction process for this oxidation is observed even at a faster scan rate (250mV/s) suggests that the rate of any chemical reaction following the oxidation is much faster than this.

Introducing an electron donating Me-substituent(s) on the phenyl (**2.7b**) or pyrazole (**2.7f**) or OMe (**2.7e**) on the phenyl of the C<sup>^</sup>N ligand gives a lower oxidation potential with respect to the unsubstituted complex **2.7a**, suggesting that these have a higher HOMO resulting in a smaller HOMO-LUMO energy gap *i.e.*  $\Delta E^{1/2}$  (**Table 2.2** entries 1, 2, 5 and 6). Alternatively, electron withdrawing substituents (CF<sub>3</sub> or NO<sub>2</sub>) on the phenyl show an increase in oxidation potential (**Table 2.2** entries 3 and 4) and

suggesting that these have a lower HOMO and larger  $\Delta E^{1/2}$ , compared to **2.7a**. Note the increase in oxidation potential from one *para* CF<sub>3</sub> is 0.28V which is almost the same as putting F-substituents in both *meta* positions (0.3V).<sup>19</sup> Replacement of ppz **2.7a** with ppy in **2.7g** leads to only minor changes in the oxidation and reduction potentials (**Table 2.2**, entries 1 and 7), which suggests that pyrazole is a similar donor to pyridine; though it does give a 0.1V increase in  $\Delta E^{1/2}$  consistent with a blue shift in emission for the ppz complex.<sup>19, 44-46</sup>

### 2.2.2.2 Photophysical properties of $[\text{Ir}(\text{C}^{\wedge}\text{N})_2(\text{bipy})]^+$ (**2.7a-f**) and $[\text{Ir}(\text{C}^{\wedge}\text{N})_2(\text{dps})]^+$ complexes (**2.8a,g**)

#### Absorption spectroscopy of $[\text{Ir}(\text{C}^{\wedge}\text{N})_2(\text{bipy})]^+$ (**2.7a-f**)

There are three bands ( $\pi \rightarrow \pi^*$ , <sup>1</sup>MLCT, <sup>3</sup>MLCT) observed in the electronic absorption spectra of cyclometallated Ir(III) complexes  $[\text{Ir}(\text{C}^{\wedge}\text{N})_2(\text{bipy})]^+$  as mentioned in the literature.<sup>47</sup> The most intense absorption bands below 300 nm are assigned to the spin allowed intraligand IL ( $\pi \rightarrow \pi^*$ ) transitions. The moderately intense absorption bands at around 300 – 400 nm are attributed to the spin allowed metal to ligand charge transfer (<sup>1</sup>MLCT) (d $\pi$  (Ir)  $\rightarrow$   $\pi^*$  (C $^{\wedge}$ N and X $^{\wedge}$ Y) transitions; these correspond to promotion of an electron from the HOMO, which resides primarily on the Ir, to the LUMO which is on the bipy. The shape and location of the HOMO and LUMO have been probed with DFT calculations.<sup>47</sup> Strong spin orbit coupling on Ir provides some intensity to the formally spin forbidden <sup>3</sup>MLCT transitions. Therefore, the weak absorption bands towards the lower energy region, *ca.* > 400 nm are tentatively assigned to the spin forbidden <sup>3</sup>MLCT (d $\pi$  (Ir)  $\rightarrow$   $\pi^*$  (C $^{\wedge}$ N and X $^{\wedge}$ Y) transitions. The absorption spectra of complexes **2.7a-f** are shown in **Fig. 2.5** with data in **Table 2.3**, the values for **2.7a** are comparable to those in the literature.<sup>19</sup>

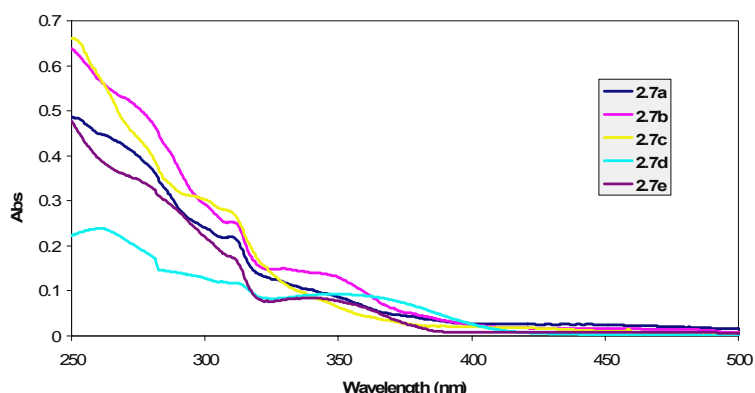


**Fig. 2.5:** Absorption spectra of complexes **2.7a-f**.

**Table 2.3: Electronic absorption spectral data of  $[\text{Ir}(\text{C}^{\wedge}\text{N})_2(\text{bipy})]^+$  complexes (2.7a-f)**

Entry	Complex	Solvent	$\lambda_{\text{abs}} \text{ [nm]} (\epsilon_{\text{max}} \text{ [dm}^3\text{mol}^{-1}\text{cm}^{-1}] )$
1	<b>2.7a</b> (ppz-H)	DCM	263 sh (44600), 311 (22100), 410 sh (2700)
2	<b>2.7b</b> (ppz-Me)	DCM	270 sh (53000), 310 (25300), 330 (15000), 448 sh (1700)
3	<b>2.7c</b> (ppz-CF <sub>3</sub> )	DCM	298 sh (30600), 310 sh (27600), 398 sh (2000)
4	<b>2.7d</b> (ppz-NO <sub>2</sub> )	DCM	261 (23860), 314 (11290), 347 (9200)
5	<b>2.7e</b> (ppz-OMe)	DCM	241 (52500), 342 (8500), 476 (500)
6	<b>2.7f</b> (pmpz-Me <sub>2</sub> )	DCM	248 (21310), 277 sh (14570), 310 sh (8000), 461 sh (270)
7	<b>2.7g</b> (ppy)	DCM	270 (57600), 389 (33200), 471 (1800)

**Emission spectroscopy of  $[\text{Ir}(\text{C}^{\wedge}\text{N})_2(\text{bipy})]^+$  (2.7a-f)**

In addition to increasing the intensity of <sup>3</sup>MLCT absorption bands, strong spin-orbit coupling leads to efficient intersystem crossing and hence emission from triplet states (phosphorescence) in cyclometallated Ir(III) complexes. As discussed in **Chapter 1**, emission from  $[\text{Ir}(\text{C}^{\wedge}\text{N})_2(\text{diimine})]^+$  commonly comes from mixed <sup>3</sup>IL ( $\pi_{(\text{C}^{\wedge}\text{N})} \rightarrow \pi^*_{(\text{C}^{\wedge}\text{N})}$ ) and <sup>3</sup>MLCT ( $\text{d}\pi_{(\text{Ir})} \rightarrow \pi^*_{(\text{diimine})}$ ) transitions.<sup>47</sup>

**Table 2.4: Emission data of  $[\text{Ir}(\text{C}^{\wedge}\text{N})_2(\text{bipy})]^+$  complexes (2.7a-g)**

Entry	Complex	Solvent	$\lambda_{\text{em}} \text{ (nm)}$	Energy (eV)
1	<b>2.7a</b> (ppz-H)	DCM	557	2.22
2	<b>2.7a</b> (ppz-H)	MeOH	565	2.19
3	<b>2.7b</b> (ppz-Me)	DCM	587	2.10
4	<b>2.7c</b> (ppz-CF <sub>3</sub> )	DCM	504	2.45
5	<b>2.7d</b> (ppz-NO <sub>2</sub> )	DCM	497	2.49
6	<b>2.7e</b> (ppz-OMe)	DCM	615	2.01
7	<b>2.7f</b> (pmpz-Me <sub>2</sub> )	DCM	583	2.12
8	<b>2.7g</b> (ppy)	DCM	580	2.13

All of the bipy complexes (2.7a-g) emit at room temperature in fluid solutions and the emission data are listed in **Table 2.4** and illustrated in **Fig 2.7**. The excitation spectra are in accordance with the absorption spectra. The observation of a shift in the emission wavelength with solvent for **2.7a** (557 nm in DCM and 565 nm in MeOH) is consistent with a charge transfer component.

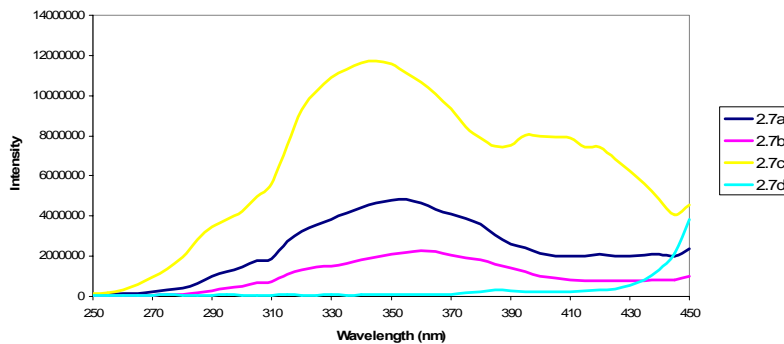


**Fig. 2.6:** Excitation spectra of **2.7a-d** complexes monitoring actual  $\lambda_{\text{em}}$  mentioned in **Table 2.4**.

<sup>a</sup>Intensity of **2.7d** is multiplied by a factor of  $10^2$ .

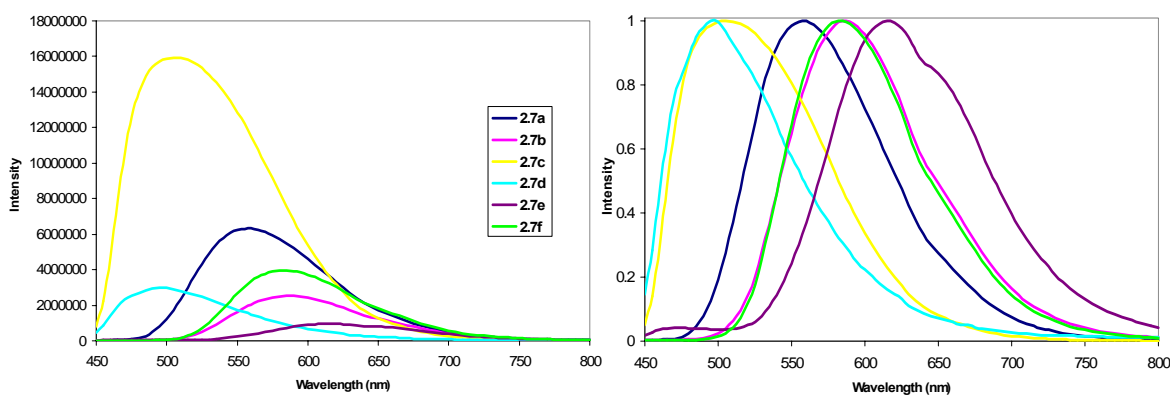


**Fig. 2.7:** Degassed emission spectra and the normalised intensity plot of **2.7a-d,f** showing the effect of changing the substituents on the C<sup>N</sup> ligand.

<sup>a</sup>All measurements were carried out at a concentration 0.01 mM in dry DCM. <sup>b</sup>Intensity of **2.7d** is multiplied by a factor of  $10^2$ . <sup>c</sup> $\lambda_{\text{ex}}$  390 nm.

A significant variation in emission wavelength (118 nm) is observed for complexes **2.7a-e**, upon changing the substituent on the phenyl ring (**Table 2.4**, **Fig. 2.7**). As mentioned above, and consistent with our electrochemical data, in these complexes, the HOMO resides on the Ir and the phenyl of the C<sup>N</sup> ligand while the LUMO is localised on the bipy. Therefore, substituting H in **2.7a** with an electron donating group, Me in **2.7b** and OMe in **2.7e**, lowers the  $\Delta E^{1/2}$  energy gap from 2.75 V (**2.7a**) to 2.63 V and 2.46 V for **2.7b** and **2.7e** respectively (**Table 2.2**, entries 1, 2 and 5), which is consistent with a red shift in the emission from 557 nm (**2.7a**) to 587 nm and 615 nm for **2.7b** and **2.7e** respectively (**Table 2.4**, entries 1, 3 and 6). The considerable red shift (58 nm, 0.21 eV) in emission upon OMe substitution in **2.7e** relative to unsubstituted complex **2.7a** is consistent with the only other para OMe

complex in the literature.<sup>19</sup> The shift is much larger than that (6 nm, 0.02 eV) found putting an OMe *meta* in  $[\text{Ir}(\text{ppy}-\text{OMe})_2(\text{bipy})]^+$ .<sup>1</sup> Conversely, replacing H with electron withdrawing groups (CF<sub>3</sub> and NO<sub>2</sub>) causes a significant blue shift (*ca.* 50-60 nm) with respect to **2.7a** (cf entries 4, 5 with 1 in **Table 2.4**). The overall range is equivalent to about 0.48 eV which compares with a range of only 0.13 eV (from OMe to F) for ppy ligands with the substituents *meta* to Ir.<sup>1</sup>

Putting electron donating methyl substituents on the pyrazole ring (**2.7f**) also results in a red shift (entries 7 and 1). This is consistent with the electrochemical data which showed an easier oxidation (raised HOMO) for this complex. This result is consistent with that reported in literature for the neutral complexes  $[\text{Ir}(\text{ppz}-\text{Me})_2(\text{iq})]$ .<sup>5</sup> Complex **2.7g** also shows a red shift with respect to **2.7a** (entries 8 and 1 **Table 2.4**) which can be ascribed to the smaller HOMO-LUMO gap for the pyridine ligand (See **Table 2.2**), as has been observed previously.<sup>19, 44-46</sup>

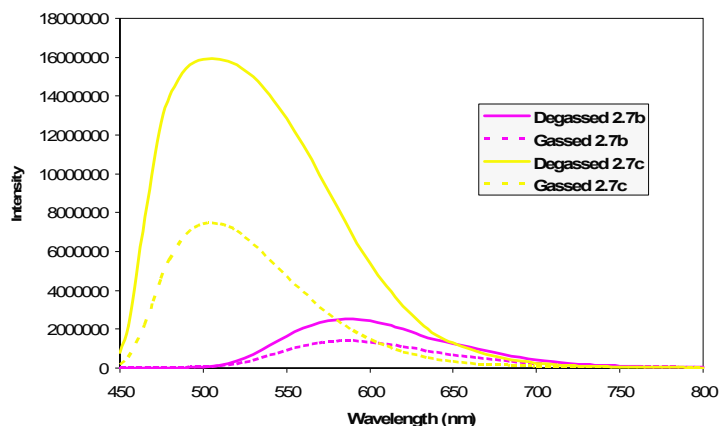


**Fig. 2.8:** Comparison of gassed and degassed emission spectra of **2.7b** and **2.7c**.

The emission for **2.7a-f** is sensitive to the presence of oxygen, for example, gassed and degassed emission spectra of **2.7b** and **2.7c** are compared in **Fig. 2.8**. This suggests that excited states for these complexes are a mixture of singlet and triplet states due to strong spin-orbit coupling which transfers its energy to the molecular oxygen in triplet state generating singlet oxygen and leads to some quenching of emission in the aerated samples.

### Absorption spectroscopy of $[\text{Ir}(\text{C}^{\wedge}\text{N})_2(\text{dps})]^+$ (**2.8a,g**)

In similarity to bipy complexes **2.7a-g**, there are three bands ( $\pi \rightarrow \pi^*$ , <sup>1</sup>MLCT, <sup>3</sup>MLCT) observed in the electronic absorption spectra of  $[\text{Ir}(\text{C}^{\wedge}\text{N})_2(\text{dps})]^+$  **2.8a,g** (**Table**

**2.5).** The most intense absorption bands below 300 nm are assigned to the spin allowed intraligand IL ( $\pi \rightarrow \pi^*$ ) transitions. The moderately intense absorption bands at around 300 – 400 nm are attributed to the spin allowed metal to ligand charge transfer ( $^1\text{MLCT}$ ) ( $d\pi(\text{Ir}) \rightarrow \pi^*(\text{C}^{\wedge}\text{N} \text{ and } \text{X}^{\wedge}\text{Y})$ ) transitions and the weak absorption bands towards the lower energy region, *ca.* > 400 nm are tentatively assigned to the spin forbidden  $^3\text{MLCT}$  ( $d\pi(\text{Ir}) \rightarrow \pi^*(\text{C}^{\wedge}\text{N} \text{ and } \text{X}^{\wedge}\text{Y})$ ) transitions.

**Table 2.5: Electronic absorption spectral data of  $[\text{Ir}(\text{C}^{\wedge}\text{N})_2(\text{dps})]^+$  complexes (2.8a,g)**

Entry	Complex	Solvent	$\lambda_{\text{abs}} [\text{nm}] (\epsilon_{\text{max}} [\text{dm}^3 \text{mol}^{-1} \text{cm}^{-1}])$
1	<b>2.8a</b>	MeOH	267 (57000), 283 (66200), 329 sh (23400), 382 sh (9100), 436 sh (3900)
2	<b>2.8a</b>	$\text{H}_2\text{O}$	264 (28120), 282 (32740), 327 sh (10890), 380 sh (3690)
3	<b>2.8g</b>	MeOH	271 (95900), 285 (88700), 334 sh (31300), 383 sh (18400), 470 sh (2900)
4	<b>2.8g</b>	$\text{H}_2\text{O}$	270 (101200), 282 (97100), 338 sh (31700), 380 sh (19100), 470 sh (2800)

**Emission spectroscopy of  $[\text{Ir}(\text{C}^{\wedge}\text{N})_2(\text{dps})]^+$  (2.8a,g)**

**Table 2.6: Emission data of  $[\text{Ir}(\text{C}^{\wedge}\text{N})_2(\text{dps})]^+$  complexes (2.8a,g)**

Entry	Complex	Solvent	$\lambda_{\text{em}} (\text{nm})$	Energy (eV)
1	<b>2.7a</b>	MeOH	565	2.19
2	<b>2.8a</b>	MeOH	576	2.15
3	<b>2.8a</b>	$\text{H}_2\text{O}$	591	2.09
4	<b>2.8g</b>	MeOH	595	2.08
5	<b>2.8g</b>	$\text{H}_2\text{O}$	594	2.08

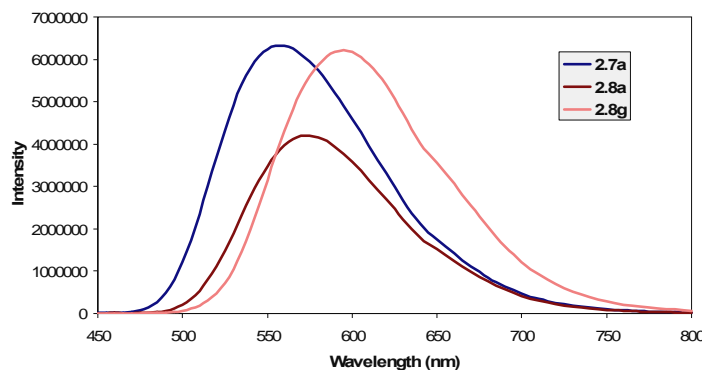


**Fig. 2.9:** Degassed emission spectra of complexes of **2.7a** and **2.8a,g** (in MeOH).

The emission of complexes **2.8a,g** is shown in **Fig. 2.9** with the data in **Table 2.6**. Complex **2.7a** emits at 565 nm while **2.8a** emits at 576 nm (**Table 2.6**, entries 1 and 2), the red shift is consistent with the increased conjugation of the dps compared to bipy, however, the substituents on dps may also be having an effect. Changing the C<sup>N</sup> ligand from ppz **2.8a** to ppy **2.8g** leads to a red shift (*cf.* 576 nm and 595 nm respectively in MeOH), as found for the bipy complexes **2.7a,g** discussed above. Complex **2.8a** shows a red shift (15 nm) in emission upon changing the solvent from MeOH to H<sub>2</sub>O (**Fig. 2.10**), however, for **2.8g** the emission is relatively unaffected by the solvent. The emission from complexes **2.8a,g** is also found to be sensitive to the presence of oxygen similar to bipy complexes **2.7a-f**, which suggests a contribution of triplet character to the excited state.

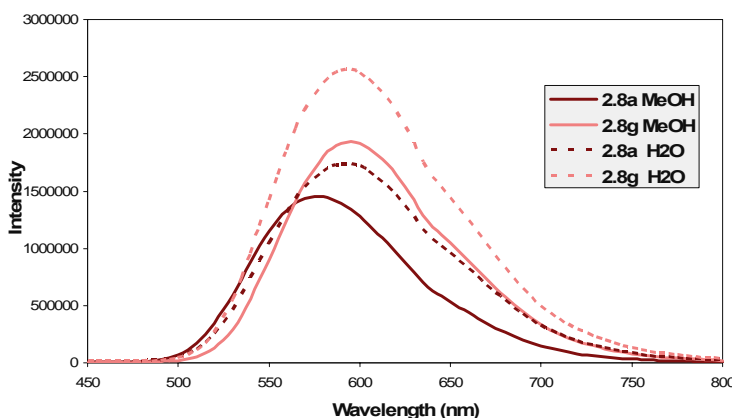


**Fig. 2.10:** Gassed emission spectra of **2.8a,g**, comparing the effect of solvent.

In conclusion, complexes **2.7a-g** and **2.8a,g** are found to be emissive at room temperature in fluid solutions. A significant variation in emission wavelength (118 nm) is observed for complexes **2.7a-e** upon changing the substituent on the phenyl ring of ppz. Substituting electron donating groups *i.e.* Me (**2.7b**) or OMe (**2.7e**) on the phenyl ring of ppz and Me on pyrazole ring of ppz (**2.7f**) causes a red shift relative to unsubstituted complex (**2.7a**), whilst electron withdrawing groups (CF<sub>3</sub> and NO<sub>2</sub>) in **2.7c,d** cause a significant blue shift (*ca.* 50-60 nm) with respect to **2.7a**. The electrochemistry and emission of complexes **2.7a-f** confirms that substituents *para* to metal have a larger impact on the HOMO than at the *meta* position. Complexes **2.8a,g** were found to be intensely luminescent in water, which indicates their potential applications in cell imaging studies discussed in **Chapter 3**.

## 2.3 Experimental

### General information and materials

All reactions were carried out under an inert atmosphere of nitrogen and under microwave irradiation unless stated otherwise. After work up all the complexes were air stable. Microwave reactions were carried out in a *CEM-Discover* commercial microwave reactor.  $^1\text{H}$ , and  $^{13}\text{C}-\{^1\text{H}\}$  NMR spectra were obtained using a DRX 400 MHz spectrometer. Chemical shifts were recorded in ppm (on  $\delta$  scale with tetramethylsilane as internal reference), and coupling constants are reported in Hz. FAB mass spectra were obtained on a Kratos concept mass spectrometer using NOBA as matrix. The electrospray (ES) mass spectra were recorded using a micromass Quattra LC mass spectrometer in HPLC grade acetonitrile except methanol for **2.6d**. UV – Vis absorption measurements were carried out on a Shimadzu UV – 1600 series spectrometer in dry DCM. Luminescence studies were performed in dry DCM using a Jobin Yvon Horiba Fluoromax-P spectrofluorimeter. All listed emission data are uncorrected for the PMT response. For emission measurements, all complexes are excited at a wavelength of 390 nm using a filter of 450 nm. Electrochemical measurements were performed with an Eco Chemie Autolab. All measurements were carried out in a one-compartment cell under  $\text{N}_2$  gas, equipped with a Pt disc working electrode, a Pt gauze counter electrode and a silver wire reference electrode. The supporting electrolyte was  $\text{Et}_4\text{NClO}_4$  (0.1 mol L<sup>-1</sup>) in acetonitrile. Elemental analyses were performed at London Metropolitan University. All starting materials were obtained from Aldrich or Alfa Aesar.

### Synthesis of Dimers

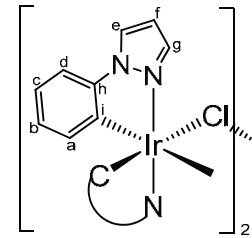
#### General procedure for synthesis of $[\text{Ir}(\text{C}^{\wedge}\text{N})_2\text{Cl}]_2$ (2.6a-i)

$\text{K}_2\text{IrCl}_6$  or  $\text{IrCl}_3\text{(H}_2\text{O})_3$ , and the appropriate cyclometallating ligand (2.4-3 equiv) were placed in a microwave vial along with a mixture of propan-2-ol/water (4 ml, 3:1). Nitrogen was bubbled through the solution for 2 mins and the vial was then sealed with a septum cap. The vial was placed in the microwave reactor and heated under microwave irradiation at 110°C for 90 minutes, at a maximum pressure of 250 psi. After this time the solvent was removed *in vacuo* leaving behind a solid which was dissolved in DCM (40 ml) and passed through celite. The filtrate was reduced in volume and hexane was added slowly to induce precipitation. The precipitate was isolated,

washed with hexane and dried *in vacuo*. The compounds could be recrystallised from DCM/hexane.

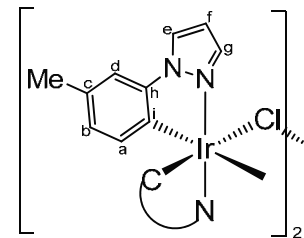
### Synthesis of $[\text{Ir}(\text{ppz})_2\text{Cl}]_2$ (2.6a)

This was prepared from  $\text{K}_2\text{IrCl}_6$  (400 mg, 0.828 mmol) and 1-phenyl-1H-pyrazole (Hppz) (358.2 mg, 0.328 ml, 2.484 mmol) and after work up gave **2.6a** as a grey solid (409 mg, 96%). The data are consistent with the literature<sup>35</sup> but full assignment of the NMR and MS is given here.  $^1\text{H}$  NMR ( $\text{CD}_2\text{Cl}_2$ ):  $\delta$  8.19 (4H, dd,  $J = 3.2, 0.8$ ,  $\text{H}_e$ ), 7.82 (4H, dd,  $J = 2.4, 0.8$ ,  $\text{H}_g$ ), 7.19 (4H, dd,  $J = 7.8, 1.2$ ,  $\text{H}_d$ ), 6.84 (4H, td,  $J = 7.4, 1.6$ ,  $\text{H}_c$ ), 6.69 (4H, m,  $\text{H}_f$ ), 6.57 (4H, td,  $J = 7.4, 1.2$ ,  $\text{H}_b$ ), 5.95 (4H, dd,  $J = 7.8, 1.2$ ,  $\text{H}_a$ ).  $^{13}\text{C}$  NMR: 141.65 ( $\text{C}_i$ ), 139.00 ( $\text{C}_g$ ), 130.97 ( $\text{C}_a$ ), 125.88 ( $\text{C}_h$ ), 124.94 ( $\text{C}_e$ ), 123.71 ( $\text{C}_b$ ), 120.43 ( $\text{C}_c$ ), 109.12 ( $\text{C}_d$ ), 105.22 ( $\text{C}_f$ ). MS (FAB):  $m/z$  1028  $[\text{M}]^+$ , 991  $[\text{M}-\text{Cl}]^+$ . MS (ES):  $m/z$  561  $[\text{Ir}(\text{ppz})_2(\text{MeCN})_2]^+$ .



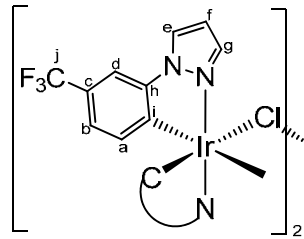
### Synthesis of $[\text{Ir}(\text{ppz-Me})_2\text{Cl}]_2$ (2.6b)

This was prepared from  $\text{IrCl}_3 \cdot (\text{H}_2\text{O})_3$  (300 mg, 0.850 mmol) and 1-*m*-tolyl-1H-pyrazole (Hppz-Me) (323 mg, 2.040 mmol) and after work up gave **2.6b** as a pale yellow solid (441 mg, 96%). Anal. Calcd for  $\text{C}_{40}\text{H}_{36}\text{Cl}_2\text{Ir}_2\text{N}_8$ : C, 44.32, H, 3.35, N, 10.34. Found: C, 44.42, H, 3.44, N, 10.19%.  $^1\text{H}$  NMR ( $\text{CDCl}_3$ ):  $\delta$  8.08 (4H, d,  $J = 2.7$ ,  $\text{H}_e$ ), 7.82 (4H, d,  $J = 2.3$ ,  $\text{H}_g$ ), 6.92 (4H, d,  $J = 1.2$ ,  $\text{H}_d$ ), 6.60 (4H, t,  $J = 2.3$ ,  $\text{H}_f$ ), 6.36 (4H, dd,  $J = 7.8, 0.8$ ,  $\text{H}_b$ ), 5.85 (4H, d,  $J = 7.8$ ,  $\text{H}_a$ ), 2.14 (12H, s, Me).  $^{13}\text{C}$  NMR: 142.86 ( $\text{C}_i$ ), 140.26 ( $\text{C}_g$ ), 132.20 ( $\text{C}_a$ ), 130.97 ( $\text{C}_h$ ), 126.22 ( $\text{C}_b$ ), 125.55 ( $\text{C}_e$ ), 123.07 ( $\text{C}_c$ ), 111.40 ( $\text{C}_d$ ), 106.14 ( $\text{C}_f$ ), 20.92 (Me). MS (FAB):  $m/z$  1084  $[\text{M}]^+$ , 1047  $[\text{M}-\text{Cl}]^+$ . MS (ES):  $m/z$  589  $[\text{Ir}(\text{ppz-Me})_2(\text{MeCN})_2]^+$ .



### Synthesis of $[\text{Ir}(\text{ppz-CF}_3)_2\text{Cl}]_2$ (2.6c)

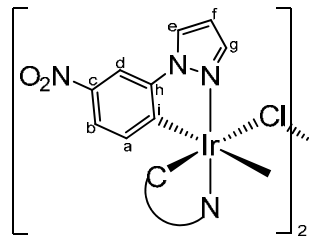
This was prepared from  $\text{IrCl}_3 \cdot (\text{H}_2\text{O})_3$  (200 mg, 0.567 mmol) and 1-(3-(trifluoromethyl)phenyl)-1H-pyrazole (Hppz-CF<sub>3</sub>) (360 mg, 1.701 mmol) and after work up gave **2.6c** as a grey solid (321 mg, 87%). Anal. Calcd for  $\text{C}_{40}\text{H}_{24}\text{Cl}_2\text{F}_{12}\text{Ir}_2\text{N}_8$ : C, 36.96, H, 1.86, N, 8.62. Found: C, 37.11, H, 1.83, N, 8.53%.  $^1\text{H}$  NMR ( $\text{CDCl}_3$ ):  $\delta$  8.24 (4H, d,  $J = 2.7$ ,  $\text{H}_e$ ), 7.85 (4H, d,  $J = 2.0$ ,  $\text{H}_g$ ), 7.35



(4H, d,  $J = 1.2$ , H<sub>d</sub>), 6.81 (4H, dd,  $J = 7.8, 0.8$ , H<sub>b</sub>), 6.76 (4H, t,  $J = 2.3$ , H<sub>f</sub>), 6.09 (4H, d,  $J = 7.8$ , H<sub>a</sub>). <sup>13</sup>C NMR: 142.99 (C<sub>h</sub>), 141.00 (C<sub>g</sub>), 126.95 (C<sub>a</sub>), 125.47 (C<sub>j</sub>), 125.03 (C<sub>c</sub>), 122.13 (C<sub>i</sub>), 122.10 (C<sub>b</sub>), 107.38, 107.34 (C<sub>d, f</sub>). MS (FAB): *m/z* 1300 [M]<sup>+</sup>, 1265 [M-Cl]<sup>+</sup>. MS (ES): *m/z* 697 [Ir(ppz-CF<sub>3</sub>)<sub>2</sub>(MeCN)<sub>2</sub>]<sup>+</sup>.

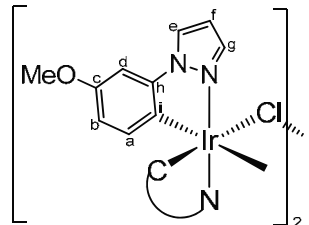
### Synthesis of [Ir(ppz-NO<sub>2</sub>)<sub>2</sub>Cl]<sub>2</sub> (2.6d)

This was prepared from IrCl<sub>3</sub>(H<sub>2</sub>O)<sub>3</sub> (100 mg, 0.284 mmol) and 1-(3-(nitrophenyl)-1H-pyrazole (Hppz-NO<sub>2</sub>) (160.7 mg, 0.852 mmol) and after work up gave **2.6d** as a pale green solid (321 mg, 87%). Anal. Calcd for C<sub>36</sub>H<sub>24</sub>Cl<sub>2</sub>Ir<sub>2</sub>N<sub>12</sub>O<sub>8</sub>: C, 35.79, H, 2.00, N, 13.91. Found: C, 35.60, H, 1.87, N, 13.88%. <sup>1</sup>H NMR (CDCl<sub>3</sub>):  $\delta$  8.37 (4H, d,  $J = 2.7$ , H<sub>e</sub>), 8.05 (4H, d,  $J = 2.5$ , H<sub>d</sub>), 7.88 (4H, d,  $J = 2.0$ , H<sub>g</sub>), 7.48 (4H, dd,  $J = 8.6, 2.3$ , H<sub>b</sub>), 6.87 (4H, t,  $J = 2.3$ , H<sub>f</sub>), 6.12 (4H, d,  $J = 8.6$ , H<sub>a</sub>). <sup>13</sup>C NMR: 144.61 (C<sub>h</sub>), 143.75 (C<sub>c</sub>), 142.01 (C<sub>g</sub>), 140.09 (C<sub>i</sub>), 132.91 (C<sub>a</sub>), 128.63 (C<sub>e</sub>), 120.52 (C<sub>b</sub>), 108.74 (C<sub>f</sub>), 106.00 (C<sub>d</sub>). MS (FAB): *m/z* 1208 [M]<sup>+</sup>. MS (ES): *m/z* 633 [Ir(ppz-NO<sub>2</sub>)<sub>2</sub>(MeOH)<sub>2</sub>]<sup>+</sup>.



### Synthesis of [Ir(ppz-OMe)<sub>2</sub>Cl]<sub>2</sub> (2.6e) major isomer (A)

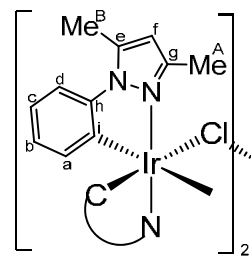
This was prepared from IrCl<sub>3</sub>(H<sub>2</sub>O)<sub>3</sub> (200 mg, 0.567 mmol) and 1-(3-(methoxyphenyl)-1H-pyrazole (Hppz-OMe) (295.8 mg, 1.701 mmol) and after work up gave **2.6e** as a grey solid (276 mg, 85%). Anal. Calcd for C<sub>40</sub>H<sub>36</sub>Cl<sub>2</sub>Ir<sub>2</sub>N<sub>8</sub>O<sub>4</sub>: C, 41.85, H, 3.16, N, 9.76. Found: C, 41.80, H, 3.18, N, 9.77%. <sup>1</sup>H NMR (CDCl<sub>3</sub>):  $\delta$  8.07 (4H, d,  $J = 3.1$ , H<sub>e</sub>), 7.83 (4H, d,  $J = 1.5$ , H<sub>g</sub>), 6.74 (4H, d,  $J = 2.7$ , H<sub>d</sub>), 6.62 (4H, t,  $J = 2.3$ , H<sub>f</sub>), 6.24 (4H, dd,  $J = 8.6, 2.7$ , H<sub>b</sub>), 5.87 (4H, d,  $J = 8.2$ , H<sub>a</sub>), 3.66 (12H, s, Me). MS (FAB): *m/z* 1148 [M]<sup>+</sup>. MS (ES): *m/z* 621 [Ir(ppz-OMe)<sub>2</sub>(MeCN)<sub>2</sub>]<sup>+</sup>.



**Minor isomer (B):** <sup>1</sup>H NMR (CDCl<sub>3</sub>):  $\delta$  8.11 (1H, d,  $J = 2.7$ ), 8.01 (1H, d,  $J = 2.7$ ), 7.87 (1H, d,  $J = 1.9$ ), 7.86 (1H, d,  $J = 1.9$ ), 7.78 (1H, d,  $J = 1.9$ ), 7.74 (1H, d,  $J = 1.9$ ), 6.85 (1H, d,  $J = 7.8$ ), 6.79 (1H, d,  $J = 7.8$ ), 6.65 (1H, t,  $J = 2.3$ ), 6.58 (1H, t,  $J = 2.3$ ), 6.56, 6.55 (2H, 2 X t,  $J = 2.3$ ), 6.20 (1H, dd,  $J = 7.8, 2.0$ ), 6.04 (1H, d,  $J = 7.8$ ), 5.84 (1H, d,  $J = 8.2$ ), 5.72 (1H, d,  $J = 8.2$ ), 3.66 (9H, s, Me), 3.13 (3H, s, Me). The remaining 8H are under the signals of major isomer, hence a detailed assignment of the minor isomer was not possible.

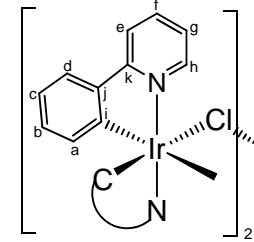
### Synthesis of $[\text{Ir}(\text{pmpz-Me}_2)_2\text{Cl}]_2$ (2.6f)

This was prepared from  $\text{IrCl}_3\cdot(\text{H}_2\text{O})_3$  (200 mg, 0.567 mmol) and 3,5-dimethyl-1-phenyl-1H-pyrazole (Hpmpz-Me<sub>2</sub>) (293 mg, 1.701 mmol) and after work up gave **2.6f** as a grey solid (297 mg, 92%). Anal. Calcd for  $\text{C}_{44}\text{H}_{44}\text{Cl}_2\text{Ir}_2\text{N}_8$ : C, 46.35, H, 3.89, N, 9.83. Found: C, 46.49, H, 3.90, N, 9.72%. <sup>1</sup>H NMR ( $\text{CDCl}_3$ ):  $\delta$  7.22 (4H, bd,  $J$  = 7.8, H<sub>d</sub>), 6.74 (4H, bt,  $J$  = 7.2, H<sub>c</sub>), 6.52 (4H, bt,  $J$  = 7.3, H<sub>b</sub>), 6.24 (4H, dd,  $J$  = 7.6, 0.7, H<sub>a</sub>), 6.13 (4H, s, H<sub>f</sub>), 2.85 (4H, s, Me<sub>B</sub>), 2.26 (4H, s, Me<sub>A</sub>). <sup>13</sup>C NMR: 152.56 (C<sub>g</sub>), 145.51 (C<sub>h</sub>), 140.20 (C<sub>e</sub>), 133.25 (C<sub>a</sub>), 127.73 (C<sub>i</sub>), 123.16 (C<sub>b</sub>), 121.53 (C<sub>c</sub>), 111.24 (C<sub>d</sub>), 110.10 (C<sub>f</sub>), 14.81 (Me<sub>A</sub> or B), 14.75 (Me<sub>A</sub> or B). MS (FAB):  $m/z$  1140 [M]<sup>+</sup>, 1105 [M-Cl]<sup>+</sup>. MS (ES):  $m/z$  617  $[\text{Ir}(\text{pmpz})_2(\text{MeCN})_2]$ <sup>+</sup>.



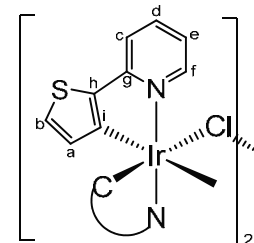
### Synthesis of $[\text{Ir}(\text{ppy})_2\text{Cl}]_2$ (2.6g)

This was prepared from  $\text{K}_2\text{IrCl}_6$  (400 mg, 0.828 mmol) and 2-phenylpyridine (Hppy) (385.5 mg, 0.355 ml, 2.484 mmol). After passing through celite the filtrate was washed with dilute HCl (3 X 20 ml). Compound **2.6g** was isolated as a yellow solid (383 mg, 86%). The NMR agrees with the literature.<sup>34</sup> <sup>1</sup>H NMR ( $\text{CD}_2\text{Cl}_2$ ):  $\delta$  9.25 (4H, bd,  $J$  = 5.5, H<sub>h</sub>), 7.92 (4H, bd,  $J$  = 7.8, H<sub>e</sub>), 7.77 (4H, td,  $J$  = 7.8, 1.6, H<sub>f</sub>), 7.55 (4H, bd,  $J$  = 7.4, H<sub>d</sub>), 6.82 – 6.79 (8H, m, H<sub>c, g</sub>), 6.59 (4H, td,  $J$  = 7.8, 1.2, H<sub>b</sub>), 5.87 (4H, bd,  $J$  = 7.4, H<sub>a</sub>). <sup>13</sup>C NMR: 168.46 (C<sub>k</sub>), 151.91 (C<sub>h</sub>), 145.28 (C<sub>j</sub>), 144.44 (C<sub>i</sub>), 137.08 (C<sub>f</sub>), 130.80 (C<sub>a</sub>), 129.50 (C<sub>b</sub>), 124.08 (C<sub>d</sub>), 123.00 (C<sub>c</sub>), 121.81 (C<sub>g</sub>), 119.13 (C<sub>e</sub>). MS (FAB):  $m/z$  1072 [M]<sup>+</sup>, 1035 [M-Cl]<sup>+</sup>. MS (ES):  $m/z$  583  $[\text{Ir}(\text{ppy})_2(\text{MeCN})_2]$ <sup>+</sup>.



### Synthesis of $[\text{Ir}(\text{thpy})_2\text{Cl}]_2$ (2.6h)

This was prepared from  $\text{IrCl}_3\cdot(\text{H}_2\text{O})_3$  (50 mg, 0.142 mmol) and 2-(thiophen-2-yl)pyridine (Hthpy) (68.5 mg, 0.425 mmol). The work up is done same to **2.6g** and gave **2.6h** as a red solid (61 mg, 79%). The NMR data agrees with that in the literature.<sup>52</sup> <sup>1</sup>H NMR ( $\text{CDCl}_3$ ):  $\delta$  9.00 (4H, d,  $J$  = 5.9, H<sub>f</sub>), 7.61 (4H, td,  $J$  = 7.8, 1.6, H<sub>d</sub>), 7.50 (4H, d,  $J$  = 8.2, H<sub>c</sub>), 7.05 (4H, d,  $J$  = 4.7, H<sub>b</sub>), 6.61 (4H, ddd,  $J$  = 7.4, 5.9, 1.6, H<sub>e</sub>), 5.91 (4H, d,  $J$  = 4.7, H<sub>a</sub>). <sup>13</sup>C NMR: 164.99 (C<sub>g</sub>), 151.68 (C<sub>f</sub>), 145.74 (C<sub>h</sub>), 136.76 (C<sub>d</sub>), 135.09 (C<sub>i</sub>), 129.34 (C<sub>a</sub>), 127.65 (C<sub>b</sub>), 119.01 (C<sub>e</sub>), 117.12 (C<sub>c</sub>). MS (FAB):  $m/z$  1096 [M]<sup>+</sup>, 1062 [M-Cl]<sup>+</sup>. MS (ES):  $m/z$  595  $[\text{Ir}(\text{thpy})_2(\text{MeCN})_2]$ <sup>+</sup>.



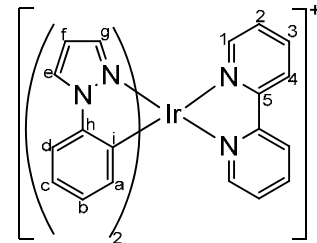
## General procedure for synthesis of bipy complexes $[\text{Ir}(\text{C}^{\wedge}\text{N})_2(\text{bipy})]\text{PF}_6$ (2.7a-f)

The appropriate dimer **2.6a-f** (1 equiv), bipy (2.2-2.4 equiv) and  $\text{KPF}_6$  (2.4 equiv) were placed in a microwave vial and methanol (3 ml) was added. Nitrogen was bubbled through the solution for 2 mins and the vial was then sealed with a septum cap. The tube was placed in the microwave reactor and heated under microwave irradiation at 60°C for 20 mins at a maximum pressure of 250 psi. After this time the solvent was removed *in vacuo* leaving behind a solid which was dissolved in DCM (15 ml) and passed through celite. The filtrate was reduced in volume and hexane was added slowly to induce precipitation. The precipitate was isolated, washed with hexane and dried *in vacuo*. The compounds could be recrystallised from DCM/hexane.

### Synthesis of $[\text{Ir}(\text{ppz})_2(\text{bipy})]\text{PF}_6$ (2.7a)

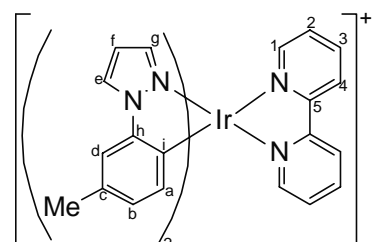
This is a known complex,<sup>19</sup> the NMR data are included here for the comparison (the  $^1\text{H}$  NMR shifts are out by 0.09 ppm relative to literature).

This was prepared from  $[\text{Ir}(\text{ppz})_2\text{Cl}]_2$  **2.6a** (50 mg, 0.048 mmol), 2,2'-bipyridyl (18.2 mg, 0.116 mmol) and  $\text{KPF}_6$  (21.3 mg, 0.116 mmol) and after work up gave **2.7a** as a yellow solid (60 mg, 81%).  $^1\text{H}$  NMR ( $\text{CD}_2\text{Cl}_2$ ):  $\delta$  8.40 (2H, dd,  $J$  = 8.2, 0.8, H<sub>4</sub>), 8.10 (2H, dd,  $J$  = 5.4, 1.5, H<sub>1</sub>), 8.08 (2H, dd,  $J$  = 2.7, H<sub>e</sub>), 8.06 (2H, td,  $J$  = 8.1, 1.7, H<sub>3</sub>) 7.39 (2H, ddd,  $J$  = 7.8, 5.5, 1.2, H<sub>2</sub>), 7.27 (2H, dd,  $J$  = 7.8, H<sub>d</sub>), 7.01 (2H, td,  $J$  = 8.9, 1.6, H<sub>c</sub>), 6.82 (2H, td,  $J$  = 8.6, 1.2, H<sub>b</sub>), 6.77 (2H, d,  $J$  = 2.3, H<sub>g</sub>), 6.47 (2H, t,  $J$  = 2.3, H<sub>f</sub>), 6.24 (2H, dd,  $J$  = 7.4, 1.2, H<sub>a</sub>). MS (FAB):  $m/z$  635 [M]<sup>+</sup>.



### Synthesis of $[\text{Ir}(\text{ppz-Me})_2(\text{bipy})]\text{PF}_6$ (2.7b)

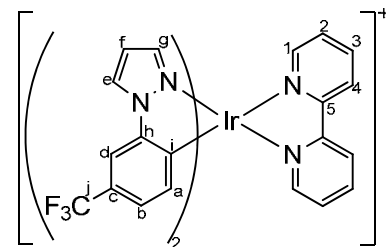
This was prepared from  $[\text{Ir}(\text{ppz-Me})_2\text{Cl}]_2$  **2.6b** (40 mg, 0.037 mmol), bipy (13.8 mg, 0.088 mmol) and  $\text{KPF}_6$  (16.2 mg, 0.088 mmol) and after work up gave **2.7b** as a yellow solid (47 mg, 80%). Anal. Calcd for  $\text{C}_{30}\text{H}_{26}\text{F}_6\text{IrN}_6\text{P}$ : C, 44.61, H, 3.24, N, 10.40. Found: C, 44.70, H, 3.16, N, 10.38%.  $^1\text{H}$  NMR ( $\text{CD}_2\text{Cl}_2$ ):  $\delta$  8.46 (2H, d,  $J$  = 8.2, H<sub>4</sub>), 8.21 (2H, ddd,  $J$  = 5.5, 1.6, 0.8, H<sub>1</sub>), 8.15 – 8.11 (4H, m, H<sub>3, e</sub>), 7.47 (2H, ddd,  $J$  = 7.4, 5.5, 1.2, H<sub>2</sub>), 7.18 (2H, s, H<sub>d</sub>), 6.83 (2H, d,  $J$  = 2.3, H<sub>g</sub>), 6.74 (2H, dd,  $J$  = 7.4, 1.6, H<sub>b</sub>), 6.53 (2H,



$t, J = 2.3, H_f)$ , 6.18 (2H, d,  $J = 7.4, H_a$ ), 2.31 (6H, s, Me).  $^{13}\text{C}$  NMR: 156.79 ( $C_5$ ), 151.54 ( $C_1$ ), 143.22 ( $C_h$ ), 139.82 ( $C_e$ ), 138.34 ( $C_g$ ), 133.62 ( $C_c$ ), 133.27 ( $C_a$ ), 128.20 ( $C_b$ ), 128.19 ( $C_2$ ), 127.83 ( $C_i$ ), 127.27 ( $C_3$ ), 124.57 ( $C_4$ ), 112.98 ( $C_d$ ), 108.46 ( $C_f$ ), 21.15 (Me). MS (FAB):  $m/z$  663 [M]<sup>+</sup>.

### Synthesis of $[\text{Ir}(\text{ppz-CF}_3)_2(\text{bipy})]\text{PF}_6$ (2.7c)

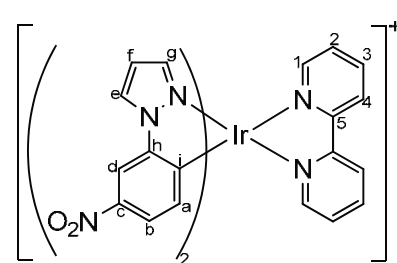
This was prepared from  $[\text{Ir}(\text{ppz-CF}_3)_2\text{Cl}]_2$  **2.6c** (50 mg, 0.038 mmol), 2,2'-bipyridyl (14.4 mg, 0.092 mmol) and  $\text{KPF}_6$  (16.9 mg, 0.092 mmol) and after work up gave **2.7c** as a yellow solid (59 mg, 84%). Anal. Calcd for  $\text{C}_{30}\text{H}_{20}\text{F}_{12}\text{IrN}_6\text{P}$ : C, 39.35, H, 2.20, N, 9.18.



Found: C, 39.42, H, 2.15, N, 9.15%.  $^1\text{H}$  NMR ( $\text{CD}_2\text{Cl}_2$ ):  $\delta$  8.54 (2H, d,  $J = 8.2, H_4$ ), 8.24 (2H, d,  $J = 3.1, H_e$ ), 8.20 (2H, td,  $J = 8.2, 1.6, H_3$ ), 8.11 (2H, ddd,  $J = 5.5, 1.6, 0.8, H_1$ ), 7.57 (2H, s,  $H_d$ ), 7.52 (2H, ddd,  $J = 7.8, 5.5, 1.2, H_2$ ), 7.16 (2H, dd,  $J = 7.8, 0.8, H_b$ ), 6.95 (2H, d,  $J = 2.3, H_g$ ), 6.65 (2H, t,  $J = 2.3, H_f$ ), 6.47 (2H, d,  $J = 7.8, H_a$ ).  $^{13}\text{C}$  NMR: 156.58 ( $C_5$ ), 151.40 ( $C_1$ ), 143.54 ( $C_h$ ), 140.59 ( $C_3$ ), 139.61 ( $C_g$ ), 137.85 ( $C_i$ ), 134.18 ( $C_a$ ), 128.58 ( $C_2$ ), 128.43 ( $C_e$ ), 126.38 ( $C_j$ ), 126.12 ( $C_c$ ), 123.82 ( $C_4$ ), 123.79 ( $C_b$ ), 109.56 ( $C_f$ ), 108.87 ( $C_d$ ). MS (FAB):  $m/z$  771 [M]<sup>+</sup>.

### Synthesis of $[\text{Ir}(\text{ppz-NO}_2)_2(\text{bipy})]\text{PF}_6$ (2.7d)

This was prepared from  $[\text{Ir}(\text{ppz-NO}_2)_2\text{Cl}]_2$  **2.6d** (50 mg, 0.041 mmol), bipy (14.2 mg, 0.091 mmol) and  $\text{KPF}_6$  (16.7 mg, 0.091 mmol) in this case heating for 65 mins was required for complete conversion and after work up gave **2.7d** as a greenish yellow solid (61 mg, 86%). Anal. Calcd for  $\text{C}_{28}\text{H}_{20}\text{F}_6\text{IrN}_8\text{O}_4\text{P}$ : C, 38.67, H, 2.32, N, 12.88. Found: C, 38.58, H, 2.27, N, 12.92%.

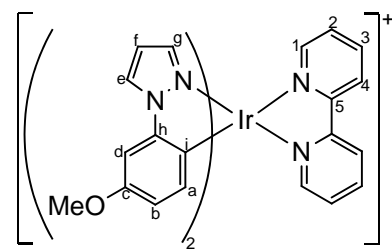


$^1\text{H}$  NMR ( $\text{CD}_2\text{Cl}_2$ ):  $\delta$  8.56 (2H, d,  $J = 8.2, H_4$ ), 8.34 (2H, d,  $J = 3.1, H_e$ ), 8.23 (2H, td,  $J = 7.8, 1.6, H_3$ ), 8.21 (2H, d,  $J = 2.3, H_d$ ), 8.08 (2H, ddd,  $J = 5.5, 1.6, 0.8, H_1$ ), 7.76 (2H, dd,  $J = 8.2, 2.3, H_b$ ), 7.54 (2H, ddd,  $J = 7.8, 5.5, 1.2, H_2$ ), 7.02 (2H, d,  $J = 2.3, H_g$ ), 6.71 (2H, t,  $J = 2.3, H_f$ ), 6.52 (2H, d,  $J = 8.2, H_a$ ).  $^{13}\text{C}$  NMR: 156.43 ( $C_5$ ), 151.32 ( $C_1$ ), 145.75 ( $C_h$ ), 143.92 ( $C_c$ ), 143.69 ( $C_i$ ), 141.00 ( $C_3$ ), 140.30 ( $C_g$ ), 134.08 ( $C_a$ ), 129.09 ( $C_2$ ), 128.79 ( $C_e$ ), 125.39 ( $C_4$ ), 121.93 ( $C_b$ ), 110.13 ( $C_f$ ), 107.09 ( $C_d$ ). MS (FAB):  $m/z$  725 [M]<sup>+</sup>.

**Minor isomer (B):**  $^1\text{H}$  NMR ( $\text{CD}_2\text{Cl}_2$ ):  $\delta$  8.49, 8.48 (2H, 2X d,  $J$  = 7.8), 7.84 (1H, dd,  $J$  = 5.5, 1.6), 7.72 (1H, t,  $J$  = 2.0), 7.29 (1H, t,  $J$  = 8.2), 6.91 (1H, d,  $J$  = 2.7), 6.88 (1H, d,  $J$  = 2.3), 6.83 (1H, d,  $J$  = 2.3), 6.80 (1H, d,  $J$  = 2.3), 6.73 (1H, d,  $J$  = 2.3), 6.69 (1H, t,  $J$  = 2.3), 6.64 (1H, t,  $J$  = 2.3), 6.57 – 6.55 (2H, m), 6.56 (1H, dd,  $J$  = 7.8, 2.0), 6.22 (1H, d,  $J$  = 7.8). The remaining 4H are under the signals of the major isomer. Hence a detailed assignment of the minor isomer was not possible.

### Synthesis of $[\text{Ir}(\text{ppz-OMe})_2(\text{bipy})]\text{PF}_6$ (2.7e)

This was prepared from  $[\text{Ir}(\text{ppz-OMe})_2\text{Cl}]_2$  **2.6e** (40 mg, 0.035 mmol), bipy (13.1 mg, 0.084 mmol) and  $\text{KPF}_6$  (15.5 mg, 0.084 mmol) and after work up gave **2.7e** as a yellow solid (43 mg, 74%). Anal. Calcd for  $\text{C}_{30}\text{H}_{26}\text{F}_6\text{IrN}_6\text{O}_2\text{P}$ : C, 42.91, H, 3.12, N, 10.01. Found:

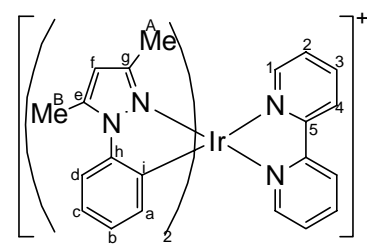


C, 43.14, H, 3.04, N, 9.90%.  $^1\text{H}$  NMR ( $\text{CD}_2\text{Cl}_2$ ):  $\delta$  8.46 (2H, d,  $J$  = 8.2,  $\text{H}_4$ ), 8.23 (2H, d,  $J$  = 5.0,  $\text{H}_1$ ), 8.16 – 8.11 (4H, m,  $\text{H}_{3, e}$ ), 7.48 (2H, m,  $\text{H}_2$ ), 6.96 (2H, d,  $J$  = 2.3,  $\text{H}_d$ ), 6.84 (2H, d,  $J$  = 1.8,  $\text{H}_g$ ), 6.59 – 6.53 (4H, m,  $\text{H}_{b, f}$ ), 6.19 (2H, d,  $J$  = 8.2,  $\text{H}_a$ ), 3.79 (6H, s, Me). MS (FAB):  $m/z$  695  $[\text{M}]^+$ .

**Minor isomer (B):**  $^1\text{H}$  NMR ( $\text{CDCl}_3$ ):  $\delta$  8.08 – 8.06 (2H, m), 7.95 (1H, d,  $J$  = 2.7), 7.07 (1H, t,  $J$  = 7.8), 6.98 (1H, d,  $J$  = 7.0), 6.89 (1H, d,  $J$  = 2.7), 6.74 – 6.73 (2H, m), 6.51 – 6.50 (2H, m), 6.42 (1H, t,  $J$  = 2.3), 6.40 (1H, d,  $J$  = 7.8), 6.06 (1H, d,  $J$  = 8.2), 3.79 (3H, s, Me), 3.25 (3H, s, Me). The remaining 7H are under the signals of the major isomer, hence a detailed assignment of the minor isomer was not possible.

### Synthesis of $[\text{Ir}(\text{pmpz-Me}_2)_2(\text{bipy})]_2$ (2.7f)

This was prepared from  $[\text{Ir}(\text{pmpz-Me}_2)_2\text{Cl}]_2$  **2.6f** (40 mg, 0.035 mmol), bipy (13.1 mg, 0.084 mmol) and  $\text{KPF}_6$  (15.5 mg, 0.084 mmol) and after work up gave **2.7f** as a yellow solid (47 mg, 81%). Anal. Calcd for  $\text{C}_{32}\text{H}_{30}\text{F}_6\text{IrN}_6\text{P}$ : C, 45.98, H, 3.62, N, 10.06. Found: C,

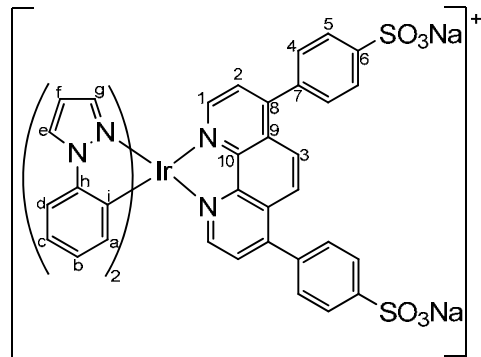


45.92, H, 3.59, N, 9.93%.  $^1\text{H}$  NMR ( $\text{CD}_2\text{Cl}_2$ ):  $\delta$  8.46 (2H, d,  $J$  = 8.2,  $\text{H}_4$ ), 8.11 (2H, td,  $J$  = 8.2, 1.6,  $\text{H}_3$ ), 8.01 (2H, dd,  $J$  = 5.4, 1.2,  $\text{H}_1$ ), 7.50 (2H, dd,  $J$  = 8.2, 0.8,  $\text{H}_d$ ), 7.44 (2H, ddd,  $J$  = 7.8, 5.5, 1.2,  $\text{H}_2$ ), 7.06 (2H, td,  $J$  = 7.8, 1.2,  $\text{H}_c$ ), 6.84 (2H, td,  $J$  = 7.4, 1.2,  $\text{H}_b$ ), 6.34 (2H, dd,  $J$  = 7.4, 1.2,  $\text{H}_a$ ), 6.03 (2H, s,  $\text{H}_f$ ), 2.80 (6H, s,  $\text{Me}_B$ ), 1.47 (6H, s,  $\text{Me}_A$ ).  $^{13}\text{C}$  NMR: 156.77 ( $\text{C}_5$ ), 151.17 ( $\text{C}_1$ ), 150.28 ( $\text{C}_g$ ), 145.01 ( $\text{C}_h$ ), 141.92 ( $\text{C}_e$ ), 139.70 ( $\text{C}_3$ ),

133.96 (C<sub>a</sub>), 133.02 (C<sub>i</sub>), 128.45 (C<sub>2</sub>), 126.09 (C<sub>b</sub>), 124.42 (C<sub>4</sub>), 123.69 (C<sub>c</sub>), 113.29 (C<sub>d</sub>), 110.62 (C<sub>f</sub>), 14.75 (Me<sub>B</sub>), 12.57 (Me<sub>A</sub>). MS (FAB): *m/z* 691 [M]<sup>+</sup>.

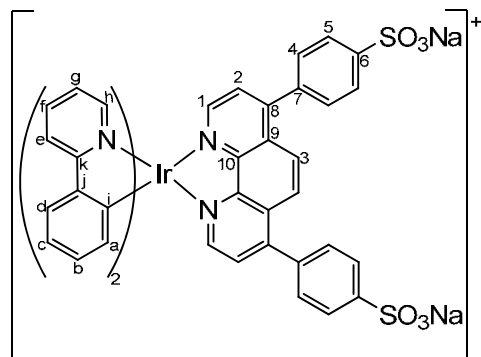
### Synthesis of 2.8a

A mixture of [Ir(ppz)<sub>2</sub>Cl]<sub>2</sub> **2.6a** (50 mg, 0.048 mmol) and 4,7-diphenyl-1,10-phenanthrolinedisulfonic acid disodium salt **dps** (59 mg, 0.110 mmol) in DCM/methanol (1:1.5) was heated under reflux, under an inert atmosphere of nitrogen for 3 hrs in dark. The mixture was then evaporated to dryness and the solid was dissolved in methanol and passed through celite. Subsequent recrystallization of the compound from methanol/diethylether mixture afforded **2.8a** as a yellow solid (82 mg, 85%). Anal. Calcd for C<sub>42</sub>H<sub>28</sub>N<sub>6</sub>O<sub>6</sub>S<sub>2</sub>Na<sub>2</sub>IrCl: C, 48.02, H, 2.69, N, 8.00. Found: C, 47.93, H, 2.73, N, 7.96%. <sup>1</sup>H NMR (MeOD):  $\delta$  8.57 (2H, d, *J* = 5.1, H<sub>1</sub>), 8.55 (2H, d, *J* = 2.7, H<sub>e</sub>), 8.22 (2H, s, H<sub>3</sub>), 8.07 – 8.03 (4H, m, H<sub>5</sub>), 7.88 (2H, d, *J* = 5.1, H<sub>2</sub>), 7.75 – 7.67 (4H, m, H<sub>4</sub>), 7.57 (2H, dd, *J* = 7.8, 0.8, H<sub>d</sub>), 7.11 – 7.07 (4H, m, H<sub>c, g</sub>), 6.91 (2H, td, *J* = 7.4, 0.8, H<sub>b</sub>), 6.56 (2H, t, *J* = 2.7, H<sub>f</sub>), 6.45 (2H, dd, *J* = 7.4, 0.8, H<sub>a</sub>). <sup>13</sup>C NMR: 150.86 (C<sub>1</sub>), 150.24 (C<sub>8</sub>), 148.08 (C<sub>10</sub>), 143.38 (C<sub>h</sub>), 138.44 (C<sub>g</sub>), 135.86 (C<sub>7</sub>), 133.07 (C<sub>a</sub>), 131.84 (C<sub>i</sub>), 131.30 (C<sub>9</sub>), 129.67 (C<sub>6</sub>), 128.87 (C<sub>4</sub>), 127.54 (C<sub>e</sub>), 126.95 (C<sub>5</sub>), 126.83 (C<sub>b</sub>), 126.51 (C<sub>2</sub>), 126.30 (C<sub>3</sub>), 123.08 (C<sub>c</sub>), 111.56 (C<sub>d</sub>), 108.00 (C<sub>f</sub>). MS (FAB): *m/z* 1015 [M]<sup>+</sup>.



### Synthesis of 2.8g

This was prepared from [Ir(ppy)<sub>2</sub>Cl]<sub>2</sub> **2.6g** (50 mg, 0.046 mmol) and 4,7-diphenyl-1,10-phenanthrolinedisulfonic acid disodium salt **dps** (49.3 mg, 0.092 mmol) using the same method as for synthesis of bipy complexes (**2.7a-f**) and after work up gave **2.8g** as a yellow solid (47 mg, 81%). Anal. Calcd for C<sub>46</sub>H<sub>30</sub>N<sub>4</sub>O<sub>6</sub>S<sub>2</sub>Na<sub>2</sub>IrCl(CH<sub>2</sub>Cl<sub>2</sub>): C, 46.40, H, 2.76, N, 4.51. Found: C, 46.34, H, 2.76, N, 4.53%. <sup>1</sup>H NMR (MeOD):  $\delta$  8.40 (2H, d, *J* = 5.1, H<sub>1</sub>), 8.20 (2H, s, H<sub>3</sub>), 8.13 (2H, d, *J* = 8.2, H<sub>h</sub>), 8.05 – 8.02 (4H, m, H<sub>5</sub>), 7.87 – 7.81 (6H, m, H<sub>2, d, g</sub>), 7.73 – 7.65 (4H, m,



H<sub>4</sub>), 7.62 (2H, d, *J* = 4.3, H<sub>e</sub>), 7.04 (2H, t, *J* = 7.5, H<sub>c</sub>), 6.97 (2H, t, *J* = 6.7, H<sub>f</sub>), 6.92 (2H, t, *J* = 7.2, H<sub>b</sub>), 6.42 (2H, d, *J* = 7.4, H<sub>a</sub>). <sup>13</sup>C NMR: 169.35 (C<sub>k</sub>), 152.00 (C<sub>1</sub>), 151.57 (C<sub>i</sub>), 150.35 (C<sub>e</sub>), 148.81 (C<sub>10</sub>), 147.57 (C<sub>6</sub>), 145.52 (C<sub>j</sub>), 139.67 (C<sub>g</sub>), 137.25 (C<sub>8</sub>), 133.01 (C<sub>a</sub>), 132.70 (C<sub>7</sub>), 131.55 (C<sub>b</sub>), 131.09 (C<sub>9</sub>), 130.29 (C<sub>4</sub>), 128.36 (C<sub>2</sub>), 128.25 (C<sub>5</sub>), 127.50 (C<sub>3</sub>), 126.07 (C<sub>d</sub>), 124.57 (C<sub>f</sub>), 123.76 (C<sub>c</sub>), 121.04 (C<sub>h</sub>). MS (FAB): *m/z* 1037 [M]<sup>+</sup>.

## 2.4 Bibliography

1. M. S. Lowry, W. R. Hudson, R. A. Pascal and S. Bernhard, *J. Am. Chem. Soc.*, 2004, **126**, 14129-14135.
2. C. H. Yang, S. W. Li, Y. Chi, Y. M. Cheng, Y. S. Yeh, P. T. Chou, G. H. Lee, C. H. Wang and C. F. Shu, *Inorg. Chem.*, 2005, **44**, 7770-7780.
3. R. Ragni, E. Orsell, G. S. Kottas, O. H. Omar, F. Badudri, A. Pedone, F. Naso, G. M. Farinola and L. De Cola, *Chem. Eur. J.*, 2009, **15**, 136-148.
4. M. L. Xu, R. Zhou, G. Y. Wang and J. Y. Yu, *Inorg. Chim. Acta*, 2009, **362**, 515-518.
5. T. H. Kwon, H. S. Cho, M. K. Kim, J. W. Kim, J. J. Kim, K. H. Lee, S. J. Park, I. S. Shin, H. Kim, D. M. Shin, Y. K. Chung and J. I. Hong, *Organometallics*, 2005, **24**, 1578-1585.
6. H. W. Hong and T. M. Chen, *Mater Chem Phys*, 2007, **101**, 170-176.
7. P. Coppo, E. A. Plummer and L. De Cola, *Chem. Commun.*, 2004, 1774-1775.
8. I. Avilov, P. Minoofar, J. Cornil and L. De Cola, *J. Am. Chem. Soc.*, 2007, **129**, 8247-8258.
9. W. C. Chang, A. T. Hu, J. P. Duan, D. K. Rayabarapu and C. H. Cheng, *J. Organomet. Chem.*, 2004, **689**, 4882-4888.
10. Y. H. Song, Y. C. Chiu, Y. Chi, Y. M. Cheng, C. H. Lai, P. T. Chou, K. T. Wong, M. H. Tsai and C. C. Wu, *Chem. Eur. J.*, 2008, **14**, 5423-5434.
11. K. Dedeian, J. Shi, N. Shepherd, E. Forsythe and D. C. Morton, *Inorg. Chem.*, 2005, **44**, 4445-4447.
12. X. N. Li, Z. J. Wu, Z. J. Si, H. J. Zhang, L. Zhou and X. J. Liu, *Inorg. Chem.*, 2009, **48**, 7740-7749.
13. Y. You and S. Y. Park, *J. Am. Chem. Soc.*, 2005, **127**, 12438-12439.
14. M. L. Xu, R. Zhou, G. Y. Wang, Q. Xiao, W. S. Du and G. B. Che, *Inorg. Chim. Acta*, 2008, **361**, 2407-2412.
15. H. Jang, C. H. Shin, N. G. Kim, K. Y. Hwang and Y. Do, *Synth. Met.*, 2005, **154**, 157-160.
16. T. Tsuzuki, N. Shirasawa, T. Suzuki and S. Tokito, *Adv. Mater.*, 2003, **15**, 1455-1458.
17. R. Terki, L. P. Simoneau and A. Rochefort, *J. Phys. Chem. A*, 2009, **113**, 534-541.
18. K. Dedeian, P. I. Djurovich, F. O. Garces, G. Carlson and R. J. Watts, *Inorg. Chem.*, 1991, **30**, 1685-1687.
19. A. B. Tamayo, S. Garon, T. Sajoto, P. I. Djurovich, I. M. Tsyba, R. Bau and M. E. Thompson, *Inorg. Chem.*, 2005, **44**, 8723-8732.
20. G. A. Tompsett, W. C. Conner and K. S. Yngvesson, *ChemPhysChem*, 2006, **7**, 296-319.
21. D. M. P. Mingos and D. R. Baghurst, *Chem. Soc. Rev.*, 1991, **20**, 1-47.

22. R. Gedye, F. Smith, K. Westaway, H. Ali, L. Baldisera, L. Laberge and J. Rousell, *Tetrahedron Lett.*, 1986, **27**, 279-282.

23. R. J. Giguere, T. L. Bray, S. M. Duncan and G. Majetich, *Tetrahedron Lett.*, 1986, **27**, 4945-4948.

24. D. R. Baghurst and D. M. P. Mingos, *J. Chem. Soc., Dalton Trans.*, 1992, 1151-1155.

25. D. R. Baghurst, D. M. P. Mingos and M. J. Watson, *J. Organomet. Chem.*, 1989, **368**, C43-C45.

26. A. S. Prakash and K. Murugan, in *Advanced Research in Physics and Engineering*, eds. O. Martin, A. Walcarus, M. Henini, A. P. F. Turner, M. Adeli and D. Lynden Bell, World Scientific and Engineering Acad and Soc, Athens, 2010, pp. 29-33.

27. R. K. Arvela and N. E. Leadbeater, *J. Org. Chem.*, 2005, **70**, 1786-1790.

28. A. Benalloum, B. Labiad and D. Villemain, *J. Chem. Soc., Chem. Commun.*, 1989, 386-387.

29. C. Gabriel, S. Gabriel, E. H. Grant, B. S. J. Halstead and D. M. P. Mingos, *Chem. Soc. Rev.*, 1998, **27**, 213-223.

30. D. L. Greene and D. M. P. Mingos, *Transition Met. Chem.*, 1991, **16**, 71-72.

31. H. Konno and Y. Sasaki, *Chem. Lett.*, 2003, **32**, 252-253.

32. K. Saito, N. Matsusue, H. Kanno, Y. Hamada, H. Takahashi and T. Matsumura, *Jpn. J. Appl. Phys., Part 1*, 2004, **43**, 2733-2734.

33. T. Matsumura-Inoue, Y. Yamamoto, N. Yoshikawa, M. Terashima, Y. Yoshida, A. Fujii and K. Yoshino, *Opt. Mater.*, 2004, **27**, 187-191.

34. S. Sprouse, K. A. King, P. J. Spellane and R. J. Watts, *J. Am. Chem. Soc.*, 1984, **106**, 6647-6653.

35. M. Nonoyama, *J. Organomet. Chem.*, 1975, **86**, 263-267.

36. M. Bandini, M. Bianchi, G. Valenti, F. Piccinelli, F. Paolucci, M. Monari, A. Umani-Ronchi and M. Marcaccio, *Inorg. Chem.*, 2010, **49**, 1439-1448.

37. P. J. Spellane, R. J. Watts and C. J. Curtis, *Inorg. Chem.*, 1983, **22**, 4060-4062.

38. A. R. McDonald, M. Lutz, L. S. von Chrzanowski, G. P. M. van Klink, A. L. Spek and G. van Koten, *Inorg. Chem.*, 2008, **47**, 6681-6691.

39. K. A. McGee and K. R. Mann, *Inorg. Chem.*, 2007, **46**, 7800-7809.

40. L. Li, W. W. Brennessel and W. D. Jones, *Organometallics*, 2009, **28**, 3492-3500.

41. L. Q. Chen, C. L. Yang and J. G. Qin, *Acta Crystallogr., Sect. C*, 2005, **61**, M513-M515.

42. L. Chen, C. Yang, M. Li, J. Qin, J. Gao, H. You and D. Ma, *Cryst. Growth Des.*, 2006, **7**, 39-46.

43. V. V. Krisyuk, A. Turgambaeva, J. Lee and S. W. Rhee, *Transition Met. Chem.*, 2005, **30**, 786-791.

44. F. Neve, M. La Deda, F. Punzoriero and S. Campagna, *Inorg. Chim. Acta*, 2006, **359**, 1666-1672.

45. J. I. Kim, I. S. Shin, H. Kim and J. K. Lee, *J. Am. Chem. Soc.*, 2005, **127**, 1614-1615.

46. J. I. Goldsmith, W. R. Hudson, M. S. Lowry, T. H. Anderson and S. Bernhard, *J. Am. Chem. Soc.*, 2005, **127**, 7502-7510.

47. Q. Zhao, S. Liu, M. Shi, C. Wang, M. Yu, L. Li, F. Li, T. Yi and C. Huang, *Inorg. Chem.*, 2006, **45**, 6152-6160.

48. F. Neve, M. La Deda, A. Crispini, A. Bellusci, F. Punzoriero and S. Campagna, *Organometallics*, 2004, **23**, 5856-5863.

49. W. A. Herrmann and C. W. Kohlpaintner, *Angew. Chem., Int. Ed.*, 1993, **32**, 1524-1544.
50. A. J. Amoroso, M. P. Coogan, J. E. Dunne, V. Fernandez-Moreira, J. B. Hess, A. J. Hayes, D. Lloyd, C. Millet, S. J. A. Pope and C. Williams, *Chem. Commun.*, 2007, 3066-3068.
51. S. V. Kukharenko, V. V. Strelets, A. R. Kudinov, A. Z. Kreidlin, M. G. Peterleitner, L. I. Denisovich and M. I. Rybinskaya, *J. Organomet. Chem.*, 1996, **519**, 1-5.
52. M. Bandini, M. Bianchi, G. Valenti, F. Piccinelli, F. Paolucci, M. Monari, A. Umani-Ronchi and M. Marcaccio, *Inorg. Chem.*, **49**, 1439-1448.

# **Chapter Three:**

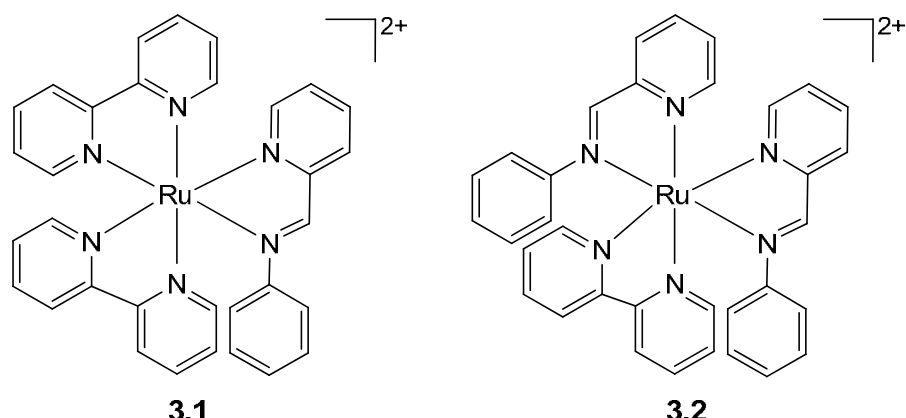
## **Synthesis, Characterisation and Properties of $[\text{Ir}(\text{C}^{\wedge}\text{N})_2(\text{X}^{\wedge}\text{Y})]^{n+}$ ( $n = 0, 1$ ); $\text{X}^{\wedge}\text{Y} = \text{pyridineimine}; \text{X}^{\wedge}\text{Y} = \text{pyrroleimine})$**

## Chapter 3 Synthesis, Characterisation and Properties of $[\text{Ir}(\text{C}^{\wedge}\text{N})_2(\text{X}^{\wedge}\text{Y})]^{n+}$ ( $n = 0, 1$ ) ( $n = 1$ , $\text{X}^{\wedge}\text{Y}$ = pyridineimine; $n = 0$ , $\text{X}^{\wedge}\text{Y}$ = pyrrolylimine)

### 3.1 Introduction

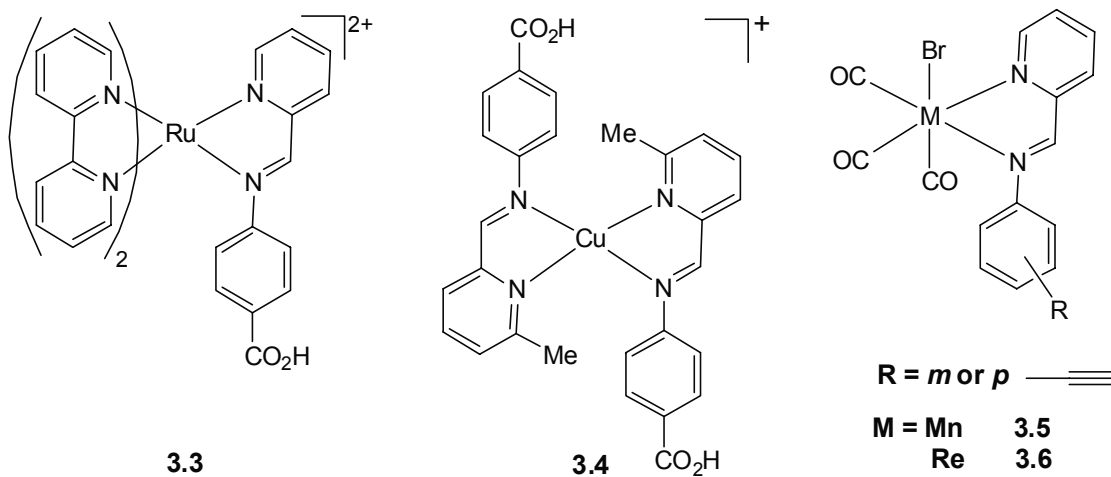
As discussed in **Chapter 1** and **2**, in cationic complexes  $[\text{Ir}(\text{C}^{\wedge}\text{N})_2(\text{bipy})]^+$  the LUMO is on the bipy whilst the HOMO is mainly on the Ir-phenyl. Hence in principle the HOMO and the LUMO can be manipulated independently by substitution on the appropriate ligand. However, changing substituents on bipy is time-consuming from a synthetic viewpoint, hence, finding an alternative to bipy ligands may expand the usefulness of these complexes. Pyridineimines are attractive alternatives since they have similar properties to bipy (NN donor set and empty  $\pi^*$ -orbitals) yet are much simpler to prepare by a simple condensation between pyridine-2-carboxaldehyde and the relevant primary amine. The ready availability of different amines and the one step preparation of pyridineimines should allow much easier access to a wide variety of different substituents in comparison to bipy ligands. Despite these attractive properties, pyridineimines are much less explored than bipy complexes.

In 2006, Hannon *et al.* reported complex **3.1** which has similar photophysical properties to  $[\text{Ru}(\text{bipy})_3]^{2+}$  demonstrating that an N-aryl pyridineimine ligand can be used as a mimic of bipy.<sup>1</sup> Complex **3.1** displays a reversible Ru(II)/(III) oxidation at +1.38 V, slightly higher than that, +1.28 V,<sup>2</sup> for  $[\text{Ru}(\text{bipy})_3]^{2+}$  suggesting that the pyridineimine slightly stabilises the Ru(II) oxidation state (compared to bipy) which may reflect enhanced  $\pi$ -back donation to this ligand. Four ligand centred reversible reductions are observed for complex **3.1** the first ligand centred reduction (-0.99 V) is more positive than for  $[\text{Ru}(\text{bipy})_3]^{2+}$  ( $E_{\text{Red}} = -1.33$  V), hence it is assigned to the pyridineimine. Upon excitation at 440 nm complex **3.1** exhibits a broad weak emission

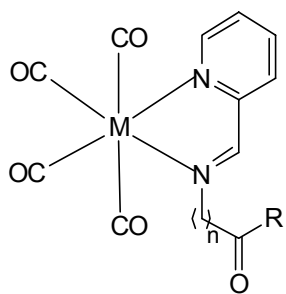


at 770 nm which is assigned to  $^3\text{MLCT}$  transition. The 155 nm red shift compared to  $[\text{Ru}(\text{bipy})_3]^{2+}$  ( $\lambda_{\text{em}} = 615$  nm) is consistent with a lower LUMO level in **3.1**<sup>3, 4</sup> with respect to  $[\text{Ru}(\text{bipy})_3]^{2+}$ . Replacing another bipy ligand with pyridineimine in complex **3.2**, shifts both the oxidation and reduction to even more anodic potentials, +1.45 V and -0.86 V respectively.<sup>5</sup> According to calculations on complex **3.2**, the LUMO of the pyridineimine ligand is about 0.2 eV lower in energy than that of bipy, therefore the first reduction was assigned to pyridineimine.<sup>5</sup>

As discussed above, the synthesis of substituted pyridineimines is very facile. Carboxylate-functionalised complexes are ubiquitous among the dyes that bind to TiO<sub>2</sub> in dye sensitized solar cells (DSSCs).<sup>6-8</sup> Very recently, Housecroft and co-workers reported carboxylate-derivatised pyridineimine complexes of Ru(II) **3.3** and Cu(I) **3.4** and demonstrated that these can be successfully employed to fabricate efficient DSSCs,<sup>9</sup> with the Cu(I) complex performing better than the Ru(II) one which was ascribed to two carboxylate anchoring groups in **3.4**. Similarly, ethynyl functionalised pyridineimine complexes of Mn(I) **3.5** and Re(I) **3.6** have been reported.<sup>10</sup> The ethynyl functionality was used for further reactivity, *e.g.* with octacarbonyl dicobalt, to afford tetrahedrane clusters.<sup>10</sup>

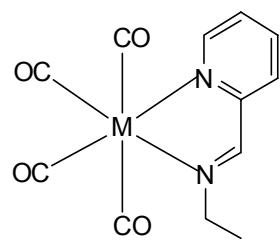


Bioconjugation of transition metal-ligand fragments has expanded over the years leading to the emerging field of bioorganometallic chemistry.<sup>11, 12</sup> As discussed in **Chapter 1 (Section 1.4.1.3)**, Meade and co-workers prepared complexes of alkyl linked pyridineimine-nucleotides which showed room temperature emission.<sup>13</sup> Incorporation of biological ligands, in particular amino acids or peptides,<sup>14, 15</sup> into organometallic systems has become a focus of chemists in recent years. A number of groups have demonstrated the incorporation of amino acid esters in pyridineimines as a way to create

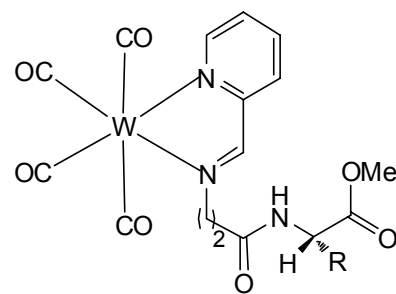


**M = Cr (3.7), W (3.8), Mo (3.9)**

**R = OEt**      **n = 1**    **a**  
**OH**              **= 2**    **b**  
                    **= 3**    **c**



**M = Mo, W 3.10**

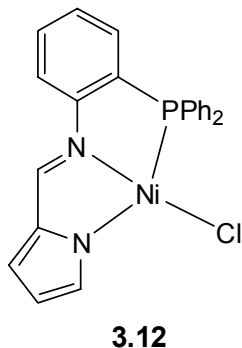


**3.11**

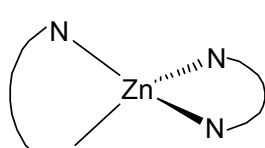
**R = *i*Pr, CH<sub>3</sub>**

biologically relevant ligands for organometallic centres.<sup>16-17, 18</sup> The first report in 1999 by Herrick *et al.* focussed on complexes **3.7-3.9** (R = OEt) which demonstrated that  $\alpha$ -,  $\beta$ - and  $\gamma$ -amino acid esters can be incorporated into pyridineimines.<sup>19</sup> Later, the same group showed that for tungsten complexes  $\beta$ - and  $\gamma$ -amino acids gave the desired complexes **3.8b,c** (R = OH) however  $\alpha$ -amino acid, glycine, underwent decarboxylation and formation of **3.10** (M = W).<sup>20</sup> Similar decarboxylation reactions have been reported for Mo.<sup>21</sup> Complexes **3.8b,c** (M = W, R = OH) were successfully coupled with L-alanine ethyl ester or L-valine methyl ester to create organometallic dipeptide complexes **3.11**.<sup>20</sup>

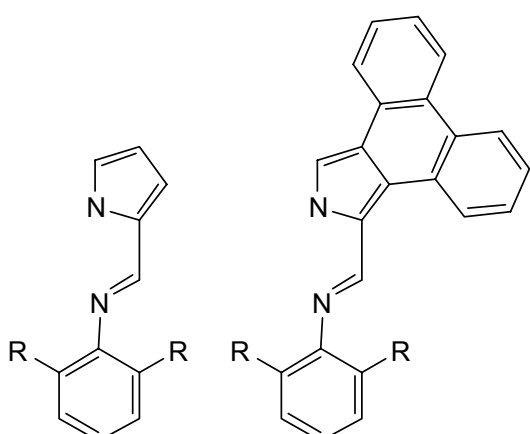
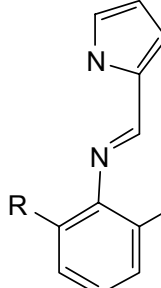
Pyrroleimines may be considered structurally similar to pyridineimines but are anionic rather than neutral when coordinated. Pyrroleimine complexes of Co(II), Ni(II), Pd(II), Cu(II) and Zn(II) were reported in the 1960s.<sup>22</sup> However, there are very few



**3.12**



**3.13**



	$\lambda_{\text{em}}$		$\lambda_{\text{em}}$	
<b>R = H</b>	<b>472</b>	<b>a</b>	<b>R = H</b>	<b>494</b>
<b>= <i>i</i>Pr</b>	<b>434</b>	<b>b</b>	<b>= <i>i</i>Pr</b>	<b>459</b>

reports on the complexes of these ligands with platinum group metals.<sup>23</sup> More recently, pyrroleimine complexes have been used as precatalysts for olefin polymerization, for example complex **3.12**, shows high activity for the polymerisation of norbornene, in the presence of methylaluminoxane (MMAO).<sup>24</sup>

Recently, Gomes *et al.* reported Zn(II) complexes **3.13** of pyrroleimines,<sup>25</sup> the luminescent properties were tuned by the modification of pyrroleimine ligands. According to DFT calculations, the LUMO resides on the pyrrole/phenanthrene ring and the imine C=N  $\pi$  bond, while the HOMO resides on the phenyl ring. The emission is red shifted upon increasing the conjugation on the pyrrole (compare **3.13a** *vs* **3.13c** and **3.13b** *vs* **3.13d**), however, it is blue shifted upon substituting H with <sup>i</sup>Pr (compare **3.13a** *vs* **3.13b** and **3.13c** *vs* **3.13d**).

This **Chapter** will investigate the synthesis and luminescent properties of  $[\text{Ir}(\text{C}^{\text{N}})^2(\text{X}^{\text{Y}})]^+$  ( $\text{X}^{\text{Y}} =$  pyridineimine) complexes to confirm their potential photoactivity and assess their applications in cell imaging. The ability to tune the emission wavelength will be explored by varying the cyclometallated ( $\text{C}^{\text{N}}$ ) ligand and/or the substituents on the imine. Neutral complexes  $[\text{Ir}(\text{C}^{\text{N}})^2(\text{pyrrolylimine})]$  are synthesised for comparison.

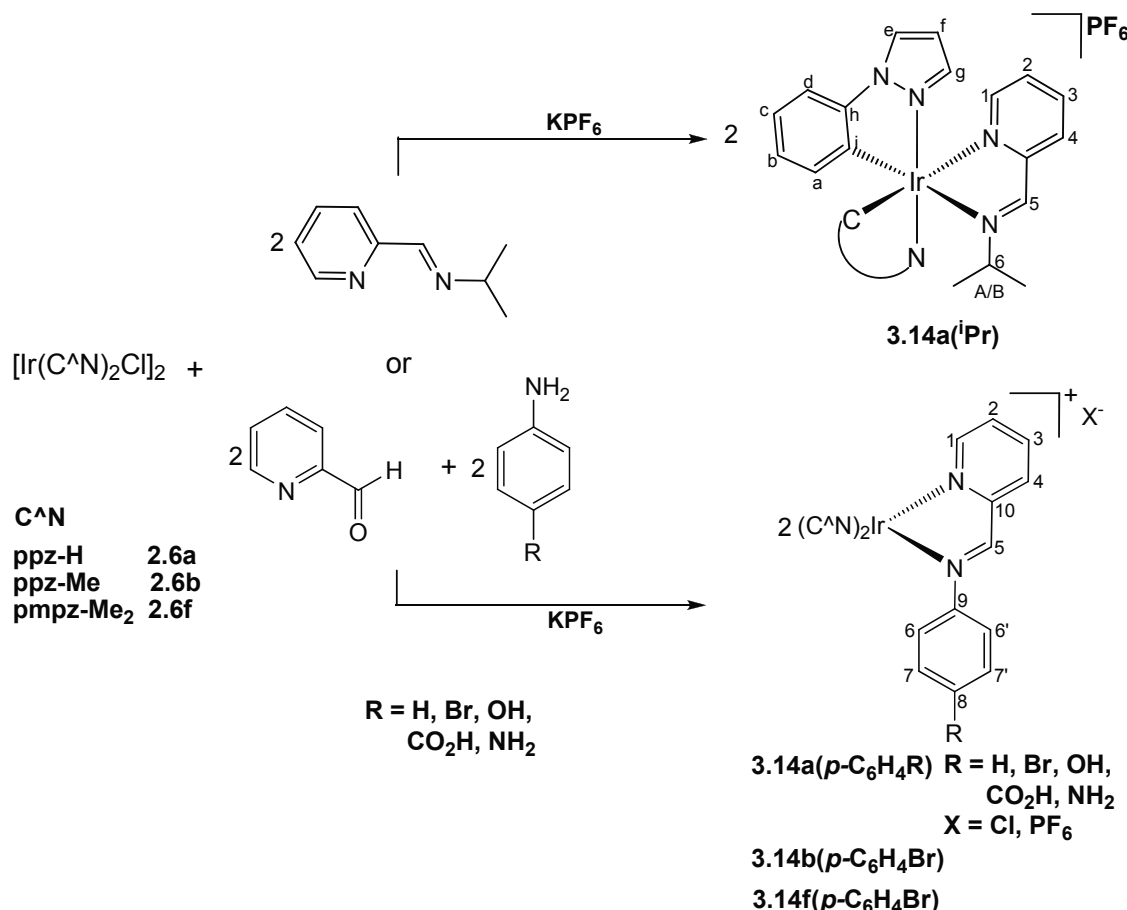
## 3.2 Results and Discussion

### 3.2.1 Synthesis and Characterisation of $[\text{Ir}(\text{C}^{\text{N}})^2(\text{pyridineimine})]^+$ (3.14)

( $\text{C}^{\text{N}} = \text{ppzR}_1, \text{pmpz-Me}_2, \text{ppy, thpy}$ )

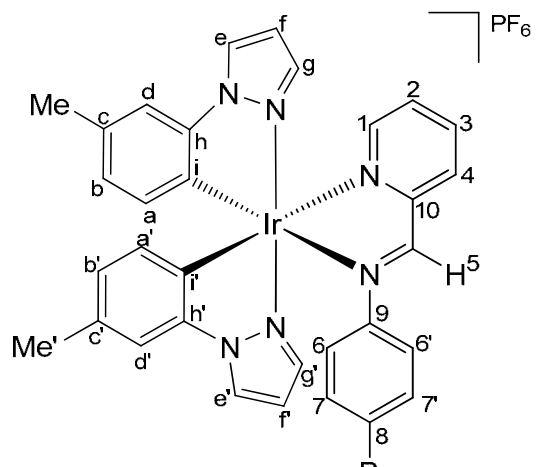
The  $\text{N}^{\text{i}}\text{Pr}$  pyridineimine was synthesized using a literature method.<sup>26</sup> The dimer **2.6a**,  $\text{KPF}_6$  and the ligand, were heated in ethanol under microwave irradiation for 30 mins at 100 °C to form compound **3.14a(iPr)** in 85% yield. Having established that the reaction worked well, the possibility of forming the ligand *in situ* was investigated. If successful this would, in principle, allow a high throughput screening approach to be used for the synthesis of analogs. The reactions of dimers **2.6a,b f** with pyridine-2-carboxaldehyde and the relevant amine ( $\text{R} = \text{H, Br, OH, CO}_2\text{H, NH}_2$ ) and  $\text{KPF}_6$  were carried out in methanol at 60 °C under microwave irradiation for 20 mins, to form compounds **3.14a(p-C}\_6\text{H}\_4\text{R)** ( $\text{R} = \text{H, Br, OH, CO}_2\text{H, NH}_2$ ), **3.14b(p-C}\_6\text{H}\_4\text{Br)** and **3.14f(p-C}\_6\text{H}\_4\text{Br)** in good yields (> 80%) (**Scheme 3.1**). Either the pyridineimine ligands were generated *in situ* or else they are formed after coordination of pyridine-2-

carboxaldehyde to the metal.<sup>27</sup> During the synthesis of **3.14a**(*p*-C<sub>6</sub>H<sub>4</sub>NH<sub>2</sub>) an excess (4 equiv) of amine was used in order to reduce the possibility of condensation of the diamine with two equivalents of pyridine-2-carboxaldehyde, which may then bridge two iridium centres. In the case of the chloride salt of **3.14b**(*p*-C<sub>6</sub>H<sub>4</sub>OH), KPF<sub>6</sub> was omitted and the complex was formed in a similar yield.



**Scheme 3.1**

The <sup>1</sup>H and <sup>13</sup>C-<sup>1</sup>H NMR spectra of complexes **3.14a(iPr)** and **3.14a(p-C<sub>6</sub>H<sub>4</sub>R)** are very complicated due to the loss of C<sub>2</sub>-symmetry present in the dimers, hence, in principle, all the protons in the complex are inequivalent. The assignment of complex **3.14b(p-C<sub>6</sub>H<sub>4</sub>Br)** is explained in detail. Important parts of the TOCSY, NOESY, COSY and HSQC spectra are shown in **Figs. 3.1-4** respectively. The TOCSY spectrum of **3.14b(p-C<sub>6</sub>H<sub>4</sub>Br)** allowed identification of two phenyls (----), two pyrazoles (—) and one pyridyl ring (---). The imine proton H<sub>5</sub> is easily identified as the most downfield singlet, at  $\delta$  9.21, and shows an NOE to one part of an [AA'BB'] system at *ca.*  $\delta$  6.8 which is therefore assigned to the N-aryl protons H<sub>6,6'</sub> the other part, at  $\delta$  7.3 is assigned to H<sub>7,7'</sub>. H<sub>5</sub> also shows an NOE to a doublet of doublets at  $\delta$  8.38 which is therefore



**3.14b(*p*-C<sub>6</sub>H<sub>4</sub>Br)**

assigned as H<sub>4</sub> and the COSY spectrum then allows assignment of protons H<sub>1</sub>, H<sub>2</sub> and H<sub>3</sub> (note H<sub>1</sub> and H<sub>3</sub> are overlapping multiplets). The imine proton H<sub>5</sub> also shows a weak NOE to the pyrazole proton H<sub>g</sub> which is a doublet at  $\delta$  7.46 which then allows assignment of the other pyrazole protons (H<sub>e</sub> and H<sub>f</sub>) using the COSY spectrum. Proton H<sub>e</sub> is a multiplet at *ca.*  $\delta$  8.1 and shows an NOE to a singlet at  $\delta$  7.16 which is therefore assigned as phenyl proton H<sub>d</sub> and then the other phenyl protons H<sub>a</sub> and H<sub>b</sub> are assigned *via* the COSY and TOCSY spectra. H<sub>a</sub> is at characteristically high field<sup>28</sup> (see **Chapter 2**) and shows an NOE to the other pyrazole ring proton H<sub>g'</sub> and the COSY spectrum then allows the assignment of the other pyrazole protons H<sub>e'</sub> and H<sub>f'</sub>. H<sub>e'</sub> is a doublet of doublets at  $\delta$  8.06 which shows an NOE to a singlet at  $\delta$  6.98 which is therefore assigned as H<sub>d'</sub>. The other phenyl protons H<sub>a'</sub> and H<sub>b'</sub> are then assigned *via* the COSY and TOCSY spectra. Having assigned H<sub>a</sub> and H<sub>a'</sub> the chemical shifts ( $\delta$  6.09 and 5.93 respectively) can be explained since H<sub>a'</sub> is affected by a neighbouring N-aryl imine substituent. Assignment of the methyls (Me and Me') is possible due to the observation of an NOE between protons H<sub>b,d</sub> and Me and between H<sub>b',d'</sub> and Me'. H<sub>g'</sub> is observed at a higher field than H<sub>g</sub> ( $\delta$  6.88 compared to  $\delta$  7.46), because it is shielded by the ring current of the pyridyl ring confirmed in the X-ray structure (H on C(1) **Fig. 3.5**). The <sup>13</sup>C- $\{{}^1\text{H}\}$  NMR spectra show the expected number of signals for the quaternary and CH carbons. Having assigned the proton spectrum, the coupled carbons were determined using the HSQC spectrum and the quaternary carbons using the HMBC spectrum. The FAB mass spectrum shows a molecular ion for the cation at *m/z* 767.

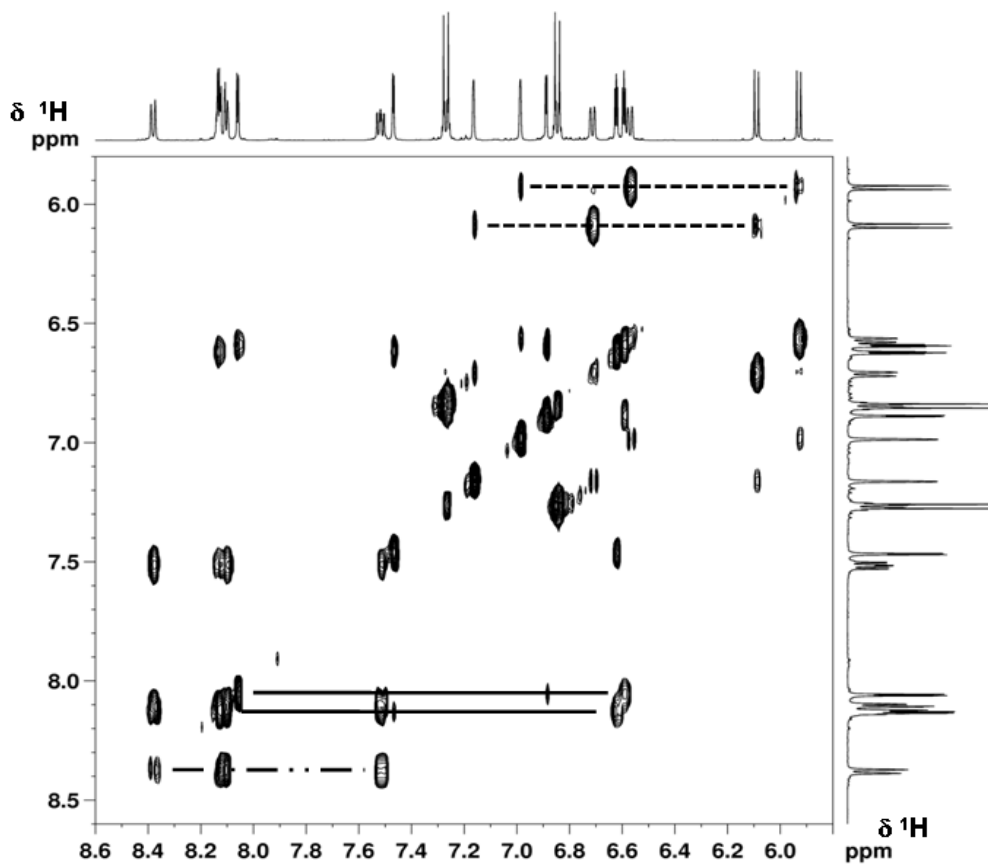


**Fig. 3.1:** Aromatic part of the TOCSY spectrum of **3.14b(p-C<sub>6</sub>H<sub>4</sub>Br)** showing identification of two cyclometallated phenyls (----), two pyrazoles (—) and one pyridine ring (---—---).

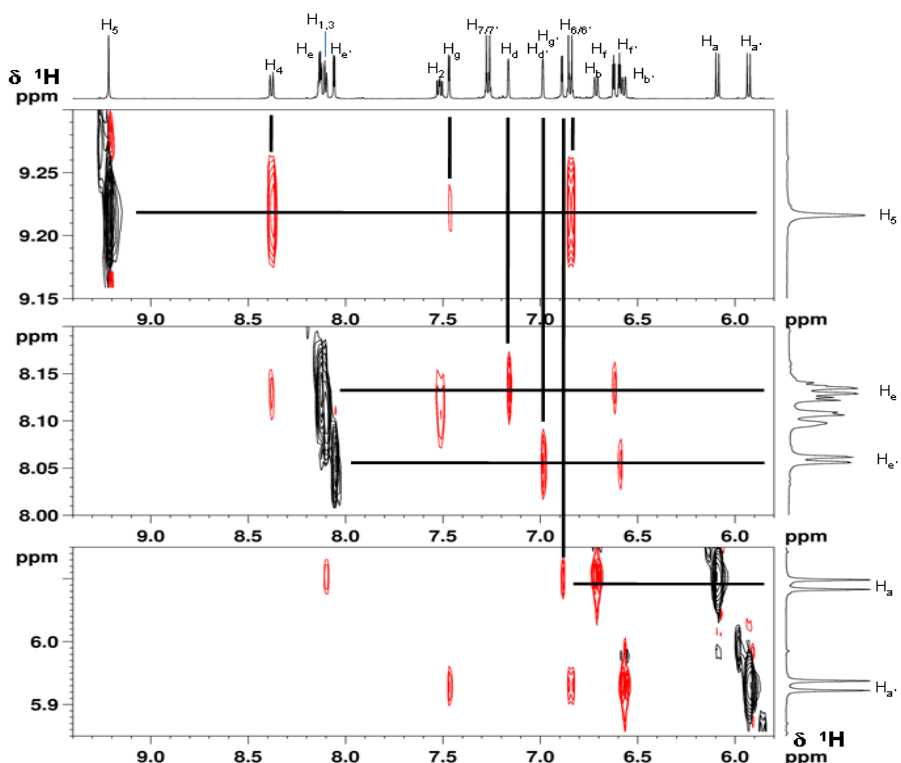


**Fig. 3.2:** NOESY spectrum of **3.14b(p-C<sub>6</sub>H<sub>4</sub>Br)** showing some key NOEs.

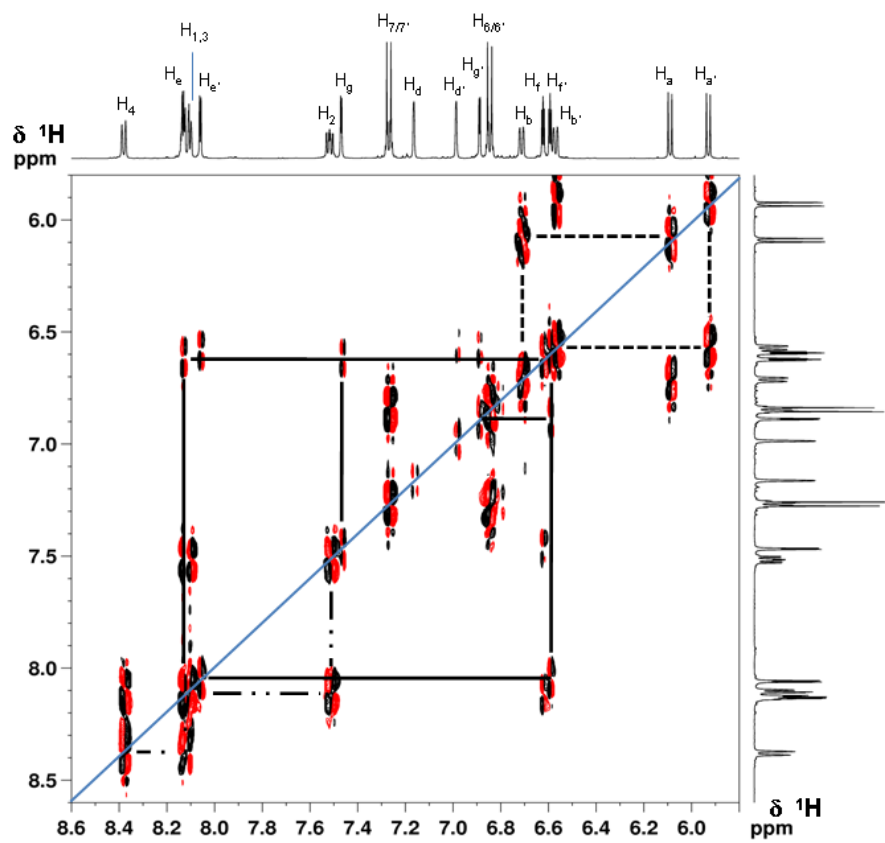


**Fig. 3.3:** COSY spectrum of **3.14b**(*p*-C<sub>6</sub>H<sub>4</sub>Br) showing one bond correlations.

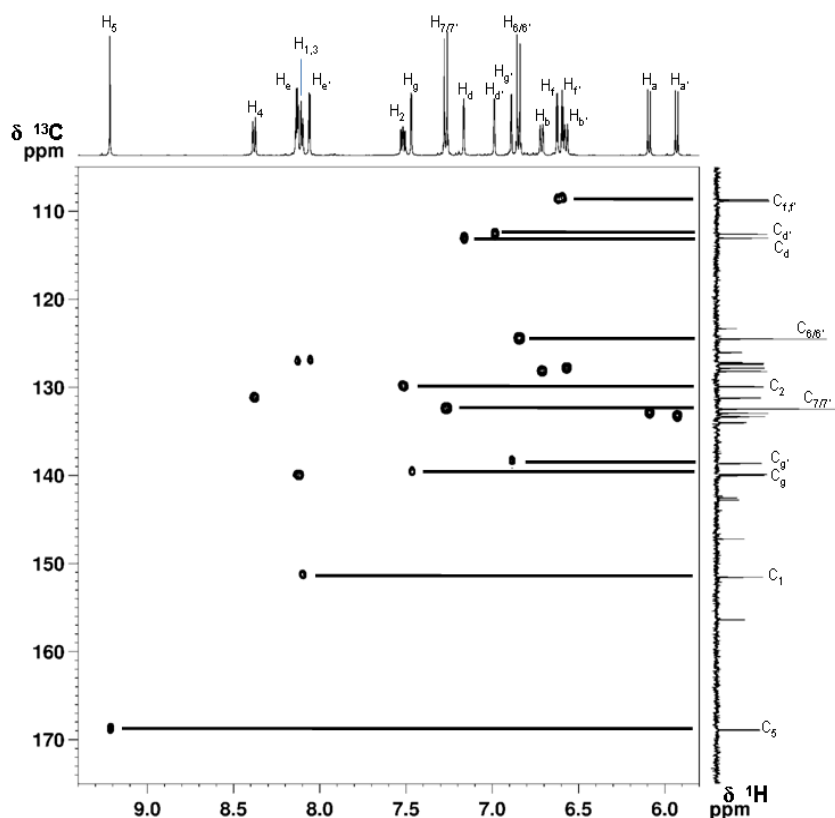


**Fig. 3.4:** HMQC spectrum of **3.14b**(*p*-C<sub>6</sub>H<sub>4</sub>Br) showing some direct C-H couplings.

Crystallisation of **3.14b(p-C<sub>6</sub>H<sub>4</sub>Br)** by slow diffusion of hexane into a DCM solution of the salt afforded crystals suitable for X-ray crystallography. The crystal structure (**Fig. 3.5**) reveals the expected distorted octahedral coordination geometry [N(1)—Ir(1)—N(3) is 171.7°] (**Fig. 3.5**), with *cis* metallated carbons and *trans* nitrogen atoms, as found for the bipy complexes. The Ir—N (N<sup>+</sup>N) bond distances [2.155(7) and 2.152(8) Å] are longer than the Ir—N (C<sup>+</sup>N) ones 2.044(7) and 2.023(6) Å] due to the *trans* influence of the Ir—C bonds similar to bipy complexes (**2.7a-f**). The phenyl ring is twisted about 50° with respect to the pyridineimine unit. The tris chelate cation is chiral and both enantiomers are observed in the unit cell. Selected bond lengths (Å) and angles (°) are shown in **Fig. 3.5**.

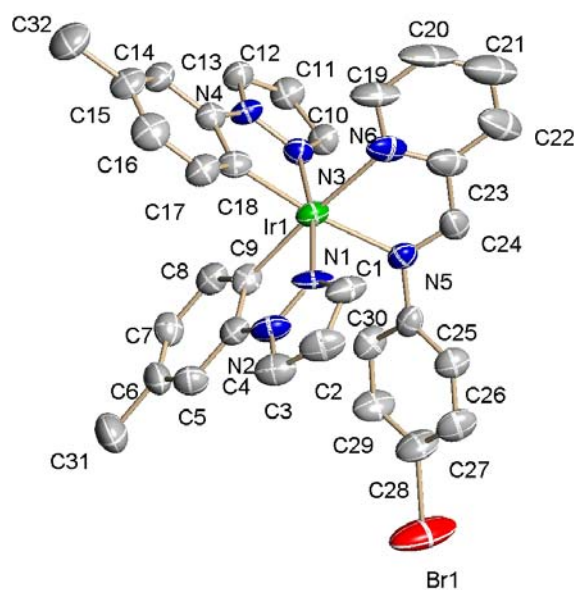


**Fig. 3.5:** X-ray crystal structure of the cation of **3.14b(p-C<sub>6</sub>H<sub>4</sub>Br)**. Selected bond lengths (Å) and bond angles (°): Ir(1)—N(1), 2.044(7); Ir(1)—N(3), 2.023(6); Ir(1)—N(5), 2.155(7); Ir(1)—N(6), 2.152(8); Ir(1)—C(9), 2.008(8); Ir(1)—C(18), 2.027(9); N(1)—Ir(1)—N(3), 172.3(3); N(1)—Ir(1)—C(9), 79.8(3); N(3)—Ir(1)—C(18), 79.6(3); N(5)—Ir(1)—N(6), 75.8(3).

<sup>a</sup>There were two independent molecules in the unit cell, therefore the data is an average of the two molecules.

The <sup>1</sup>H NMR spectra of **3.14a(p-C<sub>6</sub>H<sub>4</sub>Br)** and **3.14f(p-C<sub>6</sub>H<sub>4</sub>Br)** are similar to **3.14b(p-C<sub>6</sub>H<sub>4</sub>Br)**, notably the imine proton H<sub>5</sub> is the most downfield signal in each case ( $\delta$  9.33 and 9.20 respectively). NOEs are similar to those observed in **3.14b(p-C<sub>6</sub>H<sub>4</sub>Br)**. The phenyl signals for **3.14a(p-C<sub>6</sub>H<sub>4</sub>Br)** and **3.14f(p-C<sub>6</sub>H<sub>4</sub>Br)** are slightly

more complex having an extra proton in place of the methyl. For **3.14f(p-C<sub>6</sub>H<sub>4</sub>Br)** there are fewer pyrazole protons but there are four methyl signals, two on each pyrazole. The <sup>13</sup>C-<sup>1</sup>H NMR spectra show the expected signals and the FAB mass spectra show peaks for the cations. The X-ray crystal structures of **3.14a(p-C<sub>6</sub>H<sub>4</sub>Br)** and **3.14f(p-C<sub>6</sub>H<sub>4</sub>Br)** were determined and are shown in **Fig. 3.6** with selected bond lengths (Å) and angles (°) in **Table 3.1**.

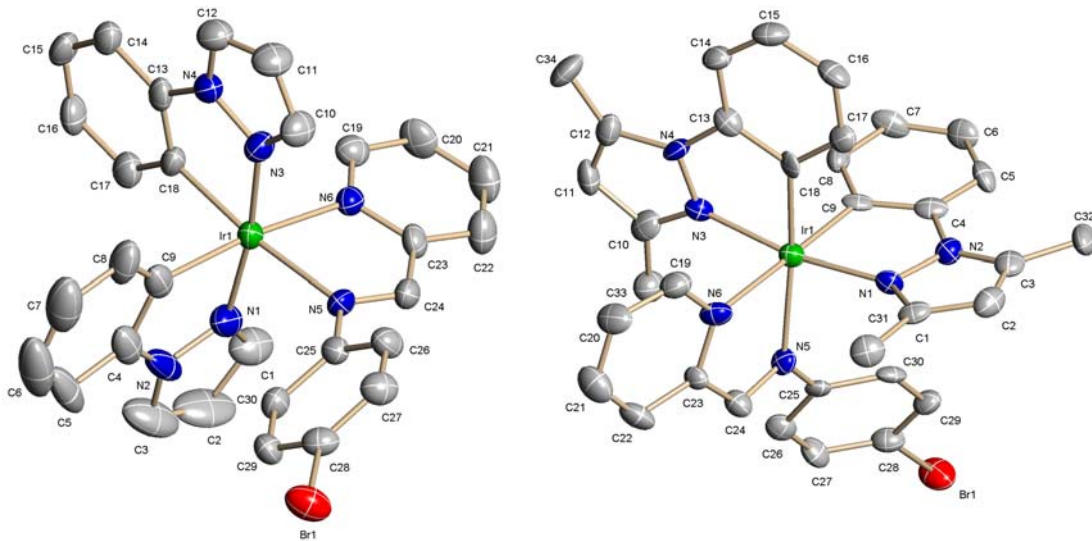


**Fig. 3.6:** X-ray crystal structures for the cations of **3.14a(p-C<sub>6</sub>H<sub>4</sub>Br)** and **3.14f(p-C<sub>6</sub>H<sub>4</sub>Br)** respectively.

**Table 3.1:** Selected bond lengths (Å) and angles (°) for **3.14a(p-C<sub>6</sub>H<sub>4</sub>Br)** and **3.14f(p-C<sub>6</sub>H<sub>4</sub>Br)** respectively.

(Å)	<b>3.14a</b> ( <i>p</i> -C <sub>6</sub> H <sub>4</sub> Br)	<b>3.14f</b> ( <i>p</i> -C <sub>6</sub> H <sub>4</sub> Br)	(°)	<b>3.14a</b> ( <i>p</i> -C <sub>6</sub> H <sub>4</sub> Br)	<b>3.14f</b> ( <i>p</i> -C <sub>6</sub> H <sub>4</sub> Br)
Ir(1)—N(1)	2.003(4)	2.019(6)	N(1)—Ir(1)—N(3)	172.28(16)	169.6(3)
Ir(1)—N(3)	2.021(4)	2.025(7)	N(1)—Ir(1)—C(9)	81.6(2)	79.4(3)
Ir(1)—N(5)	2.157(4)	2.201(6)	N(3)—Ir(1)—C(18)	80.35(18)	79.5(3)
Ir(1)—N(6)	2.135(4)	2.142(7)	N(5)—Ir(1)—N(6)	76.50(15)	75.3(2)
Ir(1)—C(9)	2.027(5)	2.007(8)			
Ir(1)—C(18)	2.023(5)	1.990(8)			

The <sup>1</sup>H and <sup>13</sup>C NMR spectra of **3.14a(p-C<sub>6</sub>H<sub>4</sub>R)**, R = H, OH, CO<sub>2</sub>H, NH<sub>2</sub> are very similar to **3.14C<sup>a</sup>N(p-C<sub>6</sub>H<sub>4</sub>Br)** (C<sup>a</sup>N = a, b, f) and also to each other except the signals of the R-groups. For all the complexes **3.14a(p-C<sub>6</sub>H<sub>4</sub>R)**, R = H, OH, CO<sub>2</sub>H, NH<sub>2</sub> the imine proton, H<sub>5</sub> is always the most downfield signal (between  $\delta$  9.43 to 9.19)

and the key NOEs which are used in the assignments of the protons are similar to those in **3.14b(p-C<sub>6</sub>H<sub>4</sub>Br)**. The phenyl protons H<sub>a,a'</sub> are always the most highfield signals ( $\delta$  6.06-6.27) due to ring current effects. The only significant difference in the spectra is the chemical shift of the N-aryl protons H<sub>7/7'</sub> which vary from ca.  $\delta$  6.5 for R = NH<sub>2</sub> and OH through to  $\delta$  7.6 (R = CO<sub>2</sub>H), consistent with similar shifts for the free arylamines.<sup>29, 30</sup> The <sup>13</sup>C- $\{{}^1\text{H}\}$  NMR spectra show the expected signals and the FAB mass spectra show peaks for the cations in each one of these. The X-ray crystal structures of **3.14a(C<sub>6</sub>H<sub>5</sub>)** and **3.14a(p-C<sub>6</sub>H<sub>4</sub>CO<sub>2</sub>H)** were determined and are shown in **Fig. 3.7** with selected bond lengths (Å) and angles (°) in **Table 3.2**.

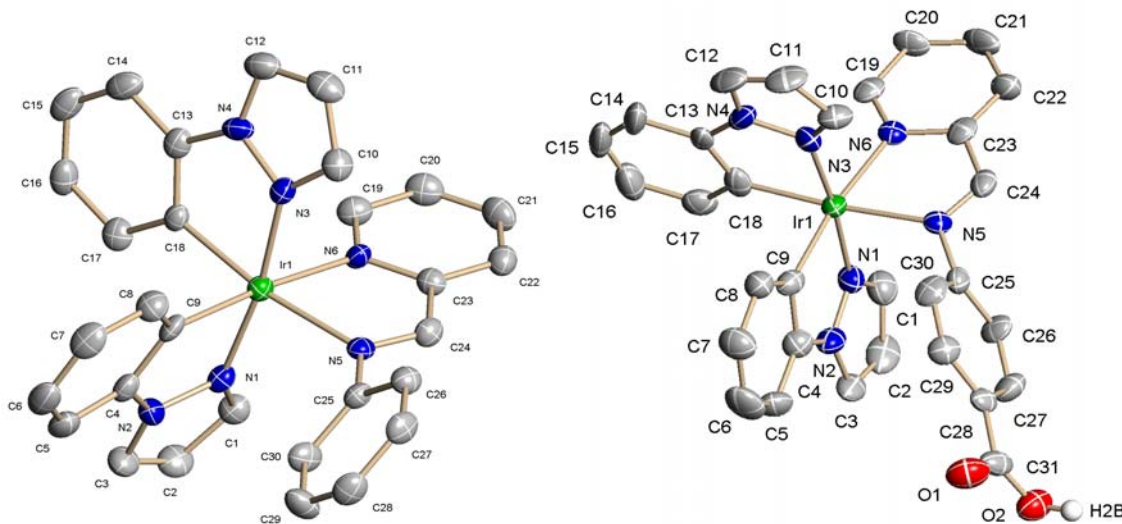


**Fig. 3.7:** X-ray crystal structure for the cations of **3.14a(C<sub>6</sub>H<sub>5</sub>)** and **3.14a(p-C<sub>6</sub>H<sub>4</sub>CO<sub>2</sub>H)** respectively.

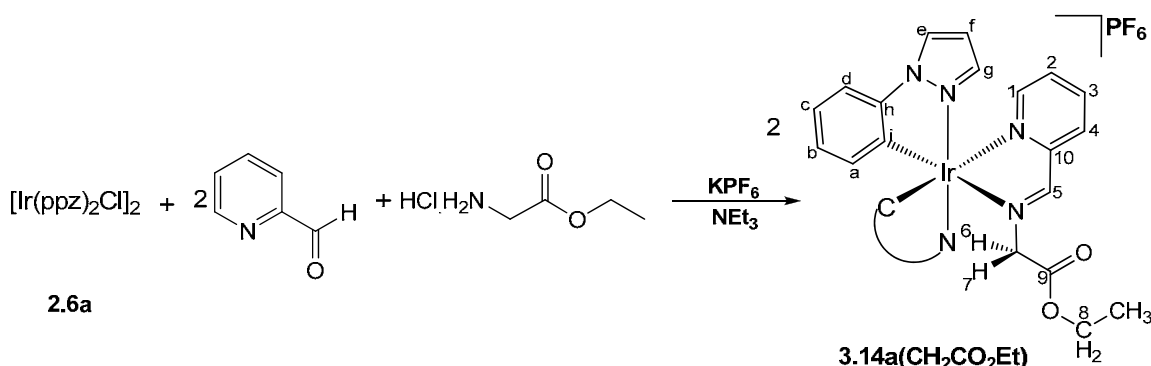
**Table 3.2:** Selected bond lengths (Å) and angles (°) for **3.14a(C<sub>6</sub>H<sub>5</sub>)** and **3.14a(p-C<sub>6</sub>H<sub>4</sub>CO<sub>2</sub>H)**.

(Å)	<b>3.14a</b> (C <sub>6</sub> H <sub>5</sub> )	<b>3.14a</b> (p-C <sub>6</sub> H <sub>4</sub> CO <sub>2</sub> H)	(°)	<b>3.14a</b> (C <sub>6</sub> H <sub>5</sub> )	<b>3.14a</b> (p-C <sub>6</sub> H <sub>4</sub> CO <sub>2</sub> H)
Ir(1)—N(1)	2.003(4)	2.035(8)	N(1)—Ir(1)—N(3)	171.40(18)	173.6(3)
Ir(1)—N(3)	2.020(4)	2.025(8)	N(1)—Ir(1)—C(9)	79.7(2)	80.7(3)
Ir(1)—N(5)	2.143(4)	2.127(7)	N(3)—Ir(1)—C(18)	79.7(2)	79.9(4)
Ir(1)—N(6)	2.124(4)	2.127(7)	N(5)—Ir(1)—N(6)	76.46(17)	76.9(3)
Ir(1)—C(9)	2.009(5)	1.997(10)			
Ir(1)—C(18)	2.020(5)	2.016(9)			

<sup>a</sup>For **3.14a(p-C<sub>6</sub>H<sub>4</sub>CO<sub>2</sub>H)** there were two independent molecules in the unit cell, therefore the data is an average of values for both molecules.

The  $^1\text{H}$  NMR spectrum of **3.14a(iPr)** is similar to **3.14a(*p*-C<sub>6</sub>H<sub>4</sub>R)** (R = H, Br, OH, CO<sub>2</sub>H, NH<sub>2</sub>) except for the signals of the R group. The imine proton H<sub>5</sub> ( $\delta$  9.28) shows an NOE to all signals of the isopropyl substituent. The two methyl groups Me<sub>A</sub> and Me<sub>B</sub> ( $\delta$  1.12 and 1.01) are inequivalent consistent with the chirality at the metal centre. The phenyl protons H<sub>a,a'</sub> are observed as doublet of doublets at high field ( $\delta$  6.22 and 6.36 respectively) The  $^{13}\text{C}$ –{ $^1\text{H}$ } NMR spectra show the expected signals and the FAB mass spectrum shows a molecular ion for the cation at *m/z* 627. The X-ray crystal structure of **3.14a(iPr)** was determined and is shown with selected bond lengths (Å) and angles (°) in **Fig. 3.8** and **Table 3.3**, respectively.

As mentioned earlier, complexes incorporating an amino acid or amino acid ester have been used as a convenient way to functionalise biological molecules.<sup>15, 18, 20</sup> Hence the synthesis of **3.14a(CH<sub>2</sub>CO<sub>2</sub>Et)** was attempted. Complex **3.14a(CH<sub>2</sub>CO<sub>2</sub>Et)** was synthesised in 77% yield *via* a similar method to **Scheme 3.1** except the temperature was reduced to 50 °C and triethylamine was added to deprotonate the hydrochloride salt used (**Scheme 3.2**).



**Scheme 3.2**

The  $^1\text{H}$  NMR spectrum of **3.14a(CH<sub>2</sub>CO<sub>2</sub>Et)** is similar to **3.14a(iPr)**, notably H<sub>a,a'</sub> are at relatively high field ( $\delta$  6.22 and 6.28 respectively). The imine proton H<sub>5</sub> is the most downfield signal ( $\delta$  9.16) and shows an NOE to the NCH<sub>2</sub> group which is observed as two mutually coupled doublets ( $\delta$  4.60 and 4.42, (H<sub>6,7</sub>) respectively) as the protons are diastereotopic due to chirality at the metal center. The  $^{13}\text{C}$ –{ $^1\text{H}$ } NMR spectra show the expected signals and the FAB mass spectrum shows a molecular ion for the cation at *m/z* 671. The X-ray crystal structure of **3.14a(CH<sub>2</sub>CO<sub>2</sub>Et)** was determined and is shown with selected bond lengths (Å) and angles (°) in **Fig. 3.8** and **Table 3.3**, respectively.

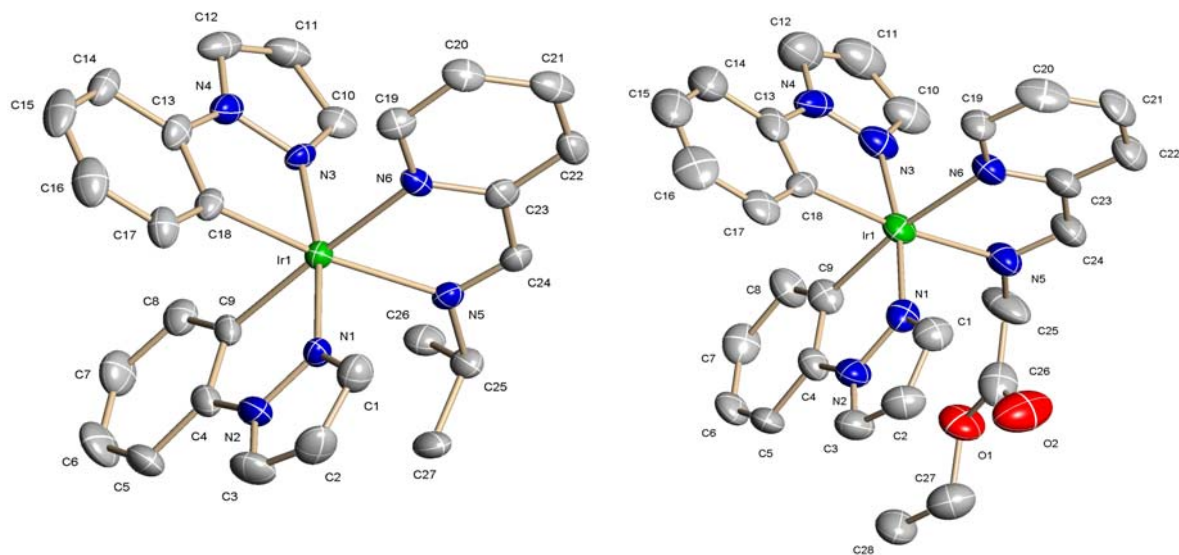
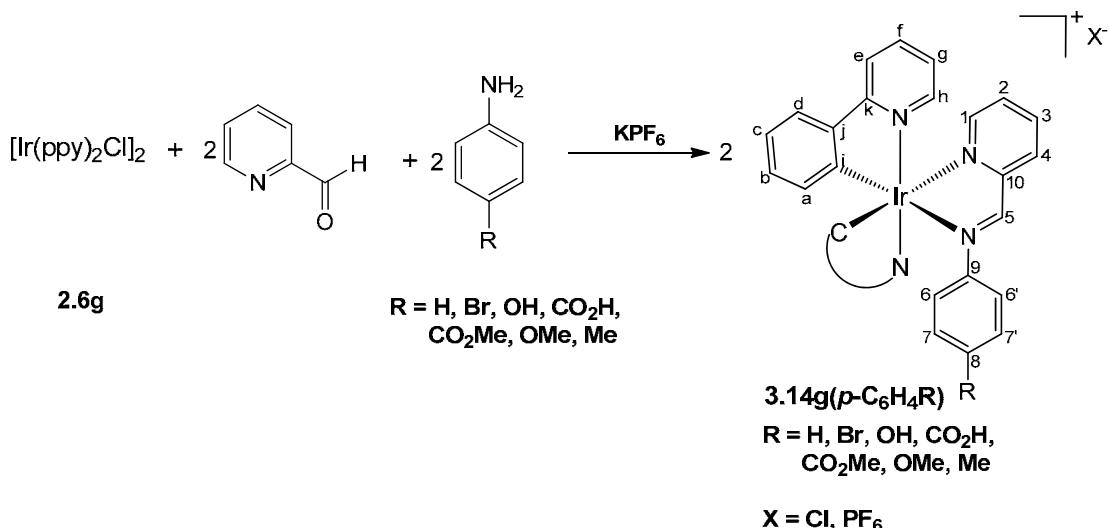


**Fig. 3.8:** X-ray crystal structure for the cations of **3.14a(iPr)** and **3.14a(CH<sub>2</sub>CO<sub>2</sub>Et)** respectively.

**Table 3.3:** Selected bond lengths (Å) and bond angles (°) for **3.14a(iPr)** and **3.14a(CH<sub>2</sub>CO<sub>2</sub>Et)**, respectively.

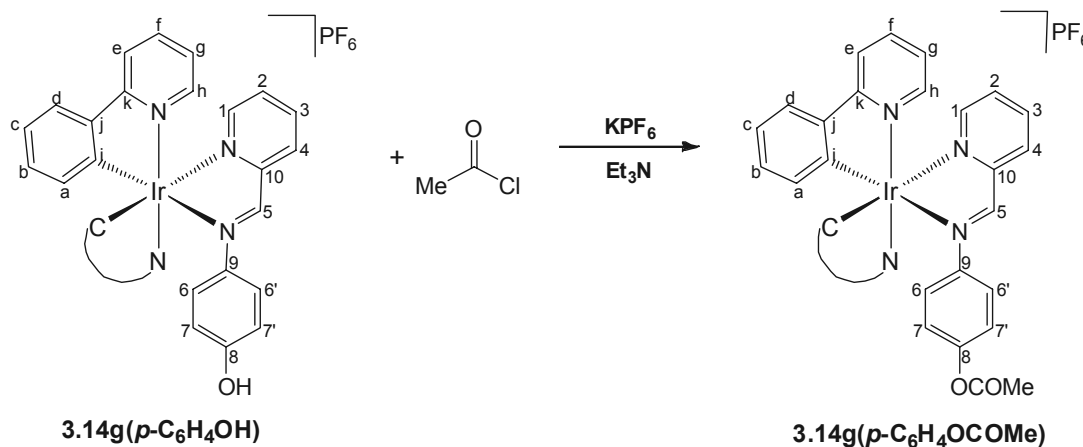
(Å)	<b>3.14a (iPr)</b>	<b>3.14a (CH<sub>2</sub>CO<sub>2</sub>Et)</b>	(°)	<b>3.14a (iPr)</b>	<b>3.14a (CH<sub>2</sub>CO<sub>2</sub>Et)</b>
Ir(1)—N(1)	2.028(5)	2.009(8)	N(1)—Ir(1)—N(3)	171.45(18)	171.7(3)
Ir(1)—N(3)	2.034(4)	2.031(9)	N(1)—Ir(1)—C(9)	79.5(2)	80.6(4)
Ir(1)—N(5)	2.166(4)	2.097(8)	N(3)—Ir(1)—C(18)	80.7(2)	79.6(4)
Ir(1)—N(6)	2.133(4)	2.158(8)	N(5)—Ir(1)—N(6)	75.76(17)	76.7(3)
Ir(1)—C(9)	2.029(6)	2.022(9)			
Ir(1)—C(18)	2.010(5)	2.038(10)			

The reactions of dimer **2.6g** with pyridine-2-carboxaldehyde and the relevant amine (R = H, Br, OH, CO<sub>2</sub>H, CO<sub>2</sub>Me, OMe, Me) and KPF<sub>6</sub> were carried out under microwave irradiation, to form compounds **3.14g(p-C<sub>6</sub>H<sub>4</sub>R)** (R = H, Br, OH, CO<sub>2</sub>H, CO<sub>2</sub>Me, OMe, Me) in good yields (>80%) (**Scheme 3.3**). Early experiments used heating for 30 mins at 100 °C in ethanol but later experiments used milder conditions (20 mins at 60 °C in methanol). In the case of Cl salts i.e **3.14g(p-C<sub>6</sub>H<sub>4</sub>OH)** and **3.14g(p-C<sub>6</sub>H<sub>4</sub>CO<sub>2</sub>H)**, the KPF<sub>6</sub> was omitted and the complexes were formed in the similar yields.



### Scheme 3.3

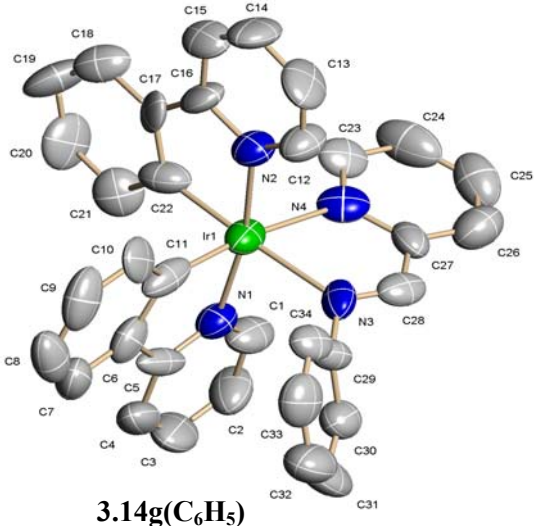
The  $^1\text{H}$  and  $^{13}\text{C}$  NMR spectra of **3.14g(p-C<sub>6</sub>H<sub>4</sub>R)**, (R = H, Br, OH, CO<sub>2</sub>H, CO<sub>2</sub>Me, OMe, Me) are similar to **3.14a(p-C<sub>6</sub>H<sub>4</sub>R)**, and also to each other but the presence of two more pyridine rings rather than pyrazoles does complicate the assignments. All the compounds **3.14g(p-C<sub>6</sub>H<sub>4</sub>R)**, show some key NOEs, for example, the imine proton H<sub>5</sub> shows NOEs to the pyridine proton H<sub>4</sub> and the N-aryl protons H<sub>6,6'</sub>, and to the pyridine proton H<sub>h</sub> of one of the cyclometallated ligands. There are also NOEs between H<sub>h</sub> and the *ortho* phenyl proton (H<sub>a'</sub>) of the other cyclometallated ligand, similarly H<sub>h'</sub> shows an NOE to H<sub>a</sub>. On each cyclometallated ligand, there is an NOE between the phenyl proton H<sub>d</sub> and the pyridine proton H<sub>e</sub> similarly (H<sub>d'</sub> and H<sub>e'</sub>). The protons H<sub>a,a'</sub> are observed as doublet of doublets between  $\delta$  6.25-6.15 and  $\delta$  6.19-6.10, for H<sub>a</sub> and H<sub>a'</sub> respectively, H<sub>a'</sub> is always observed at higher field than H<sub>a</sub> due to the ring current from the N-aryl substituent as found in **3.14a(p-C<sub>6</sub>H<sub>4</sub>R)**. The signal for H<sub>h'</sub> is upfield of that for H<sub>h</sub> due to the ring current of the pyridine ring of the pyridineimine. The variation in chemical shift of the protons (H<sub>7/7'</sub>) is consistent with the free substituted arylamines, as found in **3.14a(p-C<sub>6</sub>H<sub>4</sub>R)**.<sup>29, 30</sup> The  $^{13}\text{C}-\{^1\text{H}\}$  NMR spectra show the expected signals for CH and quaternary carbons and the FAB mass spectra show molecular ions for the cations.



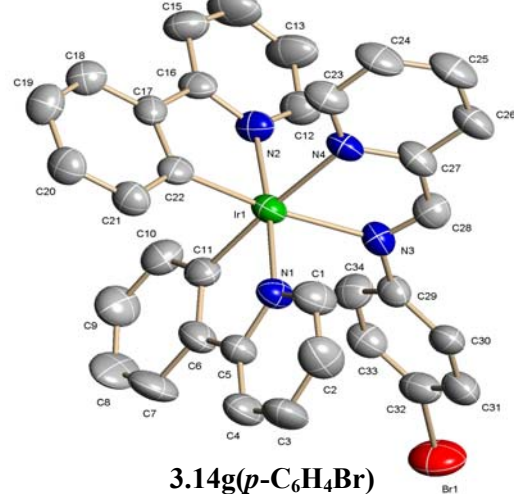
**Scheme 3.4**

A number of the complexes have reactive functional groups present (*e.g.* OH, COOH, NH<sub>2</sub>, CO<sub>2</sub>Me, Br) which provide scope for the post-coordination functionalisation of the complexes and also these may be used to attach other molecules *e.g.* for bioconjugation. Complex **3.14g(*p*-C<sub>6</sub>H<sub>4</sub>OCOMe)** was synthesised by a condensation reaction between **3.14g(*p*-C<sub>6</sub>H<sub>4</sub>OH)** and acetyl chloride using triethylamine as a base in 82% yield (**Scheme 3.4**). The identity of **3.14g(*p*-C<sub>6</sub>H<sub>4</sub>OCOMe)** was confirmed by the observation of a singlet at  $\delta$  2.21 for the methyl in the <sup>1</sup>H NMR spectrum and a molecular ion for the cation at *m/z* 741 in the FAB mass spectrum. The <sup>1</sup>H NMR spectrum of **3.14g(*p*-C<sub>6</sub>H<sub>4</sub>OCOMe)** is similar to **3.14g(*p*-C<sub>6</sub>H<sub>4</sub>R)** and the assignments are made on the same basis as for **3.14g(*p*-C<sub>6</sub>H<sub>4</sub>R)**. The imine proton H<sub>5</sub> is the most downfield signal ( $\delta$  9.30) and shows an NOE to the N-aryl protons H<sub>6,6'</sub>. The protons of N-aryl group show a [AA'BB'] system, giving rise to multiplets for H<sub>6,6'</sub> and H<sub>7,7'</sub> (*ca.*  $\delta$  6.9 and 6.8 respectively). The signal for H<sub>h'</sub> ( $\delta$  7.45) is upfield of that for H<sub>h</sub> ( $\delta$  8.28) due to its proximity to the pyridine (N<sup>+</sup>N) ring. The <sup>13</sup>C-{<sup>1</sup>H} NMR spectrum shows the expected signals for CH and quaternary carbons.

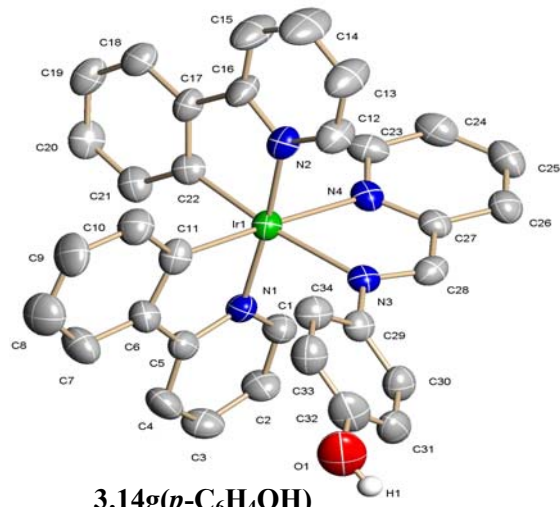
The X-ray crystal structures of **3.14g(C<sub>6</sub>H<sub>5</sub>)**, **3.14g(*p*-C<sub>6</sub>H<sub>4</sub>Br)**, **3.14g(*p*-C<sub>6</sub>H<sub>4</sub>OH)**, **3.14g(*p*-C<sub>6</sub>H<sub>4</sub>CO<sub>2</sub>H)**, **3.14g(*p*-C<sub>6</sub>H<sub>4</sub>CO<sub>2</sub>Me)** and **3.14g(*p*-C<sub>6</sub>H<sub>4</sub>OCOMe)** were determined and are shown with selected bond lengths (Å) and angles (°) in **Fig. 3.9** and **Table 3.4** respectively. The Ir(III) centre adopts an expected distorted octahedral coordination geometry in each case as the bond angle, N(1)—Ir(1)—N(3) is  $<175^\circ$  (**Table 3.4**). The Ir—N (N<sup>+</sup>N) bond distances (*ca.* 2.14 – 2.17 (Å)) are longer than the distances of Ir—N (C<sup>+</sup>N) (*ca.* 2.02 – 2.07 (Å)) for all the complexes, which can be again ascribed to the *trans* influence of the Ir—C bonds as discussed previously.



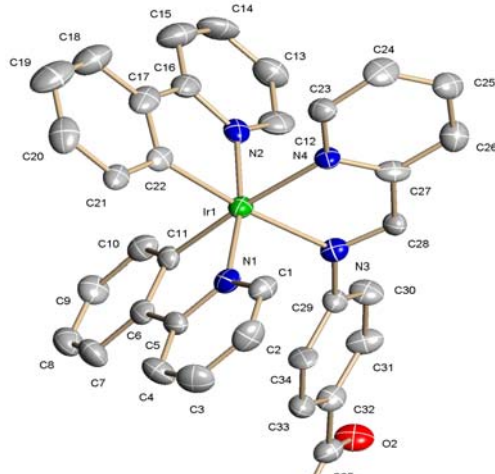
3.14g(C<sub>6</sub>H<sub>5</sub>)



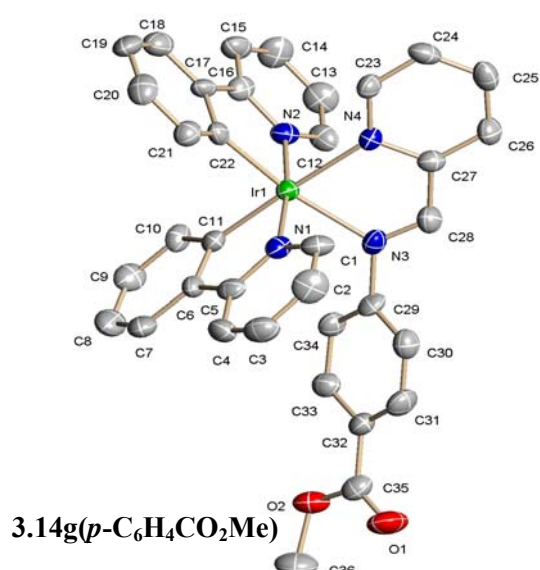
3.14g(*p*-C<sub>6</sub>H<sub>4</sub>Br)



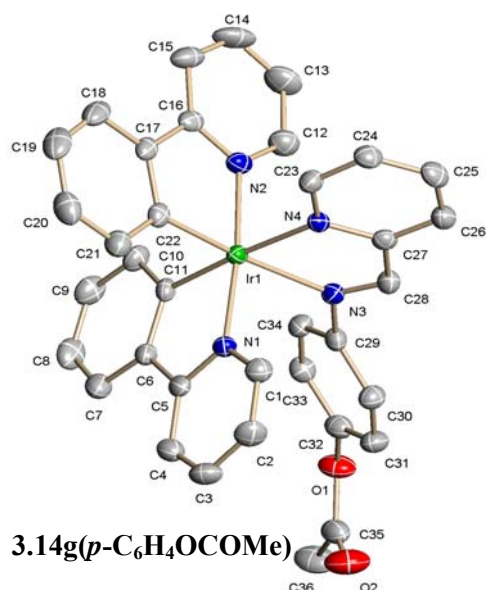
3.14g(*p*-C<sub>6</sub>H<sub>4</sub>OH)



3.14g(*p*-C<sub>6</sub>H<sub>4</sub>CO<sub>2</sub>H)



3.14g(*p*-C<sub>6</sub>H<sub>4</sub>CO<sub>2</sub>Me)



3.14g(*p*-C<sub>6</sub>H<sub>4</sub>OCOMe)

**Fig. 3.9:** X-ray crystal structures for the cations of 3.14g(C<sub>6</sub>H<sub>5</sub>), 3.14g(*p*-C<sub>6</sub>H<sub>4</sub>Br), 3.14g(*p*-C<sub>6</sub>H<sub>4</sub>OH), 3.14g(*p*-C<sub>6</sub>H<sub>4</sub>CO<sub>2</sub>H), 3.14g(*p*-C<sub>6</sub>H<sub>4</sub>CO<sub>2</sub>Me) and 3.14g(*p*-C<sub>6</sub>H<sub>4</sub>OCOMe) respectively.

**Table 3.4:** Selected bond lengths (Å) and bond angles (°) for **3.14g(C<sub>6</sub>H<sub>5</sub>)**, **3.14g(*p*-C<sub>6</sub>H<sub>4</sub>Br)**, **3.14g(*p*-C<sub>6</sub>H<sub>4</sub>OH)**, **3.14g(*p*-C<sub>6</sub>H<sub>4</sub>CO<sub>2</sub>H)**, **3.14g(*p*-C<sub>6</sub>H<sub>4</sub>CO<sub>2</sub>Me)** and **3.14g(*p*-C<sub>6</sub>H<sub>4</sub>OCOMe)** respectively.

(Å)	<b>3.14g (C<sub>6</sub>H<sub>5</sub>)</b>	<b>3.14g (<i>p</i>-C<sub>6</sub>H<sub>4</sub>Br)</b>	<b>3.14g (<i>p</i>-C<sub>6</sub>H<sub>4</sub>OH)</b>	<b>3.14g (<i>p</i>-C<sub>6</sub>H<sub>4</sub>CO<sub>2</sub>H)</b>	<b>3.14g (<i>p</i>-C<sub>6</sub>H<sub>4</sub>CO<sub>2</sub>Me)</b>	<b>3.14g (<i>p</i>-C<sub>6</sub>H<sub>4</sub>OCOMe)</b>
Ir(1)–N(1)	2.052(8)	2.053(8)	2.054(5)	2.031(7)	2.059(8)	2.047(3)
Ir(1)–N(2)	2.079(8)	2.046(8)	2.028(6)	2.047(7)	2.057(8)	2.044(3)
Ir(1)–N(3)	2.161(9)	2.175(8)	2.153(5)	2.147(6)	2.164(8)	2.173(3)
Ir(1)–N(4)	2.166(9)	2.152(8)	2.152(6)	2.141(6)	2.146(8)	2.143(3)
Ir(1)–C(11)	1.911(13)	2.046(10)	2.003(7)	1.994(8)	2.007(10)	2.018(4)
Ir(1)–C(22)	1.983(11)	2.002(10)	1.989(7)	2.011(8)	2.015(10)	1.998(4)
(°)						
N(1)–Ir(1)–N(2)	170.1(3)	175.6(3)	175.9(2)	170.4(3)	173.3(3)	174.25(12)
N(1)–Ir(1)–C(11)	79.5(4)	80.5(4)	80.8(3)	80.1(3)	80.0(4)	80.04(13)
N(2)–Ir(1)–C(22)	78.6(4)	79.6(4)	80.2(3)	80.2(3)	80.4(4)	80.39(14)
N(3)–Ir(1)–N(4)	77.3(4)	75.8(3)	75.9(2)	76.0(2)	75.2(3)	76.06(11)

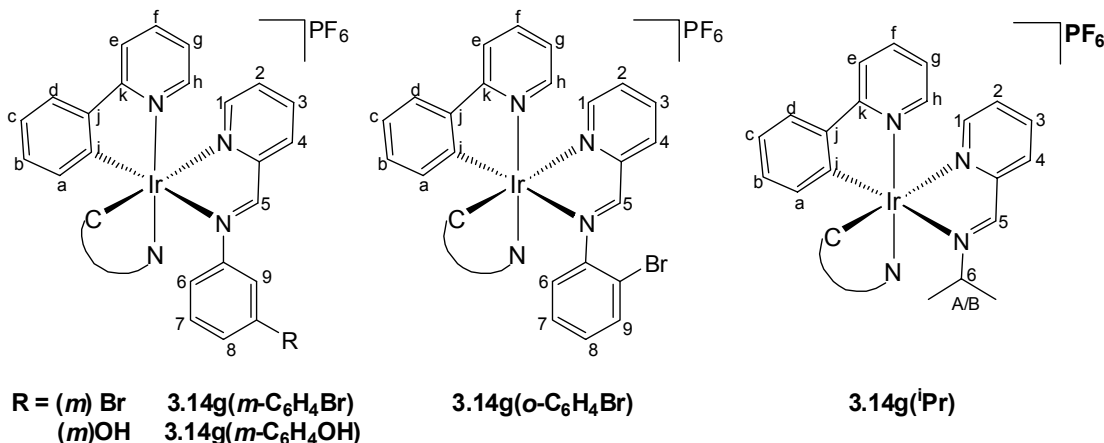


**Fig. 3.10:** Code for NMR assignments of **3.14g(*m*-C<sub>6</sub>H<sub>4</sub>Br)**, **(*m*-C<sub>6</sub>H<sub>4</sub>OH)**, **(*o*-C<sub>6</sub>H<sub>4</sub>Br)**, **(<sup>i</sup>Pr)**

Complexes **3.14g(*m*-C<sub>6</sub>H<sub>4</sub>Br)**, **3.14g(*m*-C<sub>6</sub>H<sub>4</sub>OH)**, **3.14g(*o*-C<sub>6</sub>H<sub>4</sub>Br)** and **3.14g(<sup>i</sup>Pr)** were synthesised, in good yields (61 – 80%), under microwave irradiation as for **3.14g(*p*-C<sub>6</sub>H<sub>4</sub>R)**. The code for NMR assignments is shown in **Fig. 3.10**. The <sup>1</sup>H NMR spectra of **3.14g(*m*-C<sub>6</sub>H<sub>4</sub>Br)**, **3.14g(*m*-C<sub>6</sub>H<sub>4</sub>OH)** and **3.14g(*o*-C<sub>6</sub>H<sub>4</sub>Br)** are similar to

**3.14g(*p*-C<sub>6</sub>H<sub>4</sub>R)**, notably the signals due to the cyclometallated ligands (ppy) and the pyridine ring of pyridineimine. The spectra are also similar to each other, therefore, only **3.14g(*m*-C<sub>6</sub>H<sub>4</sub>Br)** is explained in detail. The imine proton H<sub>5</sub> is the most downfield signal ( $\delta$  9.91) and shows NOEs to both the *ortho* aryl protons (H<sub>6</sub> and H<sub>9</sub>) and the COSY spectrum then allows assignment of the other N-aryl protons H<sub>7,8</sub>. The imine proton H<sub>5</sub> also shows an NOE to H<sub>4</sub> which allows the assignment of protons H<sub>1-3</sub> *via* the COSY spectrum. Proton H<sub>1</sub> shows an NOE to H<sub>a</sub> and protons H<sub>d,d'</sub> show NOEs to the protons H<sub>e,e'</sub> respectively. The protons H<sub>a,a'</sub> are observed as doublet of doublets at high field ( $\delta$  6.26 and  $\delta$  6.19 respectively) with H<sub>h,h'</sub> at  $\delta$  8.34 and 7.50 respectively. The <sup>13</sup>C- $\{{}^1\text{H}\}$  NMR spectra show the expected number of signals for CH and quaternary carbons and the FAB mass spectrum shows a molecular ion for the cation at *m/z* 761. The X-ray crystal structure of **3.14g(*m*-C<sub>6</sub>H<sub>4</sub>Br)** was determined and is shown with selected bond lengths (Å) and angles (°) in **Fig. 3.11** and **Table 3.5** respectively.

Complex **3.14g(*o*-C<sub>6</sub>H<sub>4</sub>Br)** has a similar <sup>1</sup>H NMR spectrum to **3.14g(*m*-C<sub>6</sub>H<sub>4</sub>Br)** except for the signals of N-aryl protons (H<sub>6-9</sub>). The signals for H<sub>6-8</sub> overlap and are observed as a multiplet at *ca.*  $\delta$  6.8. Pyridine proton H<sub>h</sub> shows an NOE to H<sub>6</sub> and proton H<sub>8</sub> couples to a doublet of doublets at  $\delta$  7.27 which is therefore assigned as H<sub>9</sub>. The imine proton H<sub>5</sub> ( $\delta$  9.32) shows an NOE to H<sub>4</sub> ( $\delta$  8.47). The protons H<sub>a,a'</sub> are observed as doublet of doublets at high field ( $\delta$  6.28 and  $\delta$  6.15 respectively) and H<sub>h'</sub> (*ca.*  $\delta$  7.7) is observed upfield of H<sub>h</sub> ( $\delta$  8.62) similar to the related complexes **3.14g(*m/p*-C<sub>6</sub>H<sub>4</sub>R)**. The <sup>13</sup>C- $\{{}^1\text{H}\}$  NMR spectra show the expected signals and the FAB mass spectrum shows a molecular ion for the cation at *m/z* 761. The X-ray crystal structure of **3.14g(*o*-C<sub>6</sub>H<sub>4</sub>Br)** was determined and is shown with selected bond lengths (Å) and angles (°) in **Fig. 3.11** and **Table 3.5** respectively.

The structures of **3.14g(*m*-C<sub>6</sub>H<sub>4</sub>Br)** and **3.14g(*o*-C<sub>6</sub>H<sub>4</sub>Br)**, are similar to those of **3.14g(*p*-C<sub>6</sub>H<sub>4</sub>R)** discussed above.

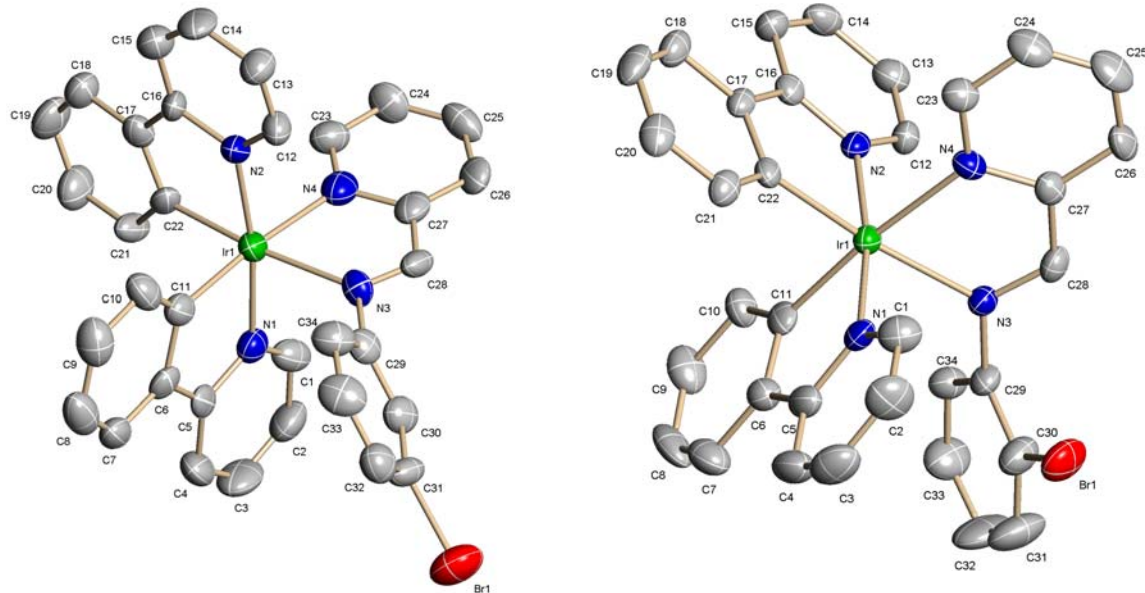


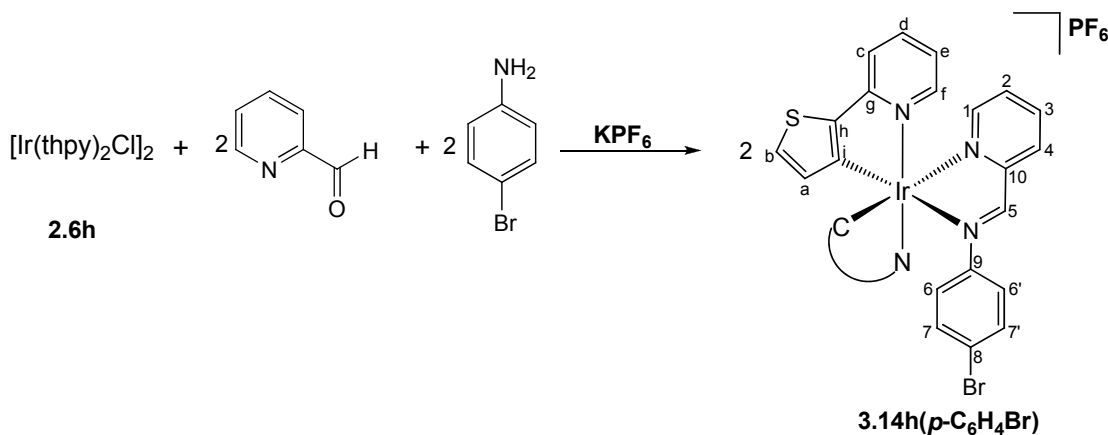
**Fig. 3.11:** X-ray crystal structure for the cations of **3.14g(*m*-C<sub>6</sub>H<sub>4</sub>Br)** and **3.14g(*o*-C<sub>6</sub>H<sub>4</sub>Br)** respectively.

**Table 3.5:** Tabulated bond lengths (Å) and bond angles (°) for the cations of **3.14g(*m*-C<sub>6</sub>H<sub>4</sub>Br)** and **3.14g(*o*-C<sub>6</sub>H<sub>4</sub>Br)**, respectively.

(Å)	<b>3.14g (<i>m</i>-C<sub>6</sub>H<sub>4</sub>Br)</b>	<b>3.14g (<i>o</i>-C<sub>6</sub>H<sub>4</sub>Br)</b>	(°)	<b>3.14g (<i>m</i>-C<sub>6</sub>H<sub>4</sub>Br)</b>	<b>3.14g (<i>o</i>-C<sub>6</sub>H<sub>4</sub>Br)</b>
Ir(1)—N(1)	2.039(9)	2.055(4)	N(1)—Ir(1)—N(2)	171.2(3)	171.64(17)
Ir(1)—N(2)	2.045(8)	2.059(4)	N(1)—Ir(1)—C(11)	79.5(4)	80.5(2)
Ir(1)—N(3)	2.155(8)	2.144(4)	N(2)—Ir(1)—C(22)	80.0(4)	80.27(19)
Ir(1)—N(4)	2.156(10)	2.154(4)	N(3)—Ir(1)—N(4)	76.8(3)	76.18(17)
Ir(1)—C(11)	1.989(11)	2.008(5)			
Ir(1)—C(22)	2.010(10)	2.015(5)			

In the <sup>1</sup>H NMR spectrum of **3.14g(*i*Pr)** the signals for the ppy are similar to those in the other complexes **3.14g**, whilst the pyridineimine signals are similar to those in **3.14a(*i*Pr)**. The most downfield signal ( $\delta$  9.73) is the imine proton H<sub>5</sub> which shows NOEs to H<sub>4</sub> (a broad doublet at  $\delta$  8.59) and to the isopropyl protons, which in turn show NOEs to the pyridine H<sub>h</sub> and the phenyl H<sub>a'</sub> protons of the two cyclometallated ligands. The methyls Me<sub>A</sub> and Me<sub>B</sub> are inequivalent due to the chirality at metal center as in **3.14a(*i*Pr)** and protons H<sub>a,a'</sub> are at characteristically high field ( $\delta$  6.17 and  $\delta$  6.35 respectively). The <sup>13</sup>C-<sup>{1}H</sup> NMR spectra show the expected number of signals for CH and quaternary carbons and the FAB mass spectrum shows a molecular ion for the

cation at  $m/z$  649. Crystals suitable for X-ray diffraction were obtained from DCM/hexane. The structure is shown with selected bond lengths (Å) and angles (°) in **Fig. 3.12** and **Table 3.6** respectively.



**Scheme 3.5**

The dimer **2.6h** reacts with pyridine-2-carboxaldehyde and the relevant amine and  $\text{KPF}_6$  under microwave irradiation to form **3.14h(p-C}\_6\text{H}\_4\text{Br)** as a red solid in 78% yield (**Scheme 3.5**). In the <sup>1</sup>H NMR spectrum of **3.14h(p-C}\_6\text{H}\_4\text{Br)** the signals due to pyridineimine are similar to those in other complexes **3.14(p-C}\_6\text{H}\_4\text{Br)**, however, four sets of doublets ( $J = 5.0$  Hz) each integrating to one proton are observed corresponding to the thiophene protons  $\text{H}_{\text{a},\text{b}}$  and  $\text{H}_{\text{a}',\text{b}'}$ . Thiopene protons  $\text{H}_{\text{a},\text{a}'}$  are the most highfield signals at  $\delta$  6.20 and  $\delta$  6.10 respectively. Proton  $\text{H}_{\text{f}'}$  is observed to high field of  $\text{H}_{\text{f}}$  ( $\delta$  7.35 and 8.14 respectively) due to a ring current effect from the pyridine of the pyridineimine. The imine proton  $\text{H}_{\text{5}}$  is the most downfield signal at  $\delta$  9.37 and the p-Br aryl substituent is an [AA'BB'] system, giving rise to multiplets for  $\text{H}_{\text{6/6}'}$  and  $\text{H}_{\text{7/7}'}$ . The <sup>13</sup>C-<sup>{1}</sup>H NMR spectra show the expected signals and the FAB mass spectrum shows a molecular ion for the cation at  $m/z$  773. Crystals suitable for X-ray diffraction were obtained from DCM/hexane. The structure is shown in **Fig. 3.12** with selected bond lengths (Å) and angles (°) in **Table 3.6** respectively.

The structures of **3.14g(iPr)** and **3.14h(p-C}\_6\text{H}\_4\text{Br)**, each show the expected distorted octahedral geometry and the Ir—N (C<sup>^</sup>N) bond distances are shorter than the distances of Ir—N (N<sup>^</sup>N) similar to **3.14(p-C}\_6\text{H}\_4\text{R)** and bipy complexes. The Ir—C bond distances to the phenyl and thiophene are statistically all the same in the two complexes.

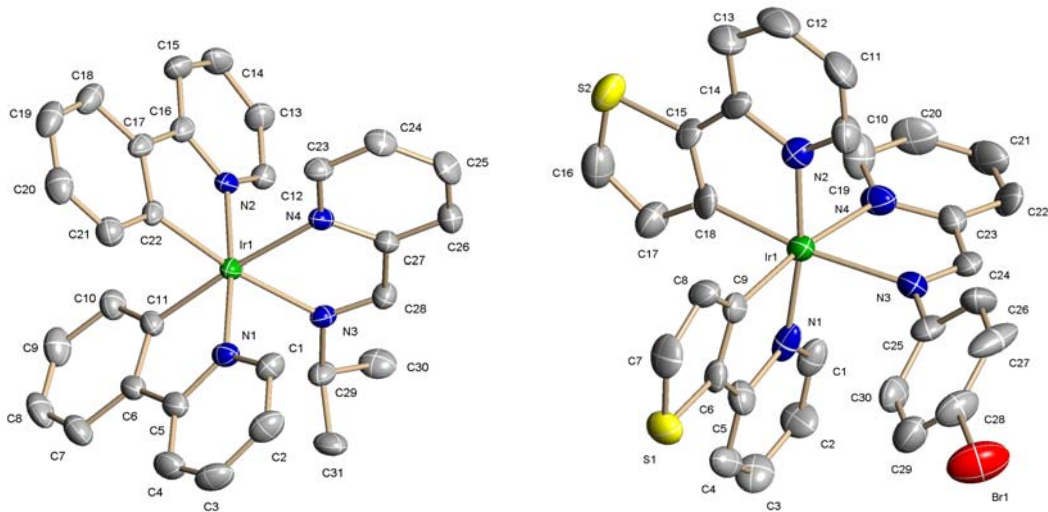


**Fig. 3.12:** X-ray crystal structure for the cations of **3.14g(iPr)** and **3.14h(*p*-C<sub>6</sub>H<sub>4</sub>Br)** respectively.

**Table 3.6:** Selected bond lengths (Å) and bond angles (°) for the cations of **3.14g(iPr)** and **3.14h(*p*-C<sub>6</sub>H<sub>4</sub>Br)**, respectively.

(Å)	<b>3.14g(iPr)</b>	(Å)	<b>3.14h(<i>p</i>-C<sub>6</sub>H<sub>4</sub>Br)</b>
Ir(1)—N(1)	2.041(4)	Ir(1)—N(1)	2.041(11)
Ir(1)—N(2)	2.055(4)	Ir(1)—N(2)	2.061(10)
Ir(1)—N(3)	2.130(4)	Ir(1)—N(3)	2.165(10)
Ir(1)—N(4)	2.154(4)	Ir(1)—N(4)	2.144(9)
Ir(1)—C(11)	2.011(4)	Ir(1)—C(9)	2.028(11)
Ir(1)—C(22)	2.009(4)	Ir(1)—C(18)	2.013(12)
(°)		(°)	
N(1)—Ir(1)—N(2)	174.78(13)	N(1)—Ir(1)—N(2)	171.7(4)
N(1)—Ir(1)—C(11)	80.18(18)	N(1)—Ir(1)—C(9)	80.3(4)
N(2)—Ir(1)—C(22)	80.50(17)	N(2)—Ir(1)—C(18)	80.7(5)
N(3)—Ir(1)—N(4)	76.21(14)	N(3)—Ir(1)—N(4)	76.4(4)

These reactions show that a range of pyridineimine complexes **3.14** were synthesised in high yields (> 75%) using microwave heating. The one pot method of synthesis, using pyridine-2-carboxaldehyde and the relevant amine, saves the need to prepare and isolate the pyridineimines first. A number of the complexes have reactive functional groups present (*e.g.* COOH, NH<sub>2</sub>, OH, CO<sub>2</sub>Me, Br) which may be used to attach other molecules *e.g.* for bioconjugation. All the complexes were fully characterised by NMR spectroscopy, mass spectrometry and microanalysis and in

several cases by X-ray crystallography. The electrochemical and photophysical properties of these complexes are discussed in the following sections.

### 3.2.1.1 Electrochemistry of $[\text{Ir}(\text{C}^{\wedge}\text{N})_2(\text{pyridineimine})]^+$ (3.14)

For cationic Ir(III) complexes, the pure metal-centred oxidation is reversible but it becomes less reversible as the contribution of the cyclometallating phenyl(s) to the HOMO, as determined by DFT calculations, increases,<sup>31, 32</sup> as discussed previously for  $[\text{Ir}(\text{C}^{\wedge}\text{N})_2(\text{bipy})]^+$  (2.7a-f) in **Chapter 2**. The electrochemical properties of  $[\text{Ir}(\text{C}^{\wedge}\text{N})_2(\text{pyridineimine})]^+$  (3.14) were examined using cyclic voltammetry and the redox data are tabulated in **Table 3.7**. Diagrams of the cyclic voltammograms for **3.14g(p-C<sub>6</sub>H<sub>4</sub>R)** (R = H, OH, OMe, CO<sub>2</sub>Me), and **3.14g<sup>i</sup>Pr**) complexes are shown in **Fig 3.13** (see later) to illustrate the effect of changing the substituent on the imine. All the complexes **3.14(p-C<sub>6</sub>H<sub>4</sub>R)** exhibit a reversible/quasi-reversible oxidative process between 1.27 and 1.41 V and a reversible reduction couple between -0.85 and -1.25 V. The relatively small range of oxidation potentials ( $\sim 0.14$  V) and the partial reversibility are consistent with the oxidation being mainly centred on the Ir and the Ir-C  $\sigma$ -bond. Thus, the HOMO mainly resides on the Ir and partially on the C $^{\wedge}$ N ligand, consistent with other cationic Ir(III) complexes mentioned above. The reduction potentials span a wider range ( $\sim 0.40$  V) than the oxidation potentials, which suggests that substitution on the pyridineimine ligand mainly affects the reduction, which is consistent with the reduction being mainly pyridineimine based similar to  $[\text{Ir}(\text{C}^{\wedge}\text{N})_2(\text{bipy})]^+$  complexes discussed in the literature<sup>31</sup> and in **Chapter 2**. In addition, some complexes, also exhibit an irreversible second reduction potential ( $E^{1/2}_{\text{Red2}}$ ) between -1.33 to -1.90 V. This can tentatively be assigned to the second reduction of the pyridineimine as no second reduction potentials were observed in bipy complexes of the same cyclometallated ligands (compare entries 1 vs 22 and 9 vs 23 in **Table 3.7**). In all the subsequent discussion only the first reduction potential ( $E^{1/2}_{\text{Red1}}$ ) is considered.

**Table 3.7:** Redox properties of  $[\text{Ir}(\text{C}^{\wedge}\text{N})_2(\text{pyridineimine})]^+$  complexes<sup>a</sup>.

Entry	Complex	$E^{1/2}_{\text{Ox}}$	$E^{1/2}_{\text{Red1}}$	$E^{1/2}_{\text{Red2}}$	$\Delta E^{1/2} (\text{V})$
1	<b>3.14a(C<sub>6</sub>H<sub>5</sub>)</b>	1.39	-0.99	-1.60 <sup>b</sup>	2.38
2	<b>3.14a(p-C<sub>6</sub>H<sub>4</sub>Br)</b>	1.41	-0.93	-1.55 <sup>b</sup>	2.34
3	<b>3.14a(p-C<sub>6</sub>H<sub>4</sub>CO<sub>2</sub>H)</b>	1.41	-0.87		2.28
4	<b>3.14a(p-C<sub>6</sub>H<sub>4</sub>NH<sub>2</sub>)</b>	1.38	-1.06		2.44
5	<b>3.14a(p-C<sub>6</sub>H<sub>4</sub>OH)</b>	1.28	-1.06		2.34
6	<b>3.14a(<sup>i</sup>Pr)</b>	1.38	-1.25		2.63
7	<b>3.14b(p-C<sub>6</sub>H<sub>4</sub>Br)</b>	1.28	-0.93	-1.54 <sup>b</sup>	2.21
8	<b>3.14f(p-C<sub>6</sub>H<sub>4</sub>Br)</b>	1.28	-0.95	-1.60 <sup>b</sup>	2.23
9	<b>3.14g(C<sub>6</sub>H<sub>5</sub>)</b>	1.38	-1.06	-1.73 <sup>b</sup>	2.44
10	<b>3.14g(p-C<sub>6</sub>H<sub>4</sub>Br)</b>	1.34	-0.92	-1.52 <sup>b</sup>	2.26
11	<b>3.14g(p-C<sub>6</sub>H<sub>4</sub>CO<sub>2</sub>H)</b>	1.34	-0.87		2.21
12	<b>3.14g(p-C<sub>6</sub>H<sub>4</sub>CO<sub>2</sub>Me)</b>	1.34	-0.85	-1.33 <sup>b</sup>	2.19
13	<b>3.14g(p-C<sub>6</sub>H<sub>4</sub>OCOMe)</b>	1.31	-0.99	-1.65 <sup>b</sup>	2.30
14	<b>3.14g(p-C<sub>6</sub>H<sub>4</sub>OMe)</b>	1.32	-1.02	-1.71 <sup>b</sup>	2.34
15	<b>3.14g(p-C<sub>6</sub>H<sub>4</sub>OH)</b>	1.27	-1.02		2.29
16	<b>3.14g(p-C<sub>6</sub>H<sub>4</sub>Me)</b>	1.38	-1.06	-1.73 <sup>b</sup>	2.44
17	<b>3.14g(m-C<sub>6</sub>H<sub>4</sub>Br)</b>	1.33	-0.91	-1.50 <sup>b</sup>	2.24
18	<b>3.14g(m-C<sub>6</sub>H<sub>4</sub>OH)</b>	1.27	-0.98		2.25
19	<b>3.14g(o-C<sub>6</sub>H<sub>4</sub>Br)</b>	1.34	-0.95	-1.50 <sup>b</sup>	2.29
20	<b>3.14g(<sup>i</sup>Pr)</b>	1.30	-1.21	-1.90 <sup>b</sup>	2.51
21	<b>3.14h(p-C<sub>6</sub>H<sub>4</sub>Br)</b>	1.22	-0.88	-1.47 <sup>b</sup>	2.10
22	<b>2.7a</b>	1.37	-1.38		2.75
23	<b>2.7g</b>	1.31	-1.35		2.66

<sup>a</sup>In dry acetonitrile (0.1 mol L<sup>-1</sup> of Et<sub>4</sub>NClO<sub>4</sub>), scan rate 100 mV s<sup>-1</sup>, all potentials are quoted vs SCE (Cp<sub>2</sub>Fe<sup>+</sup>/Cp<sub>2</sub>Fe vs SCE = +0.42 V).<sup>33</sup> A Pt disc was used as a working electrode, counter electrode was a Pt gauze and a silver wire was used as a reference. <sup>b</sup>Irreversible wave. <sup>c</sup>The energy values are calculated with respect to first reduction potential ( $E^{1/2}_{\text{Red1}}$ ).

In complexes **3.14a(p-C<sub>6</sub>H<sub>4</sub>R)**, introducing electron withdrawing substituents (Br, CO<sub>2</sub>H) on the *para* position of N-aryl ring of the pyridineimine ligand gives a more anodic reduction potential with respect to the unsubstituted complex **3.14a(C<sub>6</sub>H<sub>5</sub>)**, and hence these have a lower LUMO resulting in a smaller HOMO-LUMO energy gap *i.e.*  $\Delta E^{1/2}$  (**Table 3.7** entries 1, 2 and 3). In contrast, the NH<sub>2</sub> complex is harder to reduce and hence has a higher LUMO and larger  $\Delta E^{1/2}$  relative to **3.14a(C<sub>6</sub>H<sub>5</sub>)** (entries 1 and 4). However, the OH complex **3.14a(p-C<sub>6</sub>H<sub>4</sub>OH)**, though harder to reduce is also easier

to oxidise (by 0.11V) resulting in a slightly smaller  $\Delta E^{1/2}$  relative to **3.14a(C<sub>6</sub>H<sub>5</sub>)** (entries 1 and 5). Presumably the positive conjugative effect of the OH outweighs the negative inductive effect. Upon changing the N-aryl group (C<sub>6</sub>H<sub>5</sub>) to alkyl (iPr) in **3.14a(iPr)**, the oxidation potential is unaffected, however, the reduction potential is considerably more cathodic resulting in a larger  $\Delta E^{1/2}$  (entries 1 and 6). Introducing an electron donating Me-substituent(s) on the phenyl, **3.14b(p-C<sub>6</sub>H<sub>4</sub>Br)**, or pyrazole **3.14f(p-C<sub>6</sub>H<sub>4</sub>Br)**, of the C<sup>N</sup> ligand makes the complexes easier to oxidise as expected, but surprisingly also easier to reduce than unsubstituted complex **3.14a(C<sub>6</sub>H<sub>5</sub>)**, and hence these have a higher HOMO and a lower LUMO hence a significantly reduced  $\Delta E^{1/2}$  (**Table 3.7** entries 1, 7 and 8).

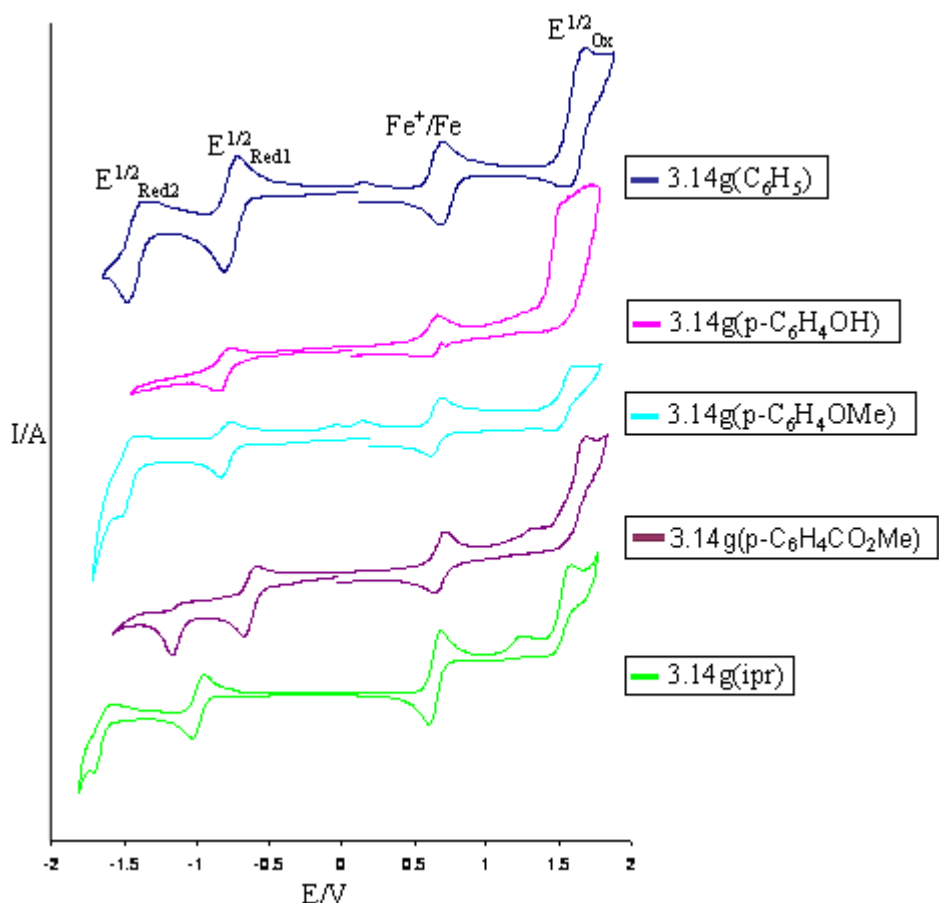


**Fig. 3.13:** Cyclic voltammograms of **3.14g(p-C<sub>6</sub>H<sub>4</sub>R)** (R = H, OH, OMe, CO<sub>2</sub>Me), and **3.14g(iPr)** complexes (scan rate 100 mV/s).

The electrochemistry of the ppy complexes **3.14g(p-C<sub>6</sub>H<sub>4</sub>R)** is not quite so straightforward. Somewhat surprisingly the Ph complex has the most anodic oxidation

potential and the most cathodic reduction potential for all these complexes; the p-Me complex has identical potentials. Introducing any other substituent makes the complex easier to oxidise (raises the HOMO) by up to 0.11V (maximum change for an OH substituent) whilst at the same time making them easier to reduce (lowers the LUMO) by up to 0.21V (maximum change for p-CO<sub>2</sub>Me). Hence in all cases substitution leads to a smaller HOMO-LUMO energy gap (*i.e.*  $\Delta E^{1/2}$ ). Changing the position of the substituents from *para* to *ortho/meta* has very little effect on the potentials (change of < 0.04V) (compare entries 10, 17, and 19 or 15 and 18). Changing the N-Ph to N-<sup>i</sup>Pr in **3.14g(<sup>i</sup>Pr)** (entries 9 and 20) makes the complex harder to reduce, as found in the ppz case, however in the ppy case the oxidation is now easier, the net effect is still an increase in  $\Delta E^{1/2}$ , of 0.07V, compared with an increase of 0.25V in the ppz complexes. Hence while some effects are as predicted the ppy series a full understanding of the electrochemistry of the ppy complexes will require more study.

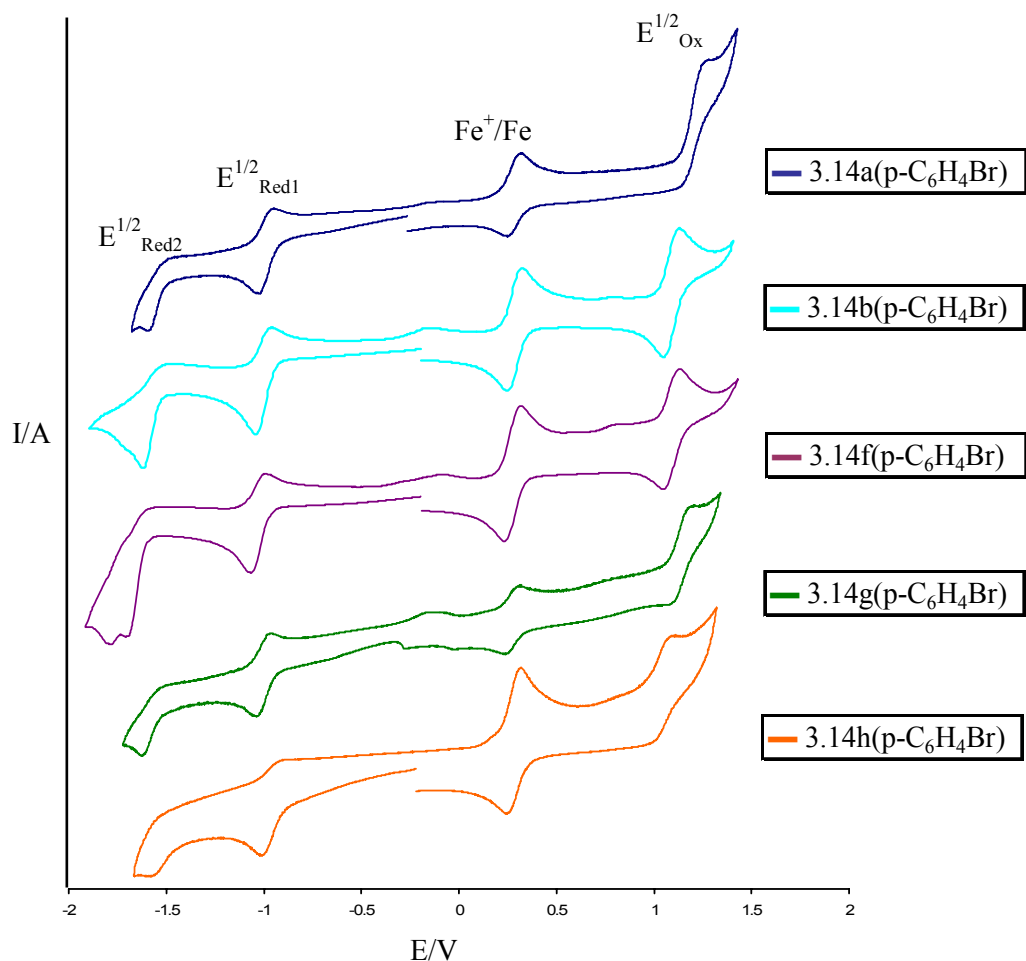


**Fig. 3.14:** Cyclic voltammograms of **3.14(C<sup>N</sup>)(p-C<sub>6</sub>H<sub>4</sub>Br)** ( $\text{C}^N = \mathbf{a}, \mathbf{b}, \mathbf{f}, \mathbf{g}, \mathbf{h}$ ) complexes (scan rate 100 mV/s).

Upon changing the cyclometallated ( $C^N$ ) ligand (ppz, ppz-Me, pmpz-Me<sub>2</sub>, ppy and thpy) in pyridineimine complexes **3.14a,b,f,g,h(p-C<sub>6</sub>H<sub>4</sub>Br)**, the oxidation potential changes more than the reduction potential (0.19V vs 0.05V) (**Table 3.7**, entries 2, 7, 8, 10 and 21 and **Fig 3.14**), which suggests that it mainly affects the HOMO. Thienyl pyridine (thpy) is more electron donating than both ppz and ppy; therefore it raises the HOMO the most, causing a smaller HOMO-LUMO energy gap  $\Delta E^{1/2}$ .

Comparing NPh pyridineimine complexes **3.14a,g(Ph)** to the cooresponding bipy complexes (**2.7a,g**), the oxidation potentials are very similar, however, the pyridineimine complexes are much easier to reduce, resulting in a smaller HOMO-LUMO energy gap  $\Delta E^{1/2}$  for the pyridineimine complexes (compare entries 1 vs 22 and 9 vs 23).

### 3.2.1.2 Photophysical properties of $[Ir(C^N)_2(\text{pyridineimine})]^+$ (3.14)

#### Absorption spectroscopy

The electronic spectra of  $[Ir(C^N)_2(\text{bipy})]^+$  (**2.7**) were discussed in **Chapter 2**. The pyridineimine complexes (**3.14**) have similar features (three bands  $\pi \rightarrow \pi^*$ ,  $^1\text{MLCT}$ ,  $^3\text{MLCT}$ ) and the absorption data are given in **Table 3.8**. The most intense absorption bands below 270 nm are assigned to the spin allowed intraligand IL ( $\pi \rightarrow \pi^*$ ) transitions. The moderately intense absorption bands at around 320 – 470 nm are attributed to the spin allowed metal to ligand charge transfer ( $^1\text{MLCT}$ ) ( $d\pi(\text{Ir}) \rightarrow \pi^*(C^N \text{ and } X^Y)$ ) transitions and the weak absorption bands towards the lower energy region, *ca.* > 470 nm are tentatively assigned to the spin forbidden  $^3\text{MLCT}$  ( $d\pi(\text{Ir}) \rightarrow \pi^*(C^N \text{ and } X^Y)$ ) transitions. Both the MLCT bands are shifted to lower energy with respect to the bipy complexes (300 – 400 nm and 400 – 480 nm for  $^1\text{MLCT}$  and  $^3\text{MLCT}$  respectively).

**Table 3.8:** Electronic absorption spectral data of  $[\text{Ir}(\text{C}^{\wedge}\text{N})_2(\text{pyridineimine})]^+$  complexes.

Entry	Complex	Solvent	$\lambda_{\text{abs}} \text{ [nm]} (\epsilon_{\text{max}} \text{ [dm}^3\text{mol}^{-1}\text{cm}^{-1}])$
1	<b>3.14a(C<sub>6</sub>H<sub>5</sub>)</b>	DCM	235 (58100), 325 (19400), 506 (100)
2	<b>3.14a(p-C<sub>6</sub>H<sub>4</sub>Br)</b>	DCM	236 (27750), 330 (9690), 508 (400)
3	<b>3.14a(p-C<sub>6</sub>H<sub>4</sub>CO<sub>2</sub>H)</b>	DCM	241 (14560), 326 (5020), 521 (90)
4	<b>3.14a(p-C<sub>6</sub>H<sub>4</sub>NH<sub>2</sub>)</b>	DCM	257 (11200), 325 sh (2570), 438 (3340)
5	<b>3.14a(p-C<sub>6</sub>H<sub>4</sub>OH)</b>	DCM	244 (24150), 326 (6360), 375 (7640), 511 (240)
6	<b>3.14a(iPr)</b>	DCM	255 (27000), 323 (6500), 473 (60)
7	<b>3.14a(CH<sub>2</sub>CO<sub>2</sub>Et)</b>	DCM	241 (23420), 321 sh (7870), 356 sh (6790), 488 (90)
8	<b>3.14b(p-C<sub>6</sub>H<sub>4</sub>Br)</b>	DCM	241 (19300), 339 (6580), 526 (180)
9	<b>3.14f(p-C<sub>6</sub>H<sub>4</sub>Br)</b>	DCM	247 (17800), 339 (5670), 547 (160)
10	<b>3.14g(C<sub>6</sub>H<sub>5</sub>)</b>	DCM	254 (53100), 267 (51400), 380 sh (13400), 408 sh (9800), 531 sh (1900)
11	<b>3.14g(p-C<sub>6</sub>H<sub>4</sub>Br)</b>	DCM	253 (11980), 268 (11010), 381 (3090), 533 (160)
12	<b>3.14g(p-C<sub>6</sub>H<sub>4</sub>CO<sub>2</sub>H)</b>	DCM	253 (52900), 267 (48500), 384 sh (10900), 529 (60)
13	<b>3.14g(p-C<sub>6</sub>H<sub>4</sub>CO<sub>2</sub>Me)</b>	DCM	254 (28530), 267 (27910), 408 sh (4050), 546 sh (310)
14	<b>3.14g(p-C<sub>6</sub>H<sub>4</sub>O<sub>COMe</sub>)</b>	DCM	253 (60500), 265 (56800), 375 sh (17000), 536 (900)
15	<b>3.14g(p-C<sub>6</sub>H<sub>4</sub>OMe)</b>	DCM	257 (10480), 388 (3840), 517 (150)
16	<b>3.14g(p-C<sub>6</sub>H<sub>4</sub>OH)</b>	DCM	255 (58400), 382 (20500), 508 (110)
17	<b>3.14g(p-C<sub>6</sub>H<sub>4</sub>Me)</b>	DCM	254 (17590), 364 (2390), 528 (80)
18	<b>3.14g(m-C<sub>6</sub>H<sub>4</sub>Br)</b>	DCM	255 (25400), 267 (24660), 378 (5400), 404 sh (4180), 552 (260)
19	<b>3.14g(m-C<sub>6</sub>H<sub>4</sub>OH)</b>	DCM	269 (25160), 377 (4730), 530 (2300)
20	<b>3.14g(o-C<sub>6</sub>H<sub>4</sub>Br)</b>	DCM	254 (29140), 266 (28120), 382 (6190), 549 (360)
21	<b>3.14g(iPr)</b>	DCM	265 (136400), 378 (25300), 469 (2200)
22	<b>3.14h(p-C<sub>6</sub>H<sub>4</sub>Br)</b>	DCM	252 (59800), 340 sh (18300), 372 (19700), 534 (60)

### Emission spectroscopy of $[\text{Ir}(\text{C}^{\wedge}\text{N})_2(\text{pyridineimine})]^+$ (3.14)

As discussed in **Chapters 1** and **2**, for  $[\text{Ir}(\text{C}^{\wedge}\text{N})_2(\text{bipy})]^+$  complexes, emission commonly comes from mixed  $^3\text{IL}$  ( $\pi_{(\text{C}^{\wedge}\text{N})} \rightarrow \pi^*_{(\text{C}^{\wedge}\text{N})}$ ) and  $^3\text{MLCT}$  ( $\text{d}\pi_{(\text{Ir})} \rightarrow \pi^*_{(\text{bipy})}$ ) transitions, owing to the strong spin-orbit coupling, which leads to efficient intersystem crossing resulting the emission from the triplet states (phosphorescence). Preliminary experiments showed that all of the pyridineimine complexes (**3.14**) emit in DCM at

room temperature though the intensity is rather weak for some of the complexes. Since the excitation spectra looked similar for all the complexes it was decided to use the same excitation wavelength (390 nm) in all cases. This means that the emission intensity is not optimized in each case. Most of the complexes (**3.14**) show dual emission, one high energy band at  $\sim$  500 nm and another lower energy band at  $\sim$  700 nm. Dual emission is not common but has been reported for Ir(III) bipy complexes<sup>34</sup> and for Ru(II) pyridineimine complexes *e.g.* **3.1**.<sup>1</sup> To try and prove that both bands are from the complex and one is not due to an impurity the emission of **3.14g(p-C<sub>6</sub>H<sub>4</sub>Br)** was run on a sample from the bulk and a single crystal sample which had been used for X-ray diffraction. These gave identical emission spectra (**Fig. 3.15**). The most likely common impurity in the samples is the starting dimer, hence the emission of dimer **2.6g** was also measured and compared with the emission of **3.14g(p-C<sub>6</sub>H<sub>4</sub>Br)**. The result is shown in **Fig 3.15**. The emission of **2.6g** is centred at 565 nm, which eliminates this as a possible trace impurity in the complex. The excitation spectra for both the emission bands of **3.14g(p-C<sub>6</sub>H<sub>4</sub>Br)** were measured and found to be very similar (**Fig. 3.15**), this again suggests that both bands arise from a single species. Hence we conclude that where there are two bands it is real dual emission.

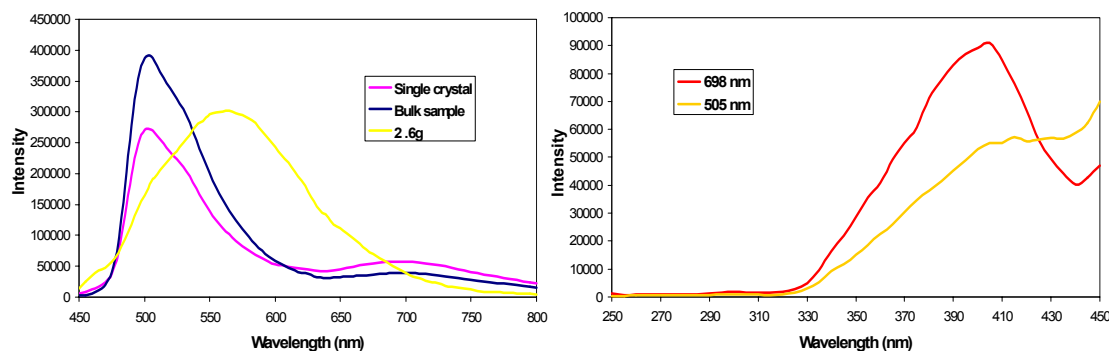


**Fig. 3.15:** Left: Degassed emission of **3.14g(p-C<sub>6</sub>H<sub>4</sub>Br)** from a single crystal and from a bulk sample and of  $[\text{Ir}(\text{ppy})_2\text{Cl}]_2$  dimer (**2.6g**). Right: Excitation spectra of **3.14g(p-C<sub>6</sub>H<sub>4</sub>Br)** monitoring emission at 505 and 698 nm.

<sup>a</sup>All measurements were carried out at a concentration 0.01 mM in dry DCM. <sup>b</sup>Intensity of dimer is multiplied by a factor of 10.

A problem in fluorescence measurements is that the detector is not uniformly sensitive across the full wavelength range. The data reported herein is uncorrected for the photomultiplier response but to try and evaluate this the uncorrected and corrected

spectra for emission of **3.14g(p-C<sub>6</sub>H<sub>4</sub>Br)** were measured and are shown in **Fig 3.16**. As can be seen the uncorrected spectra underestimate the intensities for the long wavelength bands. All subsequent emission data are uncorrected for the PMT response and are tabulated in **Table 3.9**.

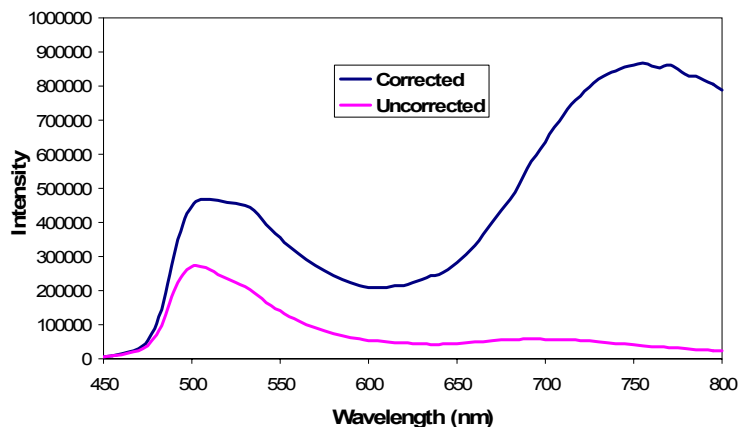


**Fig. 3.16:** Corrected for PMT response and uncorrected degassed emission spectra of **3.14g(p-C<sub>6</sub>H<sub>4</sub>Br)**.

The ppz complexes **3.14a(p-C<sub>6</sub>H<sub>4</sub>R)** generally show a strong band about 650-690 nm and some also show a weaker band at 470 nm. Complexes with the electron withdrawing substituents (Br, CO<sub>2</sub>H) are red shifted compared to R = H (**Table 3.9** entries 1, 2 and 3). An OH substituent has little effect on the wavelength but replacing H with NH<sub>2</sub> (entries 1 and 4) results in a significant blue shift to 580 nm. A blue shift is consistent with an increase in  $\Delta E^{1/2}$  of 0.06 V compared to the unsubstituted complex however the emission shifts by 0.28 eV, the reason for this large blue shift is not yet known. Replacing the N-aryl substituent on the imine with an isopropyl also leads to a significant blue shift to 611 nm, in this case the shift in emission energy compared to the NPh complex is 0.17 eV which is much closer to the change in  $\Delta E^{1/2}$  of 0.25 V (entries 1 and 7). Putting electron donating methyl substituent(s) on the cyclometallated phenyls, **3.14b(p-C<sub>6</sub>H<sub>4</sub>Br)**, or on the pyrazole, **3.14f(p-C<sub>6</sub>H<sub>4</sub>Br)**, of the C<sup>N</sup> ligand results in a considerable red shift to 710 and 723 nm respectively, relative to 680 nm for **3.14a(p-C<sub>6</sub>H<sub>4</sub>Br)** (entries 9, 10 and 2). This is consistent with the electrochemical data, which show an easier oxidation (raised HOMO) for these complexes, and with complexes **2.7b** and **2.7f** (see **Chapter 2**).

**Table 3.9:** Emission data and  $\Delta E^{1/2}$  of  $[\text{Ir}(\text{C}^{\wedge}\text{N})_2(\text{pyridineimine})]^+$  complexes (**3.14**).

Entry	Complex	Solvent	$\lambda_{\text{em}}$ (nm)		Energy (eV)	$\Delta E^{1/2}$ (V)
1	<b>3.14a(C<sub>6</sub>H<sub>5</sub>)</b>	DCM	475	670	2.60, 1.85	2.38
2	<b>3.14a(p-C<sub>6</sub>H<sub>4</sub>Br)</b>	DCM		680	1.82	2.34
3	<b>3.14a(p-C<sub>6</sub>H<sub>4</sub>CO<sub>2</sub>H)</b>	DCM	470	684	2.63, 1.81	2.28
4	<b>3.14a(p-C<sub>6</sub>H<sub>4</sub>NH<sub>2</sub>)</b>	DCM		580	2.13	2.44
5	<b>3.14a(p-C<sub>6</sub>H<sub>4</sub>OH)</b>	DCM		675	1.83	2.34
6	<b>3.14a(p-C<sub>6</sub>H<sub>4</sub>OH)</b>	MeOH	469	685	2.63, 1.81	2.34
7	<b>3.14a(iPr)</b>	DCM		611	2.02	2.63
8	<b>3.14a(CH<sub>2</sub>CO<sub>2</sub>Et)</b>	DCM	540	648	2.29, 1.91	
9	<b>3.14b(p-C<sub>6</sub>H<sub>4</sub>Br)</b>	DCM	465	710	2.69, 1.74	2.21
10	<b>3.14f(p-C<sub>6</sub>H<sub>4</sub>Br)</b>	DCM	500	723	2.47, 1.71	2.23
11	<b>3.14g(C<sub>6</sub>H<sub>5</sub>)</b>	DCM	505	694	2.45, 1.78	2.44
12	<b>3.14g(p-C<sub>6</sub>H<sub>4</sub>Br)</b>	DCM	505	698	2.45, 1.77	2.26
13	<b>3.14g(p-C<sub>6</sub>H<sub>4</sub>CO<sub>2</sub>H)</b>	DCM	505	713	2.45, 1.73	2.21
14	<b>3.14g(p-C<sub>6</sub>H<sub>4</sub>CO<sub>2</sub>Me)</b>	DCM	505, 540	710	2.45, 2.29, 1.74	2.19
15	<b>3.14g(p-C<sub>6</sub>H<sub>4</sub>OCOMe)</b>	DCM	505	700	2.45, 1.77	2.30
16	<b>3.14g(p-C<sub>6</sub>H<sub>4</sub>OMe)</b>	DCM	509, 540	685	2.43, 1.81	2.34
17	<b>3.14g(p-C<sub>6</sub>H<sub>4</sub>OH)</b>	DCM	505	687	2.45, 1.80	2.29
18	<b>3.14g(p-C<sub>6</sub>H<sub>4</sub>OH)</b>	MeOH	510	691	2.42, 1.79	2.29
19	<b>3.14g(p-C<sub>6</sub>H<sub>4</sub>Me)</b>	DCM	505	688	2.45, 1.80	2.44
20	<b>3.14g(m-C<sub>6</sub>H<sub>4</sub>Br)</b>	DCM	505	715	2.45, 1.73	2.24
21	<b>3.14g(m-C<sub>6</sub>H<sub>4</sub>OH)</b>	DCM	500	697	2.47, 1.77	2.25
22	<b>3.14g(o-C<sub>6</sub>H<sub>4</sub>Br)</b>	DCM	505	700	2.45, 1.77	2.29
23	<b>3.14g(iPr)</b>	DCM	505	651	2.45, 1.90	2.51
24	<b>3.14h(p-C<sub>6</sub>H<sub>4</sub>Br)</b>	DCM	555	595	2.23, 2.08	2.10
25	<b>2.7a (ppz)</b>	DCM		557	2.22	2.75
26	<b>2.7g (ppy)</b>	DCM		580	2.13	2.66

The ppy complexes **3.14g(p-C<sub>6</sub>H<sub>4</sub>R)** all show dual emission with a large band about 505 nm which is relatively insensitive to changing the substituent and another band between 685 and 715 nm which alters with the substituent. Substituting H with electron withdrawing substituents causes a red shift in the long wavelength band from 694 nm (R = H) to about 710 nm (R = CO<sub>2</sub>H, CO<sub>2</sub>Me), which is consistent with the electrochemical data for these complexes (**Table 3.9** entries 11-15). Alternatively, substituting H with OMe or OH results in a small blue shift to ca. 685 nm (**Table 3.9** entries 11, 16 and 17). This suggests that for these substituents in the para position the *conjugative* donor properties outweigh the inductive effects leading to a small blue shift. Note this is not consistent with the electrochemistry which predicts a red shift on the basis of a smaller  $\Delta E^{1/2}$ . In contrast, substituting OH at the *meta* position causes a small red shift of 3 nm relative to the unsubstituted complex (entries 9 and 18) which is consistent with a purely inductive effect. Substituting H with Br on any positions (*o/m/p*) on the N-aryl ring causes a red shift, however, the shift is larger with a *meta*-Br (21 nm) than with *ortho*- or *para*-Br (ca. 5 nm). Presumably for *ortho* and *para*-Br substituents the conjugative effect acts against the inductive effect leading to only a small net effect. Surprisingly replacing H with an electron donating methyl group gives a small blue shift (**Table 3.9** entries 11 and 19), however the effect is rather small which is consistent with identical electrochemical properties for these two complexes. The bands are sensitive to solvent polarity, thus, for **3.14a(p-C<sub>6</sub>H<sub>4</sub>OH)** the main emission band is at 675 nm in DCM and 685 nm in MeOH whilst for **3.14g(p-C<sub>6</sub>H<sub>4</sub>OH)** both bands shift from 505 and 687 nm in DCM to 510 and 691 nm in MeOH, these observations are consistent with a charge transfer component. Replacing the N-aryl group with an N-alkyl group (<sup>i</sup>Pr) in **3.14g(<sup>i</sup>Pr)** blue shifts the emission from 694 to 651 nm which is consistent with the electrochemical results and with the corresponding ppz complexes discussed above.

Replacement of ppz in **3.14a(p-C<sub>6</sub>H<sub>4</sub>Br)** or **3.14a(<sup>i</sup>Pr)** with ppy in **3.14g(p-C<sub>6</sub>H<sub>4</sub>Br)** and **3.14g(<sup>i</sup>Pr)** respectively leads to red shifts of 18 or 41 nm respectively consistent with decreases in  $\Delta E^{1/2}$  (**Table 3.9**). However, the thpy complex **3.14h(p-C<sub>6</sub>H<sub>4</sub>Br)** does not fit the trend, it shows dual emission at 555 and 595 nm. Thus the short wavelength band is red shifted but the long wavelength band is considerably blue shifted compared to the corresponding ppz and ppy complexes. It seems likely therefore that the origin of the bands in this complex is different and needs further study. As

expected, the pyridineimine complexes (**3.14**) are significantly red shifted relative to the bipy complexes (**2.7**) *e.g.* compare **3.14a(C<sub>6</sub>H<sub>5</sub>)** (670 nm) *vs* **2.7a** (557 nm) or **3.14g(C<sub>6</sub>H<sub>5</sub>)** (694 nm) *vs* **2.7g** (580 nm) (entries 1 *vs* 25 and 11 *vs* 26 **Table 3.9**).

As mentioned earlier, pyridineimine complexes are dual emitters. The two bands have a different response to oxygen; the shorter wavelength band (~ 500 nm) is more sensitive to oxygen than the longer wavelength band (~ 700 nm). For example the effect of oxygen on the emission of **3.14g(p-C<sub>6</sub>H<sub>4</sub>Br)** is shown in **Fig. 3.17**. This different response to oxygen may reflect different amounts of metal contribution to the orbitals involved in the two bands.

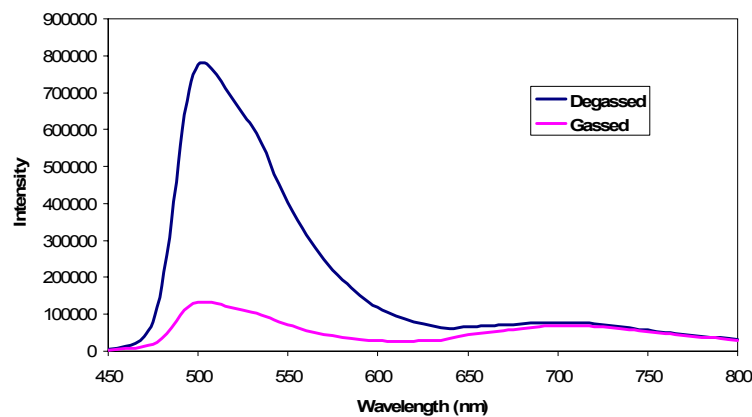
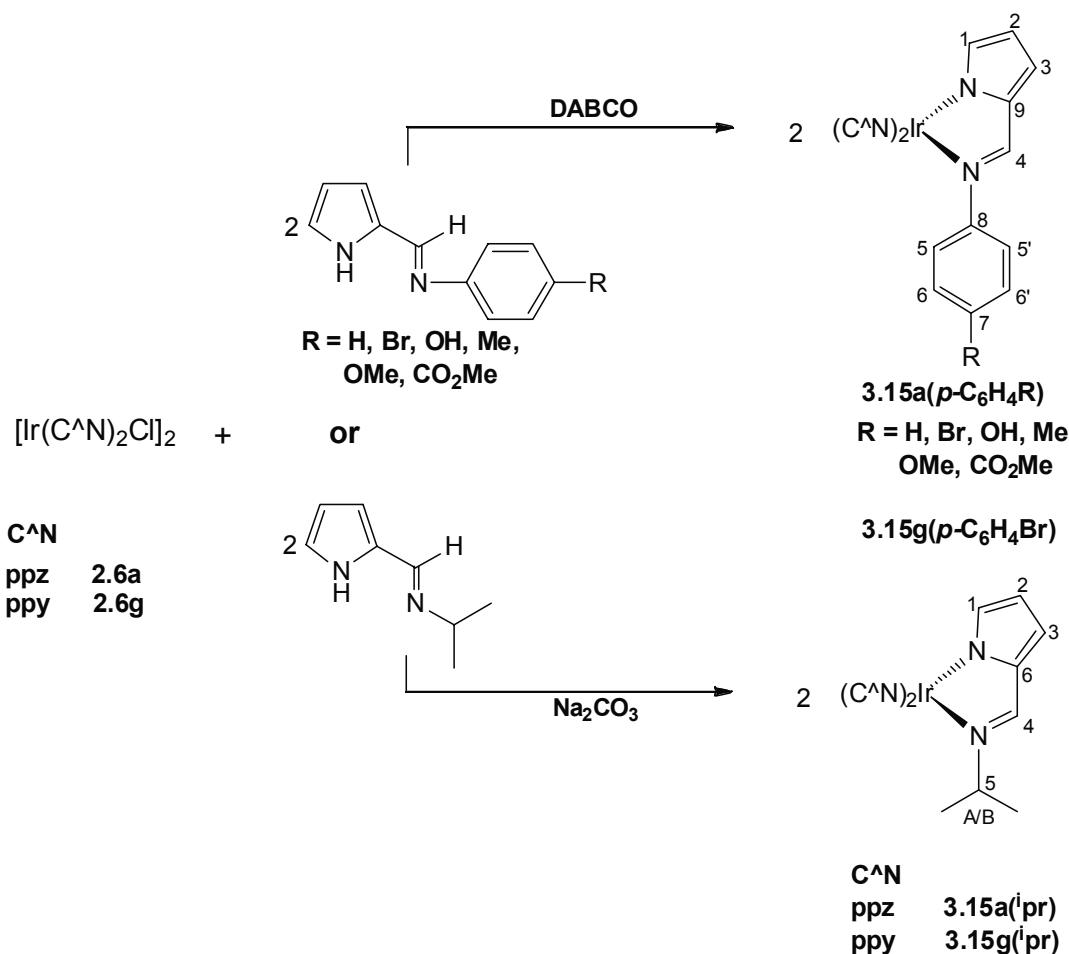


**Fig. 3.17:** A comparison of gassed and degassed emission spectra of **3.14g(p-C<sub>6</sub>H<sub>4</sub>Br)** showing the oxygen sensitivity of two bands.

In conclusion, pyridineimine complexes (**3.14**) are found to be emissive at room temperature in fluid solutions. The majority of the complexes are dual emitters showing two bands, one at ~ 500 nm and another at longer wavelength ~ 700 nm, thus covering a wide region of the visible spectrum. The longer wavelength band varies with the substituent on the imine. Bands at ~ 500 nm are found to be sensitive to oxygen however the longer wavelength bands are relatively less affected.

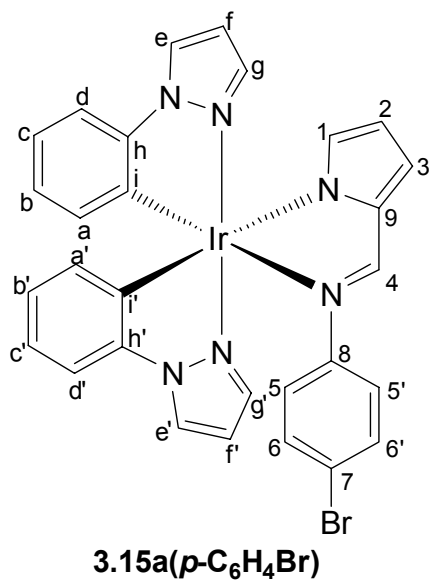
### 3.2.2 Synthesis and Characterisation of $[\text{Ir}(\text{C}^{\text{N}})_2(\text{pyrrolylimine})]$ (3.15)



**Scheme 3.6**

Pyrroleimines were synthesised using a literature method.<sup>26</sup> The dimers **2.6a,g** react with pyrroleimines and DABCO or Na<sub>2</sub>CO<sub>3</sub> under microwave irradiation to form compounds **3.15a(*p*-C<sub>6</sub>H<sub>4</sub>R)** ( $\text{R} = \text{H, Br, OH, Me, OMe, CO}_2\text{Me}$ ), **3.15h(*p*-C<sub>6</sub>H<sub>4</sub>Br)** and **3.15a,g(<sup>i</sup>Pr)** in moderate to good yields (60 - 80%) (Scheme 3.6) DABCO is preferred as a base over Na<sub>2</sub>CO<sub>3</sub> due to the limited solubility of Na<sub>2</sub>CO<sub>3</sub> in the reaction solvent (acetonitrile).

As for the pyridineimine complexes **3.14**, the <sup>1</sup>H and <sup>13</sup>C-<sup>{1}</sup>H NMR spectra of complexes **3.15a(*p*-C<sub>6</sub>H<sub>4</sub>R)** ( $\text{R} = \text{H, Br, OH, Me, OMe, CO}_2\text{Me}$ ), **3.15h(*p*-C<sub>6</sub>H<sub>4</sub>Br)** and **3.15a,g(<sup>i</sup>Pr)** are very complicated due to the loss of C<sub>2</sub>-symmetry, hence, in principle, all the protons in the complex are inequivalent. The signals due to the cyclometallated ligand (ppz) in the <sup>1</sup>H and <sup>13</sup>C NMR spectra of **3.15a(*p*-C<sub>6</sub>H<sub>4</sub>R)** are similar in all the complexes and to those for the same fragment in **3.14a(*p*-C<sub>6</sub>H<sub>4</sub>R)**,



therefore, only the assignment of **3.15a**(*p*-C<sub>6</sub>H<sub>4</sub>Br) is explained in detail. The TOCSY spectrum of **3.15a**(*p*-C<sub>6</sub>H<sub>4</sub>Br) allowed identification of two phenyls, two pyrazoles and one pyrrole ring. The imine proton H<sub>4</sub> is easily identified as the most downfield signal, a doublet at  $\delta$  8.18, and it shows an NOE to one part of an [AA'BB'] system at *ca.*  $\delta$  6.7 which is therefore assigned to the N-aryl protons H<sub>5/5'</sub> the other part at  $\delta$  7.1 is assigned to H<sub>6/6'</sub> *via* the COSY spectrum. H<sub>4</sub> also shows an NOE to a doublet of doublets at  $\delta$  6.96 which is therefore assigned as pyrrole proton H<sub>3</sub> and the COSY spectrum then allows assignment of protons H<sub>1</sub> and H<sub>2</sub>. Protons H<sub>5/5'</sub> show an NOE to a doublet of doublet of doublets at  $\delta$  6.30 which is therefore assigned as the phenyl proton H<sub>a'</sub>. The COSY spectrum then allows the assignment of all the other phenyl protons H<sub>b'-d'</sub>. H<sub>d'</sub> is a doublet of doublets at  $\delta$  7.17 which shows an NOE to a doublet of doublets at  $\delta$  8.04 which is therefore assigned as H<sub>e'</sub>. The other pyrazole protons H<sub>f'</sub> and H<sub>g'</sub> are then assigned *via* the COSY spectrum. H<sub>g'</sub> (*ca.*  $\delta$  6.8) shows an NOE to a doublet of doublet of doublets at  $\delta$  6.38 which is therefore assigned as the phenyl proton H<sub>a</sub> of the other cyclometallated ligand, and all the other phenyl protons H<sub>b-d</sub> are assigned *via* the COSY spectrum. Proton H<sub>d</sub> ( $\delta$  6.8) shows an NOE to a doublet of doublets at  $\delta$  8.12 which is therefore assigned as H<sub>e</sub>. The COSY spectrum then allows the assignment of all the other pyrazole protons H<sub>f</sub> and H<sub>g</sub>. Phenyl protons H<sub>a,a'</sub> are characteristically at high field as described earlier. The signal for H<sub>g'</sub> (*ca.*  $\delta$  6.8) is significantly upfield of that for H<sub>g</sub> ( $\delta$  7.49) due to its proximity to the pyrrole ring. The <sup>13</sup>C-*{*<sup>1</sup>H} NMR spectra show the

expected number of signals for the quaternary and CH carbons. The FAB mass spectrum shows a molecular ion at  $m/z$  726.

Crystals of **3.15a(p-C<sub>6</sub>H<sub>4</sub>Br)** were obtained from DCM/hexane and were suitable for X-ray diffraction. The crystal structure reveals the expected distorted octahedral coordination geometry [N(1)–Ir(1)–N(3) is 175.0°] (**Fig. 3.18**), with *cis* metallated carbons and *trans* nitrogen atoms, as found for the pyridineimine complexes **3.14(C<sub>6</sub>H<sub>4</sub>R)**. The Ir–N (N<sup>+</sup>N) bond distances [2.153(8) and 2.103(9) Å] are longer than the Ir–N (C<sup>+</sup>N) ones [2.015(9) and 2.023(8) Å] due to the *trans* influence of the Ir–C bonds. The structure is shown with selected bond lengths (Å) and angles (°) in **Fig. 3.18**.

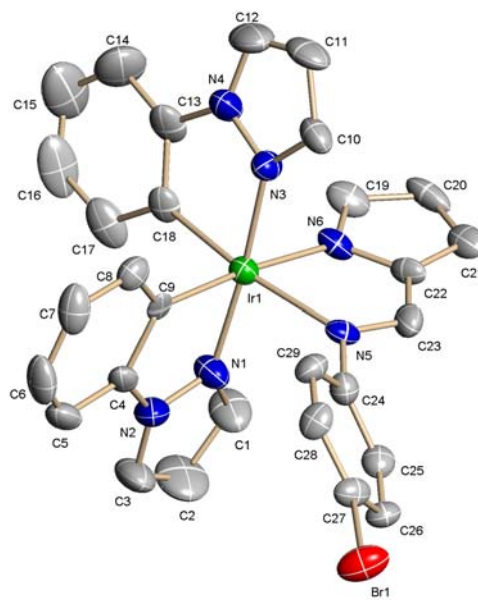


**Fig. 3.18:** X-ray crystal structure of **3.15a(p-C<sub>6</sub>H<sub>4</sub>Br)**. Selected bond lengths (Å) and bond angles (°): Ir(1)–N(1), 2.015(9); Ir(1)–N(3), 2.023(8); Ir(1)–N(5), 2.153(8); Ir(1)–N(6), 2.103(9); Ir(1)–C(9), 2.016(9); Ir(1)–C(18), 2.004(10); N(1)–Ir(1)–N(3), 175.0(4); N(1)–Ir(1)–C(9), 80.7(4); N(3)–Ir(1)–C(18), 80.7(4); N(5)–Ir(1)–N(6), 77.4(3).

As mentioned earlier, the <sup>1</sup>H NMR spectra of **3.15a(p-C<sub>6</sub>H<sub>4</sub>R)** (R = H, OH, Me, OMe, CO<sub>2</sub>Me) are similar to **3.15a(p-C<sub>6</sub>H<sub>4</sub>Br)** and similar NOE's are observed. In each case the imine proton H<sub>4</sub> is the most downfield signal ( $\delta$  8.13 – 8.20) and the phenyl protons H<sub>a,a'</sub> are at high fields characteristic of the [Ir(C<sup>+</sup>N)<sub>2</sub>] fragment.<sup>28</sup> Pyrazole protons H<sub>g'</sub> (ca.  $\delta$  6.7) are observed at higher field than H<sub>g</sub> (ca.  $\delta$  7.5). The <sup>13</sup>C–{<sup>1</sup>H} NMR spectra show the expected signals and the FAB mass spectra show molecular ions.

The  $^1\text{H}$  NMR spectrum of **3.15a(iPr)** is similar to **3.15a(*p*-C<sub>6</sub>H<sub>4</sub>R)** except for the N alkyl protons (H<sub>5</sub> and Me<sub>A/B</sub>). Proton H<sub>4</sub> ( $\delta$  8.11) is the most downfield signal and the only singlet and shows NOEs to the isopropyl protons (H<sub>5</sub> and Me<sub>A/B</sub>). The methyl protons Me<sub>A/B</sub> are inequivalent consistent with the chirality at the metal. All other assignments are done by analogy to **3.15a(*p*-C<sub>6</sub>H<sub>4</sub>Br)**. H<sub>g'</sub> (*ca.*  $\delta$  6.7) are observed at higher field than H<sub>g</sub> ( $\delta$  7.45). The  $^{13}\text{C}-\{^1\text{H}\}$  NMR spectra show the expected number of signals and the FAB mass spectrum shows a molecular ion at *m/z* 614. Crystals of **3.15a(iPr)** were obtained from DCM/hexane and were suitable for X-ray diffraction. The structure is shown in **Fig. 3.19** with selected bond lengths (Å) and angles (°) in **Table 3.10**.

The  $^1\text{H}$  NMR spectrum of **3.15g(*p*-C<sub>6</sub>H<sub>4</sub>Br)** is similar to **3.15a(*p*-C<sub>6</sub>H<sub>4</sub>Br)** except the pyrazole signals are replaced by pyridine ones. The other notable difference is that the imine proton H<sub>4</sub>, a doublet at  $\delta$  8.23, is no longer the most downfield signal. Pyridine proton H<sub>h</sub> is the most downfield signal at  $\delta$  8.45 whilst H<sub>h'</sub> is more upfield at  $\delta$  7.50 due to its proximity to the pyrrole ring. The protons H<sub>a,a'</sub> are again observed at high field ( $\delta$  6.35, 6.34 respectively) due to ring current effects. The  $^{13}\text{C}-\{^1\text{H}\}$  NMR spectra show the expected number of signals for CH and quaternary carbons and FAB mass spectrum shows a molecular ion at *m/z* 748. Crystals suitable for X-ray diffraction were obtained from DCM/hexane. The structure is shown in **Fig. 3.19** with selected bond lengths (Å) and angles (°) in **Table 3.10**.

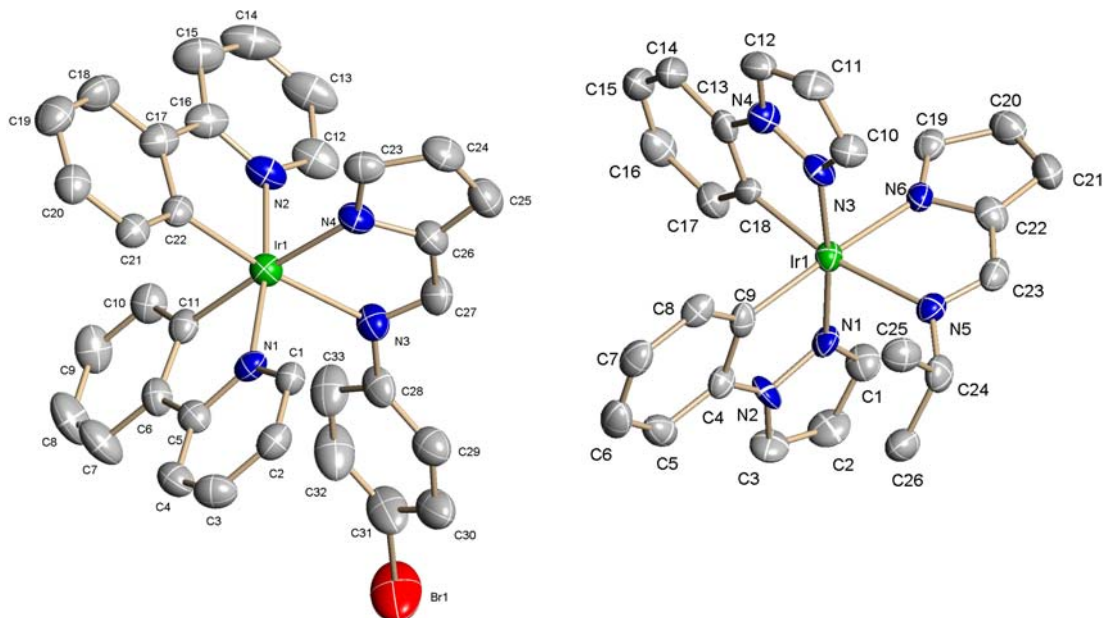


**Fig. 3.19:** X-ray crystal structure of **3.15g(*p*-C<sub>6</sub>H<sub>4</sub>Br)** and **3.15a(iPr)** respectively.

**Table 3.10:** Selected bond lengths (Å) and bond angles (°) of **3.15g(*p*-C<sub>6</sub>H<sub>4</sub>Br)** and **3.15a(<sup>i</sup>Pr)**, respectively.

(Å)	<b>3.15g (<i>p</i>-C<sub>6</sub>H<sub>4</sub>Br)</b>	(Å)	<b>3.15a(<sup>i</sup>Pr)</b>
Ir(1)—N(1)	2.040(3)	Ir(1)—N(1)	2.007(7)
Ir(1)—N(2)	2.042(4)	Ir(1)—N(3)	2.015(7)
Ir(1)—N(3)	2.192(4)	Ir(1)—N(5)	2.186(7)
Ir(1)—N(4)	2.113(3)	Ir(1)—N(6)	2.096(6)
Ir(1)—C(11)	2.012(4)	Ir(1)—C(9)	2.024(8)
Ir(1)—C(22)	2.005(4)	Ir(1)—C(18)	2.019(8)
(°)		(°)	
N(1)—Ir(1)—N(2)	172.58(15)	N(1)—Ir(1)—N(3)	172.8(3)
N(1)—Ir(1)—C(11)	79.86(16)	N(1)—Ir(1)—C(9)	80.2(3)
N(2)—Ir(1)—C(22)	80.38(17)	N(3)—Ir(1)—C(18)	79.5(3)
N(3)—Ir(1)—N(4)	76.33(14)	N(5)—Ir(1)—N(6)	76.8(3)

<sup>a</sup>For **3.15a(<sup>i</sup>Pr)** there were two independent molecules in the unit cell, therefore the data are an average of values for both structures.

The <sup>1</sup>H NMR spectrum of **3.15g(<sup>i</sup>Pr)** is similar to that of **3.15g(*p*-C<sub>6</sub>H<sub>4</sub>Br)**. Pyridine proton H<sub>h</sub> ( $\delta$  8.42) is the most downfield signal similar to **3.15g(*p*-C<sub>6</sub>H<sub>4</sub>Br)**, rather than H<sub>4</sub> in **3.15a(<sup>i</sup>Pr)**. The methyl signals (Me<sub>A/B</sub>) are inequivalent due to chirality at metal centre. The protons H<sub>a,a'</sub> are observed as doublet of doublets at high field ( $\delta$  6.26 and  $\delta$  6.49 respectively). Proton H<sub>h'</sub> ( $\delta$  7.51) is upfield of H<sub>h</sub> ( $\delta$  8.42) due to a ring current of the pyrrole ring (as found for H<sub>g'</sub> in **3.15a(<sup>i</sup>Pr)**). The <sup>13</sup>C—{<sup>1</sup>H} NMR spectra show the expected signals and FAB mass spectrum shows a molecular ion at *m/z* 636.

These reactions show that a range of pyrroleimine complexes **3.15** can be synthesised in good yields (60 - 80%) using microwave heating. The complexes were fully characterised and X-ray crystallography shows that structurally the complexes are similar to the corresponding pyridineimines ones. The electrochemical and photophysical properties of these complexes are discussed in the following sections.

### 3.2.2.1 Electrochemistry of [Ir(C<sup>N</sup>)<sub>2</sub>(pyrrolylimine)] (**3.15**)

The electrochemical properties of the pyrroleimine complexes **3.15a,g(*p*-C<sub>6</sub>H<sub>4</sub>R)** and **3.15a,g(<sup>i</sup>Pr)** were examined using cyclic voltammetry. All the complexes showed two irreversible oxidation waves. The irreversibility of the first oxidation wave was proved by reversing the scan after the first oxidation (Fig. 3.20). In the subsequent

discussion, only the first oxidation potentials ( $E^{1/2}_{\text{ox1}}$ ) are considered and are tabulated in **Table 3.11**.

**Table 3.11:** Redox properties of **3.15(p-C<sub>6</sub>H<sub>4</sub>R)** and **3.15(<sup>i</sup>Pr)** complexes<sup>a</sup>.

Entry	Complex	$E^{1/2}_{\text{ox}}\text{ b}$
1	<b>3.15a(C<sub>6</sub>H<sub>5</sub>)</b>	0.82
2	<b>3.15a(p-C<sub>6</sub>H<sub>4</sub>Me)</b>	0.77
3	<b>3.15a(p-C<sub>6</sub>H<sub>4</sub>OH)</b>	0.69
4	<b>3.15a(p-C<sub>6</sub>H<sub>4</sub>OMe)</b>	0.74
5	<b>3.15a(p-C<sub>6</sub>H<sub>4</sub>CO<sub>2</sub>Me)</b>	0.90
6	<b>3.15a(p-C<sub>6</sub>H<sub>4</sub>Br)</b>	0.83
7	<b>3.15g(p-C<sub>6</sub>H<sub>4</sub>Br)</b>	0.82
8	<b>3.15a(<sup>i</sup>Pr)</b>	0.74
9	<b>3.15g(<sup>i</sup>Pr)</b>	0.74
10	<b>2.7a</b>	1.37
11	<b>3.14a(C<sub>6</sub>H<sub>5</sub>)</b>	1.39

<sup>a</sup>In dry DCM (0.1 mol L<sup>-1</sup> of Bu<sub>4</sub>NBF<sub>4</sub>), scan rate 100 mV s<sup>-1</sup>, all potentials are quoted *vs* SCE (Cp<sub>2</sub>Fe<sup>+</sup>/Cp<sub>2</sub>Fe *vs* SCE = +0.42 V).<sup>33</sup> A Pt disc was used as a working electrode, counter electrode was a Pt gauze and a silver wire was used as a reference. <sup>b</sup>Irreversible wave.

The relatively small range of first oxidation potentials ( $E^{1/2}_{\text{ox1}} \sim 0.2$  V) and the irreversibility are consistent with the first oxidation being mainly centred on the pyrrole. Thus, the HOMO mainly resides on the pyrrole ring with, maybe, a partial contribution from the metal. This is also supported by the observation that there is no change in oxidation potential upon changing the cyclometallated ligand from ppz to ppy (**Table 3.11**, entries 6 *vs* 7 and 8 *vs* 9). In contrast for [Ir(C<sup>N</sup>)<sub>2</sub>(acac)], in which the HOMO resides on Ir and the C<sup>N</sup> ligand, the oxidation potential changes by 0.12 V upon substituting ppz with ppy.<sup>35-37</sup> However, the oxidation potentials of (**3.15**) vary (by up to 0.2V) upon changing the substituents on the N-aryl ring as expected since the pyrrole ring is in conjugation with the imine. Complex **3.15a(p-C<sub>6</sub>H<sub>4</sub>Me)** with an electron donating group *i.e.* methyl, has a lower oxidation potential than unsubstituted complex **3.15a(C<sub>6</sub>H<sub>5</sub>)** (entries 1 and 2) and hence has a higher HOMO. Replacing H with OH or OMe also lowers the oxidation potential (entries 1 *vs* 3 and 4) which indicates that these groups are acting as electron donating groups hence conjugative effects outweigh the inductive effects. Alternatively, the electron withdrawing substituent, CO<sub>2</sub>Me gives a more anodic oxidation potential (**Table 3.11**, entries 1 and 5), while replacing H with Br

has a negligible effect (entries 1 and 6). As expected, neutral pyrroleimine complexes **3.15(p-C<sub>6</sub>H<sub>4</sub>R)** are easier to oxidise in comparison to cationic bipy (**2.7a-g**) and pyridineimine **3.15(p-C<sub>6</sub>H<sub>4</sub>R)** complexes (compare entries 1, 10 and 11 **Table 3.11**).

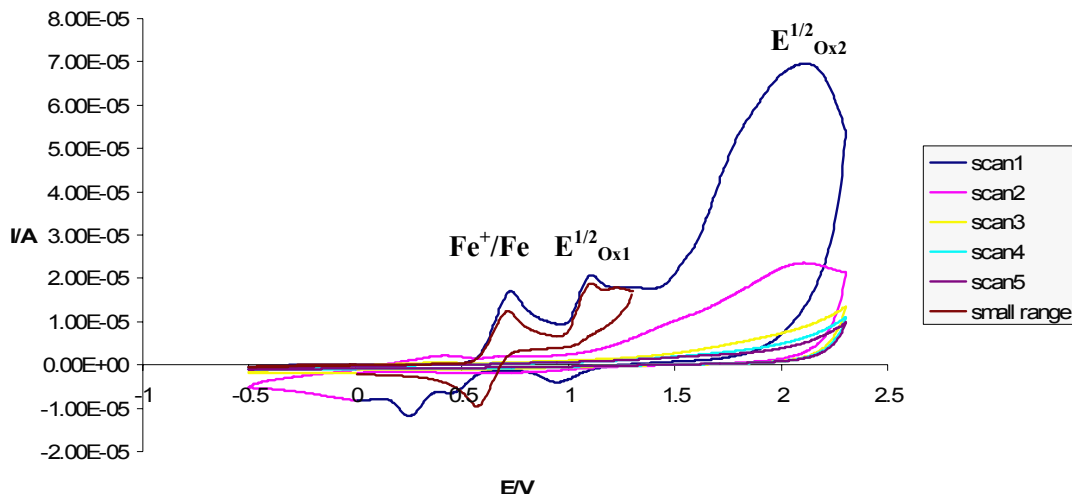


**Fig. 3.20:** Cyclic voltammogram of **3.15a(C<sub>6</sub>H<sub>5</sub>)** complex showing polymerisation of pyrrole (scan rate = 100 mV/s ).

Five consecutive scans were run on each complex (shown for **3.15a(C<sub>6</sub>H<sub>5</sub>)** in **Fig. 3.20**). It is notable that the peak current decreased with each consecutive scan and the peak for ferrocene became irreversible, which indicates that the working electrode was passivated. This may be due to polymerization of the pyrroles, after the oxidation of the pyrrole during the first scan and therefore no electron transfer either from the metal or from the ferrocene, takes place during the successive scans. This is supported with the observation that after first oxidation happening on pyrrole, the Ir-N σ-bond may rupture providing an opportunity for the polymerization of the pyrrole ring. These observations are further supported by the appearance of a yellow coloured film on the surface of the working electrode. The electropolymerisation of pyrrole is well precedented.<sup>38</sup>

No reduction waves were observed down to -2.22 V for **3.15a,g(p-C<sub>6</sub>H<sub>4</sub>R)** and **3.15a,g(<sup>i</sup>Pr)**, whilst the corresponding complexes  $[\text{Ir}(\text{ppy})_2(\text{X}^{\wedge}\text{Y})]$  ( $\text{X}^{\wedge}\text{Y}$  = acac, pic), can be reduced at  $E^{1/2}_{\text{Red}}$  -2.10 and -1.94 respectively;<sup>35, 36, 39</sup> this suggests that pyrrolylimines are better donors than acac and pic. The absence of reduction processes also means the electrochemistry provides no insight into the position of the LUMO.

### 3.2.2.2 Photophysical properties of $[\text{Ir}(\text{C}^{\wedge}\text{N})_2(\text{pyrrolylimine})]$ (3.15)

#### Absorption spectroscopy

The electronic absorption data of pyrroleimine complexes  $[\text{Ir}(\text{C}^{\wedge}\text{N})_2(\text{pyrrolylimine})]$  are given in **Table 3.12**. All *para* substituted ppz complexes **3.15a(*p*-C<sub>6</sub>H<sub>4</sub>R)** show 2 absorption bands, one at shorter wavelength (247 – 251 nm,  $\epsilon > 51,000 \text{ L mol}^{-1} \text{ cm}^{-1}$ ) and other at relatively longer wavelength (367 – 392 nm,  $\epsilon > 28,000 \text{ L mol}^{-1} \text{ cm}^{-1}$ ) (**Table 3.12**, entries 1-6). The most intense short wavelength absorption bands are assigned to the spin allowed intraligand IL ( $\pi \rightarrow \pi^*$ ) transitions, however the other band is difficult to assign. Similarly, both ppy complexes, **3.15g(<sup>i</sup>Pr)** and **3.15g(*p*-C<sub>6</sub>H<sub>4</sub>Br)** show two very similar bands, one at  $\sim 260$  nm and other at  $\sim 380$  nm. **3.15a(<sup>i</sup>Pr)** show slightly different absorption bands, the shorter wavelength band is red shifted relative to **3.15a(*p*-C<sub>6</sub>H<sub>4</sub>R)**, however, the longer wavelength band is not observed.

**Table 3.12: Electronic absorption spectral data of (3.15)**

Entry	Complex	Solvent	$\lambda_{\text{abs}} \text{ [nm]} (\epsilon_{\text{max}} \text{ [dm}^3\text{mol}^{-1}\text{cm}^{-1} \text{ ]})$
1	<b>3.15a(C<sub>6</sub>H<sub>5</sub>)</b>	DCM	248 (54600), 367 (28100)
2	<b>3.15a(<i>p</i>-C<sub>6</sub>H<sub>4</sub>Br)</b>	DCM	249 (59300), 310 sh (23500), 375 (31900)
3	<b>3.15a(<i>p</i>-C<sub>6</sub>H<sub>4</sub>OH)</b>	DCM	247 (51300), 369 (29000)
4	<b>3.15a(<i>p</i>-C<sub>6</sub>H<sub>4</sub>Me)</b>	DCM	248 (61800), 296 sh (24000), 369 (32800)
5	<b>3.15a(<i>p</i>-C<sub>6</sub>H<sub>4</sub>OMe)</b>	DCM	247 (69700), 370 (34600)
6	<b>3.15a(<i>p</i>-C<sub>6</sub>H<sub>4</sub>CO<sub>2</sub>Me)</b>	DCM	251 (73800), 315 sh (31400), 392 (36000)
7	<b>3.15a(<sup>i</sup>Pr)</b>	DCM	276 (51400), 321 (27300)
8	<b>3.15g(<sup>i</sup>Pr)</b>	DCM	264 (136400), 378 (25300)
9	<b>3.15g(<i>p</i>-C<sub>6</sub>H<sub>4</sub>Br)</b>	DCM	261 (55500), 380 (29300)

#### Emission spectroscopy of $[\text{Ir}(\text{C}^{\wedge}\text{N})_2(\text{pyrrolylimine})]$ (3.15)

All pyrroleimine complexes **3.15** are emissive at room temperature in DCM. Emission spectra of these complexes are shown in **Figs. 3.21-3.23** and the emission maxima are summarised in **Table 3.13**.

**Table 3.13: Emission data of  $[\text{Ir}(\text{C}^{\wedge}\text{N})_2(\text{pyrrolylimine})]$  complexes (3.15)**

Entry	Complex	Solvent	$\lambda_{\text{em}}$ (nm)	Energy (eV)
1	<b>3.15a(C<sub>6</sub>H<sub>5</sub>)</b>	DCM	594, 645 sh	2.08, 1.92
2	<b>3.15a(p-C<sub>6</sub>H<sub>4</sub>Br)</b>	DCM	595	2.08
3	<b>3.15a(p-C<sub>6</sub>H<sub>4</sub>OH)</b>	DCM	610, 648 sh	2.03, 1.91
4	<b>3.15a(p-C<sub>6</sub>H<sub>4</sub>Me)</b>	DCM	600	2.06
5	<b>3.15a(p-C<sub>6</sub>H<sub>4</sub>OMe)</b>	DCM	610, 645 sh	2.03, 1.92
6	<b>3.15a(p-C<sub>6</sub>H<sub>4</sub>CO<sub>2</sub>Me)</b>	DCM	595	2.08
7	<b>3.15a(<sup>i</sup>Pr)</b>	DCM	505, 540	2.45, 2.29
8	<b>3.15g(<sup>i</sup>Pr)</b>	DCM	505, 530 sh	2.45, 2.33
9	<b>3.15g(p-C<sub>6</sub>H<sub>4</sub>Br)</b>	DCM	505, 590	2.45, 2.10
10	<b>2.7a</b>	DCM	557	2.22
11	<b>3.14a(C<sub>6</sub>H<sub>5</sub>)</b>	DCM	475 sh, 670	2.60, 1.84

The complexes **3.15a(p-C<sub>6</sub>H<sub>4</sub>R)** and **3.15g(p-C<sub>6</sub>H<sub>4</sub>Br)** show broad bands at about 600 nm, some with shoulders at about 645 nm. Emission wavelengths of pyrroleimine complexes are in between bipy and pyridineimine complexes, however, probably corresponding to different transitions (mostly ligand based  $\pi \rightarrow \pi^*$  see below). There is not much shift (594-610 nm) observed in the emission maxima  $\lambda_{\text{em}}$  for **3.15a(p-C<sub>6</sub>H<sub>4</sub>R)** upon changing the substituent on the *para* position of N-aryl ring (**Fig. 3.21**). The ppz complex **3.15a(p-C<sub>6</sub>H<sub>4</sub>Br)** emits at 595 nm whilst the corresponding ppy complex **3.15g(p-C<sub>6</sub>H<sub>4</sub>Br)** emits at 590 nm with a weaker peak at 505 nm. Hence changing the cyclometallated ligand from ppz to ppy, does not affect the emission wavelength much. This is true of the N<sup>i</sup>Pr complexes thus **3.15a(<sup>i</sup>Pr)** shows two bands at 505 and 540 nm whilst **3.15g(<sup>i</sup>Pr)** has one broad intense band at 505 nm with a shoulder at 530 nm. However, as can be seen changing the imine substituent from aryl to isopropyl, whilst keeping the C<sup>W</sup>N ligand the same, leads to a pronounced blue shift (entries 2 vs 7 and 9 vs 8 in **Table 3.13** and **Fig. 3.22**). Complex **3.15a(C<sub>6</sub>H<sub>5</sub>)** emits at 594 nm which is a red shift relative to the bipy complex **2.7a** at 557 nm, but a significant blue shift compared to the pyridineimine complex **3.14a(C<sub>6</sub>H<sub>5</sub>)** at 670 nm.

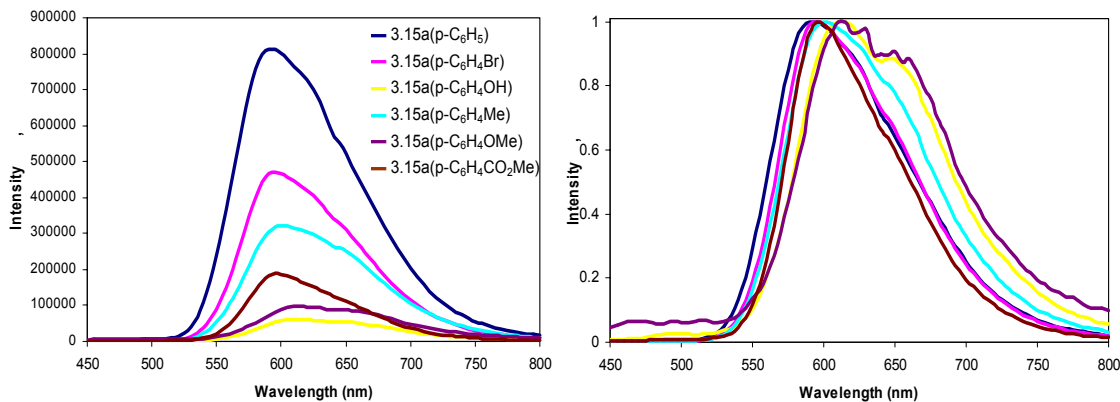


**Fig. 3.21:** Degassed emission spectra and normalised intensity plots of **3.15a(p-C<sub>6</sub>H<sub>4</sub>R)** showing the effect of changing the substituents on the pyrroleimine ligand.

<sup>a</sup>All measurements on 0.01 mM in dry DCM. <sup>b</sup>Intensity of **3.15a(p-C<sub>6</sub>H<sub>4</sub>OMe)** is multiplied by a factor of 10.

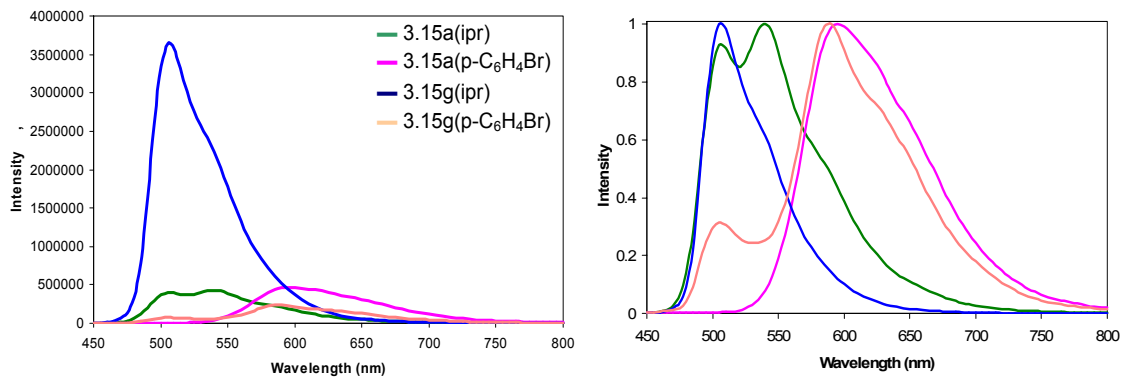


**Fig. 3.22:** Degassed emission spectra and the normalised intensity plot of pyrroleimine complexes (**3.15**) comparing the effect of changing the C<sup>N</sup> ligand and changing the substituents (alkyl vs aryl).

Pyrroleimine complexes (**3.15**) are much more sensitive to the presence of oxygen compared to the bipy (**2.7**) and pyridineimine (**3.14**) complexes. The emission intensity of pyrroleimine complexes (**3.15**) increases by a factor of 20 - 30 times upon degassing, however, for bipy complex (**2.7**) intensity is only affected by a factor of ~1.5 to 2. For pyridineimine complexes (**3.14**), the two bands have a different response to oxygen; the shorter wavelength band (~ 500 nm) is more sensitive to oxygen (response to oxygen ranges by a factor of 2 - 8) than the longer wavelength band (~ 700 nm), which remains relatively unaffected. Gassed and degassed emission of **2.7a**, **3.14a(p-C<sub>6</sub>H<sub>5</sub>)** and **3.15a(p-C<sub>6</sub>H<sub>5</sub>)** are shown in **Fig. 3.23**. This suggests that the excited states

for the pyrroleimine complexes have a higher triplet character and probably less metal character, *i.e.* a bigger proportion of  $^3\text{IL}\ \pi$  to  $\pi^*$  which is more sensitive to oxygen than MLCT bands.

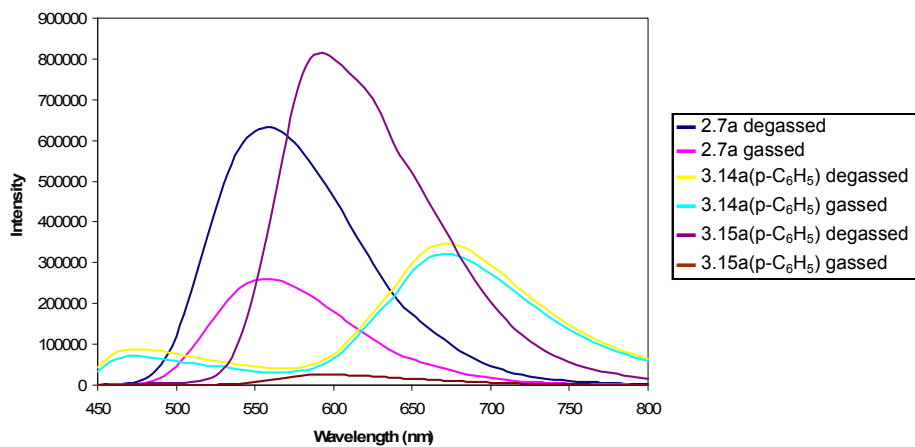
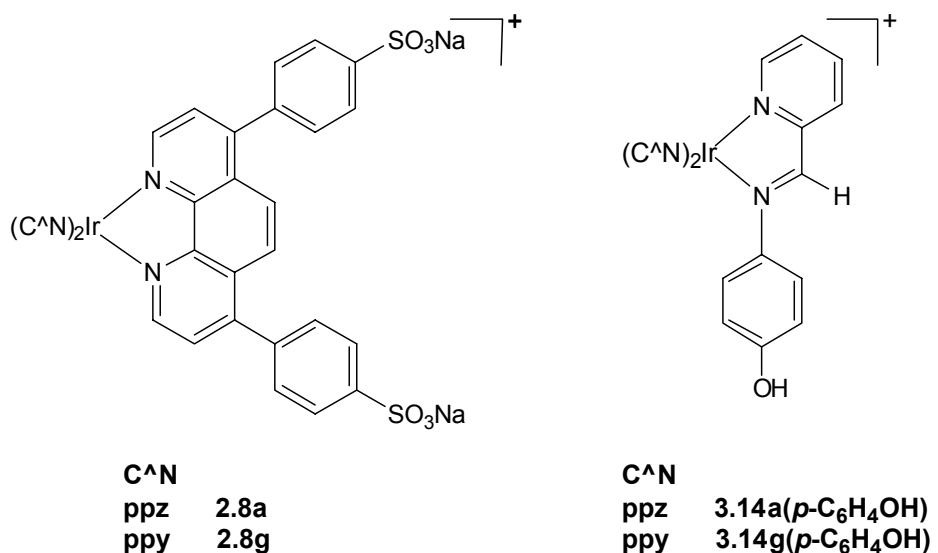


**Fig. 3.23:** A comparison of gassed and degassed emission spectra of bipy (**2.7**), pyridineimine (**3.14**) and pyrroleimine (**3.15**) complexes.

In conclusion, pyrroleimine complexes **3.15** are found to be emissive at room temperature in fluid solutions. A considerable variation in emission wavelength is observed upon changing the substituent from alkyl to aryl in pyrroleimine complexes. The emission intensity of these complexes is found to be much more sensitive to oxygen than bipy and pyridineimine complexes.

### 3.2.3 Live-cell imaging

As described in **Chapter 1**, fluorescence cell imaging offers a unique approach for visualising morphological details in tissues with sub-cellular resolution that can not be resolved by ultrasound or magnetic resonance imaging. Some prerequisite criteria for live cell imaging are that the luminescent probe must be non-toxic and cell-permeable, preferably with a distinctive compartmentalisation profile. The applications of  $d^6$  transition metal complexes in cell imaging has received considerable attention due to their attractive photophysical properties (such as relatively long lifetimes and large Stokes shifts) and thus seem to be appealing targets for avoiding auto fluorescence in bioimaging and the area has recently been reviewed.<sup>40</sup> Complexes **2.8a**, **2.8g**, **3.14a(p-C<sub>6</sub>H<sub>4</sub>OH)** and **3.14g(p-C<sub>6</sub>H<sub>4</sub>OH)** were employed for cytotoxicity assays and for live-cell imaging by our collaborators, Prof. Dr. Nils Metzler-Nolte and Annika Gross at Ruhr University Bochum.



### Cytotoxicity assays

Although relatively less explored, cytotoxicity studies of cyclometallated Ir(III) complexes are receiving increasing attention and a few reports have been published.<sup>41-43</sup> Cyclometallated Ir(III) complexes incorporating a biotin moiety were found to be non-cytotoxic (IC<sub>50</sub> values > 400  $\mu$ M),<sup>42</sup> however, the cytotoxicity of complexes bearing an indole moiety were relatively high (IC<sub>50</sub> values 1.1 to 6.3  $\mu$ M) compared with cisplatin (30.7  $\pm$  0.7  $\mu$ M).<sup>43</sup> The cytotoxicity of the complexes **2.8a**, **2.8g**, **3.14a(*p*-C<sub>6</sub>H<sub>4</sub>OH)** and **3.14g(*p*-C<sub>6</sub>H<sub>4</sub>OH)** has been studied by the Resazurin and Crystal Violet (CV) assays using three different cell lines, as PT45, HepG2 and HeLa. The Resazurin assay defines the cell viability and Crystal Violet assay defines the total cell count. The cytotoxicity data of the complexes are shown in **Table 3.14**. Complex **2.8g** is considered as non-cytotoxic (IC<sub>50</sub> values > 460  $\mu$ M) whereas IC<sub>50</sub> values for **2.8a** are more than 4.5 times lower. However, both of the complexes have significantly higher IC<sub>50</sub> values than those of cisplatin indicative of their lower cytotoxicity and hence should be suitable for live-cell imaging applications. The IC<sub>50</sub> values of the pyridineimine complexes **3.14a(*p*-C<sub>6</sub>H<sub>4</sub>OH)** and **3.14g(*p*-C<sub>6</sub>H<sub>4</sub>OH)** are comparable to those of cisplatin (**Table 3.14**) but significantly lower than those of **2.8a** and **2.8g**, suggesting that these are cytotoxic.

**Table 3.14:** Cytotoxicity ( $IC_{50}$ ) of the cyclometallated Ir(III) complexes and cisplatin toward the PT45, HepG2 and HeLa cell lines.

<b>Complex</b>	<b><math>IC_{50}/\mu M</math></b>		
	<b>PT45</b>	<b>HepG2</b>	<b>HeLa</b>
<b>2.8a</b>	$103.7 \pm 3.0$	$103.1 \pm 0.7$	$95.9 \pm 0.4$
<b>2.8g</b>	$460.8 \pm 1.9$	$> 500$	$485.2 \pm 14.9$
<b>3.14a(<i>p</i>-C<sub>6</sub>H<sub>4</sub>OH)</b>	$1.18 \pm 0.15$	$1.25 \pm 0.25$	$1.76 \pm 0.07$
<b>3.14g(<i>p</i>-C<sub>6</sub>H<sub>4</sub>OH)</b>	$0.53 \pm 0.12$	$0.73 \pm 0.28$	$1.57 \pm 0.32$
<b>cisplatin</b>	$0.9 \pm 0.2$	$2.4 \pm 0.4$	$1.8 \pm 0.1$

For PT45 and HepG2 cell lines,  $IC_{50}$  values are calculated from Crystal Violet assay and for Hela cells these are calculated from Resazurin assay.

### Cellular uptake studies

The cellular uptake characteristics of the complexes **2.8a**, **2.8g**, **3.14a(*p*-C<sub>6</sub>H<sub>4</sub>OH)** and **3.14g(*p*-C<sub>6</sub>H<sub>4</sub>OH)** have been investigated using fluorescence microscopy. Incubation of MCF7 cells with **2.8a** and **2.8g** (25  $\mu M$ ) at 37 °C under a 5% CO<sub>2</sub> atmosphere for 14 hrs led to efficient interiorization of the complex, as observed by fluorescence microscopy (see Appendix). Cellular uptake of the complexes appears to occur *via* endocytosis. The fluorescence microscopy images of **2.8a** are displayed in **Fig. 3.24**. The phase contrast image (**Fig. 3.24a**) after treatment with the compounds confirmed that the cells were viable throughout the imaging experiments. Upon UV irradiation, the vesicles (lysosomes or endosomes) of the cells exhibited bright fluorescence (**Fig. 3.24b**), indicative of localisation of the compound in vesicles. To test this, cells were treated with a lysosomal dye, *i.e.* Lysotracker Red, for 2 hrs (**Fig. 3.24c**) prior to imaging. Upon overlaying of fluorescent image of the cells (**Fig. 3.24b**) with that of Lysotracker Red labelled reference (**Fig. 3.24c**), it is observed that both, the compound and Lysotracker Red colocalise in the lysosomes of the cells (**Fig. 3.24d**). This is consistent with the Re(I) complexes of the same ligand.<sup>44</sup> Owing to the higher cytotoxicity of pyridineimine complexes **3.14a(*p*-C<sub>6</sub>H<sub>4</sub>OH)** and **3.14g(*p*-C<sub>6</sub>H<sub>4</sub>OH)**, these could not be employed for fluorescent imaging as these killed the cells even after an incubation of 30 mins. Note the high cytotoxicity of these complexes means these may have some potential as anti-cancer agents, cyclometallated ruthenium complexes have shown some anti cancer activity.<sup>45, 46</sup>

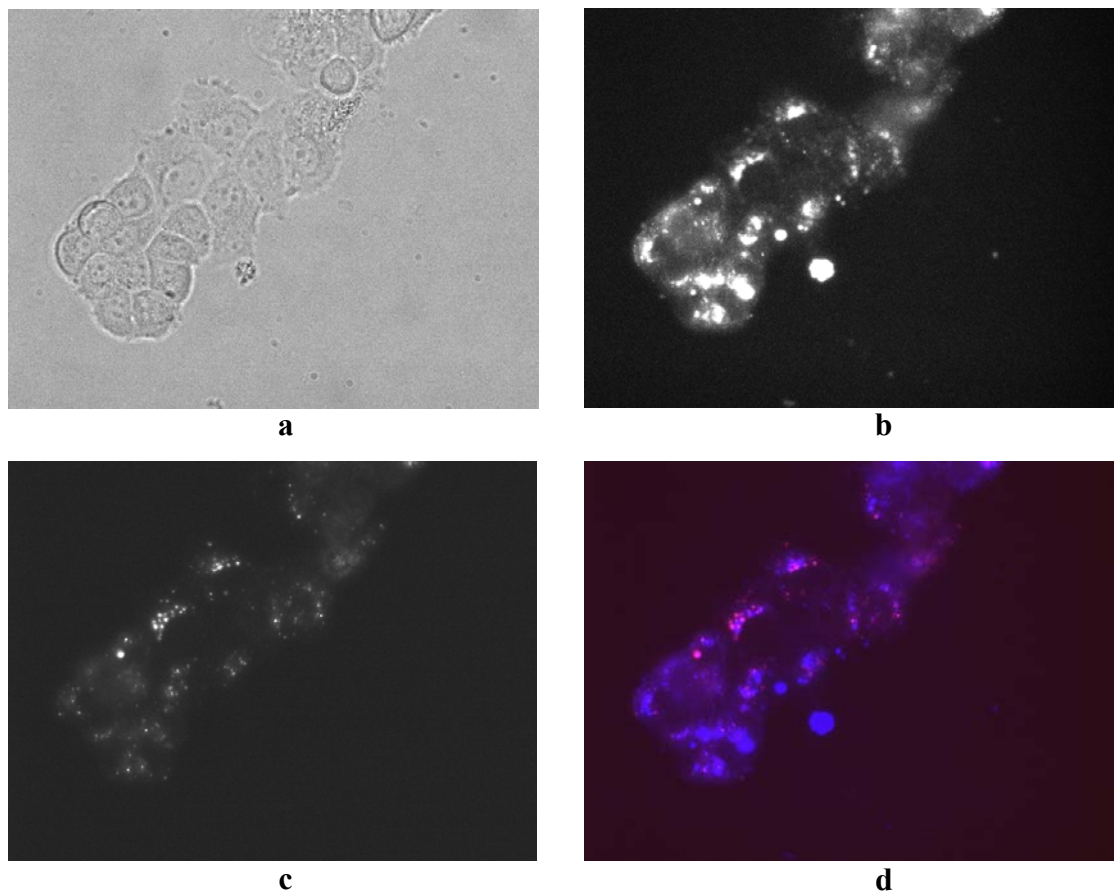


**Fig. 3.24:** Phase contrast (a), fluorescence (b), Lysotracker Red labelled reference (c) and overlays of fluorescence and Lysotracker Red (d) microscopy images of MCF7 cells incubated with complex **2.8a** (25  $\mu$ M) at 37 °C for 14 hrs.

To summarise, pyridineimines are good substitutes for bipy from a synthetic point of view. Pyridineimines can be easily generated *in situ* from pyridine-2-carboxaldehyde and the relevant amine, and hence a range of complexes containing different functional groups on the pyridineimine were easily synthesised and characterised. Electrochemical and photophysical properties of these complexes show that the  $\pi^*$  levels are lower for pyridineimine complexes relative to bipy complexes which shifts the emission to longer wavelength that may be desirable for cell imaging. Pyrroleimines are anionic analogues of neutral pyridineimines. In the complexes studied, the emission is blue shifted with respect to the pyridineimine complexes. More significantly, pyrrole is very electron rich so emission of these complexes contains a lot of  $\pi$  to  $\pi^*$  character, hence emission is relatively more sensitive to oxygen. Live-cell imaging of pyridineimine complexes **3.14a(p-C<sub>6</sub>H<sub>4</sub>OH)** and **3.14g(p-C<sub>6</sub>H<sub>4</sub>OH)** demonstrated that these types of complex can be used for such applications, however,

significant measures are required to reduce the cytotoxicity. Instead owing to their higher cytotoxicity these complexes can have some potential as anti cancer agents.

### 3.3 Experimental

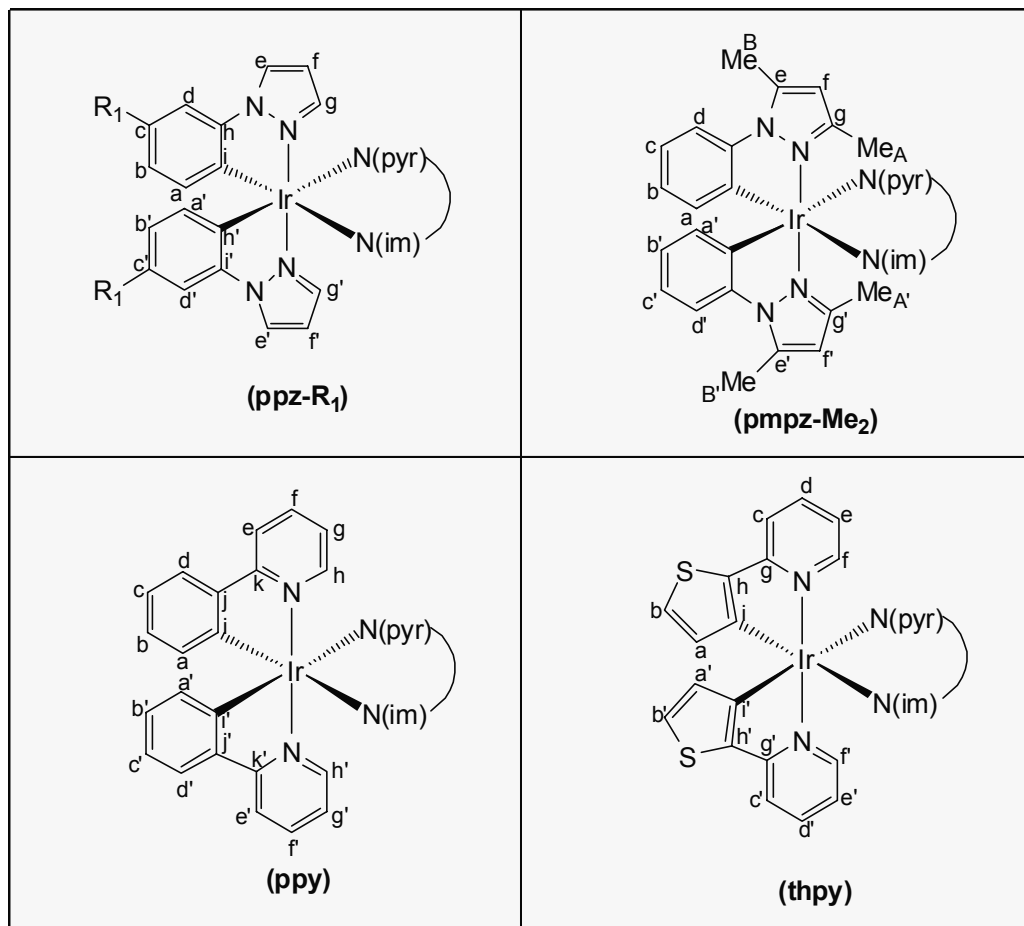
#### General information and materials

All reactions for the syntheses of pyridineimine (**3.14**) and pyrroleimine (**3.15**) complexes were carried out under an inert atmosphere of nitrogen and under microwave irradiation unless stated otherwise. After work up all the complexes were air stable. The spectroscopic techniques/instruments used were described in **Chapter 2**. All starting materials were obtained from Aldrich or Alfa Aesar with the exception of pyrroleimine ligands which are prepared according to the literature method.<sup>26</sup>

#### General procedure for synthesis of $[\text{Ir}(\text{C}^{\text{N}})_2(\text{pyridineimine})][\text{PF}_6]$ (**3.14**)

The appropriate dimer  $[\text{Ir}(\text{C}^{\text{N}})_2\text{Cl}]_2$ , pyridine-2-carboxaldehyde (2.4 equiv),  $\text{KPF}_6$  (2-2.4 equiv) and the relevant amine (2.4 equiv) were placed in a microwave vial and the solvent (3 ml) was added. Nitrogen was bubbled through the solution for 2 mins and the vial was then sealed with a septum cap. The tube was placed in the microwave reactor and heated under microwave irradiation. After this time the solvent was removed *in vacuo* leaving behind a solid which was dissolved in DCM (15 ml) and passed through celite. The filtrate was reduced in volume and hexane was added slowly to induce precipitation. The precipitate was isolated, washed with hexane and dried *in vacuo*. The compounds could be recrystallised from DCM/hexane. Early attempts were carried out at 100 °C for 30 mins in ethanol but later milder conditions (20 mins at 60 °C in methanol) were found to work just as well. Hence the reactions are done under the milder conditions unless stated otherwise. In the mass spectrometry data  $[\text{M}]^+$  will refer to just the complex cation.

**Labelling scheme for the cyclometallated ( $C^N$ ) ligands<sup>a</sup>**

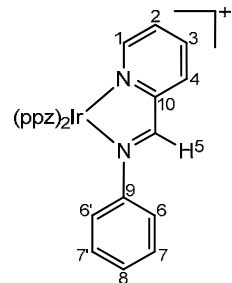


<sup>a</sup>N(pyr) represents either the pyridine or the pyrrole ring and N(im) represents the imine. In all cases the prime phenyl is *trans* to pyridine or pyrrole and the non-prime phenyl is *trans* to imine.

**Synthesis of 3.14a(C<sub>6</sub>H<sub>5</sub>)**

This was prepared from dimer **2.6a** (50 mg, 0.049 mmol), aniline (11 mg, 10.8  $\mu$ L, 0.118 mmol), pyridine-2-carboxaldehyde (12.7 mg, 12  $\mu$ L, 0.118 mmol) and KPF<sub>6</sub> (18.1 mg, 0.098 mmol) and after work up gave **3.14a(C<sub>6</sub>H<sub>5</sub>)** as a red solid (58 mg, 75%).  
Anal. Calcd for C<sub>30</sub>H<sub>24</sub>F<sub>6</sub>IrN<sub>6</sub>P: C, 44.72, H, 3.00, N, 10.43.

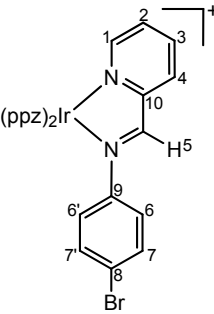
Found: C, 44.81, H, 3.07, N, 10.39%. <sup>1</sup>H NMR (CD<sub>2</sub>Cl<sub>2</sub>):  $\delta$  9.19 (1H, s, H<sub>5</sub>), 8.36 (1H, bd,  $J$  = 7.4, H<sub>4</sub>), 8.17 – 8.07 (4H, m, H<sub>1,3,e,e'</sub>), 7.54 – 7.51 (2H, m, H<sub>2,g</sub>), 7.34 (1H, bd,  $J$  = 8.2, H<sub>d</sub>), 7.21 – 7.06 (5H, m, H<sub>7,7',8,c,d'</sub>), 6.94 – 6.85 (5H, m, H<sub>6,6',b,c',g'</sub>), 6.68 (1H, td,  $J$  = 7.4, 1.2, H<sub>b</sub>), 6.65 (1H, t,  $J$  = 2.4, H<sub>f</sub>), 6.62 (1H, t,  $J$  = 2.4, H<sub>f'</sub>), 6.27 (1H, dd,  $J$  = 7.4, 1.2, H<sub>a</sub>), 6.07 (1H, dd,  $J$  = 7.4, 1.2, H<sub>a'</sub>). <sup>13</sup>C NMR: 168.55 (C<sub>5</sub>), 156.45 (C<sub>10</sub>), 151.57 (C<sub>1</sub>), 148.21 (C<sub>9</sub>), 142.90 (C<sub>h</sub>), 142.62 (C<sub>h'</sub>), 140.17 (C<sub>3</sub>), 140.05 (C<sub>g</sub>), 138.71



(C<sub>g'</sub>), 133.66 (C<sub>a'</sub>), 133.40 (C<sub>a</sub>), 131.63 (C<sub>i'</sub>), 131.02 (C<sub>4</sub>), 130.60 (C<sub>i</sub>), 129.89 (C<sub>2</sub>), 129.41 (C<sub>7, 7'</sub>), 129.36 (C<sub>8</sub>), 127.61 (C<sub>e</sub>), 127.42 (C<sub>b</sub>), 127.30 (C<sub>e'</sub>), 126.77 (C<sub>b'</sub>), 124.17 (C<sub>c</sub>), 123.41 (C<sub>c'</sub>), 122.57 (C<sub>6, 6'</sub>), 112.24 (C<sub>d</sub>), 111.65 (C<sub>d'</sub>), 108.99 (C<sub>f</sub>), 108.84 (C<sub>f'</sub>). MS (FAB): *m/z* 661 [M]<sup>+</sup>.

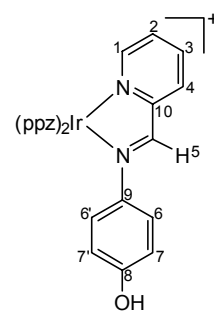
### Synthesis of 3.14a(*p*-C<sub>6</sub>H<sub>4</sub>Br)

This was prepared from dimer **2.6a** (50 mg, 0.049 mmol), 4-bromoaniline (20.3 mg, 0.118 mmol), pyridine-2-carboxaldehyde (12.7 mg, 12  $\mu$ L, 0.118 mmol) and KPF<sub>6</sub> (18.1 mg, 0.098 mmol) and after work up gave **3.14a(*p*-C<sub>6</sub>H<sub>4</sub>Br)** as a red solid (74 mg, 86%). Anal. Calcd for C<sub>31</sub>H<sub>25</sub>BrCl<sub>2</sub>F<sub>6</sub>IrN<sub>6</sub>P: C, 38.40, H, 2.60, N, 8.67. Found: C, 38.46, H, 2.51, N, 8.62%. <sup>1</sup>H NMR (CDCl<sub>3</sub>):  $\delta$  9.33 (1H, s, H<sub>5</sub>), 8.52 (1H, bd, *J* = 7.4, H<sub>4</sub>), 8.09 (2 X overlapping 1H, td, *J* = 7.4, 1.5, H<sub>3</sub>, d, *J* = 2.0, H<sub>e</sub>), 8.02 – 8.01 (2H, m, H<sub>1, e'</sub>), 7.53 (1H, d, *J* = 2.3, H<sub>g</sub>), 7.46 (1H, ddd, *J* = 7.8, 5.5, 1.2, H<sub>2</sub>), 7.27 (1H, dd, *J* = 7.8, 1.2, H<sub>d</sub>), 7.23 – 7.19 (2H, m, H<sub>7, 7'</sub>), 7.07 (1H, dd, *J* = 7.8, 1.2, H<sub>d'</sub>), 7.05 (1H, td, *J* = 7.8, 1.2, H<sub>c</sub>), 6.95 (1H, d, *J* = 2.3, H<sub>g'</sub>), 6.90 – 6.84 (4H, m, H<sub>6, 6', b, c'</sub>), 6.70 (1H, td, *J* = 7.8, 1.2, H<sub>b</sub>), 6.65 (1H, t, *J* = 2.5, H<sub>f</sub>), 6.61 (1H, t, *J* = 2.5, H<sub>f'</sub>), 6.25 (1H, dd, *J* = 7.4, 1.2, H<sub>a</sub>), 6.05 (1H, dd, *J* = 7.4, 1.2, H<sub>a'</sub>). <sup>13</sup>C NMR: 169.14 (C<sub>5</sub>), 156.29 (C<sub>10</sub>), 150.40 (C<sub>1</sub>), 146.58 (C<sub>9</sub>), 142.33 (C<sub>h</sub>), 142.02 (C<sub>h'</sub>), 139.75 (C<sub>3</sub>), 139.70 (C<sub>g</sub>), 138.55 (C<sub>g'</sub>), 133.26 (C<sub>a'</sub>), 133.07 (C<sub>a</sub>), 132.09 (C<sub>7, 7'</sub>), 131.61 (C<sub>4</sub>), 131.14 (C<sub>i'</sub>), 130.23 (C<sub>i</sub>), 129.06 (C<sub>2</sub>), 127.03 (C<sub>b</sub>), 126.69 (C<sub>b'</sub>), 126.62 (C<sub>e</sub>), 126.55 (C<sub>e'</sub>), 124.07 (C<sub>6, 6'</sub>), 123.70 (C<sub>c</sub>), 123.15 (C<sub>c'</sub>), 123.06 (C<sub>8</sub>), 111.59 (C<sub>d</sub>), 111.18 (C<sub>d'</sub>), 108.80 (C<sub>f</sub>), 108.58 (C<sub>f'</sub>). MS (FAB): *m/z* 739 [M]<sup>+</sup>.



### Synthesis of 3.14a(*p*-C<sub>6</sub>H<sub>4</sub>OH)

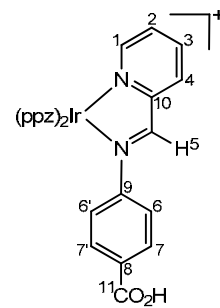
This was prepared from dimer **2.6a** (40 mg, 0.039 mmol), 4-aminophenol (10.2 mg, 0.094 mmol) and pyridine-2-carboxaldehyde (10.1 mg, 8  $\mu$ L, 0.094 mmol) and after work up gave **3.14a(*p*-C<sub>6</sub>H<sub>4</sub>OH)** as a red solid (45 mg, 87%). Anal. Calcd for C<sub>30</sub>H<sub>24</sub>ClIrN<sub>6</sub>O: C, 50.59, H, 3.40, N, 11.80. Found: C, 50.62, H, 3.31, N, 11.70%. <sup>1</sup>H NMR (MeOD):  $\delta$  9.29 (1H, s, H<sub>5</sub>), 8.57 (1H, d, *J* = 3.1, H<sub>e</sub>), 8.47 (1H, d, *J* = 2.3, H<sub>e'</sub>), 8.36 (1H, bd, *J* = 7.8, H<sub>4</sub>), 8.19 (1H, td, *J* = 7.8, 1.6, H<sub>3</sub>), 8.10 (1H, d, *J* = 5.5, H<sub>1</sub>), 7.69 (1H, d, *J* = 2.3, H<sub>g</sub>), 7.59 (1H, ddd, *J* = 7.8, 5.5, 1.2, H<sub>2</sub>), 7.53 (1H, dd, *J* = 7.8, 1.2, H<sub>d</sub>), 7.32 (1H, dd, *J* = 7.8, 1.2, H<sub>d'</sub>), 7.11 (1H, dd, *J*



$\delta$  = 2.3, 0.8, H<sub>g'</sub>), 7.06 (1H, td,  $J$  = 7.8, 1.2, H<sub>c</sub>), 6.91 – 6.87 (3H, m, H<sub>6, 6', c'</sub>), 6.84 (1H, td,  $J$  = 7.4, 1.2, H<sub>b</sub>), 6.71 (1H, t,  $J$  = 2.3, H<sub>f</sub>), 6.69 (1H, m, H<sub>b'</sub>), 6.67 (1H, t,  $J$  = 2.3, H<sub>f'</sub>), 6.51 – 6.47 (2H, m, H<sub>7, 7'</sub>), 6.26 (1H, dd,  $J$  = 7.8, 1.2, H<sub>a</sub>), 6.09 (1H, dd,  $J$  = 7.4, 1.2, H<sub>a'</sub>).  $^{13}\text{C}$  NMR: 166.03 (C<sub>5</sub>), 158.64 (C<sub>8</sub>), 156.84 (C<sub>10</sub>), 150.60 (C<sub>1</sub>), 142.85 (C<sub>h</sub>), 142.63 (C<sub>h'</sub>), 140.53 (C<sub>9</sub>), 139.34 (C<sub>3, g</sub>), 138.09 (C<sub>g'</sub>), 132.98 (C<sub>a'</sub>), 132.66 (C<sub>a</sub>), 131.80 (C<sub>i</sub>), 130.68 (C<sub>i</sub>), 129.41 (C<sub>4</sub>), 128.70 (C<sub>2</sub>), 127.58 (C<sub>e</sub>), 127.29 (C<sub>e'</sub>), 126.23 (C<sub>b</sub>), 125.72 (C<sub>b'</sub>), 123.78 (C<sub>6, 6'</sub>), 123.18 (C<sub>c</sub>), 122.45 (C<sub>c'</sub>), 114.92 (C<sub>7, 7'</sub>), 111.57 (C<sub>d</sub>), 111.07 (C<sub>d'</sub>), 108.15 (C<sub>f</sub>), 107.96 (C<sub>f'</sub>). MS (FAB):  $m/z$  677 [M]<sup>+</sup>.

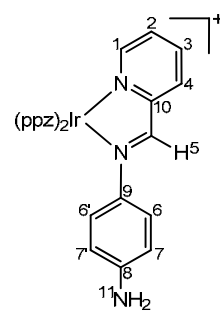
### Synthesis of 3.14a(*p*-C<sub>6</sub>H<sub>4</sub>CO<sub>2</sub>H)

This was prepared from dimer **2.6a** (100 mg, 0.097 mmol), 4-aminobenzoic acid (32 mg, 0.233 mmol), pyridine-2-carboxaldehyde (25 mg, 22  $\mu$ L, 0.233 mmol) and KPF<sub>6</sub> (49 mg, 0.233 mmol) and after work up gave **3.14a(*p*-C<sub>6</sub>H<sub>4</sub>CO<sub>2</sub>H)** as a orange-brown solid (155 mg, 94%). Anal. Calcd for C<sub>31</sub>H<sub>24</sub>F<sub>6</sub>IrN<sub>6</sub>O<sub>2</sub>P: C, 43.82, H, 2.85, N, 9.89. Found: C, 43.92, H, 2.79, N, 9.83%.  $^1\text{H}$  NMR (CD<sub>2</sub>Cl<sub>2</sub>):  $\delta$  9.36 (1H, s, H<sub>5</sub>), 8.48 (1H, d,  $J$  = 6.6, H<sub>4</sub>), 8.16 (1H, d,  $J$  = 2.7, H<sub>e</sub>), 8.07 – 8.03 (3H, m, H<sub>1, 3, e'</sub>), 7.63 – 7.61 (3H, m, H<sub>7, 7', g</sub>), 7.47 (1H, dd,  $J$  = 7.4, 5.1, H<sub>2</sub>), 7.34 (1H, dd,  $J$  = 7.8, 0.8, H<sub>d</sub>), 7.10 – 7.06 (2H, m, H<sub>c, d'</sub>), 6.94 (1H, d,  $J$  = 2.0, H<sub>g'</sub>), 6.88 – 6.80 (4H, m, H<sub>6, 6', b, c'</sub>), 6.66 – 6.63 (2H, m, H<sub>b', f</sub>), 6.60 (1H, t,  $J$  = 2.3, H<sub>f</sub>), 6.26 (1H, dd,  $J$  = 7.8, 1.2, H<sub>a</sub>), 6.06 (1H, dd,  $J$  = 7.4, 1.2, H<sub>a'</sub>).  $^{13}\text{C}$  NMR: 170.23 (C<sub>5</sub>), 168.89 (C<sub>11</sub>), 156.39 (C<sub>10</sub>), 151.42 (C<sub>1</sub>), 151.29 (C<sub>9</sub>), 142.91 (C<sub>h</sub>), 142.56 (C<sub>h'</sub>), 140.28 (C<sub>3</sub>), 140.11 (C<sub>g</sub>), 138.84 (C<sub>g'</sub>), 133.59 (C<sub>a</sub>), 133.36 (C<sub>a</sub>), 132.61 (C<sub>8</sub>), 131.68 (C<sub>4</sub>), 131.47 (C<sub>i'</sub>), 130.90 (C<sub>7, 7'</sub>), 130.53 (C<sub>i</sub>), 130.01 (C<sub>2</sub>), 127.64 (C<sub>b</sub>), 127.51 (C<sub>e</sub>), 127.23 (C<sub>e'</sub>), 126.83 (C<sub>b'</sub>), 124.16 (C<sub>c</sub>), 123.52 (C<sub>c'</sub>), 122.55 (C<sub>6, 6'</sub>), 112.24 (C<sub>d</sub>), 111.73 (C<sub>d'</sub>), 109.07 (C<sub>f</sub>), 108.87 (C<sub>f'</sub>). MS (FAB):  $m/z$  705 [M]<sup>+</sup>.



### Synthesis of 3.14a(*p*-C<sub>6</sub>H<sub>4</sub>NH<sub>2</sub>)

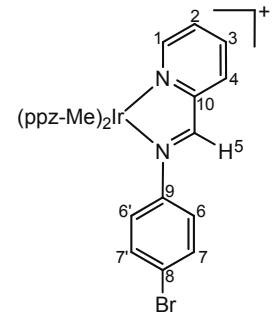
This was prepared from dimer **2.6a** (50 mg, 0.049 mmol), 4-diaminobenzene (42.4 mg, 0.392 mmol), pyridine-2-carboxaldehyde (12.7 mg, 12  $\mu$ L, 0.118 mmol) and KPF<sub>6</sub> (22 mg, 0.118 mmol) and after work up gave **3.14a(*p*-C<sub>6</sub>H<sub>4</sub>NH<sub>2</sub>)** as a red solid (58 mg, 72%). Anal. Calcd for C<sub>30</sub>H<sub>25</sub>F<sub>6</sub>IrN<sub>7</sub>P: C, 43.90, H, 3.07, N, 11.95. Found: C, 44.00, H, 3.02, N, 11.87%.  $^1\text{H}$  NMR (Acetone – D<sub>6</sub>):  $\delta$  9.43 (1H,



s, H<sub>5</sub>), 8.73 (1H, dd, *J* = 3.1, 0.8, H<sub>e</sub>), 8.65 (1H, dd, *J* = 2.7, 0.8, H<sub>e'</sub>), 8.48 (1H, d, *J* = 7.4, H<sub>4</sub>), 8.30 (1H, td, *J* = 7.8, 1.6, H<sub>3</sub>), 8.15 (1H, d, *J* = 5.5, H<sub>1</sub>), 7.78 (1H, d, *J* = 2.3, H<sub>g</sub>), 7.70 (1H, ddd, *J* = 7.8, 5.5, 1.2, H<sub>2</sub>), 7.63 (1H, dd, *J* = 7.8, 0.8, H<sub>d</sub>), 7.46 (1H, dd, *J* = 8.2, 1.2, H<sub>d'</sub>), 7.26 (1H, d, *J* = 2.3, H<sub>g'</sub>), 7.06 (1H, td, *J* = 7.4, 1.6, H<sub>c</sub>), 7.00 – 6.96 (2H, m, H<sub>6, 6'</sub>), 6.91 (1H, td, *J* = 7.8, 1.2, H<sub>c'</sub>), 6.86 (1H, td, *J* = 7.4, 1.2, H<sub>b</sub>), 6.79 (1H, t, *J* = 2.3, H<sub>f</sub>), 6.76 (1H, t, *J* = 2.3, H<sub>f'</sub>), 6.72 (1H, td, *J* = 7.4, 1.2, H<sub>b'</sub>), 6.43 – 6.39 (2H, m, H<sub>7, 7'</sub>), 6.27 (1H, dd, *J* = 7.4, 1.2, H<sub>a</sub>), 6.16 (1H, dd, *J* = 7.4, 1.2, H<sub>a'</sub>), 5.10 (2H, s, H<sub>11</sub>). <sup>13</sup>C NMR: 164.94 (C<sub>5</sub>), 158.20 (C<sub>10</sub>), 151.67 (C<sub>1</sub>), 150.94, 150.89 (C<sub>8</sub>), 143.90 (C<sub>h</sub>), 143.73 (C<sub>h'</sub>), 140.71 (C<sub>3</sub>), 140.53 (C<sub>g</sub>), 139.51 (C<sub>g'</sub>), 139.48 (C<sub>9</sub>), 134.24 (C<sub>a</sub>), 133.66 (C<sub>a'</sub>), 133.32 (C<sub>i</sub>), 131.94 (C<sub>i'</sub>), 130.25 (C<sub>4</sub>), 129.61 (C<sub>2</sub>), 128.91 (C<sub>e</sub>), 128.67 (C<sub>e'</sub>), 127.40 (C<sub>b</sub>), 126.86 (C<sub>b'</sub>), 125.21 (C<sub>6, 6'</sub>), 124.25 (C<sub>c</sub>), 123.47 (C<sub>c'</sub>), 114.37, 114.33 (C<sub>7, 7'</sub>), 112.87 (C<sub>d</sub>), 112.41 (C<sub>d'</sub>), 109.41 (C<sub>f</sub>), 109.17 (C<sub>f'</sub>). MS (FAB): *m/z* 676 [M]<sup>+</sup>.

### Synthesis of 3.14b(*p*-C<sub>6</sub>H<sub>4</sub>Br)

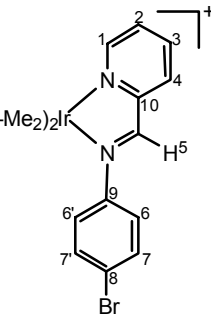
This was prepared from dimer **2.6b** (60 mg, 0.055 mmol), 4-bromoaniline (22.7 mg, 0.132 mmol), pyridine-2-carboxaldehyde (14.2 mg, 12.6  $\mu$ L, 0.132 mmol) and KPF<sub>6</sub> (24.3 mg, 0.132 mmol) and after work up gave **3.14b(*p*-C<sub>6</sub>H<sub>4</sub>Br)** as a red solid (82 mg, 82%). Anal. Calcd for C<sub>32</sub>H<sub>27</sub>BrF<sub>6</sub>IrN<sub>6</sub>P: C, 42.11, H, 2.98, N, 9.21. Found: C, 42.17, H, 3.03, N, 9.28%. <sup>1</sup>H NMR (CD<sub>2</sub>Cl<sub>2</sub>):  $\delta$  9.21 (1H, s, H<sub>5</sub>), 8.38 (1H, dd, *J* = 7.8, 1.2, H<sub>4</sub>), 8.16 – 8.10 (3H, m, H<sub>1, 3, e</sub>), 8.06 (1H, dd, *J* = 3.1, 0.8, H<sub>e</sub>), 7.52 (1H, ddd, *J* = 7.8, 5.5, 1.6, H<sub>2</sub>), 7.46 (1H, d, *J* = 2.3, H<sub>g</sub>), 7.30 – 7.26 (2H, m, H<sub>7, 7'</sub>), 7.16 (1H, s, H<sub>d</sub>), 6.98 (1H, s, H<sub>d'</sub>), 6.88 (1H, d, *J* = 2.3, H<sub>g'</sub>), 6.86 – 6.82 (2H, m, H<sub>6, 6'</sub>), 6.72 (1H, dd, *J* = 7.8, 0.8, H<sub>b</sub>), 6.63 (1H, t, *J* = 2.7, H<sub>f</sub>), 6.60 – 6.56 (2H, m, H<sub>b', f'</sub>), 6.09 (1H, d, *J* = 7.8, H<sub>a</sub>), 5.93 (1H, d, *J* = 7.8, H<sub>a'</sub>), 2.32 (3H, s, Me), 2.24 (3H, s, Me'). <sup>13</sup>C NMR: 168.90 (C<sub>5</sub>), 156.38 (C<sub>10</sub>), 151.55 (C<sub>1</sub>), 147.21 (C<sub>9</sub>), 142.79 (C<sub>h</sub>), 142.53 (C<sub>h'</sub>), 140.02 (C<sub>3</sub>), 139.90 (C<sub>g</sub>), 138.65 (C<sub>g'</sub>), 134.02 (C<sub>c</sub>), 133.36 (C<sub>c'</sub>), 133.28 (C<sub>a'</sub>), 132.93 (C<sub>a</sub>), 132.47 (C<sub>7, 7'</sub>), 131.22 (C<sub>4</sub>), 129.93 (C<sub>2</sub>), 128.18 (C<sub>f</sub>), 127.83 (C<sub>f'</sub>), 127.39 (C<sub>e</sub>), 127.26 (C<sub>e'</sub>), 127.17 (C<sub>i</sub>), 126.06 (C<sub>i'</sub>), 124.50 (C<sub>6, 6'</sub>), 123.33 (C<sub>8</sub>), 113.05 (C<sub>d</sub>), 112.61 (C<sub>d'</sub>), 108.87 (C<sub>f</sub>), 108.70 (C<sub>f'</sub>), 21.11 (Me), 21.03 (Me'). MS (FAB): *m/z* 767 [M]<sup>+</sup>.



### Synthesis of 3.14f(*p*-C<sub>6</sub>H<sub>4</sub>Br)

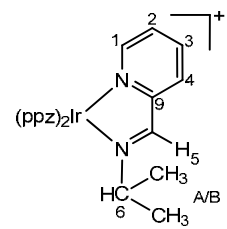
This was prepared from dimer **2.6f** (50 mg, 0.044 mmol), 4-bromoaniline (18.2 mg, 0.106 mmol), pyridine-2-carboxaldehyde (11.3 mg, 10.1  $\mu$ L, 0.106 mmol) and

KPF<sub>6</sub> (19.5 mg, 0.106 mmol) and after work up gave **3.14f(p-C<sub>6</sub>H<sub>4</sub>Br)** as a red solid (73 mg, 89%). Anal. Calcd for C<sub>34</sub>H<sub>31</sub>BrF<sub>6</sub>IrN<sub>6</sub>P: C, 43.41, H, 3.32, N, 8.93. Found: C, 43.35, H, 3.36, N, 8.84%. <sup>1</sup>H NMR (CD<sub>2</sub>Cl<sub>2</sub>): δ 9.20 (1H, s, H<sub>5</sub>), 8.39 (1H, dd, *J* = 7.8, 0.8, H<sub>4</sub>), 8.13 (1H, td, *J* = 7.8, 1.6, H<sub>3</sub>), 7.98 (1H, ddd, *J* = 5.4, 1.6, 0.8, H<sub>1</sub>), 7.53 – 7.49 (2H, m, H<sub>2</sub>, d), 7.22 – 7.18 (2H, m, H<sub>7, 7'</sub>), 7.10 (1H, dd, *J* = 8.2, 1.2, H<sub>d'</sub>), 7.06 (1H, ddd, *J* = 8.2, 7.4, 1.6, H<sub>c</sub>), 6.91 (1H, ddd, *J* = 8.2, 7.4, 1.6, H<sub>c'</sub>), 6.81 (1H, td, *J* = 7.4, 0.8, H<sub>b</sub>), 6.78 – 6.73 (3H, m, H<sub>6, 6', b'</sub>), 6.35 (1H, dd, *J* = 7.4, 1.6, H<sub>a</sub>), 6.21 (1H, dd, *J* = 7.8, 1.6, H<sub>a'</sub>), 6.14 (1H, s, H<sub>f</sub>), 6.06 (1H, s, H<sub>f'</sub>), 2.84 (3H, s, Me<sub>B</sub>), 2.56 (3H, s, Me<sub>B'</sub>), 2.13 (3H, s, Me<sub>A</sub>) 1.56 (3H, s, Me<sub>A'</sub>). <sup>13</sup>C NMR: 167.98 (C<sub>5</sub>), 156.55 (C<sub>10</sub>), 151.19 (C<sub>1</sub>), 150.69 (C<sub>g</sub>), 150.09 (C<sub>g'</sub>), 146.53 (C<sub>9</sub>), 144.72 (C<sub>i'</sub>), 144.54 (C<sub>i</sub>), 142.16 (C<sub>e</sub>), 141.71 (C<sub>e'</sub>), 139.82 (C<sub>3</sub>), 133.92 (C<sub>a</sub>), 133.84 (C<sub>a'</sub>), 132.67 (C<sub>h</sub>), 132.13 (C<sub>7, 7'</sub>), 131.19 (C<sub>4</sub>), 130.61 (C<sub>h</sub>), 130.18 (C<sub>2</sub>), 125.98 (C<sub>b</sub>), 125.81 (C<sub>b'</sub>), 124.76 (C<sub>6, 6'</sub>), 123.99 (C<sub>c</sub>), 123.55 (C<sub>c'</sub>), 123.40 (C<sub>8</sub>), 113.23 (C<sub>d</sub>), 112.83 (C<sub>d'</sub>), 110.56 (C<sub>f</sub>), 110.44 (C<sub>f'</sub>), 14.76 (Me<sub>B</sub>), 14.45 (Me<sub>B'</sub>), 14.07 (Me<sub>A</sub>), 12.47 (Me<sub>A'</sub>). MS (FAB): *m/z* 795 [M]<sup>+</sup>.



### Synthesis of **3.14a(iPr)**

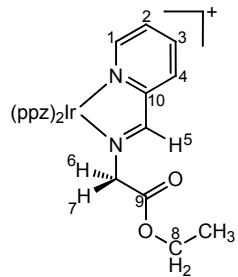
This was prepared from dimer **2.6a** (70 mg, 0.068 mmol), 2-pyridinecarbaldisopropylimine (24.2 mg, 0.164 mmol), and KPF<sub>6</sub> (25 mg, 0.136 mmol) and after work up gave **3.14a(iPr)** as a orange solid (89 mg, 85%). Anal. Calcd for C<sub>27</sub>H<sub>26</sub>F<sub>6</sub>IrN<sub>6</sub>P: C, 42.02, H, 3.40, N, 10.89. Found: C, 41.92, H, 3.30, N, 10.81%. <sup>1</sup>H NMR (CD<sub>2</sub>Cl<sub>2</sub>): δ 9.28 (1H, s, H<sub>5</sub>), 8.32 (1H, bd, *J* = 7.6, H<sub>4</sub>), 8.24 (1H, dd, *J* = 2.8, 0.6, H<sub>e</sub>), 8.18 (1H, dd, *J* = 2.8, 0.6, H<sub>e'</sub>), 8.12 (1H, td, *J* = 7.8, 1.4, H<sub>3</sub>), 8.02 (1H, dd, *J* = 5.3, 1.2, H<sub>1</sub>), 7.48 – 7.45 (2H, m, H<sub>2, g</sub>), 7.35 (1H, dd, *J* = 3.4, 0.8, H<sub>d'</sub>), 7.34 (1H, dd, *J* = 3.4, 0.8, H<sub>d</sub>), 7.11 (1H, td, *J* = 7.6, 1.4, H<sub>c</sub>), 7.05 (1H, td, *J* = 7.6, 1.4, H<sub>c'</sub>), 6.92 – 6.88 (2H, m, H<sub>b, g'</sub>), 6.86 (1H, td, *J* = 7.3, 1.2, H<sub>b'</sub>), 6.67 – 6.65 (2H, m, H<sub>f, f'</sub>), 6.36 (1H, dd, *J* = 7.5, 1.4, H<sub>a'</sub>), 6.22 (1H, dd, *J* = 7.5, 1.4, H<sub>a</sub>), 4.11 (1H, septd, *J* = 6.7, 0.8, H<sub>6</sub>), 1.12 (3H, d, *J* = 6.5, Me<sub>A</sub> or B), 1.01 (3H, d, *J* = 6.7, Me<sub>A</sub> or B). <sup>13</sup>C NMR: 166.75 (C<sub>5</sub>), 156.42 (C<sub>9</sub>), 150.66 (C<sub>1</sub>), 142.73 (C<sub>h</sub>), 142.51 (C<sub>h</sub>), 139.85 (C<sub>g</sub>), 139.64 (C<sub>3</sub>), 138.14 (C<sub>g'</sub>), 133.92 (C<sub>a'</sub>), 132.63 (C<sub>a</sub>), 131.25 (C<sub>i</sub>), 130.56 (C<sub>i'</sub>), 129.39 (C<sub>4</sub>), 128.74 (C<sub>2</sub>), 127.09 (C<sub>e</sub>), 126.93 (C<sub>e'</sub>), 126.85 (C<sub>b</sub>), 126.47 (C<sub>b'</sub>), 123.56 (C<sub>c</sub>), 123.03 (C<sub>c'</sub>), 111.67 (C<sub>d'</sub>), 111.40



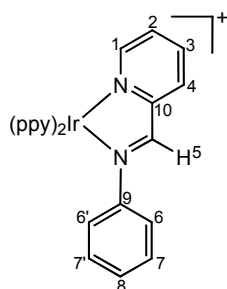
(C<sub>d</sub>), 108.40, 108.34 (C<sub>f, f'</sub>), 63.47 (C<sub>6</sub>), 22.17 (Me<sub>A</sub> or B), 21.82 (Me<sub>A</sub> or B). MS (FAB): *m/z* 627 [M]<sup>+</sup>.

### Synthesis of 3.14a(CH<sub>2</sub>CO<sub>2</sub>Et)

This was prepared from dimer **2.6a** (40 mg, 0.039 mmol), glycineethylester hydrochloride (13 mg, 0.090 mmol), pyridine-2-carboxaldehyde (10 mg, 9  $\mu$ L, 0.090 mmol), triethylamine (9 mg, 12  $\mu$ L, 0.090 mmol) and  $\text{KPF}_6$  (17 mg, 0.090 mmol) and after work up gave **3.14a**( $\text{CH}_2\text{CO}_2\text{Et}$ ) as a orange-red solid (40 mg, 63%). Anal. Calcd for  $\text{C}_{28}\text{H}_{26}\text{F}_6\text{IrN}_6\text{O}_2\text{P}$ : C, 41.23, H, 3.21, N, 10.30. Found: C, 41.30, H, 3.14, N, 10.37%.  $^1\text{H}$  NMR ( $\text{CD}_2\text{Cl}_2$ ):  $\delta$  9.16 (1H, s,  $\text{H}_5$ ), 8.26 (1H, d,  $J$  = 7.4,  $\text{H}_4$ ), 8.15 (1H, d,  $J$  = 2.3,  $\text{H}_e$ ), 8.11 – 8.07 (2H, m,  $\text{H}_{3, e}$ ), 8.05 (1H, d,  $J$  = 5.5,  $\text{H}_1$ ), 7.77 (1H, dd,  $J$  = 2.3, 0.8,  $\text{H}_g$ ), 7.49 (1H, ddd,  $J$  = 7.4, 5.5, 1.6,  $\text{H}_2$ ), 7.30 (1H, dd,  $J$  = 8.2, 0.8,  $\text{H}_d$ ), 7.27 (1H, dd,  $J$  = 8.2, 1.2,  $\text{H}_{d'}$ ), 7.06 (1H, td,  $J$  = 7.4, 1.2,  $\text{H}_c$ ), 7.03 (1H, td,  $J$  = 7.8, 1.2,  $\text{H}_c$ ), 6.89 (1H, d,  $J$  = 2.3,  $\text{H}_{g'}$ ), 6.86 (1H, td,  $J$  = 7.4, 1.2,  $\text{H}_b$ ), 6.82 (1H, td,  $J$  = 7.4, 1.2,  $\text{H}_b$ ), 6.64 (1H, t,  $J$  = 2.3,  $\text{H}_f$ ), 6.61 (1H, t,  $J$  = 2.3,  $\text{H}_f$ ), 6.28 (1H, dd,  $J$  = 7.4, 1.2,  $\text{H}_a$ ), 6.22 (1H, dd,  $J$  = 7.8, 1.2,  $\text{H}_a$ ), 4.60 (1H, dd,  $J$  = 15.6, 1.2,  $\text{H}_6$ ), 4.42 (1H, dd,  $J$  = 15.6, 1.2,  $\text{H}_7$ ), 3.84 (2H, q,  $J$  = 7.0,  $\text{H}_8$ ), 1.05 (3H, t,  $J$  = 7.0, Me).  $^{13}\text{C}$  NMR: 173.57 ( $\text{C}_5$ ), 167.19 ( $\text{C}_9$ ), 156.12 ( $\text{C}_{10}$ ), 151.50 ( $\text{C}_1$ ), 143.23 ( $\text{C}_{h'}$ ), 143.07 ( $\text{C}_h$ ), 140.53 ( $\text{C}_g$ ), 140.04 ( $\text{C}_3$ ), 138.72 ( $\text{C}_{g'}$ ), 134.10 ( $\text{C}_{a'}$ ), 133.33 ( $\text{C}_a$ ), 131.55 ( $\text{C}_i$ ), 130.33 ( $\text{C}_4$ ), 129.86 ( $\text{C}_{i'}$ ), 129.77 ( $\text{C}_2$ ), 127.33 ( $\text{C}_b$ ), 127.26 ( $\text{C}_{b'}$ ), 127.08 ( $\text{C}_e$ ), 126.89 ( $\text{C}_{e'}$ ), 124.01 ( $\text{C}_c$ ), 123.88 ( $\text{C}_{c'}$ ), 111.98 ( $\text{C}_d$ ), 111.79 ( $\text{C}_{d'}$ ), 108.79 ( $\text{C}_f$ ), 108.68 ( $\text{C}_f$ ), 62.42 ( $\text{C}_8$ ), 61.83 ( $\text{C}_{6, 7}$ ), 14.02 (Me). MS (FAB):  $m/z$  671 [ $\text{M}]^+$ .



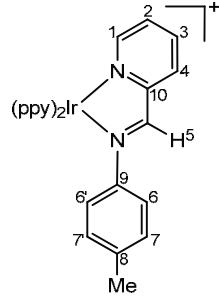
### Synthesis of 3.14g(C<sub>6</sub>H<sub>5</sub>)



7.8, 1.2, H<sub>d</sub>), 7.52 (1H, ddd,  $J$  = 7.8, 5.1, 1.2, H<sub>2</sub>), 7.46 – 7.43 (2H, m, H<sub>d'</sub>, h'), 7.21 – 7.16 (2H, m, H<sub>8,g</sub>), 7.12 – 7.05 (4H, m, H<sub>7,7',c,g</sub>), 6.92, (1H, td,  $J$  = 7.4, 1.2, H<sub>b</sub>), 6.89 – 6.84 (3H, m, H<sub>6,6',c</sub>), 6.79 (1H, td,  $J$  = 7.4, 1.5, H<sub>b</sub>), 6.25 (1H, dd,  $J$  = 7.4, 1.2, H<sub>a</sub>), 6.17 (1H, dd,  $J$  = 7.4, 1.2, H<sub>a'</sub>).  $^{13}\text{C}$  NMR: 167.70 (C<sub>k, k'</sub>), 167.30 (C<sub>5</sub>), 155.41 (C<sub>10</sub>), 150.73 (C<sub>1</sub>), 150.28 (C<sub>h</sub>), 149.54 (C<sub>i'</sub>), 148.69 (C<sub>h'</sub>), 148.01 (C<sub>i</sub>), 147.29 (C<sub>9</sub>), 143.47 (C<sub>j</sub>), 143.20 (C<sub>j'</sub>), 139.52 (C<sub>3</sub>), 138.37 (C<sub>f</sub>), 138.34 (C<sub>f'</sub>), 131.45 (C<sub>a</sub>), 131.42 (C<sub>a'</sub>), 130.95 (C<sub>4</sub>), 130.68 (C<sub>b</sub>), 130.16 (C<sub>b'</sub>), 129.78 (C<sub>2</sub>), 128.91 (C<sub>8</sub>), 128.84 (C<sub>7,7'</sub>), 124.85 (C<sub>d</sub>), 124.32 (C<sub>d'</sub>), 123.76 (C<sub>g</sub>), 123.34 (C<sub>g'</sub>), 122.99 (C<sub>c</sub>), 122.38 (C<sub>6,6'</sub>), 122.28 (C<sub>c'</sub>), 119.95 (C<sub>e</sub>), 119.41 (C<sub>e'</sub>). MS (FAB):  $m/z$  683 [M]<sup>+</sup>.

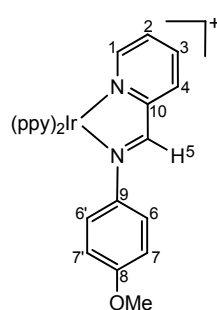
### Synthesis of 3.14g(*p*-C<sub>6</sub>H<sub>4</sub>Me)

This was prepared from dimer **2.6g** (40 mg, 0.037 mmol), *p*-toluidine (9.5 mg, 0.089 mmol), pyridine-2-carboxaldehyde (9.6 mg, 8  $\mu$ L, 0.089 mmol) and  $\text{KPF}_6$  (13.6 mg, 0.074 mmol) and after work up gave **3.14g**(*p*-C<sub>6</sub>H<sub>4</sub>Me) as a red solid (58 mg, 94%). Anal. Calcd for C<sub>35</sub>H<sub>28</sub>F<sub>6</sub>IrN<sub>4</sub>P: C, 49.94, H, 3.35, N, 6.66. Found: C, 50.04, H, 3.37, N, 6.57%. <sup>1</sup>H NMR (CD<sub>2</sub>Cl<sub>2</sub>):  $\delta$  9.19 (1H, s, H<sub>5</sub>), 8.29 (1H, d, *J* = 7.8, H<sub>4</sub>), 8.21 (1H, ddd, *J* = 5.9, 1.6, 0.8, H<sub>h</sub>), 8.02 (1H, td, *J* = 7.8, 1.2, H<sub>3</sub>), 7.89 (1H, d, *J* = 7.8, H<sub>e</sub>), 7.84 (1H, d, *J* = 5.9, H<sub>1</sub>), 7.76 (1H, td, *J* = 7.4, 1.6, H<sub>f</sub>), 7.72 – 7.70 (2H, m, H<sub>e', f'</sub>), 7.64 (1H, dd, *J* = 7.8, 1.2, H<sub>d</sub>), 7.41 – 7.37 (2H, m, H<sub>2, d'</sub>), 7.35 (1H, dt, *J* = 5.9, 1.2, H<sub>h'</sub>), 7.08 (1H, ddd, *J* = 7.0, 5.5, 1.2, H<sub>g</sub>), 7.02 – 6.96 (2H, m, H<sub>c, g'</sub>), 6.85 – 6.78 (4H, m, H<sub>7, 7', b, c'</sub>), 6.73 – 6.69 (3H, m, H<sub>6, 6', b'</sub>), 6.15 (1H, dd, *J* = 7.8, 0.8, H<sub>a</sub>), 6.10 (1H, dd, *J* = 7.4, 0.8, H<sub>a'</sub>), 2.14 (3H, s, Me). <sup>13</sup>C NMR: 168.12 (C<sub>k'</sub>), 167.67 (C<sub>k</sub>), 166.82 (C<sub>5</sub>), 155.95 (C<sub>10</sub>), 151.09 (C<sub>1</sub>), 150.69 (C<sub>h</sub>), 150.11 (C<sub>i'</sub>), 149.05 (C<sub>h'</sub>), 148.45 (C<sub>i</sub>), 145.55 (C<sub>9</sub>), 143.87 (C<sub>j</sub>), 143.62 (C<sub>j'</sub>), 140.12 (C<sub>8</sub>), 139.88 (C<sub>3</sub>), 138.70 (C<sub>f, f'</sub>), 131.86 (C<sub>a'</sub>), 131.75 (C<sub>a</sub>), 131.08 (C<sub>4</sub>), 130.56 (C<sub>b</sub>), 129.98 (C<sub>b'</sub>), 129.83 (C<sub>2, 7, 7'</sub>), 125.23 (C<sub>d</sub>), 124.80 (C<sub>d</sub>), 124.15 (C<sub>g</sub>), 123.69 (C<sub>g'</sub>), 123.37 (C<sub>c</sub>), 122.77 (C<sub>6, 6'</sub>), 122.65 (C<sub>c'</sub>), 120.33 (C<sub>e</sub>), 119.86 (C<sub>e'</sub>), 21.13 (Me). MS (FAB): *m/z* 697 [M]<sup>+</sup>.



### Synthesis of 3.14g(*p*-C<sub>6</sub>H<sub>4</sub>OMe)

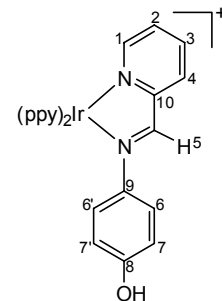
This was prepared from dimer **2.6g** (40 mg, 0.037 mmol), 4-methoxyaniline (10.9 mg, 0.089 mmol), pyridine-2-carboxaldehyde (9.6 mg, 8  $\mu$ L, 0.089 mmol) and KPF<sub>6</sub> (16.3 mg, 0.089 mmol) and after work up gave **3.14g(p-C<sub>6</sub>H<sub>4</sub>OMe)** as a red solid (53 mg, 84%).



Anal. Calcd for  $C_{35}H_{28}F_6IrN_4OP$ : C, 49.01, H, 3.29, N, 6.53. Found: C, 48.89, H, 3.26, N, 6.52%.  $^1H$  NMR ( $CD_2Cl_2$ ):  $\delta$  9.15 (1H, s,  $H_5$ ), 8.27 (1H, dd,  $J$  = 7.8, 0.8,  $H_4$ ), 8.20 (1H, ddd,  $J$  = 5.9, 1.6, 0.8,  $H_h$ ), 8.01 (1H, td,  $J$  = 7.8, 1.6,  $H_3$ ), 7.90 (1H, bd,  $J$  = 8.2,  $H_e$ ), 7.83 (1H, ddd,  $J$  = 5.5, 1.6, 0.8,  $H_1$ ), 7.76 (1H, ddd,  $J$  = 8.2, 7.4, 1.5,  $H_f$ ), 7.72 – 7.70 (2H, m,  $H_{e', f'}$ ), 7.65 (1H, dd,  $J$  = 7.4, 0.8,  $H_d$ ), 7.41 (1H, dd,  $J$  = 7.8, 1.2,  $H_{d'}$ ), 7.37 (1H, ddd,  $J$  = 7.8, 5.5, 1.6,  $H_2$ ), 7.34 (1H, dd,  $J$  = 5.9, 1.2,  $H_{h'}$ ), 7.07 (1H, ddd,  $J$  = 7.4, 5.9, 1.6,  $H_g$ ), 7.02 – 6.96 (2H, m,  $H_{c, g'}$ ), 6.85 – 6.80 (4H, m,  $H_{6, 6', b, c'}$ ), 6.73 (1H, td,  $J$  = 7.4, 1.6,  $H_{b'}$ ), 6.49 – 6.45 (2H, m,  $H_{7, 7'}$ ), 6.16 (1H, dd,  $J$  = 7.4, 0.8,  $H_a$ ), 6.12 (1H, dd,  $J$  = 7.4, 0.8,  $H_{a'}$ ) 3.62 (3H, s, Me).  $^{13}C$  NMR: 168.08 ( $C_k'$ ), 167.68 ( $C_k$ ), 165.47 ( $C_5$ ), 160.82 ( $C_8$ ), 156.13 ( $C_{10}$ ), 151.00 ( $C_1$ ), 150.69 ( $C_h$ ), 150.27 ( $C_{i'}$ ), 149.02 ( $C_{h'}$ ), 148.45 ( $C_i$ ), 143.88 ( $C_j$ ), 143.69 ( $C_{j'}$ ), 141.11 ( $C_9$ ), 139.81 ( $C_3$ ), 138.69 ( $C_{f, f'}$ ), 131.88 ( $C_a$ ), 131.80 ( $C_a$ ), 131.07 ( $C_b$ ), 130.82 ( $C_4$ ), 130.58 ( $C_{b'}$ ), 129.71 ( $C_2$ ), 125.24 ( $C_d$ ), 124.84 ( $C_{d'}$ ), 124.53 ( $C_{6, 6'}$ ), 124.15 ( $C_g$ ), 123.68 ( $C_{g'}$ ), 123.36 ( $C_c$ ), 122.69 ( $C_c$ ), 120.32 ( $C_e$ ), 119.82 ( $C_e$ ), 114.34 ( $C_{7, 7'}$ ), 55.89 (Me). MS (FAB):  $m/z$  713 [M]<sup>+</sup>.

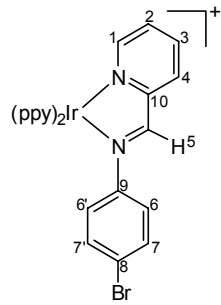
### Synthesis of 3.14g(*p*-C<sub>6</sub>H<sub>4</sub>OH)

This was prepared from dimer **2.6g** (50 mg, 0.047 mmol), 4-aminophenol (12.3 mg, 0.113 mmol) and pyridine-2-carboxaldehyde (12.1 mg, 11  $\mu$ L, 0.113 mmol) and after work up gave **3.14g(*p*-C<sub>6</sub>H<sub>4</sub>OH)** as a red solid (65 mg, 94%). Anal. Calcd for  $C_{34}H_{26}ClIrN_4O$ : C, 55.62, H, 3.57, N, 7.63. Found: C, 55.57, H, 3.49, N, 7.68%.  $^1H$  NMR (MeOD):  $\delta$  9.37 (1H, s,  $H_5$ ), 8.40 (1H, dd,  $J$  = 5.8, 0.8,  $H_h$ ), 8.36 (1H, bd,  $J$  = 7.4,  $H_4$ ), 8.18 – 8.14 (2H, m,  $H_{3, e}$ ), 7.96 – 7.82 (5H, m,  $H_{1, d, e', f, f'}$ ), 7.57 – 7.54 (3H, m,  $H_{2, d', h'}$ ), 7.22 (1H, ddd,  $J$  = 7.4, 5.8, 1.6,  $H_g$ ), 7.13 (1H, ddd,  $J$  = 7.4, 5.8, 1.6,  $H_{g'}$ ), 7.03 (1H, td,  $J$  = 7.4, 1.2,  $H_c$ ), 6.88 – 6.84 (4H, m,  $H_{6, 6', b, c'}$ ), 6.77 (1H, td,  $J$  = 7.4, 1.2,  $H_{b'}$ ), 6.42 – 6.39 (2H, m,  $H_{7, 7'}$ ), 6.23 (1H, dd,  $J$  = 7.8, 1.2,  $H_a$ ), 6.18 (1H, dd,  $J$  = 7.8, 1.2,  $H_{a'}$ ).  $^{13}C$  NMR: 168.51 ( $C_k'$ ), 168.03 ( $C_k$ ), 165.58 ( $C_5$ ), 159.65 ( $C_8$ ), 156.70 ( $C_{10}$ ), 150.69 ( $C_{1, h}$ ), 150.54 ( $C_{i'}$ ), 149.07 ( $C_{h'}$ ), 148.89 ( $C_i$ ), 144.09 ( $C_j$ ), 143.94 ( $C_{j'}$ ), 140.41 ( $C_9$ ), 139.65 ( $C_3$ ), 138.75 ( $C_f$ ), 138.61 ( $C_{f'}$ ), 131.62 ( $C_{a, a'}$ ), 130.55 ( $C_b$ ), 130.14 ( $C_{b'}$ ), 130.00 ( $C_4$ ), 129.45 ( $C_2$ ), 125.03 ( $C_d$ ), 124.64 ( $C_{d'}$ ), 124.45 ( $C_{6, 6'}$ ), 123.75 ( $C_g$ ), 123.26 ( $C_{g'}$ ), 122.92 ( $C_c$ ), 122.22 ( $C_{c'}$ ), 120.14 ( $C_e$ ), 119.62 ( $C_{e'}$ ), 115.23 ( $C_{7, 7'}$ ). MS (FAB):  $m/z$  699 [M]<sup>+</sup>.



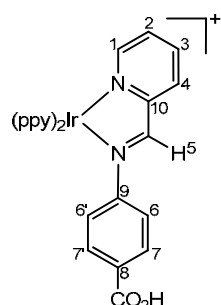
### Synthesis of 3.14g(*p*-C<sub>6</sub>H<sub>4</sub>Br)

This was prepared from dimer **2.6g** (30 mg, 0.028 mmol), 4-bromoaniline (11.5 mg, 0.067 mmol), pyridine-2-carboxaldehyde (7.2 mg, 6.4  $\mu$ L, 0.067 mmol) and  $\text{KPF}_6$  (12.4 mg, 0.067 mmol) and after work up gave **3.14g(p-C<sub>6</sub>H<sub>4</sub>Br)** as a red solid (37 mg, 74%). This compound was also synthesised using harsh conditions *i.e.* microwave heating for 30 mins at 100 °C, which resulted in a 65% yield. Anal. Calcd for  $\text{C}_{34}\text{H}_{25}\text{BrF}_6\text{IrN}_4\text{P}(\text{CH}_3\text{COCH}_3)$ : C, 46.06, H, 3.24, N, 5.81. Found: C, 45.89, H, 3.24, N, 5.90%.  $^1\text{H}$  NMR ( $\text{CD}_2\text{Cl}_2$ ):  $\delta$  9.48 (1H, s,  $\text{H}_5$ ), 8.52 (1H, bd,  $J$  = 7.8,  $\text{H}_4$ ), 8.28 (1H, bd,  $J$  = 5.5,  $\text{H}_h$ ), 8.11 (1H, td,  $J$  = 7.8, 1.2,  $\text{H}_3$ ), 7.97 (1H, bd,  $J$  = 8.2,  $\text{H}_e$ ), 7.93 (1H, dd,  $J$  = 5.1, 1.2,  $\text{H}_l$ ), 7.84 (1H, td,  $J$  = 8.2, 1.6,  $\text{H}_f$ ), 7.81 – 7.79 (2H, m,  $\text{H}_{e', f'}$ ), 7.73 (1H, dd,  $J$  = 7.8, 1.2,  $\text{H}_d$ ), 7.51 – 7.44 (3H, m,  $\text{H}_{2, d', h'}$ ), 7.19 – 7.15 (3H, m,  $\text{H}_{7, 7', g}$ ), 7.11 – 7.04 (2H, m,  $\text{H}_{c, g'}$ ), 6.91, 6.90 (2H, 2 X td,  $J$  = 7.4, 1.2,  $\text{H}_{b, c}$ ), 6.83 – 6.79 (3H, m,  $\text{H}_{6, 6', b'}$ ), 6.24 (1H, dd,  $J$  = 7.8, 1.2,  $\text{H}_a$ ), 6.17 (1H, dd,  $J$  = 7.8, 1.2,  $\text{H}_a$ ).  $^{13}\text{C}$  NMR: 169.65 ( $\text{C}_5$ ), 169.00 ( $\text{C}_{k'}$ ), 168.62 ( $\text{C}_k$ ), 156.92 ( $\text{C}_{10}$ ), 152.05 ( $\text{C}_1$ ), 151.73 ( $\text{C}_h$ ), 150.88 ( $\text{C}_i$ ), 150.20 ( $\text{C}_h$ ), 149.20 ( $\text{C}_i$ ), 147.68 ( $\text{C}_9$ ), 144.89 ( $\text{C}_j$ ), 144.65 ( $\text{C}_{j'}$ ), 140.93 ( $\text{C}_3$ ), 139.83 ( $\text{C}_f$ ), 139.79 ( $\text{C}_f'$ ), 133.31 ( $\text{C}_{7, 7'}$ ), 132.98 ( $\text{C}_4$ ), 132.88 ( $\text{C}_a$ ), 132.79 ( $\text{C}_a$ ), 132.10 ( $\text{C}_b$ ), 131.73 ( $\text{C}_{b'}$ ), 131.27 ( $\text{C}_2$ ), 126.28 ( $\text{C}_d$ ), 125.91 ( $\text{C}_{d'}$ ), 125.68 ( $\text{C}_{6, 6'}$ ), 125.27 ( $\text{C}_g$ ), 124.85 ( $\text{C}_{g'}$ ), 124.44 ( $\text{C}_c$ ), 124.29 ( $\text{C}_8$ ), 123.87 ( $\text{C}_{c'}$ ), 121.38 ( $\text{C}_e$ ), 120.93 ( $\text{C}_{e'}$ ). MS (FAB):  $m/z$  761 [M]<sup>+</sup>.



### Synthesis of 3.14g(*p*-C<sub>6</sub>H<sub>4</sub>CO<sub>2</sub>H)

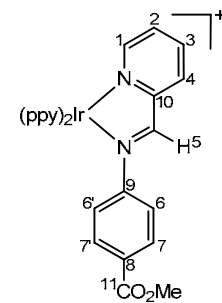
This was prepared from dimer **2.6g** (50 mg, 0.047 mmol), 4-aminobenzoic acid (15.5 mg, 0.113 mmol) and pyridine-2-carboxaldehyde (12.1 mg, 11  $\mu$ L, 0.113 mmol) and after work up gave **3.14g**(*p*-C<sub>6</sub>H<sub>4</sub>CO<sub>2</sub>H) as a red solid (58 mg, 82%). Anal. Calcd for C<sub>35</sub>H<sub>26</sub>ClIrN<sub>4</sub>O<sub>2</sub>: C, 55.15, H, 3.44, N, 7.35. Found: C, 54.99, H, 3.41, N, 7.27%. <sup>1</sup>H NMR (MeOD):  $\delta$  9.51 (1H, s, H<sub>5</sub>), 8.49 (1H, dd, *J* = 5.1, 0.8, H<sub>h</sub>), 8.44 (1H, bd, *J* = 7.4, H<sub>4</sub>), 8.22 (1H, td, *J* = 7.8, 1.5, H<sub>3</sub>), 8.16 (1H, dd, *J* = 8.2, 0.8, H<sub>e</sub>), 8.00 (1H, bd, *J* = 5.1, H<sub>1</sub>), 7.96 – 7.83 (5H, m, H<sub>1, d, e', f, f'</sub>), 7.66 – 7.62 (4H, m, H<sub>2, 7, 7', h'</sub>), 7.48 (1H, dd, *J* = 7.4, 1.2, H<sub>d'</sub>), 7.25 (1H, ddd, *J* = 7.4, 5.8, 1.6, H<sub>g</sub>), 7.16 (1H, ddd, *J* = 7.4, 5.8, 1.6, H<sub>g'</sub>), 7.03 (1H, td, *J* = 7.4, 1.2, H<sub>c</sub>), 6.93 – 6.90 (2H, m, H<sub>6, 6'</sub>) 6.87 (1H, td, *J* = 7.4, 1.6, H<sub>b</sub>) 6.82 (1H, td, *J* = 7.4, 1.2, H<sub>c'</sub>), 6.75 (1H, td, *J* = 7.4,



1.6, H<sub>b</sub>), 6.24 (1H, dd, *J* = 7.4, 1.2, H<sub>a</sub>), 6.15 (1H, dd, *J* = 7.4, 1.2, H<sub>a'</sub>). <sup>13</sup>C NMR: 170.88 (C<sub>5</sub>), 169.35 (C<sub>k'</sub>), 168.93 (C<sub>k</sub>), 157.06 (C<sub>10</sub>), 152.06 (C<sub>9</sub>), 151.93 (C<sub>1</sub>), 151.76 (C<sub>h</sub>), 150.80 (C<sub>i'</sub>), 150.37 (C<sub>h'</sub>), 149.55 (C<sub>i</sub>), 145.11 (C<sub>j</sub>), 144.83 (C<sub>j'</sub>), 140.86 (C<sub>3</sub>), 139.90 (C<sub>f</sub>), 139.88 (C<sub>f'</sub>), 132.79 (C<sub>8</sub>), 132.63 (C<sub>a, a'</sub>), 132.32 (C<sub>4</sub>), 131.58 (C<sub>b</sub>), 131.42 (C<sub>2</sub>), 131.14 (C<sub>7, 7', b'</sub>), 126.09 (C<sub>d</sub>), 125.59 (C<sub>d'</sub>), 124.88 (C<sub>g</sub>), 124.51 (C<sub>g'</sub>), 124.04 (C<sub>c</sub>), 123.63 (C<sub>6, 6'</sub>), 123.44 (C<sub>c'</sub>), 121.22 (C<sub>e</sub>), 120.70 (C<sub>e'</sub>). MS (FAB): *m/z* 727 [M]<sup>+</sup>.

### Synthesis of 3.14g(*p*-C<sub>6</sub>H<sub>4</sub>CO<sub>2</sub>Me)

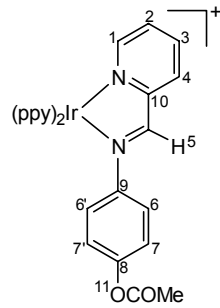
This was prepared from dimer **2.6g** (30 mg, 0.028 mmol), methyl-4-aminobenzoate (10.1 mg, 0.067 mmol), pyridine-2-carboxaldehyde (7.2 mg, 6.4  $\mu$ L, 0.067 mmol) and KPF<sub>6</sub> (12.4 mg, 0.067 mmol) and after work up gave **3.14g(*p*-C<sub>6</sub>H<sub>4</sub>CO<sub>2</sub>Me)** as a red solid (36 mg, 73%). This compound was also synthesised using harsh conditions *i.e.* microwave heating for 30 mins at 100 °C, which resulted in a comparable yield (66%). Anal. calcd for C<sub>36</sub>H<sub>28</sub>F<sub>6</sub>IrN<sub>4</sub>O<sub>2</sub>P: C, 48.80, H, 3.19, N, 6.32. Found: C, 48.78, H, 3.18, N, 6.27%. <sup>1</sup>H NMR (CDCl<sub>3</sub>):  $\delta$  9.83 (1H, s, H<sub>5</sub>), 8.84 (1H, bd, *J* = 7.9, H<sub>4</sub>), 8.36 (1H, ddd, *J* = 5.8, 1.5, 0.8, H<sub>h</sub>), 8.08 (1H, td, *J* = 7.6, 1.5, H<sub>3</sub>), 7.93 (1H, bd, *J* = 8.2, H<sub>e</sub>), 7.87 (1H, dd, *J* = 5.2, 1.5, H<sub>1</sub>), 7.82 (1H, td, *J* = 8.2, 1.5, H<sub>f</sub>), 7.75 (1H, td, *J* = 8.2, 1.5, H<sub>f'</sub>), 7.71 – 7.66 (4H, m, H<sub>7, 7', d, e'</sub>), 7.49 (1H, bd, *J* = 5.8, H<sub>b'</sub>), 7.44 (1H, ddd, *J* = 7.6, 5.5, 1.2, H<sub>2</sub>), 7.35 (1H, dd, *J* = 7.6, 1.6, H<sub>d'</sub>), 7.21 (1H, ddd, *J* = 7.3, 6.1, 1.5, H<sub>g</sub>), 7.12 (1H, ddd, *J* = 7.3, 5.8, 1.5, H<sub>g'</sub>), 7.03 (1H, td, *J* = 7.3, 1.3, H<sub>c</sub>), 7.02 – 6.99 (2H, m, H<sub>6, 6'</sub>), 6.89 (1H, td, *J* = 7.6, 1.5, H<sub>b</sub>), 6.83 (1H, td, *J* = 7.3, 1.2, H<sub>c'</sub>), 6.77 (1H, td, *J* = 7.6, 1.5, H<sub>b'</sub>), 6.23 (1H, dd, *J* = 7.6, 0.9, H<sub>a</sub>), 6.14 (1H, dd, *J* = 7.6, 0.9, H<sub>a'</sub>), 3.84 (3H, s, Me). <sup>13</sup>C NMR: 170.50 (C<sub>5</sub>), 167.83 (C<sub>k'</sub>), 167.33 (C<sub>k</sub>), 166.05 (C<sub>11</sub>), 156.22 (C<sub>10</sub>), 150.62 (C<sub>9</sub>), 150.55 (C<sub>h</sub>), 149.86 (C<sub>1</sub>), 149.67 (C<sub>i'</sub>), 148.78 (C<sub>h'</sub>), 148.27 (C<sub>i</sub>), 143.26 (C<sub>j</sub>), 142.88 (C<sub>j'</sub>), 139.50 (C<sub>3</sub>), 138.18 (C<sub>f, f'</sub>), 133.39 (C<sub>4</sub>), 131.59 (C<sub>a</sub>), 131.48 (C<sub>a'</sub>), 130.85 (C<sub>b</sub>), 130.47 (C<sub>b'</sub>), 130.29 (C<sub>7, 7'</sub>), 129.98 (C<sub>8</sub>), 129.43 (C<sub>2</sub>), 124.73 (C<sub>d</sub>), 124.40 (C<sub>d'</sub>), 123.81 (C<sub>g</sub>), 123.23 (C<sub>c</sub>), 122.94 (C<sub>6, 6', g'</sub>), 122.47 (C<sub>c'</sub>), 119.64 (C<sub>e</sub>), 119.24 (C<sub>e'</sub>), 52.25 (Me). MS (FAB): *m/z* 741 [M]<sup>+</sup>.



### Synthesis of 3.14g(*p*-C<sub>6</sub>H<sub>4</sub>OCOMe)

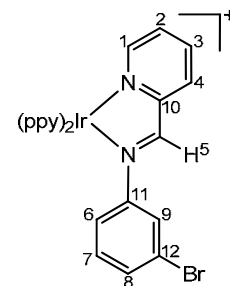
Complex **3.14g(*p*-C<sub>6</sub>H<sub>4</sub>OH)** (50 mg, 0.059 mmol) and triethylamine (6.1 mg, 9  $\mu$ L, 0.059 mmol) were dissolved in dry DCM (5 ml) and solution of acetyl chloride (7.1 mg, 6  $\mu$ L, 0.088 mmol) in DCM (2 ml) was added slowly. After stirring for an

hour, passed the clear red solution through celite and washed with water (3 x 5 ml), dried the organic layer. Subsequent recrystallization of the compound from DCM/Hexane mixture afforded **3.14g(p-C<sub>6</sub>H<sub>4</sub>OCOMe)** as a red solid (44 mg, 82%). Anal. Calcd for C<sub>36</sub>H<sub>28</sub>F<sub>6</sub>IrN<sub>4</sub>O<sub>2</sub>P: C, 48.81, H, 3.19, N, 6.32. Found: C, 48.74, H, 3.19, N, 6.27%. <sup>1</sup>H NMR (CD<sub>2</sub>Cl<sub>2</sub>):  $\delta$  9.30 (1H, s, H<sub>5</sub>), 8.40 (1H, dd, *J* = 7.8, 0.8, H<sub>4</sub>), 8.28 (1H, d, *J* = 5.5, H<sub>h</sub>), 8.13 (1H, td, *J* = 7.4, 1.2, H<sub>3</sub>), 7.98 (1H, d, *J* = 7.8, H<sub>e</sub>), 7.95 (1H, d, *J* = 5.5, H<sub>1</sub>), 7.85 (1H, td, *J* = 7.4, 1.6, H<sub>f</sub>), 7.81 – 7.80 (2H, m, H<sub>e', f'</sub>), 7.74 (1H, dd, *J* = 7.8, 1.2, H<sub>d</sub>), 7.53 – 7.47 (2H, m, H<sub>2, d'</sub>), 7.45 (1H, d, *J* = 5.9, H<sub>h'</sub>), 7.17 (1H, ddd, *J* = 7.4, 5.9, 1.2, H<sub>g</sub>), 7.12 – 7.05 (2H, m, H<sub>c, g</sub>), 6.96 – 6.88 (4H, m, H<sub>6, 6', b, c'</sub>), 6.84 – 6.79 (3H, m, H<sub>7, 7', b'</sub>), 6.25 (1H, dd, *J* = 7.8, 1.2, H<sub>a</sub>), 6.19 (1H, dd, *J* = 7.4, 1.2, H<sub>a'</sub>), 2.21 (3H, s, Me). <sup>13</sup>C NMR: 168.81 (C<sub>11</sub>), 167.61 (C<sub>k'</sub>), 167.38 (C<sub>5</sub>), 167.24 (C<sub>k</sub>), 155.35 (C<sub>10</sub>), 151.11 (C<sub>8</sub>), 150.74 (C<sub>1</sub>), 150.24 (C<sub>h</sub>), 149.47 (C<sub>i'</sub>), 148.73 (C<sub>h'</sub>), 147.77 (C<sub>i</sub>), 144.68 (C<sub>9</sub>), 143.45 (C<sub>j</sub>), 143.27 (C<sub>j'</sub>), 139.52 (C<sub>3</sub>), 138.43 (C<sub>f</sub>), 138.37 (C<sub>f'</sub>), 131.46 (C<sub>a'</sub>), 131.39 (C<sub>a</sub>), 131.10 (C<sub>4</sub>), 130.71 (C<sub>b</sub>), 130.26 (C<sub>b'</sub>), 129.85 (C<sub>2</sub>), 124.87 (C<sub>d</sub>), 124.50 (C<sub>d'</sub>), 123.83 (C<sub>g</sub>), 123.64 (C<sub>6, 6'</sub>), 123.43 (C<sub>g'</sub>), 123.04 (C<sub>c</sub>), 122.41 (C<sub>c'</sub>), 122.05 (C<sub>7, 7'</sub>), 119.98 (C<sub>e</sub>), 119.52 (C<sub>e'</sub>) 20.81 (Me). MS (FAB): *m/z* 741 [M]<sup>+</sup>.



### Synthesis of 3.14g(*m*-C<sub>6</sub>H<sub>4</sub>Br)

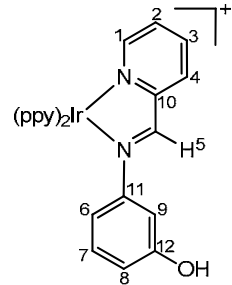
This was prepared from dimer **2.6g** (50 mg, 0.047 mmol), 3-bromoaniline (19.4 mg, 0.113 mmol), pyridine-2-carboxaldehyde (12.1 mg, 11  $\mu$ L, 0.113 mmol) and KPF<sub>6</sub> (17.3 mg, 0.094 mmol) and after work up gave **3.14g(*m*-C<sub>6</sub>H<sub>4</sub>Br)** as a red solid (73 mg, 82%). This compound was also synthesised using harsh conditions *i.e.* microwave heating for 30 mins at 100 °C, which resulted in a comparable yield (79%). Anal. Calcd for C<sub>34</sub>H<sub>25</sub>BrF<sub>6</sub>IrN<sub>4</sub>P: C, 45.04, H, 2.78, N, 6.18. Found: C, 45.17, H, 2.64, N, 6.09%. <sup>1</sup>H NMR (CDCl<sub>3</sub>):  $\delta$  9.91 (1H, s, H<sub>5</sub>), 8.94 (1H, bd, *J* = 7.8, H<sub>4</sub>), 8.34 (1H, bd, *J* = 5.8, H<sub>h</sub>), 8.11 (1H, td, *J* = 7.6, 1.2, H<sub>3</sub>), 7.95 (1H, bd, *J* = 7.7, H<sub>e</sub>), 7.89 (1H, dd, *J* = 5.4, 1.2, H<sub>1</sub>), 7.84 (1H, td, *J* = 8.2, 1.5, H<sub>f</sub>), 7.80 – 7.77 (2H, m, H<sub>e', f'</sub>), 7.69 (1H, dd, *J* = 7.8, 0.8, H<sub>d</sub>), 7.50 (1H, bd, *J* = 5.7, H<sub>h'</sub>), 7.48 – 7.45 (2H, m, H<sub>2, d'</sub>), 7.27 – 7.22 (2H, m, H<sub>6, g</sub>), 7.16 (1H, dd, *J* = 7.6, 1.5, H<sub>8</sub>), 7.13 (1H, td, *J* = 5.8, 2.6, H<sub>g'</sub>), 7.07 – 7.00 (2H, m, H<sub>7, c</sub>), 6.96 (1H, t, *J* = 1.8, H<sub>9</sub>), 6.94 – 6.83 (3H, m, H<sub>b, b', c'</sub>), 6.26 (1H, dd, *J* = 7.6, 0.8, H<sub>a</sub>), 6.19 (1H, dd, *J* = 7.6, 1.1, H<sub>a'</sub>). <sup>13</sup>C NMR: 169.89 (C<sub>5</sub>), 167.89 (C<sub>k'</sub>), 167.30



(C<sub>k</sub>), 156.15 (C<sub>10</sub>), 150.49 (C<sub>h</sub>), 149.84 (C<sub>1, i'</sub>), 148.78 (C<sub>h'</sub>), 148.24 (C<sub>i</sub>), 148.00 (C<sub>11</sub>), 143.28 (C<sub>j</sub>), 142.79 (C<sub>j'</sub>), 139.48 (C<sub>3</sub>), 138.21 (C<sub>f</sub>), 138.17 (C<sub>f'</sub>), 133.19 (C<sub>4</sub>), 131.71 (C<sub>8</sub>), 131.49 (C<sub>a</sub>), 131.45 (C<sub>a'</sub>), 130.84 (C<sub>b</sub>), 130.72 (C<sub>b'</sub>), 130.55 (C<sub>7</sub>), 129.37 (C<sub>2</sub>), 126.81 (C<sub>9</sub>), 124.72 (C<sub>d</sub>), 124.47 (C<sub>d'</sub>), 123.87 (C<sub>g</sub>), 123.24 (C<sub>g'</sub>), 122.93 (C<sub>c</sub>), 122.62 (C<sub>c'</sub>), 122.10 (C<sub>12</sub>), 120.98 (C<sub>6</sub>), 119.61 (C<sub>e</sub>), 119.22 (C<sub>e'</sub>). MS (FAB): *m/z* 761 [M]<sup>+</sup>.

### Synthesis of 3.14g(*m*-C<sub>6</sub>H<sub>4</sub>OH)

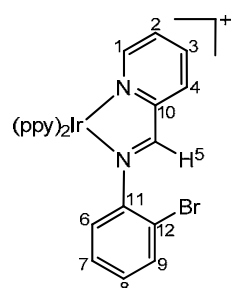
This was prepared from dimer **2.6g** (50 mg, 0.047 mmol), 3-aminophenol (12.3 mg, 0.113 mmol), pyridine-2-carboxaldehyde (12.1 mg, 11  $\mu$ L, 0.113 mmol) and  $\text{KPF}_6$  (17.3 mg, 0.094 mmol) and after work up gave **3.14g**(*m*-C<sub>6</sub>H<sub>4</sub>OH) as a red solid (66 mg, 84%). Anal. Calcd for C<sub>34</sub>H<sub>26</sub>F<sub>6</sub>IrN<sub>4</sub>OP: C, 48.40, H, 3.11, N, 6.64.



Found: C, 48.46, H, 3.05, N, 6.65%.  $^1\text{H}$  NMR (Acetone – D<sub>6</sub>):  $\delta$  9.66 (1H, s, H<sub>5</sub>), 8.64 (1H, bd,  $J$  = 5.9, H<sub>h</sub>), 8.61 (1H, bd,  $J$  = 7.4, H<sub>4</sub>), 8.34 (1H, td,  $J$  = 7.8, 1.6, H<sub>3</sub>), 8.27 (1H, bd,  $J$  = 8.2, H<sub>e</sub>), 8.09 – 8.02 (3H, m, H<sub>1</sub>, e', h'), 7.99 (1H, td,  $J$  = 8.2, 1.6, H<sub>f</sub>), 7.90 (1H, dd,  $J$  = 7.8, 0.8, H<sub>d</sub>), 7.82 – 7.77 (2H, m, H<sub>2</sub>, f'), 7.60 (1H, dd,  $J$  = 7.8, 1.2, H<sub>d'</sub>), 7.36 (1H, ddd,  $J$  = 7.4, 5.9, 1.6, H<sub>g</sub>), 7.25 (1H, ddd,  $J$  = 7.4, 5.9, 1.6, H<sub>g</sub>), 7.04 (1H, td,  $J$  = 7.8, 1.2, H<sub>c</sub>), 6.93 – 6.87 (2H, m, H<sub>7</sub>, b), 6.82 (1H, td,  $J$  = 7.8, 1.6, H<sub>c</sub>), 6.75 (1H, td,  $J$  = 7.4, 1.6, H<sub>b</sub>), 6.68 (1H, dd,  $J$  = 8.2, 1.6, H<sub>6</sub>), 6.58 (1H, dd,  $J$  = 2.3, 2.0, H<sub>9</sub>), 6.44 (1H, dd,  $J$  = 7.8, 1.2, H<sub>8</sub>), 6.28 (1H, dd,  $J$  = 7.4, 0.8, H<sub>a</sub>), 6.22 (1H, dd,  $J$  = 7.4, 0.8, H<sub>a'</sub>).  $^{13}\text{C}$  NMR: 169.86 (C<sub>5</sub>), 168.87 (C<sub>k'</sub>), 168.33 (C<sub>k</sub>), 158.82 (C<sub>12</sub>), 156.85 (C<sub>10</sub>), 151.80 (C<sub>h</sub>), 151.61 (C<sub>h'</sub>), 150.90 (C<sub>i'</sub>), 150.35 (C<sub>2</sub>), 150.13 (C<sub>11</sub>), 149.64 (C<sub>i</sub>), 144.79 (C<sub>j</sub>), 144.41 (C<sub>j'</sub>), 140.61 (C<sub>3</sub>), 139.62 (C<sub>f</sub>), 139.54 (C<sub>1</sub>), 132.40 (C<sub>a'</sub>), 132.21 (C<sub>a</sub>), 131.88 (C<sub>4</sub>), 131.22 (C<sub>f'</sub>), 131.06 (C<sub>b</sub>), 130.67 (C<sub>7</sub>), 130.29 (C<sub>b'</sub>), 125.78 (C<sub>d</sub>), 125.24 (C<sub>d'</sub>), 124.73 (C<sub>g</sub>), 124.29 (C<sub>g'</sub>), 123.58 (C<sub>c</sub>), 122.84 (C<sub>c'</sub>), 120.89 (C<sub>e</sub>), 120.38 (C<sub>e'</sub>), 116.41 (C<sub>6</sub>), 114.59 (C<sub>8</sub>), 110.61 (C<sub>9</sub>). MS (FAB):  $m/z$  699 [M]<sup>+</sup>.

### Synthesis of 3.14g(*o*-C<sub>6</sub>H<sub>4</sub>Br)

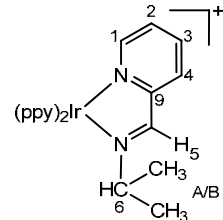
This was prepared from dimer **2.6g** (30 mg, 0.028 mmol), 2-bromoaniline (11.5 mg, 0.067 mmol), pyridine-2-carboxaldehyde (7.2 mg, 6.4  $\mu$ L, 0.067 mmol) and KPF<sub>6</sub> (12.4 mg, 0.067 mmol) and after work up gave **3.14g**(*o*-C<sub>6</sub>H<sub>4</sub>Br) as a orange/red solid (42 mg, 84%). This compound was also synthesised using harsh conditions *i.e.* microwave heating for 30 mins at 100 °C, which resulted in a



80% yield. Anal. Calcd for  $C_{34}H_{25}BrF_6IrN_4P$ : C, 46.11, H, 2.99, N, 6.15. Found: C, 46.01, H, 3.02, N, 6.07%.  $^1H$  NMR ( $CDCl_3$ ):  $\delta$  9.32 (1H, s,  $H_5$ ), 8.62 (1H, ddd,  $J$  = 5.8, 1.6, 0.8,  $H_h$ ), 8.47 (1H, bd,  $J$  = 7.4,  $H_4$ ), 8.12 (1H, td,  $J$  = 7.8, 1.6,  $H_3$ ), 8.00 (1H, dd,  $J$  = 5.5, 1.6,  $H_1$ ), 7.92 (1H, bd,  $J$  = 8.2,  $H_e$ ), 7.82 (1H, td,  $J$  = 8.2, 1.6,  $H_f$ ), 7.78 – 7.65 (4H, m,  $H_d, e', f, h'$ ), 7.51 (1H, ddd,  $J$  = 7.8, 5.5, 1.2,  $H_2$ ), 7.32 (1H, ddd,  $J$  = 7.5, 5.8, 1.6,  $H_g$ ), 7.27 (1H, dd,  $J$  = 6.3, 2.3,  $H_9$ ), 7.19 (1H, m,  $H_d'$ ), 7.07 (1H, ddd,  $J$  = 7.5, 5.8, 1.6,  $H_g'$ ), 7.02 (1H, td,  $J$  = 7.4, 1.2,  $H_c$ ), 6.88 (1H, td,  $J$  = 7.4, 1.2,  $H_b$ ), 6.86 – 6.82 (3H, m,  $H_{6, 7, 8}$ ), 6.73 – 6.71 (2H, m,  $H_{b', c'}$ ), 6.28 (1H, dd,  $J$  = 7.4, 0.8,  $H_a$ ), 6.15 (1H, m,  $H_{a'}$ ).  $^{13}C$  NMR: 172.96 ( $C_5$ ), 167.87 ( $C_k$ ), 166.88 ( $C_k$ ), 155.01 ( $C_{10}$ ), 150.75 ( $C_h$ ), 150.21 ( $C_1$ ), 150.00 ( $C_{h'}$ ), 149.40 ( $C_i$ ), 148.19 ( $C_i$ ), 144.43 ( $C_{11}$ ), 143.56 ( $C_j$ ), 142.98 ( $C_{j'}$ ), 139.67 ( $C_3$ ), 138.36 ( $C_f$ ), 138.28 ( $C_f$ ), 132.64 ( $C_9$ ), 132.05 ( $C_{a'}$ ), 131.84 ( $C_4$ ), 131.31 ( $C_a$ ), 130.53 ( $C_b$ ), 130.06 ( $C_{b'}$ ), 130.03 ( $C_2$ ), 128.49 ( $C_8$ ), 127.39 ( $C_7$ ), 125.11 ( $C_6$ ), 124.65 ( $C_d$ ), 124.04 ( $C_g$ ), 123.74 ( $C_{d'}$ ), 123.08 ( $C_{g'}$ ), 122.83 ( $C_c$ ), 122.21 ( $C_{c'}$ ), 119.44 ( $C_e$ ), 119.23 ( $C_e$ ), 114.20 ( $C_{12}$ ). MS (FAB):  $m/z$  761 [ $M]^+$ .

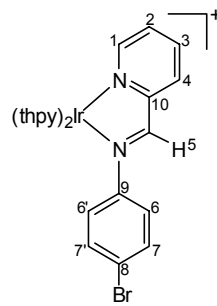
### Synthesis of **3.14g*i*Pr**

This was prepared from dimer **2.6g** (70 mg, 0.065 mmol), 2-pyridinecarbaldisopropylimine (23.2 mg, 0.157 mmol), and  $KPF_6$  (24 mg, 0.131 mmol) and after work up gave **3.14g*i*Pr** as a orange solid (91 mg, 88%). Anal. Calcd for  $C_{31}H_{28}ClIrN_4(CH_2Cl_2)(H_2O)$ : C, 48.82, H, 4.10, N, 7.12. Found; C, 48.71, H, 4.14, N, 6.99%.  $^1H$  NMR ( $CD_2Cl_2$ ):  $\delta$  9.73 (1H, s,  $H_5$ ), 8.59 (1H, bd,  $J$  = 7.6,  $H_4$ ), 8.17 (1H, ddd,  $J$  = 5.9, 1.4, 0.8,  $H_h$ ), 8.11 (1H, td,  $J$  = 7.8, 1.4,  $H_3$ ), 8.02 (1H, bd,  $J$  = 7.8,  $H_e'$ ), 7.96 (1H, bd,  $J$  = 7.8,  $H_e$ ), 7.92 – 7.83 (3H, m,  $H_{1, f, f'}$ ), 7.73 (2H, td,  $J$  = 7.6, 1.4,  $H_{d, d'}$ ), 7.46 – 7.42 (2H, m,  $H_{2, h'}$ ), 7.20 (1H, td,  $J$  = 5.9, 1.6,  $H_g$ ), 7.13 – 7.02 (3H, m,  $H_{c, c', g}$ ), 6.94 (1H, td,  $J$  = 7.6, 1.4,  $H_b$ ), 6.90 (1H, td,  $J$  = 7.6, 1.4,  $H_{b'}$ ), 6.35 (1H, ddd,  $J$  = 7.6, 1.2, 0.6,  $H_{a'}$ ), 6.17 (1H, ddd,  $J$  = 7.6, 1.2, 0.6,  $H_a$ ), 4.08 (1H, septd,  $J$  = 6.7, 0.8,  $H_6$ ), 1.19 (3H, d,  $J$  = 6.7,  $Me_A$  or  $B$ ), 0.98 (3H, d,  $J$  = 6.5,  $Me_A$  or  $B$ ).  $^{13}C$  NMR: 168.49 ( $C_k$ ), 167.83 ( $C_k$ ), 167.39 ( $C_5$ ), 156.63 ( $C_9$ ), 150.79 ( $C_h$ ), 150.62 ( $C_1$ ), 149.77 ( $C_i$ ), 149.53 ( $C_i$ ), 149.28 ( $C_h$ ), 143.97 ( $C_{j, j'}$ ), 139.85 ( $C_3$ ), 138.67 ( $C_f$ ), 138.56 ( $C_f$ ), 132.50 ( $C_a$ ), 131.31 ( $C_a$ ), 131.00 ( $C_b$ ), 130.69 ( $C_{4, b'}$ ), 129.40 ( $C_2$ ), 125.06 ( $C_d$ ), 124.97 ( $C_{d'}$ ), 123.85 ( $C_g$ ), 123.63 ( $C_{g'}$ ), 123.18 ( $C_c$ ), 122.71 ( $C_{c'}$ ), 120.14 ( $C_e$ ), 120.06 ( $C_{e'}$ ), 62.37 ( $C_6$ ), 22.82 ( $Me_A$  or  $B$ ), 22.54 ( $Me_A$  or  $B$ ). MS (FAB):  $m/z$  649 [ $M]^+$ .



### Synthesis of 3.14h(*p*-C<sub>6</sub>H<sub>4</sub>Br)

This was prepared from dimer **2.6h** (40 mg, 0.036 mmol), 4-bromoaniline (15 mg, 0.087 mmol), pyridine-2-carboxaldehyde (9.3 mg, 8.3  $\mu$ L, 0.087 mmol) and KPF<sub>6</sub> (16 mg, 0.087 mmol) and after work up gave **3.14h(*p*-C<sub>6</sub>H<sub>4</sub>Br)** as a red solid (52 mg, 78%). This compound was also synthesised using harsh conditions *i.e.* microwave heating for 30 mins at 100 °C, which resulted in a 64% yield. Anal. Calcd for C<sub>30</sub>H<sub>21</sub>BrF<sub>6</sub>IrN<sub>4</sub>PS<sub>2</sub>: C, 39.22, H, 2.30, N, 6.10. Found: C, 39.32, H, 2.20, N, 6.03%. <sup>1</sup>H NMR (CDCl<sub>3</sub>):  $\delta$  9.37 (1H, s, H<sub>5</sub>), 8.51 (1H, bd, *J* = 7.8, H<sub>4</sub>), 8.14 (1H, bd, *J* = 5.5, H<sub>f</sub>), 8.07 (1H, td, *J* = 7.8, 1.6, H<sub>3</sub>), 7.84 (1H, bd, *J* = 4.7, H<sub>1</sub>), 7.67 (1H, td, *J* = 8.2, 1.6, H<sub>d</sub>), 7.64 (1H, td, *J* = 8.2, 1.6, H<sub>d'</sub>), 7.54 (1H, bd, *J* = 7.8, H<sub>c</sub>), 7.49 (1H, ddd, *J* = 7.8, 5.5, 1.2, H<sub>2</sub>), 7.39 (1H, bd, *J* = 8.2, H<sub>c'</sub>), 7.37 (1H, d, *J* = 4.7, H<sub>b</sub>), 7.35 (1H, bd, *J* = 5.5, H<sub>f'</sub>), 7.22 (1H, d, *J* = 4.7, H<sub>b'</sub>), 7.23 – 7.20 (2H, m, H<sub>7, 7'</sub>), 6.99 (1H, ddd, *J* = 7.4, 5.8, 1.6, H<sub>e</sub>), 6.91 (1H, ddd, *J* = 7.4, 5.8, 1.6, H<sub>e'</sub>), 6.85 – 6.81 (2H, m, H<sub>6, 6'</sub>), 6.20 (1H, d, *J* = 5.1, H<sub>a</sub>), 6.10 (1H, d, *J* = 4.7, H<sub>a'</sub>). <sup>13</sup>C NMR (CD<sub>2</sub>Cl<sub>2</sub>): 168.84 (C<sub>5</sub>), 164.20 (C<sub>g</sub>), 163.90 (C<sub>g'</sub>), 155.95 (C<sub>10</sub>), 151.73 (C<sub>h</sub>), 151.63 (C<sub>1</sub>), 151.14 (C<sub>f</sub>), 149.63 (C<sub>f'</sub>), 149.47 (C<sub>h'</sub>), 146.79 (C<sub>9</sub>), 140.06 (C<sub>3</sub>), 139.38 (C<sub>d'</sub>), 139.35 (C<sub>d</sub>), 137.24 (C<sub>i</sub>), 136.84 (C<sub>i'</sub>), 132.45 (C<sub>7, 7'</sub>), 131.81 (C<sub>4</sub>), 130.89 (C<sub>a'</sub>), 130.73 (C<sub>a</sub>), 130.52 (C<sub>b</sub>), 130.45 (C<sub>2, b'</sub>), 124.53 (C<sub>6, 6'</sub>), 123.47 (C<sub>8</sub>), 121.49 (C<sub>e</sub>), 120.97 (C<sub>e'</sub>), 118.99 (C<sub>c</sub>), 118.66 (C<sub>c'</sub>). MS (FAB): *m/z* 773 [M]<sup>+</sup>.



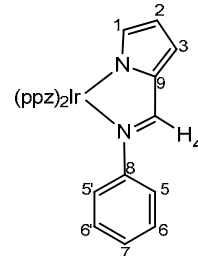
### General procedure for synthesis of [Ir(C<sup>N</sup>)<sub>2</sub>(pyrrolylimine)][PF<sub>6</sub>] (3.15)

All pyrroleimine ligands are synthesized using literature methods.<sup>26</sup> The appropriate dimer [Ir(C<sup>N</sup>)<sub>2</sub>Cl]<sub>2</sub>, pyrroleimine ligand (2.2-2.4 equiv) and DABCO/Na<sub>2</sub>CO<sub>3</sub> (2.2-2.4 equiv) were placed in a microwave vial and the acetonitrile (3 ml) was added. Nitrogen was bubbled through the solution for 2 mins and the vial was then sealed with a septum cap. The tube was placed in the microwave reactor and heated under microwave irradiation. Synthesis was started using harsh conditions such as heating for 80 mins at 80 °C but gradually transformed to milder conditions (20 mins at 70 °C). Following this, majority of the synthesis has been done under the milder conditions unless stated. After this time the solvent is removed *in vacuo* leaving behind a solid which was dissolved in DCM (15 ml) and passed through celite. The filtrate was washed with slightly acidic water (3 x 5 ml). Reduced the volume of DCM and hexane

was added slowly to induce precipitation. Precipitate was isolated, washed with hexane and dried *in vacuo*. The compounds could be recrystallised from DCM/hexane.

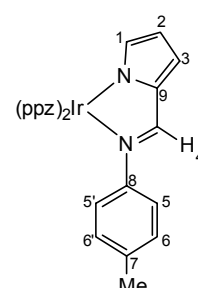
### Synthesis of 3.15a(C<sub>6</sub>H<sub>5</sub>)

This was prepared from dimer **2.6a** (70 mg, 0.068 mmol), (*E*)-((1H-pyrrol-2-yl)methylene)aniline (27.8 mg, 0.164 mmol) and DABCO (18.4 mg, 0.164 mmol) and after work up gave **3.15a(C<sub>6</sub>H<sub>5</sub>)** as a pale yellow solid (52 mg, 60%). Anal. Calcd for C<sub>29</sub>H<sub>23</sub>IrN<sub>6</sub>: C, 53.77, H, 3.58, N, 12.97. Found: C, 53.68, H, 3.50, N, 13.01%. <sup>1</sup>H NMR (CD<sub>2</sub>Cl<sub>2</sub>):  $\delta$  8.17 (1H, d, *J* = 0.8, H<sub>4</sub>), 8.07 (1H, dd, *J* = 2.7, 0.8, H<sub>e</sub>), 8.00 (1H, dd, *J* = 2.7, 0.8, H<sub>e</sub>), 7.50 (1H, dd, *J* = 2.3, 0.8, H<sub>g</sub>), 7.23 (1H, dd, *J* = 7.8, 0.8, H<sub>d</sub>), 7.12 (1H, dd, *J* = 7.8, 0.8, H<sub>d'</sub>), 7.00 – 6.91 (4H, m, H<sub>6, 6', 7, c</sub>), 6.89 (1H, dd, *J* = 3.9, 1.2, H<sub>3</sub>), 6.81 (1H, td, *J* = 7.4, 1.2, H<sub>c'</sub>), 6.77 – 6.73 (4H, m, H<sub>5, 5', b, g'</sub>), 6.63 (1H, td, *J* = 7.4, 1.2, H<sub>b'</sub>), 6.56 (1H, t, *J* = 2.3, H<sub>f</sub>), 6.49 (1H, t, *J* = 2.7, H<sub>f'</sub>), 6.42 (1H, bs, H<sub>1</sub>), 6.35 (1H, dd, *J* = 7.4, 1.2, H<sub>a</sub>), 6.25 (1H, dd, *J* = 7.4, 1.2, H<sub>a</sub>), 6.19 (1H, dd, *J* = 3.5, 1.2, H<sub>2</sub>). <sup>13</sup>C NMR: 159.93 (C<sub>4</sub>), 151.74 (C<sub>8</sub>), 144.17 (C<sub>h'</sub>), 143.91 (C<sub>h</sub>), 142.83 (C<sub>9</sub>), 139.11 (C<sub>i'</sub>), 138.89 (C<sub>g</sub>), 137.91 (C<sub>g'</sub>), 137.23 (C<sub>1</sub>), 134.73 (C<sub>a'</sub>), 133.83 (C<sub>a, i</sub>), 128.66 (C<sub>6, 6'</sub>), 125.99, 125.95, 125.89 (C<sub>b, b', e, e'</sub>), 125.00 (C<sub>7</sub>), 122.98 (C<sub>5, 5'</sub>), 121.77 (C<sub>c</sub>), 121.38 (C<sub>c'</sub>), 118.74 (C<sub>3</sub>), 112.61 (C<sub>2</sub>), 111.00 (C<sub>d</sub>), 110.88 (C<sub>d'</sub>), 107.64 (C<sub>f</sub>), 107.44 (C<sub>f'</sub>). MS (FAB): *m/z* 648 [M]<sup>+</sup>.



### Synthesis of 3.15a(*p*-C<sub>6</sub>H<sub>4</sub>Me)

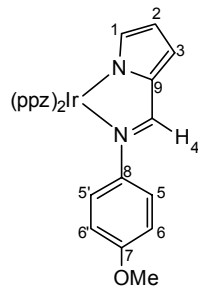
This was prepared from dimer **2.6a** (70 mg, 0.068 mmol), (*E*)-((1H-pyrrol-2-yl)methylene)-4-methylaniline (30.2 mg, 0.164 mmol) and DABCO (18.4 mg, 0.164 mmol) and after work up gave **3.15a(*p*-C<sub>6</sub>H<sub>4</sub>Me)** as a yellow solid (59 mg, 66%). Anal. Calcd for C<sub>30</sub>H<sub>25</sub>IrN<sub>6</sub>: C, 54.44, H, 3.81, N, 12.70. Found: C, 54.38, H, 3.74, N, 12.62%. <sup>1</sup>H NMR (CD<sub>2</sub>Cl<sub>2</sub>):  $\delta$  8.16 (1H, s, H<sub>4</sub>), 8.06 (1H, dd, *J* = 3.1, 0.8, H<sub>e</sub>), 8.02 (1H, dd, *J* = 3.1, 0.8, H<sub>e</sub>), 7.48 (1H, dd, *J* = 2.3, 0.8, H<sub>g</sub>), 7.23 (1H, dd, *J* = 7.8, 1.2, H<sub>d</sub>), 7.14 (1H, dd, *J* = 7.8, 1.2, H<sub>d'</sub>), 6.94 (1H, td, *J* = 7.8, 1.2, H<sub>c</sub>), 6.87 (1H, dd, *J* = 3.5, 1.2, H<sub>3</sub>), 6.83 (1H, td, *J* = 7.4, 1.6, H<sub>c'</sub>), 6.81 – 6.78 (2H, m, H<sub>6, 6'</sub>), 6.75 (1H, td, *J* = 7.4, 1.2, H<sub>b</sub>), 6.72 (1H, dd, *J* = 2.0, 0.8, H<sub>g'</sub>), 6.66 – 6.63 (2H, m, H<sub>5, 5'</sub>), 6.64 (1H, td, *J* = 7.4, 1.2, H<sub>b'</sub>), 6.55 (1H, dd, *J* = 2.3, 2.0, H<sub>f</sub>), 6.48 (1H, dd, *J* = 2.3, 2.3, H<sub>f'</sub>), 6.40 (1H, bs, H<sub>1</sub>), 6.33 (1H, dd, *J* = 7.4, 1.2, H<sub>a</sub>), 6.25 (1H, dd, *J* = 7.4, 1.2, H<sub>a'</sub>), 6.18 (1H, dd, *J* = 3.9, 1.6, H<sub>2</sub>), 2.18



(3H, s, Me).  $^{13}\text{C}$  NMR: 159.73 (C<sub>4</sub>), 149.48 (C<sub>8</sub>), 144.20 (C<sub>h</sub>), 143.91 (C<sub>h'</sub>), 142.83 (C<sub>9</sub>), 139.18 (C<sub>i'</sub>), 138.86 (C<sub>g</sub>), 137.91 (C<sub>g'</sub>), 136.94 (C<sub>1</sub>), 134.79 (C<sub>7</sub>), 134.76 (C<sub>a'</sub>), 133.89 (C<sub>i</sub>), 133.80 (C<sub>a</sub>), 129.26 (C<sub>6</sub>), 126.01, 125.98, 125.92, 125.89 (C<sub>b</sub>, b', e, e'), 122.71 (C<sub>5</sub>), 121.75 (C<sub>c</sub>), 121.35 (C<sub>c'</sub>), 118.37 (C<sub>3</sub>), 112.45 (C<sub>2</sub>), 110.98 (C<sub>d</sub>), 110.91 (C<sub>d'</sub>), 107.63 (C<sub>f</sub>), 107.43 (C<sub>f'</sub>), 20.86 (Me). MS (FAB):  $m/z$  662 [M]<sup>+</sup>.

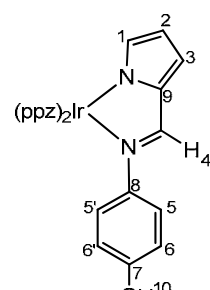
### Synthesis of 3.15a(*p*-C<sub>6</sub>H<sub>4</sub>OMe)

This was prepared from dimer **2.6a** (70 mg, 0.068 mmol), (*E*)-((1*H*-pyrrol-2-yl)methylene)-4-methoxyaniline (32.8 mg, 0.164 mmol) and DABCO (18.4 mg, 0.164 mmol) and after work up gave **3.15a(*p*-C<sub>6</sub>H<sub>4</sub>OMe)** as a yellow solid (57 mg, 62%). Anal. Calcd for C<sub>30</sub>H<sub>26</sub>IrN<sub>6</sub>O: C, 53.08, H, 3.86, N, 12.38. Found: C, 53.00, H, 3.85, N, 12.27%.  $^1\text{H}$  NMR (CD<sub>2</sub>Cl<sub>2</sub>):  $\delta$  8.14 (1H, d,  $J$  = 0.8, H<sub>4</sub>), 8.06 (1H, dd,  $J$  = 3.1, 0.8, H<sub>e</sub>), 8.00 (1H, dd,  $J$  = 3.1, 0.8, H<sub>e'</sub>), 7.48 (1H, dd,  $J$  = 2.3, 0.8, H<sub>g</sub>), 7.23 (1H, dd,  $J$  = 7.8, 1.2, H<sub>d</sub>), 7.13 (1H, dd,  $J$  = 7.8, 0.8, H<sub>d'</sub>), 6.94 (1H, td,  $J$  = 7.4, 1.2, H<sub>c</sub>), 6.85 (1H, dd,  $J$  = 3.5, 1.2, H<sub>3</sub>), 6.83 (1H, td,  $J$  = 7.8, 1.2, H<sub>c'</sub>), 6.75 (1H, td,  $J$  = 7.4, 1.2, H<sub>b</sub>), 6.72 (1H, dd,  $J$  = 2.7, 0.8, H<sub>g'</sub>), 6.72 (1H, dd,  $J$  = 2.7, 0.8, H<sub>g'</sub>), 6.69 – 6.65 (2H, m, H<sub>5, 5'</sub>), 6.64 (1H, td,  $J$  = 7.4, 1.2, H<sub>b'</sub>), 6.55 (1H, t,  $J$  = 2.3, H<sub>f</sub>), 6.52 – 6.49 (2H, m, H<sub>6, 6'</sub>), 6.48 (1H, t,  $J$  = 2.7, H<sub>f'</sub>), 6.39 (1H, bs, H<sub>1</sub>), 6.35 (1H, dd,  $J$  = 7.4, 1.2, H<sub>a</sub>), 6.26 (1H, dd,  $J$  = 7.4, 1.2, H<sub>a'</sub>), 6.17 (1H, dd,  $J$  = 3.5, 1.6, H<sub>2</sub>), 3.66 (1H, s, Me).  $^{13}\text{C}$  NMR: 159.36 (C<sub>4</sub>), 157.34 (C<sub>7</sub>), 145.24 (C<sub>8</sub>), 144.19 (C<sub>h</sub>), 143.91 (C<sub>h</sub>), 142.80 (C<sub>9</sub>), 139.18 (C<sub>i'</sub>), 138.80 (C<sub>g</sub>), 137.89 (C<sub>g'</sub>), 136.73 (C<sub>1</sub>), 134.75 (C<sub>a'</sub>), 133.99 (C<sub>i</sub>), 133.84 (C<sub>a</sub>), 126.03, 125.96, 125.92, 125.88 (C<sub>b</sub>, b', e, e'), 123.75 (C<sub>5, 5'</sub>), 121.74 (C<sub>c</sub>), 121.40 (C<sub>c'</sub>), 118.09 (C<sub>3</sub>), 113.74 (C<sub>6, 6'</sub>), 112.31 (C<sub>2</sub>), 110.98 (C<sub>d</sub>), 110.91 (C<sub>d'</sub>), 107.62 (C<sub>f</sub>), 107.42 (C<sub>f'</sub>), 55.66 (Me). MS (FAB):  $m/z$  678 [M]<sup>+</sup>.



### Synthesis of 3.15a(*p*-C<sub>6</sub>H<sub>4</sub>OH)

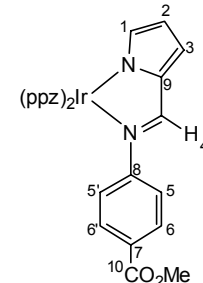
This was prepared from dimer **2.6a** (70 mg, 0.068 mmol), (*E*)-((1*H*-pyrrol-2-yl)methyleneamino)phenol (30.5 mg, 0.164 mmol) and DABCO (18.4 mg, 0.164 mmol) and after work up gave **3.15a(*p*-C<sub>6</sub>H<sub>4</sub>OH)** as a grey solid (75 mg, 83%). Anal. Calcd for C<sub>29</sub>H<sub>23</sub>IrN<sub>6</sub>O<sub>1</sub>: C, 52.48, H, 3.49, N, 12.66. Found: C, 52.48, H, 3.42, N, 12.64%.  $^1\text{H}$  NMR (CD<sub>2</sub>Cl<sub>2</sub>):  $\delta$  8.13 (1H, d,  $J$  = 0.8, H<sub>4</sub>), 8.07 (1H, d,  $J$  = 2.7, H<sub>e</sub>), 8.00 (1H, dd,  $J$  = 2.7, 0.8, H<sub>e'</sub>), 7.49 (1H, d,  $J$  = 2.3, H<sub>g</sub>), 7.23 (1H, dd,  $J$  = 7.8, 1.2, H<sub>d</sub>), 7.13 (1H, dd,  $J$  = 7.8, 0.8, H<sub>d'</sub>), 6.94 (1H, td,  $J$  = 7.4, 1.2, H<sub>c</sub>), 6.85 (1H, dd,  $J$  = 3.5, 1.2, H<sub>3</sub>), 6.83 (1H, td,  $J$  = 7.8, 1.2, H<sub>c'</sub>), 6.75 (1H, td,  $J$  = 7.4, 1.2, H<sub>b</sub>), 6.72 (1H, dd,  $J$  = 2.7, 0.8, H<sub>g'</sub>), 6.72 (1H, dd,  $J$  = 2.7, 0.8, H<sub>g'</sub>), 6.69 – 6.65 (2H, m, H<sub>5, 5'</sub>), 6.64 (1H, td,  $J$  = 7.4, 1.2, H<sub>b'</sub>), 6.55 (1H, t,  $J$  = 2.3, H<sub>f</sub>), 6.52 – 6.49 (2H, m, H<sub>6, 6'</sub>), 6.48 (1H, t,  $J$  = 2.7, H<sub>f'</sub>), 6.39 (1H, bs, H<sub>1</sub>), 6.35 (1H, dd,  $J$  = 7.4, 1.2, H<sub>a</sub>), 6.26 (1H, dd,  $J$  = 7.4, 1.2, H<sub>a'</sub>), 6.17 (1H, dd,  $J$  = 3.5, 1.6, H<sub>2</sub>), 3.66 (1H, s, Me).  $^{13}\text{C}$  NMR: 159.36 (C<sub>4</sub>), 157.34 (C<sub>7</sub>), 145.24 (C<sub>8</sub>), 144.19 (C<sub>h</sub>), 143.91 (C<sub>h</sub>), 142.80 (C<sub>9</sub>), 139.18 (C<sub>i'</sub>), 138.80 (C<sub>g</sub>), 137.89 (C<sub>g'</sub>), 136.73 (C<sub>1</sub>), 134.75 (C<sub>a'</sub>), 133.99 (C<sub>i</sub>), 133.84 (C<sub>a</sub>), 126.03, 125.96, 125.92, 125.88 (C<sub>b</sub>, b', e, e'), 123.75 (C<sub>5, 5'</sub>), 121.74 (C<sub>c</sub>), 121.40 (C<sub>c'</sub>), 118.09 (C<sub>3</sub>), 113.74 (C<sub>6, 6'</sub>), 112.31 (C<sub>2</sub>), 110.98 (C<sub>d</sub>), 110.91 (C<sub>d'</sub>), 107.62 (C<sub>f</sub>), 107.42 (C<sub>f'</sub>), 55.66 (Me). MS (FAB):  $m/z$  678 [M]<sup>+</sup>.



$\delta$  = 7.8, 1.2, H<sub>d</sub>), 7.13 (1H, dd,  $J$  = 7.8, 0.8, H<sub>d'</sub>), 6.94 (1H, td,  $J$  = 7.8, 1.2, H<sub>c</sub>), 6.85 (1H, dd,  $J$  = 3.9, 1.2, H<sub>3</sub>), 6.83 (1H, td,  $J$  = 7.8, 1.6, H<sub>c'</sub>), 6.74 (1H, td,  $J$  = 7.4, 1.2, H<sub>b</sub>), 6.73 (1H, d,  $J$  = 1.9, H<sub>g'</sub>), 6.64 (1H, td,  $J$  = 7.4, 1.2, H<sub>b'</sub>), 6.63 – 6.60 (2H, m, H<sub>5, 5'</sub>), 6.56 (1H, t,  $J$  = 2.7, H<sub>f</sub>), 6.48 (1H, t,  $J$  = 2.7, H<sub>f'</sub>), 6.45 – 6.41 (2H, m, H<sub>6, 6'</sub>), 6.39 (1H, bs, H<sub>1</sub>), 6.35 (1H, dd,  $J$  = 7.4, 1.2, H<sub>a</sub>), 6.26 (1H, dd,  $J$  = 7.4, 1.2, H<sub>a'</sub>), 6.17 (1H, dd,  $J$  = 3.5, 1.6, H<sub>2</sub>), 4.65 (1H, s, H<sub>10</sub>).  $^{13}\text{C}$  NMR: 160.37 (C<sub>4</sub>), 154.27 (C<sub>7</sub>), 146.33 (C<sub>8</sub>), 145.18 (C<sub>h'</sub>), 144.90 (C<sub>h</sub>), 143.74 (C<sub>9</sub>), 140.17 (C<sub>i'</sub>), 139.79 (C<sub>g</sub>), 138.88 (C<sub>g'</sub>), 137.75 (C<sub>1</sub>), 135.74 (C<sub>a'</sub>), 134.97 (C<sub>i</sub>), 134.84 (C<sub>a</sub>), 127.00 (C<sub>b'</sub>), 126.95 (C<sub>e'</sub>), 126.92 (C<sub>e</sub>), 126.87 (C<sub>b</sub>), 124.93 (C<sub>5, 5'</sub>), 122.73 (C<sub>c</sub>), 122.38 (C<sub>c'</sub>), 119.11 (C<sub>3</sub>), 116.20 (C<sub>6, 6'</sub>), 113.29 (C<sub>2</sub>), 111.97 (C<sub>d</sub>), 111.89 (C<sub>d'</sub>), 108.61 (C<sub>f</sub>), 108.42 (C<sub>f'</sub>). MS (FAB):  $m/z$  664 [M]<sup>+</sup>.

### Synthesis of 3.15a(*p*-C<sub>6</sub>H<sub>4</sub>CO<sub>2</sub>Me)

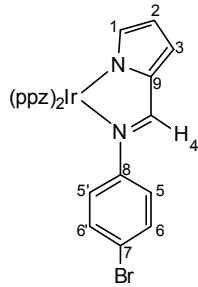
This was prepared from dimer **2.6a** (70 mg, 0.068 mmol), (*E*)-methyl-4-((1H-pyrrol-2-yl)methyleneamino)benzoate (37.4 mg, 0.164 mmol) and DABCO (18.4 mg, 0.164 mmol) and after work up gave **3.15a(*p*-C<sub>6</sub>H<sub>4</sub>CO<sub>2</sub>Me)** as a yellow solid (74 mg, 77%). Anal. Calcd for C<sub>31</sub>H<sub>26</sub>IrN<sub>6</sub>O<sub>2</sub>: C, 52.68, H, 3.71, N, 11.89. Found: C, 52.72, H, 3.71, N, 11.81%.  $^1\text{H}$  NMR (CD<sub>2</sub>Cl<sub>2</sub>):  $\delta$  8.20 (1H, d,  $J$  = 0.8, H<sub>4</sub>), 8.07 (1H, dd,  $J$  = 3.1, 0.8, H<sub>e</sub>), 7.99 (1H, dd,  $J$  = 2.7, 0.8, H<sub>e'</sub>), 7.64 – 7.60 (2H, m, H<sub>6, 6'</sub>), 7.47 (1H, dd,  $J$  = 2.7, 0.8, H<sub>g</sub>), 7.24 (1H, dd,  $J$  = 8.2, 1.2, H<sub>d</sub>), 7.12 (1H, dd,  $J$  = 7.8, 0.8, H<sub>d'</sub>), 6.97 – 6.92 (2H, m, H<sub>3, c</sub>), 6.85 – 6.80 (3H, m, H<sub>5, 5', c'</sub>), 6.77 – 6.73 (2H, m, H<sub>b, g</sub>), 6.66 (1H, td,  $J$  = 7.4, 1.2, H<sub>b'</sub>), 6.55 (1H, t,  $J$  = 2.7, H<sub>f</sub>), 6.48 (1H, t,  $J$  = 2.7, H<sub>f'</sub>), 6.46 (1H, bs, H<sub>1</sub>), 6.34 (1H, dd,  $J$  = 7.4, 1.2, H<sub>a</sub>), 6.27 (1H, dd,  $J$  = 7.4, 1.2, H<sub>a'</sub>), 6.23 (1H, dd,  $J$  = 3.9, 1.5, H<sub>2</sub>), 3.79 (1H, s, Me).  $^{13}\text{C}$  NMR: 166.86 (C<sub>10</sub>), 159.71 (C<sub>4</sub>), 155.67 (C<sub>8</sub>), 144.08 (C<sub>h'</sub>), 143.84 (C<sub>h</sub>), 143.02 (C<sub>9</sub>), 138.92 (C<sub>1</sub>), 138.70 (C<sub>i'</sub>), 138.57 (C<sub>g</sub>), 137.95 (C<sub>g'</sub>), 134.70 (C<sub>a'</sub>), 133.78 (C<sub>a</sub>), 133.14 (C<sub>i</sub>), 130.24 (C<sub>6, 6'</sub>), 126.48 (C<sub>7</sub>), 126.20 (C<sub>b'</sub>), 126.10 (C<sub>b</sub>), 126.02 (C<sub>e</sub>), 125.94 (C<sub>e'</sub>), 122.90 (C<sub>5, 5'</sub>), 121.91 (C<sub>c</sub>), 121.63 (C<sub>c'</sub>), 120.17 (C<sub>3</sub>), 113.55 (C<sub>2</sub>), 111.06 (C<sub>d'</sub>), 111.02 (C<sub>d</sub>), 107.73 (C<sub>f</sub>), 107.50 (C<sub>f'</sub>), 52.16 (Me). MS (FAB):  $m/z$  706 [M]<sup>+</sup>.



### Synthesis of 3.15a(*p*-C<sub>6</sub>H<sub>4</sub>Br)

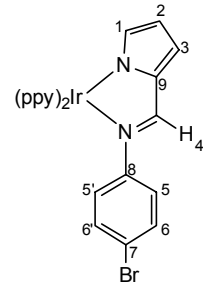
This was prepared from dimer **2.6a** (70 mg, 0.068 mmol), (*E*)-((1H-pyrrol-2-yl)methylene)-4-bromoaniline (40.7 mg, 0.164 mmol) and DABCO (18.4 mg, 0.164 mmol) and after work up gave **3.15a(*p*-C<sub>6</sub>H<sub>4</sub>Br)** as a yellow solid (75 mg, 76%). Anal.

Calcd for  $C_{29}H_{22}BrIrN_6$ : C, 47.93, H, 3.05, N, 11.57. Found: C, 47.80, H, 3.13, N, 11.38%.  $^1H$  NMR ( $CD_2Cl_2$ ):  $\delta$  8.18 (1H, d,  $J$  = 0.8,  $H_4$ ), 8.12 (1H, dd,  $J$  = 2.8, 0.6  $H_e$ ), 8.04 (1H, dd,  $J$  = 2.8, 0.6,  $H_{e'}$ ), 7.49 (1H, dd,  $J$  = 2.2, 0.8,  $H_g$ ), 7.28 (1H, dd,  $J$  = 7.9, 0.8,  $H_d$ ), 7.17 (1H, dd,  $J$  = 7.9, 0.8,  $H_{d'}$ ), 7.14 – 7.11 (2H, m,  $H_{6, 6'}$ ), 6.99 (1H, ddd,  $J$  = 7.3, 1.3, 0.6,  $H_c$ ), 6.96 (1H, dd,  $J$  = 3.9, 1.1,  $H_3$ ), 6.88 (1H, ddd,  $J$  = 7.3, 1.3, 0.6,  $H_{c'}$ ), 6.81 – 6.77 (2H, m,  $H_{b, g}$ ), 6.73 – 6.67 (3H, m,  $H_{5, 5', b'}$ ), 6.60 (1H, dd,  $J$  = 2.8, 2.2,  $H_f$ ), 6.52 (1H, dd,  $J$  = 2.8, 2.2,  $H_{f'}$ ), 6.48 (1H, m,  $H_1$ ), 6.38 (1H, ddd,  $J$  = 7.5, 1.5, 0.4,  $H_a$ ) 6.30 (1H, ddd,  $J$  = 7.5, 1.3, 0.4,  $H_{a'}$ ) 6.24 (1H, dd,  $J$  = 3.9, 1.5,  $H_2$ ).  $^{13}C$  NMR: 159.17 ( $C_4$ ), 150.39 ( $C_8$ ), 143.70 ( $C_{h'}$ ), 143.44 ( $C_h$ ), 142.41 ( $C_9$ ), 138.41 ( $C_{g, i}$ ), 137.51 ( $C_{1, g}$ ), 134.29 ( $C_a$ ), 133.38 ( $C_a$ ), 132.94 ( $C_i$ ), 131.17 ( $C_{6, 6'}$ ), 125.77 ( $C_b$ ), 125.65 ( $C_{e'}$ ), 125.58 ( $C_b$ ), 125.51 ( $C_e$ ), 124.25 ( $C_{5, 5'}$ ), 121.44 ( $C_c$ ), 121.18 ( $C_{c'}$ ), 119.03 ( $C_3$ ), 117.50 ( $C_7$ ), 112.65 ( $C_2$ ), 110.60 ( $C_{d, d'}$ ), 107.27 ( $C_f$ ), 107.05 ( $C_{f'}$ ). MS (FAB):  $m/z$  726 [M]<sup>+</sup>.



### Synthesis of 3.15g(*p*-C<sub>6</sub>H<sub>4</sub>Br)

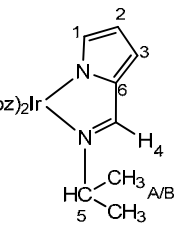
This was prepared from dimer **2.6g** (70 mg, 0.065 mmol), (*E*)-((1H-pyrrol-2-yl)methylene)-4-bromoaniline (38.9 mg, 0.156 mmol) and Na<sub>2</sub>CO<sub>3</sub> (13 mg, 0.131 mmol) and after work up gave **3.15g(*p*-C<sub>6</sub>H<sub>4</sub>Br)** as a yellow solid (70 mg, 72%). Anal. Calcd for C<sub>33</sub>H<sub>24</sub>BrIrN<sub>4</sub>: C, 52.94, H, 3.23, N, 7.48. Found: C, 52.99, H, 3.19, N, 7.31%.  $^1H$  NMR ( $CDCl_3$ ):  $\delta$  8.45 (1H, ddd,  $J$  = 5.9, 1.5, 0.8,  $H_h$ ), 8.23 (1H, d,  $J$  = 0.8,  $H_4$ ), 7.84 (1H, bd,  $J$  = 7.9,  $H_e$ ), 7.71 (1H, bd,  $J$  = 7.9,  $H_{e'}$ ), 7.66 – 7.59 (3H, m,  $H_{d, f, f'}$ ), 7.50 (1H, ddd,  $J$  = 5.9, 1.5, 0.8,  $H_{h'}$ ), 7.45 (1H, dd,  $J$  = 7.7, 1.1,  $H_{d'}$ ), 7.06 – 7.02 (2H, m,  $H_{6, 6'}$ ), 6.99 – 6.89 (4H, m,  $H_{3, c, g, g'}$ ), 7.81 (2H, 2 X td,  $J$  = 7.3, 1.3,  $H_{b, c'}$ ), 6.75 (1H, td,  $J$  = 7.3, 1.3,  $H_b$ ), 6.62 – 6.59 (2H, m,  $H_{5, 5'}$ ), 6.43 (1H, bs,  $H_1$ ), 6.35 (1H, dd,  $J$  = 7.6, 1.2,  $H_a$ ), 6.34 (1H, dd,  $J$  = 7.6, 1.2,  $H_{a'}$ ), 6.27 (1H, dd,  $J$  = 3.7, 1.5,  $H_2$ ).  $^{13}C$  NMR: 169.00 ( $C_{k'}$ ), 168.42 ( $C_k$ ), 158.01 ( $C_4$ ), 157.48 ( $C_{i'}$ ), 151.01 ( $C_i$ ), 150.51 ( $C_h$ ), 149.57 ( $C_8$ ), 149.27 ( $C_{h'}$ ), 144.19 ( $C_{j'}$ ), 144.00 ( $C_j$ ), 141.62 ( $C_9$ ), 137.79 ( $C_1$ ), 136.26 ( $C_f$ ), 135.90 ( $C_{f'}$ ), 132.42 ( $C_a$ ), 131.72 ( $C_a$ ), 131.22 ( $C_{6, 6'}$ ), 129.72 ( $C_{b'}$ ), 129.41 ( $C_b$ ), 124.07 ( $C_{5, 5', d'}$ ), 123.64 ( $C_d$ ), 122.13 ( $C_g$ ), 121.77 ( $C_g$ ), 120.74 ( $C_c$ ), 120.58 ( $C_{c'}$ ), 119.36 ( $C_3$ ), 118.56 ( $C_e$ ), 118.11 ( $C_{e'}$ ), 117.67 ( $C_7$ ), 113.30 ( $C_2$ ). MS (FAB):  $m/z$  748 [M]<sup>+</sup>.



### Synthesis of 3.15a(<sup>i</sup>Pr)

This was prepared from dimer **2.6a** (70 mg, 0.068 mmol), (*E*)-((1H-pyrrol-2-yl)methylene)propan-2-amine (22.3 mg, 0.164 mmol) and Na<sub>2</sub>CO<sub>3</sub> (13 mg, 0.136 mmol) and after work up gave **3.15a(<sup>i</sup>Pr)** as a grey solid (37 mg, 45%). Anal. Calcd for C<sub>26</sub>H<sub>25</sub>IrN<sub>6</sub>:

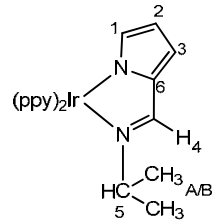
C, 50.8, H, 4.11, N, 13.7. Found: C, 50.87, H, 4.63, N, 13.62%. <sup>1</sup>H NMR (CDCl<sub>3</sub>):  $\delta$  8.11 (1H, s, H<sub>4</sub>), 8.01 (1H, dd, *J* = 2.9, 0.8, H<sub>e</sub>), 7.96 (1H, dd, *J* = 2.9, 0.6, H<sub>e</sub>), 7.45 (1H, d, *J* = 2.1, H<sub>g</sub>), 7.16 (1H, bd, *J* = 7.7, H<sub>d'</sub>), 7.13 (1H, bd, *J* = 7.4, H<sub>d</sub>), 6.89 – 6.82 (2H, m, H<sub>c, c'</sub>) 6.74 – 6.68 (4H, m, H<sub>3, b, b', g'</sub>), 6.50 (1H, dd, *J* = 7.6, 1.2, H<sub>a</sub>), 6.46 (1H, t, *J* = 2.3, H<sub>f</sub>), 6.43 (1H, t, *J* = 2.3, H<sub>f'</sub>), 6.33 (1H, bs, H<sub>1</sub>), 6.29 (1H, dd *J* = 7.3, 1.2, H<sub>a</sub>), 6.11 (1H, dd, *J* = 3.5, 1.8, H<sub>2</sub>), 3.62 (1H, sept, *J* = 6.4, H<sub>5</sub>), 0.93 (3H, d, *J* = 6.4, H<sub>A or B</sub>), 0.71 (3H, d, *J* = 6.7, H<sub>A or B</sub>). <sup>13</sup>C NMR: 158.20 (C<sub>4</sub>), 144.26 (C<sub>h</sub>), 143.37 (C<sub>h</sub>), 141.00 (C<sub>6</sub>), 138.72 (C<sub>g</sub>), 138.54 (C<sub>i</sub>), 137.49 (C<sub>g'</sub>), 135.10 (C<sub>a'</sub>), 134.76 (C<sub>i</sub>), 134.61 (C<sub>1</sub>), 133.30 (C<sub>a</sub>), 125.66, 125.53 (C<sub>b, b'</sub>), 124.98 (C<sub>e, e'</sub>), 121.09 (C<sub>c</sub>), 120.85 (C<sub>c'</sub>), 114.45 (C<sub>3</sub>), 110.31, 110.23 (C<sub>d, d'</sub>), 110.10 (C<sub>2</sub>), 106.95, 106.93 (C<sub>f, f'</sub>), 60.30 (C<sub>5</sub>), 23.41, 22.96 (C<sub>A,B</sub>). MS (FAB): *m/z* 614 [M]<sup>+</sup>.



### Synthesis of 3.15g(<sup>i</sup>Pr)

This was prepared from dimer **2.6g** (70 mg, 0.065 mmol), (*E*)-((1H-pyrrol-2-yl)methylene)propan-2-amine (21.3 mg, 0.156 mmol) and Na<sub>2</sub>CO<sub>3</sub> (13 mg, 0.136 mmol) and after work up gave **3.15g(<sup>i</sup>Pr)** as a yellow solid (66 mg, 80%). Anal. Calcd for

C<sub>30</sub>H<sub>27</sub>IrN<sub>4</sub>: C, 56.67, H, 4.28, N, 8.81. Found: C, 56.53, H, 4.29, N, 8.74%. <sup>1</sup>H NMR (CDCl<sub>3</sub>):  $\delta$  8.42 (1H, bd, *J* = 5.1, H<sub>h</sub>), 8.26 (1H, s, H<sub>4</sub>), 7.84 – 7.80 (2H, m, H<sub>e, e'</sub>), 7.67 – 7.59 (3H, m, H<sub>d', f, f'</sub>), 7.56 (1H, dd, *J* = 7.4, 0.8, H<sub>d</sub>), 7.51 (1H, dd, *J* = 5.8, 0.8, H<sub>h'</sub>), 6.98 (1H, td, *J* = 5.8, 1.6, H<sub>g</sub>), 6.93 (1H, td, *J* = 5.8, 1.6, H<sub>g'</sub>), 6.89 – 6.85 (2H, m, H<sub>c, c'</sub>), 6.81 – 6.73 (3H, m, H<sub>3, b, b'</sub>), 6.49 (1H, dd, *J* = 7.4, 0.8, H<sub>a'</sub>), 6.31 (1H, bs, H<sub>1</sub>), 6.26 (1H, dd, *J* = 7.4, 0.8, H<sub>a</sub>), 6.15 (1H, dd, *J* = 3.5, 1.6, H<sub>2</sub>), 3.64 (1H, sept, *J* = 6.6, H<sub>5</sub>), 0.92 (3H, d, *J* = 6.6, H<sub>A or B</sub>), 0.77 (3H, d, *J* = 6.4, H<sub>A or B</sub>). <sup>13</sup>C NMR: 169.30 (C<sub>k'</sub>), 168.65 (C<sub>k</sub>), 157.93 (C<sub>i'</sub>), 157.38 (C<sub>4</sub>), 152.98 (C<sub>i</sub>), 150.65 (C<sub>h</sub>), 149.67 (C<sub>h'</sub>), 144.71 (C<sub>j'</sub>), 144.02 (C<sub>j</sub>), 140.47 (C<sub>6</sub>), 136.04 (C<sub>f</sub>), 135.67 (C<sub>f</sub>), 134.47 (C<sub>1</sub>), 132.97 (C<sub>a'</sub>), 131.32 (C<sub>a</sub>), 129.43 (C<sub>b'</sub>), 129.25 (C<sub>b</sub>), 123.82 (C<sub>d'</sub>), 123.45 (C<sub>d</sub>), 121.81 (C<sub>g'</sub>), 121.67 (C<sub>g</sub>), 120.44



(C<sub>c</sub>), 120.24 (C<sub>c'</sub>), 118.38 (C<sub>e</sub>), 117.98 (C<sub>e'</sub>), 114.98 (C<sub>3</sub>), 110.75 (C<sub>2</sub>), 58.49 (C<sub>5</sub>), 23.49, 23.40 (C<sub>A,B</sub>). MS (FAB): *m/z* 636 [M]<sup>+</sup>.

### 3.4 Bibliography

1. A. C. G. Hotze, J. A. Faiz, N. Mourtzis, G. I. Pascu, P. R. A. Webber, G. J. Clarkson, K. Yannakopoulou, Z. Pikramenou and M. J. Hannon, *Dalton Trans.*, 2006, 3025-3034.
2. P. G. Bomben, K. C. D. Robson, P. A. Sedach and C. P. Berlinguette, *Inorg. Chem.*, 2009, **48**, 9631-9643.
3. J. D. Slinker, A. A. Gorodetsky, M. S. Lowry, J. J. Wang, S. Parker, R. Rohl, S. Bernhard and G. G. Malliaras, *J. Am. Chem. Soc.*, 2004, **126**, 2763-2767.
4. M. Maruyama and Y. Kaizu, *Inorg. Chim. Acta*, 1996, **247**, 155-159.
5. D. Mishra, S. Naskar, B. Adhikary, R. J. Butcher and S. K. Chattopadhyay, *Polyhedron*, 2005, **24**, 201-208.
6. M. K. Nazeeruddin, C. Klein, P. Liska and M. Gratzel, *Coord. Chem. Rev.*, 2005, **249**, 1460-1467.
7. M. Gratzel, *Inorg. Chem.*, 2005, **44**, 6841-6851.
8. S. Ardo and G. J. Meyer, *Chem Soc Rev*, 2009, **38**, 115-164.
9. B. Bozic-Weber, E. C. Constable, C. E. Housecroft, M. Neuburger and J. R. Price, *Dalton Trans.*, 2010, **39**, 3585-3594.
10. L. A. Garcia-Escudero, D. Miguel and J. A. Turiel, *J. Organomet. Chem.*, 2006, **691**, 3434-3444.
11. G. Jaouen, *Bioorganometallics: biomolecules, labelling, medicine*, Wiley-VCH, 2006.
12. R. H. Fish and G. Jaouen, *Organometallics*, 2003, **22**, 2166-2177.
13. E. S. Krider, J. J. Rack, N. L. Frank and T. J. Meade, *Inorg. Chem.*, 2001, **40**, 4002-4009.
14. R. Urban, R. Kramer, S. Mihan, K. Polborn, B. Wagner and W. Beck, *J. Organomet. Chem.*, 1996, **517**, 191-200.
15. K. Severin, R. Bergs and W. Beck, *Angew. Chem., Int. Ed.*, 1998, **37**, 1635-1654.
16. W. W. Wang, B. Spingler and R. Alberto, *Inorg. Chim. Acta*, 2003, **355**, 386-393.
17. C. M. Alvarez, R. Garcia-Rodriguez and D. Miguel, *J. Organomet. Chem.*, 2007, **692**, 5717-5726.
18. R. S. Herrick, I. Wrona, N. McMicken, G. Jones, C. J. Ziegler and J. Shaw, *Journal of Organometallic Chemistry, Second International Symposium on Bio-Organometallic Chemistry - Dedicated to Professor Richard H. Fish on the occasion of his 65th birthday*, 2004, **689**, 4848-4855.
19. R. S. Herrick, K. L. Houde, J. S. McDowell, L. P. Kiczek and G. Bonavia, *J. Organomet. Chem.*, 1999, **589**, 29-37.
20. R. S. Herrick, J. Dupont, I. Wrona, J. Pilloni, M. Beaver, M. Benotti, F. Powers and C. J. Ziegler, *J. Organomet. Chem.*, 2007, **692**, 1226-1233.
21. R. Garcia-Rodriguez and D. Miguel, *Dalton Trans.*, 2006, 1218-1225.
22. R. H. Holm, A. Chakravorty and L. J. Theriot, *Inorg. Chem.*, 1966, **5**, 625-635.
23. D. L. Davies, S. M. A. Donald, O. Al-Duaij, J. Fawcett, C. Little and S. A. Macgregor, *Organometallics*, 2006, **25**, 5976-5978.
24. F.-B. Han, Y.-L. Zhang, X.-L. Sun, B.-G. Li, Y.-H. Guo and Y. Tang, *Organometallics*, 2008, **27**, 1924-1928.

25. C. S. B. Gomes, P. T. Gomes, M. T. Duarte, R. E. Di Paolo, A. n. L. Macanita and M. J. Calhorda, *Inorg. Chem.*, 2009, **48**, 11176-11186.

26. V. V. Grushin and W. J. Marshall, *Adv. Synth. Catal.*, 2004, **346**, 1457-1460.

27. C. M. Alvarez, R. Garcia-Rodriguez and D. Miguel, *Dalton Trans.*, 2007, 3546-3554.

28. P. J. Spellane, R. J. Watts and C. J. Curtis, *Inorg. Chem.*, 1983, **22**, 4060-4062.

29. M. V. Narayana Reddy, G. C. Sekhar Reddy, K. S. Kumar, C. S. Reddy and C. N. Raju, *J. Heterocycl. Chem.*, 2010, **47**, 538-542.

30. I. Zaltsgandler, Y. Leblanc and M. A. Bernstein, *Tetrahedron Lett.*, 1993, **34**, 2441-2444.

31. Q. Zhao, S. Liu, M. Shi, C. Wang, M. Yu, L. Li, F. Li, T. Yi and C. Huang, *Inorg. Chem.*, 2006, **45**, 6152-6160.

32. G. Calogero, G. Giuffrida, S. Serroni, V. Ricevuto and S. Campagna, *Inorg. Chem.*, 1995, **34**, 541-545.

33. S. V. Kukharenko, V. V. Strelets, A. R. Kudinov, A. Z. Kreidlin, M. G. Peterleitner, L. I. Denisovich and M. I. Rybinskaya, *J. Organomet. Chem.*, 1996, **519**, 1-5.

34. K. K. W. Lo, K. Y. Zhang, S. K. Leung and M. C. Tang, *Angew. Chem., Int. Ed.*, 2008, **47**, 2213-2216.

35. B. Beyer, C. Ulbricht, D. Escudero, C. Friebe, A. Winter, L. Gonzalez and U. S. Schubert, *Organometallics*, 2009, **28**, 5478-5488.

36. J. Nishida, H. Echizen, T. Iwata and Y. Yamashita, *Chem. Lett.*, 2005, **34**, 1378-1379.

37. T. Fei, X. Gu, M. Zhang, C. L. Wang, M. Hanif, H. Y. Zhang and Y. G. Ma, *Synth. Met.*, 2009, **159**, 113-118.

38. A. Glidle, A. R. Hillman, K. S. Ryder, E. L. Smith, J. M. Cooper, R. Dalgiesh, R. Cubitt and T. Geue, *Electrochim. Acta*, 2009, **55**, 439-450.

39. A. R. McDonald, D. Mores, C. D. Donega, C. A. van Walree, R. Gebbink, M. Lutz, A. L. Spek, A. Meijerink, G. P. M. van Klink and G. van Koten, *Organometallics*, 2009, **28**, 1082-1092.

40. V. Fernandez-Moreira, F. L. Thorp-Greenwood and M. P. Coogan, *Chem. Commun.*, 2010, **46**, 186-202.

41. K. K. W. Lo, P. K. Lee and J. S. Y. Lau, *Organometallics*, 2008, **27**, 2998-3006.

42. K. Y. Zhang and K. K. W. Lo, *Inorg. Chem.*, 2009, **48**, 6011-6025.

43. J. S. Y. Lau, P. K. Lee, K. H. K. Tsang, C. H. C. Ng, Y. W. Lam, S. H. Cheng and K. K. W. Lo, *Inorg. Chem.*, 2009, **48**, 708-718.

44. A. J. Amoroso, M. P. Coogan, J. E. Dunne, V. Fernandez-Moreira, J. B. Hess, A. J. Hayes, D. Lloyd, C. Millet, S. J. A. Pope and C. Williams, *Chem. Commun.*, 2007, 3066-3068.

45. A. K. Renfrew, A. D. Phillips, A. E. Egger, C. G. Hartinger, S. S. Bosquain, A. A. Nazarov, B. K. Keppler, L. Gonsalvi, M. Peruzzini and P. J. Dyson, *Organometallics*, 2009, **28**, 1165-1172.

46. A. K. Renfrew, A. D. Phillips, E. Tapavicza, R. Scopelliti, U. Rothlisberger and P. J. Dyson, *Organometallics*, 2009, **28**, 5061-5071.

## **Chapter Four:**

### **Bis-cyclometallated Ir(III) complexes for use as Oxometallate Sensors**

## Chapter 4 Bis-cyclometallated Ir(III) complexes for use as Oxometallate Sensors

### 4.1 Introduction

A molecular sensor has to incorporate a recognition site for an analyte and a responsive portion producing a measurable output (Fig. 4.1). Luminescence is often used as an output as it is very sensitive and has been widely investigated in sensors and in imaging through fluorescence microscopy. As discussed in **Chapter 1** transition metal complexes have received much attention as lumophores. Applications of luminescent transition metal complexes as sensors for oxygen,<sup>1, 2</sup> protons,<sup>3-5</sup> metal ions,<sup>6-10</sup> anions,<sup>11, 12</sup> and chemosensors<sup>13, 14</sup> have been reported and a number of comprehensive reviews are available in this context.<sup>15-17</sup> Some of these applications are discussed below:

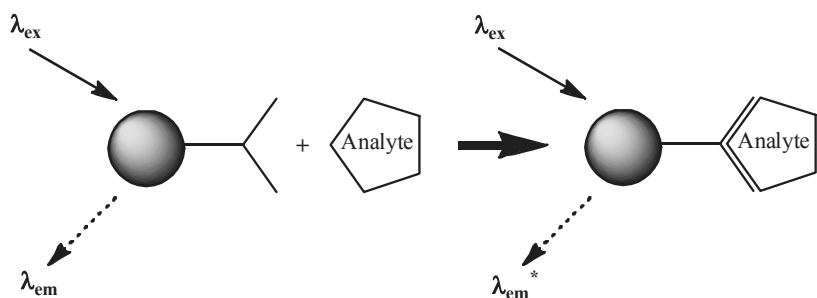
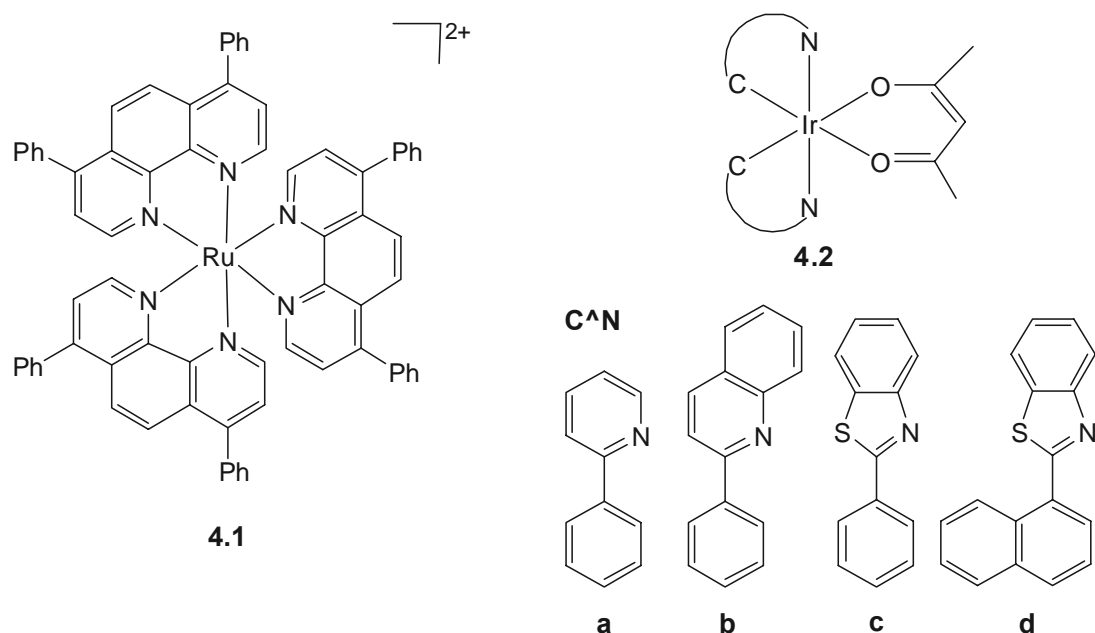


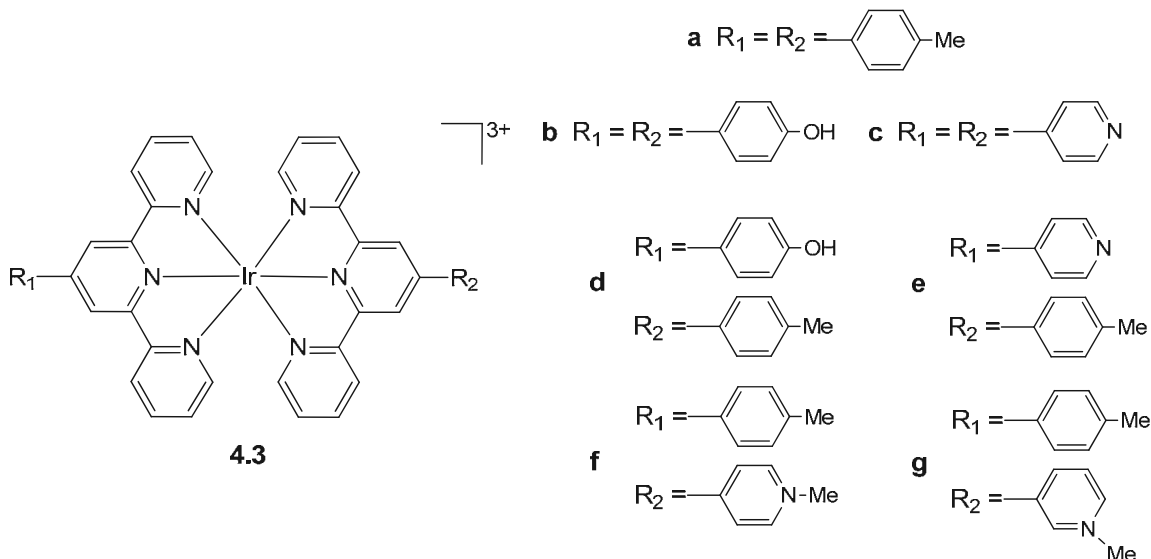
**Fig. 4.1:** Schematic representation of a molecular sensor.

A variety of transition metal based oxygen sensors have been developed of which, the most studied are Ru(II) polypyridyl complexes, particularly **4.1**.<sup>18, 19</sup> However, these probes have certain limitations such as low quantum yields, short emissive lifetimes and sensitivity to temperature. In 1977, J. N. Demas *et al.* published the first examples of Ir(III) complexes *i.e.*  $[\text{Ir}(\text{bipy})]^{3+}$  and  $[\text{Ir}(\text{phen})]^{3+}$  as oxygen sensors.<sup>20</sup> From then until now, a variety of Ir(III) complexes have been synthesised and studied as oxygen sensors.<sup>21-25</sup> The long lived triplet excited state of luminescent cyclometallated Ir(III) complexes enables efficient energy transfer to the triplet ground state of molecular oxygen, resulting in luminescence quenching and the formation of singlet oxygen.<sup>22</sup> In degassed samples, there is no intermolecular energy transfer to oxygen, hence no quenching in emission intensity is observed, thus, these complexes can be used as potential oxygen sensors. In 2007, Thompson *et al.* showed that

complexes **4.2** are efficient singlet oxygen sensitizers and could therefore in principle be used as oxygen sensors.<sup>26</sup>

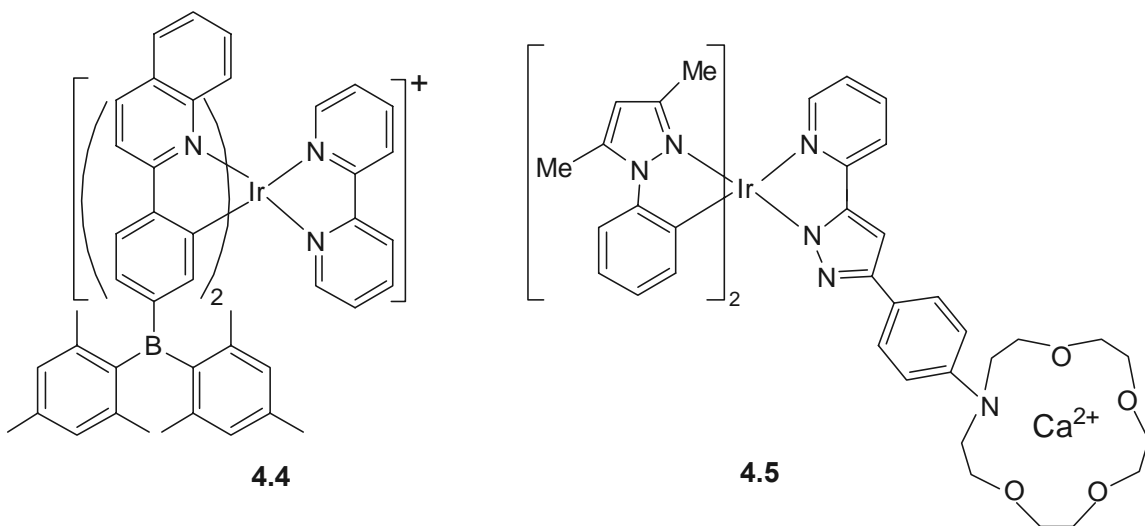


Luminescent molecules which can detect protons in aqueous solution can be used as pH sensors and pH sensors incorporating a  $[\text{Ru}(\text{bipy})_3]^{2+}$  reporter have been described in the literature.<sup>4</sup> A range of derivatives of  $[\text{Ru}(\text{bipy})_3]^{2+}$  bearing pyridyl and phenolic substituents show pH sensitive MLCT emission.<sup>5</sup> Licini and Williams have reported Ir(III) bis-terpyridine complexes **4.3a-e** incorporating pendant pyridyl and phenolic groups which can be protonated and deprotonated respectively and, hence can be used as pH sensors.<sup>3</sup> The changes in lifetime as well as intensity can be used to characterise the pH dependence. Complex **4.3e** showed pronounced pH sensitivity, hence, the emission intensity (at 507 nm) was reduced by *ca.* 8-fold on lowering the pH from 7 to 2, similarly the lifetime was reduced by a comparable factor from 4.7  $\mu\text{s}$  at pH 7 to 0.48  $\mu\text{s}$  at pH 2. Protonation of the pyridyl nitrogen lowers the energy of MLCT excited state, which leads to mixing with the emissive LC state and hence shortens the lifetimes and reduces the intensities.



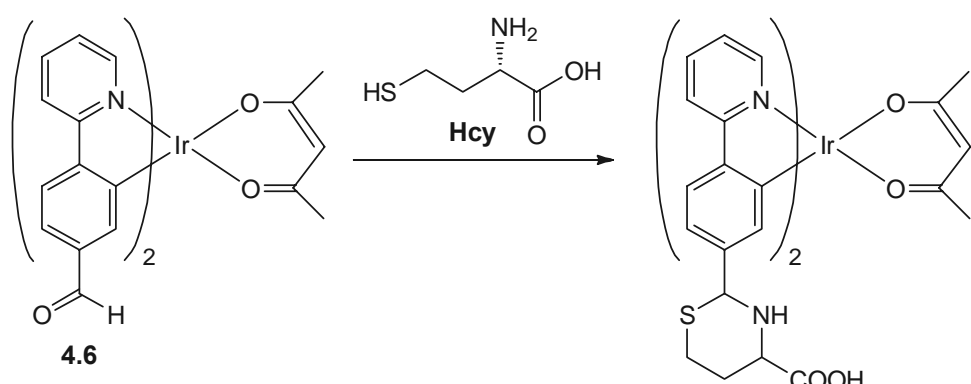
Recognition of anions is an interesting area of research because of the important roles of anions in industrial and biological processes and environmental sciences. Chloride is one of the most important ions present in the human body; it occurs both in intra-cellular (5-75 mM) and extra-cellular (100 mM) compartments of the cell and helps to maintain the osmotic pressure in the cell. Goodall and Williams reported two Ir bis-terpyridine complexes (**4.3f,g**) the emission of which are sensitive to chloride concentration.<sup>27</sup> At room temperature, aqueous solutions of both **4.3f** and **4.3g** showed intense emission at 510 nm. Addition of aqueous KCl solution led to reduction in lifetime and partial quenching of the emission for both complexes. Complex **4.3g** exhibits luminescence which is sensitive to  $\text{Cl}^-$  ion at physiologically relevant concentrations *i.e.* (34 mmol dm<sup>-3</sup>), hence, **4.3g** can be used as a potential sensory system for chloride. The site of interaction of the  $\text{Cl}^-$  ion with the complexes was expected to be the N-methylpyridinium substituent since the emission from **4.3f,g** is sensitive to  $\text{Cl}^-$  ion, whereas that of **4.3a** is not.

Zhao *et al.* reported an Ir(III) complex (**4.4**) containing bismesitylboryl groups on the cyclometallated ligands, which can act as highly selective chemosensor for fluoride ions detectable by the naked eye.<sup>28</sup> The addition of  $\text{F}^-$  ions to **4.4** induces an evident change in the solution colour from yellow to orange-red. The red shift in emission can be attributed to the switching of the excited state from LC  $\pi-\pi^*$  to CT transitions.



Chou *et al.* prepared Ir(III) complex (**4.5**) with an azacrown receptor which selectively binds to  $\text{Ca}^{2+}$  ions and that leads to a measurable and reversible change in the emission.<sup>6</sup> After addition of  $\text{Ca}^{2+}$  ions, the emission spectrum shows a blue shift (from 560 to 520 nm) accompanied by an increase of the emission intensity.

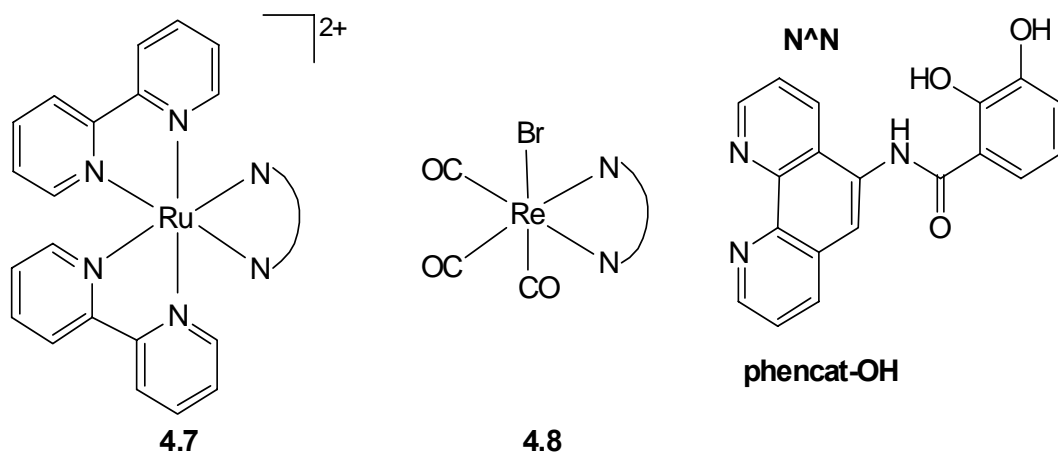
Homocysteine (Hcy) is an amino acid containing a free thiol moiety, hence, has an important role in human physiology, *e.g.* elevated levels of Hcy in blood plasma (about 6  $\mu\text{mol/L}$ ) are risk factors for thrombosis and cardiovascular diseases. Direct detection of this molecule is often hampered by the presence of other structurally-related molecules such as cysteine (Cys) or glutathione (GSH), and thus Hcy analyses are performed in conjunction with chromatographic separations or immunoassays. In 2007, Huang and co-workers reported complex **4.6** with aldehyde groups on ppy, which react selectively with Hcy to form a six-membered thiazinane ring (**Scheme 4.1**), and



### Scheme 4.1

do not react with Cys or GHS.<sup>13</sup> Upon reaction with Hcy, the observed emission wavelength changes from 615 nm (red) to 525 nm (green), with a large enhancement in emission intensity.

Metal ions in high oxidation states can form oxometalate anions in aqueous media. Environmental monitoring of molybdate is important as excessive soil molybdate causes molybdenosis in ruminants.<sup>29</sup> Medical analysis is of interest as deficiency of Mo cofactor causes neurological disorders.<sup>30</sup> Despite their importance, as yet, there are no luminescent chemosensors for oxometalates on the market though the area has recently been reviewed.<sup>31</sup> In 2007, Duhme-Klair *et al.* reported Ru(II) (**4.7**) and Re(I) (**4.8**) complexes, which proved to be highly selective sensors for molybdate, tungstate and vanadate.<sup>32</sup> The sensor system was based on two components which form discrete subunits of the same molecule, a) specific chelating units for binding to oxometalates and, b) components capable of signalling the binding by changes in the intensity of emission.<sup>33</sup> The subunits communicate with each other by photo-induced electron or energy transfer. Both complexes (**4.7** and **4.8**) signal the presence of molybdate and vanadate in aqueous acetonitrile through a decrease of emission intensity, complex **4.8** also detects tungstate. The addition of 0.5 equivalents of oxometalates to solutions of complexes **4.7** and **4.8** in acidic pH (1 to 4) result in the decrease of emission intensity. The decrease in emission intensity is attributed to the deprotonation of the catechol units upon metal ion coordination.

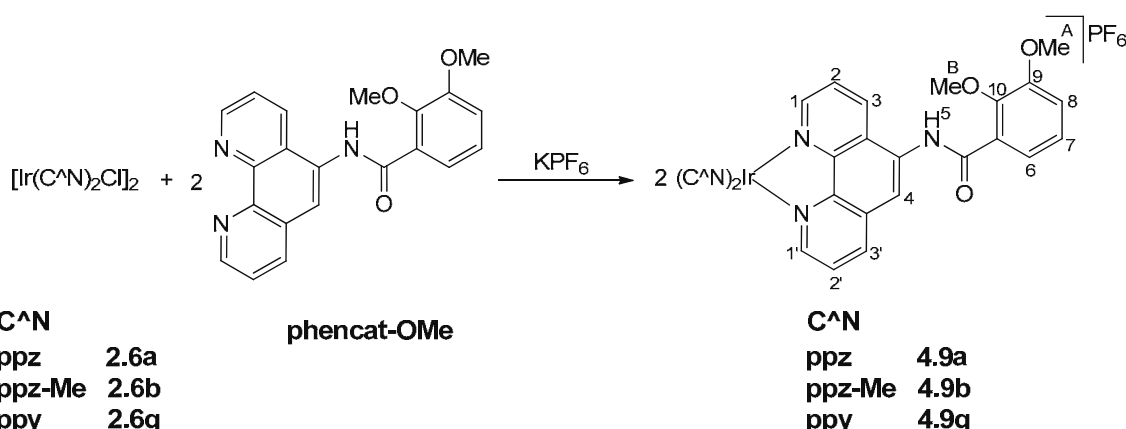


This **Chapter** will investigate the synthesis and characterisation of  $[\text{Ir}(\text{C}^{\wedge}\text{N})_2(\text{X}^{\wedge}\text{Y})]^+$  ( $\text{X}^{\wedge}\text{Y}$  = **phencat-OH**) complexes, which will be further tested as molybdate and pH sensors.

## 4.2 Results and Discussion

### 4.2.1 Synthesis and Characterisation

As discussed above, Duhme-Klair *et al.* synthesised some Ru(II) and Re(I) complexes of a phenacet-OH ligand, which are luminescent sensors for oxometalates particularly for molybdates and vanadates. Hence, we have synthesised cyclometallated Ir(III) complexes of the same ligand in order to compare their applicability as molybdate sensors.



**Scheme 4.2**

We started with the same approach as for the Ru(II) **4.7** and Re(I) **4.8** complexes *i.e.* complexation of the protected ligand (OMe in place of OH) and then deprotection of methoxy groups using BBr<sub>3</sub>. The ligand phenacet-OMe was prepared by the literature method.<sup>32</sup> The dimers **2.6a,b,g** react with phenacet-OMe and KPF<sub>6</sub> at 60 °C under microwave irradiation for 20 mins to form compounds **4.9a,b,g** as yellow solids with yields of greater than 90% (**Scheme 4.2**).

The <sup>1</sup>H and <sup>13</sup>C NMR spectra of **4.9a,b,g** are very complicated due to the lack of C<sub>2</sub>-symmetry (see **Chapter 3**) hence the assignment of **4.9a** is described in detail. In complex **4.9a**, there are two pyrazole, three phenyl and two pyridine ring systems, giving in principle, 31 inequivalent protons. However, the <sup>1</sup>H NMR spectrum shows only seventeen different signals suggesting that there is a lot of accidental overlap. The most downfield signal in the <sup>1</sup>H NMR spectrum is a singlet at δ 10.84 assigned to the amide proton H<sub>5</sub> (confirmed by no cross peak in the HSQC <sup>1</sup>H-<sup>13</sup>C) and H<sub>4</sub> is easily identified as the only other singlet at δ 9.02. H<sub>4</sub> shows an NOE to a doublet of doublets

at  $\delta$  8.69 which is therefore assigned as  $H_{3'}$  and the COSY spectrum then allows assignment of  $H_{1'}$  and  $H_{2'}$ . Similarly,  $H_5$  shows a strong NOE to a doublet of doublets at  $\delta$  8.77 which is therefore assigned as  $H_3$  and both  $H_1$  and  $H_2$  are assigned *via* the COSY spectrum. In the free ligand (phencat-OMe), the signals for  $H_{1,1'}$  are found at  $\delta$  9.16 and 9.04 respectively, but on co-ordination they shift to high field ( $\delta$  8.53 and *ca.* 8.3, respectively) due to ring current effects from the neighbouring cyclometallated phenyls.  $H_1$  shows an NOE to phenyl and pyrazole protons  $H_a$  and  $H_g$  respectively, similarly  $H_{a'}$  and  $H_g$  both show NOEs to  $H_1$  which then allows assignment of all the other protons of the phenyl ( $H_{a,a'-d,d'}$ ) and pyrazole ( $H_{e,e'-g,g'}$ ) rings using the COSY spectrum. The protons  $H_{a,a'}$  are observed as overlapping doublet of doublets at high field ( $\delta$  6.42 and  $\delta$  6.41 respectively) characteristic of the  $[\text{Ir}(\text{C}^{\text{N}})^2]$  fragment, as discussed in **Chapters 2** and **3**. The phenyl protons give rise to four signals which integrate to two protons each. Presumably, the asymmetry of the phencat-OMe ligand is too far away to make the phenyl groups sufficiently different to resolve. Similarly, the pyrazole groups are difficult to resolve but the signals for  $H_{f,f'}$  are seen as overlapping triplets at  $\delta$  6.51 and  $\delta$  6.50. The expected NOEs are observed between the phenyl protons  $H_{d,d'}$  and pyrazole protons  $H_{e,e'}$ . The remaining three protons of the phencat-OMe give rise to a doublet of doublets at  $\delta$  7.73 assigned to  $H_6$  which couples to protons  $H_7$  and  $H_8$  which are observed as overlapping multiplets at  $\delta$  7.36–7.30. The two OMe groups give rise to singlets at  $\delta$  3.98 and  $\delta$  4.11 assigned to  $\text{Me}_A$  and  $\text{Me}_B$  respectively due to NOEs to  $H_8$  and  $H_5$  respectively. The chemical shift of the amide proton  $H_5$  ( $\delta$  10.84) is consistent with an intramolecular hydrogen bond between the amide N—H and the adjacent O atom of 2,3-dimethoxybenzamide (**Fig. 4.2**) which is consistent with the literature.<sup>32</sup>

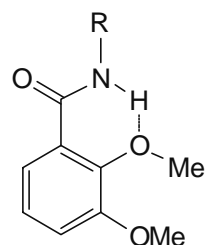


**Fig. 4.2:** Intramolecular hydrogen bond in 2,3-dimethoxybenzamide.

The  $^{13}\text{C}-\{^1\text{H}\}$  NMR spectra of **4.9a** show the expected signals though there is some overlap between signals of related groups. The FAB mass spectrum shows an ion at  $m/z$  838 due to the cation  $[\text{Ir}(\text{ppz})_2(\text{phencat-OMe})]^+$  and the microanalysis is satisfactory.

The  $^1\text{H}$  NMR spectrum of **4.9b** is similar to that of **4.9a** except the signals for the phenyl rings of cyclometallated ligand, *i.e.* in **4.9b** one proton on each phenyl has been replaced by a methyl ( $\text{Me}_{\text{C},\text{C}'}$ ), which are observed as coincident singlets at  $\delta$  2.34. The most downfield singlet signals, at  $\delta$  10.82 and  $\delta$  9.03 are assigned to  $\text{H}_5$  and  $\text{H}_4$  respectively. Most of the signals of the two ppz-Me ligands are accidentally equivalent though  $\text{H}_g$  and  $\text{H}_{g'}$  are resolved, giving two doublets at  $\delta$  6.89 and  $\delta$  6.88. The other assignments are made on the same basis as for **4.9a**. Once again protons  $\text{H}_{\text{a},\text{a}'}$  are at high field ( $\delta$  6.41) and these protons also show NOEs to  $\text{H}_1$  and  $\text{H}_{1'}$  respectively. The orientation of the amide is the same as **4.9a** as evidenced by the NOE between the amide proton  $\text{H}_5$ , and one of the OMe groups ( $\text{Me}_\text{B}$ ) at  $\delta$  4.11 and also by the intramolecular hydrogen bond between the amide N—H and the adjacent O atom of the catechol unit in the crystal structure. The  $^{13}\text{C}$ —{ $^1\text{H}$ } NMR spectra of **4.9b** show the expected signals and the FAB mass spectrum shows an ion at  $m/z$  866 due to the cation  $[\text{Ir}(\text{ppz-Me})_2(\text{phencat-OMe})]^+$ .

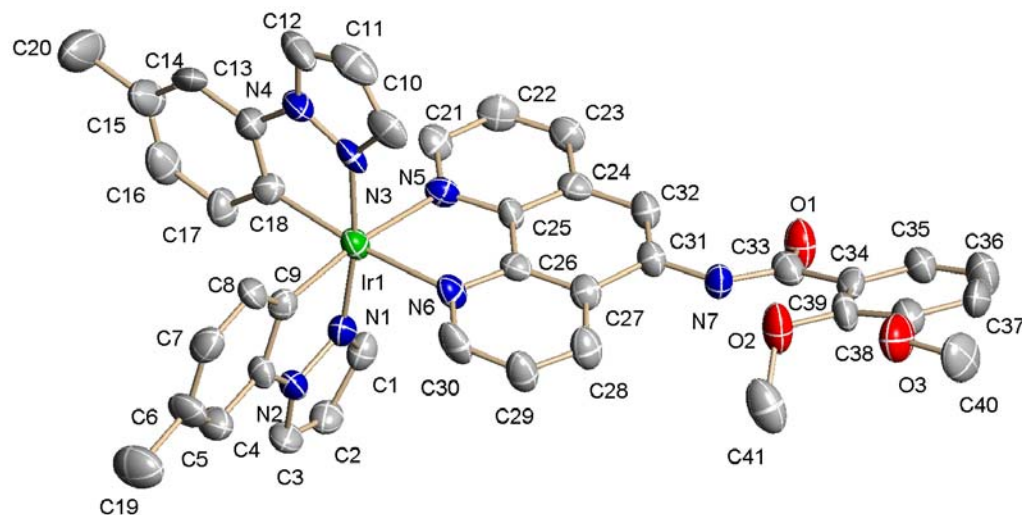


**Fig. 4.3:** X-ray crystal structure of the cation of **4.9b**. Selected bond lengths ( $\text{\AA}$ ) and bond angles ( $^\circ$ ):  $\text{Ir(1)}-\text{N(1)}$ , 2.007(5);  $\text{Ir(1)}-\text{N(3)}$ , 1.997(5);  $\text{Ir(1)}-\text{N(5)}$ , 2.128(4);  $\text{Ir(1)}-\text{N(6)}$ , 2.124(4);  $\text{Ir(1)}-\text{C(9)}$ , 2.005(6);  $\text{Ir(1)}-\text{C(18)}$ , 2.009(6);  $d(\text{N(7)}-\text{O(2)})$ , 2.680;  $\text{N(1)}-\text{Ir(1)}-\text{N(3)}$ , 171.32(19);  $\text{N(1)}-\text{Ir(1)}-\text{C(9)}$ , 80.4(2);  $\text{N(3)}-\text{Ir(1)}-\text{C(18)}$ , 80.1(2);  $\text{N(5)}-\text{Ir(1)}-\text{N(6)}$ , 77.07(18);  $\text{C(31)}-\text{N(7)}-\text{C(33)}$ , 127.8(5);  $\text{N(7)}-\text{C(33)}-\text{O(1)}$ , 122.5(6).

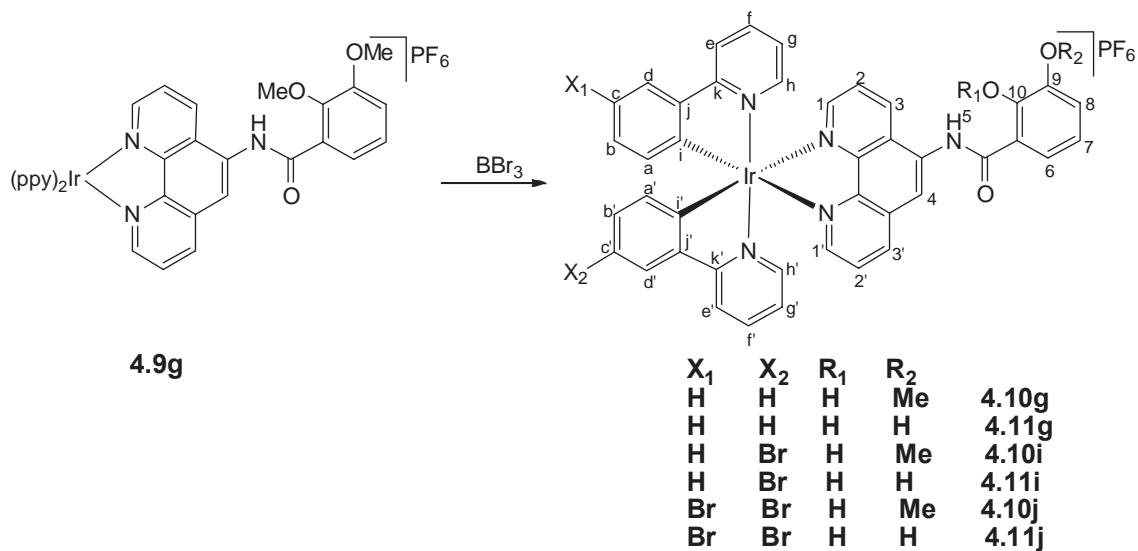
Single crystals of **4.9b** were obtained by slow diffusion of hexane into a concentrated DCM solution of the salt. The crystal structure (**Fig. 4.3**) reveals the

expected six-coordinate Ir(III) centre surrounded by two cyclometallated ligands and one phencat-OMe ligand. The Ir(III) centre adopts a distorted octahedral coordination geometry [N(1)—Ir(1)—N(3) is 171.32°], with *cis* metallated carbons and *trans* nitrogen atoms, as expected for such systems.<sup>34</sup> The catechol unit is held planar by an intramolecular hydrogen bond N—H $\cdots$ O ( $d(\text{N—O}) = 2.680 \text{ \AA}$ ) as discussed above and as observed in similar Re(I) and Ru(II) complexes ( $d(\text{N—O}) = 2.649 \text{ \AA}$  and  $2.641 \text{ \AA}$  respectively).<sup>32</sup> Selected bond lengths ( $\text{\AA}$ ) and angles (°) are shown in **Fig. 4.3**.

The  $^1\text{H}$  NMR spectrum of **4.9g** is similar to that of **4.9a**, many of the signals for the two ppy ligands overlap. The amide proton  $H_5$  is the most downfield signal, at  $\delta$  10.81, with the other singlet at  $\delta$  9.03 being assigned to  $H_4$  whilst protons  $H_{a,a'}$  are observed as doublet of doublets at characteristically high field ( $\delta$  6.40, 6.39). The  $^{13}\text{C}$ —{ $^1\text{H}$ } NMR spectra show the expected signals, and the FAB mass spectrum shows an ion at  $m/z$  860 due to  $[\text{Ir}(\text{ppy})_2(\text{phencat-OMe})]^+$ .

As mentioned earlier, the second step for the synthesis of molybdate sensor was deprotection of the methoxy groups using  $\text{BBr}_3$ . Following the literature method, complex **4.9g** was reacted with a 10-fold molar excess of  $\text{BBr}_3$  in DCM at -78 °C. **Scheme 4.3.** Monitoring by ES-MS showed that deprotection of the first methyl occurred within one hour (**4.10g**), however, deprotection of the second methyl (**4.11g**) was much slower requiring several days at room temperature (RT) and a large excess of  $\text{BBr}_3$  to go to completion, which suggests one OMe is perhaps less basic than the other as found previously.<sup>32</sup> Unfortunately, a more important problem is that bromination of one of the cyclometallated phenyls starts to occur over a period of a few days (as evidenced by peaks *ca* 80 daltons higher showing a correct isotope pattern for substitution of one hydrogen by bromine *i.e.* **4.10i** and **4.11i**). Note, a direct bromination of the phenyl ring at the *para* positon with respect to the metal in  $[\text{Ir}(\text{ppy})_2(\text{Cl})]_2$  dimer has been reported using pyridinium tribromide.<sup>35</sup> Unfortunately it was not possible to separate out a pure component from these mixtures. Similar reactions were tried with **4.9a** and **4.9b** but those also ended up in an inseparable mixture of products and bromination was evident in the ES-MS for both of the complexes. Bromination in **4.9b** suggests that there may be another site of bromination on the ppz other than the *para* position on the phenyl ring relative to the metal; however, this could not be identified, as the NMR showed very broad peaks.

Iodotrimethylsilane was also tried as a deprotecting reagent for **4.9g** instead of  $\text{BBr}_3$  however this only gave the mono deprotected product as judged by ES-MS.



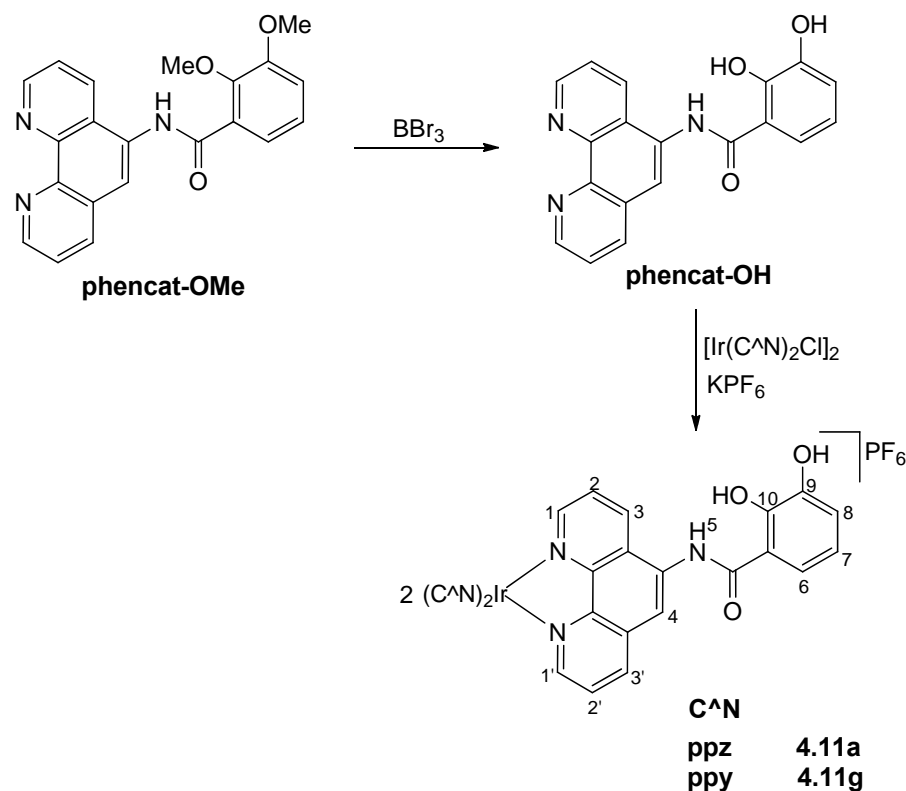
**Scheme 4.3**

Note out of all possible products shown in the scheme, only **4.11j** could be isolated and fully characterised, however all others were observed in the ES-MS. **4.11g** was synthesised from another method discussed later.

In an attempt to isolate one product from **4.9g**, a prolonged reaction with a large excess (28 equiv) of  $\text{BBr}_3$  was attempted to try and force conversion to the dibrominated product **4.11j**. The  $^1\text{H}$  and  $^{13}\text{C}$  NMR spectra of **4.11j** are similar to the protected complex **4.9g**. However, the  $^1\text{H}$  NMR spectrum of **4.11j** shows no signals for OMe groups showing that the deprotection has been successful. In addition there are only three signals for each cyclometallated phenyl, doublets for  $\text{H}_{\text{a}/\text{a}'}$  and  $\text{H}_{\text{d}/\text{d}'}$  and doublet of doublets for  $\text{H}_{\text{b}/\text{b}'}$  consistent with bromination on both phenyl rings *para* to the metal. The other signals are similar to **4.9a** (see experimental for details). The  $^{13}\text{C}$ – $\{^1\text{H}\}$  NMR spectra of **4.11j** show the expected signals though there is some overlap between signals of related groups. The FAB mass spectrum shows an ion at  $m/z$  990 with the appropriate isotope pattern due to the cation  $[\text{Ir}(\text{ppy-Br})_2(\text{phenCat-OH})]^+$  and the microanalysis is satisfactory, confirming the dibromination in **4.11j**.

Since deprotection of the complexed ligand was complicated by simultaneous bromination of the cyclometallated phenyl(s), the alternative approach of deprotecting the ligand and then complexation to the metal was attempted. The ligand phenCat-OMe was deprotected to phenCat-OH using  $\text{BBr}_3$ . Owing to the insolubility of phenCat-OH in any organic solvents or in water, it was purified by washing successively with MeOH,

DCM and diethylether, and was then reacted with the corresponding dimers *i.e.* **2.6a** and **2.6g** under microwave irradiation for 2 hrs at 70 °C to give **4.11a** and **4.11g** respectively in high yields (~ 80%) (**Scheme 4.4**).



**Scheme 4.4**

The  $^1\text{H}$  and  $^{13}\text{C}$  NMR spectra of **4.11a** and **4.11g** are similar to **4.9a** and **4.9g** respectively, except the signals due to the phenacet-ligands. The amide proton  $\text{H}_5$  is not observed for either complex, probably due to exchange with the solvent ( $\text{MeOD}$ ). The only singlet is therefore assigned to  $\text{H}_4$  ( $\delta$  8.81 and 8.87 for **4.11a** and **4.11g** respectively) which shows an NOE to  $\text{H}_{3'}$ . The catechol protons  $\text{H}_{6-8}$  are identified using the HMBC spectra as proton  $\text{H}_6$  show a cross peak to  $\text{C}_{10}$  and proton  $\text{H}_7$  show a cross peak to  $\text{C}_9$  respectively in each case. The other assignments are made on the same basis as for **4.9a**. The protons of the cyclometallated rings ( $\text{H}_{\text{a-g/h}}$  and  $\text{H}_{\text{a'-g'/h'}}$ ) are accidentally equivalent though some of them were able to resolve. Protons  $\text{H}_{\text{a,a'}}$  are again at high field and show NOEs to  $\text{H}_1$  and  $\text{H}_{1'}$  respectively. The  $^{13}\text{C}-\{^1\text{H}\}$  NMR spectra show the expected signals and the FAB mass spectra show peaks for  $[\text{Ir}(\text{C}\equiv\text{N})_2(\text{phenacet-OH})]^+$  ions at  $m/z$  810 and 832 for **4.11a** and **4.11g** respectively.

In conclusion, both the protected and the deprotected complexes (**4.9** and **4.11** respectively) have been easily synthesised using microwave heating. For complexes **4.11** deprotection of the ligand had to be done before complexation to the metal in contrast to the related Ru(II) and Re(I) complexes.<sup>32</sup> The crystal structure of **4.9b** demonstrates the presence of an intramolecular hydrogen bond between the amide N—H and the adjacent O atom of 2,3-dimethoxybenzamide. This is consistent with the NMR data and also with the literature for similar complexes of Re(I) and Ru(II).<sup>32</sup> The photophysical properties and use of these complexes for molybdate sensing are discussed in the following sections. The absorption and molybdate sensing experiments were carried out by Anne-K. Duhme-Klair and co-workers at the University of York.

#### 4.2.2 Photophysical properties of $[\text{Ir}(\text{C}^{\wedge}\text{N})_2(\text{phencat-OMe})]^+$ (**4.9**) and $[\text{Ir}(\text{C}^{\wedge}\text{N})_2(\text{phencat-OH})]^+$ (**4.11**) complexes.

The electronic absorption spectral data of the methyl protected **4.9a,b,g** and deprotected **4.11a,g,j** complexes are summarised in **Table 4.1**. They agree well with the data for  $[\text{Ir}(\text{C}^{\wedge}\text{N})_2(\text{bipy})]^+$  **2.7a,g** discussed in **Chapter 2**. By comparison with the reported spectra of  $[\text{Ir}(\text{C}^{\wedge}\text{N})_2(\text{bipy})]^+$ , the highest energy bands below 280 nm can be assigned to the spin allowed intraligand IL ( $\pi \rightarrow \pi^*$  ( $\text{C}^{\wedge}\text{N}$  and  $\text{X}^{\wedge}\text{Y}$ )) transitions and the moderately intense absorption bands between 280 to 390 nm can be attributed to a  $d\pi(\text{Ir}) \rightarrow \pi^*$  ( $\text{C}^{\wedge}\text{N}$  and  $\text{X}^{\wedge}\text{Y}$ ) charge transfer ( $^1\text{MLCT}$ ) transition. The weak absorption bands towards the lower energy region, *ca.* > 390 nm are tentatively assigned to the spin forbidden  $^3\text{MLCT}$  [ $d\pi(\text{Ir}) \rightarrow \pi^*$  ( $\text{C}^{\wedge}\text{N}$  and  $\text{X}^{\wedge}\text{Y}$ )] transitions.

**Table 4.1:** Electronic absorption spectral data of  $[\text{Ir}(\text{C}^{\wedge}\text{N})_2(\text{phencat-OMe})]^+$  (**4.9**) and  $[\text{Ir}(\text{C}^{\wedge}\text{N})_2(\text{phencat-OH})]^+$  (**4.10**) complexes.

Entry	Complex	Solvent	$\lambda_{\text{abs}} \text{ [nm]} (\epsilon_{\text{max}} \text{ [dm}^3\text{mol}^{-1}\text{cm}^{-1}] )$
1	<b>4.9a</b>	MeCN	274 (55000), 320 (26100), 386 sh (6200), 433 sh (3200)
2	<b>4.9b</b>	MeCN	249 (48700), 277 sh (39300), 323 (18070), 395 sh (2670)
3	<b>4.9g</b>	MeCN	253 (56800), 326 (19600), 376 sh (8300), 468 sh (1400)
4	<b>4.11a</b>	MeCN	253(21330), 264 sh (20500), 326 (7860), 403 sh (2790)
5	<b>4.11g</b>	MeCN	254 (50400), 267 sh(49150), 332 (17800), 381 sh (10150), 415 sh (6050)
6	<b>4.11j</b>	MeCN	254 (20960), 335 (6220), 405 sh (2730)

The absorption spectra of the protected complexes **4.9a,g** are pH independent (between pH 0.1 and 11), however, those of the deprotected ones **4.11a,g,j** show an increase in intensity with increase in pH, as shown for **4.11a** in **Fig. 4.4**. This is consistent with the Ru(II) and Re(I) complexes of the same ligand.<sup>32</sup> Due to the limited water solubility of the complexes, a mixed solvent system consisting of acetonitrile and water (20:1) was used. The absorption spectra of 2,3-dihydroxybenzamides generally show an increase in absorbance at 365 nm upon deprotonation of the *ortho* OH group of the catecholamide unit,<sup>36,37</sup> hence, the increase in absorbance of **4.11a,g,j** with pH is attributed to the deprotonation of the same OH group in the catechol unit of phenacet-OH ligand.

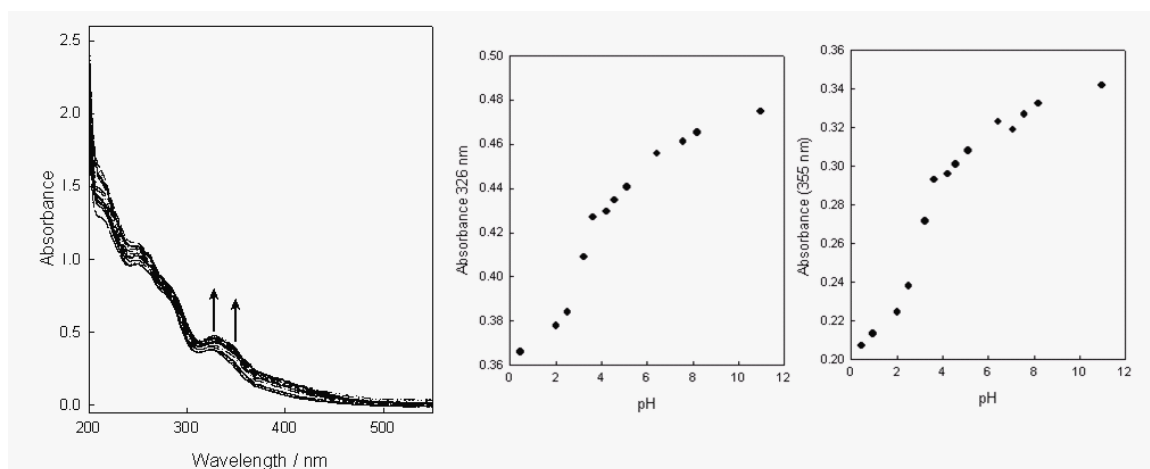


**Fig. 4.4:** Left: Absorption spectra recorded during the titrations of acidic solutions of **4.11a** (0.02 mM) in acetonitrile:water (20:1) with an aqueous tetramethyl ammonium hydroxide solution. Right: Plot of the absorbance at 326 nm and 355 nm as a function of pH.

Upon excitation both the protected and deprotected complexes **4.9** and **4.11** respectively show emission in acetonitrile and the data are tabulated in **Table 4.2**. The emission of complex **4.9a** is solvent sensitive, a red shift (10 nm) is observed upon increasing the polarity of the solvent from DCM to acetonitrile/MeOH, which is consistent with a charge transfer component in the emissive state. Each of the deprotected complexes **4.11a,g,j** also shows a red shift in emission upon changing the solvent from acetonitrile to a mixture of acetonitrile:water (20:1). For complexes **4.11a,g,j**, the emission was also investigated between pH 0.1 and 10 in a mixed solvent system of acetonitrile:water (20:1). Complexes **4.11a** and **4.11j** show only one emission band, however, complex **4.11g** shows two emission bands at 445 and 610 nm

**Table 4.2:** Emission data of  $[\text{Ir}(\text{C}^{\wedge}\text{N})_2(\text{phencat-OMe})]^+$  (**4.9**) and  $[\text{Ir}(\text{C}^{\wedge}\text{N})_2(\text{phencat-OH})]^+$  (**4.11**) complexes.

Entry	Complex	Solvent	$\lambda_{\text{em}}(\text{nm})$	Energy (eV)
1	<b>4.9a</b>	MeCN	570	2.17
2	<b>4.9a</b>	DCM	560	2.21
3	<b>4.9a</b>	MeOH	570	2.17
4	<b>4.9b</b>	MeCN	600	2.06
5	<b>4.9g</b>	MeCN	590	2.10
6	<b>4.11a</b>	MeCN	575	2.15
7	<b>4.11a</b>	MeCN:H <sub>2</sub> O	597	2.07
8	<b>4.11g</b>	MeCN	590	2.10
9	<b>4.11g</b>	MeCN:H <sub>2</sub> O	445, 610	2.77, 2.03
10	<b>4.11j</b>	MeCN	575	2.15
11	<b>4.11j</b>	MeCN:H <sub>2</sub> O	588	2.10

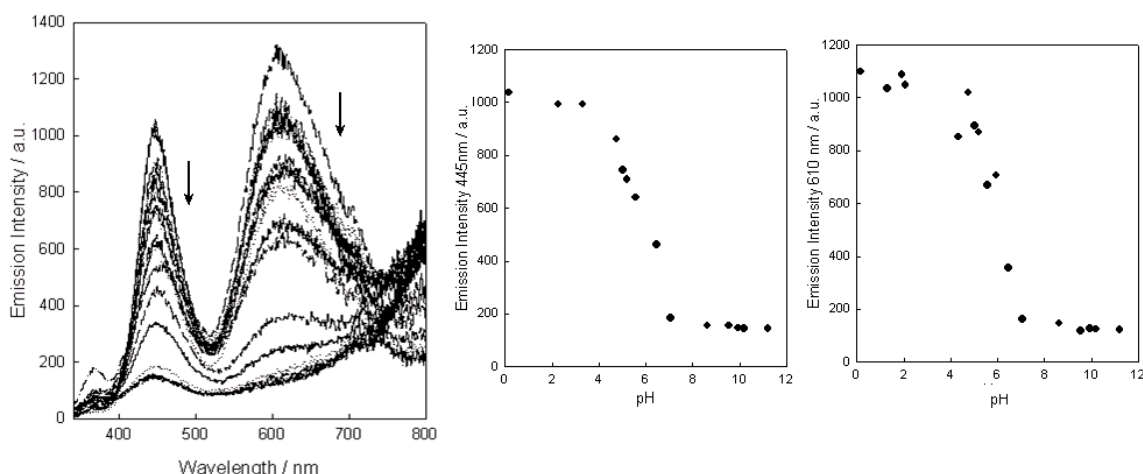


**Fig. 4.5:** Left: Emission spectrum recorded during the titrations of acidic solution of **4.11g** (0.04 mM) in aqueous acetonitrile with an aqueous tetramethyl ammonium hydroxide solution. Right: Emission intensity at maximum 445 and 610 nm vs pH for **4.11g**.

(**Fig. 4.5**). The intensity of the emission decreases sigmoidally with increasing pH for each complex (as shown for **4.11g** in **Fig. 4.5**) which is attributed to the deprotonation of the catechol unit. This assertion is further supported by the observation that the emission intensity of the protected complexes (**4.9a,g**) is pH independent. In addition, emission quenching upon deprotonation of phenolic OH groups was reported for similar systems.<sup>38, 39</sup> As a result of the pH sensitivity of these complexes, (**4.11a,g,j**) can in principle be used as pH sensors.

### 4.2.3 Molybdate sensing

The addition of 0.5 equiv of molybdate to solutions of each deprotected complex **4.11a,g,j** resulted in a decrease of the emission intensity in the acidic pH range *i.e.* up to 3.6 for **4.11a** and 6.5 for **4.11g** and **4.11j**. The effect of addition of molybdate on emission intensity of **4.11j** both in acidic and basic pH range is shown in **Fig. 4.6**. The decrease in emission intensity of the complexes **4.11a,g,j** is proportional to the concentration of molybdate, consequently, these can be used as molybdate sensors. The decrease in the emission intensity in the presence of the molybdate is due to deprotonation of the catechol units upon metal-ion coordination. The observation that the emission intensity of the methyl protected complexes **4.9a,g** is not influenced by the presence of molybdate supports this assertion and demonstrates that the decrease in emission intensity is not due to intermolecular quenching processes.

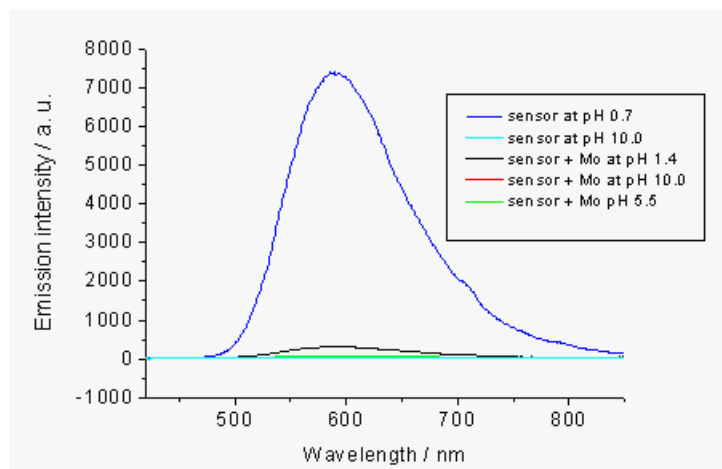


**Fig. 4.6:** Emission spectrum of **4.11j** showing the limit of pH profile and the effect of addition of molybdate (Mo) in aqueous acetonitrile both in acidic and basic pH range.

To determine the composition of the Mo complexes formed, the solutions of **4.11a,g,j** were titrated with aqueous solutions of molybdate, as shown for **4.11g** in **Fig. 4.7**. During the titrations, the solutions were buffered at pH values 4.08, 4.67 and 4.08 for **4.11a**, **4.11g** and **4.11j** respectively. Upon the addition of molybdate the emission intensity of all the three sensors decreases almost linearly until a ratio of sensor to molybdate of approximately 2:1 is reached. This ratio is consistent with the predominant formation of *cis*-dioxo-Mo(VI)-dicatecholate complexes at these pH values. Complexes of this composition are well known in the literature.<sup>40, 41</sup>

The detection limits for the quantitative analysis of molybdate with **4.11a**, **4.11g** and **4.11j** have been determined, using the spectrofluorimetric titrations and are shown in **Table 4.3**. As is evident from **Table 4.3**, **4.11a** and **4.11g** are more sensitive sensors than **4.11j**. The detection limits achieved with **4.11a** and **4.11g** are comparable with those reported for Ru(II) based sensor (Detection Limit  $1.8 \times 10^{-7}$ ), and are higher from Re(I) based sensor (Detection Limit  $1.3 \times 10^{-6}$ ).<sup>32</sup>

**Table 4.3:** Detection limits for the detection of molybdate by  $[\text{Ir}(\text{C}^{\wedge}\text{N})_2(\text{phen}^{\text{cat}}\text{-OH})]^+$  (**4.11**) complexes.

Compound	Detection Limit ( $\text{mol dm}^{-3}$ )
<b>4.11a</b>	$1.3 \times 10^{-7} - 3.3 \times 10^{-7}$
<b>4.11g</b>	$2.7 \times 10^{-7} - 6.7 \times 10^{-7}$
<b>4.11j</b>	$4.3 \times 10^{-7} - 1.1 \times 10^{-6}$

Complex **4.11g** has an advantage over the other two sensors and also over the related Ru(II) and Re(I) sensors mentioned in literature.<sup>32</sup> As said earlier **4.11g** shows two emission bands and both show a decrease in emission intensity upon deprotonation, however, only the lower energy band is quenched upon molybdate addition (**Fig. 4.7**). This suggests that this or related complexes warrant further investigation as ratiometric sensors for molybdate and can have potential applications *in vivo* studies.

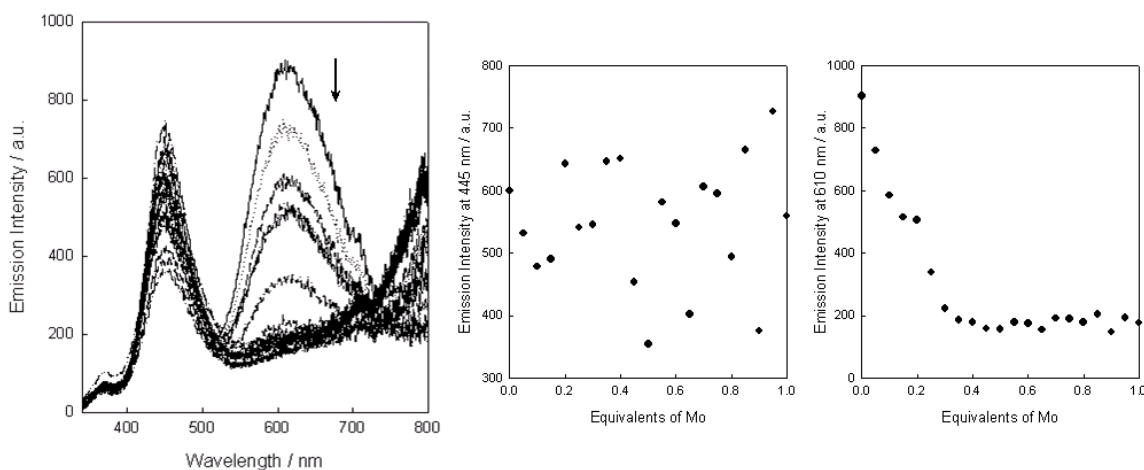


**Fig. 4.7:** Left: Emission spectra of **4.11g** (0.042 mM) in the presence of increasing molybdate concentrations in aqueous acetonitrile at pH 4.67, buffer 2,6-lutidine. Right: The emission intensity at 445 nm and at 610 nm, respectively, as a function of the molar  $\text{MoO}_4^{2-}$  fractions.

In conclusion, three new luminescent chemosensors for molybdate have been developed. The complexes **4.11a,g,j** were synthesised in high yields and can detect the presence of molybdate in solution through a decrease in emission intensity down to pH values as low as 0.4. **4.11a** and **4.11g** are more sensitive sensors than **4.11j** and show similar detection limits as Ru(II) sensor.<sup>32</sup> However, all the three sensors are proved to be better than Re(I) sensor.<sup>32</sup> The presence of dual emission for **4.11g** in which the two bands respond differently to molybdate suggests that this or related complexes warrant further investigation as ratiometric sensors for molybdate.

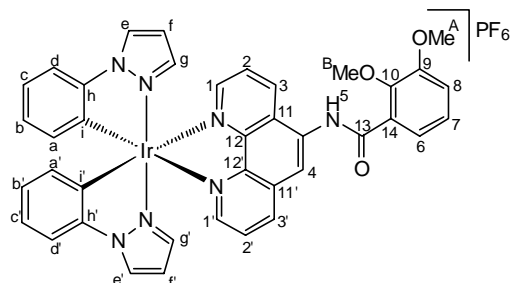
### 4.3 Experimental

#### General information and materials

Unless stated otherwise all reactions were carried out under an inert atmosphere of nitrogen and under microwave irradiation. After work up all the complexes were stable in air. The spectroscopic techniques and instruments used were as described in **Chapter 2**. All starting materials were obtained from Aldrich or Alfa Aesar with the exception of phencat-OMe ligand which was prepared according to the literature method.<sup>32</sup> The ligand phencat-OMe was deprotected to phencat-OH using BBr<sub>3</sub>. The molybdate detection and pH sensitive studies were carried out in collaboration with Dr. Anne-K. Duhme-Klair at the University of York.

#### Synthesis of **4.9a**

Dimer **2.6a** (70 mg, 0.068 mmol), phencat-OMe (59 mg, 0.164 mmol) and KPF<sub>6</sub> (25 mg, 0.136 mmol) were placed in a microwave vial and methanol (3 ml) was added to it. Nitrogen was bubbled through the

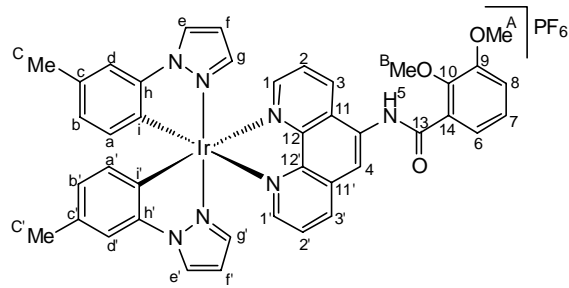


solution for 2 mins and the vial was then sealed with a septum cap. The reaction mixture was then heated under microwave irradiation for 20 mins at 60 °C. After this time the solvent was removed *in vacuo* leaving behind a solid which was dissolved in DCM (15 ml) and passed through celite. The volume of the filtrate was reduced and hexane was added slowly to induce precipitation. The precipitate was filtered, washed with hexane and dried *in vacuo* to yield **4.9a** as a yellow solid (121 mg, 91%). Anal. Calcd for C<sub>39</sub>H<sub>31</sub>N<sub>7</sub>O<sub>3</sub>IrPF<sub>6</sub>: C, 47.66, H, 3.18, N, 9.98. Found: C, 47.76, H, 3.24, N,

9.92%.  $^1\text{H}$  NMR (CD<sub>3</sub>CN):  $\delta$  10.84 (1H, s, H<sub>5</sub>), 9.02 (1H, s, H<sub>4</sub>), 8.77 (1H, dd,  $J$  = 8.6, 1.2, H<sub>3</sub>), 8.69 (1H, dd,  $J$  = 8.6, 1.6, H<sub>3'</sub>), 8.53 (1H, dd,  $J$  = 5.1, 1.2, H<sub>1</sub>), 8.38 – 8.37 (3H, m, H<sub>1'</sub>, e, e'), 7.96 (1H, dd,  $J$  = 8.2, 5.1, H<sub>2</sub>), 7.82 (1H, dd,  $J$  = 8.2, 5.1, H<sub>2'</sub>), 7.73 (1H, dd,  $J$  = 7.1, 2.7, H<sub>6</sub>), 7.53 (2H, d,  $J$  = 8.2, H<sub>d, d'</sub>), 7.36 – 7.30 (2H, m, H<sub>7, 8</sub>), 7.13 (2H, tt,  $J$  = 7.4, 1.2, H<sub>c, c'</sub>), 6.97 – 6.92 (4H, m, H<sub>b, b', g, g'</sub>), 6.51, 6.50 (2H, 2  $\times$  t,  $J$  = 2.7, H<sub>f, f'</sub>), 6.42, 6.41 (2H, 2  $\times$  dd,  $J$  = 7.4, 0.8, H<sub>a, a'</sub>), 4.11 (3H, s, Me<sub>B</sub>), 3.98 (3H, s, Me<sub>A</sub>).  $^{13}\text{C}$  NMR: 164.48 (C<sub>13</sub>), 152.94 (C<sub>9</sub>), 151.75 (C<sub>1</sub>), 150.46 (C<sub>1</sub>), 147.97 (C<sub>12</sub>), 147.56 (C<sub>10</sub>), 145.22 (C<sub>12</sub>), 143.45, 143.38 (C<sub>h, h'</sub>), 138.85 (C<sub>g, g'</sub>), 138.13 (C<sub>3'</sub>), 134.04 (C<sub>11</sub>), 133.24, 133.19 (C<sub>a, a'</sub>), 132.98 (C<sub>3</sub>), 131.85, 131.52, 131.30 (C<sub>11', 14, i, i'</sub>), 127.91 (C<sub>e, e'</sub>), 126.78 (C<sub>2'</sub>), 126.53 (C<sub>b, b'</sub>), 126.32 (C<sub>2</sub>), 124.82 (C<sub>7</sub>), 123.36 (C<sub>c, c'</sub>), 122.08 (C<sub>6</sub>), 117.99 (C<sub>4</sub>), 116.80 (C<sub>8</sub>), 111.96 (C<sub>d, d'</sub>), 108.05 (C<sub>f, f'</sub>), 61.57 (Me<sub>B</sub>), 55.91 (Me<sub>A</sub>). MS (FAB):  $m/z$  838 [M]<sup>+</sup>.

### Synthesis of 4.9b

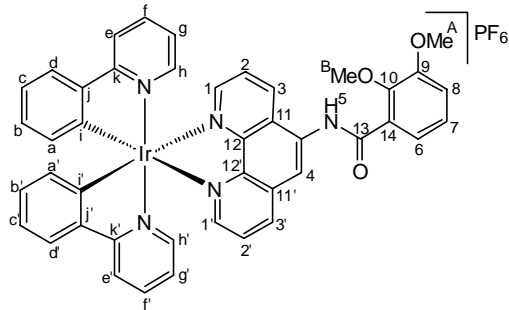
The procedure was the same as for **4.9a** using dimer **2.6b** (100 mg, 0.092 mmol), phencat-OMe (79.3 mg, 0.221 mmol) and KPF<sub>6</sub> (40.7 mg, 0.221 mmol), and after work up gave **4.9b** as a yellow solid (154 mg, 83%). Anal. Calcd for



C<sub>41</sub>H<sub>35</sub>N<sub>7</sub>O<sub>3</sub>IrPF<sub>6</sub>: C, 48.71, H, 3.49, N, 9.70. Found: C, 48.80, H, 3.57, N, 9.65%.  $^1\text{H}$  NMR (400 MHz, CD<sub>3</sub>CN):  $\delta$  10.82 (1H, s, H<sub>5</sub>), 9.03 (1H, s, H<sub>4</sub>), 8.77 (1H, dd,  $J$  = 8.6, 1.2, H<sub>3</sub>), 8.69 (1H, dd,  $J$  = 8.6, 1.6, H<sub>3'</sub>), 8.56 (1H, dd,  $J$  = 5.1, 1.2, H<sub>1</sub>), 8.40 (1H, dd,  $J$  = 5.1, 1.2, H<sub>1'</sub>), 8.34, 8.33 (2H, 2  $\times$  d,  $J$  = 2.7, H<sub>e, e'</sub>), 7.97 (1H, dd,  $J$  = 8.6, 5.1, H<sub>2</sub>), 7.83 (1H, dd,  $J$  = 8.2, 5.1, H<sub>2'</sub>), 7.74 (1H, dd,  $J$  = 7.0, 2.7, H<sub>6</sub>), 7.39 (2H, s, H<sub>d, d'</sub>), 7.36 – 7.30 (2H, m, H<sub>7, 8</sub>), 6.89, 6.88 (2H, 2  $\times$  d,  $J$  = 2.7, H<sub>g, g'</sub>), 6.79 (2H, bd,  $J$  = 7.4, H<sub>b, b'</sub>), 6.49, 6.48 (2H, 2  $\times$  t,  $J$  = 2.7, H<sub>f, f'</sub>), 6.26, 6.25 (2H, 2  $\times$  d,  $J$  = 7.4, H<sub>a, a'</sub>), 4.11 (3H, s, Me<sub>B</sub>), 3.98 (3H, s, Me<sub>A</sub>), 2.34 (6H, s, Me<sub>C, C'</sub>).  $^{13}\text{C}$  NMR: 165.50 (C<sub>13</sub>), 154.02 (C<sub>9</sub>), 152.82 (C<sub>1</sub>), 151.53 (C<sub>1'</sub>), 149.10 (C<sub>12</sub>), 148.65 (C<sub>10</sub>), 146.36 (C<sub>12</sub>), 144.52, 144.45 (C<sub>h, h'</sub>), 139.76 (C<sub>g, g'</sub>), 139.12 (C<sub>3'</sub>), 135.05 (C<sub>c, c'</sub>), 134.02 (C<sub>a, a'</sub>), 133.97 (C<sub>14</sub>), 133.89 (C<sub>3</sub>), 132.35 (C<sub>11'</sub>), 128.66 (C<sub>b, b'</sub>), 128.42 (C<sub>e, e'</sub>), 128.34 (C<sub>i, i'</sub>), 127.81 (C<sub>11</sub>), 127.61 (C<sub>2'</sub>), 127.39 (C<sub>2</sub>), 125.93 (C<sub>7</sub>), 123.18 (C<sub>6</sub>), 119.03 (C<sub>4</sub>), 117.92 (C<sub>8</sub>), 113.76 (C<sub>d, d'</sub>), 109.02 (C<sub>f, f'</sub>), 62.66 (Me<sub>B</sub>), 56.99 (Me<sub>A</sub>), 21.11 (Me<sub>C, C'</sub>). MS (FAB):  $m/z$  866 [M]<sup>+</sup>.

## Synthesis of 4.9g

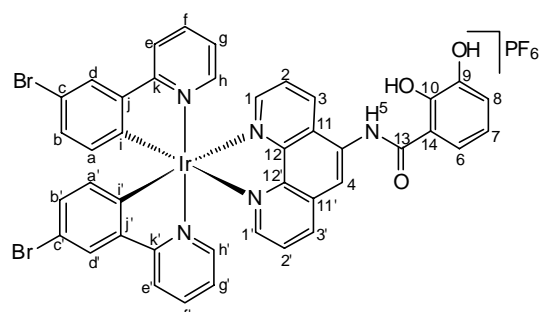
The procedure was of the same as for **4.9a** using dimer **2.6g** (70 mg, 0.065 mmol), phencat-OMe (56.1 mg, 0.156 mmol) and  $\text{KPF}_6$  (26.4 mg, 0.144 mmol), and after work up gave **4.9g** as a yellow solid (119 mg, 91%). Anal. Calcd for  $\text{C}_{43}\text{H}_{33}\text{N}_5\text{O}_3\text{IrPF}_6$ : C,



51.39, H, 3.31, N, 6.97. Found: C, 51.41, H, 3.26, N, 6.94%.  $^1\text{H}$  NMR (CD<sub>3</sub>CN): δ 10.81 (1H, s, H<sub>5</sub>), 9.03 (1H, s, H<sub>4</sub>), 8.74 (1H, dd,  $J$  = 8.6, 1.4, H<sub>3</sub>), 8.65 (1H, dd,  $J$  = 8.4, 1.4, H<sub>3'</sub>), 8.37 (1H, dd,  $J$  = 5.2, 1.4, H<sub>1</sub>), 8.22 (1H, dd,  $J$  = 5.2, 1.4, H<sub>1'</sub>), 8.06 (2H, m, H<sub>h, h'</sub>), 7.94 (1H, dd,  $J$  = 8.6, 5.2, H<sub>2</sub>), 7.84 (2H, dd,  $J$  = 7.7, 1.0, H<sub>d, d'</sub>), 7.82 – 7.76 (3H, m, H<sub>2', g, g'</sub>), 7.71 (1H, dd,  $J$  = 6.9, 2.6, H<sub>6</sub>), 7.45 (2H, ddd,  $J$  = 5.8, 2.1, 1.4, H<sub>e, e'</sub>), 7.33 – 7.27 (2H, m, H<sub>7, 8</sub>), 7.09, 7.08 (2H, 2 × td,  $J$  = 7.6, 1.4, H<sub>c, c'</sub>), 6.97, 6.96 (2H, 2 × td,  $J$  = 7.4, 1.4, H<sub>b, b'</sub>), 6.88, 6.87 (2H, 2 × td,  $J$  = 7.2, 1.2, H<sub>f, f'</sub>), 6.40, 6.39 (2H, 2 × dd,  $J$  = 7.6, 0.8, H<sub>a, a'</sub>).  $^{13}\text{C}$  NMR: 167.52, 167.47 (C<sub>k, k'</sub>), 164.44 (C<sub>13</sub>), 152.95 (C<sub>9</sub>), 151.44 (C<sub>1</sub>), 150.16 (C<sub>1'</sub>), 150.02 (C<sub>i, i'</sub>), 149.68 (C<sub>14</sub>), 149.41 (C<sub>e, e'</sub>), 147.59 (C<sub>10</sub>), 147.33 (C<sub>12</sub>), 144.53 (C<sub>11'</sub>), 144.33 (C<sub>12</sub>), 144.27 (C<sub>j, j'</sub>), 138.49 (C<sub>g, g'</sub>), 138.07 (C<sub>3'</sub>), 134.16 (C<sub>11</sub>), 132.82 (C<sub>3</sub>), 131.75, 131.70 (C<sub>a, a'</sub>), 130.37 (C<sub>b, b'</sub>), 127.00 (C<sub>2</sub>), 126.79 (C<sub>2</sub>), 124.87 (C<sub>7, d, d'</sub>), 123.40, 123.36 (C<sub>f, f'</sub>), 122.66 (C<sub>c, c'</sub>), 122.12 (C<sub>6</sub>), 119.82 (C<sub>h, h'</sub>), 118.12 (C<sub>4</sub>), 116.88 (C<sub>8</sub>), 61.59 (Me<sub>B</sub>), 55.93 (Me<sub>A</sub>). MS (FAB):  $m/z$  860 [M]<sup>+</sup>.

## Attempted deprotection of 4.9g and Synthesis of 4.11j

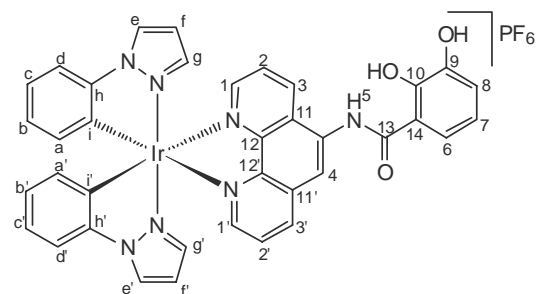
Under an inert atmosphere, **4.9g** (100 mg, 0.099 mmol) was dissolved in dry DCM (8 ml). The solution was cooled to -78 °C and a 10-fold molar excess (per methoxy) of 1.0 M  $\text{BBr}_3$  in DCM was added slowly. The reaction was stirred at -78 °C for 1 hr and then allowed to warm to room temperature. The reaction was then stirred at room temperature for a further 14 days and a total of 28 equiv (per methoxy) of 1.0 M  $\text{BBr}_3$  in DCM was added at different time intervals. The reaction was monitored via  $^1\text{H}$  NMR spectroscopy and ES mass spectrometry and the molecular ions  $[\text{M}]^+$  at  $m/z$  846, 832,



924, 910, 1004 and 990 were observed in ES-mass spectra, corresponding to complexes **4.10g**, **4.11g**, **4.10i**, **4.11i**, **4.10j** and **4.11j**. After 14 days only **4.11j** was observed as the final product in NMR and ES-MS. After completion of the reaction water was added slowly until no HBr was evolved. The reaction mixture was evaporated to dryness and the residues were taken up in methanol. KPF<sub>6</sub> (32.2 mg, 0.175 mmol) was added to the solution and stirred for 30 mins. The mixture was evaporated to dryness and the solid was dissolved in DCM (20 ml) and passed through celite. The volume of the filtrate was reduced and hexane was added slowly to induce precipitation. The precipitate was isolated, washed with hexane and dried *in vacuo* to yield **4.11j** as a yellow solid (79 mg, 75%). Anal. Calcd for C<sub>41</sub>H<sub>27</sub>N<sub>5</sub>O<sub>3</sub>Br<sub>2</sub>IrPF<sub>6</sub>: C, 43.40, H, 2.40, N, 6.17. Found: C, 43.32, H, 2.39, N, 6.14%. <sup>1</sup>H NMR (400 MHz, CD<sub>3</sub>CN):  $\delta$  10.59 (1H, s, H<sub>5</sub>), 8.84 (1H, dd, *J* = 8.6, 1.6, H<sub>3</sub>), 8.67 (1H, dd, *J* = 8.6, 1.6, H<sub>3'</sub>), 8.67 (1H, s, H<sub>4</sub>), 8.37 (1H, dd, *J* = 5.1, 1.6, H<sub>1</sub>), 8.27 (1H, dd, *J* = 5.1, 1.2, H<sub>1'</sub>), 8.08, (2H, bd, *J* = 8.2, H<sub>e, e'</sub>), 8.01 (2H, d, *J* = 1.9, H<sub>d, d'</sub>), 7.87 (1H, dd, *J* = 8.6, 5.1, H<sub>2</sub>), 7.84 – 7.78 (4H, m, H<sub>2', 6, f, f'</sub>), 7.46 (2H, m, H<sub>h, h'</sub>), 7.17 (1H, dd, *J* = 7.8, 1.6, H<sub>8</sub>), 7.11, 7.10 (2H, 2  $\times$  dd, *J* = 8.2, 1.9, H<sub>b, b'</sub>), 6.95 – 6.91 (3H, m, H<sub>7, g, g'</sub>), 6.27, 6.26 (2H, 2  $\times$  d, *J* = 8.2, H<sub>a, a'</sub>). <sup>13</sup>C NMR: 169.67 (C<sub>13</sub>), 166.89, 166.81 (C<sub>k, k'</sub>), 152.77 (C<sub>1</sub>), 151.85 (C<sub>1'</sub>), 150.84, 150.76 (C<sub>h, h'</sub>), 149.02 (C<sub>i, i'</sub>), 148.73 (C<sub>10</sub>), 148.20 (C<sub>12</sub>), 147.91, 147.85 (C<sub>j, j'</sub>), 146.87 (C<sub>9</sub>), 146.13 (C<sub>12'</sub>), 139.89 (C<sub>f, f'</sub>), 139.50 (C<sub>3'</sub>), 135.81 (C<sub>3</sub>), 134.91 (C<sub>12</sub>), 134.59, 134.56 (C<sub>a, a'</sub>), 133.76 (C<sub>b, b'</sub>), 132.29 (C<sub>11'</sub>), 129.23 (C<sub>11</sub>), 128.59, 128.56 (C<sub>d, d'</sub>), 128.10 (C<sub>2'</sub>), 127.58 (C<sub>2</sub>), 125.32 (C<sub>g, g'</sub>), 122.82 (C<sub>4</sub>), 121.52, 121.47 (C<sub>e, e'</sub>), 120.99 (C<sub>7</sub>), 120.91 (C<sub>8</sub>), 120.56 (C<sub>6</sub>), 117.40 (C<sub>14</sub>), 117.05 (C<sub>c, c'</sub>). MS (FAB): *m/z* 990 [M]<sup>+</sup>.

### Synthesis of **4.11a**

A mixture of dimer **2.6a** (70 mg, 0.068 mmol) and phenacet-OH (72.8 mg, 0.176 mmol) in methanol (2 ml) was degassed and heated under microwave irradiation for 2 hrs. at 70 °C. The orange-yellow solution was then cooled to room temperature and

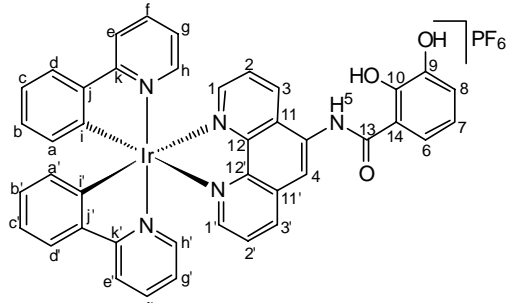


KPF<sub>6</sub> (32.3 mg, 0.176 mmol) was added to the solution and stirred for 30 mins. The mixture was evaporated to dryness and the solid was dissolved in DCM (15 ml) and passed through celite. The volume of the filtrate was reduced and hexane was added slowly to induce precipitation. The precipitate was filtered, washed with hexane and

dried *in vacuo* to yield **4.11a** as a yellow solid (101 mg, 78%). Anal. Calcd for C<sub>37</sub>H<sub>27</sub>N<sub>7</sub>O<sub>3</sub>IrPF<sub>6</sub>: C, 46.54, H, 2.85, N, 10.27. Found: C, 46.63, H, 2.76, N, 10.27%. <sup>1</sup>H NMR (400 MHz, MeOD):  $\delta$  8.87 (1H, dd, *J* = 8.6, 1.2, H<sub>3</sub>), 8.81 (1H, s, H<sub>4</sub>), 8.69 (1H, dd, *J* = 8.6, 1.2, H<sub>3'</sub>), 8.55 – 8.53 (3H, m, H<sub>1, e, e'</sub>), 8.43 (1H, dd, *J* = 5.1, 1.6, H<sub>1'</sub>), 7.94 (1H, dd, *J* = 8.6, 5.1, H<sub>2</sub>), 7.86 (1H, dd, *J* = 8.6, 5.1, H<sub>2'</sub>), 7.60 (1H, dd, *J* = 8.2, 1.2, H<sub>6</sub>), 7.55 (2H, bd, *J* = 7.8, H<sub>d, d'</sub>), 7.12 – 7.05 (3H, m, H<sub>8, c, c'</sub>), 6.96, 6.95 (2H, 2  $\times$  d, *J* = 2.3, H<sub>g, g'</sub>), 6.91, 6.90 (2H, 2  $\times$  td, *J* = 7.4, 0.8, H<sub>b, b'</sub>), 6.87 (1H, t, *J* = 8.2, H<sub>7</sub>), 6.53, 6.52 (2H, 2  $\times$  d, *J* = 2.3, H<sub>f, f'</sub>), 6.42, 6.41 (2H, 2  $\times$  dd, *J* = 7.4, 1.2, H<sub>a, a'</sub>). <sup>13</sup>C NMR: 167.78 (C<sub>13</sub>), 151.32 (C<sub>1</sub>), 150.38 (C<sub>1'</sub>), 148.00 (C<sub>12</sub>), 147.06 (C<sub>10</sub>), 146.01 (C<sub>9</sub>), 145.58 (C<sub>12'</sub>), 143.35, 143.31 (C<sub>h, h'</sub>), 138.26, 138.23 (C<sub>g, g'</sub>), 138.15 (C<sub>3</sub>), 133.87 (C<sub>11</sub>), 133.62 (C<sub>3</sub>), 133.05, 133.00 (C<sub>a, a'</sub>), 131.49 (C<sub>11'</sub>), 131.13 (C<sub>i, i'</sub>), 127.52 (C<sub>e, e'</sub>), 126.32 (C<sub>2', b, b'</sub>), 125.93 (C<sub>2</sub>), 123.16 (C<sub>c, c'</sub>), 120.21 (C<sub>4</sub>), 119.72 (C<sub>6</sub>), 119.29 (C<sub>7</sub>), 118.95 (C<sub>8</sub>), 117.14 (C<sub>14</sub>), 111.56 (C<sub>d, d'</sub>), 107.94, 107.92 (C<sub>f, f'</sub>). MS (FAB): *m/z* 810 [M]<sup>+</sup>.

## Synthesis of 4.11g

The procedure was of the same as for **4.10a** using dimer **2.6g** (60 mg, 0.056 mmol), phencat-OH (60 mg, 0.146 mmol) and KPF<sub>6</sub> (25.7 mg, 0.139 mmol) and after work up gave **4.11g** as a yellow solid (87 mg, 80%). Anal. Calcd for C<sub>41</sub>H<sub>29</sub>N<sub>5</sub>O<sub>3</sub>IrPF<sub>6</sub>: C, 50.41, H, 2.99,



N, 7.17. Found: C, 50.32, H, 2.93, N, 7.11%.  $^1\text{H}$  NMR (400 MHz, MeOD):  $\delta$  8.90 (1H, dd,  $J$  = 8.6, 1.2, H<sub>3</sub>), 8.87 (1H, s, H<sub>4</sub>), 8.69 (1H, dd,  $J$  = 8.6, 0.8, H<sub>3'</sub>), 8.41 (1H, dd,  $J$  = 5.1, 1.2, H<sub>1</sub>), 8.29 (1H, dd,  $J$  = 5.1, 1.6, H<sub>1'</sub>), 8.13 (2H, bd,  $J$  = 8.2, H<sub>e, e'</sub>), 7.96 (1H, dd,  $J$  = 8.2, 5.1, H<sub>2</sub>), 7.88 – 7.84 (3H, m, H<sub>2', d, d'</sub>), 7.82, 7.80 (2H, 2  $\times$  td,  $J$  = 7.4, 1.6, H<sub>f, f'</sub>), 7.60 (1H, dd,  $J$  = 8.2, 1.6, H<sub>6</sub>), 7.49 (2H, bd,  $J$  = 5.8, H<sub>h, h'</sub>), 7.11 – 7.03 (3H, m, H<sub>8, c, c'</sub>), 6.97 – 6.90 (4H, m, H<sub>b, b', g, g'</sub>), 6.84, (1H, t,  $J$  = 7.8, H<sub>7</sub>), 6.42, 6.40 (2H, 2  $\times$  dd,  $J$  = 7.4, 0.8, H<sub>a, a'</sub>).  $^{13}\text{C}$  NMR: 167.99, 167.95 (C<sub>k, k'</sub>), 167.73 (C<sub>13</sub>), 151.04 (C<sub>1</sub>), 150.08 (C<sub>1'</sub>), 149.74, 149.40 (C<sub>i, i'</sub>), 148.71 (C<sub>h, h'</sub>), 147.31 (C<sub>12</sub>), 147.11, (C<sub>10</sub>), 146.03 (C<sub>9</sub>), 144.84 (C<sub>12'</sub>), 144.06, 144.01 (C<sub>j, j'</sub>), 138.23 (C<sub>f, f'</sub>), 138.08 (C<sub>3'</sub>), 133.54 (C<sub>3</sub>), 131.59, 131.52 (C<sub>a, a'</sub>), 131.37 (C<sub>11'</sub>), 130.18, 130.14 (C<sub>b, b'</sub>), 127.67 (C<sub>11</sub>), 126.72 (C<sub>2</sub>), 126.32 (C<sub>2</sub>), 124.63 (C<sub>d, d'</sub>), 123.04, 123.01 (C<sub>g, g'</sub>), 122.43 (C<sub>c, c'</sub>), 120.27 (C<sub>4</sub>), 119.74 (C<sub>6</sub>), 119.61 (C<sub>e, e'</sub>), 119.24 (C<sub>7</sub>), 118.91 (C<sub>8</sub>), 116.90 (C<sub>14</sub>). MS (FAB):  $m/z$  832 [M]<sup>+</sup>.

#### 4.4 Bibliography

1. G. Di Marco, M. Lanza, A. Mamo, I. Stefio, C. Di Pietro, G. Romeo and S. Campagna, *Anal. Chem.*, 1998, **70**, 5019-5023.
2. J. N. Demas, W. Xu, K. Kneas and B. A. Degriff, *Photochem. Photobiol.*, 1997, **65**, 97S.
3. M. Licini and J. A. G. Williams, *Chem. Commun.*, 1999, 1943-1944.
4. R. Grigg, J. M. Holmes, S. K. Jones and W. Norbert, *J. Chem. Soc., Chem. Commun.*, 1994, 185-187.
5. A. Thompson, M. C. C. Smailes, J. C. Jeffery and M. D. Ward, *J. Chem. Soc., Dalton Trans.*, 1997, 737-743.
6. M. L. Ho, F. M. Hwang, P. N. Chen, Y. H. Hu, Y. M. Cheng, K. S. Chen, G. H. Lee, Y. Chi and P. T. Chou, *Org. Biomol. Chem.*, 2006, **4**, 98-103.
7. W. S. Sie, G. H. Lee, K. Y. D. Tsai, I. J. Chang and K. B. Shiu, *Journal of Molecular Structure*, 2008, **890**, 198-202.
8. M. L. Ho, Y. M. Cheng, L. C. Wu, P. T. Chou, G. H. Lee, F. C. Hsu and Y. Chi, *Polyhedron*, 2007, **26**, 4886-4892.
9. M. Schmittel and H. W. Lin, *Inorg. Chem.*, 2007, **46**, 9139-9145.
10. Q. Zhao, S. J. Liu, F. Y. Li, T. Yi and C. H. Huang, *Dalton Trans.*, 2008, 3836-3840.
11. K. K.-W. Lo, J. S.-Y. Lau, D. K.-K. Lo and L. T.-L. Lo, *Eur. J. Inorg. Chem.*, 2006, 4054-4062.
12. Q. Zhao, F. Y. Li, S. J. Liu, M. X. Yu, Z. Q. Liu, T. Yi and C. H. Huang, *Inorg. Chem.*, 2008, **47**, 9256-9264.
13. H. L. Chen, Q. Zhao, Y. B. Wu, F. Y. Li, H. Yang, T. Yi and C. H. Huang, *Inorg. Chem.*, 2007, **46**, 11075-11081.
14. D. L. Ma, W. L. Wong, W. H. Chung, F. Y. Chan, P. K. So, T. S. Lai, Z. Y. Zhou, Y. C. Leung and K. Y. Wong, *Angew. Chem., Int. Ed.*, 2008, **47**, 3735-3739.
15. J. N. Demas and B. A. DeGraff, *J. Chem. Educ.*, 1997, **74**, 690-695.
16. J. N. Demas and B. A. DeGraff, *Coord. Chem. Rev.*, 2001, **211**, 317-351.
17. C. W. Rogers and M. O. Wolf, *Coord. Chem. Rev.*, 2002, **233-234**, 341-350.
18. Z. Rosenzweig and R. Kopelman, *Anal. Chem.*, 1995, **67**, 2650-2654.
19. E. R. Carraway, J. N. Demas, B. A. Degriff and J. R. Bacon, *Anal. Chem.*, 1991, **63**, 337-342.
20. J. N. Demas, E. W. Harris and R. P. McBride, *J. Am. Chem. Soc.*, 1977, **99**, 3547-3551.
21. M. C. DeRosa, D. J. Hodgson, G. D. Enright, B. Dawson, C. E. B. Evans and R. J. Crutchley, *J. Am. Chem. Soc.*, 2004, **126**, 7619-7626.
22. R. M. Gao, D. G. Ho, B. Hernandez, M. Selke, D. Murphy, P. I. Djurovich and M. E. Thompson, *J. Am. Chem. Soc.*, 2002, **124**, 14828-14829.
23. Y. Amao, Y. Ishikawa and I. Okura, *Analytica Chimica Acta*, 2001, **445**, 177-182.
24. M. Gaetano Di, L. Maurizio, P. Marco and C. Sebastiano, *Adv. Mater.*, 1996, **8**, 576-580.
25. S. M. Borisov and I. Klimant, *Anal. Chem.*, 2007, **79**, 7501-7509.
26. P. I. Djurovich, D. Murphy, M. E. Thompson, B. Hernandez, R. Gao, P. L. Hunt and M. Selke, *Dalton Trans.*, 2007, 3763-3770.
27. W. Goodall and J. A. G. Williams, *J. Chem. Soc., Dalton Trans.*, 2000, **17**, 2893-2895.

28. Q. Zhao, F. Li, S. Liu, M. Yu, Z. Liu, T. Yi and C. Huang, *Inorg. Chem.*, 2008, **47**, 9256-9264.
29. J. Mason, *Toxicology*, 1986, **42**, 99.
30. C. Kisker, H. Schindelin, A. Pacheco, W. A. Wehbi, R. M. Garrett, K. V. Rajagopalan, J. H. Enemark and D. C. Rees, *Cell*, 1997, **91**, 973-983.
31. A. K. Duhme-Klair, *Eur. J. Inorg. Chem.*, 2009, 3689-3701.
32. H. D. Batey, A. C. Whitwood and A. K. Duhme-Klair, *Inorg. Chem.*, 2007, **46**, 6516-6528.
33. A. F. A. Peacock, H. D. Batey, C. Raendler, A. C. Whitwood, R. N. Perutz and A. K. Duhme-Klair, *Angew. Chem. Int. Ed.*, 2005, **44**, 1712-1714.
34. Q. Zhao, S. Liu, M. Shi, C. Wang, M. Yu, L. Li, F. Li, T. Yi and C. Huang, *Inorg. Chem.*, 2006, **45**, 6152-6160.
35. K.-M. Cheung, Q.-F. Zhang, K.-W. Chan, M. H. W. Lam, I. D. Williams and W.-H. Leung, *J. Organomet. Chem.*, 2005, **690**, 2913-2921.
36. T. M. Garrett, T. J. McMurry, M. W. Hosseini, Z. E. Reyes, F. E. Hahn and K. N. Raymond, *J. Am. Chem. Soc.*, 1991, **113**, 2965-2977.
37. S. M. Cohen, M. Meyer and K. N. Raymond, *J. Am. Chem. Soc.*, 1998, **120**, 6277-6286.
38. D. Burdinski, E. Bothe and K. Wieghardt, *Inorg. Chem.*, 2000, **39**, 105-116.
39. S. Y. Reece and D. G. Nocera, *J. Am. Chem. Soc.*, 2005, **127**, 9448-9458.
40. A. K. Duhme, *J. Chem. Soc., Dalton Trans.*, 1997, 773-778.
41. W. P. Griffith, H. I. S. Nogueira, B. C. Parkin, R. N. Sheppard, A. J. P. White and D. J. Williams, *J. Chem. Soc., Dalton Trans.*, 1995, 1775-1781.

## **Chapter Five:**

# **Homochiral bis-cyclometallated Ir(III) complexes**

## Chapter 5 Homochiral bis-cyclometallated Ir(III) complexes

### 5.1 Introduction

Octahedral complexes  $[M(A^{\wedge}A)_3]$  containing three identical symmetric bidentate ligands have  $D_3$  symmetry and are chiral having  $\Lambda$  (left handed twist) and  $\Delta$  (right handed twist) isomers *e.g.*  $[Ru(bipy)_3]^{2+}$  (Fig. 5.1) as discussed in **Chapter 1** (Fig. 1.11). Complexes of type  $[M(A^{\wedge}A)_2(B^{\wedge}B)]$  having two different types of symmetrical bidentate ligands or  $[M(A^{\wedge}A)_2(B)_2]$  with two symmetric bidentate and two equivalent monodentate ligands, are  $C_2$ -symmetric and exist as enantiomers in a similar way, *e.g.*  $[Ru(bipy)_2(phen)]^{2+}$  and  $[Ru(bipy)_2(py)_2]^{2+}$  respectively. Homochiral metal complexes are interesting in terms of their applications as DNA probes and cleavage agents due to their stereoselective interactions with DNA as discussed in **Chapter 1**.<sup>1-8</sup> For example, a 6-10 fold variation in the luminescence between  $\Lambda$  and  $\Delta$ - $[Ru(phen)_2(dppz)]^{2+}$  in the presence of DNA was explained in terms of a slightly different intercalation geometry of the two isomers.<sup>9</sup>

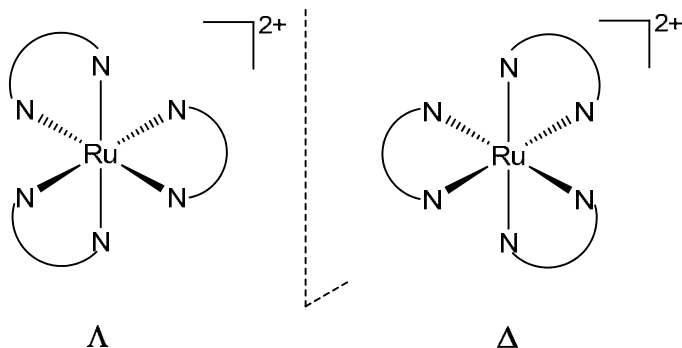


**Fig. 5.1:** View of the two enantiomers of  $[Ru(N^{\wedge}N)_3]^{2+}$  ( $N^{\wedge}N$  = bipy)

Another important goal of coordination chemistry is the development and understanding of systems that involve the enantio-selective synthesis of organic molecules.<sup>10-12</sup> In the vast majority of cases these involve chiral bidentate ligands often bisphosphines or N-donor ligands *e.g.* bisoxazolines, however tetradentate ligands *e.g.*  $N_2O_2$  salen derivatives have also been very successful.<sup>13-18</sup> In recent years there has been interest in systems in which chirality at the metal plays a more important role.<sup>19</sup>

In order to study interactions of chiral complexes with DNA and to assess the role of metal chirality in asymmetric catalysis it is necessary to be able to resolve the  $\Delta$  and  $\Lambda$  enantiomers. This can be quite challenging and is typically attempted *via*

formation of diastereomers and then separation by crystallisation or chromatography. On a small scale (a few mg) direct chromatographic separation of enantiomers using a chiral stationary phase is also feasible. Examples of the application of these methods are discussed below.

The association of chiral complex ions with enantiopure counter ions results in the formation of diastereomeric salts which in principle can be separated by crystallisation or chromatography. The most commonly employed technique for the resolution of cationic complexes is crystallisation with a chiral anion and this method has been widely reviewed.<sup>20-25</sup> To prepare complexes which are only chiral at the metal, diastereomers need to be converted back to enantiomers by the exchange of chiral anions with non-chiral anions. The separated chiral anions can be then reused. In early approaches, chiral anions derived from the chiral pool were used *e.g.* resolution of the  $\Delta$  and  $\Lambda$  isomers of  $[\text{Ru}(\text{bipy})_2(\text{py})_2]^{2+}$  was achieved using *O,O'*-dibenzoyl(*R,R*)-tartrate (**Fig. 5.2a**).<sup>26-28</sup> These chiral precursors were used further to synthesise other chiral-at-metal centre complexes by stereoretentive substitution of the two monodentate pyridine ligands followed by anion metathesis with other non-chiral anions.<sup>27, 29</sup> Recent developments in chiral anion mediated resolution of transition metal complexes have made use of new synthetic anions, *e.g.* BINOL derivatives of borates and phosphates and TRISPHAT and its derivatives (**Fig. 5.2**).<sup>21, 22, 30-32</sup> In principle, preformed ionic diastereomer mixtures are separable by chromatography; however, in practice most ion-

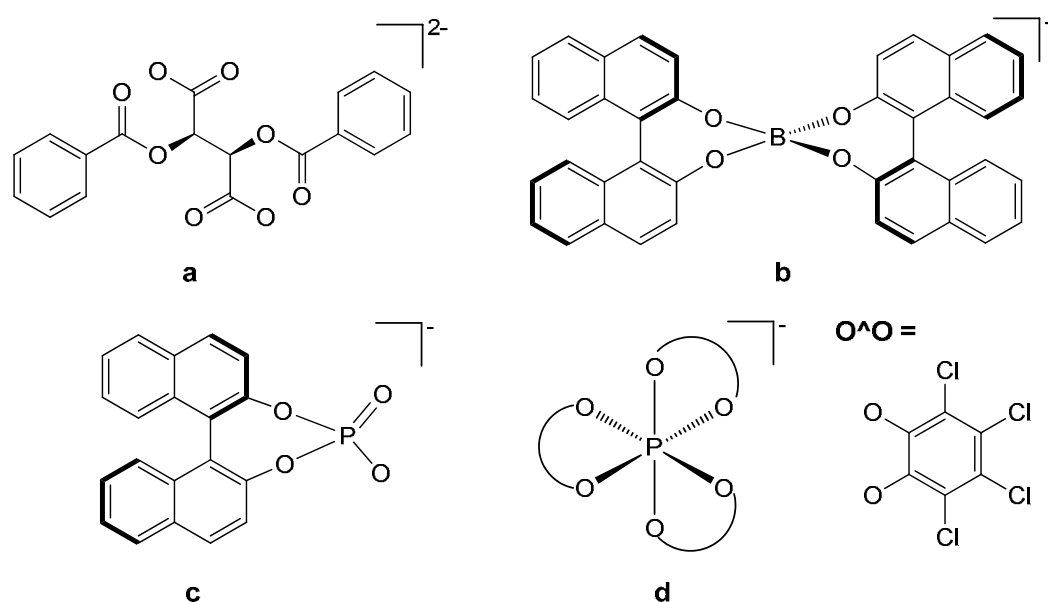


**Fig. 5.2:** Chiral anions used for the resolution of cationic coordination complexes.

pair chromatographic resolutions have involved the addition of non-racemic counterions such as those in **Fig 5.2**, to the mobile phase. For example, Gruselle *et al.* reported the resolution of *cis*-[Ru(phen)<sub>2</sub>(MeCN)<sub>2</sub>]<sup>2+</sup> complex using Δ-TRISPHAT as a chiral counterion by column chromatography on alumina.<sup>33</sup>

Another means of resolution of racemic transition metal complexes is through the synthesis of diastereomers containing a homochiral coordinating ligand; crystallisation and chromatography can then be used to attempt a separation. This strategy is equally applicable to ionic and neutral complexes. A range of chiral coordinating ligands has been used for the resolution of transition metal complexes and some of them are displayed in **Fig. 5.3**. For example, diastereomers of [M(bipy-pinen)<sub>3</sub>]<sup>2+</sup> (M = Fe, Ru, Os) were obtained using a homochiral C<sub>2</sub> symmetric ligand (**Fig. 5.3a**) and the diastereomers were separated *via* crystallisation and/or chromatography.<sup>34</sup> Another approach to homochiral transition metal complexes is by synthetic predetermination of the helicity about the metal centre, as demonstrated by von Zelewsky and co-workers using caged, CHIRAGEN-type pineno-polypyridine ligands (**Fig. 5.3c**),<sup>35</sup> only one of the two possible helical configurations, Δ or Λ at the metal, is formed. The absolute configuration depends on the choice of the enantiomer of the homochiral ligand. Hence, the judicious design of a chiral tripod ligand enables the formation of an octahedral metal complex with predetermined configuration at the metal centre.

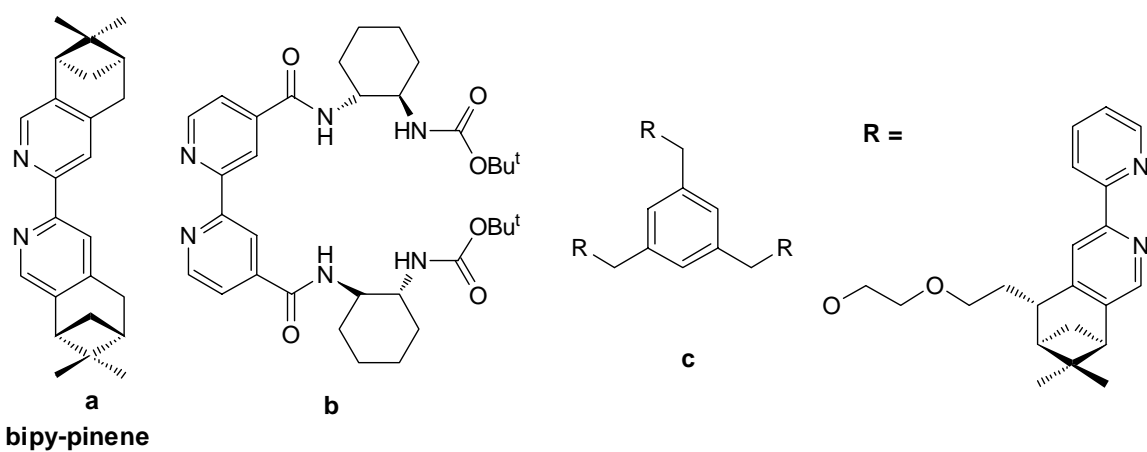


**Fig. 5.3:** Chiral coordinating ligands.

During the past two decades, direct chromatographic separation of enantiomers of coordination complexes, on chiral stationary phases (CSPs) by HPLC has been extensively developed.<sup>36-39</sup> Among more than a hundred commercially available CSPs, polysaccharide derivatives, such as cellulose esters and phenyl carbamates of cellulose,

amylose, and cyclodextrins have been widely used.<sup>38-42</sup> Resolution of the enantiomers of Ru(II) polypyridyl complexes,  $[\text{Ru}(\text{N}^{\wedge}\text{N})_3]^{2+}$  ( $\text{N}^{\wedge}\text{N}$  = bipy, phen and dppz) and  $[\text{Ru}(\text{phen})_2(\text{py})_2]^{2+}$  have been achieved using HPLC with carbamate derivatized  $\beta$ -cyclodextrin CSPs.<sup>43</sup>

The lipophilicity of the TRISPHAT anion also confers on its salts an affinity for organic solvents and, once dissolved, the ion pair do not partition in aqueous layers. This rather uncommon property was used by Lacour's group to develop a simple and practical resolution procedure of chiral cationic coordination complexes by asymmetric extraction.<sup>22</sup>

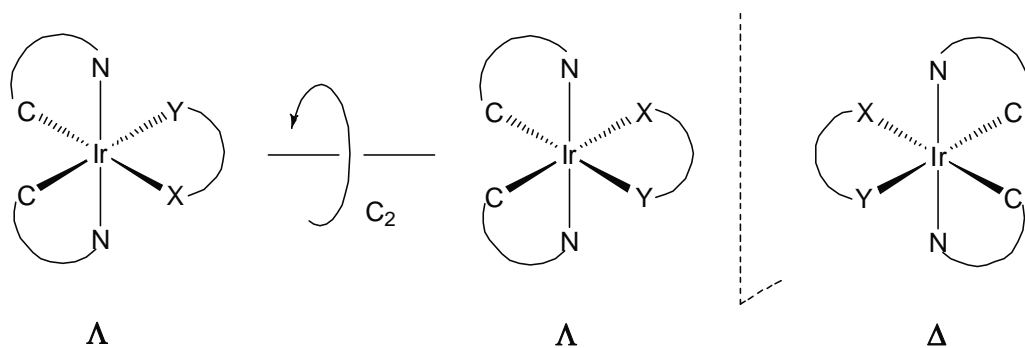
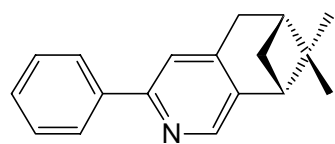


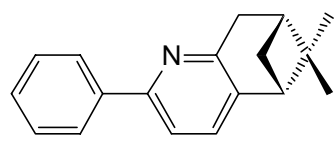
**Fig. 5.4:** View of the two enantiomers of  $[\text{Ir}(\text{C}^{\wedge}\text{N})_2(\text{X}^{\wedge}\text{Y})]$ .

As mentioned in **Chapter 1** complexes of type  $[\text{Ir}(\text{C}^{\wedge}\text{N})_2(\text{X}^{\wedge}\text{Y})]$  all occur as a single isomer with *cis* carbon atoms and *trans* nitrogen atoms of the cyclometallated ligand (**Fig. 1.7**); these complexes also exist as enantiomers (**Fig 5.4**) similar to  $[\text{Ru}(\text{bipy})_3]^{2+}$ . However, the resolution of Ir(III) complexes is still in its infancy and very few reports have been published so far,<sup>32, 44, 45</sup> the majority of which are based on the direct resolution by HPLC on a CSP. The first report of separation of the enantiomers of  $[\text{Ir}(\text{ppy})_3]$  using HPLC on a polysaccharide derived CSP was published in 2007 by Chen and co-workers,<sup>44</sup> and in 2008 Bernhard *et al.* reported the resolution of  $[\text{Ir}(\text{ppy-R})_2(\text{acac})]$  ( $\text{R} = \text{F}, \text{OMe}, \text{Ph}$ ) by HPLC.<sup>45</sup>

Another approach for the resolution of Ir(III) complexes is the use of the CHIRAGEN-type ligands, as discussed above for Ru(II) complexes. Zelewsky and co-workers reported that the reaction of  $[\text{Ir}(\text{acac})_3]$  with enantiopure ppy-pinene1 (**Fig. 5.5**) gave the *fac*- $\Lambda$ - and the *fac*- $\Delta$ - $[\text{Ir}(\text{ppy-pinene1})_3]$  in a ratio 2:3 and the two diastereomers were then separated by preparative TLC.<sup>46</sup> Recently, the same group has



**ppy-pinene1**

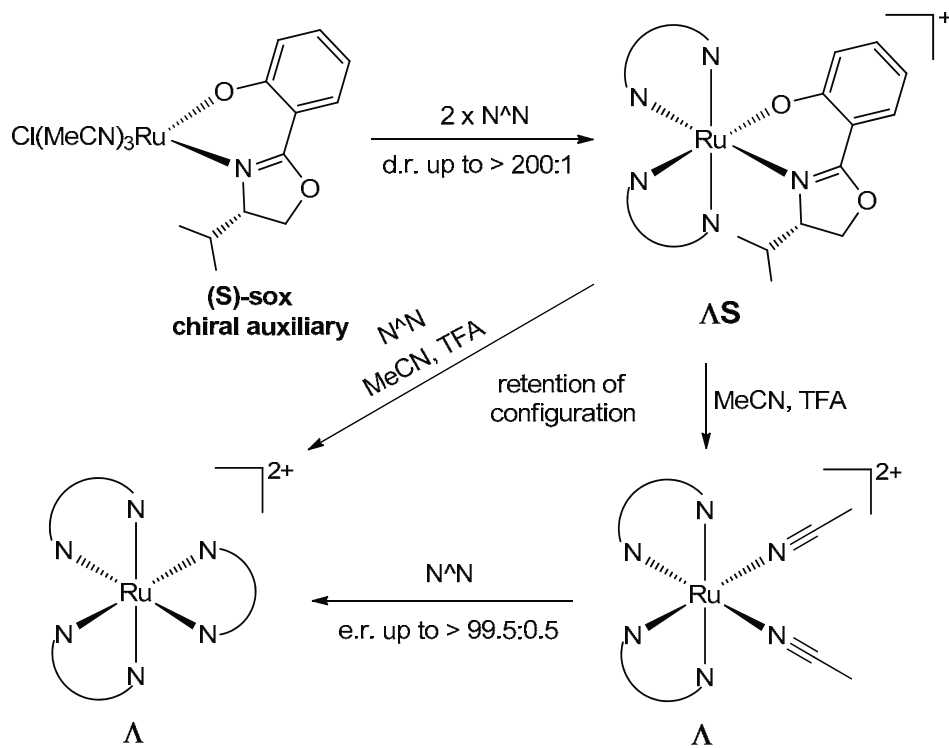


**ppy-pinene2**

**Fig. 5.5:** Chiral cyclometallating ligands.

described the diastereoselective synthesis of  $\Delta$ -[Ir(ppy-pinene2)<sub>2</sub>(acac)].<sup>47</sup> Although this strategy is successful to some degree it still gives complexes which have chirality at the ligand as well as the metal; hence, the aim of this project is to resolve the enantiomers of Ir(III) complexes on a preparative scale. This **Chapter** describes attempts to (i) synthesise diastereomeric complexes  $[\text{Ir}(\text{C}^{\Delta}\text{N})_2(\text{X}^{\Delta}\text{Y})]^{\text{n}+}$  in which  $\text{X}^{\Delta}\text{Y}$  is a homochiral bidentate ligand, (ii) separate the diastereomers on a preparative scale by selective crystallisation or chromatography, (iii) convert a single diastereomer to a homochiral dimer  $\Delta\Delta$  or  $\Lambda\Lambda$   $[\text{Ir}(\text{C}^{\Delta}\text{N})_2\text{X}]_2$  with only metal-centred chirality, (iv) synthesise a homochiral complex(es)  $[\text{Ir}(\text{C}^{\Delta}\text{N})_2(\text{bipy})]^+$ .

Whilst our work was in progress Meggers *et al.* reported a similar strategy for the resolution of Ru(II) complexes (**Scheme 5.1**) using salicyloxazolines (sox) as chiral



**Scheme 5.1**

$\text{N}^{\Delta}\text{N}$  bipy, phen  
d.r. diastereomeric ratio  
e.r. enantiomeric ratio

auxiliaries.<sup>48, 49</sup> The anionic (S)-sox provides excellent asymmetric induction ( $\Lambda$  at metal, in this case) on coordination of the  $\text{N}^{\wedge}\text{N}$  ligand ( $\text{N}^{\wedge}\text{N}$  = bipy, phen), and, can thereafter be substituted stereospecifically, with complete retention of configuration, in the presence of acid.

The intramolecular interactions in diastereomers of  $[\text{Ir}(\text{C}^{\wedge}\text{N})_2(\text{X}^{\wedge}\text{Y})]$ , containing a homochiral ligand  $\text{X}^{\wedge}\text{Y}$  can be analysed by reference to a quadrant diagram (**Fig 5.6**). Thus, in the  $\Lambda$  isomer, the substituents (*i.e.* H or methyl) on the *trans* nitrogens are directed towards quadrants 1 and 3 causing steric hindrance to any substituent on  $\text{X}^{\wedge}\text{Y}$  which would point towards these quadrants. Similarly for the  $\Delta$  isomer it is quadrants 2 and 4, that are more sterically hindered as shown in **Fig. 5.6**. Hence, chiral bidentate ligands may give some chiral discrimination of one diastereomer over the other, depending upon the steric congestion in the different quadrants.

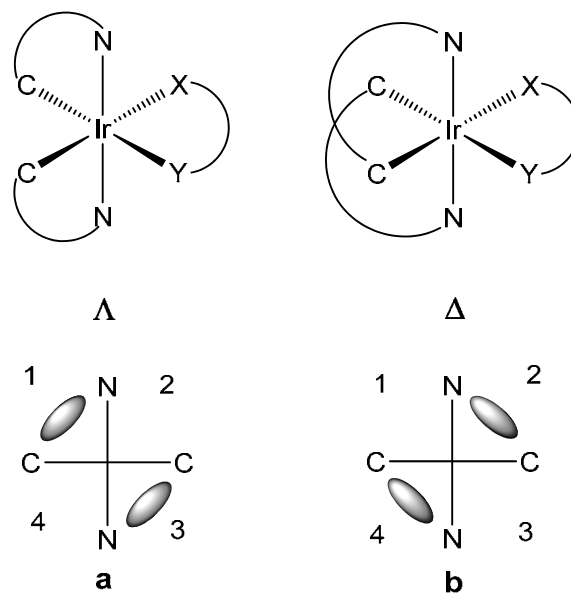


**Fig. 5.6:** Front view of the two enantiomers of  $[\text{Ir}(\text{C}^{\wedge}\text{N})_2(\text{X}^{\wedge}\text{Y})]$ .  $\text{X}^{\wedge}\text{Y}$  ligands attack from the front; shaded areas of quadrant diagrams indicate steric hindrance.

## 5.2 Results and Discussion

### 5.2.1 Synthesis and resolution of Ir(III) diastereomers

As mentioned above, the first step for the resolution of Ir(III) complexes is the synthesis of diastereomers using homochiral ligands such as (S)-soxH, (S)-pepH, (S)-phglyH, (+)-tfacH and (S)-pfea ( **Fig. 5.7**).

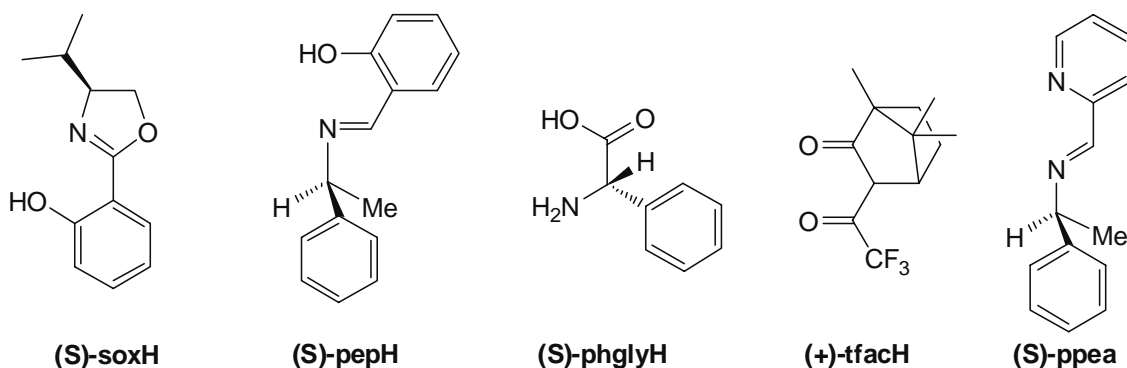
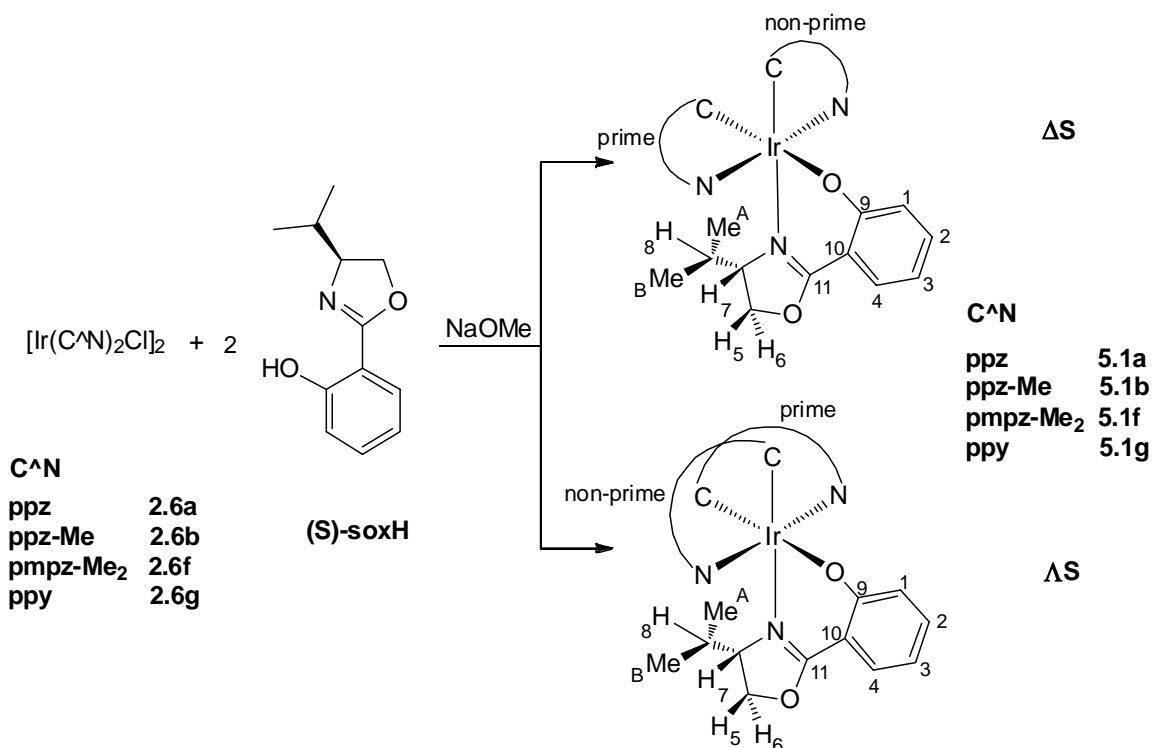


**Fig. 5.7:** Chiral coordinating ligands used in the study.

The crystal structure and NMR features of the  $[\text{Ir}(\text{C}^{\text{N}})^2]$  fragments of complexes discussed below are the same as those discussed in the **Chapter 2, 3 and 4**. For example the Ir(III) centre adopts a distorted octahedral coordination geometry [N—Ir—N ranges between  $173^{\circ}$ – $175^{\circ}$ ], with *cis* metallated carbons and *trans* nitrogen atoms, as expected for similar systems.<sup>50–52</sup> In the  $^1\text{H}$  NMR spectra all the protons in each isomer are inequivalent, and the characteristic NOEs for the  $[\text{Ir}(\text{C}^{\text{N}})^2]$  fragment are observed, *e.g.* between the phenyl protons  $\text{H}_{\text{d},\text{d}'}$  and pyrazole/pyridine protons  $\text{H}_{\text{e},\text{e}'}$ , and between  $\text{H}_{\text{a}}$  to  $\text{H}_{\text{g}'\text{ or } \text{h}'}$  and  $\text{H}_{\text{a}'}$  to  $\text{H}_{\text{g}}$  or  $\text{h}$ . Hence, only the significant features of the  $\text{X}^{\text{Y}}$  ligand interacting with  $[\text{Ir}(\text{C}^{\text{N}})^2]$  fragment, used to identify each diastereomer, will be explained below.

The ligand (S)-soxH was synthesised using a literature method.<sup>53</sup> The dimers **2.6a,b,f,g** reacted with 2.2–2.4 equiv of (S)-soxH and NaOMe in a mixture of DCM/methanol (2:1) at room temperature for 2–4 hrs, to form compounds **5.1a,b,f,g** as mixtures of diastereomers,  $\Delta\text{S}$  and  $\Delta\text{S}'$ , in good combined yields (>75%) (**Scheme 5.2**). Analysis of the  $^1\text{H}$  NMR spectra of the crude products showed the diastereomer ratio was 1:1 in each case. However, since excess ligand was used it is possible that all of one diastereomer was formed first then the other one. To test this possibility, the reaction of **2.6a** was



**Scheme 5.2**

Note: Phenyl ring with primes is *trans* to O while with non-primes is *trans* to imine N for both the isomers .

carried out with only 0.8 equiv of (S)-soxH per dimer. The <sup>1</sup>H NMR spectrum showed a 1:1 ratio of the two diastereomers of **5.1a** along with the unreacted excess dimer, which suggests that there is no diastereoselectivity in the synthesis and there is an equal probability for the formation of the two diastereomers. The diastereomers of **5.1a** were separated *via* crystallisation. Slow diffusion of hexane into a DCM solution of **5.1a** afforded pure crystals of the  $\Lambda$ S isomer, whereas the  $\Delta$ S isomer could be obtained from the mother liquor (enriched in  $\Delta$ S isomer) by crystallisation from methanol/diethyl ether. Unfortunately the  $\Lambda$ S/ $\Delta$ S diastereomers of **5.1b** could not be separated by crystallisation or chromatography; however,  $\Delta$ S-**5.1f** and  $\Lambda$ S-**5.1f** could be partially separated by flash column chromatography or preparative TLC (DCM/ethyl acetate 20:1). For **5.1g** both isomers crystallised out together from DCM/hexane or DCM/diethylether however the isomers could be separated by hand-picking due to a significant variation in colour and shape of the crystals. Partial separation of the diastereomers of **5.1g** was also achieved *via* column chromatography using alumina as a stationary phase, a pure fraction of the  $\Lambda$ S isomer eluted first with DCM/hexane (7:3), however the remaining fractions all contained both isomers, becoming increasingly enriched in the  $\Delta$ S isomer.

Determination of the relative configuration of each diastereomer relied heavily on X-ray crystallography. Fortunately for **5.1a** crystals of both diastereomers could be obtained by choosing the appropriate solvent mixtures as described above. The X-ray crystal structures are displayed in **Fig. 5.8** with selected bond lengths (Å) and angles (°) for  $\Delta S\text{-}5.1a$ . The crystal structures show that both isomers have S configuration at the chiral carbon atom of the sox ligand, one isomer has a  $\Lambda$  configuration at the Ir centre (**Fig. 5.8a**), whereas the other isomer shows a  $\Delta$  configuration at the Ir (**Fig. 5.8b**). The 6-membered  $N^{\wedge}O$  chelate angle (*ca.* 86°) is considerably larger than the 5-membered  $C^{\wedge}N$  chelate angles (*ca.* 80°) for both the isomers (**Fig. 5.8**). The major difference between the two diastereomers is that, in the  $\Lambda S$  isomer the pyrazole (non-prime) is directed towards the oxazoline nitrogen (towards quadrant 1 **Fig. 5.6a**) and is pointing towards the unsubstituted side of the oxazoline hence, the isopropyl is in a vacant quadrant (quadrant 4, **Fig. 5.6a**), whereas, in the  $\Delta S$  isomer, the same pyrazole is directed towards quadrant 4 (**Fig. 5.6b**) as is the isopropyl which leads to steric congestion. The steric congestion is clearly evident in the planarity of the sox ligand (**Fig. 5.8**). Thus, in the  $\Lambda S$  isomer the angle between the planes of the phenyl and the oxazoline is less than *ca.* 3° in the  $\Delta S$  isomer the corresponding angle is *> 20°*.

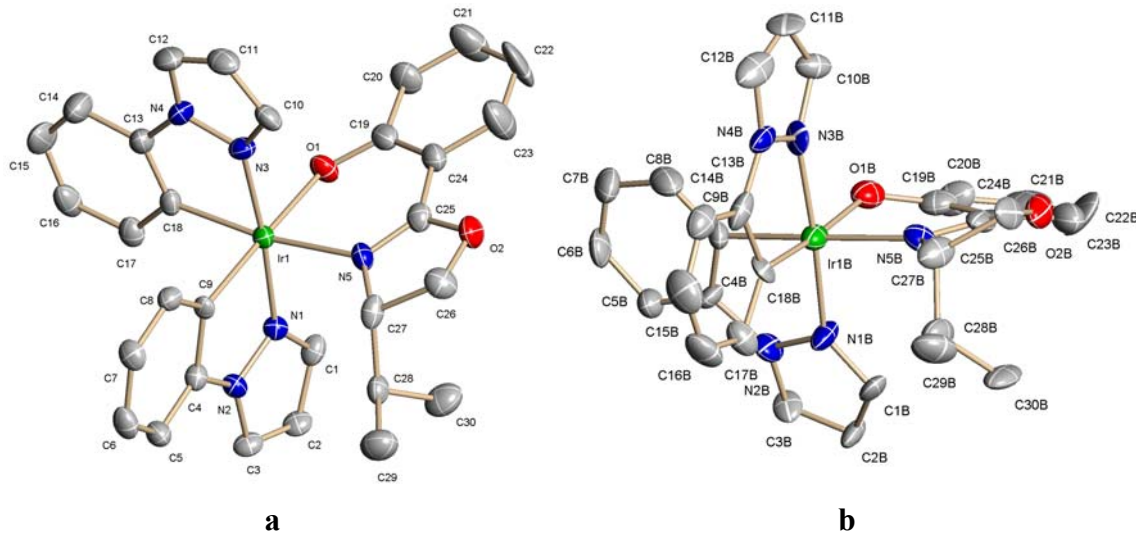


**Fig. 5.8:** X-ray crystal structures for  $\Lambda S\text{-}5.1a$  (**a**) and  $\Delta S\text{-}5.1a$  (**b**) respectively. Selected bond lengths (Å) and bond angles (°) for  $\Lambda S\text{-}5.1a$ : Ir(1)—N(1), 2.022(4); Ir(1)—N(3), 2.026(4); Ir(1)—N(5), 2.128(4); Ir(1)—O(1), 2.132(4); Ir(1)—C(9), 2.004(6); Ir(1)—C(18), 2.030(5); N(1)—Ir(1)—N(3), 174.83(18); N(1)—Ir(1)—C(9), 80.37(19); N(3)—Ir(1)—C(18), 79.8(2); N(5)—Ir(1)—O(1), 85.99(16).

<sup>a</sup>For  $\Delta S\text{-}5.1a$  there were three independent molecules in the unit cell, therefore no bond lengths/angles are quoted, isomer labelled b is shown in the **Fig. 5.8**.

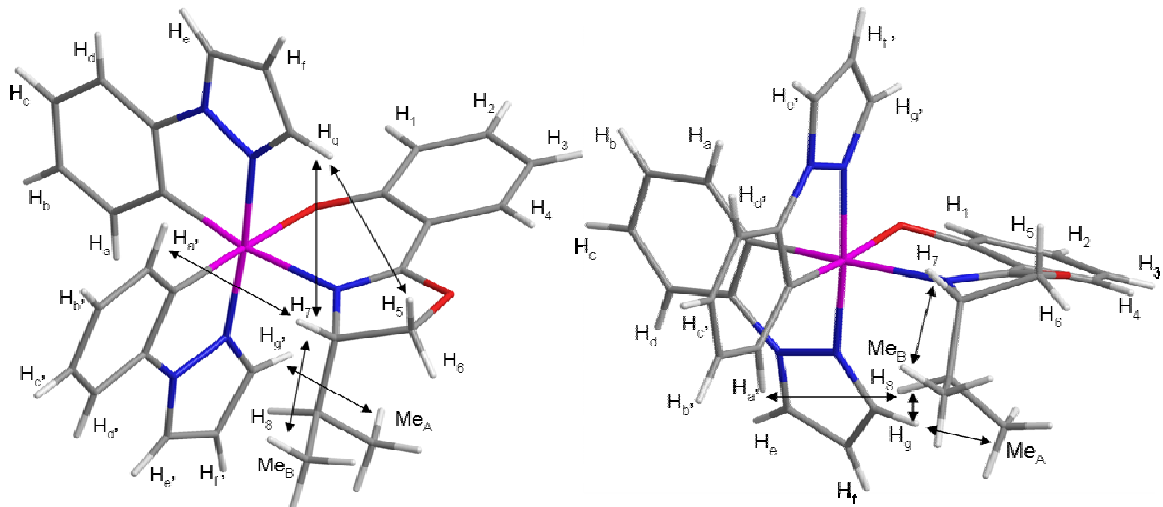


**Fig. 5.9:** Wireframe crystal structures showing key NOEs of  $\Lambda$ S-5.1a (a) and  $\Delta$ S-5.1a (b). Phenyl ring with primes is *trans* to O while with non-primes is *trans* to imine N for both the isomers.

The key NOEs used to verify that the solution structures are consistent with the solid state structures, are shown in **Fig. 5.9**. As mentioned above, in  $\Lambda$ S isomer of **5.1a**, a pyrazole (non-prime) lies over the unsubstituted side of the oxazoline, this is supported by the NOEs between the oxazoline protons  $H_5$  and  $H_7$  and the pyrazole proton  $H_g$  confirming their proximity [see Hs on C(26) and C(27) close to H on C(10), **Fig. 5.8a**]. Proton  $H_7$  also shows an NOE to  $H_{a'}$  *i.e.* the phenyl of the other ppz (prime). The isopropyl group is in quadrant 4 lying above a ppz ligand (prime) and hence is significantly affected by ring currents. This is obvious in the chemical shifts of the isopropyl group ( $\delta$  0.53, 0.20 and 0.28 for  $H_8$ ,  $Me_A$  and  $Me_B$  respectively) and is corroborated by an NOE between  $Me_A$  and  $H_{g'}$ . As stated above, in the  $\Delta$ S isomer, the isopropyl is directed towards an occupied quadrant (quadrant 4, **Fig. 5.6b**), this observation is confirmed by the NOEs between the isopropyl [ $Me_A$  and  $CH(H_8)$ ] and the pyrazole proton  $H_g$  (*ca.*  $\delta$  7.6) there is another NOE between  $H_8$  and a phenyl proton  $H_{a'}$  at  $\delta$  6.37 of the other ppz (prime). The proximity of these protons is evident in the X-ray structure [protons on C(30) close to the proton on C(1), and proton on C(28) close to those on C(1) and C(17) **Fig. 5.8b**]. The isopropyl chemical shifts are more normal ( $\delta$  2.01, 0.89 and 0.33 for  $H_8$ ,  $Me_A$  and  $Me_B$  respectively). However, protons  $H_5$  and  $H_7$  [ $\delta$  3.76 ( $H_5$ ) and 3.04 ( $H_7$ )] are now affected more by a ring current (of ppz prime) and so are at higher field than in the  $\Lambda$ S isomer [*ca.*  $\delta$  4.3 ( $H_5$ ) and 3.93 ( $H_7$ )]. Methyls ( $Me_A$  and  $Me_B$ ) are distinguished on the basis of NOEs between oxazoline proton  $H_7$  and  $Me_B$  in each isomer. Using the COSY and NOESY spectra all the other protons of the ppz

ligands can be assigned. The  $^{13}\text{C}$ -{ $^1\text{H}$ } NMR spectra of both isomers show the expected number of signals for the quaternary and CH carbons. The FAB mass spectrum of a 1:1 mixture of the two isomers shows a molecular ion at  $m/z$  683. The compounds are chiral with a specific rotation, of  $+582^\circ$  for  $\Delta\text{S}$  isomer compared to  $-593^\circ$  for the  $\Delta\text{S}$  isomer, in  $\text{CHCl}_3$  which are much higher than that of the free (S)-sox ligand ( $-29^\circ$  in  $\text{CHCl}_3$ ). This suggests that the chirality imposed by the metal has a bigger effect on the specific rotation than the chirality at the carbon of the sox ligand.

For **5.1b**, both of the diastereomers,  $\Delta\text{S}$  and  $\Delta\text{S}$ , crystallised together as a pseudoracemate in the same unit cell. This was confirmed by running the  $^1\text{H}$  NMR spectrum of a single crystal of **5.1b** which showed a 1:1 ratio of the two isomers. The crystal structures are shown in **Fig. 5.10** with selected bond lengths ( $\text{\AA}$ ) and angles ( $^\circ$ ) in **Table 5.1**. The conformations of the complexes are determined by the same steric interactions as **5.1a**, *i.e.* in the  $\Delta\text{S}$  isomer a pyrazole lies over the unsubstituted side of the oxazoline (**Fig. 5.10a**) whereas in the  $\Delta\text{S}$  isomer a pyrazole is lying over the substituted (isopropyl) side of the oxazoline (**Fig. 5.10b**). The  $\text{N}^\wedge\text{O}$  chelate angles are considerably higher than the  $\text{C}^\wedge\text{N}$  chelates for both of the isomers, as found for **5.1a**.

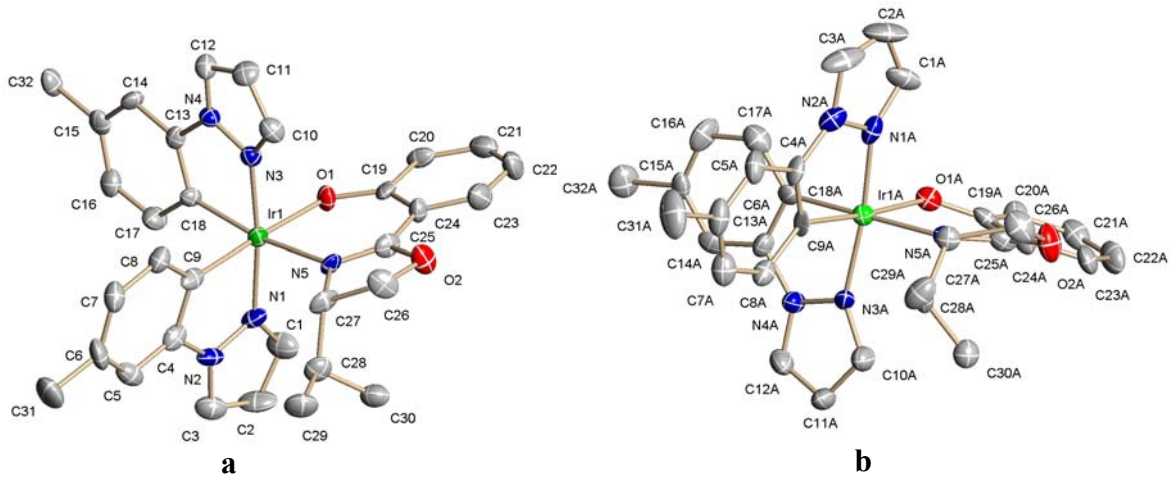


**Fig. 5.10:** X-ray crystal structures for  $\Delta\text{S}$ -**5.1b** (a) and  $\Delta\text{S}$ -**5.1b** (b) respectively.

<sup>a</sup>For **5.1b** both diastereomers are present in the same unit cell.

**Table 5.1:** Selected bond lengths (Å) and angles (°) for  $\Lambda$ S-**5.1b** (**a**) and  $\Delta$ S-**5.1b** (**b**) respectively.

(Å)	$\Lambda$ S- <b>5.1b</b>	(Å)	$\Delta$ S- <b>5.1b</b>
Ir(1)—N(1)	2.021(6)	Ir(1A)—N(1A)	2.001(7)
Ir(1)—N(3)	2.019(6)	Ir(1A)—N(3A)	2.020(6)
Ir(1)—N(5)	2.112(8)	Ir(1A)—N(5A)	2.142(9)
Ir(1)—O(1)	2.134(7)	Ir(1A)—O(1A)	2.193(7)
Ir(1)—C(9)	1.977(12)	Ir(1A)—C(9A)	2.014(9)
Ir(1)—C(18)	2.025(10)	Ir(1A)—C(18A)	2.015(11)
(°)		(°)	
N(1)—Ir(1)—N(3)	173.6(5)	N(1A)—Ir(1A)—N(3A)	173.7(4)
N(1)—Ir(1)—C(9)	79.7(4)	N(1A)—Ir(1A)—C(9A)	81.0(4)
N(3)—Ir(1)—C(18)	80.4(3)	N(3A)—Ir(1A)—C(18A)	80.0(3)
N(5)—Ir(1)—O(1)	86.5(3)	N(5A)—Ir(1A)—O(1A)	85.8(3)

As mentioned earlier,  $\Lambda$ S-**5.1b** and  $\Delta$ S-**5.1b** could not be resolved *via* crystallisation or chromatography so assignment of the  $^1\text{H}$  and  $^{13}\text{C}$ -{ $^1\text{H}$ } NMR spectra had to be done on the mixture. The  $^1\text{H}$  NMR spectra of  $\Lambda$ S-**5.1b** and  $\Delta$ S-**5.1b** are similar to  $\Lambda$ S-**5.1a** and  $\Delta$ S-**5.1a** respectively, except for **5.1b** each cyclometallated phenyl ring has one proton less than **5.1a**, and there are four additional methyl signals (two for each isomer) between  $\delta$  2.19 and 2.17, due to the substituents on the phenyl rings. The assignments are based on the same chemical shift arguments and NOEs described for **5.1a**. Thus, for the  $\Lambda$ S isomer, the oxazoline protons  $\text{H}_5$  and  $\text{H}_7$  show NOEs to the pyrazole proton  $\text{H}_g$  and the isopropyl signals are at highfield ( $\delta$  0.53, 0.19 and 0.29 for  $\text{H}_8$ ,  $\text{Me}_A$  and  $\text{Me}_B$  respectively). Whereas, in the  $\Delta$ S isomer the isopropyl  $\text{CH}$  ( $\text{H}_8$ ), shows NOEs to pyrazole proton  $\text{H}_g$  and to phenyl proton  $\text{H}_a$  of the other ppz (primes) and protons  $\text{H}_5$  and  $\text{H}_7$  are observed at higher field relative to the same protons in the  $\Lambda$ S isomer [ $\delta$  3.74 and 3.05 ( $\Delta$ S) *vs*  $\delta$  4.19 and 3.93 ( $\Lambda$ S)]. The isopropyl signals are now at more normal chemical shifts ( $\delta$  2.04, 0.88 and 0.35 for  $\text{H}_8$ ,  $\text{Me}_A$  and  $\text{Me}_B$  respectively). The  $^{13}\text{C}$ -{ $^1\text{H}$ } NMR spectra of the two isomers show the expected number of signals for the quaternary and  $\text{CH}$  carbons. The FAB mass spectrum of a 1:1 mixture of the two isomers shows a molecular ion at  $m/z$  711.

On the basis of the quadrant diagrams (Fig. 5.6b), in the  $\Delta$  isomer the protons ( $\text{H}_g$ ) on the pyrazoles are directed towards quadrants 2 and 4 causing steric congestion for the isopropyl of the (S)-sox ligand. Hence, replacing protons ( $\text{H}_g$ ) with larger groups (*e.g.* methyl) was expected to hinder formation of the  $\Delta$ S isomer. This hypothesis was

tested by reaction of (S)-soxH with dimer **2.6f**. However, the  $^1\text{H}$  NMR spectrum of **5.1f** still showed a 1:1 ratio of diastereomers. The diastereomers were partially separated by flash column chromatography or preparative TLC, using DCM/ethyl acetate (20:1) as eluent. Unfortunately, no crystals suitable for crystallography were obtained for these complexes. The  $^1\text{H}$  and  $^{13}\text{C}$ -{ $^1\text{H}$ } NMR spectra of **5.1f** are similar to **5.1a**, except for **5.1f** there are fewer pyrazole protons but there are an extra four methyl signals, two on each pyrazole, for both isomers. Again, the assignments are based on similar chemical shift arguments and NOEs as described above. The  $^1\text{H}$  NMR spectrum of the  $\Lambda\text{S}$  isomer of **5.1f**, shows NOEs between the oxazoline protons  $\text{H}_5$  and  $\text{H}_7$  and pyrazole methyl  $\text{Me}_D$  which are absent in the  $\Delta\text{S}$  isomer. The isopropyl signals are at highfield [ $\delta$  0.56 ( $\text{H}_8$ ), 0.30 and 0.29 ( $\text{Me}_A$  and  $\text{Me}_B$ )] showing they are affected by a ring current. For the  $\Delta\text{S}$  isomer, the key NOE is between the isopropyl CH ( $\text{H}_8$ ) and  $\text{Me}_A$  and pyrazole methyl  $\text{Me}_D$  it also shows an NOE to phenyl proton  $\text{H}_{a'}$  of the other ppz (prime). Protons  $\text{H}_5$  and  $\text{H}_7$  show an upfield shift ( $\delta$  3.75 and 2.91 respectively) compared to the  $\Lambda\text{S}$  isomer ( $\delta$  4.02 and 3.76 respectively) due to ring current effects, whilst the isopropyl is now at a more normal shift ( $\delta$  1.53, 0.70 and 0.17 for  $\text{H}_8$ ,  $\text{Me}_A$  and  $\text{Me}_B$  respectively) since it is no longer influenced by a ring current. The  $^{13}\text{C}$ -{ $^1\text{H}$ } NMR spectra of both isomers show the expected number of signals. The FAB mass spectrum of a 1:1 mixture of two isomers shows a molecular ion at  $m/z$  739. The specific rotations is  $-428^\circ$  in DCM for  $\Delta\text{S}$ -**5.1f**: $\Lambda\text{S}$ -**5.1f** (16:1) compared to  $+469^\circ$  for  $\Delta\text{S}$ -**5.1f**: $\Lambda\text{S}$ -**5.1f** (1:20) respectively.

As mentioned earlier, for **5.1g** the isomers crystallised together but were separated by hand picking. Crystals of the  $\Lambda\text{S}$  isomer were of X-ray quality and the structure is displayed in **Fig. 5.11** with selected bond lengths ( $\text{\AA}$ ) and angles ( $^\circ$ ); a structure could not be obtained for the  $\Delta\text{S}$  isomer. For the  $\Lambda\text{S}$  isomer, a pyridine is pointing towards the oxazoline nitrogen on the unsubstituted side of the oxazoline (quadrant 1 **Fig. 5.6a**) *i.e.* the opposite side to the isopropyl which lies in a vacant quadrant (quadrant 4, **Fig. 5.6a**) similar to  $\Lambda\text{S}$ -**5.1a,b** above. The  $\text{N}^\text{O}$  chelate angle ( $85.98^\circ$ ) is larger than the  $\text{C}^\text{N}$  chelates ( $80.4^\circ$  and  $80.5^\circ$ ), as found for **5.1a,b**.

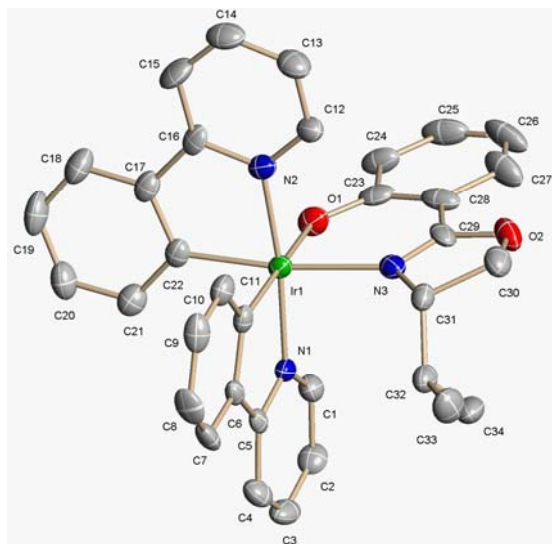


**Fig. 5.11:** X-ray crystal structure of  $\Lambda S\text{-5.1g}$ . Selected bond lengths ( $\text{\AA}$ ) and bond angles ( $^\circ$ ): Ir(1)—N(1), 2.033(4); Ir(1)—N(2), 2.042(5); Ir(1)—N(3), 2.142(5); Ir(1)—O(1), 2.123(4); Ir(1)—C(11), 1.994(5); Ir(1)—C(22), 2.002(5); N(1)—Ir(1)—N(2), 172.84(18); N(1)—Ir(1)—C(11), 80.4(2); N(2)—Ir(1)—C(22), 80.5(2); N(3)—Ir(1)—O(1), 85.98(17).

The  $^1\text{H}$  and  $^{13}\text{C}$ -{ $^1\text{H}$ } NMR spectra of **5.1g** are similar to those of **5.1a** except that each pyrazole ring of the cyclometallated ligand is replaced with a pyridine ring making the assignment slightly more complicated. The assignments are based on similar chemical shift arguments and NOEs as discussed above. Thus, for the  $\Lambda S$  isomer, the oxazoline protons H<sub>5</sub> and H<sub>7</sub> show NOEs to the pyridine proton H<sub>h</sub> whereas, in the  $\Delta S$  isomer, the main NOEs are between the isopropyl CH (H<sub>8</sub>) to pyridine proton H<sub>h</sub> and to phenyl proton H<sub>a'</sub> of the other ppz (primes). Protons H<sub>5</sub> and H<sub>7</sub> are observed at higher field relative to the same protons in the  $\Lambda S$  isomer [ $\delta$  3.65 and 3.08 ( $\Delta S$ ) *vs* *ca.*  $\delta$  4.3 and 3.95 ( $\Lambda S$ )] similar to **5.1a,b,f**. The  $^{13}\text{C}$ -{ $^1\text{H}$ } NMR spectra show the expected number of signals. The FAB mass spectrum of a 1:1 mixture of the two isomers shows a molecular ion at  $m/z$  706. The specific rotation for  $\Lambda S$  isomer is +570° in DCM compared to -532° for  $\Delta S\text{-5.1g}:\Lambda S\text{-5.1g}$  (15:1).

The optical properties of the,  $\Lambda S$  and  $\Delta S$ -**5.1a,f,g** were investigated further *via* the CD spectra which are discussed below (Fig. 5.12). The spectra of each pair of diastereomers show similar features but with opposite signs, suggesting that the chirality at the metal, which controls the relative orientation of the ligands is the determining feature of the CD spectra. As expected the spectra are not perfect mirror images since they are diastereomers rather than enantiomers. In  $\Delta 5.1a,f$  there is a positive Cotton effect at about 250 nm and a negative one at 280 nm (the reverse for the

AS isomers) however, these effects seem to be reversed in **5.1g** hence there appear to be no features that can easily be assigned to the configuration imposed by the metal.

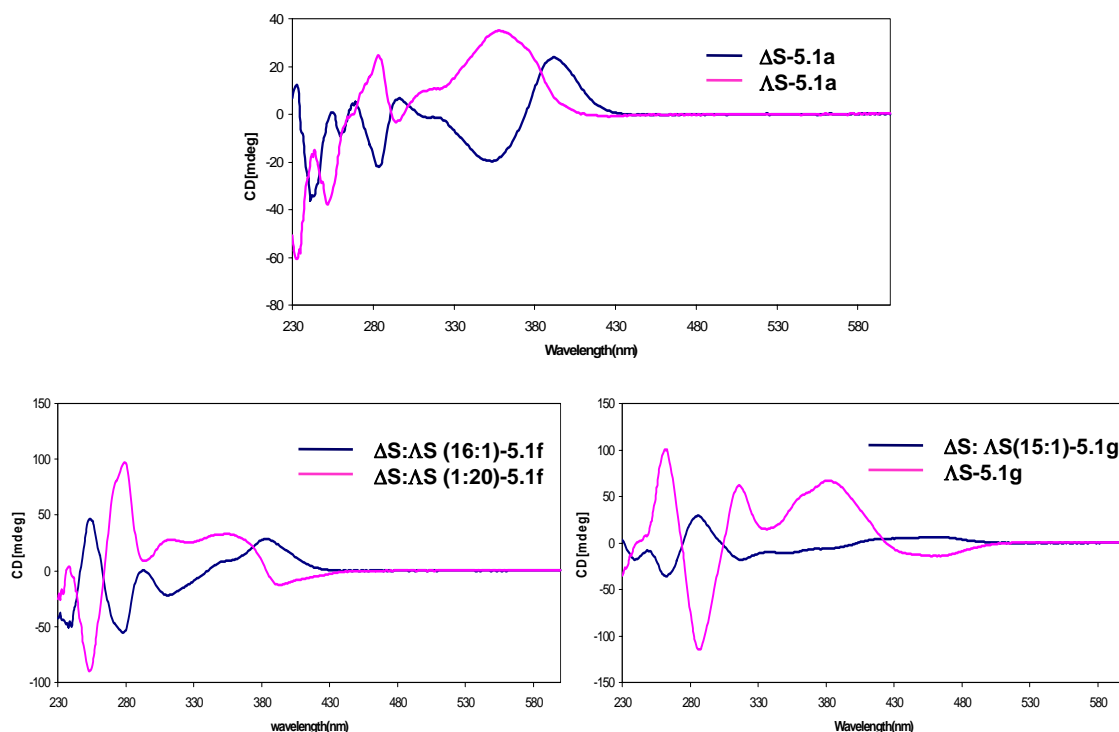
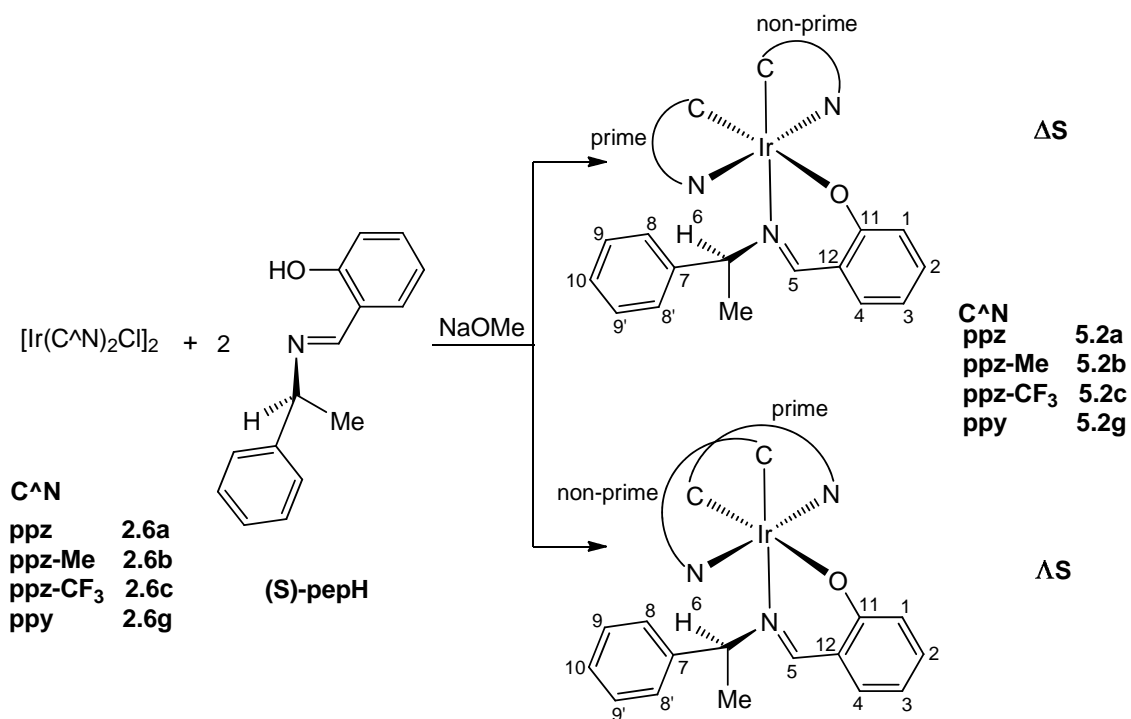


**Fig. 5.12:** CD spectra of AS/ΔS-**5.1a,f,g** respectively.

The ligand (S)-pepH was synthesised *via* a condensation reaction between salicylaldehyde and (S)-(-)-1-phenylethylamine.<sup>54</sup> The reactions of dimers **2.6a-c, g** with (S)-pepH and NaOMe were carried out in a mixture of DCM/methanol (2:1) at room temperature for 2-4 hrs, to form compounds ΔS/AS-**5.2a-c, g** as a 1:1 ratio of diastereomers, ΔS and AS, in good combined yield (>75%) (**Scheme 5.3**). The <sup>1</sup>H NMR spectrum of the crude products showed a 1:1 ratio of diastereomers along with the excess ligand and this ratio was maintained after work up. Since the isomers do not interconvert at room temperature (see below) the formation of a 1:1 mixture is presumably because there is no chiral discrimination in the synthesis as for the sox ligand described above. For most of the complexes **5.2** it was found that one diastereomer could be crystallised pure by selection of a suitable solvent, (**5.2a**, ΔS crystallised from methanol, **5.2b** and **5.2c**, AS crystallised from DCM/isopropanol and DCM/methanol mixtures respectively). However, for **5.2g** (also for **5.2b**) both isomers crystallised out together in methanol but they could be separated by hand-picking due to a significant variation in colour and shape of the crystals. The <sup>1</sup>H NMR spectrum of the mother liquors after recrystallisation of ΔS-**5.2a** and AS-**5.2b,c** showed signals that

were significantly enriched in the other diastereomer, *i.e.*  $\Delta S$ -**5.2a** and  $\Delta S$ -**5.2b,c** which suggests that the chirality at the metal is stable.



**Scheme 5.3**

Note: Phenyl ring with primes is *trans* to O while with non-primes is *trans* to imine N for both the isomers .

For **5.2b** crystallisation from methanol gave a mixture of crystals from which single crystals of the  $\Delta S$  isomer were obtained by hand picking, whereas crystals of the  $\Delta S$  isomer were obtained from DCM/isopropanol. The crystal structures are displayed in **Fig. 5.13**. Selected bond lengths ( $\text{\AA}$ ) and angles ( $^\circ$ ) are shown in **Table 5.2**. The 6-membered  $\text{N}^{\text{O}}$  chelate angle is considerably larger than the 5-membered  $\text{C}^{\text{N}}$  chelate angles (**Table 5.2**) similar to compounds **5.1**. Unlike complexes **5.1**, in complexes **5.2** there is free rotation about the  $\text{N}-\text{CH}(\text{Me})\text{Ph}$  bond of the (S)-pep ligand which can help alleviate any steric congestion. The crystal structures show that both isomers have S configuration at the chiral carbon atom of the pep ligand, one isomer has a  $\Delta$  configuration at the Ir centre (**Fig. 5.13a**), whereas the other isomer shows a  $\Lambda$  configuration at the Ir (**Fig. 5.13b**).

In pep complexes, owing to the free rotation about the  $\text{N}-\text{CH}(\text{Me})\text{Ph}$  bond, the conformations of complexes with this ligand are often influenced by attractive interactions of the phenyl with other aromatic groups in the molecule (face-to-face or

edge-to-face, for example in arene ruthenium complexes\*).<sup>55</sup> A significant feature of the  $\Delta S$  isomer is the face-on orientation of the phenyl ring [C(28)-C(33)] relative to the cyclometallated ligand [C(1)-C(9) including N(1) and N(2)], the angle between the planes is less than 10°. This causes the methyl, C(27), to be almost eclipsed with the imine hydrogen and the hydrogen on the chiral carbon, C(26), to be pointing in towards the ligands on Ir. However in the  $\Lambda S$  isomer to accommodate a similar phenyl-ppz interaction would put the methyl group into the crowded position pointing inwards. Hence, the conformation of the  $\Lambda S$  isomer is determined more by simple steric interactions with the H on C(26) being directed almost directly towards the Ir, trans to the imine H, so that the methyl and phenyl substituents can both point back away from the Ir.

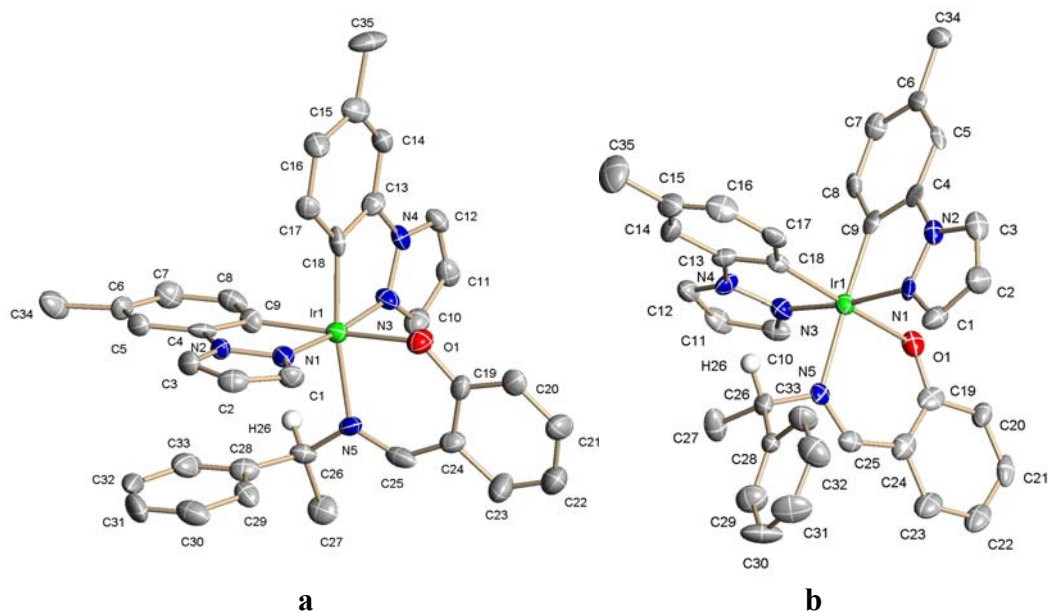


**Fig. 5.13:** X-ray crystal structures for  $\Delta S$ -**5.2b** (a) and  $\Lambda S$ -**5.2b** (b) respectively.

**Table 5.2:** Selected bond lengths ( $\text{\AA}$ ) and bond angles ( $^\circ$ ) for  $\Delta S$ -**5.2b** and  $\Lambda S$ -**5.2b** respectively.

( $\text{\AA}$ )	$\Delta S$ - <b>5.2b</b>	$\Lambda S$ - <b>5.2b</b>	( $^\circ$ )	$\Delta S$ - <b>5.2b</b>	$\Lambda S$ - <b>5.2b</b>
Ir(1)—N(1)	2.005(6)	2.000(8)	N(1)—Ir(1)—N(3)	174.2(2)	174.1(3)
Ir(1)—N(3)	2.019(5)	1.989(8)	N(1)—Ir(1)—C(9)	79.5(3)	79.7(3)
Ir(1)—N(5)	2.143(6)	2.140(7)	N(3)—Ir(1)—C(18)	79.5(3)	80.3(3)
Ir(1)—O(1)	2.126(6)	2.123(6)	N(5)—Ir(1)—O(1)	88.3(2)	88.1(3)
Ir(1)—C(9)	2.011(8)	1.997(9)			
Ir(1)—C(18)	1.993(9)	1.992(9)			

<sup>a</sup>For  $\Lambda S$ -**5.2b** there were two independent molecules in the unit cell, therefore the data is an average of values for both molecules.

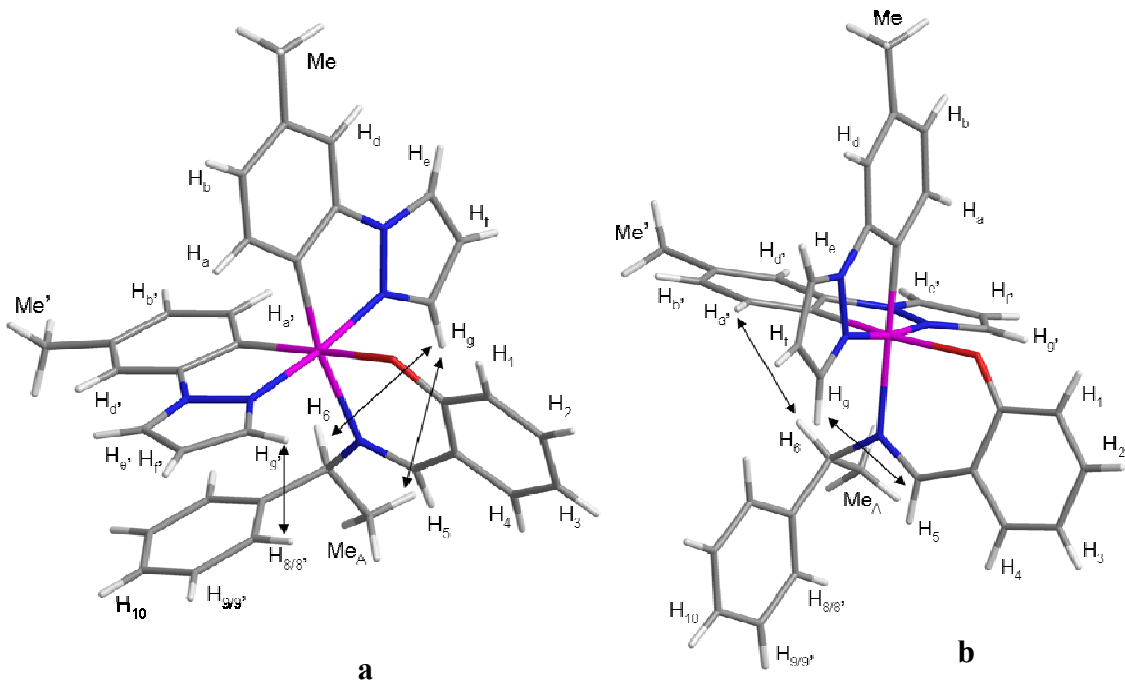


**Fig. 5.14:** Wireframe crystal structures showing key NOEs of  $\Delta S\text{-}5.2\mathbf{b}$  (a) and  $\Lambda S\text{-}5.2\mathbf{b}$  (b). Phenyl ring with primes is *trans* to O while with non-primes is *trans* to imine N for both the isomers.

The key NOEs and features used to verify that the solution structures are consistent with the solid state structures are shown in **Fig. 5.14**. In the  $^1\text{H}$  NMR spectrum of the  $\Delta S$  isomer the imine proton  $\text{H}_5$  is easily identified as the most downfield signal, a singlet at  $\delta$  8.02. As discussed above, in the crystal structure (**Fig. 5.13a**) the ppz (primes) is oriented almost parallel to the phenyl ring of the (S)-pep ligand, this is supported by the NOEs between the phenyl protons  $\text{H}_{8,8'}$  and the pyrazole proton  $\text{H}_{g'}$  (**Fig. 5.14a**) confirming their proximity. Consequently, protons  $\text{H}_{8,8'}$  (*ca.*  $\delta$  6.3) and  $\text{H}_{9,9',10}$  (*ca.*  $\delta$  6.9-7.0) are at relatively highfield consistent with a ring current from the ppz (primes). For the same reason,  $\text{H}_{d'}$  and  $\text{H}_{e'}$  ( $\delta$  6.59 and 7.67 respectively) are to higher field than  $\text{H}_d$  and  $\text{H}_e$  (*ca.*  $\delta$  7.0 and 7.99 respectively), consistent with a ring current from the phenyl ring of the (S)-pep ligand. The methyl,  $\text{Me}_A$  and  $\text{H}_6$  show NOEs to the pyrazole proton  $\text{H}_g$  (a doublet at  $\delta$  7.51) confirming their proximity (see Hs on C(26) and C(27) close to H on C(10), **Fig. 5.13a**).

As mentioned above, in the  $\Lambda S\text{-}5.2\mathbf{b}$  isomer,  $\text{H}_6$  [on C(26)] is oriented towards Ir, this is supported by an NOE between  $\text{H}_6$  and the phenyl proton  $\text{H}_{a'}$  [on C(17)] (**Fig. 5.14b**). The imine proton  $\text{H}_5$  shows an NOE to the pyrazole proton  $\text{H}_g$  (non primes) which is different to the  $\Delta S$  isomer as in the latter, the same proton points away from both of the

ppz ligands (**Fig. 5.13a**) and hence, does not show any NOE to any proton of  $[\text{Ir}(\text{C}^{\wedge}\text{N})_2]$  fragment. In contrast to the  $\Delta\text{S}$  isomer, the imine proton,  $\text{H}_5$  (*ca.*  $\delta$  7.9), is not the most downfield signal consistent with a shielding effect from the phenyl [ $\text{H}_{8-10}$ ] which is now pointing away from the Ir (see **Fig. 5.13b**). In addition,  $\text{Me}_\text{A}$  [ $\text{C}(27)$ ] lies under a ppz (prime) ligand and is observed at  $\delta$  0.80, considerably higher field than that,  $\delta$  1.50, in the  $\Delta\text{S}$  isomer, due to a ring current effect. As mentioned above, the phenyl [ $\text{H}_{8-10}$ ] points to the imine so is not affected by a ring current from a ppz so occurs at a more normal chemical shift (*ca.*  $\delta$  7.3) compared to the  $\Delta\text{S}$  isomer ( $\delta$  6.3 -7.0). For the same reason  $\text{H}_{\text{d}^{'}}$  and  $\text{H}_{\text{e}^{'}}$  are *ca.* 0.4 ppm downfield from the corresponding protons in  $\Delta\text{S-5.2b}$ . Using the COSY and NOESY spectra all the other protons of the ppz ligands can be assigned. The  $^{13}\text{C}-\{^1\text{H}\}$  NMR spectra of both isomers show the expected number of signals for the quaternary and CH carbons. The FAB mass spectrum of a 1:1 mixture of the two isomers shows a molecular ion at  $m/z$  731. The compounds are chiral with a specific rotation, of  $+658^\circ$  for  $\Delta\text{S}$  isomer compared to  $-560^\circ$  for the  $\Delta\text{S}$  isomer, in DCM which are much higher than that of the free (S)-pep ligand ( $+187^\circ$  in  $\text{CHCl}_3$ ). This suggests that the chirality imposed by the metal has a bigger effect on the specific rotation than the chirality at the carbon of the pep ligand similar to compounds **5.2**.

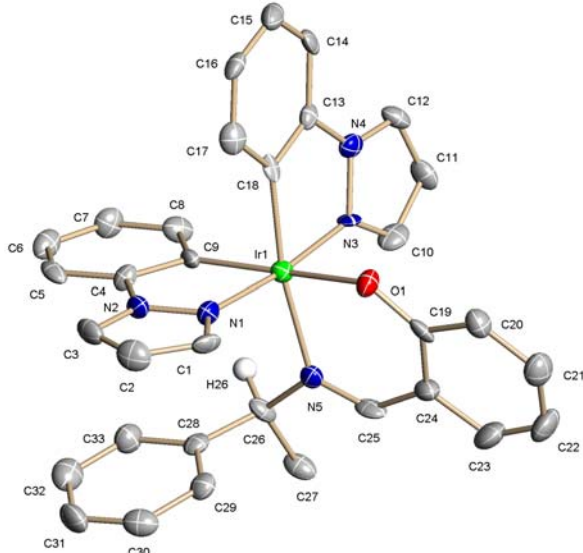


**Fig. 5.15:** X-ray crystal structure of  $\Delta\text{S-5.2a}$ . Selected bond lengths ( $\text{\AA}$ ) and bond angles ( $^\circ$ ):  $\text{Ir}(1)-\text{N}(1)$ , 1.997(6);  $\text{Ir}(1)-\text{N}(3)$ , 2.012(6);  $\text{Ir}(1)-\text{N}(5)$ , 2.139(7);  $\text{Ir}(1)-\text{O}(1)$ , 2.120(5);  $\text{Ir}(1)-\text{C}(9)$ , 2.000(8);  $\text{Ir}(1)-\text{C}(18)$ , 2.001(8);  $\text{N}(1)-\text{Ir}(1)-\text{N}(3)$ , 173.5(3);  $\text{N}(1)-\text{Ir}(1)-\text{C}(9)$ , 80.4(3);  $\text{N}(3)-\text{Ir}(1)-\text{C}(18)$ , 79.8(3);  $\text{N}(5)-\text{Ir}(1)-\text{O}(1)$ , 88.6(3).

Single crystals of one isomer of **5.2a** were obtained selectively by the slow evaporation of a concentrated solution of a racemic mixture of **5.2a** in methanol. The

structure is shown in **Fig. 5.15** with selected bond lengths (Å) and angles (°). The N<sup>^</sup>O chelate angle (88.6°) is considerably higher than the C<sup>^</sup>N chelates (80.4° and 79.8°), as found for **5.2b**. The structure reveals an S configuration at the pep ligand and Δ configuration at the metal. A face on interaction between phenyl ring [C(28)-C(33)] and ppz [C(1)-C(9) including N(1) and N(2)] is present, as observed for **ΔS-5.2b**.

The <sup>1</sup>H and <sup>13</sup>C-<sup>{1}</sup>H NMR spectra of **ΔS-5.2a** are similar to those of **ΔS-5.2b**. In the ΔS isomer, the ppz (primes) is oriented parallel to the phenyl ring of the (S)-pep ligand causing the phenyl protons H<sub>8-10</sub> to be observed at relatively high field (ca. δ 6.4-7.0), in addition there is an NOE between the phenyl protons H<sub>8,8'</sub> and the pyrazole proton H<sub>g'</sub> confirming their proximity (see Hs on C(29) and C(33) close to H on C(1), **Fig. 5.15**). As expected H<sub>d'</sub> and H<sub>e'</sub> (δ 6.77 and 7.66 respectively) are to higher field than H<sub>d</sub> and H<sub>e</sub> (δ 7.12 and 8.02 respectively), due to ring current of the phenyl ring of the (S)-pep ligand. The methyl and H<sub>6</sub> show NOEs to the pyrazole proton H<sub>g</sub> (δ 7.52) confirming their proximity (see Hs on C(26) and C(27) close to H on C(10), **Fig. 5.15**). The imine proton H<sub>5</sub> is the most downfield signal, a singlet at δ 8.06 and does not show any NOE to any proton of the [Ir(C<sup>^</sup>N)<sub>2</sub>] fragment similar to **ΔS-5.2b**.

The <sup>1</sup>H NMR spectrum of the mother liquor after recrystallisation of **ΔS-5.2a** showed signals that were significantly enriched in the other diastereomer, **ΔS-5.2a** (ΔS:ΔS 10:1). In **ΔS-5.2a**, proton H<sub>6</sub> is oriented towards Ir and shows an NOE to the phenyl proton H<sub>a'</sub>, the methyl is observed at δ 0.82, considerably higher field than that, δ 1.51, in the ΔS isomer due to the ring currents from the ppz (with prime). As for **ΔS-5.2b** the imine proton, at δ 7.96, is not the most downfield signal and shows an NOE to the pyrazole proton H<sub>g</sub> (non primes). The other assignments are made using the COSY and NOESY spectra. The <sup>13</sup>C-<sup>{1}</sup>H NMR spectra of both isomers show the expected number of signals for the quaternary and CH carbons. The FAB mass spectrum of a 1:1 mixture of the two isomers shows a molecular ion at *m/z* 703. The specific rotation is -631 for ΔS isomer compared to +480° (c = 1, CHCl<sub>3</sub>) for **ΔS-5.2a:ΔS-5.2a** 1:10.

The stability of the isomers in solid and solution was tested *via* running <sup>1</sup>H NMRs from the same batch of solid at different times and by running the same NMR sample at different times and it was observed that no racemisation took place. To test the stability of the chirality at the metal centre with respect to temperature in solution, complex **ΔS-5.2a** was dissolved in DMSO-d<sub>6</sub> and heated in stages to 140 °C. No racemisation was observed up to 120 °C, however, after heating at 140 °C for 3 hrs, another methyl signal and new

signals in the aromatic region were observed in the  $^1\text{H}$  NMR spectrum which may be due to some decomposition of the compound. Therefore it is concluded that the chirality is stable up to 120 °C. This is consistent with interconversion of *mer* to *fac* isomers of  $[\text{Ir}(\text{ppy})_3]$  requiring heating to > 200 °C.<sup>56, 57</sup> Note racemisation at the metal requires either both nitrogens of the C<sup>N</sup> to dissociate and exchange places or breaking of an M-C bond so that the carbon atoms can change places.

As mentioned above crystallisation of **5.2c** gave crystals of the  $\Delta\text{S}$  isomer and the structure is shown in **Fig. 5.16** with selected bond lengths (Å) and angles (°). The conformation is similar to  $\Delta\text{S}$ -**5.2b** with the H on C(26) being directed towards the Ir, so that the methyl and phenyl substituents can both point away from the Ir. The N<sup>O</sup> chelate angle (87.53°) is considerably higher than the 5-membered C<sup>N</sup> chelates (80.74° and 80.11°), as for **5.2a** and **5.2b**.

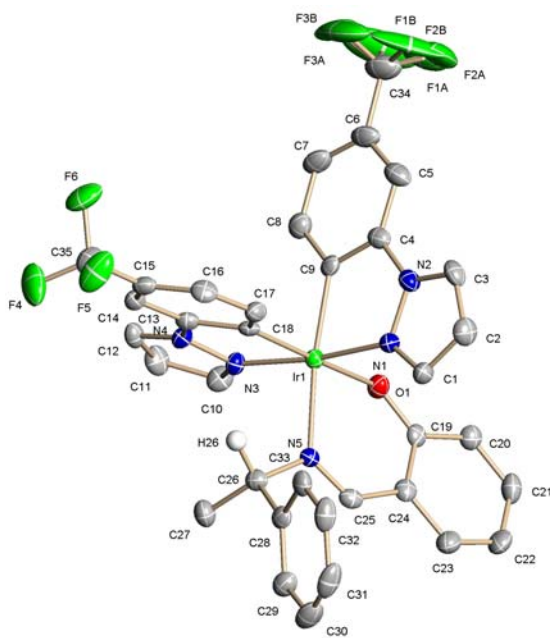


**Fig. 5.16:** X-ray crystal structure of  $\Delta\text{S}$ -**5.2c**. Selected bond lengths (Å) and bond angles (°):  
 Ir(1)—N(1), 2.018(3); Ir(1)—N(3), 2.026(3); Ir(1)—N(5), 2.135(3); Ir(1)—O(1), 2.130(3);  
 Ir(1)—C(9), 2.024(4); Ir(1)—C(18), 1.999(4); N(1)—Ir(1)—N(3), 172.62(15);  
 N(1)—Ir(1)—C(9), 80.74(16); N(3)—Ir(1)—C(18), 80.11(16); N(5)—Ir(1)—O(1), 87.53(12).

<sup>a</sup>One of the  $\text{CF}_3$  groups is highly disordered and the disordered F atoms have been split.

The  $^1\text{H}$  and  $^{13}\text{C}$ -{ $^1\text{H}$ } NMR spectra of **5.2c** are similar to those of **5.2a** and **5.2b**. In the spectrum of the  $\Delta\text{S}$  isomer, the phenyl protons  $\text{H}_{8,8'}$  show NOEs to the pyrazole

proton H<sub>g'</sub> and, the methyl and H<sub>6</sub> show NOEs to the pyrazole proton H<sub>g</sub>. Whereas, in the spectrum of the  $\Delta S$  isomer proton H<sub>6</sub> shows an NOE to the phenyl proton H<sub>a'</sub>. The phenyl protons H<sub>8-10</sub> ( $\delta$  6.20) and H<sub>9,9',10</sub> (*ca.*  $\delta$  6.9-7.0) are at higher field in  $\Delta S$  isomer ( $\delta$  6.2-7.0) than in the  $\Delta S$  isomer ( $\delta$  7.1 - 7.3) consistent with a face-to-face interaction between the phenyl H<sub>8-10</sub> and ppz (prime) in the  $\Delta S$  isomer. The methyl is observed at  $\delta$  0.93 in **AS-5.2c**, (*cf.*  $\delta$  1.55, in the  $\Delta S$  isomer) due to the ring currents from the ppz (prime). The COSY and the NOESY spectra are used for other assignments of ppz ligands. The  $^{13}\text{C}$ -{ $^1\text{H}$ } NMR spectra of both isomers show the expected number of signals. The FAB mass spectrum of a 1:1 mixture of the two isomers shows a molecular ion at *m/z* 839. The specific rotation is +563° for the  $\Delta S$  isomer and -473° for  $\Delta S:\Delta S$  17:1, in DCM.

For **5.2g** both isomers crystallised together from methanol and were separated by hand-picking due to a significant variation in colour and shape of the crystals. The structures are shown in **Fig. 5.17** with selected bond lengths (Å) and angles (°) in **Table 5.3**. As found for **5.2a,b** in the ΔS isomer, the phenyl [C(32)-C(37)] and ppy [C(1)-C(11) including N(1)] are in a face to face orientation no such interaction is found in the ΛS isomer. The N<sup>+</sup>O chelate angle is larger in the ΔS isomer than the ΛS isomer (88.50(19)° vs 85.90(11)° respectively) but both of these are higher than the C<sup>+</sup>N chelates (80.2° to 80.7° for ΔS and ΛS respectively).

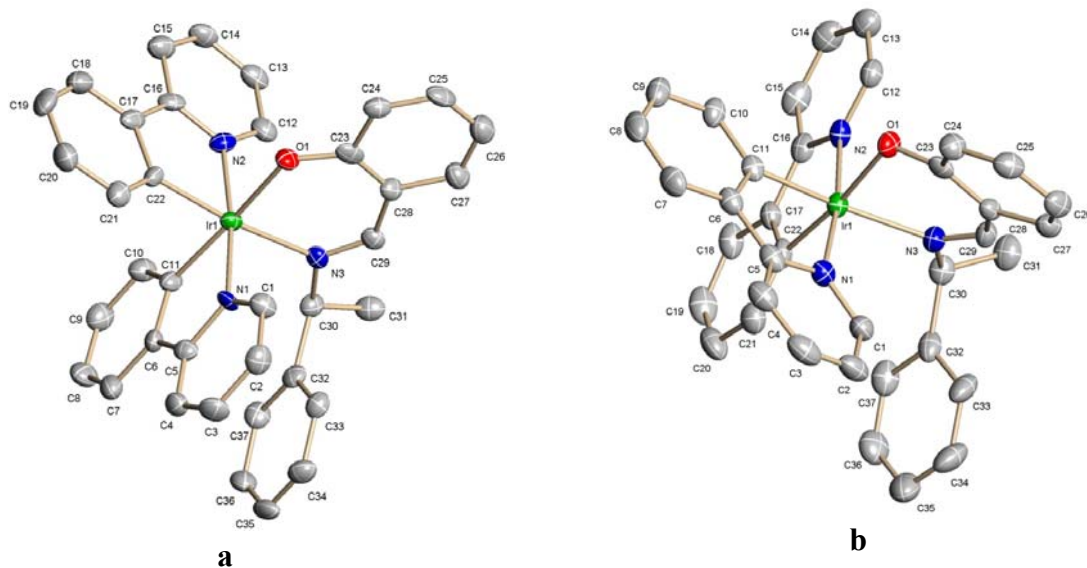


**Fig. 5.17:** X-ray crystal structures for  $\Delta S\text{-}5.2\text{g}$  (a) and  $\Delta S\text{-}5.2\text{g}$  (b) respectively.

**Table 5.3:** Selected bond lengths (Å) and bond angles (°) for  $\Delta S\text{-5.2g}$  and  $\Lambda S\text{-5.2g}$  respectively.

(Å)	$\Delta S\text{-5.2g}$	$\Lambda S\text{-5.2g}$	(°)	$\Delta S\text{-5.2g}$	$\Lambda S\text{-5.2g}$
Ir(1)—N(1)	2.041(5)	2.045(3)	N(1)—Ir(1)—N(2)	172.9(2)	173.15(12)
Ir(1)—N(2)	2.040(6)	2.025(3)	N(1)—Ir(1)—C(11)	80.2(2)	80.36(14)
Ir(1)—N(3)	2.132(6)	2.157(3)	N(2)—Ir(1)—C(22)	80.6(3)	80.70(14)
Ir(1)—O(1)	2.145(4)	2.140(3)	N(3)—Ir(1)—O(1)	88.50(19)	85.90(11)
Ir(1)—C(11)	2.001(6)	1.999(4)			
Ir(1)—C(22)	2.006(6)	1.999(4)			

The  $^1\text{H}$  and  $^{13}\text{C}$ -{ $^1\text{H}$ } NMR spectra of **5.2g** are similar to those of **5.2a-c** except the pyrazole protons of the cyclometallated ligand are replaced with pyridine protons. As a result the imine proton  $\text{H}_5$  is not the most downfield signal for either isomer. The other assignments and NOEs for **5.2g** are made on the same basis as for **5.2a-c**. The phenyl protons  $\text{H}_{8/8'}$  in the  $\Delta S$  isomer are observed at *ca.*  $\delta$  6.3 compared to *ca.*  $\delta$  7.2 in the  $\Lambda S$  isomer, consistent with the face-to-face interaction between phenyl [C(32)-C(37)] and the ppy (prime) as discussed above. Conversely, the methyl is observed at considerably higher field in the  $\Lambda S$  isomer than in the  $\Delta S$  isomer ( $\delta$  0.73 vs 1.45 for  $\Lambda S$  and  $\Delta S$  respectively) due to the ring currents from the ppy (prime). The  $^{13}\text{C}$ -{ $^1\text{H}$ } NMR spectra show the expected signals for the CH and quaternary carbons. The stability of chirality at the metal was checked by heating a mixture of  $\Delta S\text{-5.2g}/\Lambda S\text{-5.2g}$  (1:1.4) in stages to 150 °C in  $\text{DMSO-d}_6$  and no change in the ratio was observed by  $^1\text{H}$  NMR spectroscopy up to 120 °C. The FAB mass spectrum shows a molecular ion at  $m/z$  725 for a 1:1 mixture of **5.2g**. The specific rotation is -535° for the  $\Delta S$  isomer and +654° for  $\Lambda S$  isomer in DCM.

The optical properties of  $\Delta S$  and  $\Lambda S\text{-5.2a-c, g}$  were also investigated *via* circular dichroism. The CD spectra of each pair of isomers (**Fig. 5.18**) show similar features but with opposite signs, similar to compounds **5.1**. All of the  $\Delta S$  isomers of compounds **5.2a-c, g** have a negative Cotton effect at about 270 nm and 380 nm, and a positive one at about 370 nm (the reverse for the  $\Lambda S$  isomers). Hence it is possible that these bands may be diagnostic of the metal configuration in this range of complexes however further work would be needed to confirm the generality of this observation.

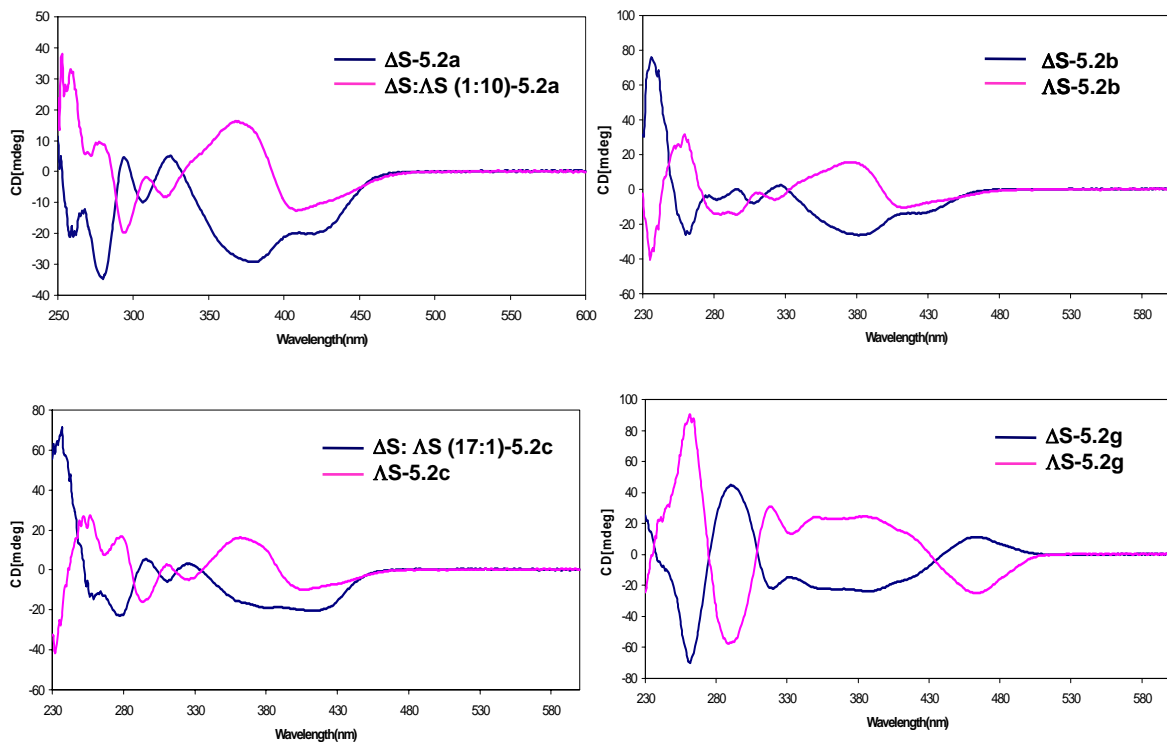
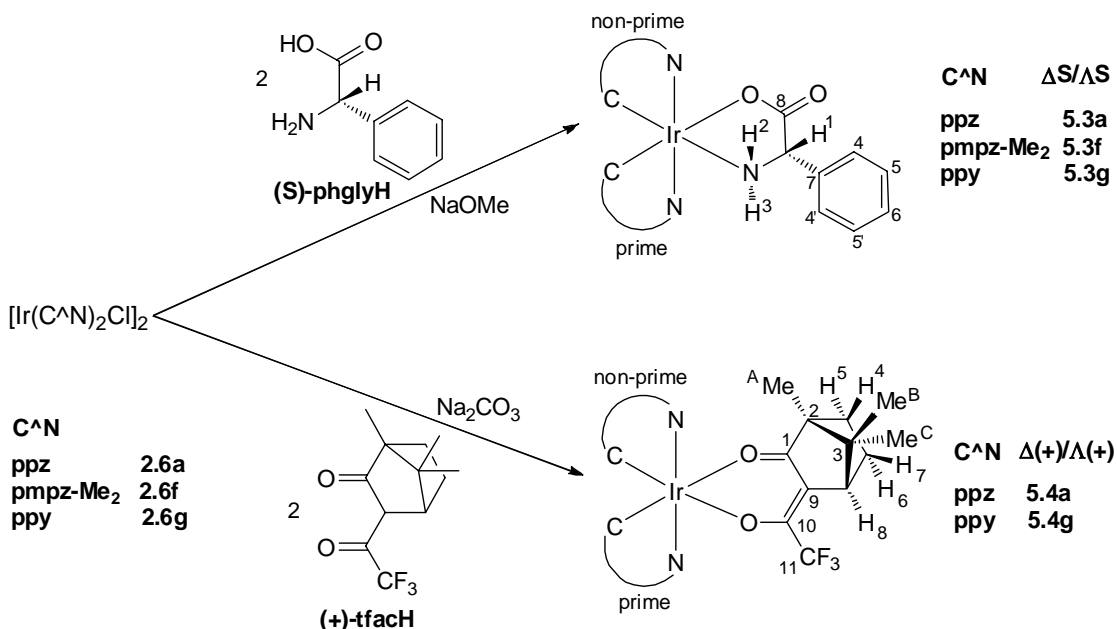


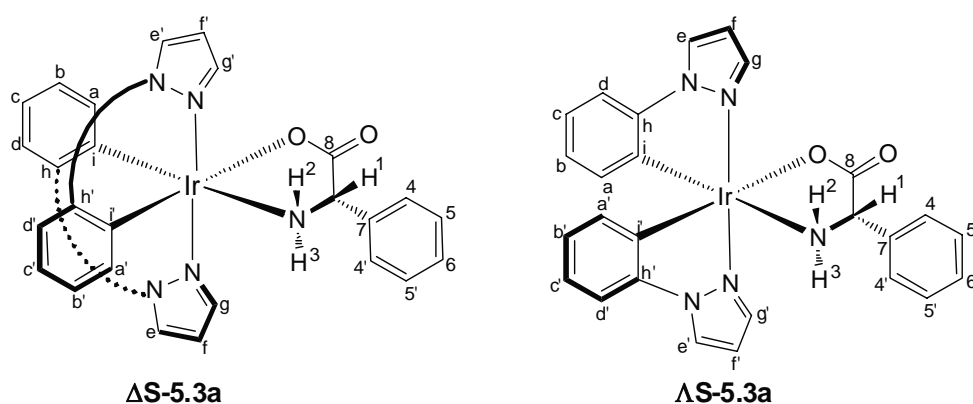
**Fig. 5.18:** CD spectra of  $\Delta S/\Delta S$ -5.2a-c, g respectively.

The dimers **2.6a,f,g** reacted with (S)-phglyH and NaOMe in a mixture of DCM/methanol (2:1) at room temperature for 2-4 hrs, to form compounds **5.3a,f,g** as a 1:1 ratio of diastereomers ( $\Delta S$  and  $\Delta S$ ), in good combined yields (>75%) (**Scheme 5.4**).



**Scheme 5.4**

Similarly compounds  $\Delta(+)/\Lambda(+)$ -**5.4a,g** were synthesised *via* the reaction of dimers **2.6a,g** with (+)-tfacH and  $\text{Na}_2\text{CO}_3$  in a mixture of DCM/methanol (2:1) at room temperature for 1-2 hrs. None of the diastereomers ( $\Delta\text{S}/\Delta\text{S}$ -**5.3a,f,g** or  $\Delta(+)/\Lambda(+)$ -**5.4a,g**) could be separated by any of the techniques attempted (crystallisation or chromatography), however, a ratio of 2:3 ( $\Delta\text{S}:\Delta\text{S}$ ) was observed for **5.3a** after a crystallisation of the product. This ratio did not alter with time (5 days), monitored by  $^1\text{H}$  NMR spectroscopy.



The  $^1\text{H}$  and  $^{13}\text{C}$ -{ $^1\text{H}$ } NMR spectra of complexes  $\Delta\text{S}/\Delta\text{S}$ -**5.3a,f,g** and  $\Delta(+)/\Lambda(+)$ -**5.4a,g** are very complicated due to the presence of both isomers and hence a detailed assignment of the mixture was not possible. However it was possible (see later) to prepare selectively just the  $\Delta\text{S}$  isomer of **5.3a** which helped in the assignment of the spectrum of the mixture. In **5.3a**, the chiral CH protons ( $\text{H}_1$ ) are observed as doublets of doublets at  $\delta$  4.48 ( $\Delta\text{S}$ ) and at *ca.*  $\delta$  4.7 ( $\Delta\text{S}$ ). After several days, the  $\text{NH}_2$  protons ( $\text{H}_2$  and  $\text{H}_3$ ) exchange with  $\text{D}_2\text{O}$  in the MeOD and the  $\text{H}_1$  protons collapse into singlets. The  $\text{H}_1$  signals can also be differentiated from the  $\text{NH}_2$  protons since they show a cross peak in the HSQC spectrum which the  $\text{NH}_2$  do not.  $\text{H}_1$  shows an NOE to only one of the  $\text{NH}_2$  protons ( $\text{H}_2$ ) which helped to distinguish between  $\text{H}_2$  and  $\text{H}_3$ . In the  $\Delta\text{S}$  isomer  $\text{H}_3$  shows an NOE to the pyrazole proton  $\text{H}_g$  (a doublet of doublets at  $\delta$  7.90) confirming their proximity (see H(5B) on N(5) close to H on C(10), **Fig. 5.19**). Proton  $\text{H}_2$  is observed at a higher field in the  $\Delta\text{S}$  isomer ( $\delta$  5.32) relative to the  $\Delta\text{S}$  ( $\delta$  5.93) due to the ring current from the ppz (primes). For the  $\Delta\text{S}$  isomer  $\text{H}_1$  shows an NOE to the pyrazole proton  $\text{H}_g$  ( $\delta$  8.30) and now proton  $\text{H}_3$  is observed at a higher field ( $\delta$  3.86) than in  $\Delta\text{S}$  isomer (*ca.*  $\delta$  4.7) due to ring currents. The  $^{13}\text{C}$ -{ $^1\text{H}$ } NMR spectra show the expected number of signals for the quaternary and CH carbons. The FAB mass spectrum of a 1:1 mixture of the two isomers shows a molecular ion at  $m/z$  630 for  $[\text{M}+\text{H}]^+$ . The specific

rotation for  $\Delta S\text{-5.3a}$  is  $-516.5^\circ$  in MeOH. The X-ray crystal structure of  $\Delta S\text{-5.3a}$  synthesised from  $\Delta\Delta\text{-5.6a}$  was determined and is shown in **Fig. 5.19** with selected bond lengths ( $\text{\AA}$ ) and angles ( $^\circ$ ). CD spectra of  $\Delta S\text{-5.3a}$  and  $\Delta S\text{-5.3a}:\Delta S\text{-5.3a}$  (1:1) are recorded and are displayed in **Fig. 5.20**.

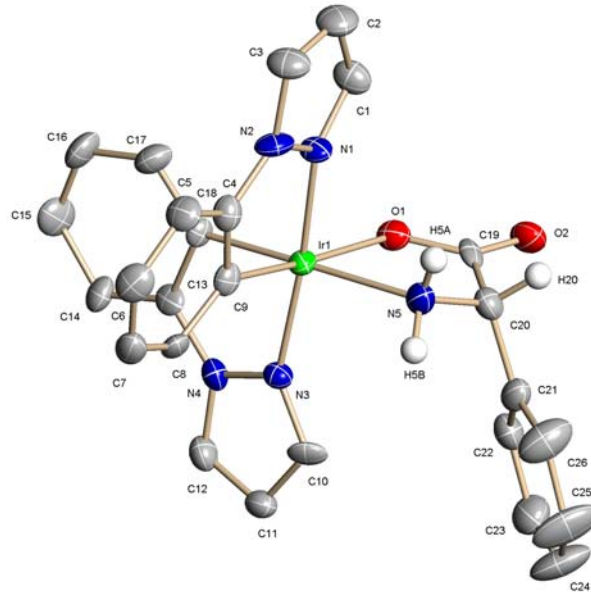


**Fig. 5.19:** X-ray crystal structure of  $\Delta S\text{-5.3a}$ . Selected bond lengths ( $\text{\AA}$ ) and bond angles ( $^\circ$ ): Ir(1)—N(1), 2.015(5); Ir(1)—N(3), 2.024(5); Ir(1)—N(5), 2.198(6); Ir(1)—O(1), 2.168(5); Ir(1)—C(9), 1.994(6); Ir(1)—C(18), 2.010(6); N(1)—Ir(1)—N(3), 175.2(2); N(1)—Ir(1)—C(9), 80.6(3); N(3)—Ir(1)—C(18), 80.4(2); N(5)—Ir(1)—O(1), 77.7(2).

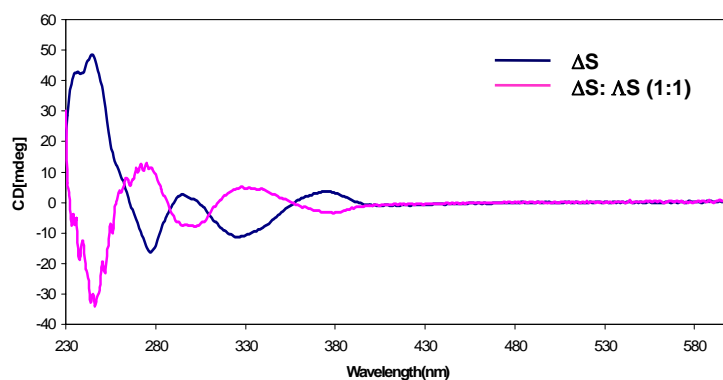
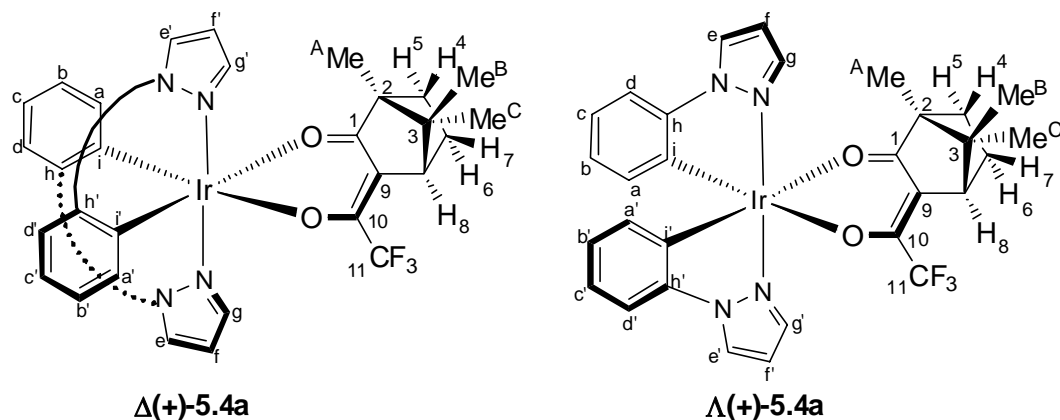


**Fig. 5.20:** CD spectra of  $\Delta S\text{-5.3a}$  and  $\Delta S\text{-5.3a}:\Delta S\text{-5.3a}$  (1:1).

The  $^1\text{H}$  and  $^{13}\text{C}$  NMR spectra of  $\Delta S/\Delta S\text{-5.3f,g}$  are very similar to  $\Delta S/\Delta S\text{-5.3a}$  and also to each other except the signals of the cyclometallated ligands. All assignments were done on the same basis as  $\Delta S/\Delta S\text{-5.3a}$  and the expected NOEs are observed. Proton  $\text{H}_2$  is observed at higher field in the  $\Delta S$  than the  $\Delta S$ , conversely  $\text{H}_3$  is observed at

a lower field in  $\Delta S$  isomer. The  $^{13}\text{C}-\{^1\text{H}\}$  NMR spectra show the expected number of signals for the quaternary and CH carbons. The FAB mass spectra of a 1:1 mixture of the two isomers show molecular ions  $[\text{M}+\text{H}]^+$  at  $m/z$  686 and 652 for **5.3f** and **5.3g** respectively.



Complexes  $\Delta(+)/\Lambda(+)$ -**5.4a,g** have similar  $^1\text{H}$  NMR spectra to  $\Delta\text{S}/\Lambda\text{S}$ -**5.1, 5.2**, **5.3a,g** except for the signals of  $\text{X}^{\text{Y}}$  ligand, (+)-tfac. As for **5.3a** the  $\Delta(+)$  isomer of **5.4a** could be synthesised selectively (see below) which helped in the assignment of the spectrum of the mixture. In the  $\Delta(+)$  isomer, proton  $\text{H}_8$  is identified as the pseudotriplet at  $\delta$  2.85, which shows NOEs to protons  $\text{H}_6$  and  $\text{H}_7$ , and methyls  $\text{Me}_\text{B}$  and  $\text{Me}_\text{C}$ . Proton  $\text{H}_4$  is identified using the COSY and NOESY spectra (shows correlations to  $\text{H}_7$ ) and  $\text{H}_5$  is assigned using the HSQC spectrum.  $\text{Me}_\text{B}$  and  $\text{Me}_\text{C}$  can be differentiated from  $\text{Me}_\text{A}$  as it is the remained only methyl. The methyl signals,  $\text{Me}_\text{B}$  and  $\text{Me}_\text{C}$  can be distinguished by their NOE interactions. Thus  $\text{Me}_\text{C}$  shows correlations to  $\text{H}_4$  and  $\text{H}_7$  whilst  $\text{Me}_\text{B}$  shows an NOE to the pyrazole proton  $\text{H}_\text{g'}$ , which allows the assignment of  $[\text{Ir}(\text{C}^{\text{N}})_2]$  fragment using the COSY and NOESY spectra. The assignment of  $\text{Me}_\text{B}$  and  $\text{Me}_\text{C}$  is confirmed since they both show a cross peak to one carbon signal ( $\text{C}_3$ ) in the HMBC spectrum. In the  $\Lambda(+)$  isomer, the assignment of the (+)-tfac protons is carried out by analogy to the  $\Delta(+)$  isomer, however, now  $\text{Me}_\text{B}$  shows an NOE to  $\text{H}_\text{g}$  rather than  $\text{H}_\text{g'}$ . The chemical shifts are very similar for the same protons in both the isomers, particularly most of the signals for the  $[\text{Ir}(\text{C}^{\text{N}})_2]$  fragment and protons  $\text{H}_4$ ,  $\text{H}_6$  and  $\text{H}_7$  of (+)-tfac, are overlapping multiplets. However,  $\text{H}_5$  is observed at higher field in the  $\Delta(+)$  isomer relative to the  $\Lambda(+)$  isomer ( $\delta$  0.88 vs  $\delta$  1.59 in  $\Delta(+)$ -**5.4a** and  $\Lambda(+)$ -**5.4a** respectively) which is presumably due to the ring currents from a ppz (non-primes) in the  $\Delta(+)$  isomer. The  $^{13}\text{C}-\{^1\text{H}\}$  NMR spectra show the expected number of signals for the

quaternary and CH carbons. The FAB mass spectrum of a 1:1 mixture of the two isomers shows a molecular ion at  $m/z$  726. The specific rotation for  $\Delta(+)$ -**5.4a** is  $-538^\circ$  in DCM and the CD spectra of  $\Delta(+)$ -**5.4a** and  $\Delta(+)$ -**5.4a**: $\Lambda(+)$ -**5.4a** (1:1) are displayed in **Fig. 5.21**. As can be seen the spectrum of the 1:1 mixture of diastereomers is almost a straight line which emphasises that the CD spectrum is dominated by the chirality at the metal rather than at the tfac ligand.

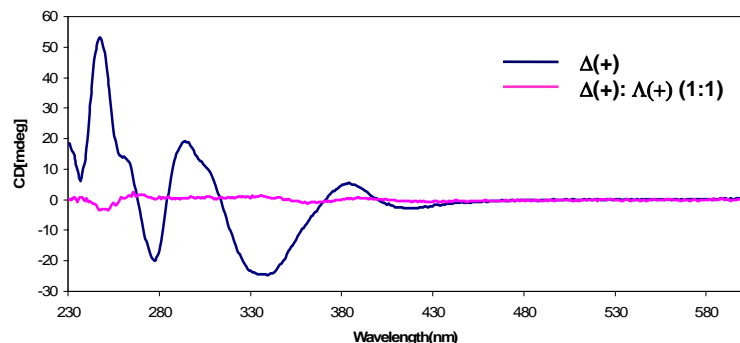
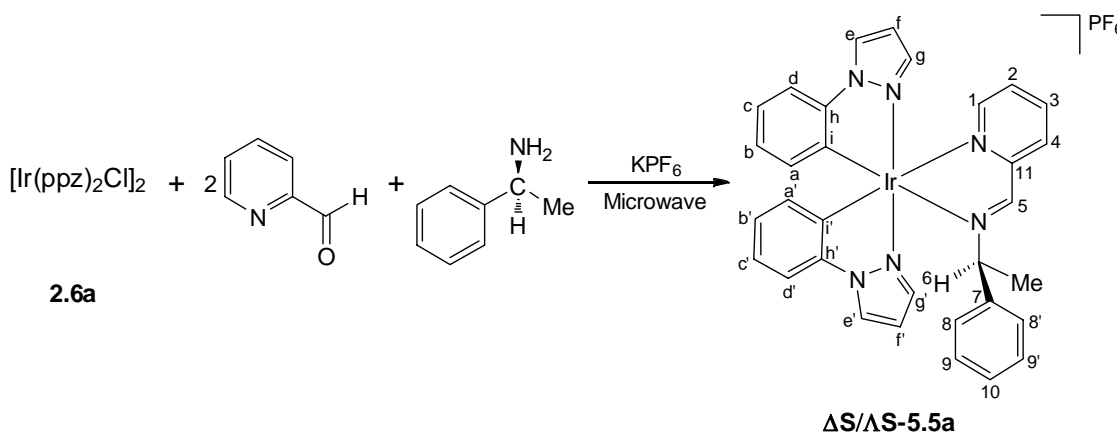


**Fig. 5.21:** CD spectra of  $\Delta(+)$ -**5.4a** and  $\Delta(+)$ -**5.4a**: $\Lambda(+)$ -**5.4a** (1:1).

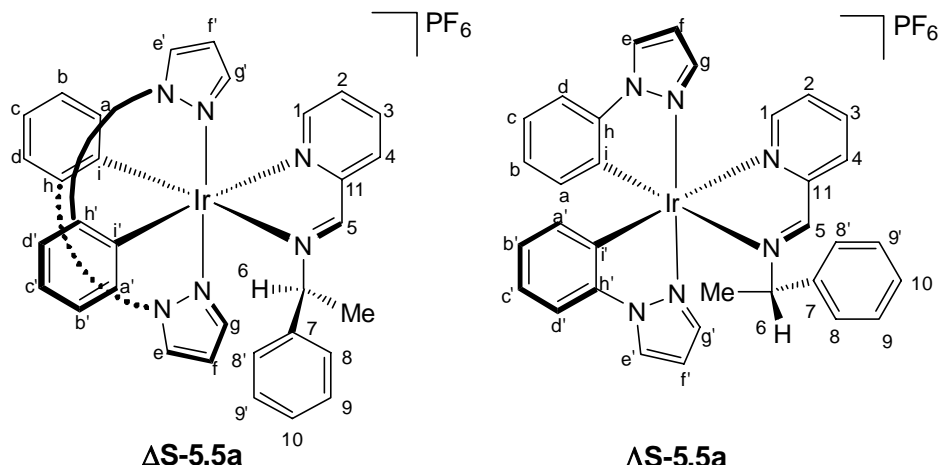
In complex **5.4g** the pyridine rings replaced the pyrazoles of **5.4a**. The  $^1\text{H}$  NMR spectrum of **5.4g** resembles **5.4a** for the signals of (+)-tfac ligand. All the expected NOEs were observed and the assignments were done by analogy to **5.4a**.  $\text{Me}_\text{B}$  shows an NOE to pyridine proton  $\text{H}_\text{h}$  in  $\Delta(+)$  isomer and to  $\text{H}_\text{h}$  in  $\Lambda(+)$  isomer and other ppy protons are assigned *via* the COSY and NOESY spectra.  $\text{H}_8$  shows NOEs to protons  $\text{H}_6$  and  $\text{H}_7$ , and methyls  $\text{Me}_\text{B}$  and  $\text{Me}_\text{C}$  in each isomer. The  $^{13}\text{C}$ -{ $^1\text{H}$ } NMR spectra show the expected number of signals for the quaternary and CH carbons. The FAB mass spectrum of a 1:1 mixture of the two isomers shows a molecular ion at  $m/z$  748.

The complexes discussed above, all contain an anionic  $\text{X}^\wedge\text{Y}$  ligand leading to neutral complexes  $[\text{Ir}(\text{C}^\wedge\text{N})_2(\text{X}^\wedge\text{Y})]$ . It is also possible to use neutral ligands giving cationic complexes. One might expect that stability of the chirality at the metal may be even stronger at a cationic metal centre since dissociation of a ligand is likely to be more difficult. Hence, reaction of the dimer **2.6a** with a chiral pyridineimine was attempted (**Scheme 5.5**).



### Scheme 5.5

The reaction of dimer **2.6a** with pyridine-2-carboxaldehyde, KPF<sub>6</sub> and (S)-phenylethylamine was carried out in methanol at 60 °C under microwave irradiation for 20 mins, and gave **5.5a** in 65% yield (**Scheme 5.5**).



The  $^1\text{H}$  NMR spectrum of **5.5a** shows a 1:1 ratio of diastereomers. As for **5.3a** and **5.4a** it was possible (see later) to prepare selectively just the  $\Delta\text{S}$  isomer which helped in the assignment of the spectrum of the mixture. The imine protons  $\text{H}_5$  are easily identified as the most downfield signals, at  $\delta$  10.76 in  $\Delta\text{S-5.5a}$ , and  $\delta$  10.84 in  $\Delta\text{S-5.5a}$  and show NOEs to two doublets at  $\delta$  9.44 and 9.37 which are therefore assigned as  $\text{H}_4$  and the COSY spectrum then allows assignment of protons  $\text{H}_1$ ,  $\text{H}_2$  and  $\text{H}_3$  for each isomer. For the  $\Delta\text{S}$  isomer,  $\text{H}_5$  also shows NOEs to  $\text{H}_6$ ,  $\text{H}_{8,8'}$  and the methyl, however, for the  $\Delta\text{S}$  isomer  $\text{H}_5$  shows NOEs only to  $\text{H}_6$  and  $\text{H}_{8,8'}$ , which helped to assign all protons of (S)-phenylethylimine ligand for both of the isomers. In the  $\Delta\text{S}$

isomer the ppz (non-prime) is pointing towards the imine substituent. This gives rise to NOEs between the pyrazole proton  $H_g$  and both the methyl and  $H_6$ .  $H_6$  also show an NOE to  $H_{a'}$  on the other ppz (prime). In the  $\Delta S$  isomer the corresponding NOE is between the ppz proton (prime)  $H_{a'}$  and the methyl. Unlike in the pep complexes **5.2**, in neither diastereomer of **5.5a** is there any evidence for ring currents having a marked effect on the chemical shifts of  $H_6$  or the methyl. This is probably because the pyridineimine forms a 5-membered chelate, compared with a 6-membered chelate for **5.2**, hence the  $CH(Me)Ph$  substituent is angled more away from the metal. All other assignments of the ppz ligands are made using the COSY and the NOESY spectra. The  $^{13}C-\{^1H\}$  NMR spectra show the expected number of signals for the quaternary and CH carbons. The FAB mass spectrum of a 1:1 mixture of the two isomers shows a molecular ion at  $m/z$  689. The specific rotation is  $-614^\circ$  (in DCM) for  $\Delta S$ -**5.5a** and the CD spectra of  $\Delta S$ -**5.5a** and  $\Delta S$ -**5.5a**: $\Delta S$ -**5.5a** (1:1) are shown in **Fig. 5.22**.

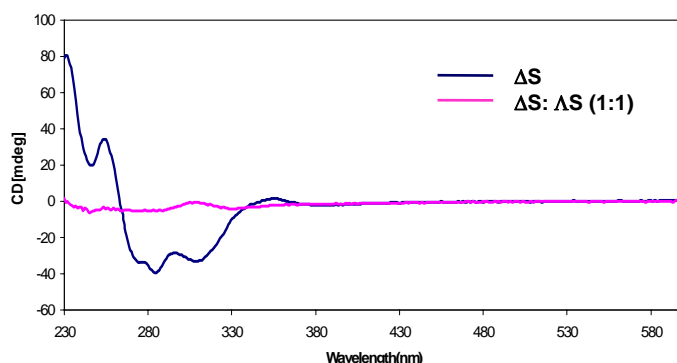
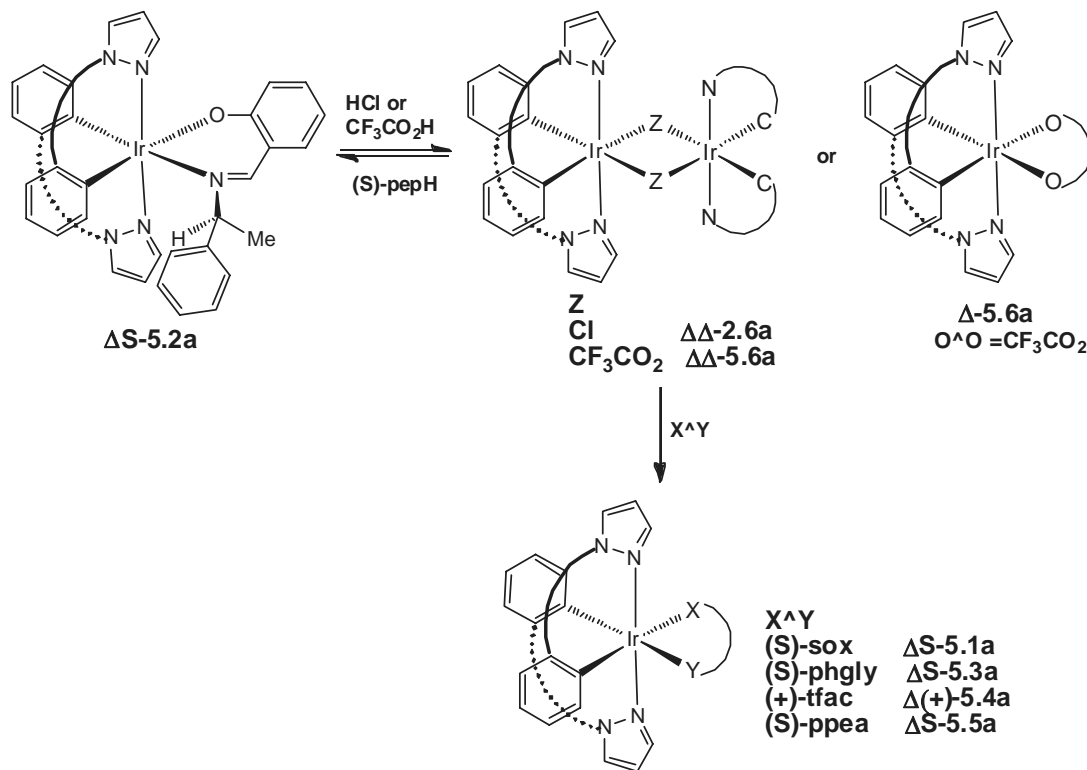


**Fig. 5.22:** CD spectra of  $\Delta S$ -**5.5a** and  $\Delta S$ -**5.5a**: $\Delta S$ -**5.5a** (1:1).

In conclusion, neutral complexes **5.1-5.4** and the cationic one **5.5** can be easily synthesised in high yields, in all cases a 1:1 mixture of diastereomers was seen in the NMR spectra of the crude reaction mixtures. Diastereomers of the (S)-soxH and (S)-pepH ligands can often be separated *via* crystallisation and in some cases by column chromatography, hence, these ligands are regarded as useful for separating the  $\Delta$  and  $\Lambda$  forms of  $[Ir(C^N_2(X^Y)]$  complexes. In terms of cyclometallated ligands, in general, with complexes of ppz or substituted ppz ligands (*i.e.* ppz- $R_1$ ) one isomer could be crystallised selectively by selecting appropriate conditions, however with ppy complexes separation of diastereomers often relied on crystal picking. For both **5.2a** and **5.2g** the chirality at the metal is stable up to  $120^\circ C$  in solution and for none of the complexes was any racemisation noted even though no precautions were taken to

protect the solutions from light. Having separated single diastereomers the next step was to see if these could be converted back to enantiomers by removal of the  $X^Y$  ligand without racemisation at the metal. These experiments are described below.

### 5.2.2 Synthesis of homochiral dimers and homochiral complexes



**Scheme 5.6**

As stated earlier, the next step is to convert a single diastereomer to a homochiral dimer  $\Delta\Delta$  or  $\Lambda\Lambda$   $[\text{Ir}(\text{C}^{\text{N}})^2\text{X}]_2$  with only metal-centred chirality. To do this, the anionic  $X^Y$  ligand is removed by treatment with an acid. The first attempt involved bubbling  $\text{HCl(g)}$  through a DCM solution of pure **5.2a** for 2 mins. The product was isolated and identified as  $[\text{Ir}(\text{ppz})_2\text{Cl}]_2$  (**2.6a**) by  $^1\text{H}$  NMR spectroscopy and ESMS. The chirality at metal centre was not determined at this stage, as the two enantiomers can not be distinguished by simple NMR spectroscopy. To determine the chirality at the metal the dimer obtained in the previous step was reacted with (S)-pepH which gave **5.2a** in a diastereomeric ratio (*d.r.*) of 1.3:1,  $\Delta\text{S}:\Delta\text{S}$ . Hence, some racemisation has occurred, probably due to the protonation of a metallated carbon(s) on treatment with  $\text{HCl}$  (Fig. 5.23). In order to racemise at the metal centre it is necessary to either dissociate both N

donors or to break one M-C bond. As mentioned previously (**Chapter 2**) *mer/fac* isomerisation of  $[\text{Ir}(\text{C}^{\wedge}\text{N})_3]$  complexes<sup>58, 59</sup> requires breaking an M-C bond and is accelerated in the presence of acid. Reversal of cyclometallation by treatment with acid is also known for half-sandwich cyclometallated complexes of Ir.<sup>60</sup> Hence the high acidity of  $\text{HCl(g)}$  may be opening a  $\text{C}^{\wedge}\text{N}$  chelate as shown in **Fig. 5.23**. In support of this explanation, reducing the bubbling time from 2 mins to 1 min improved the d.r. to 4:1 ( $\Delta\text{S}:\Delta\text{S}$ ), *i.e.* lead to less racemisation. Hence a weaker acid is required as discussed below.

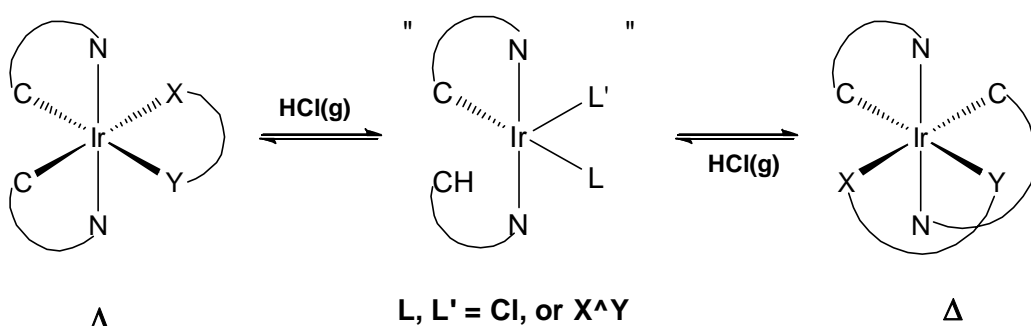


**Fig. 5.23:** Possible mechanism for racemisation in  $[\text{Ir}(\text{C}^{\wedge}\text{N})_2(\text{X}^{\wedge}\text{Y})]$  complexes.

**ΔS-5.2a** was reacted with TFA (pH 2) in a biphasic mixture of DCM: $\text{H}_2\text{O}$  (1:1) at room temperature for 48 hrs. Monitoring the reaction by  $^1\text{H}$  NMR spectroscopy showed a spectrum very similar to that of **2.6a** discussed in **Chapter 2**, however, the chemical shifts vary slightly, possibly since this contains  $\text{CF}_3\text{CO}_2$  rather than Cl. Pyrazole proton  $\text{H}_e$  is observed as a doublet and is the most downfield signal at  $\delta$  8.10 similar to **2.6a** ( $\delta$  8.19).  $\text{H}_e$  shows an NOE to a doublet of doublets at  $\delta$  7.13 which is assigned as  $\text{H}_d$  ( $\delta$  7.19 in **2.6a**). Having assigned  $\text{H}_d$  and  $\text{H}_e$  other phenyl ( $\text{H}_{a-c}$ ) and pyrazole ( $\text{H}_{f,g}$ ) protons are assigned using the COSY spectrum. The FAB mass spectrum shows an ion at  $m/z$  1071 corresponding to  $[\text{Ir}_2(\text{ppz})_4\text{CF}_3\text{CO}_2]^+$  hence the product is proposed to be dimer **5.6a**, which is formed in high yield (81%) (**Scheme 5.6**). Note, it is possible that **5.6a** could be a monomer with a chelating trifluoroacetate ( $\text{CF}_3\text{CO}_2$ ), however the mass spectrum favours a dimer. During the reaction the (S)-pep decomposed slowly to give salicylaldehyde and (S)-(-)-1-phenylethylammonium trifluoroacetate (confirmed by the independent reaction of the ligand (S)-pepH with TFA), which were separated from **5.6a** through precipitation of **5.6a** from DCM/hexane.

A sample of **5.6a** was crystallised from DCM/hexane and gave crystals suitable for X-ray diffraction. Surprisingly the structure showed a monomeric complex **Δ-5.7a** containing one  $\text{CF}_3\text{CO}_2$  and one water molecule as the X/Y ligands. The X-ray crystal structure is shown in **Fig. 5.24** with selected bond lengths ( $\text{\AA}$ ) and angles ( $^\circ$ ).

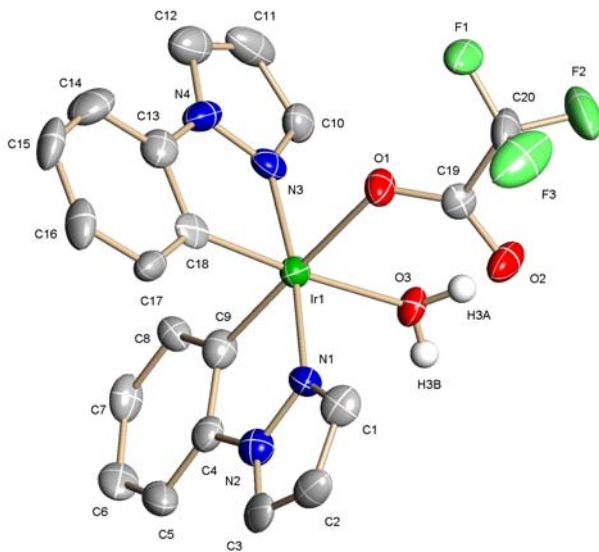


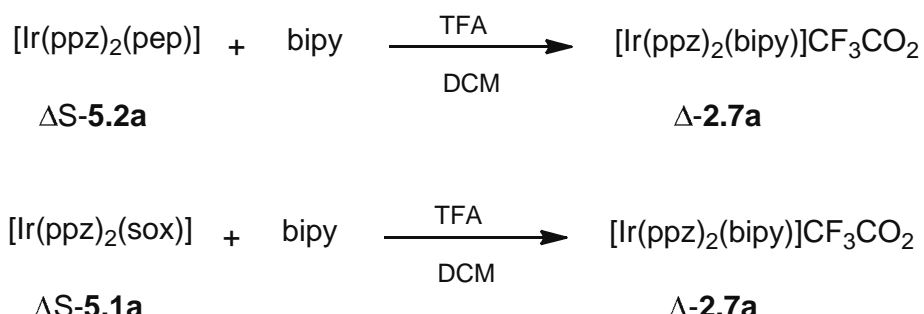
**Fig. 5.24:** X-ray crystal structure of **Δ-5.7a**. Selected bond lengths ( $\text{\AA}$ ) and bond angles ( $^\circ$ ): Ir(1)—N(1), 2.014(9); Ir(1)—N(3), 1.991(9); Ir(1)—O(1), 2.185(7); Ir(1)—O(3), 2.222(7); Ir(1)—C(9), 1.964(10); Ir(1)—C(18), 1.983(12); N(1)—Ir(1)—N(3), 172.8(4); N(1)—Ir(1)—C(9), 80.3(4); N(3)—Ir(1)—C(18), 80.9(4); O(1)—Ir(1)—O(3), 86.8(3).

To determine the chirality at the metal centre, the sample of **5.6a** was reacted with (S)-soxH and (S)-pepH which gave **ΔS-5.1a** and **ΔS-5.2a** respectively, in good yields (>70%), in each case as a single diastereomer. There was no evidence by  $^1\text{H}$  NMR spectroscopy for any AS isomer in either case. Thus, the overall process has occurred with retention of configuration at the metal with no racemisation.

To further prove the enantiopurity of **ΔΔ-5.6a** it was reacted with (S)-phglyH, (+)-tfacH and (S)-ppea (generated *in situ* from pyridine-2-carboxaldehyde and (S)-phenylethylamine) to form pure compounds **ΔS-5.3a**, **Δ(+)-5.4a** and **ΔS-5.5a** in good yields (>72%). In each case the  $^1\text{H}$  NMR spectrum of the crude products showed no evidence for the other diastereomer which suggests that the starting **ΔΔ-5.6a** was of high optical purity and that therefore the chirality at the metal centre is stable to TFA at least for 3 days. The  $^1\text{H}$  NMR spectra of **ΔS-5.3a**, **Δ(+)-5.4a** and **ΔS-5.5a** were used in

the assignment of the inseparable mixtures *i.e.*  $\Delta S/\Delta S\text{-5.3a}$ ,  $\Delta(+)/\Delta(+)\text{-5.4a}$  and  $\Delta S/\Delta S\text{-5.5a}$  and have been discussed above.

To try and access  $\Lambda\Lambda\text{-5.6a}$  a  $\Lambda$  starting material is required. Since  $\Delta S\text{-5.1a}$  crystallises readily (see above) this was chosen for reaction with TFA. Monitoring the reaction by  $^1\text{H}$  NMR spectroscopy showed formation of **5.6a** and (S)-soxH which was stable and did not decompose in the presence of TFA and  $\text{H}_2\text{O}$ . The reaction mixture was washed with water ( $3 \times 5$  ml) to remove TFA. Unfortunately, this led to the starting material *i.e.*  $\Delta S\text{-5.1a}$ , presumably due to the deprotonation of the (S)-soxH ligand, however, no racemisation was observed. Hence this reaction works but a different work up procedure is required.



**Scheme 5.7**

Having established that a homochiral dimer is easily accessible, it only remained to convert it into a complex with an achiral bidentate ligand to make a complex in which the only chirality is at the metal. In an attempt to improve the overall process it was decided to attempt this in one pot (**Scheme 5.7**). Thus,  $\Delta S\text{-5.2a}$  was reacted with TFA then bipy in one pot to form  $\Delta\text{-2.7a}$  in 72% yield. Using a similar procedure  $\Lambda\text{-2.7a}$  was synthesised from  $\Lambda S\text{-5.1a}$ . Clearly in the presence of TFA and bipy recoordination of the sox ligand is not a problem. The complexes  $\Delta\text{-2.7a}$  and  $\Lambda\text{-2.7a}$  were purified by precipitation from DCM/hexane. The  $^1\text{H}$  NMR spectrum of the enantiomers  $\Delta\text{-2.7a}$  and  $\Lambda\text{-2.7a}$  are identical, as expected, however, they differ to the NMR spectrum of **2.7a** discussed in **Chapter 2** which can be ascribed to the different counterions in the two complexes ( $\text{PF}_6$  in **Chapter 2** and  $\text{CF}_3\text{CO}_2$  in  $\Delta\text{-2.7a}$  and  $\Lambda\text{-2.7a}$ ). The major differences in chemical shifts are observed for the bipy protons  $\text{H}_3$  and  $\text{H}_4$ . Thus  $\text{H}_3$  and  $\text{H}_4$  are observed at  $\delta$  8.06 and 8.40 for the  $\text{PF}_6$  salt *vs*  $\delta$  8.23 and 9.23 in the  $\text{CF}_3\text{CO}_2$ . The shift to lower field for the  $\text{CF}_3\text{CO}_2$  is consistent with hydrogen

bonding between proton H<sub>4</sub> and the CF<sub>3</sub>CO<sub>2</sub>. The enantiomers have equal and opposite specific rotation, -471° for  $\Delta$ -**2.7a** and +473° for  $\Lambda$ -**2.7a** in DCM. The CD spectra of  $\Delta$ -**2.7a** and  $\Lambda$ -**2.7a** are displayed in **Fig. 5.25** and are mirror images in contrast to the diastereomers **5.1** and **5.2** discussed above.

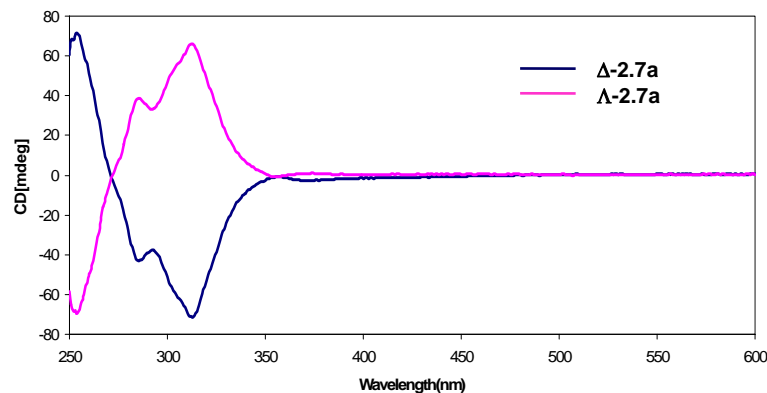


**Fig. 5.25:** CD spectra of  $\Delta$ -**2.7a** and  $\Lambda$ -**2.7a**.

In conclusion, these results demonstrate that sox and pep ligands can be easily removed from the metal by treatment with an acid. Use of HCl(g) was accompanied by some racemisation at the metal, however using TFA gave a homochiral dimer ( $\Delta\Delta$ -**5.6a** or  $\Lambda\Lambda$ -**5.6a**). The homochiral dimer,  $\Delta\Delta$ -**5.6a** was then used to synthesise diastereomerically pure complexes (**5.1a**, **5.2a**, **5.3a**, **5.4a** and **5.5a**). The enantiomerically pure complexes  $\Lambda$ -**2.7a** and  $\Delta$ -**2.7a** were synthesised from the diastereomers  $\Delta S$ -**5.1a** and  $\Delta S$ -**5.2a** respectively. The sequence of protonation of X<sup>Y</sup> then addition of another ligand can be done in one pot as shown for  $\Lambda$ -**2.7a** and  $\Delta$ -**2.7a**. The chirality at the metal in complexes  $[\text{Ir}(\text{C}^{\text{N}})_2(\text{X}^{\text{Y}})]^{n+}$  ( $n = 0, 1$ ) is stable at room temperature in solution and in many cases up to 120 °C. In addition, there was no evidence for photochemical racemisation at least under natural sunlight. This work will pave the way for the use of enantiopure Ir(III) complexes in many fields such as DNA probes which have previously relied heavily on Ru(II) polypyridine complexes. The greater synthetic flexibility of the Ir(III) complexes  $[\text{Ir}(\text{C}^{\text{N}})_2(\text{X}^{\text{Y}})]^{n+}$  suggests more sophisticated experiments may be possible with these complexes.

### 5.3 Experimental

#### General information and materials

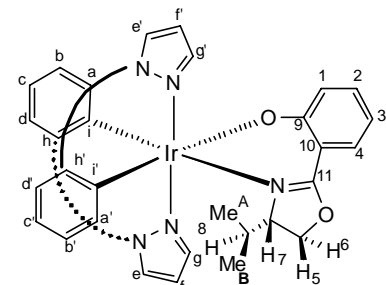
All reactions involving the syntheses of chiral Ir(III) complexes (**5.1-5.4**) were carried out at room temperature in air unless stated otherwise. After work up all the complexes were air- and photo-stable. The spectroscopic techniques/instruments used were as described in **Chapter 2** except the CD spectra were recorded on a JASCO J-715 CD spectropolarimeter (230-600 nm, 1 nm band width, scanning speed of 50 nm/min, accumulation of 2 scans) and the specific rotation values were determined with a Perkin-Elmer 341 polarimeter using a 10 cm cell and at a concentration 1 mM. All starting materials were obtained from Aldrich or Alfa Aesar with the exception of (S)-soxH and (S)-pepH ligands which were prepared according to the literature methods.<sup>53, 54</sup>

#### General procedure for synthesis of $[\text{Ir}(\text{C}^{\wedge}\text{N})_2(\text{X}^{\wedge}\text{Y})]$ ( $\text{X}^{\wedge}\text{Y} = (\text{S})\text{-pep, (S)-sox, (S)-phgly, (+)-tfac}$ )

The general procedure was as follows unless stated otherwise. A mixture of the chiral ligand ( $\text{X}^{\wedge}\text{Y} = (\text{S})\text{-pepH, (S)-soxH, (S)-phglyH, (+)-tfacH}$ ) (2.2-2.4 equiv) and an equimolar amount of NaOMe ( $\text{Na}_2\text{CO}_3$  in tfac complexes  $\Delta(+)/\Lambda(+)$ -**5.4a,g**) in methanol (3 ml) was warmed gently at 40 °C for 15 mins. A solution of the appropriate dimer  $[\text{Ir}(\text{C}^{\wedge}\text{N})_2\text{Cl}]_2$  **2.1a,b** (1 equiv) in DCM (6 ml) was added and the mixture was stirred for 2-4 hrs at room temperature. After this time the solvent was removed *in vacuo* and the residue was dissolved in DCM (15 ml) and passed through celite. The filtrate was reduced in volume and hexane was added slowly to induce precipitation. The precipitate was isolated, washed with hexane and dried *in vacuo*.

#### Synthesis of $\Delta\text{S}/\Lambda\text{S}$ -**5.1a**

This was prepared from dimer **2.6a** (140 mg, 0.136 mmol), (S)-soxH (61.3 mg, 0.299 mmol), and NaOMe (16.2 mg, 0.299 mmol) and after work up gave  $\Delta\text{S}/\Lambda\text{S}$ -**5.1a** as a grey solid (combined yield 157 mg, 85%). Slow diffusion of hexane into a DCM solution of **5.1a** afforded selectively crystals of  $\Lambda\text{S}$  isomer, the  $\Delta\text{S}$  isomer was obtained from the mother liquor, which was enriched in the  $\Delta\text{S}$ -**5.1a** isomer, by recrystallisation from methanol/diethylether. Anal. Calcd for  $\text{C}_{30}\text{H}_{28}\text{IrN}_5\text{O}_2$ : C,

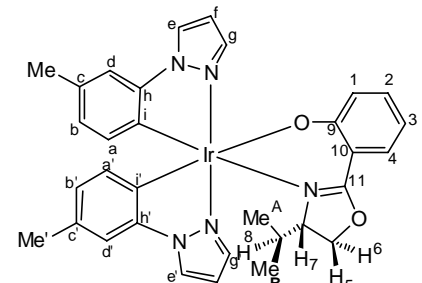
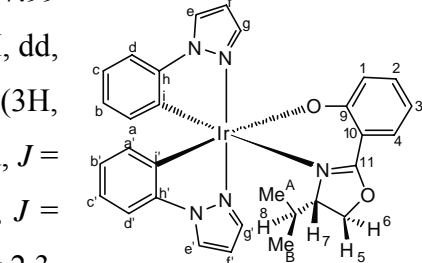


52.77, H, 4.13, N, 10.26. Found ( $\Delta S$ ): C, 52.68, H, 4.12, N, 10.17%.  $^1\text{H}$  NMR ( $\text{CDCl}_3$ )  $\Delta S$ :  $\delta$  8.05, 8.03 (2H, 2  $\text{X}$  d,  $J$  = 2.7,  $\text{H}_{\text{e}, \text{e}'}$ ), 7.63 (1H, d,  $J$  = 2.3,  $\text{H}_{\text{g}}$ ), 7.60 – 7.57 (2H, m,  $\text{H}_{\text{4, g}}$ ), 7.17 – 7.09 (3H, m,  $\text{H}_{\text{2, d, d}'}$ ), 6.84 (1H, td,  $J$  = 7.4, 1.2,  $\text{H}_{\text{c}}$ ), 6.80 (1H, td,  $J$  = 7.8, 1.2,  $\text{H}_{\text{c}}$ ), 6.67 (1H, d,  $J$  = 7.8,  $\text{H}_{\text{l}}$ ), 6.64 – 6.58 (3H, m,  $\text{H}_{\text{b, b', f}}$ ), 6.52 (1H, t,  $J$  = 2.7,  $\text{H}_{\text{f}}$ ), 6.37 (1H, dd,  $J$  = 7.8, 1.6,  $\text{H}_{\text{a}}$ ), 6.33 (1H, ddd,  $J$  = 7.8, 6.7, 1.2,  $\text{H}_{\text{3}}$ ), 6.21 (1H, dd,  $J$  = 7.4, 1.2,  $\text{H}_{\text{a}}$ ), 4.18 (1H, dd,  $J$  = 8.9, 3.9,  $\text{H}_{\text{6}}$ ), 3.76 (1H, t,  $J$  = 8.9,  $\text{H}_{\text{5}}$ ), 3.04 (1H, ddd,  $J$  = 9.4, 3.5, 1.9,  $\text{H}_{\text{7}}$ ), 2.01 (1H, septd,  $J$  = 7.0, 1.9,  $\text{H}_{\text{8}}$ ), 0.89 (3H, d,  $J$  = 7.0,  $\text{Me}_{\text{A}}$ ), 0.33 (3H, d,  $J$  = 7.0,  $\text{Me}_{\text{B}}$ ).  $^{13}\text{C}$  NMR: 169.82 ( $\text{C}_{\text{9}}$ ), 161.58 ( $\text{C}_{\text{11}}$ ), 144.06 ( $\text{C}_{\text{h}}$ ), 143.87 ( $\text{C}_{\text{h}'}$ ), 139.13 ( $\text{C}_{\text{g}}$ ), 138.26 ( $\text{C}_{\text{g}'}$ ), 135.89 ( $\text{C}_{\text{a}'}$ ), 134.84 ( $\text{C}_{\text{i}}$ ), 134.28 ( $\text{C}_{\text{a}}$ ), 132.96 ( $\text{C}_{\text{2}}$ ), 130.23 ( $\text{C}_{\text{i}'}$ ), 129.39 ( $\text{C}_{\text{4}}$ ), 125.77, ( $\text{C}_{\text{b}}$ ), 125.62 ( $\text{C}_{\text{b}'}$ ), 125.23 ( $\text{C}_{\text{e}, \text{e}'}$ ), 124.76 ( $\text{C}_{\text{l}}$ ), 121.52 ( $\text{C}_{\text{c}}$ ), 120.78 ( $\text{C}_{\text{c}'}$ ), 112.33 ( $\text{C}_{\text{3}}$ ), 110.59, 110.43 ( $\text{C}_{\text{d, d}'}$ ), 110.25 ( $\text{C}_{\text{10}}$ ), 107.07 ( $\text{C}_{\text{f}}$ ), 106.84 ( $\text{C}_{\text{f}}$ ), 70.74 ( $\text{C}_{\text{7}}$ ), 66.41 ( $\text{C}_{\text{5, 6}}$ ), 28.89 ( $\text{C}_{\text{8}}$ ), 19.21 ( $\text{Me}_{\text{B}}$ ), 14.37 ( $\text{Me}_{\text{A}}$ ).  $[\alpha]_{\text{D}} -593^\circ$  in  $\text{CHCl}_3$ .

$^1\text{H}$  NMR ( $\text{CDCl}_3$ )  $\Delta S$ :  $\delta$  8.07 (1H, d,  $J$  = 2.9,  $\text{H}_{\text{e}'}$ ), 7.99 (1H, d,  $J$  = 2.9,  $\text{H}_{\text{e}}$ ), 7.80 (1H, d,  $J$  = 2.1,  $\text{H}_{\text{g}'}$ ), 7.62 (1H, dd,  $J$  = 7.9, 1.8,  $\text{H}_{\text{4}}$ ), 7.43 (1H, d,  $J$  = 2.3,  $\text{H}_{\text{g}}$ ), 7.15 – 7.09 (3H, m,  $\text{H}_{\text{2, d, d}'}$ ), 6.84 (1H, td,  $J$  = 7.6, 1.5,  $\text{H}_{\text{c}}$ ), 6.80 (1H, td,  $J$  = 7.6, 1.5,  $\text{H}_{\text{c}}$ ), 6.73 – 6.67 (2H, m,  $\text{H}_{\text{l, b}}$ ), 6.63 (1H, t,  $J$  = 2.3,  $\text{H}_{\text{f}}$ ), 6.61 (1H, td,  $J$  = 7.3, 1.2,  $\text{H}_{\text{b}}$ ), 6.52 (1H, t,  $J$  = 2.3,  $\text{H}_{\text{f}}$ ), 6.34 (1H, ddd,  $J$  = 7.8, 6.7, 0.8,  $\text{H}_{\text{3}}$ ), 6.29 (1H, dd,  $J$  = 7.6, 1.5,  $\text{H}_{\text{a}'}$ ), 6.18 (1H, dd,  $J$  = 7.6, 1.5,  $\text{H}_{\text{a}}$ ), 4.29 – 4.18 (2H, m,  $\text{H}_{\text{5, 6}}$ ), 3.93 (1H, ddd,  $J$  = 8.8, 4.4, 3.2,  $\text{H}_{\text{7}}$ ), 0.53 (1H, septd,  $J$  = 7.0, 3.1,  $\text{H}_{\text{8}}$ ), 0.28 (3H, d,  $J$  = 7.0,  $\text{Me}_{\text{B}}$ ), 0.20 (3H, d,  $J$  = 6.7,  $\text{Me}_{\text{A}}$ ).  $^{13}\text{C}$  NMR: 170.08 ( $\text{C}_{\text{9}}$ ), 161.66 ( $\text{C}_{\text{11}}$ ), 144.60 ( $\text{C}_{\text{h}'}$ ), 143.89 ( $\text{C}_{\text{h}}$ ), 138.19 ( $\text{C}_{\text{g}'}$ ), 137.01 ( $\text{C}_{\text{g}}$ ), 135.14 ( $\text{C}_{\text{i}}$ ), 134.25 ( $\text{C}_{\text{a}'}$ ), 133.83 ( $\text{C}_{\text{a}}$ ), 133.16 ( $\text{C}_{\text{2}}$ ), 129.95 ( $\text{C}_{\text{i}'}$ ), 129.61 ( $\text{C}_{\text{4}}$ ), 125.78, 125.75 ( $\text{C}_{\text{1, b}'}$ ), 125.49 ( $\text{C}_{\text{b}}$ ), 125.27 ( $\text{C}_{\text{e}}$ ), 124.55 ( $\text{C}_{\text{e}'}$ ), 121.55 ( $\text{C}_{\text{c}}$ ), 120.91 ( $\text{C}_{\text{c}'}$ ), 112.42 ( $\text{C}_{\text{3}}$ ), 110.54 ( $\text{C}_{\text{d}}$ ), 110.36 ( $\text{C}_{\text{10}}$ ), 110.21 ( $\text{C}_{\text{d}'}$ ), 107.04 ( $\text{C}_{\text{f}}$ ), 106.73 ( $\text{C}_{\text{f}}$ ), 71.75 ( $\text{C}_{\text{7}}$ ), 66.51 ( $\text{C}_{\text{5, 6}}$ ), 28.42 ( $\text{C}_{\text{8}}$ ), 18.58 ( $\text{Me}_{\text{B}}$ ), 12.87 ( $\text{Me}_{\text{A}}$ ).  $[\alpha]_{\text{D}} +582^\circ$  in  $\text{CHCl}_3$ . MS (FAB):  $m/z$  683  $[\text{M}]^+$ .

### Synthesis of $\Delta S/\Delta S\text{-5.1b}$

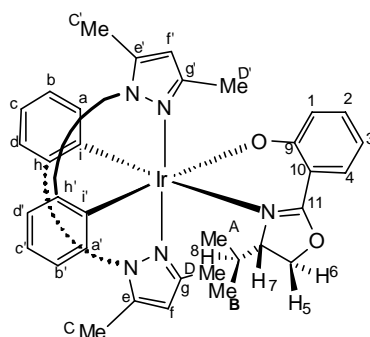
This was prepared from dimer **2.6b** (70 mg, 0.065 mmol), (S)-soxH (29.3 mg, 0.143 mmol), and NaOMe (7.7 mg, 0.143 mmol) and after work up gave  $\Delta S/\Delta S\text{-5.1b}$  as a yellow solid (combined yield



78 mg, 85%). **ΔS/ΔS-5.1b** could not be separated. Anal. Calcd for  $C_{32}H_{32}IrN_5O_2$ : C, 54.07, H, 4.54, N, 9.85. Found (ΔS:ΔS 1:1): C, 53.97, H, 4.47, N, 9.80%.  $^1H$  NMR (CDCl<sub>3</sub>): δ 8.03 (1H, dd,  $J$  = 2.7, 0.8, H<sub>e'(ΔS)</sub>), 8.00 – 7.99 (2H, m, H<sub>e, e'(ΔS)</sub>), 7.94 (1H, dd,  $J$  = 2.7, 0.8, H<sub>e(ΔS)</sub>), 7.78 (1H, dd,  $J$  = 2.3, 0.8, H<sub>g'(ΔS)</sub>), 7.63 – 7.57 (3H, m, H<sub>4, g'(ΔS), 4(ΔS)</sub>), 7.55 (1H, d,  $J$  = 2.3, H<sub>g(ΔS)</sub>), 7.40 (1H, d,  $J$  = 2.7, H<sub>g(ΔS)</sub>), 7.10 (2H, 2 X ddd,  $J$  = 8.6, 6.7, 1.9, H<sub>2(ΔS), 2(ΔS)</sub>), 6.98 – 6.97 (2H, m, H<sub>d, d'(ΔS)</sub>), 6.95 (1H, d,  $J$  = 0.8, H<sub>d'(ΔS)</sub>), 6.92 (1H, d,  $J$  = 0.8, H<sub>d(ΔS)</sub>), 6.68, 6.67 (2H, 2 X dd,  $J$  = 8.6, 1.2, H<sub>1(ΔS), 1(ΔS)</sub>), 6.59 (1H, t,  $J$  = 2.3, H<sub>f(ΔS)</sub>), 6.55 – 6.44 (7H, m, H<sub>b, b', f(ΔS), b, b', f(ΔS)</sub>), 6.34 – 6.29 (2H, m, H<sub>3(ΔS), 3(ΔS)</sub>), 6.24 (1H, d,  $J$  = 7.4, H<sub>a'(ΔS)</sub>), 6.15 (1H, d,  $J$  = 7.8, H<sub>a'(ΔS)</sub>), 6.07 (1H, d,  $J$  = 7.4, H<sub>a(ΔS)</sub>), 6.05 (1H, d,  $J$  = 7.4, H<sub>a(ΔS)</sub>), 4.25 (1H, dd,  $J$  = 8.9, 3.9, H<sub>6(ΔS)</sub>), 4.19 (1H, t,  $J$  = 8.9, H<sub>5(ΔS)</sub>), 4.16 (1H, dd,  $J$  = 8.9, 3.9, H<sub>6(ΔS)</sub>), 3.93 (1H, ddd,  $J$  = 9.4, 4.3, 3.1, H<sub>7(ΔS)</sub>), 3.74 (1H, t,  $J$  = 8.9, H<sub>5(ΔS)</sub>), 3.05 (1H, ddd,  $J$  = 9.4, 3.5, 1.2, H<sub>7(ΔS)</sub>), 2.19 – 2.17 (12H, m, Me, Me<sub>(ΔS)</sub>, Me, Me<sub>(ΔS)</sub>), 2.04 (1H, septd,  $J$  = 7.0, 1.9, H<sub>8(ΔS)</sub>), 0.88 (3H, d,  $J$  = 7.0, Me<sub>A(ΔS)</sub>), 0.53 (1H, septd,  $J$  = 7.0, 3.1, H<sub>8(ΔS)</sub>), 0.35 (3H, d,  $J$  = 7.0, Me<sub>B(ΔS)</sub>), 0.29 (3H, d,  $J$  = 7.0, Me<sub>B(ΔS)</sub>), 0.19 (3H, d,  $J$  = 7.0, Me<sub>A(ΔS)</sub>).  $^{13}C$  NMR: 170.03 (C<sub>9(ΔS)</sub> or C<sub>9(ΔS)</sub>), 169.80 (C<sub>9(ΔS)</sub> or C<sub>9(ΔS)</sub>), 139.05 (C<sub>g(ΔS)</sub>), 138.17 (C<sub>g'(ΔS)</sub>), 138.05 (C<sub>g'(ΔS)</sub>), 136.88 (C<sub>g(ΔS)</sub>), 135.55 (C<sub>a'(ΔS)</sub>), 133.85 (C<sub>a(ΔS), a(ΔS)</sub>), 133.38 (C<sub>a'(ΔS)</sub>), 133.08, 132.89 (C<sub>2(ΔS), 2(ΔS)</sub>), 129.61, 129.40 (C<sub>4(ΔS), 4(ΔS)</sub>), 126.77, 126.68, 126.50, 126.27 (C<sub>b, b'(ΔS), b, b'(ΔS)</sub>), 125.56 (C<sub>1(ΔS), 1(ΔS)</sub>), 125.03, 124.97, 124.75, 124.52 (C<sub>e, e'(ΔS), e, e'(ΔS)</sub>), 112.32, 112.22 (C<sub>3(ΔS), 3(ΔS)</sub>), 111.58, 111.37, 111.16 (C<sub>d, d'(ΔS), d, d'(ΔS)</sub>), 106.91, 106.88, 106.71, 106.59 (C<sub>f, f(ΔS), f, f(ΔS)</sub>), 71.71 (C<sub>7(ΔS)</sub>), 70.67 (C<sub>7(ΔS)</sub>), 66.47 (C<sub>5, 6(ΔS)</sub>), 66.35 (C<sub>5, 6(ΔS)</sub>), 28.82 (C<sub>8(ΔS)</sub>), 28.34 (C<sub>8(ΔS)</sub>), 21.09, 21.07, 20.99 (Me, Me<sub>(ΔS)</sub>, Me, Me<sub>(ΔS)</sub>), 19.21 (Me<sub>B(ΔS)</sub>), 18.56 (Me<sub>A(ΔS)</sub>), 14.38 (Me<sub>B(ΔS)</sub>), 12.88 (Me<sub>A(ΔS)</sub>) (quaternary C could not be assigned). MS (FAB):  $m/z$  711 [M]<sup>+</sup>.

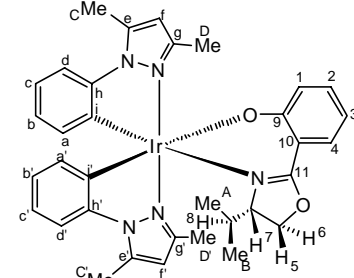
## **zSynthesis of ΔS/ΔS-5.1f**

This was prepared from dimer **2.6f** (100 mg, 0.088 mmol), (S)-soxH (39.7 mg, 0.194 mmol), and NaOMe (10.5 mg, 0.194 mmol) and after work up gave  $\Delta S/\Delta S$ -**5.1f** as a grey solid (combined yield 102 mg, 79%).  $\Delta S/\Delta S$ -**5.1f** were separated by flash column chromatography (DCM/ethyl acetate 20:1). Anal. Calcd for  $C_{34}H_{36}IrN_5O_2$ : C, 55.27, H, 4.91, N, 9.48. Found ( $\Delta S:\Delta S$  20:1): C, 55.14, H, 4.82, N,



9.50%.  $^1\text{H}$  NMR ( $\text{CDCl}_3$ )  $\Delta\text{S}$ :  $\delta$  7.46 (1H, dd,  $J$  = 8.2, 1.9, H<sub>4</sub>), 7.30 – 7.26 (2H, m, H<sub>d</sub>, d'), 7.05 (1H, ddd,  $J$  = 8.6, 7.0, 1.9, H<sub>2</sub>), 6.80 (1H, td,  $J$  = 7.4, 1.2, H<sub>c</sub>), 6.75 (1H, td,  $J$  = 7.0, 1.6, H<sub>c'</sub>), 6.61 (2H, td,  $J$  = 7.4, 0.8, H<sub>b</sub>), 6.58 – 6.54 (2H, m, H<sub>1, b'</sub>), 6.48 (1H, dd,  $J$  = 7.4, 1.6, H<sub>a'</sub>), 6.33 (1H, ddd,  $J$  = 7.8, 6.7, 0.8, H<sub>3</sub>), 6.15 – 6.13 (2H, m, H<sub>a, f</sub>), 5.97 (1H, s, H<sub>f</sub>), 4.24 (1H, dd,  $J$  = 8.6, 3.5, H<sub>6</sub>), 3.75 (1H, t,  $J$  = 8.9, H<sub>5</sub>), 2.91 (1H, ddd,  $J$  = 9.4, 3.5, 1.6, H<sub>7</sub>), 2.84 (3H, s, Me<sub>C'</sub>), 2.76 (3H, s, Me<sub>C</sub>), 2.45 (3H, s, Me<sub>D'</sub>), 2.23 (3H, s, Me<sub>D</sub>), 1.53 (1H, septd,  $J$  = 7.0, 1.6, H<sub>8</sub>), 0.70 (3H, d,  $J$  = 7.0, Me<sub>A</sub>), 0.17 (3H, d,  $J$  = 6.6, Me<sub>B</sub>).  $^{13}\text{C}$  NMR: 169.70 (C<sub>9</sub>), 162.54 (C<sub>11</sub>), 150.37 (C<sub>e'</sub>), 149.51 (C<sub>e</sub>), 146.20 (C<sub>h</sub>), 145.61 (C<sub>h'</sub>), 139.76, 139.67 (C<sub>g, g'</sub>), 136.35 (C<sub>a'</sub>), 134.24, 134.20 (C<sub>a, i</sub>), 132.74 (C<sub>2</sub>), 130.90 (C<sub>i'</sub>), 128.67 (C<sub>4</sub>), 124.32 (C<sub>b'</sub>), 124.11 (C<sub>1</sub>), 124.00 (C<sub>b</sub>), 121.56 (C<sub>c</sub>), 120.65 (C<sub>c'</sub>), 112.23 (C<sub>3</sub>), 111.99 (C<sub>10</sub>), 111.45, 111.38 (C<sub>d, d'</sub>), 109.24 (C<sub>f</sub>), 108.26 (C<sub>f</sub>), 71.01 (C<sub>7</sub>), 67.18 (C<sub>5, 6</sub>), 29.20 (C<sub>8</sub>), 20.48 (Me<sub>A</sub>), 14.90 (Me<sub>C</sub>), 14.64 (Me<sub>B</sub>), 14.44 (Me<sub>C'</sub>), 13.95 (Me<sub>D</sub>), 11.73 (Me<sub>D'</sub>).  $[\alpha]_D$  -428° (for  $\Delta\text{S}:\text{AS}$  16:1) in DCM.

$^1\text{H}$  NMR ( $\text{CDCl}_3$ )  $\Delta\text{S}$ :  $\delta$  7.63 (1H, dd,  $J$  = 7.8, 1.6, H<sub>4</sub>), 7.27 – 7.23 (2H, m, H<sub>d</sub>, d'), 7.05 (1H, ddd,  $J$  = 8.6, 6.7, 1.9, H<sub>2</sub>), 6.79 (1H, ddd,  $J$  = 8.2, 7.4, 1.6, H<sub>c</sub>), 6.75 (1H, ddd,  $J$  = 8.2, 7.4, 1.6, H<sub>c'</sub>), 6.65 (1H, td,  $J$  = 7.4, 1.2, H<sub>b</sub>), 6.61 – 6.56 (2H, m, H<sub>1, b'</sub>), 6.51 (1H, dd,  $J$  = 7.4, 1.2, H<sub>a'</sub>), 6.26 (1H, ddd,  $J$  = 8.2, 7.0, 1.6, H<sub>3</sub>), 6.13 (1H, s, H<sub>f</sub>), 6.05 (1H, dd,  $J$  = 7.4, 1.6, H<sub>a</sub>), 5.95 (1H, s, H<sub>f</sub>), 4.15 (1H, dd,  $J$  = 8.6, 3.5, H<sub>6</sub>), 4.02 (1H, t,  $J$  = 8.9, H<sub>5</sub>), 3.76 (1H, dt,  $J$  = 8.9, 3.1, H<sub>7</sub>), 2.86 (3H, s, Me<sub>C'</sub>), 2.73 (3H, s, Me<sub>C</sub>), 2.45 (3H, s, Me<sub>D'</sub>), 2.33 (3H, s, Me<sub>D</sub>), 0.56 (1H, septd,  $J$  = 7.4, 2.7, H<sub>8</sub>), 0.30, 0.29 (6H, 2 X d,  $J$  = 7.0, Me<sub>A, B</sub>).  $^{13}\text{C}$  NMR: 169.93 (C<sub>9</sub>), 161.93 (C<sub>11</sub>), 150.63 (C<sub>e'</sub>), 148.55 (C<sub>e</sub>), 146.34, 146.32 (C<sub>h, h'</sub>), 139.86 (C<sub>g</sub>), 139.74 (C<sub>g'</sub>), 136.32 (C<sub>i</sub>), 134.83 (C<sub>a</sub>), 133.85 (C<sub>a</sub>), 132.91 (C<sub>2</sub>), 130.41 (C<sub>i'</sub>), 129.77 (C<sub>4</sub>), 124.50 (C<sub>b'</sub>), 124.32 (C<sub>1</sub>), 124.28 (C<sub>b</sub>), 121.58 (C<sub>c</sub>), 120.70 (C<sub>c'</sub>), 112.18 (C<sub>3</sub>), 111.60, 111.14 (C<sub>d, d'</sub>), 110.29 (C<sub>10</sub>), 109.47 (C<sub>f</sub>), 109.39 (C<sub>f</sub>), 71.52 (C<sub>7</sub>), 65.87 (C<sub>5, 6</sub>), 28.54 (C<sub>8</sub>), 18.82 (Me<sub>A</sub> or B), 14.72 (Me<sub>C</sub>), 14.36 (Me<sub>C'</sub>), 13.32 (Me<sub>A</sub> or B), 13.01 (Me<sub>D</sub>), 12.55 (Me<sub>D'</sub>).  $[\alpha]_D$  +469° (for  $\Delta\text{S}:\text{AS}$  1:20) in DCM. MS (FAB):  $m/z$  739 [M]<sup>+</sup>.

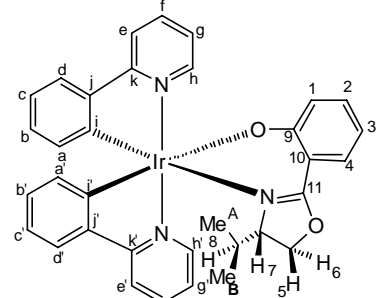
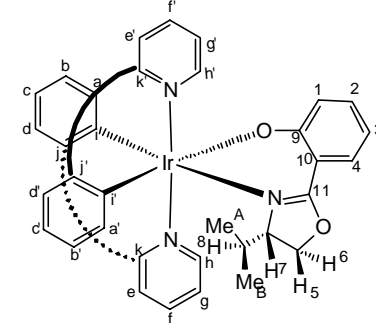


### Synthesis of $\Delta\text{S}/\text{AS}$ -5.1g

This was prepared from dimer **2.6g** (70 mg, 0.065 mmol), (S)-soxH (29.3 mg, 0.143 mmol), and NaOMe (7.7 mg, 0.143 mmol) and after work up gave  $\Delta\text{S}/\text{AS}$ -**5.1g** as a yellow solid (combined yield 68 mg, 75%). Both isomers crystallised out together in

DCM/hexane or DCM/diethylether solvent mixtures but they could be separated by hand picking due to significant variation in colour and shape of the crystals. Anal. Calcd for  $C_{34}H_{30}IrN_3O_2\cdot NaCl$ : C, 53.50, H, 3.96, N, 5.51. Found ( $\Delta S$ ): C, 54.69, H, 3.35, N, 5.40%.  $^1H$  NMR ( $CDCl_3$ )  $\Delta S$ :  $\delta$  8.87 (1H, ddd,  $J$  = 5.4, 1.6, 0.8,  $H_h$ ), 8.59 (1H, ddd,  $J$  = 5.8, 1.6, 0.8,  $H_h$ ), 7.85 – 7.82 (2H, m,  $H_e, e'$ ), 7.72 (1H, td,  $J$  = 7.4, 1.6,  $H_f$ ), 7.65 (1H, td,  $J$  = 7.4, 1.6,  $H_f$ ), 7.58 – 7.53 (3H, m,  $H_{4, d, d'}$ ), 7.13 – 7.07 (2H, m,  $H_{2, g'}$ ), 6.92 (1H, ddd,  $J$  = 7.4, 5.8, 1.6,  $H_g$ ), 6.82 (1H, td,  $J$  = 7.8, 1.2,  $H_c$ ), 6.79 (1H, td,  $J$  = 7.8, 1.2,  $H_c$ ), 6.70 (1H, td,  $J$  = 7.4, 1.2,  $H_b$ ), 6.66 – 6.62 (2H, m,  $H_{1, b'}$ ), 6.40 (1H, dd,  $J$  = 7.8, 1.2,  $H_{a'}$ ), 6.34 (1H, ddd,  $J$  = 7.8, 6.7, 1.2,  $H_3$ ), 6.19 (1H, dd,  $J$  = 7.4, 1.2,  $H_a$ ), 4.18 (1H, dd,  $J$  = 8.9, 3.5,  $H_6$ ), 3.65 (1H, t,  $J$  = 8.9,  $H_5$ ), 3.08 (1H, ddd,  $J$  = 9.7, 3.9, 1.9,  $H_7$ ), 1.79 (1H, septd,  $J$  = 7.0, 1.9,  $H_8$ ), 0.84 (3H, d,  $J$  = 6.6,  $Me_A$ ), 0.20 (3H, d,  $J$  = 7.0,  $Me_B$ ).  $^{13}C$  NMR: 169.30 ( $C_k$ ), 169.06 ( $C_9$ ), 168.23 ( $C_{k'}$ ), 161.55 ( $C_{11}$ ), 152.54 ( $C_i$ ), 155.33 ( $C_{i'}$ ), 150.12 ( $C_h$ ), 149.17 ( $C_{h'}$ ), 144.64 ( $C_j$ ), 144.05 ( $C_{j'}$ ), 136.63 ( $C_f$ ), 136.36 ( $C_f$ ), 134.20 ( $C_{a'}$ ), 132.89 ( $C_2$ ), 132.21 ( $C_a$ ), 129.48 ( $C_b$ ), 129.07 ( $C_4$ ), 128.99 ( $C_{b'}$ ), 125.18 ( $C_1$ ), 123.91, 123.80 ( $C_{d, d'}$ ), 121.83 ( $C_g$ ), 121.04 ( $C_g$ ), 120.91 ( $C_c$ ), 120.14 ( $C_c$ ), 118.54, 117.88 ( $C_{e, e'}$ ), 112.30 ( $C_3$ ), 110.51 ( $C_{10}$ ), 69.82 ( $C_7$ ), 66.86 ( $C_{5, 6}$ ), 28.85 ( $C_8$ ), 19.65 ( $Me_A$ ), 14.50 ( $Me_B$ ).  $[\alpha]_D$  -532° (for  $\Delta S:\Delta S$  15:1) in DCM.

$^1H$  NMR ( $CDCl_3$ )  $\Delta S$ :  $\delta$  9.02 (1H, ddd,  $J$  = 5.8, 1.6, 0.8,  $H_{h'}$ ), 8.41 (1H, d,  $J$  = 5.8,  $H_h$ ), 7.87 (1H, d,  $J$  = 8.2,  $H_{e'}$ ), 7.80 (1H, d,  $J$  = 8.2,  $H_e$ ), 7.72 (1H, td,  $J$  = 8.2, 1.6,  $H_f$ ), 7.65 (1H, dd,  $J$  = 8.2, 1.9,  $H_4$ ), 7.63 (1H, td,  $J$  = 8.2, 1.6,  $H_f$ ), 7.54 (1H, dd,  $J$  = 8.2, 1.2,  $H_d$ ), 7.51 (1H, dd,  $J$  = 8.2, 1.6,  $H_{d'}$ ), 7.14 – 7.09 (2H, m,  $H_{2, g'}$ ), 7.03 (1H, ddd,  $J$  = 7.4, 5.9, 1.6,  $H_g$ ), 6.83 (1H, td,  $J$  = 7.4, 1.2,  $H_c$ ), 6.79 (1H, td,  $J$  = 7.8, 0.8,  $H_{c'}$ ), 6.75 (1H, td,  $J$  = 7.4, 1.6,  $H_b$ ), 6.69 (1H, dd,  $J$  = 8.6, 1.2,  $H_1$ ), 6.66 (1H, td,  $J$  = 7.4, 1.2,  $H_{b'}$ ), 6.37 (1H, dd,  $J$  = 7.4, 1.2,  $H_{a'}$ ), 6.34 (1H, ddd,  $J$  = 7.8, 6.7, 1.2,  $H_3$ ), 6.08 (1H, dd,  $J$  = 7.4, 1.2,  $H_a$ ), 4.27 – 4.19 (2H, m,  $H_{5, 6}$ ), 3.95 (1H, ddd,  $J$  = 8.2, 4.7, 3.1,  $H_7$ ), 0.73 (1H, septd,  $J$  = 7.0, 3.1,  $H_8$ ), 0.24 (3H, d,  $J$  = 7.0,  $Me_B$ ), 0.06 (3H, d,  $J$  = 7.0,  $Me_A$ ).  $^{13}C$  NMR: 169.28 ( $C_k$ ), 169.19 ( $C_9$ ), 168.62 ( $C_{k'}$ ), 161.67 ( $C_{11}$ ), 153.39 ( $C_i$ ), 148.86 ( $C_{h'}$ ), 148.72 ( $C_{i'}$ ), 147.73 ( $C_h$ ), 145.11 ( $C_{j'}$ ), 144.48 ( $C_j$ ), 136.63

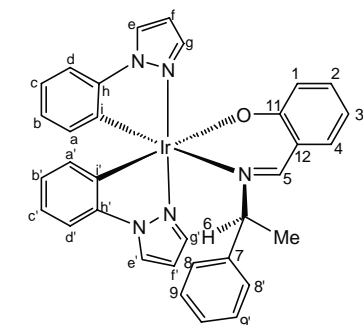
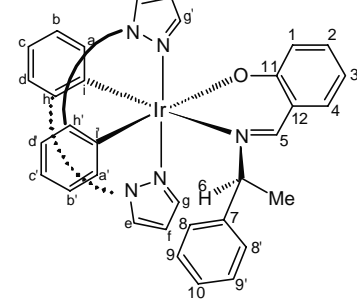


(C<sub>f</sub>), 136.56 (C<sub>f</sub>), 133.31 (C<sub>2</sub>), 132.45 (C<sub>a'</sub>), 131.35 (C<sub>a</sub>), 129.78 (C<sub>4</sub>), 129.37 (C<sub>b, b'</sub>), 124.79 (C<sub>1</sub>), 123.84, 123.77 (C<sub>d, d'</sub>), 121.68 (C<sub>g</sub>), 121.63 (C<sub>g</sub>), 121.19 (C<sub>c</sub>), 120.28 (C<sub>c</sub>), 119.03 (C<sub>e</sub>), 118.18 (C<sub>e'</sub>), 112.68 (C<sub>3</sub>), 109.98 (C<sub>10</sub>), 72.04 (C<sub>7</sub>), 66.77 (C<sub>5, 6</sub>), 28.82 (C<sub>8</sub>), 18.58 (Me<sub>B</sub>), 12.75 (Me<sub>A</sub>).  $[\alpha]_D +570^\circ$  in DCM. MS (FAB): *m/z* 706 [M+H]<sup>+</sup>.

### Synthesis of $\Delta S/\Delta S\text{-5.2a}$

This was prepared from dimer **2.6a** (70 mg, 0.068 mmol), (S)-pepH (36.8 mg, 0.164 mmol), and NaOMe (8.8 mg, 0.164 mmol) and after work up gave  $\Delta S/\Delta S\text{-5.2a}$  as a yellow solid (combined yield 71 mg, 75%).  $\Delta S$  isomer was selectively crystallised from methanol, hence, the two isomers were separated *via* fractional crystallisation from methanol until a ratio of 1:10 was attained for  $\Delta S:\Delta S$ . Anal. Calcd for C<sub>33</sub>H<sub>28</sub>IrN<sub>5</sub>O: C, 56.39, H, 4.02, N, 9.96. Found ( $\Delta S$ ): C, 56.28, H, 3.98, N, 9.87%. <sup>1</sup>H NMR (CDCl<sub>3</sub>)  $\Delta S$ :  $\delta$  8.06 (1H, s, H<sub>5</sub>), 8.02 (1H, d, *J* = 3.1, H<sub>e</sub>), 7.66 (1H, d, *J* = 3.5, H<sub>e'</sub>), 7.65 (1H, d, *J* = 2.3, H<sub>g'</sub>), 7.52 (1H, d, *J* = 2.3, H<sub>g</sub>), 7.19 (1H, ddd, *J* = 8.6, 6.7, 1.6, H<sub>2</sub>), 7.12 (1H, d, *J* = 7.4, H<sub>d</sub>), 7.05 (1H, dd, *J* = 7.8, 1.6, H<sub>4</sub>), 7.01 – 6.92 (3H, m, H<sub>9, 9', 10</sub>), 6.82 (1H, td, *J* = 7.4, 0.8, H<sub>c</sub>), 6.77 (1H, dd, *J* = 7.8, 1.2, H<sub>d'</sub>), 6.73 – 6.66 (3H, m, H<sub>1, b, c'</sub>), 6.61 (1H, td, *J* = 7.8, 1.6, H<sub>b'</sub>), 6.53 (1H, t, *J* = 2.7, H<sub>f</sub>), 6.49 (1H, t, *J* = 2.7, H<sub>f'</sub>), 6.39 – 6.34 (3H, m, H<sub>3, 8, 8'</sub>), 6.27 (1H, dd, *J* = 7.4, 1.2, H<sub>a'</sub>), 6.13 (1H, dd, *J* = 7.4, 1.2, H<sub>a</sub>), 4.94 (1H, q, *J* = 7.0, H<sub>6</sub>), 1.51 (3H, d, *J* = 7.0, Me). <sup>13</sup>C NMR: 166.41 (C<sub>11</sub>), 161.08 (C<sub>5</sub>), 144.24 (C<sub>h'</sub>), 143.88 (C<sub>h</sub>), 141.99 (C<sub>7</sub>), 137.87 (C<sub>g'</sub>), 137.81 (C<sub>g</sub>), 135.21 (C<sub>4</sub>), 134.63 (C<sub>i</sub>), 134.39 (C<sub>a'</sub>), 134.17 (C<sub>a</sub>), 133.70 (C<sub>2</sub>), 131.10 (C<sub>i'</sub>), 127.92 (C<sub>9, 9'</sub>), 126.19 (C<sub>10</sub>), 125.96 (C<sub>8, 8'</sub>), 125.85 (C<sub>e</sub>), 125.63 (C<sub>b</sub>), 125.43 (C<sub>b'</sub>), 125.23 (C<sub>e'</sub>), 123.71 (C<sub>1</sub>), 121.68 (C<sub>c</sub>), 121.42 (C<sub>12</sub>), 120.75 (C<sub>c</sub>), 112.89 (C<sub>3</sub>), 110.54 (C<sub>d</sub>), 110.47 (C<sub>d'</sub>), 106.87 (C<sub>f</sub>), 106.71 (C<sub>f'</sub>), 66.97 (C<sub>6</sub>), 22.81 (Me).  $[\alpha]_D -631^\circ$  in CHCl<sub>3</sub>.

<sup>1</sup>H NMR (CDCl<sub>3</sub>)  $\Delta S$ :  $\delta$  8.11 (1H, d, *J* = 2.7, H<sub>e'</sub>), 7.97 (1H, d, *J* = 2.7, H<sub>e</sub>), 7.96 (1H, s, H<sub>5</sub>), 7.83 (1H, d, *J* = 2.3, H<sub>g'</sub>), 7.36 – 7.22 (5H, m, H<sub>8, 8', 9, 9', 10</sub>), 7.20 (1H, dd, *J* = 7.8, 0.8, H<sub>d'</sub>), 7.18 (1H, d, *J* = 2.3, H<sub>g</sub>), 7.14 – 7.10 (2H, m, H<sub>2, d</sub>), 6.89 (1H, dd, *J* = 7.8, 1.9, H<sub>4</sub>), 6.87 – 6.81 (2H, m, H<sub>c, c'</sub>), 6.72 – 6.68 (2H, m, H<sub>b, b'</sub>), 6.67 (1H, t, *J* = 2.3, H<sub>f</sub>), 6.61 (1H, d, *J* = 8.2, H<sub>1</sub>), 6.42 (1H, dd, *J* = 7.4, 1.6, H<sub>a'</sub>), 6.38 (1H, t, *J* = 2.3, H<sub>f'</sub>), 6.30 (1H, ddd, *J* = 7.8, 6.7, 1.2, H<sub>3</sub>), 6.22 (1H, dd, *J* = 7.4, 1.6, H<sub>a</sub>),

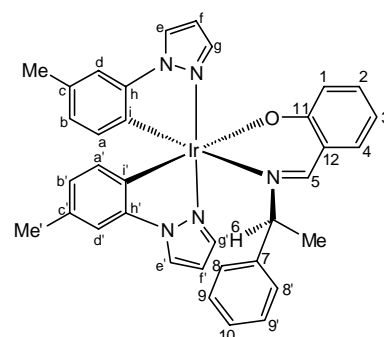
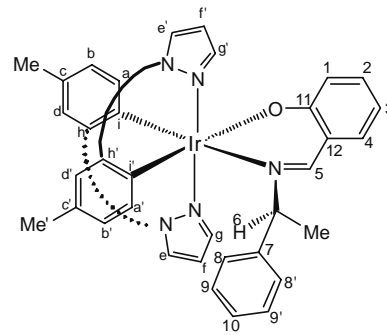


4.80 (1H, q,  $J = 7.0$ , H<sub>6</sub>), 0.82 (3H, d,  $J = 7.0$ , Me). <sup>13</sup>C NMR: 166.69 (C<sub>11</sub>), 162.25 (C<sub>5</sub>), 144.31 (C<sub>h'</sub>), 143.93 (C<sub>h</sub>), 142.04 (C<sub>7</sub>), 138.78 (C<sub>g</sub>), 138.27 (C<sub>g'</sub>), 135.21 (C<sub>a'</sub>), 134.88 (C<sub>4</sub>), 134.27 (C<sub>i</sub>), 134.17 (C<sub>a</sub>), 133.58 (C<sub>2</sub>), 132.03 (C<sub>i'</sub>), 128.60 (C<sub>9, 9'</sub>), 127.97 (C<sub>8, 8'</sub>), 127.56 (C<sub>10</sub>), 125.93 (C<sub>e</sub>), 125.61 (C<sub>b, b'</sub>), 125.45 (C<sub>e'</sub>), 123.66 (C<sub>1</sub>), 121.97 (C<sub>12</sub>), 121.72 (C<sub>c</sub>), 121.06 (C<sub>c'</sub>), 112.76 (C<sub>3</sub>), 110.66 (C<sub>d</sub>), 110.47 (C<sub>d'</sub>), 107.16 (C<sub>f</sub>), 106.61 (C<sub>f'</sub>), 64.93 (C<sub>6</sub>), 20.33 (Me).  $[\alpha]_D +480^\circ$  (for  $\Delta S:\Lambda S$  1:10) in CHCl<sub>3</sub>. MS (FAB): *m/z* 703 [M]<sup>+</sup>.

### Synthesis of $\Delta S/\Lambda S$ -5.2b

This was prepared from dimer **2.6b** (70 mg, 0.065 mmol), (S)-pepH (32.2 mg, 0.143 mmol), and NaOMe (7.7 mg, 0.143 mmol) and after work up gave  $\Delta S/\Lambda S$ -**5.2b** as a yellow solid (combined yield 79 mg, 83%).  $\Lambda S$  isomer crystallised out selectively in DCM/isopropanol mixture and crystals of  $\Delta S$  isomer were obtained from methanol which also gave some of the  $\Lambda S$  isomer. Anal. Calcd for C<sub>35</sub>H<sub>32</sub>IrN<sub>5</sub>O: C, 57.52, H, 4.41, N, 9.58. Found ( $\Lambda S$ ): C, 57.51, H, 4.39, N, 9.57%. <sup>1</sup>H NMR (CDCl<sub>3</sub>)  $\Delta S$ :  $\delta$  8.02 (1H, s, H<sub>5</sub>), 7.99 (1H, d,  $J = 2.7$ , H<sub>e</sub>), 7.67 (1H, d,  $J = 2.7$ , H<sub>e'</sub>), 7.64 (1H, d,  $J = 2.0$ , H<sub>g'</sub>), 7.51 (1H, d,  $J = 2.0$ , H<sub>g</sub>), 7.17 (1H, ddd,  $J = 8.6, 6.7, 1.6$ , H<sub>2</sub>), 7.03 – 6.92 (5H, m, H<sub>4, 9, 9', 10, d</sub>), 6.69 (1H, d,  $J = 8.6$ , H<sub>1</sub>), 6.59 (1H, s, H<sub>d'</sub>), 6.51 – 6.48 (3H, m, H<sub>b, f, f'</sub>), 6.45 (1H, dd,  $J = 7.4, 0.8$ , H<sub>b'</sub>), 6.36 – 6.32 (3H, m, H<sub>3, 8, 8'</sub>), 6.14 (1H, d,  $J = 7.4$ , H<sub>a'</sub>), 6.02 (1H, d,  $J = 7.4$ , H<sub>a</sub>), 4.91 (1H, q,  $J = 7.0$ , H<sub>6</sub>), 2.18 (3H, s, Me), 2.13 (3H, s, Me'), 1.50 (3H, d,  $J = 7.0$ , Me<sub>A</sub>). <sup>13</sup>C NMR: 166.71 (C<sub>11</sub>), 161.08 (C<sub>5</sub>), 144.21 (C<sub>h'</sub>), 143.87 (C<sub>h</sub>), 142.19 (C<sub>7</sub>), 137.82 (C<sub>g</sub>), 137.73 (C<sub>g'</sub>), 135.13 (C<sub>4</sub>), 134.07 (C<sub>a'</sub>), 133.82 (C<sub>a</sub>), 133.49 (C<sub>2</sub>), 130.76 (C<sub>j</sub>), 130.32 (C<sub>i</sub>), 129.83 (C<sub>j'</sub>), 127.83 (C<sub>9, 9'</sub>), 126.69 (C<sub>b</sub>), 126.57 (C<sub>i'</sub>), 126.48 (C<sub>b'</sub>), 126.16 (C<sub>10</sub>), 126.07 (C<sub>8, 8'</sub>), 125.55 (C<sub>e</sub>), 124.98 (C<sub>e'</sub>), 123.88 (C<sub>1</sub>), 121.59 (C<sub>12</sub>), 112.60 (C<sub>3</sub>), 111.49, 111.47 (C<sub>d, d'</sub>), 106.67, 106.55 (C<sub>f, f'</sub>), 66.65 (C<sub>6</sub>), 22.62 (Me<sub>A</sub>), 21.08 (Me), 20.98 (Me').  $[\alpha]_D -560^\circ$  in DCM.

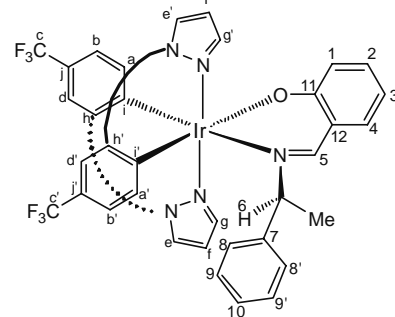
<sup>1</sup>H NMR (CDCl<sub>3</sub>)  $\Lambda S$ :  $\delta$  8.08 (1H, dd,  $J = 2.7, 0.8$ , H<sub>e'</sub>), 7.94 – 7.93 (2H, m, H<sub>5, e</sub>), 7.80 (1H, dd,  $J = 2.3, 0.8$ , H<sub>g</sub>), 7.36 – 7.23 (5H, m, H<sub>8, 8', 9, 9', 10</sub>), 7.16 (1H, dd,  $J = 2.3, 0.8$ , H<sub>g</sub>), 7.10 (1H, ddd,  $J = 8.6, 6.7, 1.9$ ,



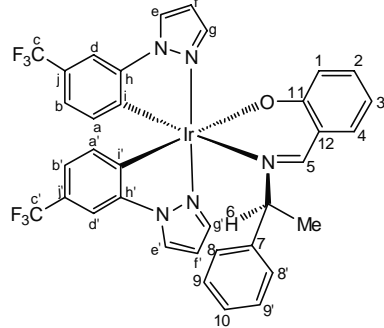
$\text{H}_2$ ), 7.01 (1H, s,  $\text{H}_{\text{d}'}$ ), 6.95 (1H, s,  $\text{H}_{\text{d}}$ ), 6.87 (1H, dd,  $J$  = 7.8, 1.9,  $\text{H}_4$ ), 6.64 (1H, t,  $J$  = 2.7,  $\text{H}_{\text{f}}$ ), 6.60 (1H, d,  $J$  = 8.2,  $\text{H}_1$ ), 6.55 – 6.51 (2H, m,  $\text{H}_{\text{b}}, \text{b}'$ ), 6.35 (1H, t,  $J$  = 2.7,  $\text{H}_{\text{f}}$ ), 6.29 (1H, d,  $J$  = 7.8,  $\text{H}_{\text{a}'}$ ), 6.27 (1H, ddd,  $J$  = 7.8, 6.7, 1.2,  $\text{H}_3$ ), 6.10 (1H, d,  $J$  = 7.4,  $\text{H}_{\text{a}}$ ), 4.83 (1H, q,  $J$  = 7.0,  $\text{H}_6$ ), 2.20, 2.19 (6H, 2  $\times$  s, Me, Me $\cdot$ ), 0.80 (3H, d,  $J$  = 7.0,  $\text{Me}_{\text{A}}$ ).  $^{13}\text{C}$  NMR: 166.82 ( $\text{C}_{11}$ ), 162.10 ( $\text{C}_5$ ), 144.48 ( $\text{C}_{\text{h}'}$ ), 143.91 ( $\text{C}_{\text{h}}$ ), 142.19 ( $\text{C}_7$ ), 138.64 ( $\text{C}_{\text{g}}$ ), 138.10 ( $\text{C}_{\text{g}}$ ), 134.81 ( $\text{C}_{4, \text{a}'}$ ), 133.77 ( $\text{C}_{\text{a}}$ ), 133.38 ( $\text{C}_2$ ), 130.83 ( $\text{C}_{\text{j}}$ ), 130.21 ( $\text{C}_{\text{j}'}$ ), 130.02 ( $\text{C}_{\text{i}}$ ), 128.56 ( $\text{C}_{9, 9'}$ ), 128.05 ( $\text{C}_{8, 8'}$ ), 127.50 ( $\text{C}_{10}$ ), 127.39 ( $\text{C}_{\text{i}'}$ ), 127.05 ( $\text{C}_{\text{b}'}$ ), 126.67 ( $\text{C}_{\text{b}}$ ), 125.34 ( $\text{C}_{\text{e}}$ ), 125.18 ( $\text{C}_{\text{e}'}$ ), 123.78 ( $\text{C}_1$ ), 122.05 ( $\text{C}_{12}$ ), 112.50 ( $\text{C}_3$ ), 111.64 ( $\text{C}_{\text{d}'}$ ), 111.44 ( $\text{C}_{\text{d}}$ ), 106.97 ( $\text{C}_{\text{f}'}$ ), 106.43 ( $\text{C}_{\text{f}}$ ), 64.54 ( $\text{C}_6$ ), 21.09 (Me, Me $\cdot$ ), 20.22 ( $\text{Me}_{\text{A}}$ ).  $[\alpha]_D$  +658° in DCM. MS (FAB):  $m/z$  731 [ $\text{M}$ ] $^+$ .

## Synthesis of $\Delta$ S/ $\Delta$ S-5.2c

This was prepared from dimer **2.6c** (70 mg, 0.054 mmol), (S)-pepH (26.7 mg, 0.118 mmol), and NaOMe (6.4 mg, 0.118 mmol) and after work up gave  $\Delta S/\Delta S\text{-5.2c}$  as a yellow solid (combined yield 71 mg, 79%).  $\Delta S$  isomer was selectively crystallised from DCM/methanol, hence, the two isomers were separated *via* fractional crystallisation from DCM/methanol until a ratio of 17:1 was attained for  $\Delta S:\Delta S$ . Anal. Calcd for  $C_{35}H_{26}F_6IrN_5O$ : C, 50.11, H, 3.12, N, 8.35. Found ( $\Delta S$ ): C, 50.08, H, 3.07, N, 8.40%.  $^1H$  NMR ( $CDCl_3$ )  $\Delta S$ :  $\delta$  8.17 (1H, s,  $H_5$ ), 8.08 (1H, d,  $J$  = 2.7,  $H_{e'}$ ), 7.59 – 7.57 (3H, m,  $H_{e, g, g'}$ ), 7.30 (1H, s,  $H_{d'}$ ), 7.24 (1H, ddd,  $J$  = 8.6, 7.0, 1.9,  $H_2$ ), 7.14 (1H, dd,  $J$  = 7.8, 1.6,  $H_4$ ), 6.98 (1H, t,  $J$  = 7.4,  $H_{10}$ ), 6.88 – 6.84 (4H, m,  $H_{9, 9', b, b'}$ ), 6.74 (2H, m,  $H_{1, d}$ ), 6.61 (1H, t,  $J$  = 2.7,  $H_f$ ), 6.52 (1H, t,  $J$  = 2.7,  $H_f$ ), 6.45 (1H, td,  $J$  = 7.8, 1.2,  $H_3$ ), 6.33 (1H, d,  $J$  = 7.8,  $H_a$ ), 6.20 (2H, d,  $J$  = 7.4,  $H_{8, 8'}$ ), 6.17 (1H, d,  $J$  = 7.8,  $H_{a'}$ ), 5.03 (1H, q,  $J$  = 7.0,  $H_6$ ), 1.55 (3H, d,  $J$  = 7.0, Me).  $^{13}C$  NMR: 166.47 ( $C_{11}$ ), 161.08 ( $C_5$ ), 144.46 ( $C_h$ ), 143.99 ( $C_h$ ), 141.51 ( $C_7$ ), 140.51 ( $C_j$ ), 138.81, 138.33 ( $C_{g, g'}$ ), 137.72 ( $C_j$ ), 135.51 ( $C_4$ ), 135.14, 134.30, 134.19 ( $C_{2, a, a'}$ ), 128.73 ( $C_i$ ), 128.06 ( $C_{9, 9'}$ ), 127.53 ( $C_{i'}$ ), 126.78 ( $C_{e'}$ ), 126.07 ( $C_{10}$ ), 125.97 ( $C_e$ ), 124.96 ( $C_{8, 8'}$ ), 123.62 ( $C_1$ ), 123.00, 122.26 ( $C_{b, b'}$ ), 121.05 ( $C_{12}$ ), 113.49 ( $C_3$ ), 107.43 ( $C_f$ ), 107.27 ( $C_f$ ), 107.24 ( $C_{d'}$ ), 106.71 ( $C_d$ ), 68.18 ( $C_6$ ), 23.90 (Me).  $[\alpha]_D$  -473° (for  $\Delta S:\Delta S$  17:1) in DCM.

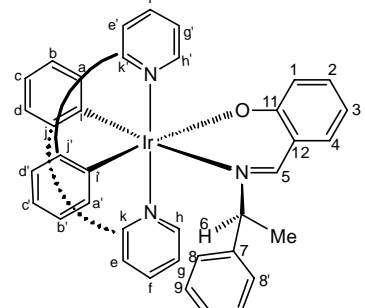


<sup>1</sup>H NMR (CDCl<sub>3</sub>)  $\Delta\delta$ :  $\delta$  8.15 (1H, d,  $J$  = 2.3, H<sub>e'</sub>), 8.05 (1H, d,  $J$  = 2.3, H<sub>e</sub>), 7.99 (1H, s, H<sub>5</sub>), 7.82 (1H, d,  $J$  = 2.3, H<sub>g</sub>), 7.37 (1H, d,  $J$  = 1.2, H<sub>d'</sub>), 7.34 – 7.28 (4H, m, H<sub>9, 9', 10, d</sub>), 7.24 (1H, d,  $J$  = 2.3, H<sub>g</sub>), 7.17 – 7.11 (3H, m, H<sub>2, 8, 8'</sub>), 6.95 – 6.90 (3H, m, H<sub>4, b, b'</sub>), 6.74 (1H, t,  $J$  = 2.3, H<sub>f</sub>), 6.59 (1H, d,  $J$  = 8.6, H<sub>1</sub>), 6.51 (1H, d,  $J$  = 7.8, H<sub>a'</sub>), 6.46 (1H, t,  $J$  = 2.3, H<sub>f</sub>), 6.35 (1H, ddd,  $J$  = 7.8, 6.7, 1.2, H<sub>3</sub>), 6.26 (1H, d,  $J$  = 7.8, H<sub>a</sub>), 4.68 (1H, q,  $J$  = 7.0, H<sub>6</sub>), 0.93 (3H, d,  $J$  = 7.0, Me). <sup>13</sup>C NMR: 166.58 (C<sub>11</sub>), 162.69 (C<sub>5</sub>), 144.45 (C<sub>h'</sub>), 143.97 (C<sub>h</sub>), 141.45 (C<sub>7</sub>), 140.22 (C<sub>j</sub>), 139.71 (C<sub>g</sub>), 139.10 (C<sub>g'</sub>), 138.65 (C<sub>j'</sub>), 135.47 (C<sub>a'</sub>), 135.01 (C<sub>4</sub>), 134.26 (C<sub>a</sub>), 134.11 (C<sub>2</sub>), 128.73 (C<sub>9, 9'</sub>), 127.71 (C<sub>10</sub>), 127.56 (C<sub>8, 8'</sub>), 126.41 (C<sub>e</sub>), 126.33 (C<sub>e'</sub>), 125.78 (C<sub>i'</sub>), 123.62 (C<sub>i</sub>), 123.50 (C<sub>1</sub>), 122.44, 122.29 (C<sub>b, b'</sub>), 121.55 (C<sub>12</sub>), 113.30 (C<sub>3</sub>), 107.93 (C<sub>f</sub>), 107.44 (C<sub>f</sub>), 107.28 (C<sub>d'</sub>), 107.16 (C<sub>d</sub>), 66.41 (C<sub>6</sub>), 20.63 (Me).  $[\alpha]_D$  +563° in DCM. MS (FAB): *m/z* 839 [M]<sup>+</sup>.



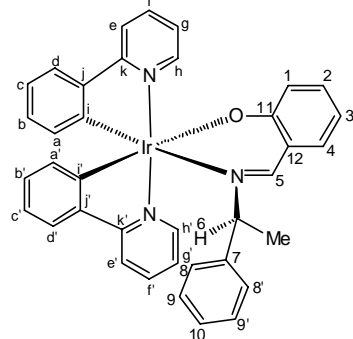
### Synthesis of $\Delta\delta/\Delta\delta\text{-5.2g}$

This was prepared from dimer **2.6g** (70 mg, 0.065 mmol), (S)-pepH (35.1 mg, 0.156 mmol), and NaOMe (8.4 mg, 0.156 mmol) and after work up gave  $\Delta\delta/\Delta\delta\text{-5.2g}$  as a yellow solid (combined yield 74 mg, 79%). Both isomers crystallised out together in methanol but they could be separated by hand picking due to significant variation in colour and shape of the crystals. Anal. Calcd for C<sub>37</sub>H<sub>30</sub>IrN<sub>3</sub>O: C, 61.27, H, 4.17, N, 5.80. Found ( $\Delta\delta$ ): C, 61.37, H, 4.23, N, 5.83%. <sup>1</sup>H NMR (CDCl<sub>3</sub>)  $\Delta\delta$ :  $\delta$  8.90 (1H, dt,  $J$  = 5.5, 1.2, H<sub>h'</sub>), 8.53 (1H, d,  $J$  = 5.5, H<sub>h</sub>), 8.03 (1H, s, H<sub>5</sub>), 7.83 (1H, d,  $J$  = 8.2, H<sub>e</sub>), 7.65 (1H, td,  $J$  = 7.4, 1.6, H<sub>f</sub>), 7.62 – 7.59 (2H, m, H<sub>e', f'</sub>), 7.53 (1H, dd,  $J$  = 7.8, 1.2, H<sub>d</sub>), 7.39 (1H, dd,  $J$  = 7.8, 1.2, H<sub>d'</sub>), 7.12 (1H, ddd,  $J$  = 8.2, 7.1, 1.2, H<sub>2</sub>), 7.10 (1H, ddd,  $J$  = 8.6, 5.8, 2.7, H<sub>g</sub>), 7.02 – 6.91 (5H, m, H<sub>4, 9, 9', 10, g</sub>), 6.81 (1H, td,  $J$  = 7.4, 1.2, H<sub>c</sub>), 6.78 (1H, td,  $J$  = 7.8, 1.2, H<sub>c'</sub>), 6.72 – 6.66 (2H, m, H<sub>b, b'</sub>), 6.60 (1H, d,  $J$  = 7.8, H<sub>1</sub>), 6.42 (1H, dd,  $J$  = 7.4, 0.8, H<sub>a</sub>), 6.35 – 6.31 (3H, m, H<sub>3, 8, 8'</sub>), 6.13 (1H, dd,  $J$  = 7.4, 0.8, H<sub>a</sub>), 4.70 (1H, q,  $J$  = 7.0, H<sub>6</sub>), 1.45 (3H, d,  $J$  = 7.0, Me). <sup>13</sup>C NMR: 169.08 (C<sub>k</sub>), 168.34 (C<sub>k'</sub>), 166.17 (C<sub>11</sub>), 161.13 (C<sub>5</sub>), 153.09 (C<sub>i</sub>), 150.93 (C<sub>i'</sub>), 148.95 (C<sub>h</sub>), 148.58 (C<sub>h'</sub>), 144.73 (C<sub>j'</sub>), 144.46 (C<sub>j</sub>), 142.12 (C<sub>7</sub>), 136.50 (C<sub>f</sub>), 136.46 (C<sub>f'</sub>), 134.96 (C<sub>4</sub>), 133.56 (C<sub>2</sub>), 133.13 (C<sub>a'</sub>), 131.91 (C<sub>a</sub>), 129.27 (C<sub>b, b'</sub>), 127.90 (C<sub>9, 9'</sub>),



126.79 (C<sub>8, 8'</sub>), 126.63 (C<sub>10</sub>), 124.40 (C<sub>1</sub>), 124.16 (C<sub>d'</sub>), 123.63 (C<sub>d</sub>), 121.50 (C<sub>12</sub>), 121.45 (C<sub>g'</sub>), 121.33 (C<sub>g</sub>), 121.14 (C<sub>c</sub>), 120.12 (C<sub>c'</sub>), 118.87 (C<sub>e</sub>), 118.25 (C<sub>e'</sub>), 112.83 (C<sub>3</sub>), 65.84 (C<sub>6</sub>), 22.15 (Me). [α]<sub>D</sub> -535° in DCM.

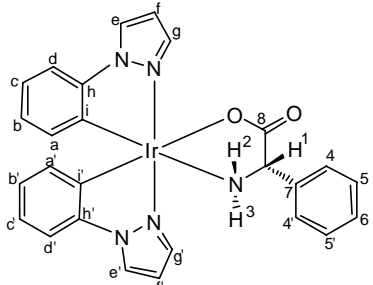
<sup>1</sup>H NMR (CDCl<sub>3</sub>) ΔS: δ 9.02 (1H, ddd, *J* = 5.8, 1.4, 0.8, H<sub>h'</sub>), 8.19 (1H, ddd, *J* = 5.8, 1.4, 0.8, H<sub>h</sub>), 8.11 (1H, s, H<sub>5</sub>), 7.93 (1H, d, *J* = 8.2, H<sub>e'</sub>), 7.80 – 7.75 (2H, m, H<sub>e, f'</sub>), 7.63 (1H, dd, *J* = 7.6, 1.2, H<sub>d'</sub>), 7.60 – 7.52 (2H, m, H<sub>d, f</sub>), 7.35 – 7.27 (3H, m, H<sub>9, 9', 10</sub>), 7.22 – 7.11 (3H, m, H<sub>2, 8, 8'</sub>), 6.92 (1H, dd, *J* = 7.8, 1.8, H<sub>4</sub>), 6.86 – 6.81 (2H, m, H<sub>c, c'</sub>), 6.78 – 6.69 (3H, m, H<sub>b, b', g</sub>), 6.58 (1H, d, *J* = 8.5, H<sub>1</sub>), 6.47 (1H, dd, *J* = 7.6, 1.2, H<sub>a'</sub>), 6.30 (1H, ddd, *J* = 8.2, 6.7, 0.8, H<sub>3</sub>), 6.22 (1H, dd, *J* = 7.6, 1.2, H<sub>a</sub>), 4.73 (1H, q, *J* = 7.0, H<sub>6</sub>), 0.73 (3H, d, *J* = 7.0, Me). <sup>13</sup>C NMR: 169.79 (C<sub>k, k'</sub>), 167.13 (C<sub>11</sub>), 163.03 (C<sub>5</sub>), 154.10 (C<sub>i</sub>), 152.97 (C<sub>i'</sub>), 151.35 (C<sub>h</sub>), 150.09 (C<sub>h'</sub>), 146.45, 146.35 (C<sub>j, j'</sub>), 143.22 (C<sub>7</sub>), 138.58 (C<sub>f'</sub>), 138.11 (C<sub>f</sub>), 136.56 (C<sub>4</sub>), 135.02 (C<sub>2</sub>), 134.77 (C<sub>a'</sub>), 133.29 (C<sub>a</sub>), 131.01 (C<sub>b'</sub>), 130.18 (C<sub>b</sub>), 129.91 (C<sub>9, 9'</sub>), 129.43 (C<sub>8, 8'</sub>), 129.08 (C<sub>10</sub>), 125.90 (C<sub>d'</sub>), 125.14 (C<sub>d</sub>), 124.69 (C<sub>1</sub>), 123.40 (C<sub>g</sub>), 123.18 (C<sub>12</sub>), 122.77 (C<sub>g</sub>), 122.56, 121.90 (C<sub>c, c'</sub>), 120.27 (C<sub>e</sub>), 119.82 (C<sub>e'</sub>), 114.18 (C<sub>3</sub>), 65.71 (C<sub>6</sub>), 22.49 (Me). [α]<sub>D</sub> +654° in DCM. MS (FAB): *m/z* 725 [M]<sup>+</sup>.



### Synthesis of ΔS/ΔS-5.3a

This was prepared from dimer **2.6a** (70 mg, 0.068 mmol), (S)-phglyH (24.7 mg, 0.164 mmol), and NaOMe (8.8 mg, 0.164 mmol) and after work up gave ΔS/ΔS-**5.3a** as a grey solid (combined yield 66 mg, 78%). ΔS/ΔS-**5.3a** could not be separated. Anal. Calcd for C<sub>26</sub>H<sub>22</sub>IrN<sub>5</sub>O<sub>2</sub>: C, 49.67, H, 3.53, N, 11.14. Found

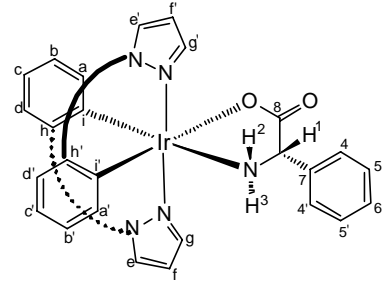
(ΔS:AS 1:1): C, 49.76, H, 3.64, N, 11.07%. <sup>1</sup>H NMR (MeOD): δ 8.55 – 8.54 (2H, m, H<sub>e' (ΔS), e' (AS)</sub>), 8.48 – 8.47 (2H, m, H<sub>e (ΔS), e (AS)</sub>), 8.30 (1H, d, *J* = 2.3, H<sub>g (AS)</sub>), 7.99 (1H, d, *J* = 2.3, H<sub>g' (AS)</sub>), 7.91 (1H, d, *J* = 2.3, H<sub>g (ΔS)</sub>), 7.86 (1H, d, *J* = 2.3, H<sub>g' (ΔS)</sub>), 7.40 – 7.26 (14H, m, H<sub>4, 4', 5, 5', 6, d, d' (ΔS), 4, 4', 5, 5', 6, d, d' (AS)</sub>), 6.88 – 6.75 (7H, m, H<sub>c, c', f (ΔS), c, c', f (AS)</sub>), 6.72 (1H, t, *J* = 2.3, H<sub>f (ΔS)</sub>), 6.62 – 6.49 (4H, m, H<sub>b, b' (ΔS), b, b' (AS)</sub>), 6.22 (1H, dd, *J* = 7.8, 1.2, H<sub>a' (AS)</sub>), 6.15 – 6.09 (3H, m, H<sub>a, a' (ΔS), a (AS)</sub>), 5.93 (1H, dd, *J* = 11.3, 8.6, H<sub>2 (AS)</sub>), 5.32 (1H, dd, *J* = 11.7, 8.6, H<sub>2 (ΔS)</sub>), 4.72 – 4.65 (2H, m, H<sub>3 (ΔS), 1 (AS)</sub>), 4.48 (1H, dd, *J* = 8.2, 7.0, H<sub>1 (AS)</sub>), 3.86 (1H, dd, *J* = 11.3, 8.9, H<sub>3 (ΔS)</sub>). <sup>13</sup>C NMR: 186.37 (C<sub>8 (ΔS)</sub>), 185.91



(C<sub>8(ΔS)</sub>), 140.83 (C<sub>g(ΔS)</sub>), 140.66 (C<sub>g'(ΔS)</sub>), 138.86 (C<sub>g(ΔS)</sub>), 138.74 (C<sub>g(ΔS)</sub>), 135.26, 135.19, 135.17, 135.14 (C<sub>a, a'(ΔS)</sub>, a, a'(ΔS)), 129.96, 129.90, 129.55, 129.42, 129.12, 128.86, 128.70, 128.66, 128.36, 128.29, 128.22 (C<sub>e, e', 4, 4', 5, 5', 6(ΔS)</sub>, e, e', 4, 4', 5, 5', 6(ΔS)), 126.57, 126.41, 126.33, 126.10 (C<sub>b, b'(ΔS)</sub>, b, b'(ΔS)), 122.83, 122.26, 122.22 (C<sub>c, c'(ΔS)</sub>, c, c'(ΔS)), 112.03, 111.92, 111.86 (C<sub>d, d'(ΔS)</sub>, d, d'(ΔS)), 108.82, 108.72, 108.67, 108.37 (C<sub>f, f'(ΔS)</sub>, f, f'(ΔS)), 62.24 (C<sub>1(ΔS)</sub>), 61.36 (C<sub>1(ΔS)</sub>) (quaternary C could not be assigned). MS (FAB): *m/z* 630 [M+H]<sup>+</sup>.

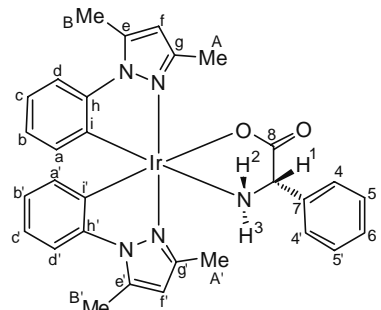
### Synthesis of ΔS-5.3a

This was prepared from dimer ΔΔ-5.6a (30 mg, 0.025 mmol), (S)-phglyH (9.2 mg, 0.061 mmol), and NaOMe (3.3 mg, 0.061 mmol) and after work up gave ΔS-5.3a as a grey solid (23 mg, 72%). <sup>1</sup>H NMR (MeOD): δ 8.54 (1H, dd, *J* = 2.3, 0.8, H<sub>e</sub>), 8.49 (1H, dd, *J* = 2.3, 0.8, H<sub>e</sub>), 7.90 (1H, dd, *J* = 2.3, 0.8, H<sub>g</sub>), 7.87 (1H, dd, *J* = 2.3, 0.8, H<sub>g</sub>), 7.39 – 7.29 (7H, m, H<sub>4, 4', 5, 5', 6, d, d'</sub>), 6.88 (1H, t, *J* = 2.3, H<sub>f</sub>), 6.83 (1H, td, *J* = 7.8, 1.2, H<sub>c'</sub>), 6.77 (1H, td, *J* = 7.4, 1.6, H<sub>c</sub>), 6.72 (1H, t, *J* = 2.3, H<sub>f</sub>), 6.60 (1H, td, *J* = 7.4, 1.2, H<sub>b'</sub>), 6.51 (1H, td, *J* = 7.4, 1.2, H<sub>b</sub>), 6.13, 6.11 (2H, 2 X dd, *J* = 7.4, 1.2, H<sub>a, a'</sub>), 5.34 (1H, dd, *J* = 11.7, 8.9, H<sub>2</sub>), 4.70 (1H, dd, *J* = 11.7, 6.7, H<sub>3</sub>), 4.48 (1H, dd, *J* = 8.6, 7.0, H<sub>1</sub>). <sup>13</sup>C NMR: 186.39 (C<sub>8</sub>), 145.52 (C<sub>h'</sub>), 145.38 (C<sub>h</sub>), 140.67 (C<sub>g</sub>), 138.75 (C<sub>g'</sub>), 135.29, 135.17 (C<sub>a, a'</sub>), 134.05 (C<sub>7</sub>), 129.98, 129.50, 129.14, 128.53 (C<sub>4, 4', 5, 5', 6, i'</sub>), 128.38 (C<sub>e</sub>), 128.23 (C<sub>e'</sub>), 126.60 (C<sub>i</sub>), 126.35 (C<sub>b'</sub>), 126.12 (C<sub>b</sub>), 122.86 (C<sub>c'</sub>), 122.23 (C<sub>c</sub>), 112.03, 111.87 (C<sub>d, d'</sub>), 108.72 (C<sub>f</sub>), 108.38 (C<sub>f</sub>), 61.38 (C<sub>1</sub>). [α]<sub>D</sub> -516.5° in MeOH.



### Synthesis of ΔS/ΔS-5.3f

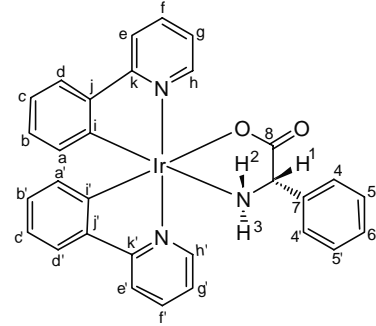
This was prepared from dimer 2.6f (50 mg, 0.044 mmol), (S)-phglyH (16.1 mg, 0.106 mmol), and NaOMe (5.8 mg, 0.106 mmol) and after work up gave ΔS/ΔS-5.3f as a grey solid (combined yield 52 mg, 87%). ΔS/ΔS-5.3f could not be separated. Anal. Calcd for C<sub>30</sub>H<sub>30</sub>IrN<sub>5</sub>O<sub>2</sub>: C, 52.62, H, 4.42, N, 10.23. Found (ΔS:ΔS 1:1): C, 52.57, H, 4.39, N, 10.19%. <sup>1</sup>H NMR (CDCl<sub>3</sub>): δ 7.33 – 7.19 (14H, m, H<sub>4, 4', 5, 5', 6, d, d'(ΔS)</sub>, 4, 4', 5, 5', 6, d, d'(ΔS)), 6.84 – 6.76 (4H, m,



$H_c, c'(\Delta S), c, c'(\Delta S))$ , 6.64 – 6.57 (4H, m,  $H_b, b'(\Delta S), b, b'(\Delta S)$ ), 6.49 (1H, dd,  $J = 7.8, 1.6$ ,  $H_{a'(\Delta S)}$ ), 6.44 (1H, dd,  $J = 7.4, 1.6$ ,  $H_{a(\Delta S)}$ ), 6.28 (1H, s,  $H_{f(\Delta S)}$ ), 6.26 (1H, s,  $H_{f'(\Delta S)}$ ), 6.19 (1H, s,  $H_{f(\Delta S)}$ ), 6.19 – 6.15 (2H, m,  $H_{a'(\Delta S)}, a(\Delta S)$ ), 6.14 (1H, s,  $H_{f'(\Delta S)}$ ), 4.64 (1H, dd,  $J = 9.8, 7.8$ ,  $H_{l(\Delta S)}$ ), 4.28 (1H, dd,  $J = 9.8, 7.8$ ,  $H_{l(\Delta S)}$ ), 4.04 – 3.94 (2H, m,  $H_{3(\Delta S)}, 2(\Delta S)$ ), 3.21 (1H, dd,  $J = 10.9, 7.4$ ,  $H_{2(\Delta S)}$ ), 2.92 (1H, m,  $H_{3(\Delta S)}$ ), 2.87 (3H, s,  $Me_{B(\Delta S)}$ ), 2.84 (3H, s,  $Me_{B'(\Delta S)}$ ), 2.81 (3H, s,  $Me_{B'(\Delta S)}$ ), 2.80 (3H, s,  $Me_{B(\Delta S)}$ ), 2.66 (3H, s,  $Me_{A'(\Delta S)}$ ), 2.64 (3H, s,  $Me_{A(\Delta S)}$ ), 2.62 (3H, s,  $Me_{A(\Delta S)}$ ), 2.42 (3H, s,  $Me_{A'(\Delta S)}$ ).  $^{13}C$  NMR: 178.93, 178.85 ( $C_{8(\Delta S)}, C_{8(\Delta S)}$ ), 135.30 ( $C_{a(\Delta S)}$ ), 135.00 ( $C_{a'(\Delta S)}$ ), 133.99, 133.83 ( $C_{a'(\Delta S)}, a(\Delta S)$ ), 129.16, 129.08, 128.17, 128.03, 127.98, 127.51, 127.39, 127.24 ( $C_{4, 4', 5, 5', 6(\Delta S)}, 4, 4', 5, 5', 6(\Delta S)$ ), 124.49, 124.37, 124.35 ( $C_b, b'(\Delta S), b, b'(\Delta S)$ ), 121.88, 121.77, 121.24 ( $C_c, c'(\Delta S), c, c'(\Delta S)$ ), 111.95, 111.86, 111.71, 111.67 ( $C_d, d'(\Delta S), d, d'(\Delta S)$ ), 110.12, 109.97, 109.68, 109.47 ( $C_f, f(\Delta S), f, f'(\Delta S)$ ), 61.44 ( $C_{l(\Delta S)}$ ), 60.71 ( $C_{1(\Delta S)}$ ), 14.72, 14.69, 14.56, 13.77, 13.53, 12.87 ( $Me_{A, A'}, B, B'(\Delta S), Me_{A, A'}, B, B'(\Delta S)$ ) (quaternary C could not be assigned). MS (FAB):  $m/z$  686 [M+H]<sup>+</sup>.

### Synthesis of $\Delta S/\Delta S\text{-5.3g}$

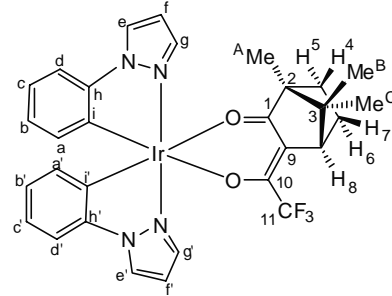
This was prepared from dimer **2.6g** (70 mg, 0.065 mmol), (S)-phglyH (23.6 mg, 0.157 mmol), and NaOMe (8.5 mg, 0.157 mmol) and after work up gave  $\Delta S/\Delta S\text{-5.3g}$  as a yellow solid (combined yield 63 mg, 74%).  $\Delta S/\Delta S\text{-5.3g}$  could not be separated. Anal. Calcd for  $C_{30}H_{24}IrN_3O_2$ : C, 55.37, H, 3.72, N, 6.46. Found ( $\Delta S:\Delta S$  1:1): C, 55.31, H, 3.68, N, 6.33%.  $^1H$  NMR ( $CDCl_3$ ):  $\delta$  9.09 (1H, d,  $J = 5.4$ ,  $H_{h'(\Delta S)}$ ), 8.98 (1H, d,  $J = 5.4$ ,  $H_{h(\Delta S)}$ ), 8.82 (1H, d,  $J = 5.8$ ,  $H_{h(\Delta S)}$ ), 8.12 (1H, d,  $J = 5.8$ ,  $H_{h'(\Delta S)}$ ), 7.93 – 7.79 (6H, m,  $H_e, e', f(\Delta S), e, e', f'(\Delta S)$ ), 7.75 (1H, td,  $J = 8.2, 1.6$ ,  $H_{f(\Delta S)}$ ), 7.68 (1H, td,  $J = 8.2, 1.2$ ,  $H_{f'(\Delta S)}$ ), 7.56 – 7.49 (4H, m,  $H_d, d'(\Delta S), d, d'(\Delta S)$ ), 7.34 – 7.06 (13H, m,  $H_{4, 4', 5, 5', 6, g(\Delta S)}, 4, 4', 5, 5', 6, g, g'(\Delta S)$ ), 6.95 (1H, ddd,  $J = 7.4, 5.9, 1.6$ ,  $H_{g'(\Delta S)}$ ), 6.86 – 6.76 (4H, m,  $H_c, c'(\Delta S), c, c'(\Delta S)$ ), 6.72 – 6.60 (4H, m,  $H_b, b'(\Delta S), b, b'(\Delta S)$ ), 6.34 (1H, d,  $J = 7.4$ ,  $H_{a'(\Delta S)}$ ), 6.26 (1H, d,  $J = 7.8$ ,  $H_{a(\Delta S)}$ ), 6.15 (1H, d,  $J = 7.8$ ,  $H_{a(\Delta S)}$ ), 6.12 (1H, d,  $J = 7.8$ ,  $H_{a'(\Delta S)}$ ), 4.72 (1H, dd,  $J = 9.3, 8.6$ ,  $H_{l(\Delta S)}$ ), 4.51 (1H, dd,  $J = 8.6, 5.9$ ,  $H_{l(\Delta S)}$ ), 4.28 (1H, dd,  $J = 11.7, 8.2$ ,  $H_{2(\Delta S)}$ ), 3.34 (1H, dd,  $J = 11.3, 8.2$ ,  $H_{2(\Delta S)}$ ), 3.16 (1H, dd,  $J = 11.3, 5.8$ ,  $H_{3(\Delta S)}$ ), 2.39 (1H, m,  $H_{3(\Delta S)}$ ).  $^{13}C$  NMR: 180.31, 180.25 ( $C_{8(\Delta S)}, C_{8(\Delta S)}$ ), 149.70 ( $C_{h'(\Delta S)}$ ), 149.26, 148.87, 148.78 ( $C_{h, h'(\Delta S)}, h(\Delta S)$ ), 137.76, 137.63, 137.19 ( $C_{f, f'(\Delta S)}, f, f'(\Delta S)$ ), 133.09, 133.05, 132.21 ( $C_a, a'(\Delta S), a, a'(\Delta S)$ ), 129.57, 129.53, 129.45, 129.27, 129.02, 128.59, 128.42, 127.84, 127.76 ( $C_{4, 4', 5, 5', 6, b, b'(\Delta S)}, 4, 4', 5, 5', 6, b, b'(\Delta S)$ ),



124.31, 124.20, 124.13, 124.04 (C<sub>d</sub>, d'(ΔS), d, d'(ΔS)), 122.62, 122.53, 122.08, 121.40, 121.33, 120.83, 120.68 (C<sub>c</sub>, c', g, g'(ΔS), c, c', g, g'(ΔS)), 119.14, 119.10, 118.89, 118.75 (C<sub>e</sub>, e'(ΔS), e, e'(ΔS)), 59.73 (C<sub>1(ΔS)</sub>), 59.42 (C<sub>1(ΔS)</sub>) (quaternary C could not be assigned). MS (FAB): *m/z* 652 [M+H]<sup>+</sup>.

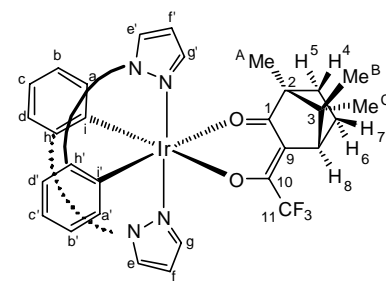
### Synthesis of Δ(+)/Λ(+)-5.4a

This was prepared from dimer **2.6a** (80 mg, 0.078 mmol), (+)-tfacH (38.7 mg, 33 μL, 0.156 mmol), and Na<sub>2</sub>CO<sub>3</sub> (33.1 mg, 0.312 mmol) and after work up gave Δ(+)/Λ(+)-**5.4a** as a yellow solid (combined yield 92 mg, 82%). Δ(+)/Λ(+)-**5.4a** could not be separated. Anal. Calcd for C<sub>30</sub>H<sub>29</sub>F<sub>3</sub>IrN<sub>4</sub>O<sub>2</sub>: C, 49.58, H, 4.02, N, 7.71. Found (Δ(+):Λ(+): 1:1): C, 49.62, H, 3.89, N, 7.61%. <sup>1</sup>H NMR (CDCl<sub>3</sub>): δ 8.06 – 8.02 (4H, m, H<sub>e</sub>, e'(ΔS), e, e'(ΔS)), 7.54 (1H, d, *J* = 2.7, H<sub>g(ΔS)</sub>), 7.53 (1H, d, *J* = 2.7, H<sub>g'(ΔS)</sub>), 7.46 (1H, d, *J* = 2.3, H<sub>g(ΔS)</sub>), 7.42 (1H, d, *J* = 2.3, H<sub>g'(ΔS)</sub>), 7.15 – 7.12 (4H, m, H<sub>d</sub>, d'(ΔS), d, d'(ΔS)), 6.85 – 6.80 (4H, m, H<sub>c</sub>, c'(ΔS), c, c'(ΔS)), 6.68 – 6.60 (8H, m, H<sub>b</sub>, b', f, f'(ΔS), b, b', f, f'(ΔS)), 6.24 – 6.21 (4H, m, H<sub>a</sub>, a'(ΔS), a, a'(ΔS)), 2.85 (1H, t, *J* = 3.1, H<sub>8(ΔS)</sub>), 2.82 (1H, t, *J* = 3.1, H<sub>8(ΔS)</sub>), 2.07 – 1.96 (2H, m, H<sub>7(ΔS)</sub>, 7(ΔS)), 1.59 (1H, dd, *J* = 11.0, 3.9, H<sub>5(ΔS)</sub>), 1.44 – 1.28 (4H, m, H<sub>4, 6(ΔS)</sub>, 4, 6(ΔS)), 0.88 – 0.82 (1H, m, H<sub>5(ΔS)</sub>), 0.87 (3H, s, Me<sub>B(ΔS)</sub>), 0.84 (3H, s, Me<sub>C(ΔS)</sub>), 0.82 (3H, s, Me<sub>C(ΔS)</sub>), 0.81 (3H, s, Me<sub>A(ΔS)</sub>), 0.73 (3H, s, Me<sub>A(ΔS)</sub>), 0.65 (3H, s, Me<sub>B(ΔS)</sub>). <sup>13</sup>C NMR: 203.54 (C<sub>1(ΔS)</sub>, C<sub>1(ΔS)</sub>), 137.84, 137.29, 137.22, 136.84 (C<sub>g</sub>, g'(ΔS), g, g'(ΔS)), 135.06, 134.95, 134.85 (C<sub>a</sub>, a'(ΔS), a, a'(ΔS)), 126.12, 126.00, 125.90, 125.84, 125.72, 125.16, 125.12 (C<sub>b</sub>, b', e, e'(ΔS), b, b', e, e'(ΔS)), 121.57, 121.48, 121.44 (C<sub>c</sub>, c'(ΔS), c, c'(ΔS)), 110.43, 110.35, 110.32 (C<sub>d</sub>, d'(ΔS), d, d'(ΔS)), 106.90, 106.81, 106.73, 106.70 (C<sub>f</sub>, f'(ΔS), f, f'(ΔS)), 49.54 (C<sub>8(ΔS)</sub>), 48.73 (C<sub>8(ΔS)</sub>), 30.33 (C<sub>4, 5(ΔS)</sub>), 30.18 (C<sub>4, 5(ΔS)</sub>), 28.18 (C<sub>6, 7(ΔS)</sub>, 6, 7(ΔS)), 20.09 (Me<sub>B(ΔS)</sub>), 19.74 (Me<sub>B(ΔS)</sub>), 19.11 (Me<sub>C(ΔS)</sub>), 19.08 (Me<sub>C(ΔS)</sub>), 9.56 (Me<sub>A(ΔS)</sub>, Me<sub>A(ΔS)</sub>) (quaternary C could not be assigned). MS (FAB): *m/z* 726 [M]<sup>+</sup>.



### Synthesis of Δ(+)-5.4a

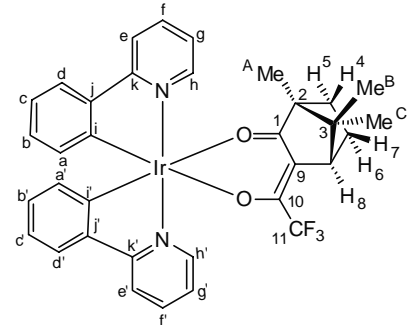
This was prepared from dimer ΔΔ-**5.6a** (20 mg, 0.017 mmol), (+)-tfacH (10 mg, 8.6 μL, 0.041 mmol), and Na<sub>2</sub>CO<sub>3</sub> (7.2 mg, 0.068 mmol) and after work up gave Δ(+)-**5.4a** as a yellow solid (18 mg, 73%). <sup>1</sup>H NMR (CDCl<sub>3</sub>): δ 8.05 (1H, dd, *J* = 2.7, 0.8, H<sub>e</sub>), 8.02



(1H, dd,  $J = 2.3, 0.8$ , H<sub>e</sub>), 7.53 (1H, dd,  $J = 1.9, 0.8$ , H<sub>g'</sub>), 7.46 (1H, dd,  $J = 2.3, 0.8$ , H<sub>g</sub>), 7.13 (2H, 2X dd,  $J = 7.8, 1.2$ , H<sub>d, d'</sub>), 6.85 – 6.79 (2H, m, H<sub>c, c'</sub>), 6.68 – 6.60 (4H, m, H<sub>b, b', f, f'</sub>), 6.23 (1H, dd,  $J = 7.4, 1.2$ , H<sub>a'</sub>), 6.22 (1H, dd,  $J = 7.4, 1.2$ , H<sub>a</sub>), 2.85 (1H, t,  $J = 2.7$ , H<sub>8</sub>), 2.00 (1H, m, H<sub>7</sub>), 1.41 – 1.31 (2H, m, H<sub>4, 6</sub>), 0.88 – 0.82 (1H, m, H<sub>5</sub>), 0.87 (3H, s, Me<sub>B</sub>), 0.84 (3H, s, Me<sub>C</sub>), 0.81 (3H, s, Me<sub>A</sub>).  $^{13}\text{C}$  NMR: 206.96 (C<sub>10</sub>), 203.52 (C<sub>1</sub>), 144.40, 144.25 (C<sub>h, h'</sub>), 137.28, 137.20 (C<sub>g, g'</sub>), 135.05, 134.84 (C<sub>a, a'</sub>), 127.17, 126.14 (C<sub>i, i'</sub>), 125.90, 125.71 (C<sub>e, e'</sub>), 125.15 (C<sub>b, b'</sub>), 121.56, 121.43 (C<sub>c, c'</sub>), 112.74 (C<sub>11</sub>), 110.43, 110.35 (C<sub>d, d'</sub>), 106.89, 106.69 (C<sub>f, f'</sub>), 58.43 (C<sub>9</sub>), 49.50 (C<sub>3</sub>), 48.66 (C<sub>8</sub>), 30.93 (C<sub>2</sub>), 30.18 (C<sub>4, 5</sub>), 28.18 (C<sub>6, 7</sub>), 20.09 (Me<sub>B</sub>), 19.08 (Me<sub>C</sub>), 9.55 (Me<sub>A</sub>).  $[\alpha]_D$  -538° in DCM. MS (FAB):  $m/z$  726 [M]<sup>+</sup>.

## Synthesis of $\Delta(+)$ / $\Lambda(+)$ -5.4g

This was prepared from dimer **2.6g** (80 mg, 0.075 mmol), (+)-tfacH (37.2 mg, 31.8  $\mu$ L, 0.150 mmol), and  $\text{Na}_2\text{CO}_3$  (31.8 mg, 0.300 mmol) and after work up gave  $\Delta(+)/\Lambda(+)$ -**5.4g** as a yellow solid (combined yield 92 mg, 82%).  $\Delta(+)/\Lambda(+)$ -**5.4g** could not be separated. Anal. Calcd for  $\text{C}_{34}\text{H}_{31}\text{F}_3\text{IrN}_2\text{O}_2$ : C,

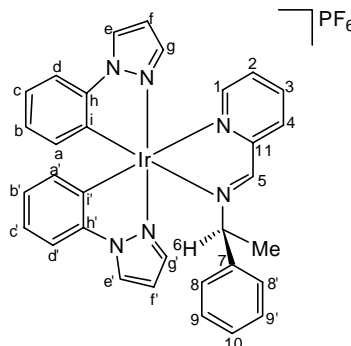


54.53, H, 4.17, N, 3.74. Found ( $\Delta(+)$ ): $\Lambda(+)$  1:1): C, 54.45, H, 4.11, N, 3.73%.  $^1\text{H}$  NMR (CDCl<sub>3</sub>):  $\delta$  8.44 – 8.42 (2H, m, H<sub>h'(\Delta S)</sub>, H<sub>h'(\Lambda S)</sub>), 8.33 (1H, ddd,  $J$  = 5.5, 1.6, 0.8, H<sub>h(\Delta S)</sub>), 8.25 (1H, ddd,  $J$  = 5.9, 1.6, 0.8, H<sub>h(\Lambda S)</sub>), 7.86 – 7.80 (4H, m, H<sub>e, e'(\Delta S)</sub>, H<sub>e, e'(\Lambda S)</sub>), 7.74 – 7.68 (4H, m, H<sub>f, f'(\Delta S)</sub>, H<sub>f, f'(\Lambda S)</sub>), 7.54 – 7.52 (4H, m, H<sub>d, d'(\Delta S)</sub>, H<sub>d, d'(\Lambda S)</sub>), 7.12 – 7.06 (4H, m, H<sub>g, g'(\Delta S)</sub>, H<sub>g, g'(\Lambda S)</sub>), 6.84 – 6.79 (4H, m, H<sub>c, c'(\Delta S)</sub>, H<sub>c, c'(\Lambda S)</sub>), 6.72 – 6.65 (4H, m, H<sub>b, b'(\Delta S)</sub>, H<sub>b, b'(\Lambda S)</sub>), 6.30 – 6.25 (4H, m, H<sub>a, a'(\Delta S)</sub>, H<sub>a, a'(\Lambda S)</sub>), 2.83 (1H, t,  $J$  = 3.1, H<sub>8(\Delta S)</sub>), 2.79 (1H, t,  $J$  = 3.1, H<sub>8(\Lambda S)</sub>), 2.05 – 1.93 (2H, m, H<sub>7(\Delta S)</sub>, H<sub>7(\Lambda S)</sub>), 1.59 – 1.53 (1H, m, H<sub>5(\Delta S)</sub>), 1.39 – 1.23 (4H, m, H<sub>4, 6(\Delta S)</sub>, H<sub>4, 6(\Lambda S)</sub>), 0.84 (3H, s, Me<sub>B(\Delta S)</sub>), 0.82 (3H, s, Me<sub>C(\Delta S)</sub>), 0.80 (3H, s, Me<sub>C(\Lambda S)</sub>), 0.78 (3H, s, Me<sub>A(\Delta S)</sub>), 0.69 (3H, s, Me<sub>A(\Lambda S)</sub>), 0.64 – 0.57 (1H, m, H<sub>5(\Delta S)</sub>), 0.52 (3H, s, Me<sub>B(\Lambda S)</sub>).  $^{13}\text{C}$  NMR: 203.38, 202.97 (C<sub>1(\Delta S)</sub>, C<sub>1(\Lambda S)</sub>), 148.13, 147.75 (C<sub>h'(\Delta S)</sub>, C<sub>h'(\Lambda S)</sub>), 147.59 (C<sub>h(\Delta S)</sub>), 147.00 (C<sub>h(\Lambda S)</sub>), 137.20, 137.18, 137.15, 137.11 (C<sub>f, f'(\Delta S)</sub>, C<sub>f, f'(\Lambda S)</sub>), 133.46, 133.29, 133.20, 133.14 (C<sub>a, a'(\Delta S)</sub>, C<sub>a, a'(\Lambda S)</sub>), 128.98, 128.86 (C<sub>b, b'(\Delta S)</sub>, C<sub>b, b'(\Lambda S)</sub>), 123.75, 123.71, 123.64 (C<sub>d, d'(\Delta S)</sub>, C<sub>d, d'(\Lambda S)</sub>), 121.33, 121.20, 120.92, 120.86, 120.83, 120.35 (C<sub>c, c'</sub>, C<sub>c, c'(\Delta S)</sub>, C<sub>c, c'(\Lambda S)</sub>), 118.66, 118.63, 118.25, 118.12 (C<sub>e, e'(\Delta S)</sub>, C<sub>e, e'(\Lambda S)</sub>), 48.70, 48.60 (C<sub>8(\Delta S)</sub>, C<sub>8(\Lambda S)</sub>), 30.08 (C<sub>4, 5(\Delta S)</sub>), 29.94 (C<sub>4, 5(\Lambda S)</sub>), 28.29, 28.10 (C<sub>6, 7(\Delta S)</sub>, C<sub>6, 7(\Lambda S)</sub>), 19.96 (Me<sub>B(\Delta S)</sub>), 19.47

(Me<sub>B(ΔS)</sub>), 19.16, 19.07 (Me<sub>C(ΔS)</sub>, Me<sub>C(ΔS)</sub>), 9.52, 9.49 (Me<sub>A(ΔS)</sub>, Me<sub>A(ΔS)</sub>) (quaternary C could not be assigned). MS (FAB): *m/z* 748 [M]<sup>+</sup>.

### Synthesis of ΔS/ΔS-5.5a

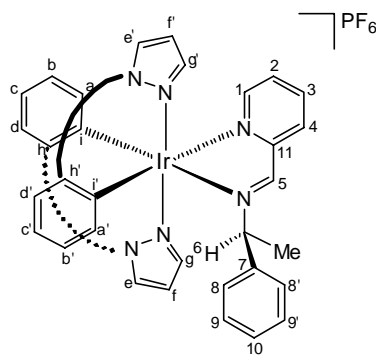
The dimer **2.6a** (35 mg, 0.034 mmol), pyridine-2-carboxaldehyde (8.4 mg, 7.4 μL, 0.078 mmol), (S)-phenylethylamine (9.5 mg, 10.1 μL, 0.078 mmol) and KPF<sub>6</sub> (14.3 mg, 0.078 mmol) were placed in a microwave vial and methanol (1 ml) was added. Nitrogen was bubbled through the solution for 2 mins and the vial was then sealed with a septum cap. The tube was placed in the microwave reactor and heated under microwave irradiation at 60 °C for 20 mins. After this time the solvent was removed *in vacuo* leaving behind a solid which was dissolved in DCM (5 ml) and passed through celite. The filtrate was reduced in volume and hexane was added slowly to induce precipitation. The precipitate was isolated, washed with hexane and dried *in vacuo* to give ΔS/ΔS-**5.5a** as a yellow solid (combined yield 37 mg, 65%). <sup>1</sup>H NMR (CDCl<sub>3</sub>): δ 10.84 (1H, s, H<sub>5(ΔS)</sub>), 10.76 (1H, s, H<sub>5(ΔS)</sub>), 9.44, 9.37 (2H, 2 X d, *J* = 7.8, H<sub>4(ΔS)</sub>, 4(ΔS)), 8.10 – 8.04 (3H, m, H<sub>3</sub>, e(ΔS), 3(ΔS)), 8.01 (1H, d, *J* = 2.7, H<sub>e(ΔS)</sub>), 7.92 (1H, dd, *J* = 5.4, 1.2, H<sub>1(ΔS)</sub>), 7.80 – 7.78 (2H, m, H<sub>1</sub>, e'(ΔS)), 7.55 (1H, d, *J* = 2.7, H<sub>e'(ΔS)</sub>), 7.37 (1H, dd, *J* = 7.4, 5.4, H<sub>2(ΔS)</sub>), 7.32 (1H, dd, *J* = 7.4, 5.4, H<sub>2(ΔS)</sub>), 7.26 (1H, m, H<sub>g(ΔS)</sub>), 7.24 (1H, d, *J* = 2.3, H<sub>g(ΔS)</sub>), 7.21 – 7.19 (2H, m, H<sub>d(ΔS)</sub>, d(ΔS)), 7.13 – 6.74 (18H, m, H<sub>9</sub>, 9', 10, b, b', c, c', d'(ΔS), 8, 8', 9, 9', 10, b, b', c, c', d'(ΔS)), 6.65 (1H, d, *J* = 1.9, H<sub>g'(ΔS)</sub>), 6.63 (1H, d, *J* = 2.3, H<sub>g'(ΔS)</sub>), 6.59 (1H, t, *J* = 2.3, H<sub>f(ΔS)</sub>), 6.46 – 6.41 (4H, m, H<sub>8</sub>, 8'(ΔS), f, f(ΔS)), 6.35 (1H, t, *J* = 2.3, H<sub>f(ΔS)</sub>), 6.23 (1H, dd, *J* = 7.4, 1.2, H<sub>a'(ΔS)</sub>), 6.21 (1H, dd, *J* = 7.4, 1.2, H<sub>a'(ΔS)</sub>), 6.07 (1H, dd, *J* = 7.4, 1.2, H<sub>a(ΔS)</sub>), 6.02 (1H, dd, *J* = 7.4, 1.2, H<sub>a(ΔS)</sub>), 5.28 (1H, q, *J* = 7.0, H<sub>6(ΔS)</sub>), 5.10 (1H, q, *J* = 7.0, H<sub>6(ΔS)</sub>), 1.77 (3H, d, *J* = 7.0, Me<sub>(ΔS)</sub>), 1.72 (3H, d, *J* = 7.0, Me<sub>(ΔS)</sub>). <sup>13</sup>C NMR: 170.82 (C<sub>5(ΔS)</sub>), 169.76 (C<sub>5(ΔS)</sub>), 149.76 (C<sub>1(ΔS)</sub>), 149.68 (C<sub>1(ΔS)</sub>), 140.54 (C<sub>3(ΔS)</sub>), 139.62 (C<sub>3(ΔS)</sub>), 139.37, 139.12, 137.49, 137.18 (C<sub>g</sub>, g'(ΔS), g, g'(ΔS)), 132.87, 132.45, 132.23, 131.81 (C<sub>a</sub>, a'(ΔS), a, a'(ΔS)), 128.61, 128.34, 128.12, 127.80, 127.69, 126.96, 126.86, 126.57 (C<sub>2</sub>, 4, 8, 8', 9, 9', 10, b, b'(ΔS), 2, 4, 8, 8', 9, 9', 10, b, b'(ΔS)), 126.43, 126.21 (C<sub>e</sub>, e'(ΔS), e, e'(ΔS)), 123.40, 122.83, 122.74 (C<sub>c</sub>, c'(ΔS), c, c'(ΔS)), 111.68, 111.41 (C<sub>d</sub>, d'(ΔS), d, d'(ΔS)), 108.51, 108.17, 107.91, 107.63 (C<sub>f</sub>, f(ΔS), f, f(ΔS)), 69.90 (C<sub>6(ΔS)</sub>), 69.81 (C<sub>6(ΔS)</sub>), 22.98 (Me<sub>(ΔS)</sub>), 20.81 (Me<sub>(ΔS)</sub>) (quaternary C could not be assigned). MS (FAB): *m/z* 689 [M]<sup>+</sup>.



## Synthesis of $\Delta S\text{-5.5a}$

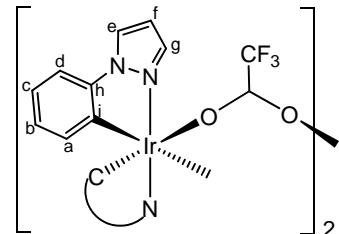
The procedure was carried out same as that described for the preparation of  $\Delta S/\Delta S\text{-5.5a}$ . This was prepared from dimer  $\Delta\Delta\text{-5.6a}$  (20 mg, 0.017 mmol), pyridine-2-carboxaldehyde (4.4 mg, 3.9  $\mu$ L, 0.041 mmol), (S)-phenylethylamine (4.9 mg, 5.2  $\mu$ L, 0.041 mmol) and  $\text{KPF}_6$  (7.5 mg, 0.041 mmol) and after work up gave  $\Delta S\text{-5.5a}$  as a yellow solid (22 mg, 78%).

Anal. Calcd for  $\text{C}_{32}\text{H}_{28}\text{F}_6\text{IrN}_6\text{P}$ : C, 46.10, H, 3.38, N, 10.08. Found ( $\Delta S$ ): C, 45.99, H, 3.40, N, 10.04%.  $^1\text{H}$  NMR ( $\text{CDCl}_3$ ):  $\delta$  9.71 (1H, d,  $J$  = 1.2,  $\text{H}_5$ ), 8.69 (1H, d,  $J$  = 7.8,  $\text{H}_4$ ), 8.06 (1H, td,  $J$  = 7.8, 1.6,  $\text{H}_3$ ), 8.04 (1H, d,  $J$  = 2.7,  $\text{H}_e$ ), 7.95 (1H, dd,  $J$  = 5.1, 0.8,  $\text{H}_1$ ), 7.56 (1H, d,  $J$  = 2.7,  $\text{H}_{e'}$ ), 7.38 (1H, ddd,  $J$  = 7.8, 5.5, 1.2,  $\text{H}_2$ ), 7.29 (1H, d,  $J$  = 2.3,  $\text{H}_g$ ), 7.19 (1H, dd,  $J$  = 7.8, 0.8,  $\text{H}_d$ ), 7.02 – 6.95 (2H, m,  $\text{H}_{10, c}$ ), 6.93 – 6.89 (3H, m,  $\text{H}_{9, 9', c'}$ ), 6.82 – 6.76 (3H, m,  $\text{H}_{b, b', d'}$ ), 6.70 (1H, d,  $J$  = 2.3,  $\text{H}_{g'}$ ), 6.61 (1H, t,  $J$  = 2.3,  $\text{H}_f$ ), 6.38 – 6.36 (3H, m,  $\text{H}_{8, 8', f}$ ), 6.22 (1H, dd,  $J$  = 7.4, 1.6,  $\text{H}_a$ ), 6.07 (1H, dd,  $J$  = 7.4, 1.2,  $\text{H}_a$ ), 5.25 (1H, q,  $J$  = 7.0,  $\text{H}_6$ ), 1.69 (3H, d,  $J$  = 7.0, Me).  $^{13}\text{C}$  NMR: 167.77 ( $\text{C}_5$ ), 156.94 ( $\text{C}_{11}$ ), 150.07 ( $\text{C}_1$ ), 142.83 ( $\text{C}_{b'}$ ), 142.52 ( $\text{C}_h$ ), 139.68 ( $\text{C}_3$ ), 139.20 ( $\text{C}_g$ ), 138.63 ( $\text{C}_7$ ), 137.31 ( $\text{C}_{g'}$ ), 132.98 ( $\text{C}_{a'}$ ), 132.70 ( $\text{C}_a$ ), 131.57 ( $\text{C}_i$ ), 130.93 ( $\text{C}_4$ ), 130.85 ( $\text{C}_{i'}$ ), 128.42 ( $\text{C}_2$ ), 128.37 ( $\text{C}_{9, 9'}$ ), 126.94 ( $\text{C}_{10}$ ), 126.86 ( $\text{C}_b$ ), 126.58 ( $\text{C}_b$ ), 126.34 ( $\text{C}_e$ ), 126.19 ( $\text{C}_e$ ), 126.09 ( $\text{C}_{8, 8'}$ ), 123.36 ( $\text{C}_c$ ), 122.70 ( $\text{C}_c$ ), 111.35 ( $\text{C}_{d, d'}$ ), 108.60 ( $\text{C}_f$ ), 107.70 ( $\text{C}_f$ ), 69.43 ( $\text{C}_6$ ), 22.33 (Me).  $[\alpha]_D$  -614° in DCM. MS (FAB):  $m/z$  689 [ $\text{M}]^+$ .



## Synthesis of $\Delta\Delta\text{-5.6a}$

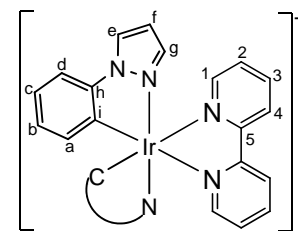
TFA (162 mg, 109.7  $\mu$ L, 1.423 mmol) was added to a solution of  $\Delta S\text{-5.2a}$  (50 mg, 0.071 mmol) in DCM (2 ml).  $\text{H}_2\text{O}$  (2 ml) was added to this reaction mixture after stirring it for an hour. Deep yellow colour changed successively to pale yellow and colourless after stirring for 48 hrs at room temperature. After this time, aqueous layer is separated and organic layer is passed through celite. Reduced the volume of filtrate and hexane was added slowly to induce precipitation. The precipitate was isolated, washed with hexane and dried *in vacuo* to give  $\Delta\Delta\text{-5.6a}$  as a grey solid (34 mg, 81%).  $^1\text{H}$  NMR ( $\text{CDCl}_3$ ):  $\delta$  8.10 (4H, d,  $J$  = 2.3,  $\text{H}_e$ ), 7.88 (4H, d,  $J$  = 2.0,  $\text{H}_g$ ), 7.13 (4H, dd,  $J$  = 7.8, 1.2,  $\text{H}_d$ ), 6.85 (4H, td,  $J$  = 7.4,



1.2, H<sub>c</sub>), 6.75 (4H, t, *J* = 2.7, H<sub>f</sub>), 6.63 (4H, td, *J* = 7.4, 1.2, H<sub>b</sub>), 6.10 (4H, dd, *J* = 7.8, 1.2, H<sub>a</sub>). MS (FAB): *m/z* 1071 [M-CF<sub>3</sub>CO<sub>2</sub>]<sup>+</sup>. MS (ES): *m/z* 561 [Ir(ppz)<sub>2</sub>(MeCN)<sub>2</sub>]<sup>+</sup>.

### Synthesis of $\Delta$ -2.7a

TFA (40.5 mg, 27.4  $\mu$ L, 0.356 mmol) was added to a solution of  $\Delta$ S-5.2a (50 mg, 0.071 mmol) and bipy (12.2 mg, 0.078 mmol) in DCM (2 ml). Stirred the reaction mixture for an hour and after that washed the reaction mixture with water (3  $\times$  5 ml). Separated the organic layer and dried with anh.



MgSO<sub>4</sub>. Reduced the volume of filtrate and hexane was added slowly to induce precipitation. The precipitate was isolated, washed with hexane and dried *in vacuo* to give  $\Delta$ -2.7a as a yellow solid (38 mg, 72%). <sup>1</sup>H NMR (CD<sub>2</sub>Cl<sub>2</sub>):  $\delta$  9.23 (2H, d, *J* = 8.2, H<sub>4</sub>), 8.23 (2H, td, *J* = 8.2, 0.8, H<sub>3</sub>), 8.11 (2H, d, *J* = 2.7, H<sub>e</sub>), 8.07 (2H, dd, *J* = 5.4, 1.2, H<sub>1</sub>), 7.40 (2H, dd, *J* = 7.0, 5.8, H<sub>2</sub>), 7.29 (2H, dd, *J* = 7.8, 0.8, H<sub>d</sub>), 7.05 (2H, td, *J* = 7.8, 1.2, H<sub>c</sub>), 6.87 (2H, td, *J* = 7.4, 1.2, H<sub>b</sub>), 6.84 (2H, d, *J* = 2.0, H<sub>g</sub>), 6.54 (2H, t, *J* = 2.7, H<sub>f</sub>), 6.31 (2H, dd, *J* = 7.4, 1.2, H<sub>a</sub>).  $[\alpha]_D$  -471° in DCM. MS (FAB): *m/z* 635 [M]<sup>+</sup>.

Being enantiomer  $\Lambda$ -2.7a has the same NMR assignment as that of  $\Delta$ -2.7a.  $[\alpha]_D$  +473° in DCM.

### 5.4 Bibliography

1. K. E. Erkkila, D. T. Odom and J. K. Barton, *Chem. Rev.*, 1999, **99**, 2777-2795.
2. K. K. W. Lo, *Photofunctional transition metal complexes*, 2007, **123**, 205-245
3. C. Metcalfe and J. A. Thomas, *Chem. Soc. Rev.*, 2003, **32**, 215-224.
4. K. K. W. Lo, W. K. Hui, C. K. Chung, K. H. K. Tsang, D. C. M. Ng, N. Y. Zhu and K. K. Cheung, *Coord. Chem. Rev.*, 2005, **249**, 1434-1450.
5. K. K. W. Lo, C. K. Chung and N. Y. Zhu, *Chem. Eur. J.*, 2006, **12**, 1500-1512.
6. F. Pierard and A. Kirsch-De Mesmaeker, *Inorg. Chem. Commun.*, 2006, **9**, 111-126.
7. L. Herman, S. Ghosh, E. Defrancq and A. K. D. Mesmaeker, *J. Phys. Org. Chem.*, 2008, **21**, 670-681.
8. F. Li, W. Chen, C. F. Tang and S. S. Zhang, *Talanta*, 2008, **77**, 1-8.
9. G. N. Grimm, A. S. Boutorine, P. Lincoln, B. Norden and C. Helene, *Chembiochem*, 2002, **3**, 324-331.
10. J. M. Fisher, R. J. Potter and C. F. J. Barnard, *Applications of Coordination Complexes*, 2003.
11. H.-U. Blaser, *Tetrahedron: Asymmetry*, 1991, **2**, 843-866.
12. W. A. Herrmann and C. W. Kohlpaintner, *Angew. Chem., Int. Ed.*, 1993, **32**, 1524-1544.
13. B. J. Cowen and S. J. Miller, *Chem. Soc. Rev.*, 2009, **38**, 3102-3116.
14. M. Wills and H. Tye, *J. Chem. Soc., Perkin Trans. 1*, 1999, 1109-1132.

15. A. K. Ghosh, M. Packiarajan and J. Cappiello, *Tetrahedron-Asymmetry*, 1998, **9**, 1-45.
16. A. W. Kleij, *Eur. J. Inorg. Chem.*, 2009, 193-205.
17. H. U. Blaser, C. Malan, B. Pugin, F. Spindler, H. Steiner and M. Studer, *Adv. Synth. Catal.*, 2003, **345**, 103-151.
18. S. E. Denmark, N. Nakajima, C. M. Stiff, O. J. C. Nicaise and M. Kranz, *Adv. Synth. Catal.*, 2008, **350**, 1023-1045.
19. P. D. Knight and P. Scott, *Coord. Chem. Rev.*, 2003, **242**, 125-143.
20. J. Lacour and D. Moraleda, *Chem Commun (Camb)*, 2009, 7073-7089.
21. J. Lacour and R. Frantz, *Org. Biomol. Chem.*, 2005, **3**, 15-19.
22. J. Lacour and V. Hebbe-Viton, *Chem. Soc. Rev.*, 2003, **32**, 373-382.
23. J. Lacour, *Chimia*, 2003, **57**, 168-168.
24. J. Lacour, *Chimia*, 2002, **56**, 672-675.
25. F. R. Keene, *Chem. Soc. Rev.*, 1998, **27**, 185-193.
26. X. Hua and A. G. Lappin, *Inorg. Chem.*, 1995, **34**, 992-994.
27. O. Morgan, S. Wang, S. A. Bae, R. J. Morgan, A. D. Baker, T. C. Strekas and R. Engel, *J. Chem. Soc., Dalton Trans.*, 1997, 3773-3776.
28. J. A. A. Sagües, R. D. Gillard, D. J. Smalley and P. A. Williams, *Inorg. Chim. Acta*, 1980, **43**, 211-216.
29. X. Hua and A. von Zelewsky, *Inorg. Chem.*, 1995, **34**, 5791-5797.
30. F. Favarger, C. Goujon-Ginglinger, D. Monchaud and J. Lacour, *J. Org. Chem.*, 2004, **69**, 8521-8524.
31. S. Constant, R. Frantz, J. Muller, G. Bernardinelli and J. Lacour, *Organometallics*, 2007, **26**, 2141-2143.
32. A. Auffrant, A. Barbieri, F. Barigelli, J. Lacour, P. Mobian, J. P. Collin, J. P. Sauvage and B. Ventura, *Inorg. Chem.*, 2007, **46**, 6911-6919.
33. M. Gruselle, R. Thouvenot, W. Caspar, K. Boubekeur, H. Amouri, M. Ivanov and K. Tonsuaadu, *Mendeleev Commun.*, 2004, 282-283.
34. D. Drahonovsky, U. Kno, L. Jungo, T. Belser, A. Neels, G. C. Labat, H. Stoeckli-Evans and A. von Zelewsky, *Dalton Trans.*, 2006, 1444-1454.
35. C. Hamann, A. von Zelewsky, A. Neels and H. Stoeckli-Evans, *Dalton Trans.*, 2004, 402-406.
36. B. Chankvetadze, C. Yamamoto and Y. Okamoto, *Combinatorial Chemistry & High Throughput Screening*, 2000, **3**, 497-508.
37. B. Chankvetadze and G. Blaschke, *J. Chromatogr. A*, 2001, **906**, 309-363.
38. E. Yashima, *J. Chromatogr. A*, 2001, **906**, 105-125.
39. K. Lorenz, E. Yashima and Y. Okamoto, *Angew. Chem., Int. Ed.*, 1998, **37**, 1922-1925.
40. B. Chankvetadze, M. Saito, E. Yashima and Y. Okamoto, *Chirality*, 1998, **10**, 134-139.
41. Y. Okamoto, E. Yashima and C. Yamamoto, *Abstracts of Papers of the American Chemical Society*, 1999, **217**, 279-POLY.
42. T. Kubota, T. Kusano, C. Yamamoto, E. Yashima and Y. Okamoto, *Chem. Lett.*, 2001, 724-725.
43. P. Sun, A. Krishnan, A. Yadav, S. Singh, F. M. MacDonnell and D. W. Armstrong, *Inorg. Chem.*, 2007, **46**, 10312-10320.
44. X. M. Chen, Y. Okamoto, T. Yano and J. Otsuki, *J. Sep. Sci.*, 2007, **30**, 713-716.
45. F. J. Coughlin, M. S. Westrol, K. D. Oyler, N. Byrne, C. Kraml, E. Zysman-Colman, M. S. Lowry and S. Bernhard, *Inorg. Chem.*, 2008, **47**, 2039-2048.
46. C. Schaffner-Hamann, A. von Zelewsky, A. Barbieri, F. Barigelli, G. Muller, J. P. Riehl and A. Neels, *J. Am. Chem. Soc.*, 2004, **126**, 9339-9348.

47. L. R. Yang, A. von Zelewsky, H. P. Nguyen, G. Muller, G. Labat and H. Stoeckli-Evans, *Inorg. Chim. Acta*, 2009, **362**, 3853-3856.
48. L. Gong, S. P. Mulcahy, K. Harms and E. Meggers, *J. Am. Chem. Soc.*, 2009, **131**, 9602-9603.
49. L. Gong, S. P. Mulcahy, D. Devarajan, K. Harms, G. Frenking and E. Meggers, *Inorg. Chem.*, 2010, **49**, 7692-7699.
50. A. B. Tamayo, S. Garon, T. Sajoto, P. I. Djurovich, I. M. Tsyba, R. Bau and M. E. Thompson, *Inorg. Chem.*, 2005, **44**, 8723-8732.
51. F. Neve, M. La Deda, A. Crispini, A. Bellusci, F. Puntiliero and S. Campagna, *Organometallics*, 2004, **23**, 5856-5863.
52. Q. Zhao, S. Liu, M. Shi, C. Wang, M. Yu, L. Li, F. Li, T. Yi and C. Huang, *Inorg. Chem.*, 2006, **45**, 6152-6160.
53. D. Franco, M. Gómez, F. Jiménez, G. Muller, M. Rocamora, M. A. Maestro and J. Mahía, *Organometallics*, 2004, **23**, 3197-3209.
54. H. Nozaki, H. Takaya, S. Moriuti and R. Noyori, *Tetrahedron*, 1968, **24**, 3655-3669.
55. H. Brunner, R. Oeschey and B. Nuber, *J. Chem. Soc., Dalton Trans.*, 1996, 1499-1508.
56. A. B. Tamayo, B. D. Alleyne, P. I. Djurovich, S. Lamansky, I. Tsyba, N. N. Ho, R. Bau and M. E. Thompson, *J. Am. Chem. Soc.*, 2003, **125**, 7377-7387.
57. H.-C. Böttcher, M. Graf, H. Krüger and C. Wagner, *Inorg. Chem. Commun.*, 2005, **8**, 278-280.
58. A. R. McDonald, M. Lutz, L. S. von Chrzanowski, G. P. M. van Klink, A. L. Spek and G. van Koten, *Inorg. Chem.*, 2008, **47**, 6681-6691.
59. K. A. McGee and K. R. Mann, *Inorg. Chem.*, 2007, **46**, 7800-7809.
60. L. Li, W. W. Brennessel and W. D. Jones, *Organometallics*, 2009, **28**, 3492-3500.

# **Appendix**

## Appendix

### Live-cell imaging

The live-cell imaging and cytotoxicity studies were carried out by our collaborators, Prof. Dr. Nils Metzler-Nolte and Annika Gross at the Ruhr University Bochum.

MCF7 cells were grown on Ibidi 8 well slides and incubated at 37 °C under a 5% CO<sub>2</sub> atmosphere for 24 hrs. The culture medium was removed and replaced with a medium containing the Ir(III) complexes (**2.8a** or **2.8g**) at a concentration of 25 µM and incubated for 14 hrs. After this time, the cells were further incubated with Lysotracker Red for 2h, then the medium was removed and the cell layer is washed gently with PBS. Further, PBS was exchanged against medium without phenol red or supplements and imaging was carried out using a fluorescence microscope, as discussed below.

### Microscope and Filter information

Imaging was performed using a fluorescence microscope (OLYMPUS IX81, IX81S1F-3) with a lamp X-Cite (120Q) and filter set UV: U-MWU. Details are as follows: Excitation filter: 330-395 nm, long pass filter: 420nm-long pass, Dichroic mirror: 400 nm, Texas red filter: U-MNG, Excitation filter: 530-550nm, Barrier Filter: 590nm- long pass, Dichroic mirror: 570 nm.

### Cell Culture

The human HepG2 cell line was obtained from “Deutsche Sammlung von Mikroorganismen und Zellkultur ACC 180”. The cell lines Hela and PT45 were provided by Prof. Hahn (Molekular Onkology, Ruhr-University Bochum). Cells were grown in RPMI 1640 medium with 1 mM Sodium pyruvate, 2 mM L-Glutamin, 100 units/ml Pen Strep, 10% fetal calf serum. The cells were maintained at 37 °C in a humidified incubator under an atmosphere containing 5% CO<sub>2</sub>.

### Cytotoxicity assays

To determine the activity of the compounds, two antiproliferative assays, Resazurin and Crystal Violet were performed. PT45, HepG2 and HeLa were seeded in 96-well flat-bottomed microtiter plates (6000-9000 cells/well) in growth medium and incubated at 37 °C under a 5% CO<sub>2</sub> atmosphere for 48 hrs. The different compounds were diluted directly in culture medium with 0.5% DMSO from 0.05 µM to 10 µM

concentration and 100  $\mu$ l per well of each solution was then applied to the microtiter plates. After 48h, the medium was removed. The cells were washed twice with 1x PBS and 100  $\mu$ l 10% Resazurin in colourless medium (RPMI 1640) was applied to each well. The initial absorbance was immediately measured at 600 nm in a Tecan Sapphire reader. After 2h of incubation at 37 °C and 5% CO<sub>2</sub> atmosphere, the measurement was repeated. The difference in absorbance gave the viability. Resazurin was removed and cells were fixated with 2% (w/v) glutardialdehyde in PBS for 25 min at room temperature for the Crystal Violet assay. Glutardialdehyde was eluted with two times PBS and cells were permealized with a 0.1% (v/v) Triton-X100 solution in PBS. Afterwards a 0.04% (w/v) aqueous Crystal Violet solution was applied and the microtiter plates were mechanically shaken for 30 min. Excess Crystal Violet was eliminated by repeated elution with H<sub>2</sub>O. The microtiter plates were dried at room temperature and Crystal Violet was eluted from the cells with 96% Ethanol for 4 h at room temperature. The absorbance was measured at 570 nm. 24h pre-substance incubation values were subtracted for normalization for the Crystal Violet assay. IC<sub>50</sub> values were determined by plotting the obtained absorbance values against the compound concentration in half-logarithmical scale, and applying a sigmoidal fit function with Origin 7 Software (Originlab, Northhampton, USA).

### **pH dependent absorption/emission studies and Molybdate sensing**

The pH dependent absorption and emission studies and molybdate sensing were carried out by Dr. Anne-K. Duhme-Klair *et al.* at the University of York.

### **General Titration protocol**

The solvent system used consisted of a mixture of acetonitrile and water (20:1). Adjustments to the pH were carried out with 0.6 M and 0.1 M solutions of HCl in this solvent system and 0.6 M, 0.1 M and 0.05 M solutions of tetramethyl ammonium hydroxide [(Me<sub>4</sub>N)OH] in water. The concentrations of **4.11a**, **4.11g** and **4.11j** were made to 0.02 mM, 0.04 mM and 0.08 mM respectively. These concentrations gave an absorbance within the Beer-Lambert range. The excitation wavelength were set to 326nm, 330 nm and 400 nm for **4.11a**, **4.11g** and **4.11j** respectively, and the emission spectra were recorded between 350 and 800 nm for **4.11a** and **4.11g** and between 450 and 800 nm for **4.11j**.

## Determination of pH profiles

The solution of the sensors was adjusted to the starting pH value in acidic range (1) using the standard acid (mentioned above) and a spectrum was recorded. Small aliquots of base were added to the sample. The pH of the solution was allowed to stabilize before a spectrum was recorded. The spectra were recorded at intervals of approximately 0.5 pH units, across the pH range of *ca.* 1-10. Analogous titrations were conducted in the presence of stoichiometric quantities of molybdate. Aqueous standard solution of  $\text{Na}_2\text{MoO}_4$  was used for this purpose.

## Metal-to-Sensor titrations

Titrations for the determination of the composition of the complexes were conducted using the following procedure. The standard sample solutions (0.015 mM, 0.042 mM and 0.083 mM for **4.11a**, **4.11g** and **4.11j** respectively) of the sensors (**4.11a,g,j**) were buffered with 10  $\mu\text{L}$  of lutidine, and the pH were adjusted to the required value (4.08 for **4.11a** and **4.11j**, and 4.67 for **4.11g**) with standard acid and base solutions. To the above solutions, 5  $\mu\text{L}$  aliquots of the standard solution of  $\text{Na}_2\text{MoO}_4$  (0.6 mM, 1.26 mM and 2.49 mM for **4.11a**, **4.11g** and **4.11j** respectively) were added. After each addition, the sample was stirred for *ca.* 3 min to allow the solution to equilibrate before the emission was recorded. Aliquots of  $\text{Na}_2\text{MoO}_4$  were added until an approximate 2:1 ratio was reached.

## Detection Limit

The detection limit (DL), is defined as the smallest concentration of the analyte that can be reported with a certain level of confidence and is calculated using equation 1.<sup>i</sup>

$$DL = ks_b / m \quad (1)$$

where  $k$  is chosen to be 3, and corresponds to a confidence level of 98.3%, respectively;  $s_b$  is the standard deviation of the blank and  $m$  is the calibration sensitivity.

---

<sup>i</sup>. D. A. Skoog, D. M. West, F. J. Holler and S. R. Crouch, *Fundamentals of Analytical Chemistry*, (Chapters 6 & 8), Thomson Brooks/Coke, Australia, Eighth Edition.

## Postgraduate activities

### Internal seminars-External speakers

30/04/07 Mini symposium “*Metals in Medicine*”  
Dr Sofia Pascu (University of Oxford)  
“*Designing Small Molecule-based Probes for In Vitro Fluorescence Imaging*”  
Prof. Nils Metzler-Nolte (Rhur-Universitaet Bochum, Germany)  
“*Labelling of Bioactive Peptide with organometallic Compounds: From Basic Chemistry to Biomedical Application*”  
Dr Gareth Williams (Durham University)  
“*Sensing and Imaging with Cell-permeable Luminescent Platinum and Iridium Complexes*”  
Prof. Chris Orvig (University of British Columbia, Canada)  
“*Carbohydrate Conjugates in Medicinal Inorganic Chemistry*”

09/05/07 Mini-symposium “Aspects of catalysis”  
Dr Ian Fairlamb (University of York)  
“*Ligand effects in Pd catalysed processes: Importance of conformational flexibility and the exploitation of non-innocent alkene ligands*”  
Prof. Simon Woodward (University of Nottingham)  
“*Organic 'Couplings'via New Metallic Chemistry of Al, Ni, Cu and Zn*”  
Dr David Willock (University of Cardiff)  
“*Simulation of adsorption and Reaction at catalyst surfaces*”

06/05/08 The RSC Centenary Lecture by Professor Don Tilley (University of California Berkeley)  
"New bond activations at transition metal centres: Fundamental studies and applications to Catalysis"

27/06/08 Anniversary research day in the University of Leicester  
Dr Rob Brown (University of Huddersfield)  
“*Cleaner Chemistry with Solid Acid Catalysts*”

Dr Kevin Hughes (University of Leeds)  
“*Mechanism Reduction: Methodologies and Examples*”

Dr Peter Holliman (University of Wales, Bangor)  
“*Super leaves - using materials chemistry to make clean up with solar energy*”

Dr Karl Coleman (University of Durham)  
“*Chemistry of Carbon Nanotubes*”

Dr Craig Rice (University of Huddersfield)  
“*Reprogrammable Ligands*”

Dr Bill Henderson (Waikato University)  
“*180 Degrees of Coordination Chemistry*”

Dr Mike Coogan (Cardiff University)  
“*Design and Application of Luminescent Rhenium Complexes in Cell Imaging*”

Prof Emma Raven (University of Leicester)  
“*The reactivity of heme in biological systems*”

Dr Andrew Russell (University of Reading)  
“*Symmetry in Synthesis; Obvious and Hidden*”

Dr Sean Bew (University of East Anglia)  
“*Small Rings to Big Rings: Adventures in Asymmetric Synthesis*”

Dr Sally Freeman (University of Manchester)  
“*Phosphorus Chemistry-To Leicester and Beyond*”

29/10/08	Dr George Britovsek (Imperial College) "Tuning the Reactivity of Non-heme Iron Catalysts for the Oxidation of Alkanes"
05/11/08	Dr Paul Davies (Birmingham) "Organic Synthesis by Gold Catalysed Alkyne Activation"
25/02/09	Prof Martin Wills (University of Warwick) "Asymmetric Catalysts for the Asymmetric Reduction of Ketones and Imines"

11/03/09 Prof Joe Harrity (University of Sheffield)  
"Development of New Strategies for the Synthesis of Functionalised Synthetic Intermediates"

06/05/09 James Clark (University of York)  
"Green Chemistry and the Biorefinery"

09/12/09 Prof Steve Nolan Clark (University of St Andrews)  
"The use of N-heterocyclic Carbenes (NHC) in late transition metal catalysis"

**Symposia, Conferences and Poster sessions attended**

27/03/08 **DALTON Division Midlands Postgraduate Symposium, University of Warwick**  
Poster title: "Cyclometallated Iridium Complexes: Applications as (bio)sensors"

29-30/06/09 **Coordination Chemistry Discussion Group, University of Leeds**  
Poster title: "Luminescent Cyclometallated Iridium Complexes: Synthesis, Characterisation and Applications" **Received prize out of 67 posters.**